UNIVERSITÀ
DEGLI STUDI
DI BRESCIA

UNIVERSITÀ DEGLI STUDI DI BRESCIA

DOTTORATO DI RICERCA IN
Ingegneria Meccanica e Industriale

settore scientifico disciplinare
ING-IND/13 Meccanica Applicata alle Macchine

CICLO XXXIII

Advanced Dynamic Model and Analysis of Serial Robotics

NOME DEL DOTTORANDO:
Lei HAO

NOME DEL RELATORE:
Giovanni Legnani

Abstract

Questa tesi si occupa dello studio di modelli dinamici e dei comportamenti derivanti da fenomi d'attrito durante le movimentazioni di manipolatori seriali a sei assi. Il modello dinamico viene discusso in primo luogo con la sua linearizzazione e successivamente viene introdotto un nuovo tipo di modello d'attrito. Le traiettorie utilizzate durante gli esperimenti sono state progettate allo scopo di identificare i parametri dinamici ed il comportamento dell'attrito dalla condizione di macchina fredda a quella di macchina calda. Al fine di creare una traiettoria di eccitazione appropriata per l'identificazione, sono stati applicati due differenti metodi per l'ottimizzazione. Successivamente le traiettorie sono state modificate ulteriormente per risolvere il problema del mancato raggiungimento della velocità massima. Una speciale sequenza di movimentazioni è stata configurata per misurare la coppia di attrito a diverse velocità ed a diverse temperature. Le traiettorie realizzate per gli esperimenti sono state eseguite ripetutamente su due robot dello stesso modello, e quindi teoricamente identici, con lo scopo di effettuare poi un confronto dei risultati ottenuti.

Abstract

This thesis deals with the study of dynamic models and friction phenomena during the movements of six-axis serial manipulators. The dynamic model is first discussed with its linearization, and then a new type of friction model is introduced. The trajectories used during the experiments were designed to identify the dynamic parameters of the model and the behaviour of friction from cold to hot machine. In order to create an appropriate excitation trajectory for identification, two different optimization methods were applied. Subsequently, the trajectories were further modified to solve the problem of not reaching the maximum speed of the robot. A special sequence of movements was configured to measure the friction torque at different velocities and temperatures. The trajectories created for the experiments were repeatedly performed on two robots of the same model (theoretically identical), to make a comparison of the results obtained.

Acknowledgements

This thesis is completed with many helps. In particular, I would like to thank:

Giovanni Legnani, my advisor, who guides me in the path of study, with many suggestions and conversations in the study, showing me the direction in the knowledge of robotics, providing the information in the living, and everything else. Roberto Pagani, who gives many helps in the study, and provides me with some of his previous works, which has helped me much to finish the working.

The companies of EFORT, ROBOX, CMA and EVOLUT, and the wonderful people who are in these companies. I would like to thank EFORT firstly, which provides this opportunity of study, and gives me a choice to touch the treasure hide in the knowledge. Then I would like to thank everyone from these companies who help me in the study with great supports.

And everyone else in the University of Brescia, who provide a fantastic environment of studying.

At last, I would like to thank my parents and my wife. Without your supports, this study would be lonely. Thanks to my wife, who brings us a daughter. This makes the life full of laughter.

Best wishes with everyone mentioned above, in this special period and for the future.

Contents

List of Tables

List of Figures

Chapter 1

Introduction

1.1 Motivation And Background

Due to the industry growth, the intelligent manufacturing is introduced in the traditional manufacturing. As an integral part of intelligent manufacturing, the automatic machine in production lines has earned an increasing amount of attention. Specifically, the robot is becoming popular due to the flexible and multi-purpose usage. Generally, the industry robot refers to a machine with multi-degree-of-freedom or multi-joint manipulators in the industrial field, which is mainly applied in welding, processing, assembly, handling, painting, polishing and so on. Producing a robot requires the technologies of modern manufacturing, new material and control system. The research and development, manufacturing and applications of the industry robot have become important indicators of the manufacturing and technological innovation capabilities of a country or region.

In the traditional industrial field, such as auto manufacturing and metallurgy, the applications with the 6-serial-axis manipulator are in great demand. Recently, new applications, such as laser cutting and the 3D scanning, have obtained more attention with the development of new manufacturing processes. All these applications rely on high precision trajectory control with high velocity movement. In the early stage of development, the nonlinear elements of robot dynamics are not counted due to the computing performance, which includes the frictions and gravity. Usually, the robot drivers are simply controlled by PID regulator only to simplify the controller system design. However, this choice creates a disadvantage of the accuracy of the robot at high velocity movement. Additionally, to increase efficiency and reduce product cost, the equipment is configured at the highest operating rate. This requires robots to ensure accuracy in the trajectory with the shortest working cycle. To solve this problem, some methodologies are introduced for estimation and compensation of the torque. These methodologies include importing nonlinear elements in the dynamic model and creating the feed-forward control loop. These methods cause the benefits of reducing the errors created by the controllers and increasing the convergence rate of the errors inside the drivers, which improves the dynamic response of robot. However, the implementation of these methods relies on the accuracy of the robot dynamic parameters.

In China's market, the demand of industrial robot is arising. With the production growing, and with the problem of the shortage of labour, the demand of automation in industrial manufactures is increasing. The industrial robots have become the first choice for upgrading new and old production lines due to its wide applicability, controllable cost, and stability. Because of that, China becomes an indispensable part of the global robot market, which total annual sales exceed 50,000 units. Therefore, a large number of studies related to robotics have been performed by robotic companies and research departments. However, most of them focused on the field of traditional control methodologies. In terms of basic motion planning and control algorithms, theoretical research and virtual simulation are the main focus, which cannot solve and verify system flexibility and nonlinear problems.

This thesis focuses on the study and experiments of robotic dynamics. The dynamic model is based the Newton-Euler functions. Additionally, for the purpose of increasing accuracy of the dynamic model, the nonlinear coefficients are introduced into the friction model. In this study, an optimal excitation trajectory has been found. In order to solve the problem that the gearbox temperature cannot be measured directly, a time-based friction observation model is introduced and discussed. Simultaneously, to observe whether the above test was repeatable, the tests were conducted in two robots and the results are compared.

1.2 Technical Review

1.2.1 Dynamic Model

The accuracy of dynamic parameters is crucial for establishing a robot dynamics model. The values extracted from general CAD files are not sufficient accurate for the actual calculation. This issue comes from nonlinear elements which cannot be obtained by the measurement of the CAD drawing, such as friction and dimension errors. Therefore, parameter identification through experimental data is the only reliable method to accurately obtain dynamic parameters. There are massive researches and studies of dynamic parameter identification, which parts of results have been applied to the actual production.

The work of Calafiore [8] and Indri [21] describe a procedure useful to obtain the dynamical parameters of a SCARA robot, which includes the parameter estimation and experiment trajectory optimization. Both articles are important because they provide a standard method for the dynamic parameter identification based on the fundamental concept of dynamic identification. This method demonstrates the calculation of robot dynamic model with the Newton-Euler equation, and also the creation of the excitation trajectory optimization. Additionally, the results are discussed in the articles with the figures and RMS values. Moreover, in the case of 6-axis manipulators, the base parameters are required to avoid complex calculation. This work is illustrated in many other papers [3, 7, 16–18, 24, 26, 27, 35, 36, 61]. These preview works create a complete method to estimate the dynamic parameters on 6-axis robots.

Due to the sensor size decreases, it becomes possible to insert torque sensors into the robot body. Therefore, the output torque can be measured directly in the recent released collaborative robot, such as KUKA LBR iiwa [29] and UR series of Universal Robots [58].

Jubien [23] studied the dynamic identification with the robot KUKA LWR, which the torque of robot joints can be obtained directly from the build-in sensors. He used two methods for the identification, one was established from the joint position and the motor current, and the other one was created by the data measured from the torque sensors. The comparison results proved that the above two methods were consistent in the identification results of dynamic parameters.

Memar [37] discussed parameter identification with a 6 DOF robot SCHUNK Powerball LWA 4P. The methods presented in this paper were based on the inverse kinetic model and least square. The results were verified with a designed experimental trajectory. It should point that there was a warm-up motion in the designed experiment to avoid reducing of the viscous friction due to the changes of the temperature of the lubrication, which means the results were calculated based on the warm conditions of the robot.

Toward the various researches based on dynamic parameters identification and friction of robots, it has been found that most of the studies were based on traditional robot dynamics models, which are Newton-Euler and Lagrange models. After the model established, the linearization has been down with the selected base parameters. Additionally, high-precision friction model is also essential for estimating the torque output. Recently, with the introduction of robots with build-in joint torque sensors, the data obtained from these sensors can be used in the parameter identification. The results of both methods are identical and proved by the

Jubien [23].

In these studies, the physical elements are mainly focused, such as mass and inertia. However, the nonlinear coefficients are not described in the simplified model, therefore their impact on dynamic identification is ignored. This leads to future studies for these nonlinear elements to improve the robot performance with new control methodologies.

1.2.2 Friction

Friction is a complex phenomenon and it could be influenced by many factors. For example, the shape and roughness of the object surface, the velocity and pressure between the surface, the temperature and humidity, lubrication, and so on [4, 48]. The mainly used friction models are based on the velocity. The classic friction model includes static friction and dynamic friction. The static friction presents the force between two solid objects that are not moving. The dynamic friction is the resistance force that appear when there is a relative motion between two materials. The most used friction model is based on the coulomb model and the viscous model. However, the precision of these models is low in complex scenarios, especially when the operations are affected by the alterations of the environment, for example, the temperature. Therefore, some models based on temperature changes have been studied in several papers [34, 38, 42].

The common friction models are also used in the study of dynamic model of the robots. Some models are introduced and created based on the Stribeck model [7, 47, 49, 50], which includes exponential coefficients. New friction models are introduced in the later last century with new theories, such as Dahl model [12], LuGre model [10] and Maxwell-Slip model [30, 51].

With respect to the mechanical structure of robotics, the assembly and contents of the robot joint effect the friction in the robot motions [4,34]. The assembly influences the pressure between the object surface, which creates friction in the movement due to the roughness and shape. However, this influence is controllable due to the usage of new tools and standardized production. Moreover, this influence may have negligible changes in the life cycle of the machine. Another issue could be linked with the inside and outside environment, for example, the temperature and lubrication. This situation has been examined with the temperature-based friction model. Many studies show that the most fiction changes during the motion depend on the lubrication. Since the lubrication has its own performance and it is linked with the temperature, the friction-temperature affection related the internal lubrication has been studied.

Many papers and studies discussed the friction behaviours with temperature change. Bittencourt [5, 6] discussed the friction model with temperature effects. Both papers discussed the friction in robotics designed as the LuGre model with the influence of temperature. The book [4] discussed the friction and all possible influences in the theories and physics, including the relationship between friction and lubrication, and its behaviours with different temperatures. In addition, there are no temperature sensors in the most industrial robot due to the cost, which leads to the impossibility of obtaining the temperature values directly to establish the relationship between temperature and friction. To solve this problem, Pagani [39] provides an option for studying friction behaviour with a time-based friction model.

Since the inability of obtaining the temperature directly from the robot gearbox, alternative methods have been studied. Based on the studies of temperature-based friction model, it is assured that, using a specific protocol, the temperature rising can be estimated by time. In the paper of Simoni [47] and Pagani [39], a time-based friction observation model is introduced and discussed with some experiments, which describe the behaviour between the friction and time within the robot operations, with the purpose of trying to solve the problem that the temperature inside the gearboxes cannot be directly measured.

Based on the previews researches, Calafiore [8] provides a simplified friction model, but it can only describe the friction behaviour at specific range of velocity. Therefore, to provide a better description of the friction, a third order polynomial model is introduced by Visioli [59], and then continuously implemented in the paper of Indri [21], Legnani [32], Simoni [48] and

Pagani [39]. These studies show a good estimation results with this new friction model, which is discussed in Section 3.1.2. The paper of Legnani [32], Simoni [47,48] and Pagani [39] demonstrate the basic theory and the methodologies. They described the relationship between the friction and temperature with a designed trajectory. Simoni [47, 48] also analysed and modelled this thermal-friction effect. These studies provided the basic ideas of experiment design and they will be discussed in Section 4.

1.3 Overview Of This Thesis

This thesis provides a new methodology to investigate the relationship between the friction and the dynamic model, which is presented by the results of designed experiments. This thesis is organized into 7 parts, which include 6 chapters and an appendix. The introduction has been presented previously and shown the motivation and previews work reviews. The 2^{nd} chapter demonstrates the based knowledge and mathematical theories used in this thesis. The study of robot dynamics is presented in Chapter 3, in which the creation of the information matrix of the dynamic model and the base parameter selection are explained. The experimental design is introduced in details in the Chapter 4. It is also presented the method and reason to create the experimental trajectory. In addition, a problem in excitation trajectory creation is illustrated and solved. The data obtained from the experimental trajectory have been calculated and presented in Chapter 5. The dynamic parameters found with the identification are verified and compared between the tests and robots. The friction behaviour during the experiments is discussed. The last chapter is the conclusion. Due to the larger number of the figures and tables, they are listed and described in the appendixes. Additionally, the code used in MATLAB and some calculation details are also presented in the appendixes.

Furthermore, the robots used in experiments are provided by EFORT and they are installed in the robotics laboratory at the university of Brescia. The mechanical characters of the manipulator are introduced in Section 2.1.1, and the robot movement configurations in experiments are demonstrated in Section 4.4. The experimental environment is explained in Section 4.6. In experiments, the position, velocity and acceleration of motion are collected. The related software and built-in functions that introduction in Section 4.6.

Chapter 2

The Theories And Mathematics

2.1 The Robot

2.1.1 The Structure

There are several types of robots used in manufacturing. The most popular manipulator is the anthropomorphic arm with Spherical Wrist as shown in Figure 2.1, which has 6 axes. In this thesis, the robot used is the ER3A from EFORT [14] and it is shown in Figure 2.2. The robot specifications are listed in Table 2.1.

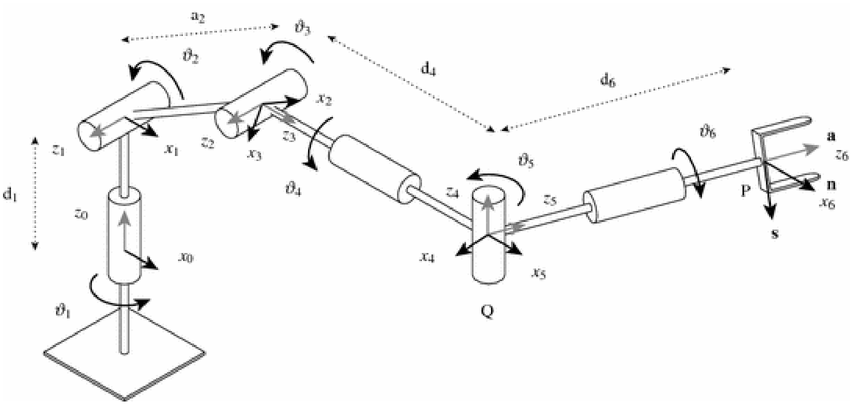

Figure 2.1: The anthropomorphic arm with the spherical wrist

Figure 2.2: The robot of ER3A from EFORT

Table 2.1: The specifications of ER3A

Joint	Position ($degree$)	Maximum Velocity ($degree/s$)	Maximum Acceleration ($degree/s^2$)	Rated Torque of Motor (Nm)	Gear ratio
1	140 ∼ -140	230	510	0.64	121
2	90 ∼ -130	230	495	0.64	121
3	100 ∼ -70	250	510	0.318	101
4	180 ∼ -180	320	1080	0.318	75.48
5	110 ∼ -110	320	1080	0.159	81
6	360 ∼ -360	420	1080	0.159	50

2.1.2 Denavit-Hartenberg Parameters

The mathematical method of Denavit-Hartenberg [13], called DH from now on, is introduced to describe the relationship between all links. There are two types of DH methods, which are standard DH method [13] and modified DH method (MDH) [25]. There are four parameters used in both methods, which are a, α, d and θ. The most important difference between them is the definition of the θ angle, as shown in Figure 2.3. In the standard DH method, θ is defined as the angle between the X axis of Joint i and $i+1$. Then this method leads to a_i and α_i, which are the distance and the angel between the Z axis of the same joint pairs respectively. By contrast, in the modified DH method, θ is defined as the angle between the X axis of Joint $i-1$ and i. This change results to a_{i-1} and α_{i-1}, which have the same meanings as a_i and α_i respectively but with different joint pairs. These parameters are used in the calculation of the direct kinematic and the dynamic model of the robot, but they will be elaborated in Section 2.1.4 and Chapter 3 respectively.

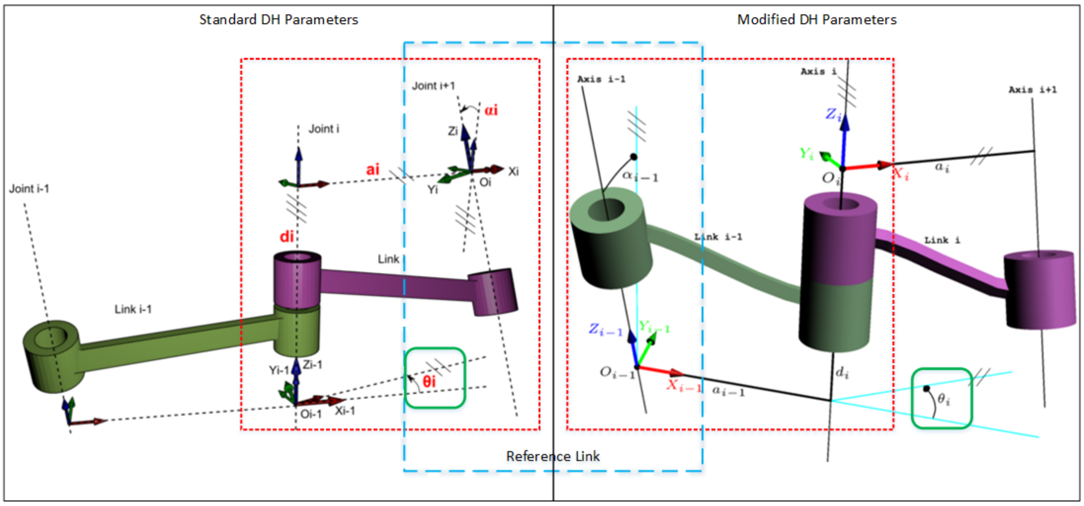

Figure 2.3: The DH & MDH with their difference

In this thesis the MDH has been used as default due to the data provided by EFORT. The MDH parameters of ER3A are shown in Table 2.2, and their scheme is show in Figure 2.4. In this thesis, the MDH values are used to calculate the robot joint position with the link transformation matrix, see Section 2.1.3.

2.1.3 The Link Transformation Matrix

The link transformation matrix relocates the position of one link frame to another link frame. With the modified DH system, the DH parameters are built with three pre-defined

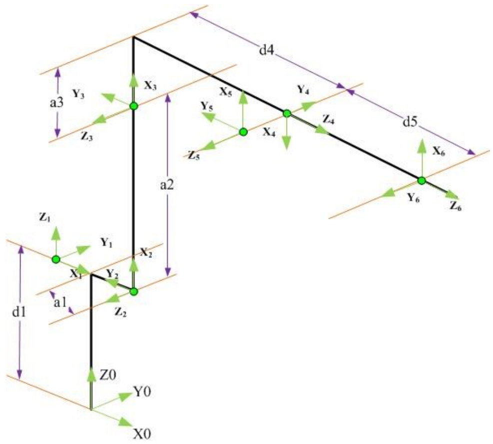

Figure 2.4: The Schematic of MDH frame

Table 2.2: MDH parameters of ER3A

Link	a_{i-1} (m)	α_{i-1} $(degree)$	d (m)	θ $(degree)$
1	0	0	0.32	0
2	0.05	90	0	90
3	0.27	0	0	0
4	0.07	90	0.3	180
5	0	90	0	180
6	0	90	0.0785	0

frames (Figure 2.5), which are Frame R located on the Axis $i-1$, Frame Q located on the Axis i, and frame P based on the position of the link $i-1$ and link i.

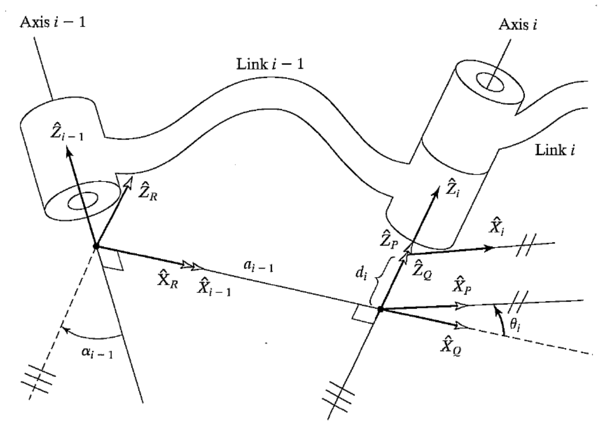

Figure 2.5: The frame P, Q and R, and the MDH parameters

As stated in [11, 45], the transfer function that describes the vector defined by link i in the frame of link $i-1$ can be written as:

$$\boldsymbol{p}^{i-1} = \boldsymbol{T}_i^{i-1}\boldsymbol{p}^i = \boldsymbol{R}_{x,\alpha_{i-1}}\boldsymbol{D}_{x,a_{i-1}}\boldsymbol{R}_{z,\theta_i}\boldsymbol{D}_{z,d_i}\boldsymbol{p}^i \tag{2.1}$$

And the transfer elements of $\boldsymbol{T}_i^{i-1}$ can be written in a matrix form as follows:

$$\boldsymbol{T}_i^{i-1} = \boldsymbol{R}_{x,\alpha_{i-1}} \boldsymbol{D}_{x,a_{i-1}} \boldsymbol{R}_{z,\theta_i} \boldsymbol{D}_{z,d_i} = \begin{bmatrix} \cos\theta_i & -\sin\theta_i & 0 & a_{i-1} \\ \sin\theta_i \cos\alpha_{i-1} & \cos\theta_i \cos\alpha_{i-1} & -\sin\alpha_{i-1} & -d_i \sin\alpha_{i-1} \\ \sin\theta_i \sin\alpha_{i-1} & \cos\theta_i \sin\alpha_{i-1} & \cos\alpha_{i-1} & d_i \cos\alpha_{i-1} \\ 0 & 0 & 0 & 1 \end{bmatrix} \tag{2.2}$$

Where the $\boldsymbol{D}$ is the displacement matrix [62, 67] and $\boldsymbol{T}$ is the transfer matrix from one frame to the next one with a given distance and rotation angles.

2.1.4 The Direct Kinematic

The direct Kinematic is used to calculate the robot end positions. It is based on the MDH parameters which are introduced in Section 2.1.3. Based on the previous references, the direct kinematic transfer matrix from Joint 0 to Joint 6 is shown as Equation 2.3 [11].

$$\boldsymbol{T}_6^0 = \begin{bmatrix} \boldsymbol{R} & \boldsymbol{p} \\ \boldsymbol{0}_{1*3} & 1 \end{bmatrix} = \begin{bmatrix} r_{11} & r_{12} & r_{13} & p_x \\ r_{21} & r_{22} & r_{23} & p_y \\ r_{31} & r_{32} & r_{33} & p_z \\ 0 & 0 & 0 & 1 \end{bmatrix} \tag{2.3}$$

with

$$r_{11} = c_1 \left[c_{23} \left(c_4 c_5 c_6 - s_4 s_6\right) - s_{23} s_5 c_6\right] + s_1 \left(s_4 c_5 c_6 + c_4 s_6\right) \tag{2.3a}$$
$$r_{21} = s_1 \left[c_{23} \left(c_4 c_5 c_6 - s_4 s_6\right) - s_{23} s_5 c_6\right] - c_1 \left(s_4 c_5 c_6 + c_4 s_6\right) \tag{2.3b}$$
$$r_{31} = -s_{23} \left(c_4 c_5 c_6 - s_4 s_6\right) - c_{23} s_5 c_6 \tag{2.3c}$$
$$r_{12} = c_1 \left[-c_{23} \left(c_4 c_5 s_6 + s_4 c_6\right) + s_{23} s_5 s_6\right] + s_1 \left(c_4 c_6 - s_4 c_5 s_6\right) \tag{2.3d}$$
$$r_{22} = s_1 \left[-c_{23} \left(c_4 c_5 s_6 + s_4 c_6\right) + s_{23} s_5 s_6\right] - c_1 \left(c_4 c_6 - s_4 c_5 c_6\right) \tag{2.3e}$$
$$r_{32} = s_{23} \left(c_4 c_5 s_6 + s_4 c_6\right) + s_{23} s_5 s_6 \tag{2.3f}$$
$$r_{13} = -c_1 \left(c_{23} c_4 s_5 + s_{23} c_5\right) - s_1 s_4 s_5 \tag{2.3g}$$
$$r_{23} = -s_1 \left(c_{23} c_4 s_5 + s_{23} c_5\right) + c_1 s_4 s_5 \tag{2.3h}$$
$$r_{33} = s_{23} c_4 s_5 - c_{23} c_5 \tag{2.3i}$$
$$p_x = c_1 \left(a_2 c_2 + a_3 c_{23} - d_4 s_{23}\right) - d_2 s_1 \tag{2.3j}$$
$$p_y = s_1 \left(a_2 c_2 + a_3 c_{23} - d_4 s_{23}\right) + d_2 c_1 \tag{2.3k}$$
$$p_z = -a_3 c_{23} - a_2 s_2 - d_4 c_{23} \tag{2.3l}$$

Where $\boldsymbol{T}_6^0$ is the transfer matrix from the Joint 0 to Joint 6, and c_i and s_i stands for $\cos(\theta_i)$ and $\sin(\theta_i)$ respectively. For example, c_{23} is $\cos(\theta_2 + \theta_3)$.

2.2 The Mathematics

The mathematics used during the identification and raw data processing are explained below. Least Square is used in the identification, and Feature Scaling is used to improve the accuracy of the results and to reduce the sensitivity from the data dither.

2.2.1 The Least Squares

The Least Squares is used to identify the system dynamic parameters. It is an approach in regression analysis to obtain the optimal solution based on given data and equations. This method follows a linear system described as Equation 2.4:

$$\boldsymbol{y}(t) = \boldsymbol{\varphi}(t)\boldsymbol{\theta} \tag{2.4}$$

Where the $\boldsymbol{y}(t)$ and $\boldsymbol{\varphi}(t)$ is the vector of system output and input at time t respectively, and $\boldsymbol{\theta}$ is the system parameters to identify. The Least Squares procedure starts with the collected data of $\boldsymbol{y}$ and $\boldsymbol{\varphi}$ with the time series $\bar{\boldsymbol{t}}$ (from 1 to k), then it used the estimated parameters $\boldsymbol{\theta}^*$, the differences between the estimated results and desired results are:

$$\boldsymbol{\varepsilon} = \boldsymbol{y} - \boldsymbol{\varphi}\boldsymbol{\theta}^* \tag{2.5}$$

Minimizing j, which is the sum of squared residuals as shown in Equation 2.6, it is possible to find the optimal parameters $\boldsymbol{\theta}^*$.

$$j = \sum_{i=1}^{k} [\varepsilon(i)]^2 \tag{2.6}$$

In this process, the minimized j can be obtained by setting the partial derivative to zero as follows:

$$\left.\frac{\partial j}{\partial \boldsymbol{\theta}}\right|_{\boldsymbol{\theta}=\boldsymbol{\theta}^*} = 0 \tag{2.7}$$

Then:

$$\begin{aligned} j &= \sum_{i=1}^{k} [\varepsilon(i)]^2 = \boldsymbol{\varepsilon}^T\boldsymbol{\varepsilon} \\ &= [\boldsymbol{y} - \boldsymbol{\varphi}\boldsymbol{\theta}^*]^T [\boldsymbol{y} - \boldsymbol{\varphi}\boldsymbol{\theta}^*] \\ &= \boldsymbol{y}^T\boldsymbol{y} - 2(\boldsymbol{\theta}^*)^T\boldsymbol{\varphi}^T\boldsymbol{y} + (\boldsymbol{\theta}^*)^T\boldsymbol{\varphi}^T\boldsymbol{\theta}^* \end{aligned} \tag{2.8}$$

$$\begin{aligned} \left.\frac{\partial j}{\partial \boldsymbol{\theta}}\right|_{\boldsymbol{\theta}=\boldsymbol{\theta}^*} = 0 \Rightarrow \left.\frac{\partial j}{\partial \boldsymbol{\theta}}\right|_{\boldsymbol{\theta}=\boldsymbol{\theta}^*} &= -2\boldsymbol{\varphi}^T\boldsymbol{y} + 2\boldsymbol{\varphi}^T\boldsymbol{\varphi}\boldsymbol{\theta}^* = 0 \\ \Rightarrow \boldsymbol{\theta}^* &= \left[\boldsymbol{\varphi}^T\boldsymbol{\varphi}\right]^{-1}\boldsymbol{\varphi}^T\boldsymbol{y} \end{aligned} \tag{2.9}$$

$\boldsymbol{\theta}^*$ is obtained finally under the condition of $\boldsymbol{\varphi}^T\boldsymbol{\varphi} \neq 0$.

The Least Square method is used to identify the dynamic parameters in this work, and they are illustrated in Section 5.1.1.

2.2.2 Feature Scaling

The data collected have been feature-scaled by the method of L2-Norm (Euclidean Length) normalization [63] to reduce the noise and increase the redundancy of the data and the accuracy of the identification.

The normalization for a given vector $\boldsymbol{x} = \begin{bmatrix} x_1 & x_2 & \cdots & x_i \end{bmatrix}$ is:

$$\bar{\boldsymbol{x}} = \frac{\boldsymbol{x}}{\|\boldsymbol{x}\|} \tag{2.10}$$

Where $\|x\|$ is the Euclidean Norm of vector $\boldsymbol{x}$:

$$\|x\| = norm(x) = \sqrt{x_1^2 + x_2^2 + \cdots + x_i^2} = \sqrt{\sum_{1}^{i} x_i^2} \tag{2.11}$$

For the given data $\boldsymbol{K}_{n*m}$, shown in matrix form as below:

$$\boldsymbol{K}_{n*m} = \begin{bmatrix} \boldsymbol{k}_1 & \boldsymbol{k}_2 & \cdots & \boldsymbol{k}_m \end{bmatrix} \tag{2.12}$$

where $\boldsymbol{k}_i$ is an $n * 1$ column vector:

$$\begin{aligned}\boldsymbol{K}_{n*m} = \frac{\boldsymbol{K}}{\|\boldsymbol{K}\|} = \boldsymbol{K}\frac{1}{\|\boldsymbol{K}\|} &= \boldsymbol{K}\begin{bmatrix}\frac{1}{\|\boldsymbol{k}_1\|} & 0 & 0 & \cdots & 0\\ 0 & \frac{1}{\|\boldsymbol{k}_2\|} & 0 & \cdots & 0\\ 0 & 0 & \frac{1}{\|\boldsymbol{k}_3\|} & \cdots & 0\\ \vdots & \vdots & \vdots & \ddots & \vdots\\ 0 & 0 & 0 & \cdots & \frac{1}{\|\boldsymbol{k}_m\|}\end{bmatrix}\\ &= \boldsymbol{K}\begin{bmatrix}h_1 & 0 & 0 & \cdots & 0\\ 0 & h_2 & 0 & \cdots & 0\\ 0 & 0 & h_3 & \cdots & 0\\ \vdots & \vdots & \vdots & \ddots & \vdots\\ 0 & 0 & 0 & \cdots & h_m\end{bmatrix} = \boldsymbol{K}\boldsymbol{H}\end{aligned} \tag{2.13}$$

$\boldsymbol{H}$ is a normalization matrix with:

$$h_i = \begin{cases}\|\boldsymbol{k}_i\|^{-1}, & if\|\boldsymbol{k}_i\| \neq 0\\ 1, & if\|\boldsymbol{k}_i\| = 0\end{cases} \tag{2.14}$$

The dynamic Equation 3.17, using a normalization matrix $\boldsymbol{H}$, can be written as:

$$\boldsymbol{\tau} = \boldsymbol{K}\boldsymbol{\Phi} = (\boldsymbol{K}\boldsymbol{H})\left(\boldsymbol{H}^{-1}\boldsymbol{\Phi}\right) = \bar{\boldsymbol{K}}\bar{\boldsymbol{\Phi}} \tag{2.15}$$

Therefore the Least Square method can be used for parameters identification. At the end, a reveres of normalization is needed:

$$\boldsymbol{\Phi} = \boldsymbol{H}\bar{\boldsymbol{\Phi}} \tag{2.16}$$

Chapter 3

Dynamic Study

3.1 Information Matrix

3.1.1 The Newton–Euler Method (NE)

There are two models for establishing the robot dynamic model. They are based on the Lagrange formulations [19] and Newton–Euler formulation [33]. Silver [46] proved that both models can be equivalent. However, based on the other analysis [46], the computation cost of the robot dynamic model coming from Lagrange formula is higher than the model built from Newton–Euler. Therefore, in this thesis, the dynamic model of the robot is built from the Newton–Euler formulation. It contains two sets of recursions: forward and backward recursions. The forward recursions transfer the arms' velocities and accelerations from the base to the end-effector; the backward recursions instead, transfer the forces of the joints from the end-effector to the base. The complete formulations [11, 33] are:

- Forward recursions, from Link 0 → 5:

$$\boldsymbol{\omega}_{i+1} = \boldsymbol{R}_i^{i+1}\boldsymbol{\omega}_i + \dot{\boldsymbol{\theta}}_{i+1}\boldsymbol{z}_{i+1}^{i+1} \tag{3.1}$$

$$\dot{\boldsymbol{\omega}}_{i+1} = \boldsymbol{R}_i^{i+1}\dot{\boldsymbol{\omega}}_i + \boldsymbol{R}_i^{i+1}\boldsymbol{\omega}_i \times \dot{\boldsymbol{\theta}}_{i+1}\boldsymbol{z}_{i+1}^{i+1} + \ddot{\boldsymbol{\theta}}_{i+1}\boldsymbol{z}_{i+1}^{i+1} \tag{3.2}$$

$$\dot{\boldsymbol{v}}_{i+1} = \boldsymbol{R}_i^{i+1}\left[\dot{\boldsymbol{\omega}}_i \times \boldsymbol{p}_{i+1}^{i} + \boldsymbol{\omega}_i \times \left(\boldsymbol{\omega}_i \times \boldsymbol{p}_{i+1}^{i}\right) + \dot{\boldsymbol{v}}_i\right] \tag{3.3}$$

$$\dot{\boldsymbol{v}}_{c_{i+1}} = \dot{\boldsymbol{\omega}}_{i+1} \times \boldsymbol{p_c}_{i+1}^{i+1} + \boldsymbol{\omega}_{i+1} \times \left(\boldsymbol{\omega}_{i+1} \times \boldsymbol{p_c}_{i+1}^{i+1}\right) + \dot{\boldsymbol{v}}_{i+1} \tag{3.4}$$

$$\hat{\boldsymbol{f}}_{i+1} = m_{i+1}\dot{\boldsymbol{v}}_{c_{i+1}} \tag{3.5}$$

$$\hat{\boldsymbol{n}}_{i+1} = \boldsymbol{I}_{i+1}^{c_{i+1}}\dot{\boldsymbol{\omega}}_{i+1} + \boldsymbol{\omega}_{i+1} \times \boldsymbol{I}_{i+1}^{c_{i+1}}\boldsymbol{\omega}_{i+1} \tag{3.6}$$

  with $\boldsymbol{\omega}_0 = \dot{\boldsymbol{\omega}}_0 = \boldsymbol{0}$.

- Backward recursions, from Link 6 → 1:

$$\boldsymbol{f}_i = \boldsymbol{R}_{i+1}^{i}\boldsymbol{f}_{i+1} + \hat{\boldsymbol{f}}_i \tag{3.7}$$

$$\boldsymbol{n}_i = \hat{\boldsymbol{n}}_i + \boldsymbol{R}_{i+1}^{i}\boldsymbol{n}_{i+1} + \boldsymbol{p_c}_i^{i} \times \hat{\boldsymbol{f}}_i + \boldsymbol{p}_{i+1}^{i} \times \boldsymbol{R}_{i+1}^{i}\boldsymbol{f}_{i+1} \tag{3.8}$$

$$\boldsymbol{\tau}_i = (\boldsymbol{n_i})^T\boldsymbol{z}_i^i \tag{3.9}$$

Where:

$\boldsymbol{R}_i^{i+1}$ is the rotation matrix from link i to link $i+1$.
$\dot{\boldsymbol{\theta}}_i$ and $\ddot{\boldsymbol{\theta}}_i$ are the angle speed and acceleration of link i.
$\boldsymbol{\omega}_i$, $\dot{\boldsymbol{\omega}}_i$ and $\ddot{\boldsymbol{\omega}}_i$ are the angular position, speed and acceleration vector of link i.
$\dot{\boldsymbol{v}}_i$ is the linear acceleration of the origin of the link coordination system.
$\dot{\boldsymbol{v}}_{\boldsymbol{c}i}$ is the linear acceleration of the centre of mass of the link i.
$\hat{\boldsymbol{f}}_i$ is the inertial force of the centre of mass of the link i.

$\hat{\boldsymbol{n}}_i$ is the inertial torque of the centre of mass of the link i.
$\boldsymbol{f}_i$ is the force on link i exerted from the link $i-1$.
$\boldsymbol{n}_i$ is the torque on link i exerted from the link $i-1$.
$\boldsymbol{\tau}_i$ is linear actuator force of the link i.
$\boldsymbol{p}_{i+1}^i$ is the transformation vector of the link i, which is pointed from the origin of link i to link $i-1$.
m_i is the mass of link i.
$\boldsymbol{I}_{i+1}^{c_{i+1}}$ is the inertia tensor of link $i+1$ based on its own centre of mass coordinate.
$\boldsymbol{p}_{\boldsymbol{c}_i}^i$ is the vector of the central of mass of the link i in coordination with link i.
$\boldsymbol{z}_i^i = \begin{bmatrix} 0 & 0 & 1 \end{bmatrix}^T$, with the meaning of selecting the value followed the z-axis of DH coordinates.

It should be pointed out that with $\dot{\boldsymbol{v}}_i = \boldsymbol{g}$, the gravity acceleration of each link will be counted into the recursions process.

3.1.2 Friction Model And Motor Inertia

Friction can be modelled from the coulomb friction and viscous friction, and it could be assumed the following polynomial function [21,32,39,48,59]:

$$\tau_f = f_1 sign(\dot{\theta}) + f_2\dot{\theta} + f_3\dot{\theta}^2 sign(\dot{\theta}) + f_4\dot{\theta}^3 \tag{3.10}$$

which $\dot{\theta}$ is the velocity of the joints, and f_1, f_2, f_3 and f_4 are the coefficients of the friction model.

Equation 3.10 can be rewritten in matrix form as:

$$\tau_f = \begin{bmatrix} sign(\dot{\theta}) & \dot{\theta} & \dot{\theta}^2 sign(\dot{\theta}) & \dot{\theta}^3 \end{bmatrix} \begin{bmatrix} f_1 \\ f_2 \\ f_3 \\ f_4 \end{bmatrix} = \boldsymbol{K}_f \boldsymbol{\phi}_f \tag{3.11}$$

Where $\boldsymbol{K}_f$ is the friction information matrix that can be used in the robot dynamic model, and $\boldsymbol{\phi}_f$ is the friction coefficients.

The motor inertia equation can be written in matrix form as:

$$\tau_m = I_m \ddot{\theta} \tag{3.12}$$

$$\Rightarrow \quad \tau_m = \begin{bmatrix} I_m \end{bmatrix} \begin{bmatrix} \ddot{\theta} \end{bmatrix} = \boldsymbol{K}_m \boldsymbol{\phi}_m \tag{3.13}$$

which I_m is the inertia of the motor, and $\ddot{\theta}$ is the angle acceleration.

3.1.3 Information Matrix Formula

Using the Newton-Euler equation, discussed in Section 3.1.1 and also in Appendix C, and the friction model and motor inertia previously shown in Section 3.1.2, the parameters of each joint to identify become:

$$\boldsymbol{\phi}_d = \begin{bmatrix} m & mP_x & mP_y & mP_z & I_{xx} & I_{xy} & I_{xz} & I_{yy} & I_{yz} & I_{zz} \end{bmatrix}^T \tag{3.14}$$

$$\boldsymbol{\phi}_f = \begin{bmatrix} f_1 & f_2 & f_3 & f_4 \end{bmatrix}^T \tag{3.15}$$

$$\boldsymbol{\phi}_m = \begin{bmatrix} I_m \end{bmatrix} \tag{3.16}$$

and the matrix equation can be written as:

$$\boldsymbol{\tau}_{dynamic} = \begin{bmatrix} \tau_{Joint1} \\ \tau_{Joint2} \\ \tau_{Joint3} \\ \tau_{Joint4} \\ \tau_{Joint5} \\ \tau_{Joint6} \end{bmatrix} = \boldsymbol{K}_d\boldsymbol{\phi} + \boldsymbol{\tau}_f + \boldsymbol{\tau}_m = \boldsymbol{K}_d\boldsymbol{\phi}_d + \boldsymbol{K}_f\boldsymbol{\phi}_f + \boldsymbol{K}_m\boldsymbol{\phi}_m$$

$$= \begin{bmatrix} \boldsymbol{K}_d & \boldsymbol{K}_f & \boldsymbol{K}_m \end{bmatrix} \begin{bmatrix} \boldsymbol{\phi}_d \\ \boldsymbol{\phi}_f \\ \boldsymbol{\phi}_m \end{bmatrix} = \boldsymbol{K}_{infor}\boldsymbol{\Phi}_{infor} \tag{3.17}$$

Where:

$$\boldsymbol{K}_d = \begin{bmatrix} \boldsymbol{u}_{11} & \boldsymbol{u}_{12} & \boldsymbol{u}_{13} & \boldsymbol{u}_{14} & \boldsymbol{u}_{15} & \boldsymbol{u}_{16} \\ 0_{1*10} & \boldsymbol{u}_{22} & \boldsymbol{u}_{23} & \boldsymbol{u}_{24} & \boldsymbol{u}_{25} & \boldsymbol{u}_{26} \\ 0_{1*10} & 0_{1*10} & \boldsymbol{u}_{33} & \boldsymbol{u}_{34} & \boldsymbol{u}_{35} & \boldsymbol{u}_{36} \\ 0_{1*10} & 0_{1*10} & 0_{1*10} & \boldsymbol{u}_{44} & \boldsymbol{u}_{45} & \boldsymbol{u}_{46} \\ 0_{1*10} & 0_{1*10} & 0_{1*10} & 0_{1*10} & \boldsymbol{u}_{55} & \boldsymbol{u}_{56} \\ 0_{1*10} & 0_{1*10} & 0_{1*10} & 0_{1*10} & 0_{1*10} & \boldsymbol{u}_{66} \end{bmatrix} \tag{3.17a}$$

$$\boldsymbol{K}_f = \begin{bmatrix} \boldsymbol{k}_{f,\ J1} & 0_{1*4} & 0_{1*4} & 0_{1*4} & 0_{1*4} & 0_{1*4} \\ 0_{1*4} & \boldsymbol{k}_{f,\ J2} & 0_{1*4} & 0_{1*4} & 0_{1*4} & 0_{1*4} \\ 0_{1*4} & 0_{1*4} & \boldsymbol{k}_{f,\ J3} & 0_{1*4} & 0_{1*4} & 0_{1*4} \\ 0_{1*4} & 0_{1*4} & 0_{1*4} & \boldsymbol{k}_{f,\ J4} & 0_{1*4} & 0_{1*4} \\ 0_{1*4} & 0_{1*4} & 0_{1*4} & 0_{1*4} & \boldsymbol{k}_{f,\ J5} & 0_{1*4} \\ 0_{1*4} & 0_{1*4} & 0_{1*4} & 0_{1*4} & 0_{1*4} & \boldsymbol{k}_{f,\ J6} \end{bmatrix} \tag{3.17b}$$

$$\boldsymbol{K}_m = \begin{bmatrix} k_{m,\ J1} & 0 & 0 & 0 & 0 & 0 \\ 0 & k_{m,\ J2} & 0 & 0 & 0 & 0 \\ 0 & 0 & k_{m,\ J3} & 0 & 0 & 0 \\ 0 & 0 & 0 & k_{m,\ J4} & 0 & 0 \\ 0 & 0 & 0 & 0 & k_{m,\ J5} & 0 \\ 0 & 0 & 0 & 0 & 0 & k_{m,\ J6} \end{bmatrix} \tag{3.17c}$$

$$\boldsymbol{\phi}_d = \begin{bmatrix} \boldsymbol{\phi}_{d,\ J1} & \boldsymbol{\phi}_{d,\ J2} & \boldsymbol{\phi}_{d,\ J3} & \boldsymbol{\phi}_{d,\ J4} & \boldsymbol{\phi}_{d,\ J5} & \boldsymbol{\phi}_{d,\ J6} \end{bmatrix}^T \tag{3.17d}$$

$$\boldsymbol{\phi}_f = \begin{bmatrix} \boldsymbol{\phi}_{f,\ J1} & \boldsymbol{\phi}_{f,\ J2} & \boldsymbol{\phi}_{f,\ J3} & \boldsymbol{\phi}_{f,\ J4} & \boldsymbol{\phi}_{f,\ J5} & \boldsymbol{\phi}_{f,\ J6} \end{bmatrix}^T \tag{3.17e}$$

$$\boldsymbol{\phi}_m = \begin{bmatrix} \phi_{m,\ J1} & \phi_{m,\ J2} & \phi_{m,\ J3} & \phi_{m,\ J4} & \phi_{m,\ J5} & \phi_{m,\ J6} \end{bmatrix}^T \tag{3.17f}$$

and the subscripts of "d", "f" and "m" present the first letter of "dynamic", "friction" and "motor" respectively. The elements of "u" in Equation 3.17a are vectors of the z-direction of "U" in Equation C.26.

3.1.4 Information Matrix In The Identification

Based o the discussion of the Least Square in Section 2.2.1, the estimated dynamic parameters $\hat{\boldsymbol{\phi}}$ can be obtained from the given data $\hat{\boldsymbol{K}}$. The data can be reorganized as a matrix with series points, which are:

$$\hat{\boldsymbol{K}}_{point1}, \hat{\boldsymbol{K}}_{point2}, \cdots, \hat{\boldsymbol{K}}_{pointn} \tag{3.18}$$

To give an example, the information matrix $\boldsymbol{K}$ and the estimated parameters $\hat{\boldsymbol{\phi}}$ of joint 1, based on Equation 3.17, can be determined as follows:

$$\boldsymbol{K}_{d,\ Joint\ 1} = \begin{bmatrix} \boldsymbol{u}_{11,Point\ 1} & \boldsymbol{u}_{12,Point\ 1} & \boldsymbol{u}_{13,Point\ 1} & \boldsymbol{u}_{14,Point\ 1} & \boldsymbol{u}_{15,Point\ 1} & \boldsymbol{u}_{16,Point\ 1} \\ \boldsymbol{u}_{11,Point\ 1} & \boldsymbol{u}_{12,Point\ 1} & \boldsymbol{u}_{13,Point\ 1} & \boldsymbol{u}_{14,Point\ 1} & \boldsymbol{u}_{15,Point\ 1} & \boldsymbol{u}_{16,Point\ 1} \\ \vdots & \vdots & \vdots & \vdots & \vdots & \vdots \\ \boldsymbol{u}_{11,Point\ n} & \boldsymbol{u}_{12,Point\ n} & \boldsymbol{u}_{13,Point\ n} & \boldsymbol{u}_{14,Point\ n} & \boldsymbol{u}_{15,Point\ n} & \boldsymbol{u}_{16,Point\ n} \end{bmatrix}_{n*60} \tag{3.19a}$$

$$\boldsymbol{K}_{f,\ Joint\ 1} = \begin{bmatrix} \boldsymbol{k}_{f,1,Point\ 1} & 0_{1*4} & 0_{1*4} & 0_{1*4} & 0_{1*4} & 0_{1*4} \\ \boldsymbol{k}_{f,1,Point\ 2} & 0_{1*4} & 0_{1*4} & 0_{1*4} & 0_{1*4} & 0_{1*4} \\ \vdots & \vdots & \vdots & \vdots & \vdots & \vdots \\ \boldsymbol{k}_{f,1,Point\ n} & 0_{1*4} & 0_{1*4} & 0_{1*4} & 0_{1*4} & 0_{1*4} \end{bmatrix}_{n*24} \tag{3.19b}$$

$$\boldsymbol{K}_{m,\ Joint\ 1} = \begin{bmatrix} k_{m,1,Point\ 1} & 0 & 0 & 0 & 0 & 0 \\ k_{m,1,Point\ 2} & 0 & 0 & 0 & 0 & 0 \\ \vdots & \vdots & \vdots & \vdots & \vdots & \vdots \\ k_{m,1,Point\ n} & 0 & 0 & 0 & 0 & 0 \end{bmatrix}_{n*6} \tag{3.19c}$$

$$\hat{\boldsymbol{\phi}}_{d,\ Joint\ 1} = \begin{bmatrix} \boldsymbol{\phi}_{d,1} & \boldsymbol{\phi}_{d,2} & \boldsymbol{\phi}_{d,3} & \boldsymbol{\phi}_{d,4} & \boldsymbol{\phi}_{d,5} & \boldsymbol{\phi}_{d,6} \end{bmatrix}^T_{1*60} \tag{3.19d}$$

$$\hat{\boldsymbol{\phi}}_{f,\ Joint\ 1} = \begin{bmatrix} \boldsymbol{\phi}_{f,1} & \boldsymbol{\phi}_{f,2} & \boldsymbol{\phi}_{f,3} & \boldsymbol{\phi}_{f,4} & \boldsymbol{\phi}_{f,5} & \boldsymbol{\phi}_{f,6} \end{bmatrix}^T_{1*24} \tag{3.19e}$$

$$\hat{\boldsymbol{\phi}}_{m,\ Joint\ 1} = \begin{bmatrix} \phi_{m,1} & \phi_{m,2} & \phi_{m,3} & \phi_{m,4} & \phi_{m,5} & \phi_{m,6} \end{bmatrix}^T_{1*6} \tag{3.19f}$$

And then the equation used in identification can be rewritten as:

$$[\boldsymbol{\tau}_{Joint\ 1}]_{n*1} = \begin{bmatrix} \tau_{Joint\ 1,\ Point\ 1} \\ \tau_{Joint\ 1,\ Point\ 2} \\ \vdots \\ \tau_{Joint\ 1,\ Point\ n} \end{bmatrix} = \boldsymbol{K}_{Joint\ 1,\ n*90} \hat{\boldsymbol{\Phi}}_{Joint\ 1,\ 90*1} \tag{3.20}$$

$$\Rightarrow \quad \hat{\boldsymbol{\Phi}}_{Joint\ 1} = (\boldsymbol{K}^T_{Joint\ 1} \boldsymbol{K}_{Joint\ 1})^{-1} \boldsymbol{K}^T_{Joint\ 1} [\boldsymbol{\tau}_{Joint\ 1}] \tag{3.21}$$

Using all the joints, the information matrix and the estimated parameters created from the Equation 3.17 are:

$$\boldsymbol{K} = \begin{bmatrix} \boldsymbol{\tau}_{Joint\ 1,\ Point\ 1} \\ \boldsymbol{\tau}_{Joint\ 2,\ Point\ 1} \\ \boldsymbol{\tau}_{Joint\ 3,\ Point\ 1} \\ \boldsymbol{\tau}_{Joint\ 4,\ Point\ 1} \\ \boldsymbol{\tau}_{Joint\ 5,\ Point\ 1} \\ \boldsymbol{\tau}_{Joint\ 6,\ Point\ 1} \\ \boldsymbol{\tau}_{Joint\ 1,\ Point\ 2} \\ \boldsymbol{\tau}_{Joint\ 2,\ Point\ 2} \\ \boldsymbol{\tau}_{Joint\ 3,\ Point\ 2} \\ \boldsymbol{\tau}_{Joint\ 4,\ Point\ 2} \\ \boldsymbol{\tau}_{Joint\ 5,\ Point\ 2} \\ \boldsymbol{\tau}_{Joint\ 6,\ Point\ 2} \\ \boldsymbol{\tau}_{Joint\ 1,\ Point\ 3} \\ \vdots \\ \boldsymbol{\tau}_{Joint\ 6,\ Point\ n-1} \\ \boldsymbol{\tau}_{Joint\ 1,\ Point\ n} \\ \boldsymbol{\tau}_{Joint\ 2,\ Point\ n} \\ \boldsymbol{\tau}_{Joint\ 3,\ Point\ n} \\ \boldsymbol{\tau}_{Joint\ 4,\ Point\ n} \\ \boldsymbol{\tau}_{Joint\ 5,\ Point\ n} \\ \boldsymbol{\tau}_{Joint\ 6,\ Point\ n} \end{bmatrix} = \begin{bmatrix} \boldsymbol{K}_d & \boldsymbol{K}_f & \boldsymbol{K}_m \end{bmatrix} \tag{3.22}$$

$$
\boldsymbol{\phi} = \begin{bmatrix} \boldsymbol{\phi}_{d,\ Point\ 1} \\ \boldsymbol{\phi}_{f,\ Point\ 1} \\ \boldsymbol{\phi}_{m,\ Point\ 1} \\ \boldsymbol{\phi}_{d,\ Point\ 2} \\ \boldsymbol{\phi}_{f,\ Point\ 2} \\ \boldsymbol{\phi}_{m,\ Point\ 2} \\ \boldsymbol{\phi}_{d,\ Point\ 3} \\ \vdots \\ \boldsymbol{\phi}_{m,\ Point\ n-1} \\ \boldsymbol{\phi}_{d,\ Point\ n} \\ \boldsymbol{\phi}_{f,\ Point\ n} \\ \boldsymbol{\phi}_{m,\ Point\ n} \end{bmatrix} \tag{3.23}
$$

and for the $\boldsymbol{K}_d$, $\boldsymbol{K}_f$ and $\boldsymbol{K}_m$:

$$
\boldsymbol{K}_d = \begin{bmatrix}
\boldsymbol{u}_{11,\ Point\ 1} & \boldsymbol{u}_{12,\ Point\ 1} & \boldsymbol{u}_{13,\ Point\ 1} & \boldsymbol{u}_{14,\ Point\ 1} & \boldsymbol{u}_{15,\ Point\ 1} & \boldsymbol{u}_{16,\ Point\ 1} \\
0_{1*10} & \boldsymbol{u}_{22,\ Point\ 1} & \boldsymbol{u}_{23,\ Point\ 1} & \boldsymbol{u}_{24,\ Point\ 1} & \boldsymbol{u}_{25,\ Point\ 1} & \boldsymbol{u}_{26,\ Point\ 1} \\
0_{1*10} & 0_{1*10} & \boldsymbol{u}_{33,\ Point\ 1} & \boldsymbol{u}_{34,\ Point\ 1} & \boldsymbol{u}_{35,\ Point\ 1} & \boldsymbol{u}_{36,\ Point\ 1} \\
0_{1*10} & 0_{1*10} & 0_{1*10} & \boldsymbol{u}_{44,\ Point\ 1} & \boldsymbol{u}_{45,\ Point\ 1} & \boldsymbol{u}_{46,\ Point\ 1} \\
0_{1*10} & 0_{1*10} & 0_{1*10} & 0_{1*10} & \boldsymbol{u}_{55,\ Point\ 1} & \boldsymbol{u}_{56,\ Point\ 1} \\
0_{1*10} & 0_{1*10} & 0_{1*10} & 0_{1*10} & 0_{1*10} & \boldsymbol{u}_{66,\ Point\ 1} \\
\boldsymbol{u}_{11,\ Point\ 2} & \boldsymbol{u}_{12,\ Point\ 2} & \boldsymbol{u}_{13,\ Point\ 2} & \boldsymbol{u}_{14,\ Point\ 2} & \boldsymbol{u}_{15,\ Point\ 2} & \boldsymbol{u}_{16,\ Point\ 2} \\
0_{1*10} & \boldsymbol{u}_{22,\ Point\ 2} & \boldsymbol{u}_{23,\ Point\ 2} & \boldsymbol{u}_{24,\ Point\ 2} & \boldsymbol{u}_{25,\ Point\ 2} & \boldsymbol{u}_{26,\ Point\ 2} \\
0_{1*10} & 0_{1*10} & \boldsymbol{u}_{33,\ Point\ 2} & \boldsymbol{u}_{34,\ Point\ 2} & \boldsymbol{u}_{35,\ Point\ 2} & \boldsymbol{u}_{36,\ Point\ 2} \\
0_{1*10} & 0_{1*10} & 0_{1*10} & \boldsymbol{u}_{44,\ Point\ 2} & \boldsymbol{u}_{45,\ Point\ 2} & \boldsymbol{u}_{46,\ Point\ 2} \\
0_{1*10} & 0_{1*10} & 0_{1*10} & 0_{1*10} & \boldsymbol{u}_{55,\ Point\ 2} & \boldsymbol{u}_{56,\ Point\ 2} \\
0_{1*10} & 0_{1*10} & 0_{1*10} & 0_{1*10} & 0_{1*10} & \boldsymbol{u}_{66,\ Point\ 2} \\
\boldsymbol{u}_{11,\ Point\ 3} & \boldsymbol{u}_{12,\ Point\ 3} & \boldsymbol{u}_{13,\ Point\ 3} & \boldsymbol{u}_{14,\ Point\ 3} & \boldsymbol{u}_{15,\ Point\ 3} & \boldsymbol{u}_{16,\ Point\ 3} \\
\vdots & \vdots & \vdots & \vdots & \vdots & \vdots \\
0_{1*10} & 0_{1*10} & 0_{1*10} & 0_{1*10} & 0_{1*10} & \boldsymbol{u}_{66,\ Point\ n-1} \\
\boldsymbol{u}_{11,\ Point\ n} & \boldsymbol{u}_{12,\ Point\ n} & \boldsymbol{u}_{13,\ Point\ n} & \boldsymbol{u}_{14,\ Point\ n} & \boldsymbol{u}_{15,\ Point\ n} & \boldsymbol{u}_{16,\ Point\ n} \\
0_{1*10} & \boldsymbol{u}_{22,\ Point\ n} & \boldsymbol{u}_{23,\ Point\ n} & \boldsymbol{u}_{24,\ Point\ n} & \boldsymbol{u}_{25,\ Point\ n} & \boldsymbol{u}_{26,\ Point\ n} \\
0_{1*10} & 0_{1*10} & \boldsymbol{u}_{33,\ Point\ n} & \boldsymbol{u}_{34,\ Point\ n} & \boldsymbol{u}_{35,\ Point\ n} & \boldsymbol{u}_{36,\ Point\ n} \\
0_{1*10} & 0_{1*10} & 0_{1*10} & \boldsymbol{u}_{44,\ Point\ n} & \boldsymbol{u}_{45,\ Point\ n} & \boldsymbol{u}_{46,\ Point\ n} \\
0_{1*10} & 0_{1*10} & 0_{1*10} & 0_{1*10} & \boldsymbol{u}_{55,\ Point\ n} & \boldsymbol{u}_{56,\ Point\ n} \\
0_{1*10} & 0_{1*10} & 0_{1*10} & 0_{1*10} & 0_{1*10} & \boldsymbol{u}_{66,\ Point\ n}
\end{bmatrix} \tag{3.24}
$$

$$
\boldsymbol{K}_f = \begin{bmatrix}
\boldsymbol{k}_{f,J1,\ Point\ 1} & 0_{1*4} & 0_{1*4} & 0_{1*4} & 0_{1*4} & 0_{1*4} \\
0_{1*4} & \boldsymbol{k}_{f,J2,\ Point\ 1} & 0_{1*4} & 0_{1*4} & 0_{1*4} & 0_{1*4} \\
0_{1*4} & 0_{1*4} & \boldsymbol{k}_{f,J3,\ Point\ 1} & 0_{1*4} & 0_{1*4} & 0_{1*4} \\
0_{1*4} & 0_{1*4} & 0_{1*4} & \boldsymbol{k}_{f,J4,\ Point\ 1} & 0_{1*4} & 0_{1*4} \\
0_{1*4} & 0_{1*4} & 0_{1*4} & 0_{1*4} & \boldsymbol{k}_{f,J5,\ Point\ 1} & 0_{1*4} \\
0_{1*4} & 0_{1*4} & 0_{1*4} & 0_{1*4} & 0_{1*4} & \boldsymbol{k}_{f,J6,\ Point\ 1} \\
\boldsymbol{k}_{f,J1,\ Point\ 2} & 0_{1*4} & 0_{1*4} & 0_{1*4} & 0_{1*4} & 0_{1*4} \\
0_{1*4} & \boldsymbol{k}_{f,J2,\ Point\ 2} & 0_{1*4} & 0_{1*4} & 0_{1*4} & 0_{1*4} \\
0_{1*4} & 0_{1*4} & \boldsymbol{k}_{f,J3,\ Point\ 2} & 0_{1*4} & 0_{1*4} & 0_{1*4} \\
0_{1*4} & 0_{1*4} & 0_{1*4} & \boldsymbol{k}_{f,J4,\ Point\ 2} & 0_{1*4} & 0_{1*4} \\
0_{1*4} & 0_{1*4} & 0_{1*4} & 0_{1*4} & \boldsymbol{k}_{f,J5,\ Point\ 2} & 0_{1*4} \\
0_{1*4} & 0_{1*4} & 0_{1*4} & 0_{1*4} & 0_{1*4} & \boldsymbol{k}_{f,J6,\ Point\ 2} \\
\boldsymbol{k}_{f,J1,\ Point\ 3} & 0_{1*4} & 0_{1*4} & 0_{1*4} & 0_{1*4} & 0_{1*4} \\
\vdots & \vdots & \vdots & \vdots & \vdots & \vdots \\
0_{1*4} & 0_{1*4} & 0_{1*4} & 0_{1*4} & 0_{1*4} & \boldsymbol{k}_{f,J6,\ Point\ n-1} \\
\boldsymbol{k}_{f,J1,\ Point\ n} & 0_{1*4} & 0_{1*4} & 0_{1*4} & 0_{1*4} & 0_{1*4} \\
0_{1*4} & \boldsymbol{k}_{f,J2,\ Point\ n} & 0_{1*4} & 0_{1*4} & 0_{1*4} & 0_{1*4} \\
0_{1*4} & 0_{1*4} & \boldsymbol{k}_{f,J3,\ Point\ n} & 0_{1*4} & 0_{1*4} & 0_{1*4} \\
0_{1*4} & 0_{1*4} & 0_{1*4} & \boldsymbol{k}_{f,J4,\ Point\ n} & 0_{1*4} & 0_{1*4} \\
0_{1*4} & 0_{1*4} & 0_{1*4} & 0_{1*4} & \boldsymbol{k}_{f,J5,\ Point\ n} & 0_{1*4} \\
0_{1*4} & 0_{1*4} & 0_{1*4} & 0_{1*4} & 0_{1*4} & \boldsymbol{k}_{f,J6,\ Point\ n}
\end{bmatrix} \tag{3.25}
$$

$$
\boldsymbol{K}_m = \begin{bmatrix}
k_{m,J1,\ Point\ 1} & 0 & 0 & 0 & 0 & 0 \\
0 & k_{m,J2,\ Point\ 1} & 0 & 0 & 0 & 0 \\
0 & 0 & k_{m,J3,\ Point\ 1} & 0 & 0 & 0 \\
0 & 0 & 0 & k_{m,J4,\ Point\ 1} & 0 & 0 \\
0 & 0 & 0 & 0 & k_{m,J5,\ Point\ 1} & 0 \\
0 & 0 & 0 & 0 & 0 & k_{m,J6,\ Point\ 1} \\
k_{m,J1,\ Point\ 2} & 0 & 0 & 0 & 0 & 0 \\
0 & k_{m,J2,\ Point\ 2} & 0 & 0 & 0 & 0 \\
0 & 0 & k_{m,J3,\ Point\ 2} & 0 & 0 & 0 \\
0 & 0 & 0 & k_{m,J4,\ Point\ 2} & 0 & 0 \\
0 & 0 & 0 & 0 & k_{m,J5,\ Point\ 2} & 0 \\
0 & 0 & 0 & 0 & 0 & k_{m,J6,\ Point\ 2} \\
k_{m,J1,\ Point\ 3} & 0 & 0 & 0 & 0 & 0 \\
\vdots & \vdots & \vdots & \vdots & \vdots & \vdots \\
0 & 0 & 0 & 0 & 0 & k_{m,J6,\ Point\ n-1} \\
k_{m,J1,\ Point\ n} & 0 & 0 & 0 & 0 & 0 \\
0 & k_{m,J2,\ Point\ n} & 0 & 0 & 0 & 0 \\
0 & 0 & k_{m,J3,\ Point\ n} & 0 & 0 & 0 \\
0 & 0 & 0 & k_{m,J4,\ Point\ n} & 0 & 0 \\
0 & 0 & 0 & 0 & k_{m,J5,\ Point\ n} & 0 \\
0 & 0 & 0 & 0 & 0 & k_{m,J6,\ Point\ n}
\end{bmatrix} \tag{3.26}
$$

3.2 Base Parameters Selection

Parameter selection is useful to determine the minimum number of identifiable robot dynamic parameters, and to eliminate the parameters that have no effect on the dynamic model. It increases the robustness of the identification process and reduces the computation cost. Additionally, it eliminates the linearly dependent elements, which results in a higher rank of the information matrix. At the very first beginning, the selection was made by mathematical and mechanical analysis [7, 17, 27, 35, 36, 61], and the regrouping of initial parameters [18, 24, 26]. With the rising in electrical computing science, the selection can be carried out by using QR factorization and SVD decomposition [3,7,16,27], which results are presented by the relationship among the links.

The purpose of both decompositions is to factorize a matrix into a product of matrices. QR decomposition [65] is used to decompose a real matrix $\boldsymbol{A}$ into a product as:

$$
\boldsymbol{A} = \boldsymbol{Q}\boldsymbol{R} \tag{3.27}
$$

Where:

$\boldsymbol{Q}$ is an orthogonal matrix.
$\boldsymbol{R}$ is an upper triangular matrix.

This decomposition is often introduced to solve linear least square problems. Moreover, with QR decomposition, it is easy to solve the system with the equation $\boldsymbol{Ax} = \boldsymbol{b}$:

$$
\boldsymbol{Ax} = \boldsymbol{b} \xrightarrow{\boldsymbol{A}=\boldsymbol{QR}} \boldsymbol{QRx} = \boldsymbol{b} \xrightarrow{\boldsymbol{Q}^T\boldsymbol{Q}=\boldsymbol{I}} \boldsymbol{Q}^T\boldsymbol{QRx} = \boldsymbol{Q}^T\boldsymbol{b} \Rightarrow \boldsymbol{Rx} = \boldsymbol{Q}^T\boldsymbol{b} \tag{3.28}
$$

Meanwhile, SVD factorization [66], as know as singular value decomposition, is a general eigenvalue decomposition of a matrix into any $m * n$ matrix through an extension of the polar decomposition. It can be explained with an $m * n$ real matrix $\boldsymbol{A}$ as:

$$
\boldsymbol{A} = \boldsymbol{U}\boldsymbol{\Sigma}\boldsymbol{V}^T \tag{3.29}
$$

Where:

$\boldsymbol{U}$ and $\boldsymbol{V}$ are $m * m$ and $n * n$ complex unitary matrix respectively.

$\boldsymbol{\Sigma}$ is an $m * n$ rectangular diagonal matrix with non-negative real numbers on the diagonal.

The diagonal elements of $\boldsymbol{\Sigma}$ are the singular values of $\boldsymbol{A}$, and they are uniquely determined. Whereas $\boldsymbol{U}$ and $\boldsymbol{V}$ are not necessary to be unique.

In this section, there is a brief introduction and discussion in Subsection 3.2.1 and 3.2.2. The results are presented and discussed in Appendix D. Appendix E shows the MATLAB code.

3.2.1 QR Factorization

The QR factorization is used to search the zero-elements-columns of Matrix $\boldsymbol{R}$ in Equation 3.31. The corresponded parameter can be eliminated during the identification of the dynamic model because they are unrecognizable or because they have a linear relationship with other parameters. The torque of each joint can be explained as follows:

$$\boldsymbol{\tau} = \boldsymbol{K}\boldsymbol{\phi} \tag{3.30}$$

where $\boldsymbol{K}$ is the information matrix and $\boldsymbol{\phi}$ is a vector containing the set of the dynamic parameters of the links.

The matrix $\boldsymbol{K}$ can be factorized by QR decomposition in the following form:

$$\boldsymbol{K} = \boldsymbol{Q}\boldsymbol{R} = \begin{bmatrix}\boldsymbol{Q}_1 & \boldsymbol{Q}_2\end{bmatrix}\begin{bmatrix}\boldsymbol{R}_1 \\ [\boldsymbol{0}]\end{bmatrix} = \boldsymbol{Q}_1\boldsymbol{R}_1 \tag{3.31}$$

Where $\boldsymbol{R}_1$ is an upper triangular matrix:

$$\boldsymbol{R}_1 = \begin{bmatrix} r_{1,1} & r_{1,2} & r_{1,3} & \cdots & r_{1,60} \\ 0 & r_{2,2} & r_{2,3} & \cdots & r_{2,60} \\ 0 & 0 & r_{3,3} & \cdots & r_{3,60} \\ \vdots & \vdots & \vdots & \ddots & \vdots \\ 0 & 0 & 0 & \cdots & r_{60,60} \end{bmatrix} \tag{3.32}$$

The vector of main diagonal of $\boldsymbol{R}_1$ is:

$$\boldsymbol{r}_{1,diag} = \begin{bmatrix} r_{1,1} & r_{2,2} & r_{3,3} & \cdots & r_{60,60} \end{bmatrix} \tag{3.33}$$

The identifiable parameters of matrix $\boldsymbol{\Phi}$ are selected by the position of the no-zeros elements on the diagonal of the matrix $\boldsymbol{R}_1$. It is worth noting that also the elements below a certain threshold are considered equal to zero. For more details see Appendix D.

3.2.2 SVD Decomposition

The SVD decomposition is applied to solve the rank deficiency problem of $\boldsymbol{K}$. Its result can be used to verify the QR results. The main purpose of SVD decomposition is to obtain different values in matrix $\boldsymbol{V}$ with large condition number of the matrix $\boldsymbol{S}$. The computing routine starts with Equation 3.34:

$$\boldsymbol{K} = \boldsymbol{U}\boldsymbol{\Sigma}\boldsymbol{V}^T = \boldsymbol{U}\begin{bmatrix}\boldsymbol{S} \\ [\boldsymbol{0}]\end{bmatrix}\boldsymbol{V}^T \tag{3.34}$$

Where:

1, $\boldsymbol{K}$ is the information matrix, and has a dimension of $m * n$.

2, $\boldsymbol{S}$ is a diagonal matrix with non-negative real numbers, and its form is:

$$\boldsymbol{S} = \begin{bmatrix} r_{1,1} & 0 & 0 & \cdots & 0 \\ 0 & r_{2,2} & 0 & \cdots & 0 \\ 0 & 0 & r_{3,3} & \cdots & 0 \\ \vdots & \vdots & \vdots & \ddots & \vdots \\ 0 & 0 & 0 & \cdots & r_{n,n} \end{bmatrix} \tag{3.35}$$

or

$$\boldsymbol{s}_{diag} = \begin{bmatrix} r_{1,1} & r_{2,2} & r_{3,3} & \cdots & r_{n,n} \end{bmatrix} \tag{3.36}$$

with:

a, The size of matrix $\boldsymbol{S}$ has been decided by the dimension of matrix $\boldsymbol{K}$.
b, All values of matrix $\boldsymbol{S}$ are non-negative real number.
c, The values on the diagonal are sorted by decreasing sequence, which is $r_{1,1} > r_{2,2} > r_{3,3} > \cdots > r_{n,n}$.
d, $\boldsymbol{s}_{diag}$ is the vector of diagonal elements of $\boldsymbol{S}$.

A larger condition number of matrix $\boldsymbol{S}$ indicates that there are some parameters needed to be cancelled. They can be found by the location of some particularly different values in the column of matrix $\boldsymbol{V}$, which is the same as the minimum value in matrix $\boldsymbol{s}_{diag}$. To avoid the zero rank, it should be pointed out that the friction elements should be introduced in the SVD decomposition. An example is provided in Appendix D.

3.2.3 Base Set Of Dynamic Parameters

The parameters defined from the Equation 3.14, 3.15 and 3.16 for each link of the 6-axis manipulator, are listed as follows:

$$m \quad mP_x \quad mP_y \quad mP_z \quad I_{xx} \quad I_{xy} \quad I_{xz} \quad I_{yy} \quad I_{yz} \quad I_{zz} \quad f_1 \quad f_2 \quad f_3 \quad f_4 \quad I_m$$

After the QR and SVD decomposition in Subsection 3.2.1 and 3.2.2, and Appendix D, the merged results are shown in Table D.3. Based on this table the selected dynamic parameters involved in the identification process are shown in the Table 3.1 below.

Table 3.1: The Base Set of Dynamic Parameters

		The Dynamic Parameters														
		m	mP_x	mP_y	mP_z	I_{xx}	I_{xy}	I_{xz}	I_{yy}	I_{yz}	I_{zz}	f_1	f_2	f_3	f_4	I_m
Joints	1										✓	✓	✓	✓	✓	
	2		✓	✓		✓	✓	✓		✓	✓	✓	✓	✓	✓	
	3		✓	✓		✓	✓	✓		✓	✓	✓	✓	✓	✓	✓
	4		✓	✓		✓	✓	✓		✓	✓	✓	✓	✓	✓	✓
	5		✓	✓		✓	✓	✓		✓	✓	✓	✓	✓	✓	✓
	6		✓	✓		✓	✓	✓		✓	✓	✓	✓	✓	✓	✓

Chapter 4

Experimental Design

4.1 The Test Trajectory Creation

The main purpose of the test trajectory is to obtain the data needed for the dynamic parameter identification and to observe the related influences in the long-duration operation. Since the friction elements are the only factors that may be affected by the temperature in these operations, the test trajectory has to be appropriately short to avoid a high increase in the temperature. To better understand the influences of friction, a warming trajectory was inserted between each motion. Therefore, the test trajectory is designed with three stages, which are: the excitation trajectory for the identification, the friction trajectory to understand the friction behaviour, and the warming trajectory to warm the robot. An example of one cycle of the full test trajectory is shown in Figure 4.1.

The excitation trajectory is specifically designed to excite the model parameters with the high range of velocity between zero and the maximum velocity. The second stage is specially designed for friction measurement and estimation. The last stage is the warming up procedure to prepare the robot for the next cycle. These three stages are explained in the following sections. The complete test trajectory has 24 cycles and lasts about 2 hours.

4.2 The Excitation Trajectory

There are two methods to create an appropriate excitation trajectory. The 1^{st} one, illustrated below in Section 4.2.1, is a finite sum of N harmonic sine function. This method creates a high and sudden acceleration at the start of the trajectory, which results in the non-smooth movement. The 2^{nd} one is a finite Fourier series formula [3,22,52,53,55] presented in Section 4.2.2. To obtain the optimized excitation trajectory, it is important to select an appropriate cost function. By the literature, there are several options, which are the condition number of the information matrix [22, 28, 52], the determinant of the information matrix [22, 54, 55], and a specific formula that mix the condition number and the determinant with different weights [1,9,60], as explained in Section 4.2.3. In this thesis, the excitation trajectory has been obtained and optimized by minimizing the condition number and the reciprocal of the determinant of the information matrix.

It is possible to use two different algorithms to optimize the excitation trajectory. They are the genetic algorithm “ga” [57] and the constrained nonlinear multivariable function “fmincon” [56]. Both are functions provided by the optimal toolbox in MATLAB.

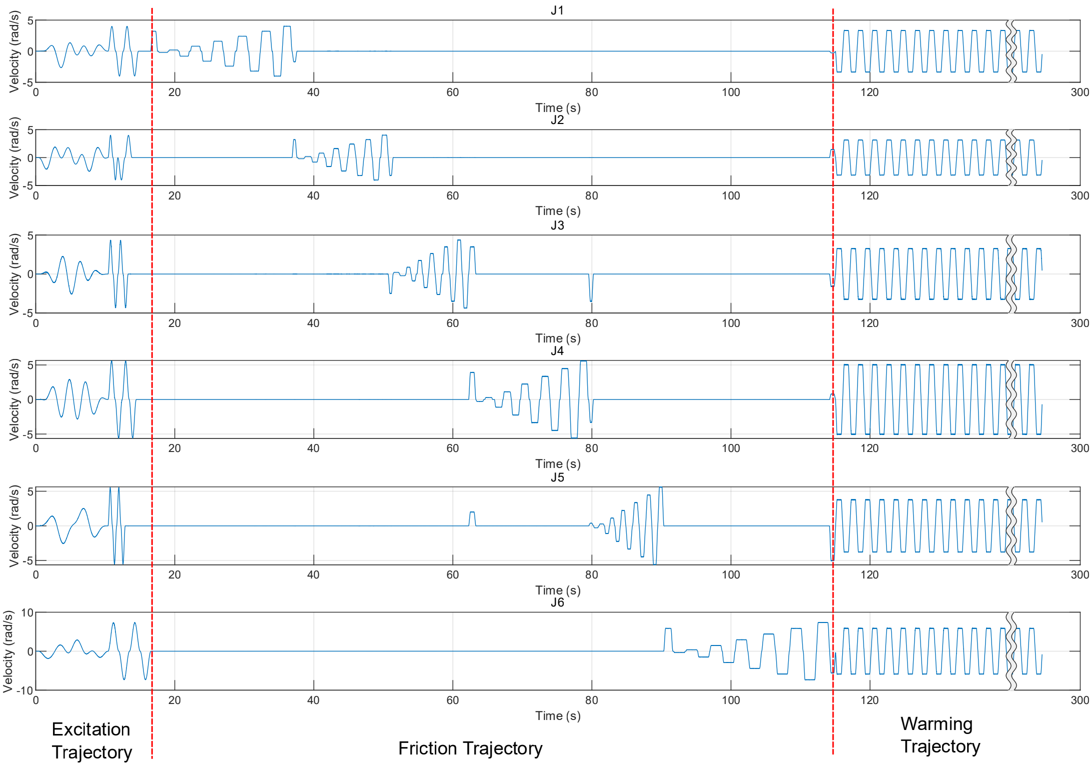

Figure 4.1: The velocity of one cycle in full test trajectory

4.2.1 The 1st Excitation Trajectory

The first excitation trajectory introduced is created by the finite sum of N harmonic sine function :

$$q(t) = \sum_{k=1}^{N} a_k \sin(k\omega_f t) \tag{4.1}$$

Where:

t is the time sequence.
$q(t)$ is the joint angle at time t.
ω_f is the base frequency.
N is the number of elements introduced in the calculation.

The boundary applied in Equation 4.1 are:

$$q_{min} \leqslant q(t) \leqslant q_{max} \tag{4.2}$$

$$\dot{q}_{min} \leqslant \dot{q}(t) \leqslant \dot{q}_{max} \tag{4.3}$$

$$\ddot{q}_{min} \leqslant \ddot{q}(t) \leqslant \ddot{q}_{max} \tag{4.4}$$

The upper limit of the Equation 4.1 is:

$$|q(t)| = \left| \sum_{k=1}^{N} a_k \sin(k\omega_f t) \right| \leqslant \sum_{k=1}^{N} |a_k \sin(k\omega_f t)| \leqslant \sum_{k=1}^{N} |a_k| \leqslant N a_{k,\ max} \tag{4.5}$$

Due to the limitation of Equation 4.2, it is possible to write:

$$a_{k,\ max} \leqslant \frac{q_{max}}{N} \tag{4.6}$$

Similar, for the angle velocity and acceleration in Equation 4.3 and 4.4 respectively:

$$\dot{q}(t) = \sum_{k=1}^{N} a_k k\omega_f \cos(k\omega_f t) \tag{4.7}$$

$$\begin{aligned} |\dot{q}(t)| &= \left|\sum_{k=1}^{N} a_k k\omega_f \cos(k\omega_f t)\right| \leqslant \sum_{k=1}^{N} |a_k k\omega_f \cos(k\omega_f t)| \leqslant \sum_{k=1}^{N} |a_k k\omega_f| \leqslant N a_{k,\ max} k\omega_f \\ &= N\frac{q_{max}}{N} k\omega_f = q_{max} k\omega_f \leqslant \dot{q}_{max} \\ &\Rightarrow k\omega_f \leqslant \frac{\dot{q}_{max}}{q_{max}} \end{aligned} \tag{4.8}$$

$$\ddot{q}(t) = -\sum_{k=1}^{N} a_k (k\omega_f)^2 \sin(k\omega_f t) \tag{4.9}$$

$$\begin{aligned} |\ddot{q}(t)| &= \left|-\sum_{k=1}^{N} a_k (k\omega_f)^2 \sin(k\omega_f t)\right| \leqslant \sum_{k=1}^{N} \left|a_k (k\omega_f)^2 \sin(k\omega_f t)\right| \leqslant \sum_{k=1}^{N} \left|a_k (k\omega_f)^2\right| \\ &= N\frac{q_{max}}{N} (k\omega_f)^2 = q_{max} (k\omega_f)^2 \leqslant \ddot{q}_{max} \\ &\Rightarrow k\omega_f \leqslant \sqrt{\frac{\ddot{q}_{max}}{q_{max}}} \end{aligned} \tag{4.10}$$

In conclusion, the limitation of a_k and $k\omega_f$ of the Equation 4.1 are:

$$a_k \leqslant \frac{q_{max}}{N} \tag{4.11}$$

$$k\omega_f \leqslant \min\left(\frac{\dot{q}_{max}}{q_{max}},\ \frac{\ddot{q}_{max}}{q_{max}}\right) \tag{4.12}$$

Then, knowing the value of $q(t)$, $\dot{q}(t)$ and $\ddot{q}(t)$, the value of a_k and $k\omega_f$ is obtained.

Using $N = 3$, Equation 4.1 can be rewritten as follows:

$$q(t) = a_1 \sin(\omega t) + a_2 \sin(2\omega t) + a_3 \sin(4\omega t) \tag{4.13}$$

$$\dot{q}(t) = a_1\omega \cos(\omega t) + 2a_2\omega \cos(2\omega t) + 4a_3\omega \cos(4\omega t) \tag{4.14}$$

$$\ddot{q}(t) = -\left[a_1\omega^2 \cos(\omega t) + 4a_2\omega^2 \cos(2\omega t) + 16a_3\omega^2 \cos(4\omega t)\right] \tag{4.15}$$

Where $a_1 = a_2 = a_3 = a$, $N = 3$, and ω is the abbreviation of ω_f;

$$|q(t)| \leqslant |a_1 \sin(\omega t)| + |a_2 \sin(2\omega t)| + |a_3 \sin(4\omega t)| \leqslant a_1 + a_2 + a_3 = Na \Rightarrow |q(t)| \leqslant Na \tag{4.16}$$

With the same logic for $\dot{q}(t)$ and $\ddot{q}(t)$, it is possible to write:

$$|\dot{q}(t)| \leqslant Na4\omega \tag{4.17}$$

$$|\ddot{q}(t)| \leqslant Na(4\omega)^2 \tag{4.18}$$

Using $k = 4$, a small value of ω is obtained. It is clear that increasing the value of ω, the related joint velocity, acceleration and output torque will rise too during the movement. Hence, it is important to find the optimized ω with the given limitation of $q_{min} \leqslant q(t) \leqslant q_{max}$, $\dot{q}_{min} \leqslant \dot{q}(t) \leqslant \dot{q}_{max}$ and $\ddot{q}_{min} \leqslant \ddot{q}(t) \leqslant \ddot{q}_{max}$. The values of a_1, a_2 and a_3 follow the same reasoning. In MATLAB, the functions "fmincon" and "ga" can easily provide the optimized value of ω, and a_1, a_2, a_3. Meanwhile, the bounds applied in the optimization are discussed and demonstrated in Equation 4.2, 4.3 and 4.4.

There was an acceleration problem at the start of the experiments using this excitation trajectory, which leads to inappropriate results of the identification. This is because the excitation trajectory has not been smooth enough. Therefore, the 2^{nd} excitation trajectory creation method is introduced in the Section 4.2.2.

4.2.2 The 2nd Excitation Trajectory

To solve the problem of the 1st excitation trajectory, the Equation 4.1 has been modified as follows:

$$\theta_i(t) = q_{i,0} + \sum_{l=1}^{N} \left[\frac{a_{l,i}}{w_f l} \sin(w_f l t) - \frac{b_{l,i}}{w_f l} \cos(w_f l t) \right] \tag{4.19}$$

and $\dot{\theta}_i(t)$, $\ddot{\theta}_i(t)$ are:

$$\dot{\theta}_i(t) = \sum_{l=1}^{N} \left[a_{l,i} \cos(w_f l t) + b_{l,i} \sin(w_f l t) \right] \tag{4.20}$$

$$\ddot{\theta}_i(t) = w_f \sum_{l=1}^{N} \left[-a_{l,i} \sin(w_f l t) + b_{l,i} \cos(w_f l t) \right] \tag{4.21}$$

Where:

$\theta_i(t)$, $\dot{\theta}_i(t)$, $\ddot{\theta}_i(t)$ are the joint position, velocity and acceleration, respectively.
The subscript i is the joint index.
t is the time sequence.
q_0 is the initial position of joint.
a and b is the elements of excitation trajectory, which has been obtained from the optimal algorithms.
N is the total number of elements a or b.
w_f is the base frequency used to create the trial trajectory in optimal algorithm.

Based on [22, 28, 52, 55], N and w_f are equal to 5 and $2\pi * 0.1$Hz respectively. The bounds of the MATLAB functions applied in optimization are the same as before, explained in Section 4.2.1. The optimization results are shown in Table 4.1.

Table 4.1: The optimization results of Equation 4.20, 4.20 and 4.21

	Joint 1	Joint 2	Joint 3	Joint 4	Joint 5	Joint 6
a_1	0.2428	-0.1795	0.0607	-0.0039	-0.0470	-1.2177
a_2	0.3845	-0.0369	-0.2272	0.0725	0.0722	0.2676
a_3	-0.6092	-0.1851	0.6706	0.0023	-0.0035	0.3225
a_4	-0.1870	-0.2343	-0.8226	0.0022	0.0203	0.5088
a_5	0.1689	0.6358	0.3185	-0.0731	-0.0419	0.1188
b_1	-0.3678	0.4024	0.0005	0.2701	-0.3227	0.0210
b_2	0.2845	-0.9426	-0.1154	0.4287	1.5358	0.0139
b_3	0.0154	-0.6795	-0.2170	0.4011	-0.5949	-0.5578
b_4	-0.7440	-0.2190	0.7542	-1.7803	-0.5858	0.8056
b_5	0.5457	0.8795	-0.4271	0.9581	0.2758	-0.3196
q_0	-0.4732	-0.2773	-0.0420	0.5805	0.2477	-0.0327

4.2.3 The Optimization Of Excitation Trajectory

The target of optimization is to find the best trajectory that excites the robot. The optimization has been performed using the functions “fmincon” and “ga” provided by MATLAB. As mentioned at the beginning of Section 4.1, the optimization has been applied using the condition number and the determinant of the information matrix. Subsequently, the results are compared together to choose the best one, which is the result that provides the highest velocities in each joint without exceeding the limitations. In the following discussion, one excitation trajectory, optimized with the genetic algorithm minimizing the condition number of the information matrix, is implemented. A low value of the condition number indicates that the maximum velocity and acceleration are reached without exceeding the joint position limitations. Here, the robot workspace is fully covered during the movement. Additionally, it also provides large torque output values. As a result, the best result of dynamic parameter estimation is achieved. The applied excitation trajectory is shown in Figure 4.2 with the coefficient value shown in Table 4.1.

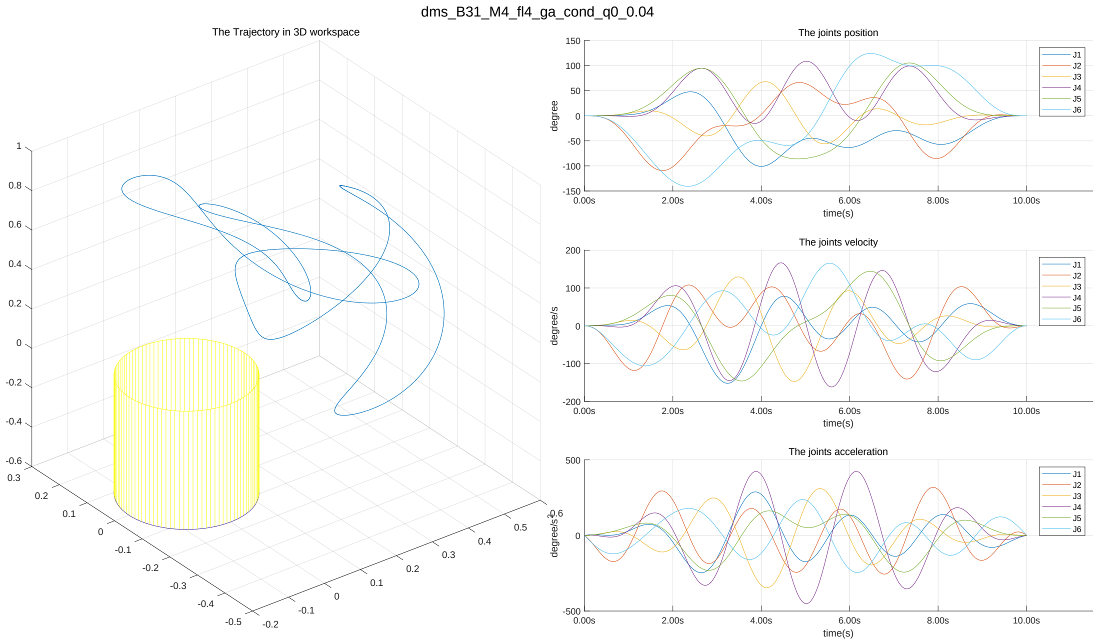

Figure 4.2: The robot movement with the related position, velocity and acceleration of applied excitation trajectory

However, in the experiments, there are some errors between the measured torque and the estimated torque, which are marked with numbers in Figure 4.3. After the analysis and discussions, it has been found that these errors occurred in the path when the joint velocity exceeds the maximum velocity of the test excitation trajectory. Due to this issue, the estimation results during these higher velocity are significantly abnormal compared with the measurement data. Additionally, another possible reason for this situation could depend on the robot specifications. The maximum velocity of some joints in the optimal trajectories based on these robot specifications can not reach the limitations. In this case, it is possible that the optimization cannot achieve the best excitation trajectory during the calculations. In light of this an additional part for the trajectory has been added in Section 4.3.

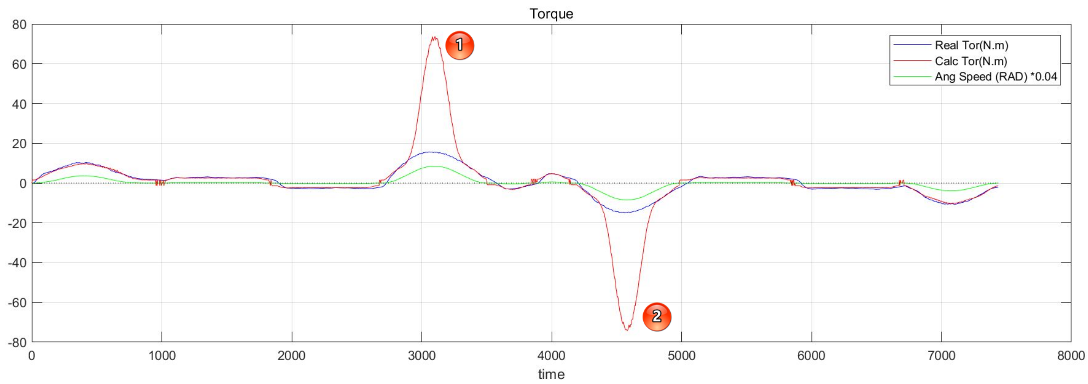

Figure 4.3: The comparison between the measured torque and the estimated torque with the 2^{nd} excitation trajectory, the data is from Joint 5.

4.3 Additional Excitation Trajectory

Due to the high errors illustrated in Section 4.2.3 and in Figure 4.3, an additional excitation trajectory is introduced. The equations are the following [31]:

$$\theta = \theta_0 + \mathit{\Delta}\theta \left[\frac{t}{T} - \frac{1}{2\pi} \sin\left(\frac{2\pi t}{T} \right) \right] \tag{4.22}$$

$$\dot{\theta} = \frac{\mathit{\Delta}\theta}{T} \left[1 - \cos\left(\frac{2\pi t}{T} \right) \right] \tag{4.23}$$

$$\ddot{\theta} = \frac{2\pi \mathit{\Delta}\theta}{T^2} \sin\left(\frac{2\pi t}{T} \right) \tag{4.24}$$

Where:

θ, $\dot{\theta}$ and $\ddot{\theta}$ are the position, velocity and acceleration of joint of the additional excitation trajectory.

θ_0 is the joint initial position, here is 0.

t, T are the time series in total time and the time duration, respectively.

$\mathit{\Delta}\theta$ is the maximum position range of joint in movement.

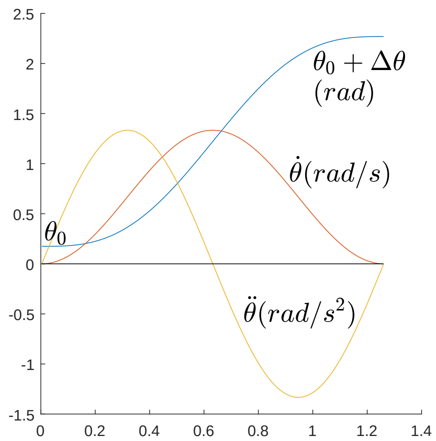

Figure 4.4: The position, velocity and acceleration of the additional trajectory

The robot starts and ends in the same position with zero velocity for all joints, moreover the trajectory is executed in both positive and negative directions. Furthermore, this additional trajectory is attached after the 2^{nd} excitation trajectory. The merged excitation trajectory is shown in Figure 4.5. It should be noted that some idle movements have been added for some joints due to the different duration of the created trajectories.

4.4 The Friction Measure Trajectory

The friction measurements have been used to understand the behaviour of friction in the long-term movement. As mentioned in Section 1.2.2, with the same mechanical structure, the same contents, the same trajectory, and environment, the friction changes depend only on the temperature. The best method to obtain the temperature is to use internal sensors. However, the robot usually does not have temperature sensors inside its structure. Therefore, finding a way to measure the statement inside the robot body becomes a crucial task. Since the motor output torque can be easily obtained and monitored from the motor current with some calculations, this problem can be solved by collecting the motor torque.

The torque depends on the velocity and temperature. Therefore, referring to the experiments of [32, 39, 48], a trajectory with 6 constant velocities has been designed, which contains the

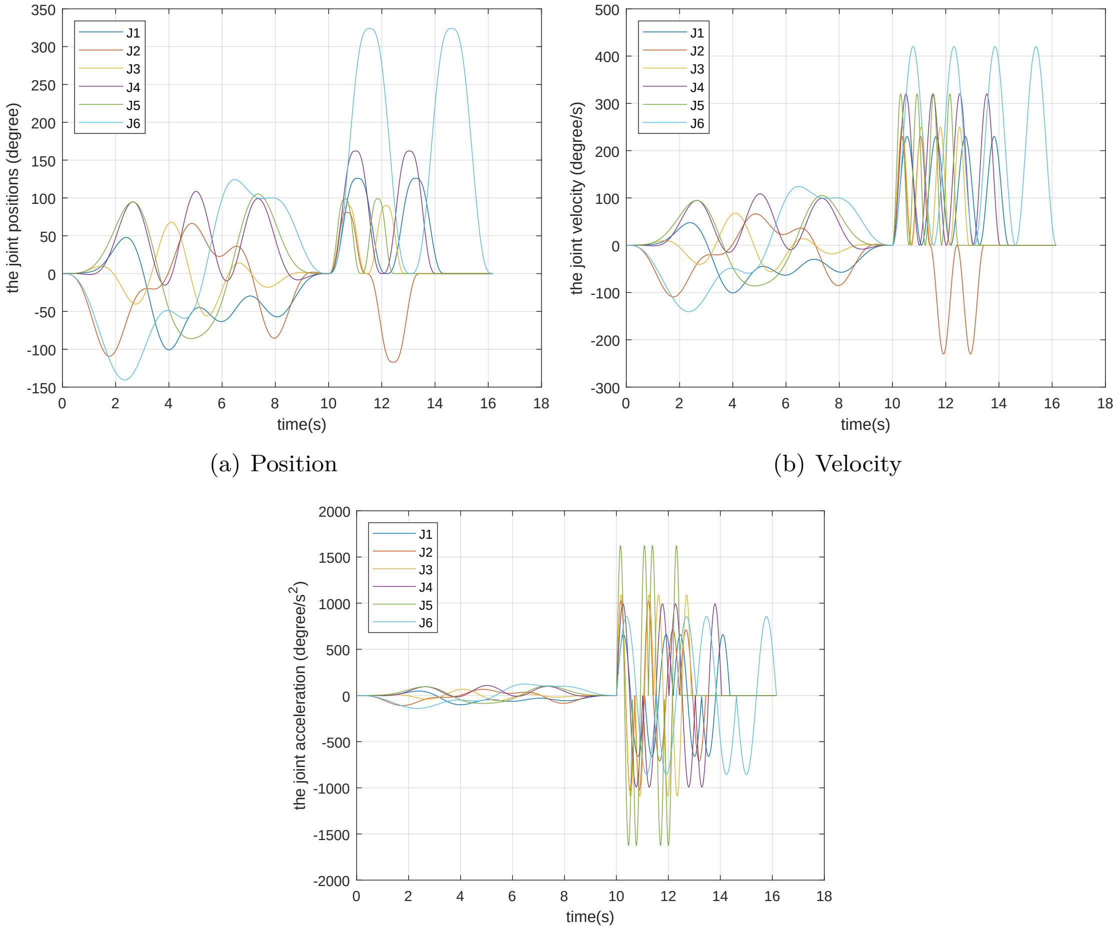

(a) Position (b) Velocity

(c) Acceleration

Figure 4.5: The merged excitation trajectory

velocities at 5%, 20%, 40%, 60%, 80% and 100% of the maximum speed of each joint. The motion is created individually for each joint, which means that the idle joints are fixed at a designed position while the test joint is moving. This design is clearly shown in Figure 4.1 at the "Friction Trajectory" section, and Figure 4.6. In Figure 4.6, the subplots show that the joint rotated repeatedly from one position to another. Also, a zoomed plot is shown in Figure 4.7 as an example. Besides, the movements for each velocity segment are specially calculated and configured to maintain the same duration for each segment. This configuration will provide the same quantity of data for each joint in the dynamic calculation, which will be discussed in Chapter 5.

To avoid the gravity contribution in torque, a special configuration is introduced during the friction measurement stage. This idea comes from the study of Simoni [47] and Pagani [39]. The main principle of this configuration is to maintain the joint test with horizontal motion, which leads to the elimination of the gravity effect. This configuration can be applied to Joint 1 (Figure 4.6(a)), 4 (Figure 4.6(d)), 5 (Figure 4.6(e)), which are clearly that all joints are moved horizontally. It should be pointed that the motion of Joint 6 (Figure 4.6(f)) is based on the horizontal movement of Joint 5, which the gravity effect are calculated. Due to the robot structure, the data collected from Joint 2 (Figure 4.6(b)) and 3 (Figure 4.6(c)) have been influenced by the gravity effect. The method used to remove the gravity contribution has been discussed in Section 5.2.2. An example of results for friction measurement is illustrated in Figure 4.8.

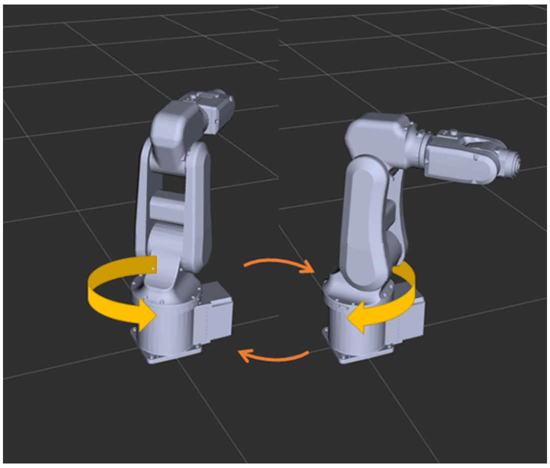

(a) Joint 1

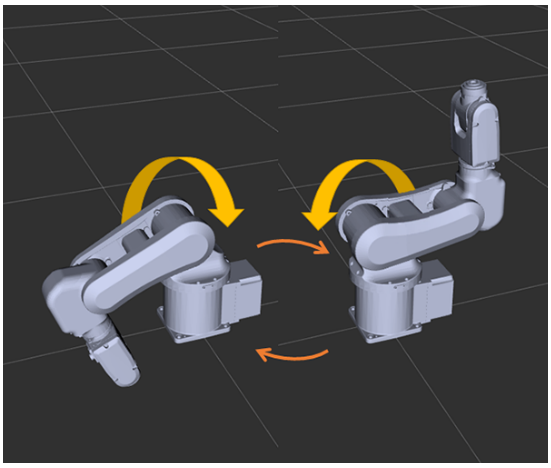

(b) Joint 2

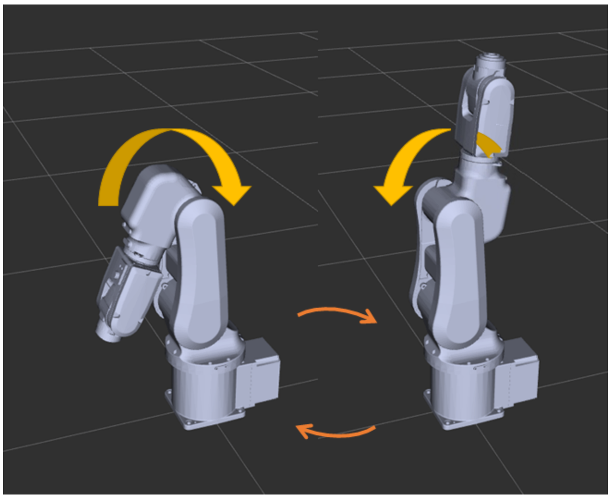

(c) Joint 3

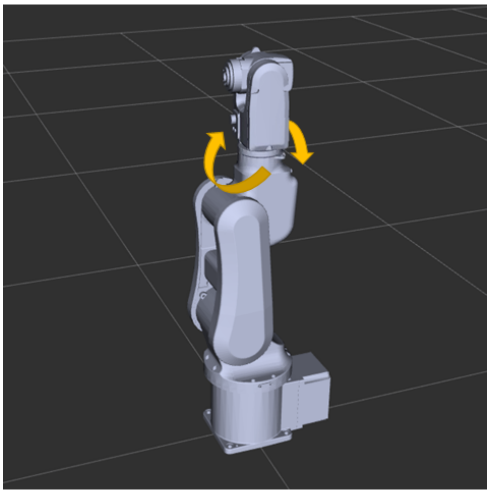

(d) Joint 4

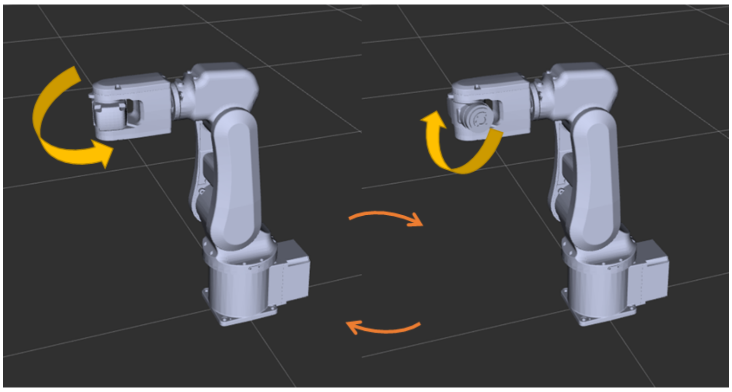

(e) Joint 5

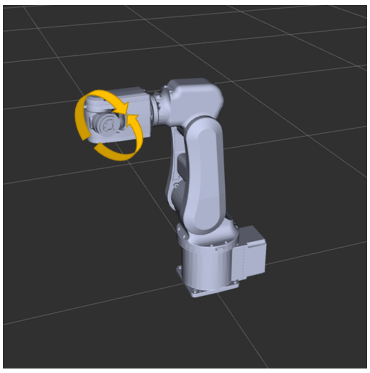

(f) Joint 6

Figure 4.6: The joint movement in friction measurement. The thick yellow arrows show the rotation directions, and the thin brown arrows show the position changes.

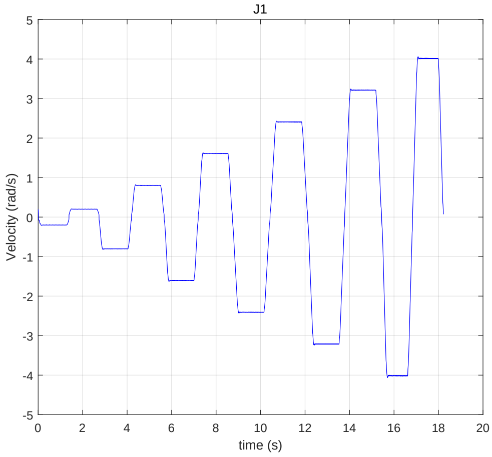

Figure 4.7: The velocity of one joint in the friction measure stage

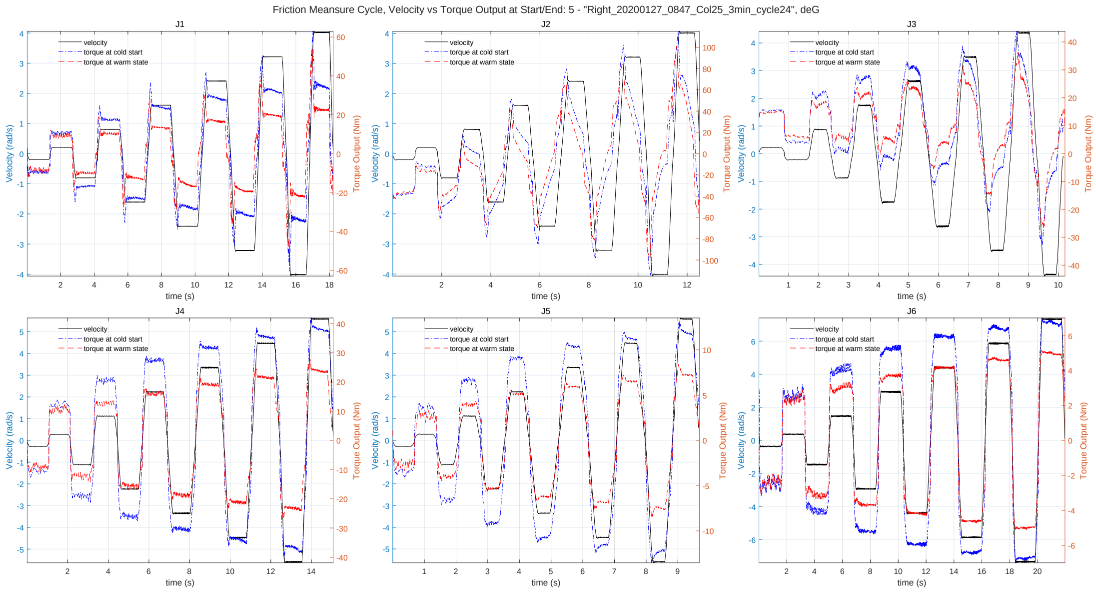

Figure 4.8: The velocity and torque versus time of obtained experimental data in the friction measure stage with the cold and warm conditions, from Joint 1 to 6

4.5 The Warming Stage Trajectory

The warming section of the trajectory was designed specifically to increase the internal temperature of the robot joints. As the discussed in Section 1.2.2 and 4.4, the temperature is one of the major factor that causes changing in friction. During the warming stage, all the joints move at their maximum speed simultaneously, as the trajectory shown in Figure 4.1 in the "Warming Trajectory" section, and the repeated movements between two positions shown in Figure 4.9. In experiment, all joints are configured about the 80% of angular limitations with 80% velocity. To capture the details of the friction changing and avoid that the temperature increases excessively, the duration of this stage has been chosen carefully. Base on the study of Simoni [47] and Pagani [39], and the results coming from the tests in the laboratory, the optimal duration for this warming stage is about 3 minutes. This leads to a 5 minutes duration in total considering all the trajectories of one cycle. To gather sufficient data for the feature analysis, the cycle has been repeated 24 times obtaining an experiment lasting 2 hours. To ensure the same condition at the start of each experiment, it is important to let the robot cool down after each experiment.

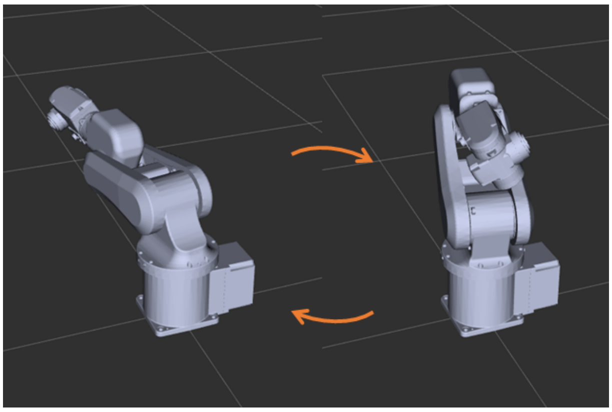

Figure 4.9: The joint movement in warming stage

4.6 The Software And Environment Of The Experiment

The robot model ER3A from EFORT has been used in the experiments, which is introduced in Chapter 2. The controller of the robot is an RP1 from ROBOX [44], which is shown in Figure 4.11. The experimental trajectory has been created using the proprietary software of Robox Development Environment (RDE) (Figure 4.10) [43]. This software also provides the built-in function for data collection (Figure 4.12).

Figure 4.10: The Robox Development Environment (RDE)

The experiments have been repeated on two robots of the very same model, called “Left” and “Right” with the index number of 1 and 2 respectively. For each robot, 4 experiments have been executed, and they have been numbered from 1 to 4 following the sequence of experiments. The data have been collected under an environment temperature of roughly 20°C, which results in the same execution condition at the start of the experiment. It is worth noting that this temperature depends only on the robot’s location. In other words, in real applications, the environment temperature should be various. Moreover, the experiment is executed once only in a day to guarantee enough time for cooling down the robot. Additionally, the data of position, velocity and torque of each joint are collected in experiment. The signals to separate the different stages are also recorded. All these data are collected by built-in oscillator (Figure 4.12) and then export to the CSV files for the future calculation. The connection diagram is shown in Figure 4.13. The communications between computer and controller is made just using and internet cable, while the EtherCAT bus is used to connect the controller and the robot.

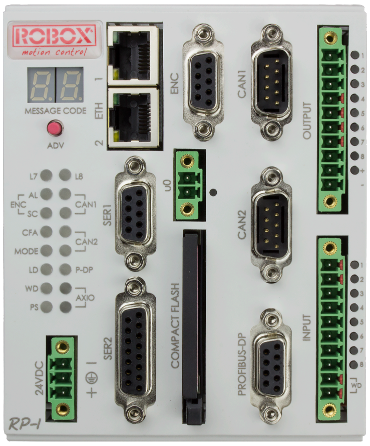

Figure 4.11: The robot controller of RP1

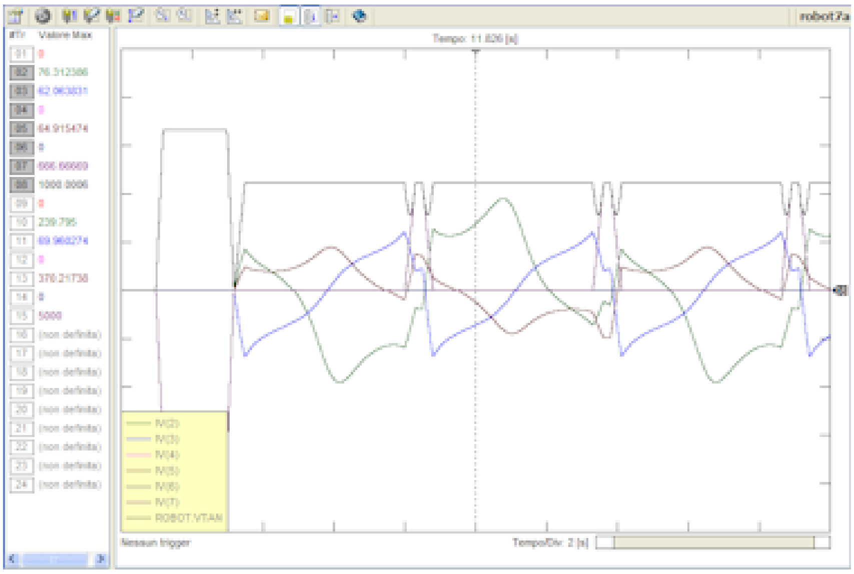

Figure 4.12: The oscillator in RDE

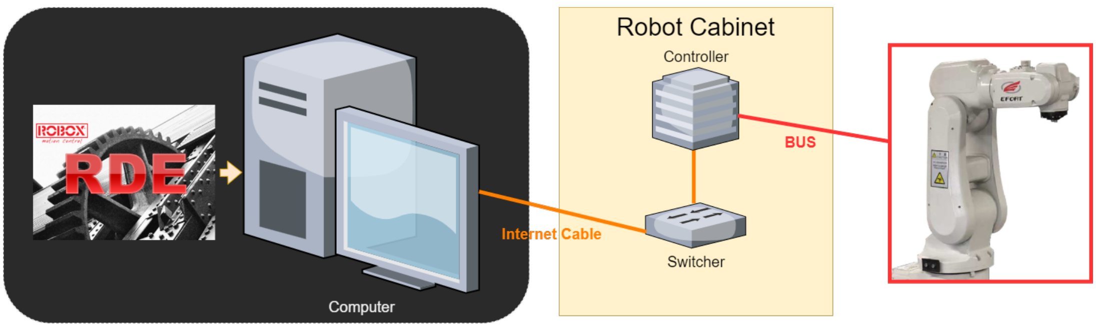

Figure 4.13: The communication between PC and robot

Chapter 5

Data Process And Analysis

5.1 The Dynamic Parameters

5.1.1 The Identification Process

As discussed in Section 3.1 and illustrated in Appendix C, the identification is carried out using the collected data, the creation of an information matrix, and then the calculation from the Least Square algorithm [2, 15, 20, 40, 41]. Figures 5.1 and 5.2 (or Figure K.1 in Appendix K and L.1 in Appendix L) show examples of the identification results between the collected torque and estimated torque. Base on these figures, the results clearly show that the errors between the estimated torque and the obtained torque are acceptable except for the very low-velocity. The errors on the low speed are clearly highlighted in Stage 2 of Figure 5.2 and more details are shown in Figure 5.3. These errors are due to the insufficient precision of the friction model at the low-velocity domain, which has been discussed in Section 5.2. The plots of the identification result of all dynamic parameters are shown in Appendix G.

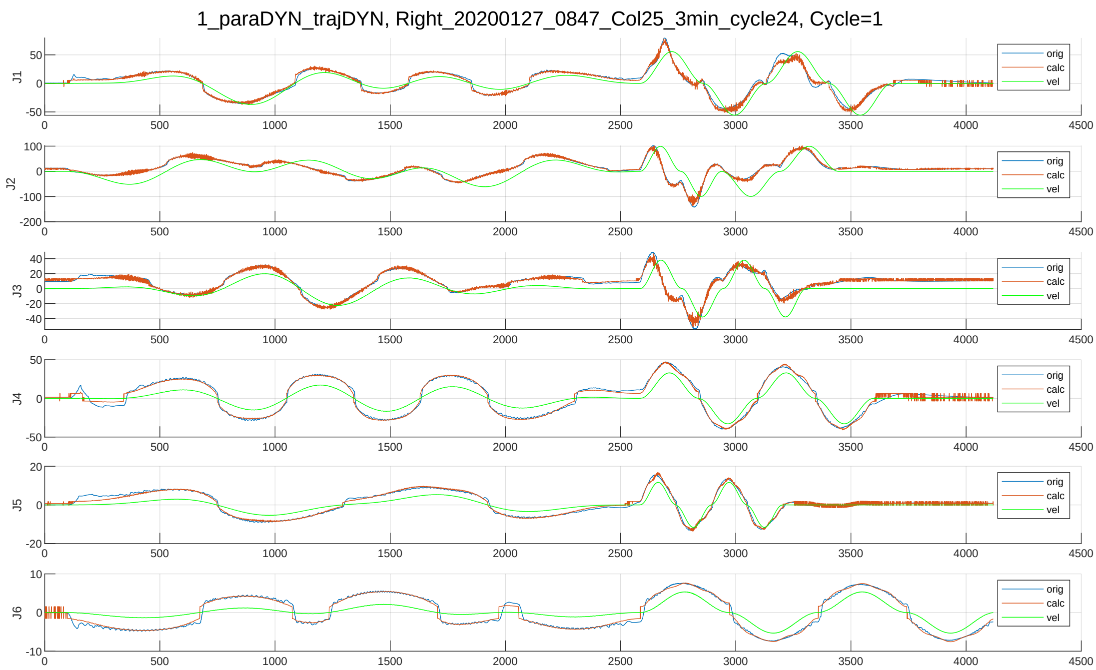

Figure 5.1: The measured torque and estimated torque of the 1st stage from the Cycle 1 of the Test 1 of the Robot 2

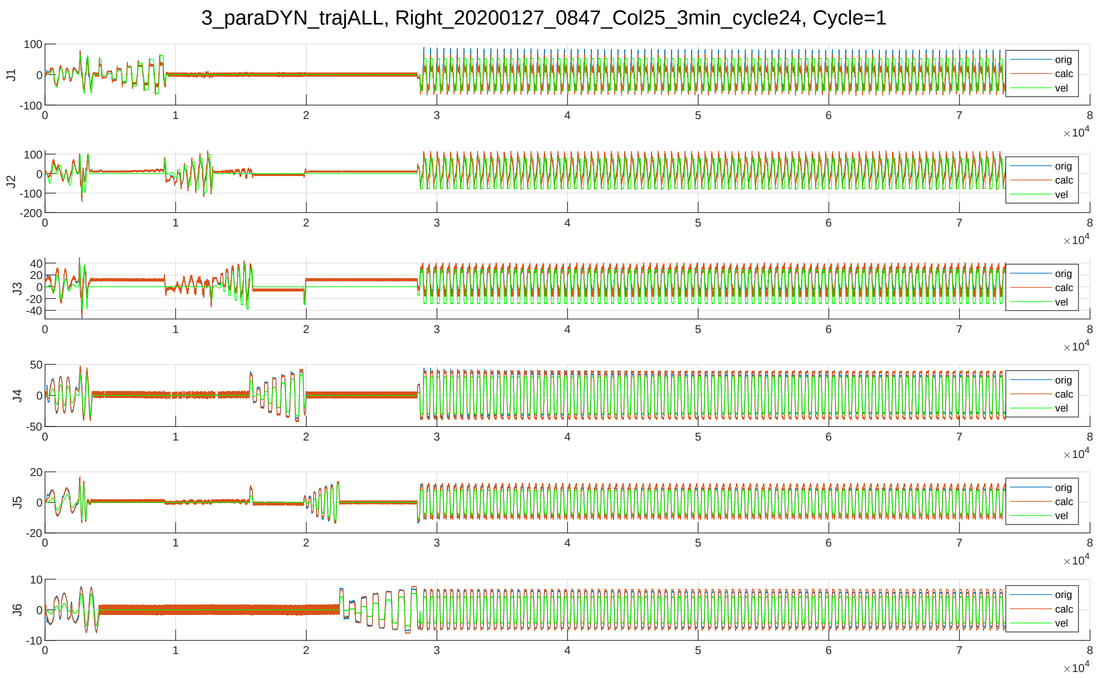

Figure 5.2: The measured torque and estimated torque from the Cycle 1 of the Test 1 of the Robot 2

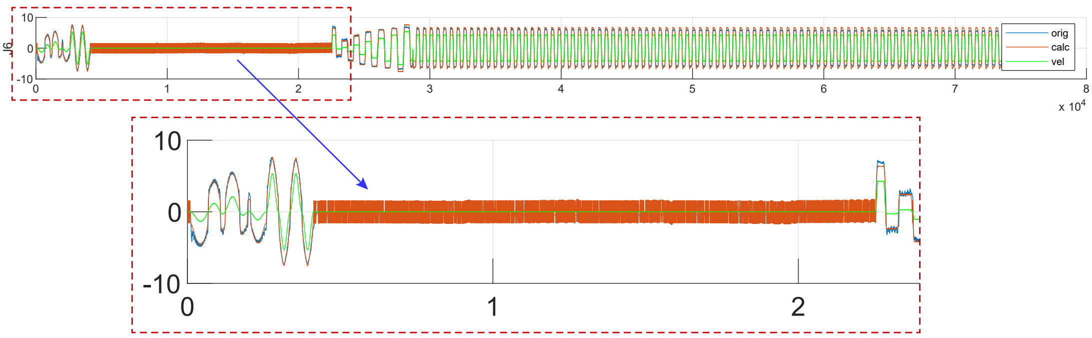

Figure 5.3: The estimation errors at the low velocity duration of Joint 6 in Figure 5.2

5.1.2 The Verification

To understand the accuracy of the identification results, the verification is introduced and indicated by the root-mean-square deviation, or RMSD. The RMSD equation is shown in Equation 5.1. This value represents the measurement of the errors between the estimated values and the collected values. The RMSD values can be easily obtained by the function of "rms" in MATLAB.

$$\tau_{RMSD} = \sqrt{\frac{1}{N}\sum_{n=1}^{N}(\tau_{n,\ estimated} - \tau_{n,\ collected})^2} \tag{5.1}$$

Figures 5.1 and 5.2 (or Figure K.1 in Appendix K and L.1 in Appendix L) shown the collected torque in blue, and the corresponding estimated torque in red. The green curves are the joint velocity. It should be emphasized that the velocity curves are scaled to make them more clear, as mentioned in Section 5.1.1 and also explained in Section 5.1.3. Additionally, the verification based on the identification results on other tests are implemented to demonstrate the accuracy of the identification in general robot operation cases. To make a clear description, the verification based on the identification trajectory are named "self-verification", while the verification based on the identification on other tests are named “cross-verification”. The data analysis has been carried out in Section 5.1.4.

The results of self-verification are shown in Table F.1 in Appendix F. It should be pointed that the values in those tables are the relative value with the unit of 100%, and the values highlighted in yellow are grated than 10%, which means the error presented with this value is considered bigger. Figures 5.4 and 5.5 represent the plots of the self-verification of each joint for all tests on both robots. Similarly, the tables of cross-verification are shown in Table F.3, F.4, F.5 and F.6 in the same appendix. Figures 5.6 and 5.7 represent the plot of the cross-verification with the 1st identification results on both robots. All tables and plots of the self-verification results and the cross-verification results are shown in Appendix F. The verification results of the excitation trajectory and the merged trajectory are plotted in Appendix K and L. It is worth noting that the figures shown in these appendixes are from the data of the 1st test of Robot 2.

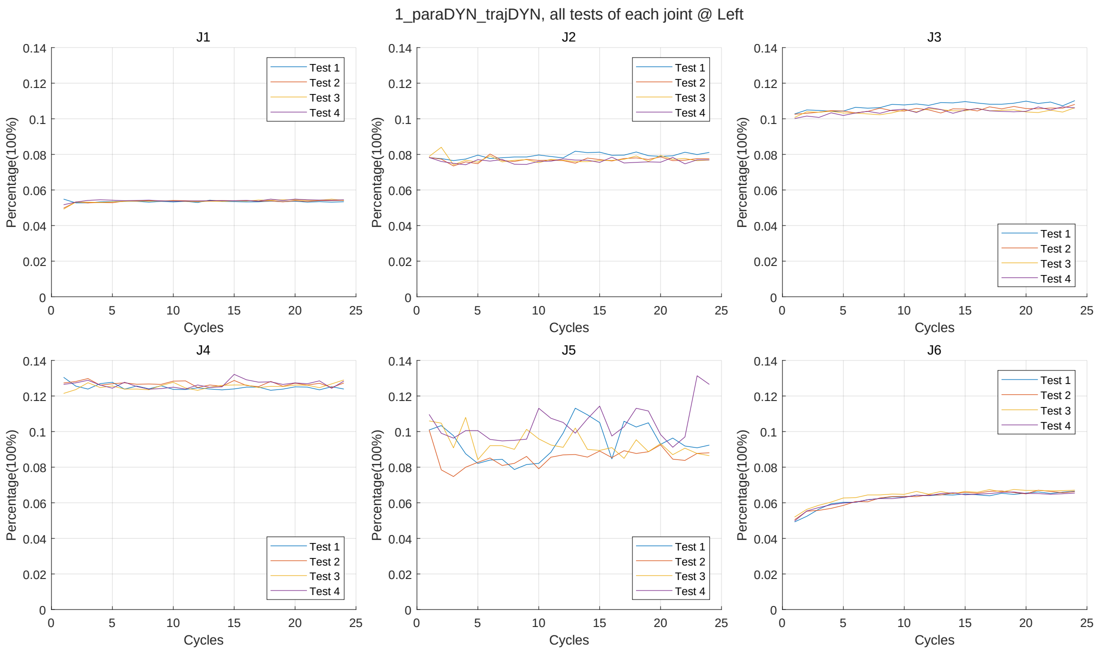

Figure 5.4: The self verification of each joint of all tests of Robot 1

5.1.3 The Low Velocity Results Filter

As mentioned in Section 5.1.1, 5.1.2, and in Figure 5.3, large errors appear when the joint velocity is slow or equal to zero because of the low precision of the friction model during the low velocity motion (Figure 5.8 and 5.9). Since the joint at low speed can be assumed firm, the torque output can be considered constant in these situations. Therefore, the errors have been eliminated. The RMSD values without the low-velocity result have been calculated and then they are shown in Table F.2 in Appendix F.

It is worth noting that Figure 5.9 also proved that the friction is effected by the temperature, and it can be presented by the time. This aspect has been discussed in Section 5.2.3.

5.1.4 The Results Of The Verification

5.1.4.1 The Self Verification

Table F.2 shows the relative error between estimated and measured torque. The values greater than 10% and less than 15% are highlighted in yellow. The remaining values are less than 10%. It should be noted that these values are calculated without the data related to

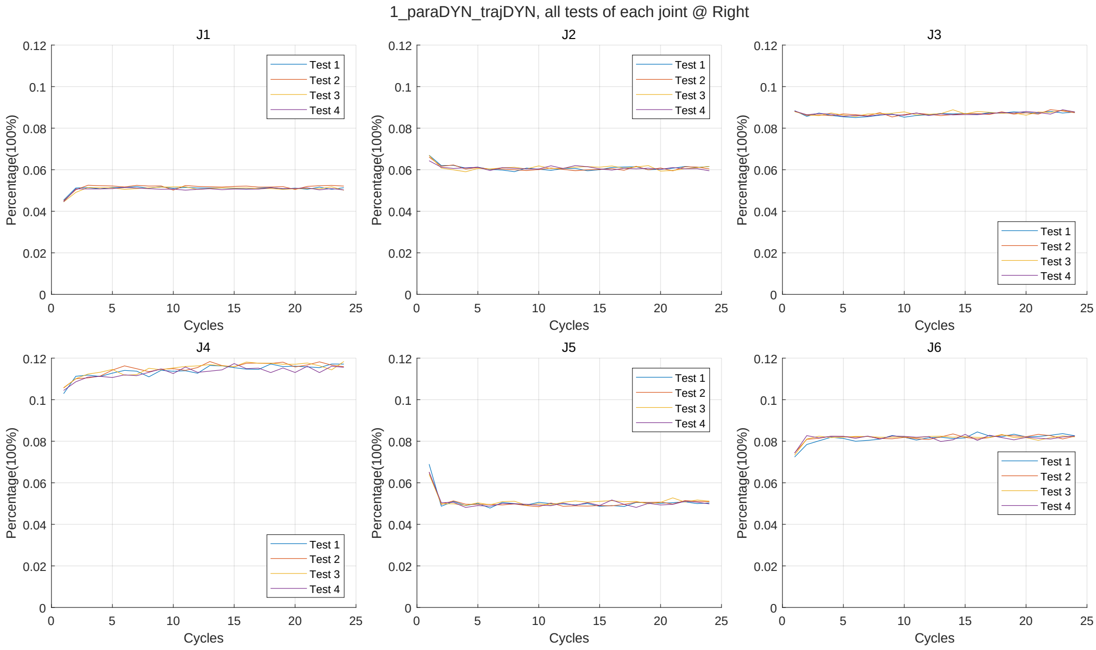

Figure 5.5: The self verification of each joint of all tests of Robot 2

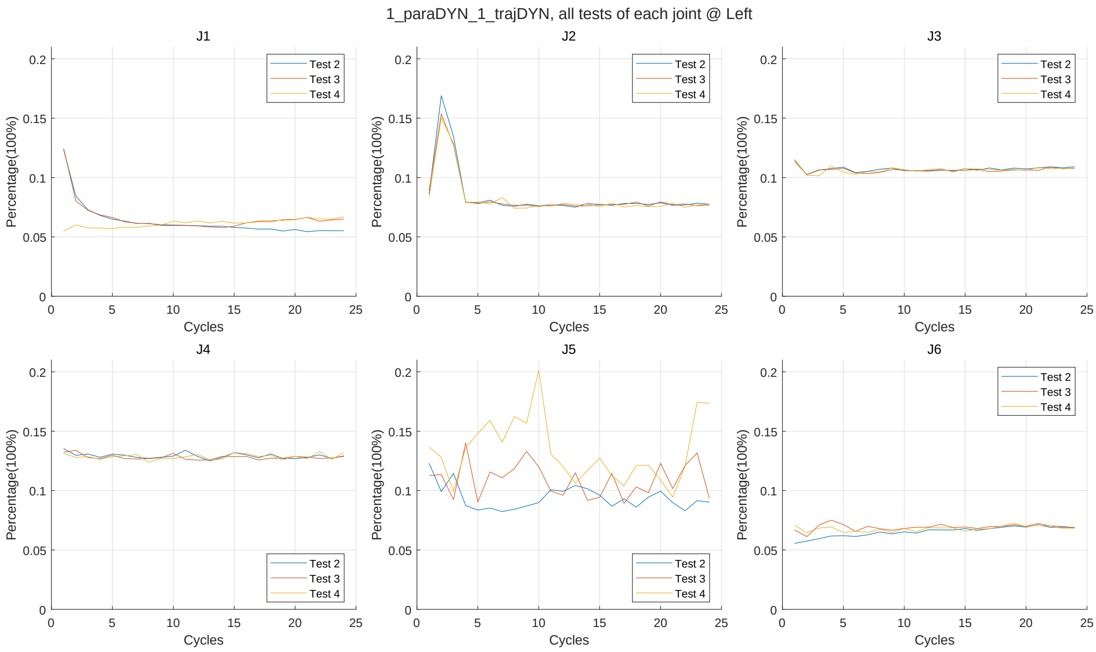

Figure 5.6: The cross verification with the 1st identification results of Robot 1

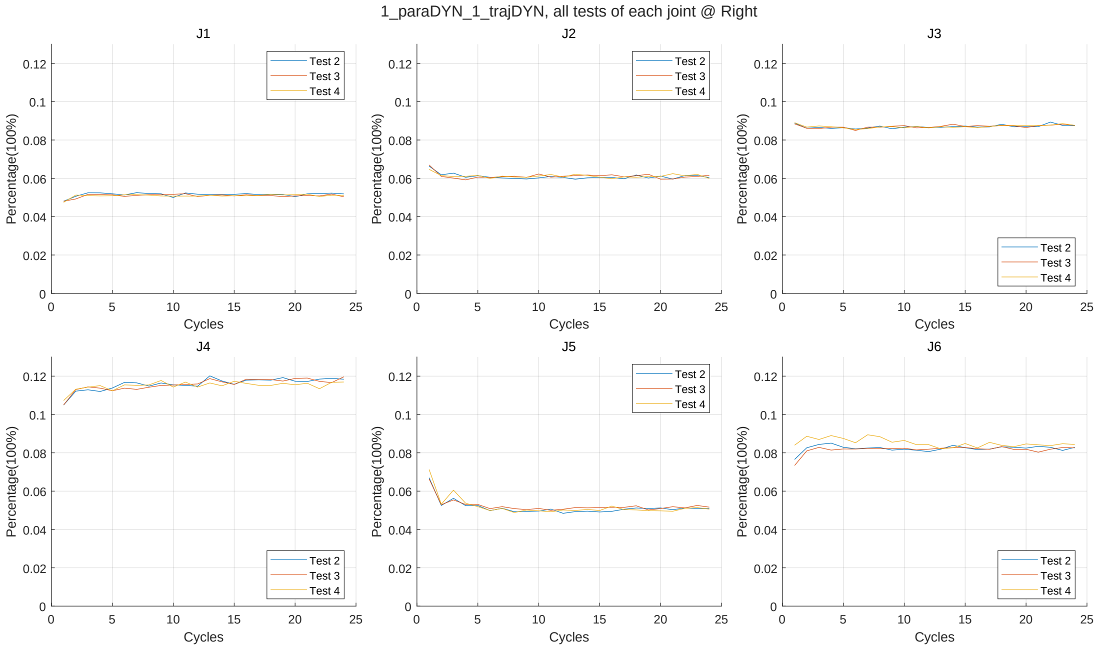

Figure 5.7: The cross verification with the 1st identification results of Robot 2

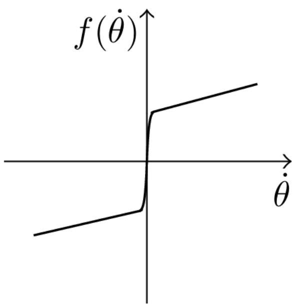

Figure 5.8: The ideal friction model

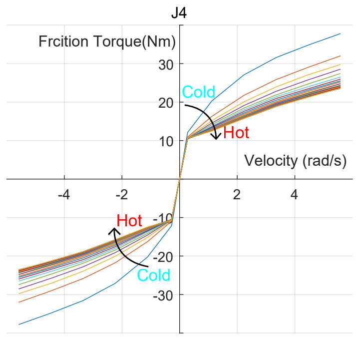

Figure 5.9: The friction observed experimentally from Joint 4 in a test

low velocities, where the robot has been considered stationary (Section 5.1.3). The results are plotted in the Figures 5.4 and 5.5 to better understand the value development with cycles. All plots have the same scale on the y-axis.

Based on the results shown in Figures 5.4 and 5.5, it is possible to see that the verification results of the Joint 3 and 4 on Robot 1, and Joint 4 on Robot 2 are higher than 10%, which have the range of 0.1 and 0.12, 0.12 and 0.14, 0.1 and 0.12 respectively. According to Table F.2, the maximum differences between the start cycle and end cycle are 7.3%, 6.2% and 13.8% respectively. The statistic data of the joints mentioned before and also Joint 5 of Robot 1 are shown in Table 5.1. The standard deviation values in this table demonstrate that the fluctuations of Joint 5 of Robot 1 are much bigger than other joints, which are confirmed in Figure 5.4. This situation illustrates that the Joint 5 of Robot 1 has some problems, which turns out with larger noise in the experiments. This requires future examination to find the causes. The plots of other joints show the acceptable identification results because that the self-verification values are less than 10%. The statistical data of all joints and robots are analysed with other tables in Appendix F.

Table 5.1: Some statistical values of Joint 3, 4 and 5 of Robot 1, and Joint 4 of Robot 2

		Tests	The Range in Plots		The Values in Tables								
			Minmum	Maxmum	Minmum		Maxmum		difference bwteen MAX/MIN		difference bwteen	Standard Deviation	
					Test	All Tests	Test	All Tests	Test	All Tests	Start/End Cycle	Test	All Tests
Unit			100%	100%	100%	100%	100%	100%	-	-	-	100%	100%
Robot 1	Joint 3	1	0.1	0.12	0.1027	0.1001	0.1102	0.1102	0.0679	0.0913	0.0728	0.002	0.0021
		2			0.1026		0.1081		0.0512		0.0540	0.001308	
		3			0.1008		0.1062		0.0513		0.0540	0.001188	
		4			0.1001		0.1067		0.0617		0.0599	0.001736	
	Joint 4	1	0.12	0.14	0.1232	0.1214	0.1277	0.1322	0.0352	0.0810	0.0505	0.001609	0.0018
		2			0.1248		0.1287		0.0308		0.0001	0.00128	
		3			0.1214		0.1290		0.0587		0.0623	0.001599	
		4			0.1238		0.1322		0.0629		0.0145	0.001997	
	Joint 5	1	0.07	0.13	0.0787	0.0748	0.1131	0.1314	0.3045	0.4309	0.0841	0.009751	0.0105
		2			0.0748		0.0926		0.1924		0.1281	0.00512	
		3			0.0842		0.1020		0.1742		0.1841	0.006487	
		4			0.0912		0.1314		0.3057		0.1539	0.00992	
Robot 2	Joint 4	1	0.1	0.12	0.1029	0.1029	0.1172	0.1184	0.1218	0.1307	0.1384	0.002978	0.0030
		2			0.1057		0.1183		0.1065		0.0958	0.002949	
		3			0.1055		0.1184		0.1082		0.1213	0.00291	
		4			0.1044		0.1174		0.1103		0.1068	0.002739	

5.1.4.2 The Cross Verification

Additional verifications are implemented on the identification, using other tests coming from the same robot, to verify the accuracy of the results. The calculation is very similar to self-verification. The results of cross-verification on the 1st test are shown in Figure 5.6 and 5.7 for the Robot 1 and 2 respectively. The ranges shown in these figures are summarized in Table 5.2, and the average values of these figures, without first 5 cycles, are listed in Table 5.3. It should be pointed that the data of the self-verification from Figure 5.4 and 5.5 are also concluded in these tables. The complete results with tables and figures are listed in Appendix F.

As shown in these figures and tables, it is easy to see that the identification results for each joint are similar between the self-verification and cross-verification. Looking at the data in Table 5.2, it is possible to see that the range differences in figures are small for Robot 1, and are zero for Robot 2. This leads to a conclusion that the self-verification results are sufficient to describe the accuracy of the identification due to the similar results between the self-verification and cross-verification. A comparable and powerful evidence can be obtained from Table 5.3, which contains the data considered from each experiment without the first 5 cycles. This is because that there is a drastic change in the first 5 cycles of each sub-plot on these figures, which demonstrates the low accuracy of the identification results during the first few cycles. This phenomenon depends on the effects of friction, but it will be discussed in detail in the next sections. Moreover, the differences between Robot 1 and 2 in Table 5.2 and 5.3 show that Robot 2 has higher accuracy of the estimation compared to Robot 1.

There is a strong oscillation in the sub-plot of Joint 5 of Robot 1 in Figure 5.6, and a similar situation is also shown in Figure 5.4. Additionally, this problem can be observed in the friction behaviours analysis in Figure N.1 and N.2. The causes of this situation require future studies as mentioned in Section 5.1.4.2.

Table 5.2: The range of plots of joints in Figure 5.4, 5.6, 5.5 and 5.7

	Robot 1			Robot 2		
	Figure 5.4	Figure 5.6	**Difference**	Figure 5.5	Figure 5.7	**Difference**
Joint 1	0.05∼0.06	0.05∼0.08	**0∼0.02**	0.05	0.05	**0**
Joint 2	0.07∼0.08	0.08	**0∼0.01**	0.06	0.06	**0**
Joint 3	0.1∼0.11	0.12	**0.01∼0.02**	0.09	0.09	**0**
Joint 4	0.12∼0.13	0.14	**0.01∼0.02**	0.1∼0.12	0.1∼0.12	**0**
Joint 5	0.07∼0.11	0.08∼0.13	**0.01∼0.02**	0.05	0.05	**0**
Joint 6	0.05∼0.07	0.05∼0.08	**0∼0.01**	0.08	0.08	**0**

Table 5.3: The average value of plots of joints in Figure 5.4, 5.6, 5.5 and 5.7 without the first 5 cycles

	Robot 1			Robot 2		
	Figure 5.4	Figure 5.6	**Difference**	Figure 5.5	Figure 5.7	**Difference**
Joint 1	0.05	0.06	**0.01**	0.05	0.05	**0**
Joint 2	0.075	0.08	**0.005**	0.06	0.06	**0**
Joint 3	0.105	0.1	**0.005**	0.085	0.08	**0.005**
Joint 4	0.13	0.13	**0**	0.115	0.115	**0**
Joint 5	/	/	/	0.05	0.05	**0**
Joint 6	0.06	0.07	**0.01**	0.08	0.08	**0**

5.1.5 The Results Of Dynamic Parameters

5.1.5.1 The Plots of Dynamic Parameters

To better understand the identification results, each parameter has been plotted. The examples are shown in Figures 5.10 and 5.11. It is possible to see that the identified dynamic parameters are different in each cycle. In these figures, there is a dramatic increase during the first 5 cycles, and then the curves gradually stabilize with fluctuations. Subplot B is the representation of subplot A with a widening on the y-axis to better evaluate the values. After the scaling of the y-axis, it is easy to understand that the fluctuation is small and the steady-state value is reached after approximately 15 cycles. Besides, the steady-state of the dynamic parameters can be observed by the standard deviation values shown in Table 5.4 with the picked parameters.

In Table 5.4, the values of the column "Last 19 Cycles" are the standard deviation of the last 19 cycles. The values in the column "All Cycles" are higher than those in the "Last 19 Cycles". This means that the parameters in last cycles have less fluctuation. This can be observed in Figure 5.10 and 5.11. The curve amplitude is reduced and it tends to be stable after 10 cycles in Figure 5.10(b), and 5 cycles in Figure 5.11(b).

However, despite the negative values show in the column of "Difference" in Table 5.4, the plots of f_1 (Figure 5.12) show large oscillations without the steady-state values. A possible reason for this could be the different attributes between mP_x, I_{xx}, and f_1. Theoretically, the mP_x and I_{xx} have physical meaning, which are constants. But f_1 is one of the friction coefficients, which change during in the movement, due to internal temperature, lubrication, pressure and stress between parts, undetectable damages, and so on.

The figures of all the identified dynamic parameters and the tables of the related statistical data are listed in Appendix G and H.

Table 5.4: The standard deviation of the identification results of selected parameters

				All Cycles	Last 19 Cycles	Difference *
2	mP_x of Joint 2	Robot 1	T1	0.0524	0.0299	-0.0225
			T2	0.0618	0.0289	-0.0329
			T3	0.0537	0.0268	-0.0269
			T4	0.0560	0.0249	-0.0311
		Robot 2	T1	0.0367	0.0113	-0.0255
			T2	0.0345	0.0092	-0.0253
			T3	0.0365	0.0113	-0.0252
			T4	0.0374	0.0086	-0.0288
4	I_{xx} of Joint 2	Robot 1	T1	0.0694	0.0377	-0.0317
			T2	0.0686	0.0507	-0.0179
			T3	0.0813	0.0502	-0.0311
			T4	0.0691	0.0343	-0.0348
		Robot 2	T1	0.0459	0.0214	-0.0245
			T2	0.0485	0.0166	-0.0319
			T3	0.0369	0.0118	-0.0251
			T4	0.0410	0.0161	-0.0249
37	$f1$ of Joint 1	Robot 1	T1	0.2516	0.0954	-0.1562
			T2	0.2064	0.0885	-0.1179
			T3	0.1317	0.1070	-0.0248
			T4	0.2168	0.0920	-0.1248
		Robot 2	T1	0.1615	0.1241	-0.0374
			T2	0.1603	0.0868	-0.0735
			T3	0.1170	0.0753	-0.0417
			T4	0.1367	0.1327	-0.0040

* The equation is "$Differences = Last\ 19\ Cycles - All\ Cycles$"

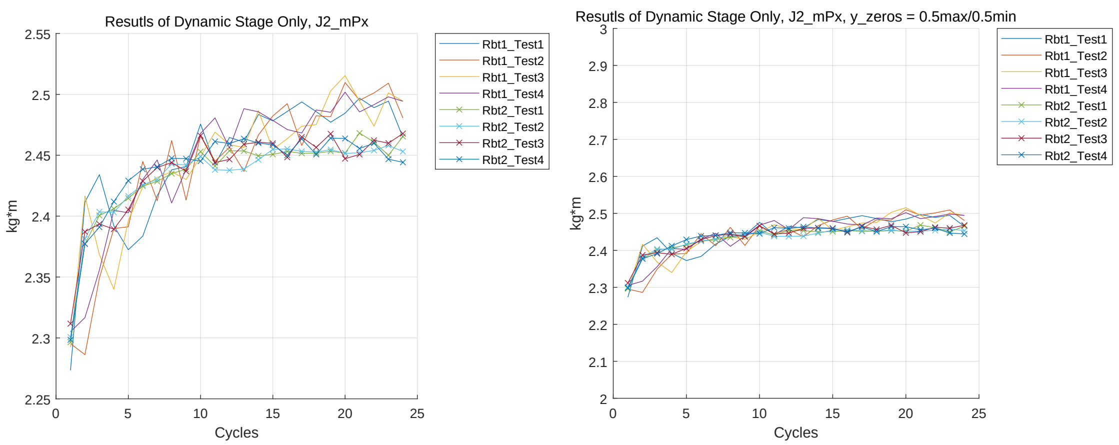

(a) Labelled automatically

(b) Labelled with the widening scale of y-axis

Figure 5.10: mP_x of Joint 2

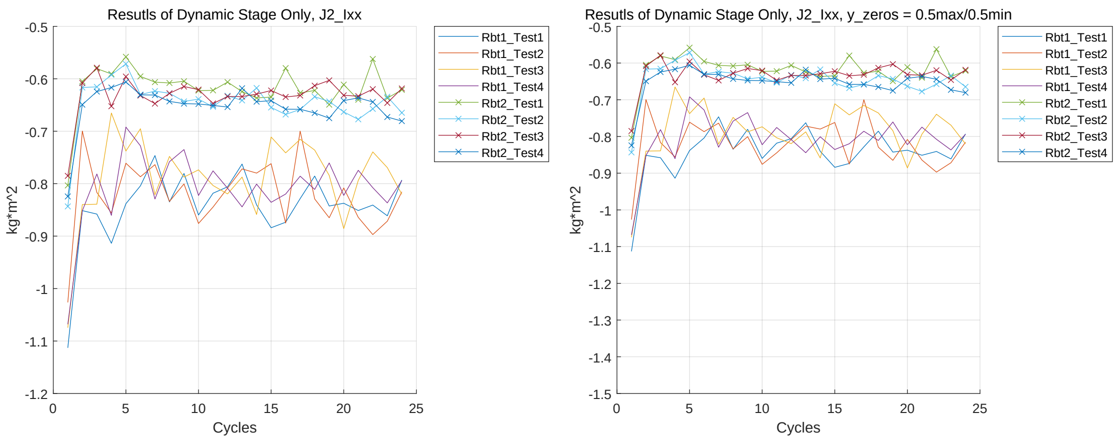

(a) Labelled automatically (b) Labelled with the widening scale of y-axis

Figure 5.11: I_{xx} of Joint 2

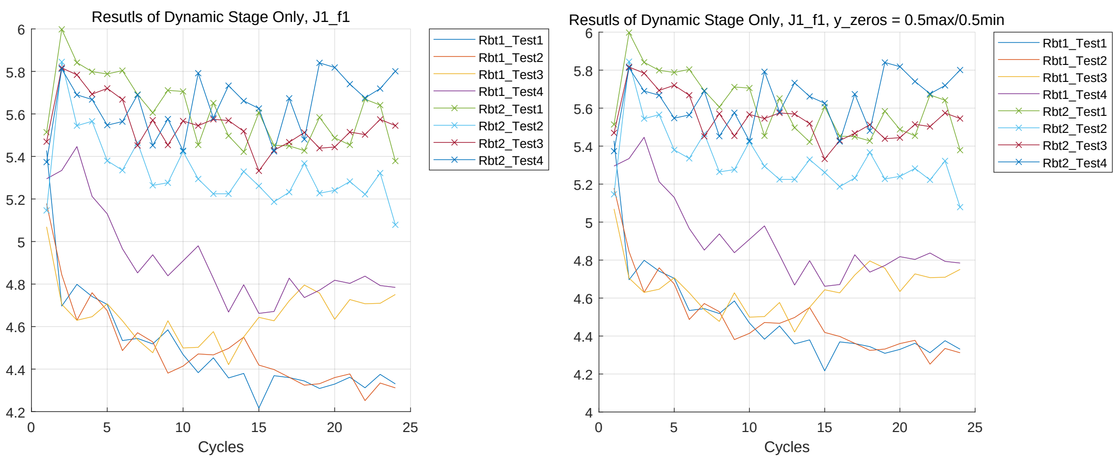

(a) Labelled automatically (b) Labelled with the widening scale of y-axis

Figure 5.12: f_1 of Joint 1

5.1.5.2 The Multiple Selected Cycles

The identifications with few selected cycles have been carried out to make a clear demonstration of dynamic parameter behaviour during the robot operations. There are three groups of selected cycles, which are Cycle 10, 15, and 20 for Group 1, Cycle 3, 9, 16, and 22 for Group 2, and Cycle 3, 5, and 10 for Group 3. The results are shown in Table 5.5. The identification results of these groups have been named as "***Unit***" results.

Table 5.5 contains the cycle selection of the identification ordered from Unit 1 to 3. The cycles selected for Unit 1 are located at the later period of the experiment, and its identification result is closed to the results obtained at the end of the cycles. Similarly, the identification result of Unit 3 is closed to the results of the initial cycles. Due to the drastic change of curves in the first few cycles, this result has a larger error than other two groups. For Unit 2, due to the evenly selected cycles, the result is between the values of Unit 1 and 3. Moreover, the result of Unit 2 also can be regarded as the average value of identification result of experiments. These conclusions are also shown in Figures 5.13 and 5.14 highlighted by straight lines. Again, subplot B in these figures is the representation of subplot A with a widening on the y-axis to better evaluate the values. These lines show the tendency of curve development in a simple way, which is from low value at the beginning, to stable value at the ending. They also demonstrate that the magnitude of the curve amplitude changes from the beginning to the ending, which meet the size of gaps between lines. Moreover, this situation also illustrates the poor accuracy in the identification.

All the plots of the identification results are shown in Appendix I and J.

Table 5.5: The cycles selected in groups in unit identification

Cycles	1	2	3	4	5	6	7	8	9	10	11	12	13	14	15	16	17	18	19	20	21	22	23	24	25	Name
Group 1																										Unit 1
Group 2																										Unit 2
Group 3																										Unit 3

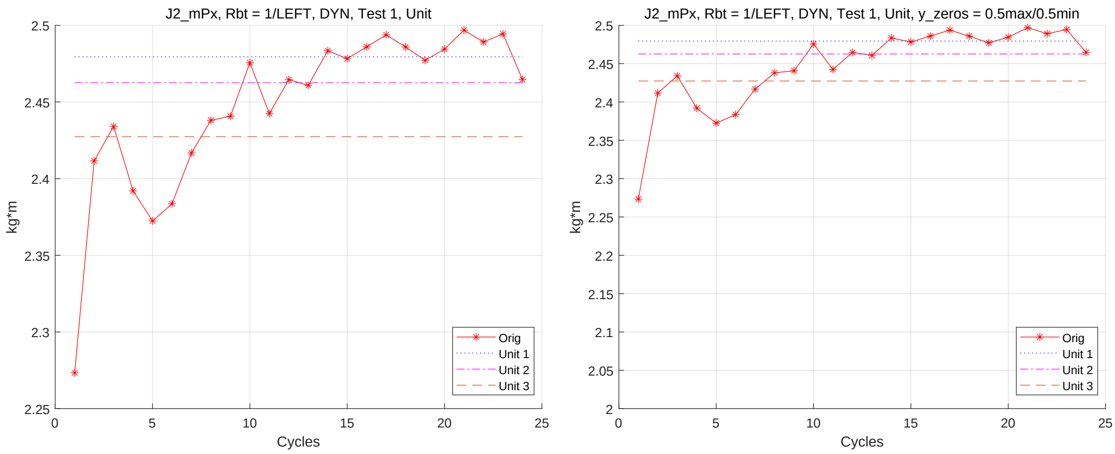

(a) Labelled automatically

(b) Labelled with the widening scale of y-axis

Figure 5.13: mP_x of Joint 2 of the Robot LEFT, the identified results and the related results of selected cycles

5.1.6 The Errors Of Start And End Of Cycles

As shown in Appendix L, it is clear that the verification results changed in the warming up stage between start and end in 1st cycle. This is demonstrated in Figure 5.15 as an example from the 1st cycle of one test. It is easy to note that the errors between the estimated torque

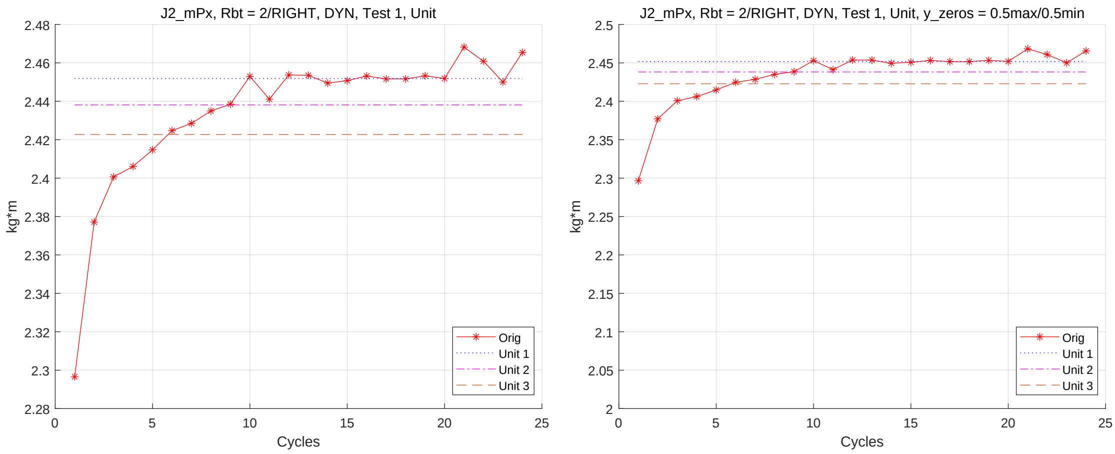

(a) Labelled automatically (b) Labelled with the widening scale of y-axis

Figure 5.14: mP_x of Joint 2 of the Robot RIGHT, the identified results and the related results of selected cycles

and measured torque at the start of the warming stage are smaller than the ones at the end. This can be explained because friction changes dramatically in the first few cycles of the tests. This aspect has been discussed in Section of 5.2.

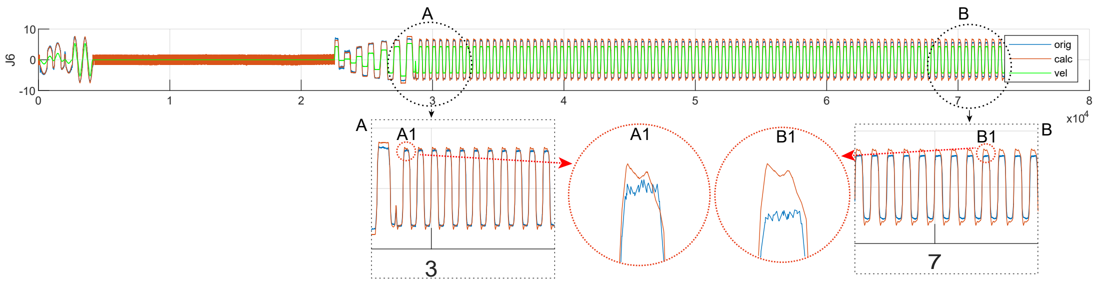

Figure 5.15: The identification errors at the start and the end of the warming stage in the 1^{st} cycle

5.1.7 Summary

In this section, the identification results of dynamic parameters are discussed and demonstrated. Generally, there is a drastic change at the first few cycles for the all identification results, except for figures made from the friction coefficients. This situation leads to the important conclusion that the identification result relies on the mechanism conditions, which accuracy changes during the operation. This could be caused by temperatures, lubrication, and so on. The similar conclusion can be found and observed from the figures in this chapter and in the related appendixes.

5.2 The Friction

This section analyses the friction behaviours in long-time duration movement. At first, the measuring method is discussed. Subsequently, the procedure applied to compensate the gravity contribution is explained. In the end, the curve fitting is implemented for the analysis. The related results of this section are listed and shown in the Appendix M, N and O.

5.2.1 Friction Measure

The friction measure stage is introduced in Section 4.4 with the trajectory example in Figure 4.7. The measurement is carried out on each joint separately while other joints maintain their designed position. The measurement trajectory is created with the selected velocity at 5%, 20%, 40%, 60%, 80%, 100% of the maximum speed. To avoid the effect of gravity and the affection from the movement of the other links, the joints' positions have been carefully designed. For example, Joints 1, 4, 5, and 6 are configured as a horizontal movement in the friction measurement stage. Due to the robot structure and installation, it is not possible to design the same movement for Joints 2 and 3, which leads to the feature process of removing the gravity effect as explained in Section 5.2.2.

Figure 5.16 shows an example of the friction measure results at the Velocity 60% of Test 1 from Robot 2. These plots clearly show that the torque output decreases from the start to the end of the cycles. This situation indicates the torque output of motor is reduced gradually in the friction trajectories of an experiment. For each joint, there are some constant sections in the torque output, corresponding to the constant velocity, except for Joints 2 and 3. To find the friction torque on Joint 2 and 3, a gravity effect compensation was needed and it was applied in the Section 5.2.2.

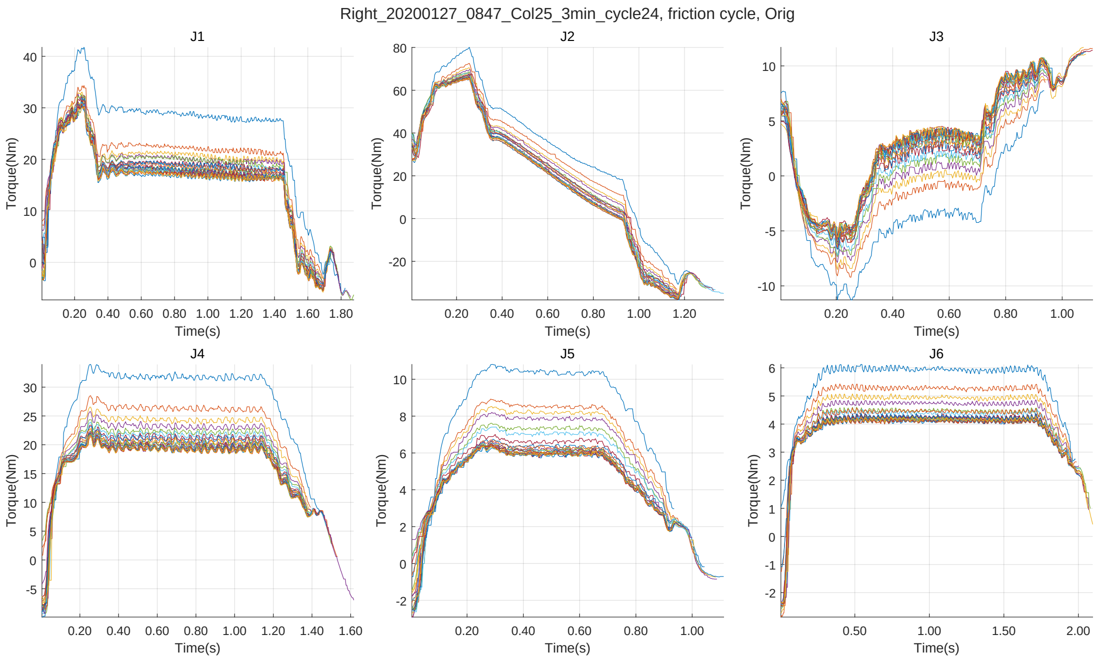

Figure 5.16: The motor torque output measured in the friction stage, separated by the joints with the velocity of 60%

To visualize the friction changing, the mean value of the torque output duration has been calculated and then it has been plotted as shown in Figure 5.17. Base on this figure, it is clear that the friction torque decrease during the cycles. And there is a dramatic decrease at the first $5 \sim 10$ cycles and then the curve becomes stable and maintains its value until the end of the test, which is similar to the situation mentioned in Section 5.1.7.

5.2.2 Reduce The Gravity Effect

As mentioned before, because of the robot structure (Figure 5.18), the torque output of Joint 2 and 3 contains the gravity contribution. An identification method using the Least Squares algorithm has been used to remove the gravity effect. The Equation 5.2 [39, 48] is used in this

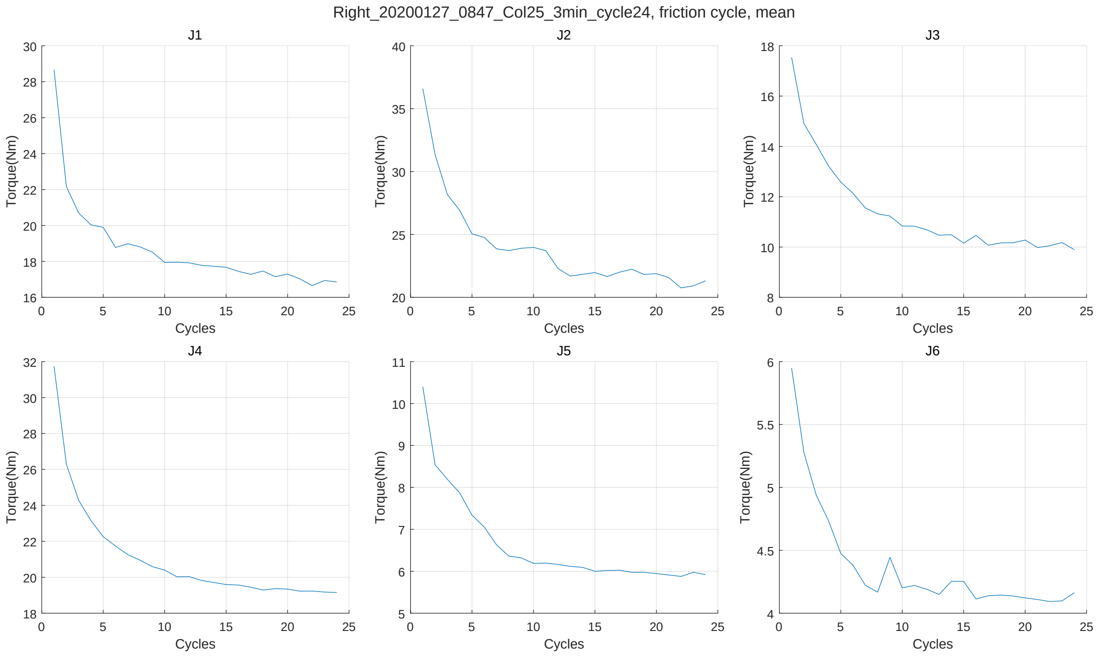

Figure 5.17: The mean value of each cycle of motor torque output measured in the friction stage, separated by the joints with the velocity of 60%, base the data shown in Figure 5.16

stage.

$$\tau_{no-gravity} = \tau_{motor} - mP_x sin(\theta) - mP_y cos(\theta) \tag{5.2}$$

Where θ is the position of joint and the mP_x and mP_y are the parameters to identify. To increase the accuracy, the friction coefficients are introduced in this identification. This leads to the Equation 5.3 for the identification.

$$\begin{aligned}\tau_{no-gravity} &= I_{motor}\ddot{\theta} - mP_x sin(\theta) - mP_y cos(\theta) + f_1 sign(\dot{\theta}) + f_2\dot{\theta} + f_3\dot{\theta}^2 sign(\dot{\theta}) + f_4\dot{\theta}^3 \\ &= \begin{bmatrix}\ddot{\theta} & -sin(\theta) & -cos(\theta) & sign(\dot{\theta}) & \dot{\theta} & \dot{\theta}^2 sign(\dot{\theta}) & \dot{\theta}^3\end{bmatrix} \begin{bmatrix} I_{motor} \\ mP_x \\ mP_y \\ f_1 \\ f_2 \\ f_3 \\ f_4 \end{bmatrix}\end{aligned} \tag{5.3}$$

Where θ, $\dot{\theta}$, and $\ddot{\theta}$ are the position, velocity, and acceleration of joints respectively. f_1 to f_4 are the friction coefficients that are not used in computing. After the identification, the friction measurement without gravity effect of Joint 2 and 3 can be obtained by the Equation 5.3. The results of Joint 2 and 3 after the removing gravity effect are shown in Figure 5.19, where the steady torque output is clearly shown.

All the plots of the friction measurement are listed in Appendix M. It should be noted that the gravity effect of Joint 2 and 3 is removed in these figures.

5.2.3 The Friction And Velocities

To better understand the friction behaviours with the different velocities, see Figures 5.9 and 5.20. These plots illustrate the friction changes based the velocities in different cycles. Friction decreases during the test from the cold to the hot condition, hence from the 1^{st} cycle to the end. Because of these plots are generated from the same trajectory on one robot, it is possible to

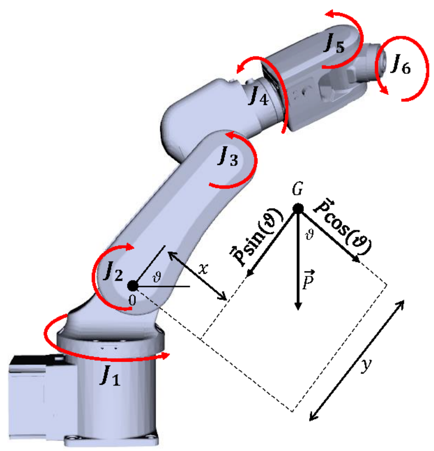

Figure 5.18: The gravity effect in joints

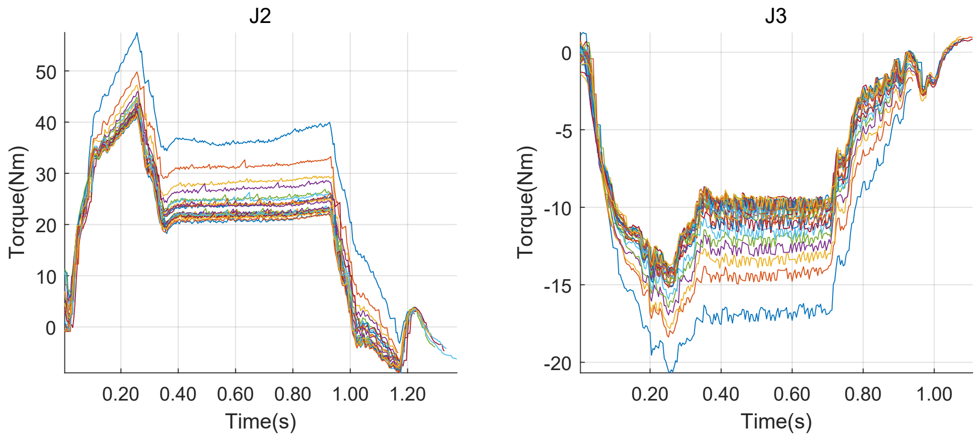

Figure 5.19: The plots of friction measurement of Joint 2 and 3 after the removed gravity effect, base the Figure 5.16

consider that each curve corresponds to a specific temperature. Therefore, friction changes with the temperature. Again, the gaps between the cycles in these plots illustrates the magnitude of the change, which has been already mentioned. Furthermore, with the same reasons as before, the temperature can be considered related to the time because the temperature rises during the operation. This results in a time-based temperature model. Additionally, due to the precision of measurement and robot system limitation, the details of low velocities are loss. This problem can be solved by applying embedded sensors and high precision equipment, which will be implemented in the future studies. All the plots of the friction versus velocities are listed in Appendix O.

5.2.4 The Curve Fitting Of Friction

To describe the results of the friction measurement, the curve fitting is introduced with a double exponential equation which is shown in the following Equation:

$$\tau = a + be^{-\frac{t}{t_1}} + ce^{-\frac{t}{t_2}} \tag{5.4}$$

Where the t_1 and t_2 are the time constants in minutes, and a, b, and c are specific coefficients. This will help to establish the time-based friction model in the future and therefore, a dynamic model of robot developed by time could be realized.

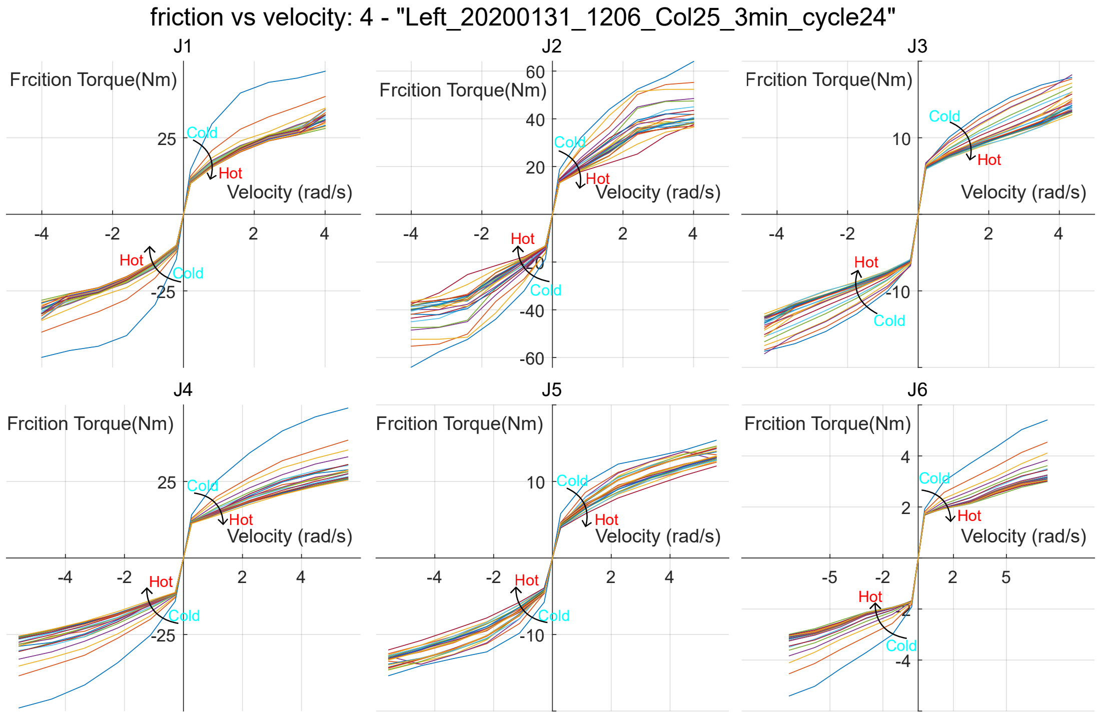

Figure 5.20: The friction versus velocities in diffident cycles of all joints

With the help of Curve Fitting Toolbox in MATLAB (Figure 5.21), the fitted results of Figure 5.17 are shown in Figure 5.22. The related coefficient values and the time constants are shown in Table 5.6. The same curve fitting operations are carried out for all the joints in all tests, and the results are shown in Appendix N.

Table 5.6: The values of the curve fitting results related with the Figure 5.22

	a	b	t_1 *	c	t_2 *
J1	16.60894	4.87445	40.94343	8.56154	2.88916
J2	20.25689	6.46293	56.55044	11.05555	7.43387
J3	10.01373	6.35484	23.01969	8.42142	0.53915
J4	19.10495	7.17766	25.88962	7.98374	3.76450
J5	5.89756	3.85085	20.28498	19.59727	0.46770
J6	4.14913	1.92346	12.83307	33.80185	0.31042

* The unit is minutes.

An additional curve fitting operation is carried out with all 4 tests of one robot to obtain a better result. The results are labelled with "***mix***" data. An example is shown in Figure 5.23. In this figure, subplot A shows the mean values of friction cycle on each test, subplot B demonstrates the curve fitting results of subplot A. Subplot C indicates the curve fitting result of mixed data with the green curve, and the "*" are points from the mixed data. Subplot D shows the curve fitting results from both subplot B and C. From these plots, it is clear that the curve fitting results of Test 2, 3, and 4 are similar to the results of the mixed data. There is a small difference between the curves fitting result of Test 1 and the others at the first 20 minutes, which includes approximately 5 cycles. These curves indicate the friction behaviours can be described by a time-based model. This finding was the reason for using Equation 5.4.

All the plots and coefficients of this section are shown in Appendix N.

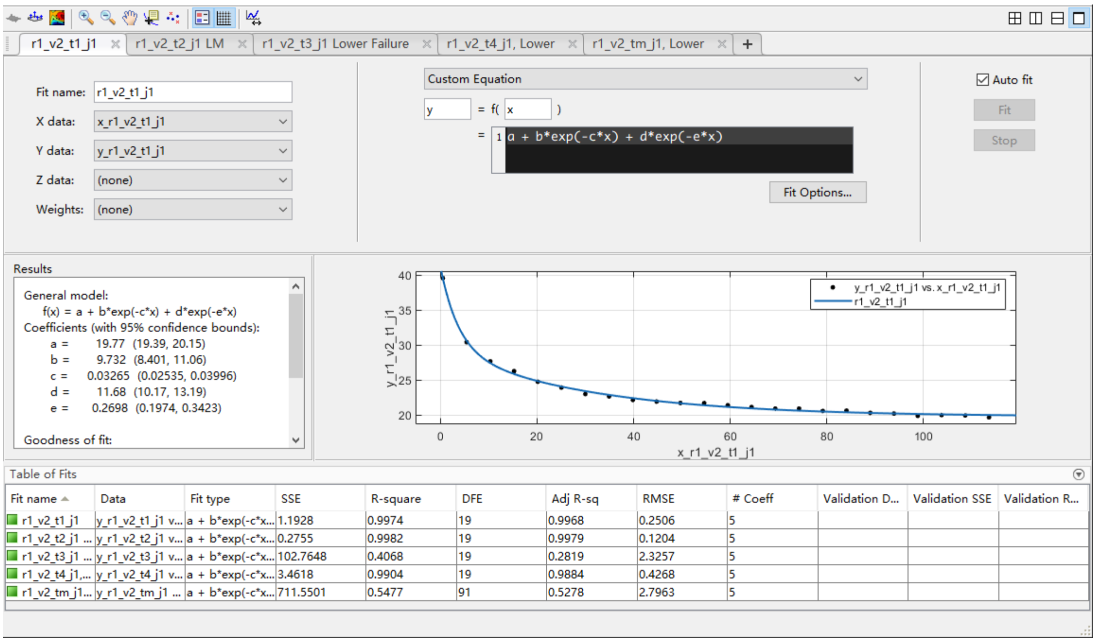

Figure 5.21: The Curve Fitting Toolbox in MATLAB

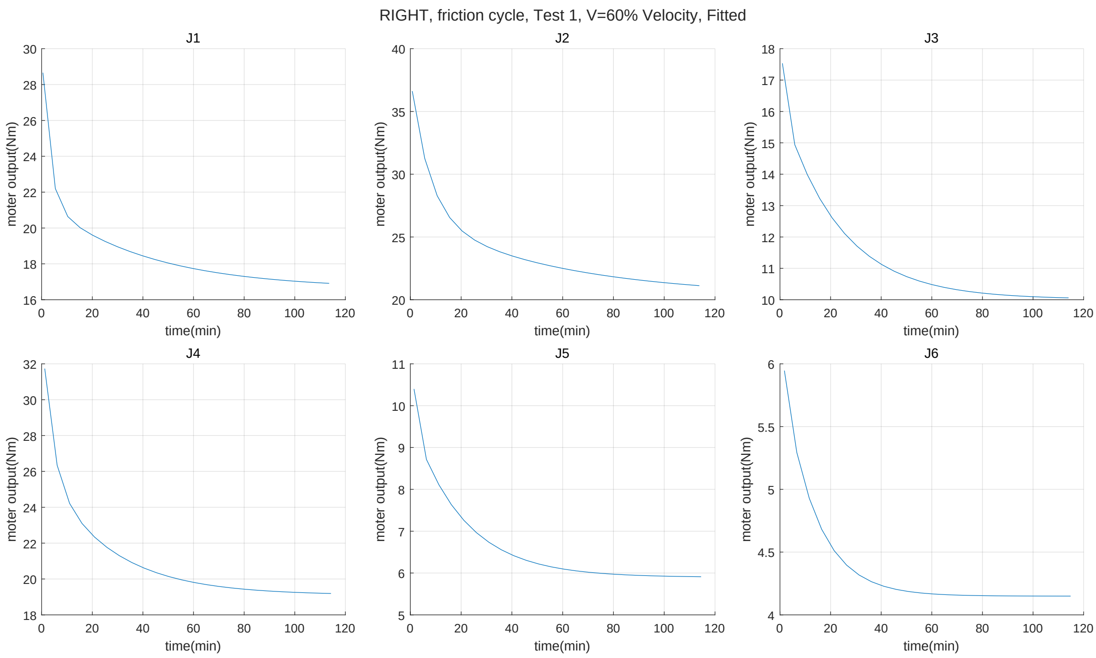

Figure 5.22: The curve fitting results of Figure 5.17

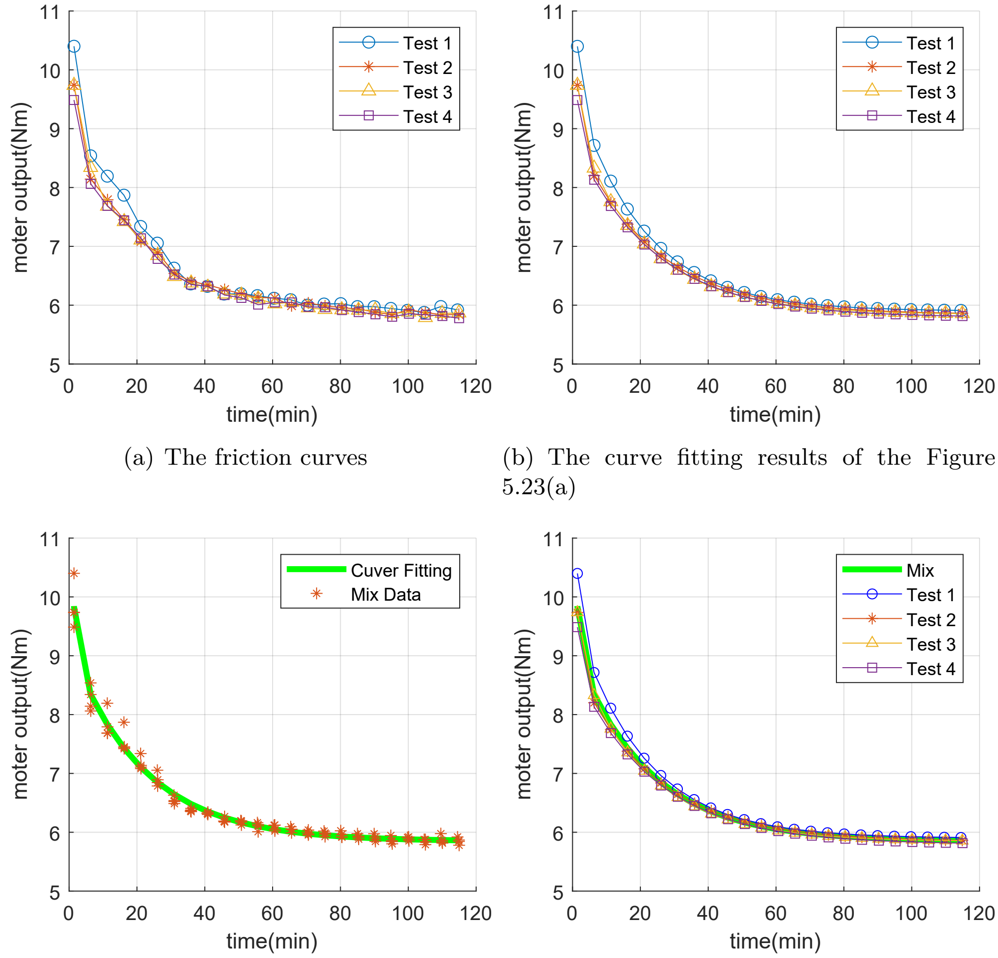

(a) The friction curves

(b) The curve fitting results of the Figure 5.23(a)

(c) The mixed points of tests and the curve fitting results

(d) The results of the Figure 5.23(c) and 5.23(b)

Figure 5.23: The curve fitting results of Joint 5 of Robot 2

Chapter 6

Conclusion And Future Work

6.1 Conclusion

The purpose of this thesis is to create the dynamic model of a specific industrial manipulator and to analyse its behaviours during robot operations. Moreover, the results of the dynamic estimation on two robots are compared. The identification and verification of the found parameters have been illustrated after the linearization of the dynamic model. To find the optimal trajectory that excites the robot, three excitation trajectories have been created and then they are combined to improve the results. The experiments have been designed to identify the dynamic parameters. Meanwhile, the behaviours of these dynamic parameters have been observed exploiting the motor torque output. It was observed that one of the most influencing factors on friction estimation is the lubrication in the gearbox. The results of the friction analysis are modelled as a time-based model. The results of the data analysis have been compared between two robots of the very same model.

The main contribution of this thesis is the experimental process specially designed to identify the dynamic and friction parameters of the robot model, as discussed in Chapter 4 and 5. The process is used to detect the robot's dynamic behaviours in any operation conditions, which is generally from the cold condition (environment temperature) to the hot condition because the robot warms up after the movements. The results of the analysis also provide that the dynamic parameter are approximately equivalent in the same robot for multiple tests.

In Chapter 3, the dynamic model of robot is illustrated. The model is formulated from the Newton Euler equations. To increase the accuracy of identification results, a new friction model has been designed. After that, the base parameters set are selected using QR and SVD analysis to reduce the complexity in the calculation.

The experimental design is explained in Chapter 4. The trajectories have been designed with three different purposes, which are the excitation trajectory to identify the dynamic parameter, the friction trajectory to observe the motor torque changing in the long-term operations, and the warming-up trajectory to arise the temperature inside the gearboxes. Three excitation trajectory have been created. The 1st was made to find the optimal trajectory that contains the larger acceleration at the start; the 2nd excitation trajectory can not provide the appropriate result with the maximum speed of joints; therefore, the trajectory used in the experiments was a merged motion coming from the 2nd excitation trajectory with an additional section. To observe the friction changing behaviours, the friction trajectory is designed to obtain the motor output torque with the different velocities. The warming-up stage was executed to raise the temperature inside the robot. It is worth noting that the trajectory created has been executed repeatedly to obtain and capture the torque changes.

The results have been analysed in Chapter 5. The dynamic parameters have been calculated firstly from the identification and then the results have been verified. The least-square method has been used in the identification process. The RMSD value is introduced to verify and evaluate the results. It should point that the estimated torque at the low velocities has been filtered because the friction model was imprecise at the very low speed. Another important issue was that the error between the estimated and measured torque at the start of the cycle was larger than the one calculated at the end of the cycle. This is because friction changed during the movement, hence the friction behaviour has been observed. Based on the idea provided by Simoni [47] and Pagani [39], a time-based friction model has been used and then it has been analysed with the curve fitting toolbox in MATLAB. It should be pointed that the data coming from Joint 2 and 3, has been modified with the least square method to remove the gravity contribution.

6.2 Future Work

This thesis was focused on the dynamic parameter identification and the friction variation due to the transmission temperature changes. In future, more aspects could be included to improve the quality of the identification. At this stage the fact that the friction changes in dependence of the temperature is confirmed, but there are no sufficient knowledge to insert this effect in the model. The algorithm used in the identification assumes a static model of robot. The effect of the temperature has been highlighted by successive estimation of the friction at different time instants while the robot was working in standard cycles. However, the incorporation of this effect in the model requires more investigation to be able to model the heat generation and its accumulation in the structure. This extension would require the use of extra sensors (namely temperature sensors) and a more complex model that would be time-dependent. That would increase the computation cost of the real time-control algorithms.

Additionally, due to the installation of robots and the seasons of winter, all tests are executed in-room with constant temperature of about 20°C. However, in real scenes, the environmental conditions could vary according to the locations and seasons. Additional experimental activity is necessary to include these factors. Moreover, the effects of different installation of robot, such as wall installation, and hanging installation, should be included in future studies.

Further research is also required to understand some unexpected and nearly instantaneous variation of friction that has been experienced in some circumstances (e.g. Figure G.43) and friction fitting results (e.g. Figure N.2), and larger oscillations in Joint 5 of identification results (e.g. Figure 5.4 and 5.6). These unexpected behaviours seem related to mechanical problem of the robot, but at the moment a final word cannot be told. An analysis of these factors could support the development of models for predictive maintenance.

Moreover, during this thesis, data collected on two theoretically identical robot specimens were compared. An extension of the work could include experimentation on additional robot specimens in order to analyse the variability of production and allow bettering understanding how to adapt a general model to individual manipulators and how to use the collected data to organize preventive maintenance.

References

[1] G. Antonelli, F. Caccavale, and P. Chiacchio. A systematic procedure for the identification of dynamic parameters of robot manipulators. *Robotica*, 17(4):427–435, 1999.

[2] B. Armstrong. On finding 'exciting' trajectories for identification experiments involving systems with non-linear dynamics. In *Proceedings. 1987 IEEE International Conference on Robotics and Automation*, volume 4, pages 1131–1139, March 1987.

[3] Christopher G. Atkeson, Chae H. An, and John M. Hollerbach. Estimation of inertial parameters of manipulator loads and links. *The International Journal of Robotics Research*, 5(3):101–119, 1986.

[4] Bharat Bhushan. *Modern tribology handbook, two volume set.* CRC press, 2000.

[5] A. C. Bittencourt, E. Wernholt, S. Sander-Tavallaey, and T. Brogårdh. An extended friction model to capture load and temperature effects in robot joints. In *2010 IEEE/RSJ International Conference on Intelligent Robots and Systems*, pages 6161–6167, Oct 2010.

[6] André Carvalho Bittencourt and Svante Gunnarsson. Static friction in a robot joint - modeling and identification of load and temperature effects. *Journal of Dynamic Systems, Measurement, and Control*, 134(5), Jul 2012. 051013.

[7] Nikolaos A Bompos, Panagiotis K Artemiadis, Apollon S Oikonomopoulos, and Kostas J Kyriakopoulos. Modelling, full identification and control of the mitsubishi pa-10 robot arm. pages 1–6, 2007.

[8] G Calafiore, Marina Indri, and Basilio Bona. Robot dynamic calibration: Optimal excitation trajectories and experimental parameter estimation. *Journal of robotic systems*, 18(2):55–68, 2001.

[9] A. Calanca, L. M. Capisani, A. Ferrara, and L. Magnani. Mimo closed loop identification of an industrial robot. *IEEE Transactions on Control Systems Technology*, 19(5):1214–1224, 2011.

[10] C. Canudas de Wit, H. Olsson, K. J. Astrom, and P. Lischinsky. A new model for control of systems with friction. *IEEE Transactions on Automatic Control*, 40(3):419–425, 1995.

[11] John J Craig. *Introduction to robotics: mechanics and control, 3/E.* Pearson Education India, 2009.

[12] Phil R Dahl. A solid friction model. Technical report, Aerospace Corp El Segundo Ca, 1968.

[13] J. Denavit and R. S. Hartenberg. A kinematic notation for lower-pair mechanisms based on matrices. *Trans. ASME E, Journal of Applied Mechanics*, 22:215–221, June 1955.

[14] EFORT Intelligent Equipment Co., Ltd. Efort. `https://efort.com.cn/en/`, 2021. [Online; accessed 2021-FEB-27].

[15] M. Gautier and W. Khalil. Exciting trajectories for the identification of base inertial parameters of robots. In *[1991] Proceedings of the 30th IEEE Conference on Decision and Control*, pages 494–499 vol.1, Dec 1991.

[16] Maxime Gautier. Numerical calculation of the base inertial parameters of robots. *Journal of robotic systems*, 8(4):485–506, 1991.

[17] Maxime Gautier and Wisama Khalil. Identification of the minimum inertial parameters of robots. pages 1529–1530, 1989.

[18] Maxime Gautier and Wisama Khalil. Direct calculation of minimum set of inertial parameters of serial robots. *IEEE Transactions on robotics and Automation*, 6(3):368–373, 1990.

[19] J. M. Hollerbach. A recursive lagrangian formulation of manipulator dynamics and a comparative study of dynamics formulation complexity. *IEEE Transactions on Systems, Man, and Cybernetics*, 10(11):730–736, 1980.

[20] G. E. Hovland, E. Berglund, and Ole Jakob Sørdalen. Identification of joint elasticity of industrial robots. In *The Sixth International Symposium on Experimental Robotics VI*, page 455–464, Berlin, Heidelberg, 1999. Springer-Verlag.

[21] M Indri, G Calafiore, G Legnani, F Jatta, and A Visioli. Optimized dynamic calibration of a scara robot. *IFAC Proceedings Volumes*, 35(1):431–436, 2002.

[22] Jingfu Jin and Nicholas Gans. Parameter identification for industrial robots with a fast and robust trajectory design approach. *Robotics and Computer-Integrated Manufacturing*, 31:21–29, 2015.

[23] Anthony Jubien, Maxime Gautier, and Alexandre Janot. Dynamic identification of the kuka lwr robot using motor torques and joint torque sensors data. *IFAC Proceedings Volumes*, 47(3):8391–8396, 2014.

[24] H. Kawasaki and K. Kanzaki. Minimum dynamics parameters of robot models. *IFAC Proceedings Volumes*, 24(9):33–38, 1991. 3rd IFAC Symposium on Robot Control 1991 (SYROCO'91), Vienna, Austria, 16-18 September 1991.

[25] W. Khalil and J. Kleinfinger. A new geometric notation for open and closed-loop robots. 3:1174–1179, April 1986.

[26] W. Khalil, J. Kleinfinger, and M. Gautier. Reducing the computational burden of the dynamic models of robots. In *IEEE International Conference on Robotics and Automation (ICRA)*, volume 3 of *IEEE International Conference on Robotics and Automation (ICRA)*, pages 525–531, San Francisco, CA, USA, 1986. IEEE. Conference Proceedings ER.

[27] Wisama Khalil and Etienne Dombre. *Modeling, identification and control of robots.* Butterworth-Heinemann, 2004.

[28] D. Kostic, Bram de Jager, M. Steinbuch, and R. Hensen. Modeling and identification for high-performance robot control: an rrr-robotic arm case study. *IEEE Transactions on Control Systems Technology*, 12(6):904–919, 2004.

[29] KUKA AG. Lbr iiwa kuka ag. `https://www.kuka.com/en-de/products/robot-systems/industrial-robots/lbr-iiwa`, 2021. [Online; accessed 2021-FEB-27].

[30] V. Lampaert, J. Swevers, and F. Al-Bender. Modification of the leuven integrated friction model structure. *IEEE Transactions on Automatic Control*, 47(4):683–687, 2002.

[31] G. Legnani and I. Fassi. *Robotica industriale.* Città Studi, 2019.

[32] Giovanni Legnani, Luca Simoni, Manuel Beschi, and Antonio Visioli. A new friction model for mechanical transmissions considering joint temperature. 50183:V006T09A020, 2016.

[33] John YS Luh, Michael W Walker, and Richard PC Paul. On-line computational scheme for mechanical manipulators. *Journal of Dynamic Systems, Measurement, and Control*, 102(2):69–76, Jun 1980.

[34] Lőrinc Márton and Franciscus van der Linden. Temperature dependent friction estimation: Application to lubricant health monitoring. *Mechatronics*, 22(8):1078–1084, 2012.

[35] H. Mayeda, K. Yoshida, and K. Ohashi. Base parameters of dynamic models for manipulators with rotational and translational joints. In *Proceedings, 1989 International Conference on Robotics and Automation*, pages 1523–1528 vol.3, 1989.

[36] H. Mayeda, K. Yoshida, and K. Osuka. Base parameters of manipulator dynamic models. In *Proceedings. 1988 IEEE International Conference on Robotics and Automation*, pages 1367–1372 vol.3, 1988.

[37] Amirhossein H Memar and Ehsan T Esfahani. Modelling and dynamic parameter identification of the schunk powerball robotic arm. 2015.

[38] Matthias Neubauer, Hubert Gattringer, and Hartmut Bremer. A persistent method for parameter identification of a seven-axes manipulator. *Robotica*, 33(5):1099–1112, 2015.

[39] Roberto Pagani, Giovanni Legnani, Giovanni Incerti, and Matteo Gheza. Evaluation and modelling of the friction in robotic joints considering thermal effects. *Journal of Mechanisms and Robotics*, 12(2), 2020.

[40] M. T. Pham, M. Gautier, and P. Poignet. Identification of joint stiffness with bandpass filtering. In *Proceedings 2001 ICRA. IEEE International Conference on Robotics and Automation (Cat. No.01CH37164)*, volume 3, pages 2867–2872 vol.3, May 2001.

[41] M. T. Pham, M. Gautier, and P. Poignet. Accelerometer based identification of mechanical systems. In *Proceedings 2002 IEEE International Conference on Robotics and Automation (Cat. No.02CH37292)*, volume 4, pages 4293–4298 vol.4, May 2002.

[42] D.M. Pirro, M. Webster, and E. Daschner. *Lubrication Fundamentals, Revised and Expanded.* CRC Press, 2016.

[43] Robox Spa. Rde — robox development environment. `http://www.robox.it/en-US/showprod.php?idpro=RDE`, 2021. [Online; accessed 2021-FEB-27].

[44] Robox Spa. Rp-1. `http://www.robox.it/en-US/showprod.php?idpro=AS1017.004`, 2021. [Online; accessed 2021-FEB-27].

[45] Bruno Siciliano, Lorenzo Sciavicco, Luigi Villani, and Giuseppe Oriolo. *Robotics: modelling, planning and control.* Springer Science & Business Media, 2010.

[46] William M. Silver. On the equivalence of lagrangian and newton-euler dynamics for manipulators. *The International Journal of Robotics Research*, 1(2):60–70, 1982.

[47] Luca Simoni, Manuel Beschi, Giovanni Legnani, and Antonio Visioli. On the inclusion of temperature in the friction model of industrial robots. *IFAC-PapersOnLine*, 50(1):3482–3487, 2017.

[48] Luca Simoni, Manuel Beschi, Giovanni Legnani, and Antonio Visioli. Modelling the temperature in joint friction of industrial manipulators. *Robotica*, 37(5):906–927, 2019.

[49] R Stribeck. Kugellager für beliebige belastungen (ball bearings for arbitrary loads). *Mitteilungen aus der Centralstelle für wissenschaftlichtechnische Untersuchungen, HS Hermann, Berlin*, 1900.

[50] Richard Stribeck. Die wesentlichen eigenschaften der gleit-und rollenlager. *Zeitschrift des Vereines Deutscher Ingenieure*, 46:1341–1348, 1902.

[51] J. Swevers, F. Al-Bender, C. G. Ganseman, and T. Projogo. An integrated friction model structure with improved presliding behavior for accurate friction compensation. *IEEE Transactions on Automatic Control*, 45(4):675–686, 2000.

[52] J. Swevers, C. Ganseman, J. De Schutter, and H. Van Brussel. Experimental robot identification using optimised periodic trajectories. *Mechanical Systems and Signal Processing*, 10(5):561–577, 1996.

[53] J. Swevers, C. Ganseman, J. De Schutter, and H. Van Brussel. Generation of periodic trajectories for optimal robot excitation. *Journal of Manufacturing Science and Engineering*, 119(4A):611–615, Nov 1997.

[54] J. Swevers, C. Ganseman, D. B. Tukel, J. de Schutter, and H. Van Brussel. Optimal robot excitation and identification. *IEEE Transactions on Robotics and Automation*, 13(5):730–740, 1997.

[55] J. Swevers, W. Verdonck, and J. De Schutter. Dynamic model identification for industrial robots. *IEEE Control Systems Magazine*, 27(5):58–71, 2007.

[56] The MathWorks, Inc. Find minimum of constrained nonlinear multivariable function. `https://www.mathworks.com/help/optim/ug/fmincon.html`, 2021. [Online; accessed 2021-FEB-27].

[57] The MathWorks, Inc. Find minimum of function using genetic algorithm. `https://www.mathworks.com/help/gads/ga.html`, 2021. [Online; accessed 2021-FEB-27].

[58] Universal Robots A/S. Collaborative robots from ur: Products overview. `https://www.universal-robots.com/products/`, 2021. [Online; accessed 2021-FEB-27].

[59] Antonio Visioli and Giovanni Legnani. Experiments on model identification and control of an industrial robot manipulator. *IFAC Proceedings Volumes*, 33(27):285–290, 2000.

[60] N.D. Vuong and M.H. Ang Jr. Dynamic model identification for industrial robots. 2009.

[61] Wei Huo. New formulas for complete determining base parameters of robots. In *Proceedings of 1995 IEEE International Conference on Robotics and Automation*, volume 3, pages 3021–3026 vol.3, 1995.

[62] Wikipedia contributors. Displacement (geometry) — Wikipedia, the free encyclopedia. `https://en.wikipedia.org/w/index.php?title=Displacement_(geometry)&oldid=1006120237`, 2021. [Online; accessed 10-March-2021].

[63] Wikipedia contributors. Euclidean distance — Wikipedia, the free encyclopedia. `https://en.wikipedia.org/w/index.php?title=Euclidean_distance&oldid=1007398353`, 2021. [Online; accessed 2021-FEB-27].

[64] Wikipedia contributors. Parallel axis theorem — Wikipedia, the free encyclopedia. https://en.wikipedia.org/w/index.php?title=Parallel_axis_theorem&oldid=1010787717, 2021. [Online; accessed 10-March-2021].

[65] Wikipedia contributors. Qr decomposition — Wikipedia, the free encyclopedia. https://en.wikipedia.org/w/index.php?title=QR_decomposition&oldid=1023213167, 2021. [Online; accessed 20-May-2021].

[66] Wikipedia contributors. Singular value decomposition — Wikipedia, the free encyclopedia. https://en.wikipedia.org/w/index.php?title=Singular_value_decomposition&oldid=1022188613, 2021. [Online; accessed 20-May-2021].

[67] Wikipedia contributors. Translation (geometry) — Wikipedia, the free encyclopedia. https://en.wikipedia.org/w/index.php?title=Translation_(geometry)&oldid=1002714403, 2021. [Online; accessed 10-March-2021].

[68] Wikipedia contributors. Triple product — Wikipedia, the free encyclopedia. https://en.wikipedia.org/w/index.php?title=Triple_product&oldid=1005995193, 2021. [Online; accessed 10-March-2021].

Appendix A

The Dot Product And Cross Product

In the vector and matrix calculation, the dot product and cross product are needed. With the given vectors of $\boldsymbol{\omega}$ and $\boldsymbol{\alpha}$:

$$\boldsymbol{\omega} = \begin{bmatrix}\omega_x & \omega_y & \omega_z\end{bmatrix}^T \qquad and \qquad \boldsymbol{\alpha} = \begin{bmatrix}\alpha_1 & \alpha_2 & \alpha_3\end{bmatrix}^T \tag{A.1}$$

And the given matrix $\boldsymbol{I}$:

$$\boldsymbol{I} = \begin{bmatrix} I_{xx} & I_{xy} & I_{xz} \\ I_{yx} & I_{yy} & I_{yz} \\ I_{zx} & I_{zy} & I_{zz} \end{bmatrix} \tag{A.2}$$

The cross product of $\boldsymbol{\omega}$ and $\boldsymbol{\alpha}$ will be:

$$\boldsymbol{\omega} \times \boldsymbol{\alpha} = \begin{bmatrix} -\omega_z\alpha_2 + \omega_y\alpha_3 \\ \omega_z\alpha_1 - \omega_x\alpha_3 \\ -\omega_y\alpha_1 + \omega_z\alpha_2 \end{bmatrix} \xRightarrow{in\ matrix\ form} \begin{bmatrix} 0 & -\omega_z & \omega_y \\ \omega_z & 0 & -\omega_x \\ -\omega_y & \omega_x & 0 \end{bmatrix} \begin{bmatrix} \alpha_1 \\ \alpha_2 \\ \alpha_3 \end{bmatrix} \triangleq [\boldsymbol{\omega}\times]\boldsymbol{\alpha} \tag{A.3}$$

And:

$$\boldsymbol{\omega} \times \boldsymbol{\alpha} = [\boldsymbol{\omega}\times]\boldsymbol{\alpha} = -[\boldsymbol{\alpha} \times \boldsymbol{\omega}] = -[\boldsymbol{\alpha}\times]\boldsymbol{\omega} \tag{A.4}$$

The dot product of $\boldsymbol{\omega}$ and $\boldsymbol{I}$ will be:

$$\boldsymbol{I} \cdot \boldsymbol{\omega} = \begin{bmatrix} \omega_x I_{xx} + \omega_y I_{xy} + \omega_z I_{xz} \\ \omega_x I_{xy} + \omega_y I_{yy} + \omega_z I_{yz} \\ \omega_x I_{xz} + \omega_y I_{yz} + \omega_z I_{zz} \end{bmatrix} = \begin{bmatrix} \omega_x & \omega_y & \omega_z & 0 & 0 & 0 \\ 0 & \omega_x & 0 & \omega_y & \omega_z & 0 \\ 0 & 0 & \omega_x & 0 & \omega_y & \omega_z \end{bmatrix} \begin{bmatrix} I_{xx} \\ I_{xy} \\ I_{xz} \\ I_{yy} \\ I_{yz} \\ I_{zz} \end{bmatrix} \triangleq [\boldsymbol{\omega}\cdot]\boldsymbol{I} \tag{A.5}$$

In the test code, the cross product and dot product are used as an operator in matrix computation, thus these product matrix are pre-defined necessarily. It should be noted that $[\boldsymbol{\omega}\times]$, $[\boldsymbol{\alpha}\times]$ and $[\boldsymbol{\omega}\cdot]$ are matrices.

Appendix B

The Rotation Matrix And Transformation Matrix

A mathematics description has been used for the coordination transformation from the robot base to the end-effector to express the robot pose in the space. This description is based on linear algebra and divided into rotation and transformation matrices.

The rotation matrix describes the rotated coordination in the reference frame. It is shown by each reference XYZ axis. The general form is:

$$\boldsymbol{R} = \begin{bmatrix} x'_x & y'_x & z'_x \\ x'_y & y'_y & z'_y \\ x'_z & y'_z & z'_z \end{bmatrix} \tag{B.1}$$

Here x'_x presents the cosines of the unit vectors of the rotated frame axes based the reference one.

In elementary rotations, it will be shown based the axis as:

$$\boldsymbol{R}_z(\alpha) = \begin{bmatrix} \cos\alpha & -\sin\alpha & 0 \\ \sin\alpha & \cos\alpha & 0 \\ 0 & 0 & 1 \end{bmatrix} \tag{B.1a}$$

$$\boldsymbol{R}_y(\beta) = \begin{bmatrix} \cos\beta & 0 & \sin\beta \\ 0 & 1 & 0 \\ -\sin\beta & 0 & \cos\beta \end{bmatrix} \tag{B.1b}$$

$$\boldsymbol{R}_x(\gamma) = \begin{bmatrix} 1 & 0 & 0 \\ 0 & \cos\gamma & -\sin\gamma \\ 0 & \sin\gamma & \cos\gamma \end{bmatrix} \tag{B.1c}$$

The transformation matrix shows the transformation from the reference coordination to a new one by each XYZ axis:

$$\boldsymbol{p} = \begin{bmatrix} p_x & p_y & p_z \end{bmatrix}^T \tag{B.2}$$

In this thesis $\boldsymbol{R}$ and $\boldsymbol{p}$ are the rotation matrix and transformation vector respectively. In the form of Homogeneous Transformations, it can be written as (example from base joint to the first joint):

$$\boldsymbol{T}_0^1 = \begin{bmatrix} \boldsymbol{R} & \boldsymbol{p} \\ 0_{1*3} & 1 \end{bmatrix} = \begin{bmatrix} x'_x & y'_x & z'_x & p_x \\ x'_y & y'_y & z'_y & p_y \\ x'_z & y'_z & z'_z & p_z \\ 0 & 0 & 0 & 1 \end{bmatrix} \tag{B.3}$$

Then the general description of transformation from a given point in a given frame to the reference frame is:

$$\boldsymbol{a}_{new} = \boldsymbol{T}_1^0 \boldsymbol{T}_2^1 \boldsymbol{T}_3^2 \cdots \boldsymbol{T}_n^{n-1} \boldsymbol{a}_{ref} \tag{B.4}$$

Appendix C

The Newton-Euler (NE) Recursions Algorithm

The Newton-Euler (NE) can be implemented into MATLAB. The linearization is started from Equation 3.8:

$$\boldsymbol{n}_i = \hat{\boldsymbol{n}}_i + \boldsymbol{R}^i_{i+1}\boldsymbol{n}_{i+1} + \boldsymbol{p_c}^i_i \times \hat{\boldsymbol{f}}_i + \boldsymbol{p}^i_{i+1} \times \boldsymbol{R}^i_{i+1}\boldsymbol{f}_{i+1} \tag{C.1}$$

with

$$\hat{\boldsymbol{f}}_i = m_i\dot{\boldsymbol{v}}_{c_i} \tag{C.2}$$

$$\dot{\boldsymbol{v}}_{c_{i+1}} = \dot{\boldsymbol{\omega}}_{i+1} \times \boldsymbol{p_c}^{i+1}_{i+1} + \boldsymbol{\omega}_{i+1} \times \left(\boldsymbol{\omega}_{i+1} \times \boldsymbol{p_c}^{i+1}_{i+1}\right) + \dot{\boldsymbol{v}}_{i+1} \tag{C.3}$$

$$\hat{\boldsymbol{n}}_{i+1} = \boldsymbol{I}^{c_{i+1}}_{i+1}\dot{\boldsymbol{\omega}}_{i+1} + \boldsymbol{\omega}_{i+1} \times \boldsymbol{I}^{c_{i+1}}_{i+1}\boldsymbol{\omega}_{i+1} \tag{C.4}$$

Then, taking Equation C.3 into Equation C.2, and rewriting Equation C.4:

$$\hat{\boldsymbol{f}}_i = m_i\left[\dot{\boldsymbol{\omega}}_i \times \boldsymbol{p_c}^i_i + \boldsymbol{\omega}_i \times \left(\boldsymbol{\omega}_i \times \boldsymbol{p_c}^i_i\right) + \dot{\boldsymbol{v}}_i\right] \tag{C.5}$$

$$\hat{\boldsymbol{n}}_i = \boldsymbol{I}^{c_i}_i\dot{\boldsymbol{\omega}}_i + \boldsymbol{\omega}_i \times \boldsymbol{I}^{c_i}_i\boldsymbol{\omega}_i \tag{C.6}$$

Then Equation C.1 can be written with Equation C.5 and Equation C.6:

$$\begin{aligned}
\boldsymbol{n}_i =& \boldsymbol{I}^{c_i}_i\dot{\boldsymbol{\omega}}_i + \boldsymbol{\omega}_i \times \boldsymbol{I}^{c_i}_i\boldsymbol{\omega}_i + \boldsymbol{R}^i_{i+1}\boldsymbol{n}_{i+1} + \boldsymbol{p}^i_{i+1} \times \boldsymbol{R}^i_{i+1}\boldsymbol{f}_{i+1} \\
&+ \boldsymbol{p_c}^i_i \times m_i\left[\dot{\boldsymbol{\omega}}_i \times \boldsymbol{p_c}^i_i + \boldsymbol{\omega}_i \times \left(\boldsymbol{\omega}_i \times \boldsymbol{p_c}^i_i\right) + \dot{\boldsymbol{v}}_i\right] \\
=& \boldsymbol{I}^{c_i}_i\dot{\boldsymbol{\omega}}_i + \boldsymbol{\omega}_i \times \boldsymbol{I}^{c_i}_i\boldsymbol{\omega}_i + \boldsymbol{R}^i_{i+1}\boldsymbol{n}_{i+1} + \boldsymbol{p}^i_{i+1} \times \boldsymbol{R}^i_{i+1}\boldsymbol{f}_{i+1} \\
&+ m_i\left\{\boldsymbol{p_c}^i_i \times \left(\dot{\boldsymbol{\omega}}_i \times \boldsymbol{p_c}^i_i\right) + \boldsymbol{p_c}^i_i \times \left[\boldsymbol{\omega}_i \times \left(\boldsymbol{\omega}_i \times \boldsymbol{p_c}^i_i\right)\right] + \boldsymbol{p_c}^i_i \times \dot{\boldsymbol{v}}_i\right\} \\
=& \boldsymbol{I}^{c_i}_i\dot{\boldsymbol{\omega}}_i + \boldsymbol{\omega}_i \times \boldsymbol{I}^{c_i}_i\boldsymbol{\omega}_i + \boldsymbol{R}^i_{i+1}\boldsymbol{n}_{i+1} + \boldsymbol{p}^i_{i+1} \times \boldsymbol{R}^i_{i+1}\boldsymbol{f}_{i+1} \\
&+ m_i\left[\boldsymbol{p_c}^i_i \times \left(\dot{\boldsymbol{\omega}}_i \times \boldsymbol{p_c}^i_i\right)\right] + m_i\left\{\boldsymbol{p_c}^i_i \times \left[\boldsymbol{\omega}_i \times \left(\boldsymbol{\omega}_i \times \boldsymbol{p_c}^i_i\right)\right]\right\} + m_i\left(\boldsymbol{p_c}^i_i \times \dot{\boldsymbol{v}}_i\right)
\end{aligned} \tag{C.7}$$

For the part of "$m_i\left[\boldsymbol{p_c}^i_i \times \left(\dot{\boldsymbol{\omega}}_i \times \boldsymbol{p_c}^i_i\right)\right] + m_i\left\{\boldsymbol{p_c}^i_i \times \left[\boldsymbol{\omega}_i \times \left(\boldsymbol{\omega}_i \times \boldsymbol{p_c}^i_i\right)\right]\right\} + m_i\left(\boldsymbol{p_c}^i_i \times \dot{\boldsymbol{v}}_i\right)$" in Equation C.7, with the cross product properties and the vector triple product [68] introduced in Appendix A, the below equations will easy the linearization:

$$\begin{aligned}
& a \times [b \times (b \times a)] = b \times (a^T a\boldsymbol{I}_{3*3} - aa^T)b \\
\Rightarrow \quad & a \times (b \times a) = (a^T a\boldsymbol{I}_{3*3} - aa^T)b
\end{aligned} \tag{C.8}$$

Here $\boldsymbol{I}_{3*3}$ is the 3 by 3 identical matrix. Then:

$$m_i\left[\boldsymbol{p_c}^i_i \times \left(\dot{\boldsymbol{\omega}}_i \times \boldsymbol{p_c}^i_i\right)\right] = m_i\left(\boldsymbol{p_c}^{iT}_i\boldsymbol{p_c}^i_i\boldsymbol{I}_{3*3} - \boldsymbol{p_c}^i_i\boldsymbol{p_c}^{iT}_i\right)\dot{\boldsymbol{\omega}}_i \tag{C.9}$$

$$m_i\left\{\boldsymbol{p_{c}}_i^i \times \left[\boldsymbol{\omega}_i \times \left(\boldsymbol{\omega}_i \times \boldsymbol{p_{c}}_i^i\right)\right]\right\} = m_i\left[\boldsymbol{\omega}_i \times \left(\boldsymbol{p_{c}}_i^{iT}\boldsymbol{p_{c}}_i^i\boldsymbol{I}_{3*3} - \boldsymbol{p_{c}}_i^i\boldsymbol{p_{c}}_i^{iT}\right)\boldsymbol{\omega}_i\right]$$
$$= m_i\boldsymbol{\omega}_i \times \left(\boldsymbol{p_{c}}_i^{iT}\boldsymbol{p_{c}}_i^i\boldsymbol{I}_{3*3} - \boldsymbol{p_{c}}_i^i\boldsymbol{p_{c}}_i^{iT}\right)\boldsymbol{\omega}_i \quad (C.10)$$

take the parallel axis theorem [64] below into above two equations:

$$\boldsymbol{I}_i^i = \boldsymbol{I}_i^{c_i} + m_i\left(\boldsymbol{p_{c}}_i^{iT}\boldsymbol{p_{c}}_i^i\boldsymbol{I}_{3*3} - \boldsymbol{p_{c}}_i^i\boldsymbol{p_{c}}_i^{iT}\right) \Rightarrow m_i\left(\boldsymbol{p_{c}}_i^{iT}\boldsymbol{p_{c}}_i^i\boldsymbol{I}_{3*3} - \boldsymbol{p_{c}}_i^i\boldsymbol{p_{c}}_i^{iT}\right) = \boldsymbol{I}_i^i - \boldsymbol{I}_i^{c_i} \quad (C.11)$$

Then:

$$m_i\left[\boldsymbol{p_{c}}_i^i \times \left(\dot{\boldsymbol{\omega}}_i \times \boldsymbol{p_{c}}_i^i\right)\right] = m_i\left(\boldsymbol{p_{c}}_i^{iT}\boldsymbol{p_{c}}_i^i\boldsymbol{I}_{3*3} - \boldsymbol{p_{c}}_i^i\boldsymbol{p_{c}}_i^{iT}\right)\dot{\boldsymbol{\omega}}_i$$
$$= \left(\boldsymbol{I}_i^i - \boldsymbol{I}_i^{c_i}\right)\dot{\boldsymbol{\omega}}_i \quad (C.12)$$

$$m_i\left\{\boldsymbol{p_{c}}_i^i \times \left[\boldsymbol{\omega}_i \times \left(\boldsymbol{\omega}_i \times \boldsymbol{p_{c}}_i^i\right)\right]\right\} = m_i\left[\boldsymbol{\omega}_i \times \left(\boldsymbol{p_{c}}_i^{iT}\boldsymbol{p_{c}}_i^i\boldsymbol{I}_{3*3} - \boldsymbol{p_{c}}_i^i\boldsymbol{p_{c}}_i^{iT}\right)\boldsymbol{\omega}_i\right]$$
$$= m_i\boldsymbol{\omega}_i \times \left(\boldsymbol{p_{c}}_i^{iT}\boldsymbol{p_{c}}_i^i\boldsymbol{I}_{3*3} - \boldsymbol{p_{c}}_i^i\boldsymbol{p_{c}}_i^{iT}\right)\boldsymbol{\omega}_i$$
$$= \boldsymbol{\omega}_i \times m_i\left(\boldsymbol{p_{c}}_i^{iT}\boldsymbol{p_{c}}_i^i\boldsymbol{I}_{3*3} - \boldsymbol{p_{c}}_i^i\boldsymbol{p_{c}}_i^{iT}\right)\boldsymbol{\omega}_i \quad (C.13)$$
$$= \boldsymbol{\omega}_i \times \left(\boldsymbol{I}_i^i - \boldsymbol{I}_i^{c_i}\right)\boldsymbol{\omega}_i$$

Now Equation C.7 can be written as follows and then expanded, merged and eliminated:

$$\boldsymbol{n}_i = \boldsymbol{I}_i^{c_i}\dot{\boldsymbol{\omega}}_i + \boldsymbol{\omega}_i \times \boldsymbol{I}_i^{c_i}\boldsymbol{\omega}_i + \boldsymbol{R}_{i+1}^i\boldsymbol{n}_{i+1} + \boldsymbol{p}_{i+1}^i \times \boldsymbol{R}_{i+1}^i\boldsymbol{f}_{i+1}$$
$$+ m_i\left[\boldsymbol{p_{c}}_i^i \times \left(\dot{\boldsymbol{\omega}}_i \times \boldsymbol{p_{c}}_i^i\right)\right] + m_i\left\{\boldsymbol{p_{c}}_i^i \times \left[\boldsymbol{\omega}_i \times \left(\boldsymbol{\omega}_i \times \boldsymbol{p_{c}}_i^i\right)\right]\right\} + m_i\left(\boldsymbol{p_{c}}_i^i \times \dot{\boldsymbol{v}}_i\right)$$
$$= \boldsymbol{I}_i^{c_i}\dot{\boldsymbol{\omega}}_i + \boldsymbol{\omega}_i \times \boldsymbol{I}_i^{c_i}\boldsymbol{\omega}_i + \boldsymbol{R}_{i+1}^i\boldsymbol{n}_{i+1} + \boldsymbol{p}_{i+1}^i \times \boldsymbol{R}_{i+1}^i\boldsymbol{f}_{i+1} \quad (C.14)$$
$$+ \left(\boldsymbol{I}_i^i - \boldsymbol{I}_i^{c_i}\right)\dot{\boldsymbol{\omega}}_i + \boldsymbol{\omega}_i \times \left(\boldsymbol{I}_i^i - \boldsymbol{I}_i^{c_i}\right)\boldsymbol{\omega}_i + m_i\left(\boldsymbol{p_{c}}_i^i \times \dot{\boldsymbol{v}}_i\right)$$
$$= \boldsymbol{R}_{i+1}^i\boldsymbol{n}_{i+1} + \boldsymbol{p}_{i+1}^i \times \boldsymbol{R}_{i+1}^i\boldsymbol{f}_{i+1} + \boldsymbol{I}_i^i\dot{\boldsymbol{\omega}}_i + \boldsymbol{\omega}_i \times \boldsymbol{I}_i^i\boldsymbol{\omega}_i + m_i\boldsymbol{p_{c}}_i^i \times \dot{\boldsymbol{v}}_i$$

For the Joint 6, Equation 3.7, Equation C.5 and C.14 can be written as:

$$\boldsymbol{f}_6 = \hat{\boldsymbol{f}}_6 = m_6\left[\dot{\boldsymbol{\omega}}_6 \times \boldsymbol{p_{c}}_6^6 + \boldsymbol{\omega}_6 \times \left(\boldsymbol{\omega}_6 \times \boldsymbol{p_{c}}_6^6\right) + \dot{\boldsymbol{v}}_6\right]$$
$$= m_6\dot{\boldsymbol{\omega}}_6 \times \boldsymbol{p_{c}}_6^6 + m_6\boldsymbol{\omega}_6 \times \left(\boldsymbol{\omega}_6 \times \boldsymbol{p_{c}}_6^6\right) + m_6\dot{\boldsymbol{v}}_6 \quad (C.15)$$
$$= m_6\dot{\boldsymbol{v}}_6 + m_6\dot{\boldsymbol{\omega}}_6 \times \boldsymbol{p_{c}}_6^6 + m_6\boldsymbol{\omega}_6 \times \left(\boldsymbol{\omega}_6 \times \boldsymbol{p_{c}}_6^6\right)$$

$$\boldsymbol{n}_6^6 = \boldsymbol{I}_6^6\dot{\boldsymbol{\omega}}_6 + \boldsymbol{\omega}_6 \times \boldsymbol{I}_6^6\boldsymbol{\omega}_6 + m_6\boldsymbol{p_{c}}_6^6 \times \dot{\boldsymbol{v}}_6$$
$$= -\dot{\boldsymbol{v}}_6 \times m_6\boldsymbol{p_{c}}_6^6 + \boldsymbol{I}_6^6\dot{\boldsymbol{\omega}}_6 + \boldsymbol{\omega}_6 \times \boldsymbol{I}_6^6\boldsymbol{\omega}_6 \quad (C.16)$$

It should be pointed that $\boldsymbol{R}_{i+1}^i\boldsymbol{f}_{i+1}$ in Equation 3.7 and $\boldsymbol{R}_{i+1}^i\boldsymbol{n}_{i+1} + \boldsymbol{p}_{i+1}^i\boldsymbol{R}_{i+1}^i\boldsymbol{f}_{i+1}$ in Equation 3.8 for Joint 6 is 0 because there is no forward axis.

Transfer Equation C.15 and C.16 to matrix form:

$$\begin{bmatrix} \boldsymbol{f}_6 \\ \boldsymbol{n}_6^6 \end{bmatrix} = \begin{bmatrix} \dot{\boldsymbol{v}}_6 & [\dot{\boldsymbol{\omega}}_6 \times] + [\boldsymbol{\omega}_6 \times][\boldsymbol{\omega}_6 \times] & 0 \\ 0 & -[\dot{\boldsymbol{v}}_6 \times] & [\dot{\boldsymbol{\omega}}_6 \cdot] + [\boldsymbol{\omega}_6 \times][\boldsymbol{\omega}_6 \cdot] \end{bmatrix} \begin{bmatrix} m_6 \\ m_6 p_{c6}^6|_x \\ m_6 p_{c6}^6|_y \\ m_6 p_{c6}^6|_z \\ I_{xx} \\ I_{xy} \\ I_{xz} \\ I_{yy} \\ I_{yz} \\ I_{zz} \end{bmatrix} \triangleq \boldsymbol{A}_6 \boldsymbol{\phi}_6 \tag{C.17}$$

For Joint 5:

$$\begin{aligned} \boldsymbol{f}_5 &= m_5 \dot{\boldsymbol{v}}_5 + \boldsymbol{R}_5^6 \boldsymbol{f}_6 \\ &= \hat{\boldsymbol{f}}_5 + \boldsymbol{R}_5^6 \boldsymbol{f}_6 \end{aligned} \tag{C.18}$$

$$\begin{aligned} \boldsymbol{n}_5^5 &= \boldsymbol{I}_5^5 \dot{\boldsymbol{\omega}}_5 + \omega_5 \times \boldsymbol{I}_5^5 \omega_5 + m_5 \boldsymbol{p}_{\boldsymbol{c}5}^5 \times \dot{v}_5 + \boldsymbol{R}_6^5 \boldsymbol{n}_6 + \boldsymbol{p}_6^5 \times \boldsymbol{R}_6^5 \boldsymbol{f}_6 \\ &= -\dot{v}_5 \times m_5 \boldsymbol{p}_{\boldsymbol{c}5}^5 + \boldsymbol{I}_5^5 \dot{\boldsymbol{\omega}}_5 + \omega_5 \times \boldsymbol{I}_5^5 \omega_5 + \boldsymbol{R}_6^5 \boldsymbol{n}_6 + \boldsymbol{p}_6^5 \times \boldsymbol{R}_6^5 \boldsymbol{f}_6 \end{aligned} \tag{C.19}$$

and then the matrix form is:

$$\begin{bmatrix} \boldsymbol{f}_5 \\ \boldsymbol{n}_5^5 \end{bmatrix} = \boldsymbol{A}_5 \boldsymbol{\phi}_5 + \begin{bmatrix} \boldsymbol{R}_6^5 & 0 \\ [\boldsymbol{p}_6^5 \times] \boldsymbol{R}_6^5 & \boldsymbol{R}_6^5 \end{bmatrix} \begin{bmatrix} \boldsymbol{f}_6 \\ \boldsymbol{n}_6^6 \end{bmatrix} \triangleq \boldsymbol{A}_5 \boldsymbol{\phi}_5 + T_{56} \boldsymbol{A}_6 \boldsymbol{\phi}_6 \tag{C.20}$$

Thus, similar for other joints:

$$\begin{bmatrix} \boldsymbol{f}_4 \\ \boldsymbol{n}_4^4 \end{bmatrix} = \boldsymbol{A}_4 \boldsymbol{\phi}_4 + \boldsymbol{T}_{45} \boldsymbol{A}_5 \boldsymbol{\phi}_5 + \boldsymbol{T}_{45} \boldsymbol{T}_{56} \boldsymbol{A}_6 \boldsymbol{\phi}_6 \tag{C.21}$$

$$\begin{bmatrix} \boldsymbol{f}_3 \\ \boldsymbol{n}_3^3 \end{bmatrix} = \boldsymbol{A}_3 \boldsymbol{\phi}_3 + \boldsymbol{T}_{34} \boldsymbol{A}_4 \boldsymbol{\phi}_4 + \boldsymbol{T}_{34} \boldsymbol{T}_{45} \boldsymbol{A}_5 \boldsymbol{\phi}_5 + \boldsymbol{T}_{34} \boldsymbol{T}_{45} \boldsymbol{T}_{56} \boldsymbol{A}_6 \boldsymbol{\phi}_6 \tag{C.22}$$

$$\begin{bmatrix} \boldsymbol{f}_2 \\ \boldsymbol{n}_2^2 \end{bmatrix} = \boldsymbol{A}_2 \boldsymbol{\phi}_2 + \boldsymbol{T}_{23} \boldsymbol{A}_3 \boldsymbol{\phi}_3 + \boldsymbol{T}_{23} \boldsymbol{T}_{34} \boldsymbol{A}_4 \boldsymbol{\phi}_4 + \boldsymbol{T}_{23} \boldsymbol{T}_{34} \boldsymbol{T}_{45} \boldsymbol{A}_5 \boldsymbol{\phi}_5 + \boldsymbol{T}_{23} \boldsymbol{T}_{34} \boldsymbol{T}_{45} \boldsymbol{T}_{56} \boldsymbol{A}_6 \boldsymbol{\phi}_6 \tag{C.23}$$

$$\begin{aligned} \begin{bmatrix} \boldsymbol{f}_1 \\ \boldsymbol{n}_1^1 \end{bmatrix} &= \boldsymbol{A}_1 \boldsymbol{\phi}_1 + \boldsymbol{T}_{12} \boldsymbol{A}_2 \boldsymbol{\phi}_2 + \boldsymbol{T}_{12} \boldsymbol{T}_{23} \boldsymbol{A}_3 \boldsymbol{\phi}_3 + \boldsymbol{T}_{12} \boldsymbol{T}_{23} \boldsymbol{T}_{34} \boldsymbol{A}_4 \boldsymbol{\phi}_4 + \boldsymbol{T}_{12} \boldsymbol{T}_{23} \boldsymbol{T}_{34} \boldsymbol{T}_{45} \boldsymbol{A}_5 \boldsymbol{\phi}_5 \\ &+ \boldsymbol{T}_{12} \boldsymbol{T}_{23} \boldsymbol{T}_{34} \boldsymbol{T}_{45} \boldsymbol{T}_{56} \boldsymbol{A}_6 \boldsymbol{\phi}_6 \end{aligned} \tag{C.24}$$

Concluding from Equation C.17 to Equation C.24 and then transfer to matrix form:

$$\begin{bmatrix} \boldsymbol{f}_1 \\ \boldsymbol{n}_1^1 \\ \boldsymbol{f}_2 \\ \boldsymbol{n}_2^2 \\ \boldsymbol{f}_3 \\ \boldsymbol{n}_3^3 \\ \boldsymbol{f}_4 \\ \boldsymbol{n}_4^4 \\ \boldsymbol{f}_5 \\ \boldsymbol{n}_5^5 \\ \boldsymbol{f}_6 \\ \boldsymbol{n}_6^6 \end{bmatrix} = \begin{bmatrix} \bar{\boldsymbol{U}}_{11} & \bar{\boldsymbol{U}}_{12} & \bar{\boldsymbol{U}}_{13} & \bar{\boldsymbol{U}}_{14} & \bar{\boldsymbol{U}}_{15} & \bar{\boldsymbol{U}}_{16} \\ 0_{6*10} & \bar{\boldsymbol{U}}_{22} & \bar{\boldsymbol{U}}_{23} & \bar{\boldsymbol{U}}_{24} & \bar{\boldsymbol{U}}_{25} & \bar{\boldsymbol{U}}_{26} \\ 0_{6*10} & 0_{6*10} & \bar{\boldsymbol{U}}_{33} & \bar{\boldsymbol{U}}_{34} & \bar{\boldsymbol{U}}_{35} & \bar{\boldsymbol{U}}_{36} \\ 0_{6*10} & 0_{6*10} & 0_{6*10} & \bar{\boldsymbol{U}}_{44} & \bar{\boldsymbol{U}}_{45} & \bar{\boldsymbol{U}}_{46} \\ 0_{6*10} & 0_{6*10} & 0_{6*10} & 0_{6*10} & \bar{\boldsymbol{U}}_{55} & \bar{\boldsymbol{U}}_{56} \\ 0_{6*10} & 0_{6*10} & 0_{6*10} & 0_{6*10} & 0_{6*10} & \bar{\boldsymbol{U}}_{66} \end{bmatrix} \begin{bmatrix} \boldsymbol{\phi}_1 \\ \boldsymbol{\phi}_2 \\ \boldsymbol{\phi}_3 \\ \boldsymbol{\phi}_4 \\ \boldsymbol{\phi}_5 \\ \boldsymbol{\phi}_6 \end{bmatrix} = \bar{\boldsymbol{K}}_{36*60} \boldsymbol{\psi}_{60*1} \tag{C.25}$$

Here:

$$\bar{\boldsymbol{U}}_{ij} = \begin{cases} \boldsymbol{A}_i, & i = j \\ \boldsymbol{T}_{i,i+1}\boldsymbol{T}_{i+1,i+2}\cdots\boldsymbol{T}_{j-1,j}\boldsymbol{A}_j, & i \neq j \end{cases} \tag{C.26}$$

$$\boldsymbol{\psi} = \begin{bmatrix}\boldsymbol{\phi}_1 & \boldsymbol{\phi}_2 & \boldsymbol{\phi}_3 & \boldsymbol{\phi}_4 & \boldsymbol{\phi}_5 & \boldsymbol{\phi}_6\end{bmatrix}^T \tag{C.27}$$

Because only the torque in the z-axis direction is considered, we have:

$$\tau_i = \begin{bmatrix}0 & 0 & 0 & 0 & 0 & 1\end{bmatrix}\begin{bmatrix}\boldsymbol{f}_i \\ \boldsymbol{n}_i^i\end{bmatrix} = \begin{bmatrix}0 & 0 & 0 & 0 & 0 & 1\end{bmatrix} \times \begin{bmatrix}f_{ix} & f_{iy} & f_{iz} & n_{ix}^i & n_{iy}^i & n_{iz}^i\end{bmatrix}^T = n_{iz}^i \tag{C.28}$$

Thus the concluded matrix can be written as:

$$\boldsymbol{\tau}_{dynamic} = \begin{bmatrix}\tau_{Joint1} \\ \tau_{Joint2} \\ \tau_{Joint3} \\ \tau_{Joint4} \\ \tau_{Joint5} \\ \tau_{Joint6}\end{bmatrix}_{6*1} = \boldsymbol{K}_{6*60}\boldsymbol{\psi}_{60*1} = \begin{bmatrix}\boldsymbol{U}_{11} & \boldsymbol{U}_{12} & \boldsymbol{U}_{13} & \boldsymbol{U}_{14} & \boldsymbol{U}_{15} & \boldsymbol{U}_{16} \\ 0_{6*10} & \boldsymbol{U}_{22} & \boldsymbol{U}_{23} & \boldsymbol{U}_{24} & \boldsymbol{U}_{25} & \boldsymbol{U}_{26} \\ 0_{6*10} & 0_{6*10} & \boldsymbol{U}_{33} & \boldsymbol{U}_{34} & \boldsymbol{U}_{35} & \boldsymbol{U}_{36} \\ 0_{6*10} & 0_{6*10} & 0_{6*10} & \boldsymbol{U}_{44} & \boldsymbol{U}_{45} & \boldsymbol{U}_{46} \\ 0_{6*10} & 0_{6*10} & 0_{6*10} & 0_{6*10} & \boldsymbol{U}_{55} & \boldsymbol{U}_{56} \\ 0_{6*10} & 0_{6*10} & 0_{6*10} & 0_{6*10} & 0_{6*10} & \boldsymbol{U}_{66}\end{bmatrix}\begin{bmatrix}\boldsymbol{\phi}_1 \\ \boldsymbol{\phi}_2 \\ \boldsymbol{\phi}_3 \\ \boldsymbol{\phi}_4 \\ \boldsymbol{\phi}_5 \\ \boldsymbol{\phi}_6\end{bmatrix} \tag{C.29}$$

Here: $\boldsymbol{K}$ is the matrix of $\bar{\boldsymbol{K}}$ with the values of z-axis direction only.

It should be pointed that, the total torque of motor output is presented by joints is:

$$\tau_{total} = \tau_{dynamic} + \tau_{motor} \tag{C.30}$$

Moreover, the $\tau_{dynamic}$ can be separated by τ_{ne} and $\tau_{friction}$, which the subscript of ne is the abbreviation of Newton-Euler.

Appendix D

The QR And SVD Decomposition

As described in Section 3.2, the QR and SVD decomposition are used to recognize the identifiable dynamic parameters. In this appendix the explanations of both methods are demonstrated in Section D.1 and D.2. The results are shown in Section D.3.

D.1 QR Factorization

The positions of no-zeros values in vector $\boldsymbol{r}_{1,diag}$ (Equation D.1) of Equation 3.33 in Section 3.2.1 are recorded. The example $\boldsymbol{r}_{1,diag}$ of all joints is shown in Table D.1. It should be pointed that the small value is considered as a zero value.

$$\boldsymbol{r}_{1,diag} = \begin{bmatrix} r_{1,1} & r_{2,2} & r_{3,3} & \cdots & r_{60,60} \end{bmatrix} \tag{D.1}$$

In Table D.1, the parameters that have not highlighted in yellow are identifiable with the corresponded link. For example, the parameter $I_{5,xx}$ of Joint 1 is identifiable due to its value of -168.5869. On the other hand, the parameter m_3 of Joint 2 is unidentifiable due to its value of 5.08E-14, which is less than 1/10000 (small value).

D.2 SVD Decomposition

As shown in Section 3.2.2, the information matrix $\boldsymbol{K}$ has been analysed by the SVD decomposition (Equation 3.34 and Equation D.2). The matrix $\boldsymbol{\Sigma}$ is diagonal and contains the singular values of $\boldsymbol{K}$ organized in descending value order. When $\boldsymbol{K}$ is ill-defined, $\boldsymbol{\Sigma}$ has a high condition number. To easy the discussion, the sub-matrix $\boldsymbol{S}$ (Equation 3.35 and Equation D.3) of $\boldsymbol{\Sigma}$ is used. Mathematically, the condition number of $\boldsymbol{S}$ can be easily obtained in Equation D.4. In our case, the threshold of high condition number is 100. And the singular values with smaller value are associated to parameters that cannot be reliably estimated. These parameters will be eliminated by the model.

$$\boldsymbol{K} = \boldsymbol{U}\boldsymbol{\Sigma}\boldsymbol{V}^T = \boldsymbol{U}\begin{bmatrix} \boldsymbol{S} \\ [\boldsymbol{0}] \end{bmatrix}\boldsymbol{V}^T \tag{D.2}$$

$$\boldsymbol{S} = \begin{bmatrix} r_{1,1} & 0 & 0 & \cdots & 0 \\ 0 & r_{2,2} & 0 & \cdots & 0 \\ 0 & 0 & r_{3,3} & \cdots & 0 \\ \vdots & \vdots & \vdots & \ddots & \vdots \\ 0 & 0 & 0 & \cdots & r_{n,n} \end{bmatrix} \tag{D.3}$$

$$cond(\boldsymbol{S}) = r_{1,1}/r_{n,n} \tag{D.4}$$

Table D.1: The values of $\boldsymbol{r}_{1,diag}$ from QR results

	Items ↓↘	Link →	1	2	3	4	5	6
Link 1	1	m	0	0	0	0	0	0
	2	mP_x	0	0	0	0	0	0
	3	mP_y	0	0	0	0	0	0
	4	mP_z	0	0	0	0	0	0
	5	I_{xx}	0	0	0	0	0	0
	6	I_{xy}	0	0	0	0	0	0
	7	I_{xz}	0	0	0	0	0	0
	8	I_{yy}	0	0	0	0	0	0
	9	I_{yz}	0	0	0	0	0	0
	10	I_{zz}	-228.6174	0	0	0	0	0
Link 2	11	m	-4.52E-16	0	0	0	0	0
	12	mP_x	9.8627	253.4396	0	0	0	0
	13	mP_y	2.4353	593.2077	0	0	0	0
	14	mP_z	2.52E-14	0	0	0	0	0
	15	I_{xx}	2.7684	-56.3891	0	0	0	0
	16	I_{xy}	23.0138	-97.8936	0	0	0	0
	17	I_{xz}	130.5884	-211.0123	0	0	0	0
	18	I_{yy}	3.12E-14	5.69E-14	0	0	0	0
	19	I_{yz}	62.9039	81.4132	0	0	0	0
	20	I_{zz}	-1.98E-15	-122.6476	0	0	0	0
Link 3	21	m	-2.07E-15	5.08E-14	0	0	0	0
	22	mP_x	37.9513	-334.7127	467.3072	0	0	0
	23	mP_y	-33.2534	354.3488	455.3911	0	0	0
	24	mP_z	-4.90E-14	5.30E-14	0	0	0	0
	25	I_{xx}	-100.5171	-47.7176	-66.8431	0	0	0
	26	I_{xy}	174.542	103.1597	112.4557	0	0	0
	27	I_{xz}	253.2117	-99.1836	-164.7055	0	0	0
	28	I_{yy}	6.53E-14	-5.46E-15	-3.16E-14	0	0	0
	29	I_{yz}	-248.5508	101.679	152.7053	0	0	0
	30	I_{zz}	-1.28E-14	-206.4943	-281.2688	0	0	0
Link 4	31	m	2.70E-14	-8.97E-14	-7.50E-14	0	0	0
	32	mP_x	-108.4773	-386.0355	-286.5489	-398.1636	0	0
	33	mP_y	-123.4907	-472.5241	374.8688	-335.879	0	0
	34	mP_z	-7.44E-14	-2.67E-13	-2.09E-13	0	0	0
	35	I_{xx}	-144.5376	-187.3428	-197.3844	-107.9234	0	0
	36	I_{xy}	280.2405	-365.3538	-383.3898	190.8098	0	0
	37	I_{xz}	108.9514	-162.0417	-247.1844	239.729	0	0
	38	I_{yy}	1.22E-13	2.17E-13	-1.50E-13	6.28E-14	0	0
	39	I_{yz}	94.7208	224.0334	274.2623	-246.0824	0	0
	40	I_{zz}	-228.3691	78.9371	-108.739	-431.3956	0	0
Link 5	41	m	-1.62E-14	5.48E-14	3.45E-14	0	0	0
	42	mP_x	110.3607	407.323	315.8836	65.6913	396.6561	0
	43	mP_y	126.9043	-404.1635	-281.1052	208.6213	394.49	0
	44	mP_z	6.67E-14	-3.01E-13	9.77E-14	1.77E-13	0	0
	45	I_{xx}	-168.5834	-171.4806	-186.6335	212.6078	201.7761	0
	46	I_{xy}	389.4686	-306.1781	-318.4133	513.4559	-399.6391	0
	47	I_{xz}	289.3772	-315.7677	-322.641	363.8805	-411.4982	0
	48	I_{yy}	1.91E-13	-1.86E-13	1.53E-13	1.59E-13	-1.91E-14	0
	49	I_{yz}	319.6101	334.8672	341.2031	368.3976	468.6476	0
	50	I_{zz}	161.8988	-205.6505	-215.2295	142.2798	-463.0538	0
Link 6	51	m	2.08E-14	-6.87E-14	-4.33E-14	2.36E-14	7.80E-15	0
	52	mP_x	426.2574	1068.3319	699.9122	295.3725	292.5512	417.3724
	53	mP_y	-434.786	-1079.0873	-704.9352	303.1425	-347.0608	407.0301
	54	mP_z	-1.11E-13	-2.31E-13	-2.41E-13	-6.23E-14	-1.29E-13	0
	55	I_{xx}	339.3361	-408.1584	-413.338	-238.2624	-476.7573	190.3695
	56	I_{xy}	679.9189	824.2461	829.0289	-506.5916	913.3395	-362.6816
	57	I_{xz}	452.786	-637.3979	-635.4993	617.0631	-1038.9653	445.405
	58	I_{yy}	2.44E-13	-3.99E-13	3.25E-13	2.28E-13	3.06E-13	-1.21E-13
	59	I_{yz}	507.4218	593.0612	551.2006	-655.9884	1109.9515	-479.4588
	60	I_{zz}	320.3927	293.4021	310.0073	558.9444	279.1904	-875.2979

An example of matrix $\boldsymbol{S}$ and $\boldsymbol{V}$ of Link 2 is given in Table D.2. The condition number of matrix $\boldsymbol{S}$ is 1.5742E+16, which is more than 100. This leads to the minimum value of 1.15E-16 in the column of I_m in matrix $\boldsymbol{S}$, which is highlighted in yellow. In this case, there are some minimum values in the column of I_m in matrix $\boldsymbol{V}$, which are significantly different with others, and also they are located in row I_{zz} and I_m. This means that the parameter I_{zz} is unidentifiable. And it is clear that I_{zz} and I_m are paralleled in this link.

Two things should be pointed before the SVD decomposition process, which are:

1, The friction elements should be introduced, which means $\boldsymbol{\phi_f}$ will be used in the identification.

2, The results of QR decomposition should be applied. Thus based the results of QR factorization, the parameters of m, mP_x, mP_y, mP_z, I_{xx}, I_{xy}, I_{xz}, I_{yy}, I_{yz} and I_{zz} of Link 1 will be eliminated in the decomposition process due to the value of zero.

The parameters selected from the results of the SVD Decomposition are marked in red in Table D.1.

Table D.2: The values of matrix of $\boldsymbol{S}$ and $\boldsymbol{V}$ form SVD results of Link 2

Matrix	Items		12	13	15	16	17	19	20	***61***	***62***	***63***	***64***	***65***
			mP_x	mP_y	I_{xx}	I_{xy}	I_{xz}	I_yz	I_{zz}	f_1	f_2	f_3	f_4	I_m
$\boldsymbol{S}$	12	mP_x	1.8091	0	0	0	0	0	0	0	0	0	0	0
	13	mP_y	0	1.6202	0	0	0	0	0	0	0	0	0	0
	15	I_{xx}	0	0	1.3755	0	0	0	0	0	0	0	0	0
	16	I_{xy}	0	0	0	1.0627	0	0	0	0	0	0	0	0
	17	I_{xz}	0	0	0	0	0.9735	0	0	0	0	0	0	0
	19	I_yz	0	0	0	0	0	0.8861	0	0	0	0	0	0
	20	I_{zz}	0	0	0	0	0	0	0.7574	0	0	0	0	0
	61	f_1	0	0	0	0	0	0	0	0.6295	0	0	0	0
	62	f_2	0	0	0	0	0	0	0	0	0.4606	0	0	0
	63	f_3	0	0	0	0	0	0	0	0	0	0.3673	0	0
	64	f_4	0	0	0	0	0	0	0	0	0	0	0.1751	0
	65	I_m	0	0	0	0	0	0	0	0	0	0	0	1.15E-16
$\boldsymbol{V}$	12	mP_x	0.0662	0.4319	-0.077	0.4367	-0.1928	0.0309	-0.4601	0.4576	-0.3493	-0.1423	-0.1043	0
	13	mP_y	0.528	0.0052	0.0411	0.013	0.0136	0.002	-0.2685	0.0935	0.2735	0.2362	0.7125	7.22E-16
	15	I_{xx}	-0.0254	-0.3267	0.1676	-0.5606	0.3815	0.1256	-0.3665	0.3981	-0.2928	-0.0967	-0.0319	9.96E-17
	16	I_{xy}	-0.4229	-0.0017	-0.0172	-0.0448	-0.1181	0.1145	-0.7078	-0.4626	0.2751	-0.0308	0.0157	1.98E-16
	17	I_{xz}	-0.0355	0.2506	0.238	-0.3055	-0.1477	-0.8693	-0.0864	-0.0116	-0.0303	0.0057	0.0003	-8.37E-16
	19	I_yz	-0.0924	-0.0885	-0.0035	0.4957	0.7856	-0.3221	-0.0924	-0.0708	0.055	0.0189	-0.0067	-2.44E-16
	20	I_{zz}	-0.0153	0.5584	-0.0663	-0.2435	0.2835	0.1729	0.0728	-0.0719	0.0531	0.0182	0.0201	-0.7071
	61	f_1	-0.3428	-0.0481	-0.5192	-0.0547	-0.0207	-0.1039	0.0719	-0.1208	-0.5559	0.2106	0.4725	-1.95E-16
	62	f_2	-0.3016	-0.0415	-0.5067	-0.0902	-0.0246	-0.1343	0.0454	0.5468	0.5665	-0.0422	-0.0026	3.23E-16
	63	f_3	0.405	-0.0612	-0.4304	-0.1158	0.0245	-0.0883	-0.2091	-0.1258	-0.0349	0.5553	-0.506	-1.64E-15
	64	f_4	0.3932	-0.0681	-0.4325	-0.1027	0.0428	-0.1199	-0.0578	-0.2539	-0.0313	-0.747	0.0066	7.77E-16
	65	I_m	-0.0153	0.5584	-0.0663	-0.2435	0.2835	0.1729	0.0728	-0.0719	0.0531	0.0182	0.0201	0.7071

D.3 Result

Based on the introduction of Section 3.2.1 and 3.2.2, the results are shown in Table D.3. The table clearly shows the linear relationship between the parameters. The non-zero values, highlighted in yellow and red, indicate that the corresponded parameter are linear with the others. This means that the information matrix created by these parameter pairs has not full rank, and results in unrecognizable parameters for the identification. This problem can be solved by select the parameters that could create the full rank information matrix, which is the base set of the dynamic parameters, called base parameters. These parameters are shown in Table 3.1.

Table D.3: The merged decomposition result

Link	Items		Joint 1	Joint 2	Joint 3	Joint 4	Joint 5	Joint 6
1	1	m	1	1	1	1	1	1
	2	mP_x	1	1	1	1	1	1
	3	mP_y	1	1	1	1	1	1
	4	mP_z	1	1	1	1	1	1
	5	I_{xx}	1	1	1	1	1	1
	6	I_{xy}	1	1	1	1	1	1
	7	I_{xz}	1	1	1	1	1	1
	8	I_{yy}	1	1	1	1	1	1
	9	I_{yz}	1	1	1	1	1	1
	10	I_{zz}	1	1	1	1	1	1
2	11	m	1	1	1	1	1	1
	12	mP_x	0	0	1	1	1	1
	13	mP_y	0	0	1	1	1	1
	14	mP_z	1	1	1	1	1	1
	15	I_{xx}	0	0	1	1	1	1
	16	I_{xy}	0	0	1	1	1	1
	17	I_{xz}	0	0	1	1	1	1
	18	I_{yy}	1	1	1	1	1	1
	19	I_{yz}	0	0	1	1	1	1
	20	I_{zz}	1	1	1	1	1	1
3	21	m	1	1	1	1	1	1
	22	mP_x	0	0	0	1	1	1
	23	mP_y	0	0	0	1	1	1
	24	mP_z	1	1	1	1	1	1
	25	I_{xx}	0	0	0	1	1	1
	26	I_{xy}	0	0	0	1	1	1
	27	I_{xz}	0	0	0	1	1	1
	28	I_{yy}	1	1	1	1	1	1
	29	I_{yz}	0	0	0	1	1	1
	30	I_{zz}	1	0	0	1	1	1
4	31	m	1	1	1	1	1	1
	32	mP_x	0	0	0	0	1	1
	33	mP_y	0	0	0	0	1	1
	34	mP_z	1	1	1	1	1	1
	35	I_{xx}	0	0	0	0	1	1
	36	I_{xy}	0	0	0	0	1	1
	37	I_{xz}	0	0	0	0	1	1
	38	I_{yy}	1	1	1	1	1	1
	39	I_{yz}	0	0	0	0	1	1
	40	I_{zz}	0	0	0	0	1	1
5	41	m	1	1	1	1	1	1
	42	mP_x	0	0	0	0	0	1
	43	mP_y	0	0	0	0	0	1
	44	mP_z	1	1	1	1	1	1
	45	I_{xx}	0	0	0	0	0	1
	46	I_{xy}	0	0	0	0	0	1
	47	I_{xz}	0	0	0	0	0	1
	48	I_{yy}	1	1	1	1	1	1
	49	I_{yz}	0	0	0	0	0	1
	50	I_{zz}	0	0	0	0	0	1
6	51	m	1	1	1	1	1	1
	52	mP_x	0	0	0	0	0	0
	53	mP_y	0	0	0	0	0	0
	54	mP_z	1	1	1	1	1	1
	55	I_{xx}	0	0	0	0	0	0
	56	I_{xy}	0	0	0	0	0	0
	57	I_{xz}	0	0	0	0	0	0
	58	I_{yy}	1	1	1	1	1	1
	59	I_{yz}	0	0	0	0	0	0
	60	I_{zz}	0	0	0	0	0	0

Appendix E

The MATLAB Code of Parameters Selection Analysis

The code shown in this appendix is the main part of MATLAB code used to calculate the results of the base parameters of the dynamic model.

```
%% QR decomposition
QR_Zeros_temp = zeros( size(K,2), 6+1+7 ); % size predefinition

for i = 1:6
    [¬, R] = qr( K(:,:,i), 0); % QR decomposition
    % Select the upper triangular matrix in the R matrix as R1
    % Select the diagonal elements in R1
    % Then select all zero values, or values close to zero and very different ...
        from
    % other values (here, the value less than 0.0001 is considered as zero)
    % Find the location of these values and record (the corresponding position is
    % assigned the value zero)
    % The parameters corresponded to these positions are unrecognizable or are
    % linearized with other parameters
    % ------------------------------------------------------------
    % QR_Zeros_temp is the result aggregation matrix.
    % Each line corresponds to one parameter:
    %     - Each 10 rows corresponds to a parameter set in one axis;
    %     - In each set, in order, it has (1 mass, 2 centroid moment X, 3 ...
        centroid
    %       moment Y, 4 centroid moment Z, 5 moment of inertia XX, 6 moment of
    %       inertia XY, 7 moment of inertia XZ, 8 moment of inertia YY , 9 moment
    %       of inertia YZ, 10 moment of inertia ZZ).
    % Columns 1 to 6 correspond to the parameter correlation of the 1st to 6th
    % axes, respectively.
    % Columns 7 & 8 are statistical columns. Used to view the relevance of each
    % parameter globally.
    QR_Zeros_temp(:,i) = logical( abs( diag(R) ) ≤ 0.0001 ) .* (1:1:size(K, 2))';
    QR_Zeros_temp(:,i+7) = logical( QR_Zeros_temp(:,i) == 0 ) .* (1:1:size(K, ...
        2))';
end

% Product of array elements in rows
QR_Zeros_temp(:, 7) = prod( QR_Zeros_temp(:,1:6), 2 );
% the no-zero value will be replaced by its row number
QR_Zeros_temp(:, 7) = logical( QR_Zeros_temp(:,7) ≠ 0 ) .* ( 1:1:size(K,2) )';
QR_Zeros_temp(:, 14) = logical( QR_Zeros_temp(:,7) == 0 ) .* ( 1:1:size(K,2) )';

% Positive order display, which is the last 7 columns of QR_Zeros
QR_Zeros = QR_Zeros_temp(:, 8:end);
```

```
% Negative order display, which is the first 7 columns of QR_Zeros
QR_Zeros_I = QR_Zeros_temp(:, 1:7);

%% SVD decomposition A
KFs_CndNum_A = zeros(6, 8);
for k = 1:size(KFs_CndNum_A, 2)
    for i = 1:6
        switch k % create KFs matrix
            %The following analysis is based on the combined QR results for ...
                comparison only
            case 1 % Independent analysis of parameter sets for each axis - ...
                QR_Zeros(:,end)
                KFs = [K(:, QR_Zeros(:,end) ≥ ( i ∗ 10 - 9 ) & ( ...
                    QR_Zeros(:,end) ≤ i ∗ 10 ), i ), Kf(:,1:5,i)];

            case 2 % 1¬2, 2¬3, 3¬4 4¬5, 5¬6, 6¬6 axis group analysis. (Note: ...
                For calculation convenience, the calculated value range in the ...
                6th axis is 51¬70)
                KFs = [K(:, QR_Zeros(:,end) ≥ ( i ∗ 10 - 9 ) & ( ...
                    QR_Zeros(:,end) ≤ ( i + 1 ) ∗ 10 ), i ), Kf(:,1:5,i)];

            case 3 % 1¬3 2¬3 3 4¬65¬66¬6 axis group analysis
                if i ≤ 3
                    KFs = [K(:, QR_Zeros(:,end) ≥ ( i ∗ 10 - 9 ) & ( ...
                        QR_Zeros(:,end) ≤ 30 ), i ), Kf(:,1:5,i)];
                else
                    KFs = [K(:, QR_Zeros(:,end) ≥ ( i ∗ 10 - 9 ) & ( ...
                        QR_Zeros(:,end) ≤ 60 ), i ), Kf(:,1:5,i)];
                end

            case 4 % 1¬6 2¬6 3¬6 4¬65¬66¬6 axis group analysis
                KFs = [K(:, QR_Zeros(:,end) ≥ ( i ∗ 10 - 9 ) & ( ...
                    QR_Zeros(:,end) ≤ 60 ), i ), Kf(:,1:5,i)];

            % The following is an analysis based on the QR results of each ...
                axis (theoretically based on this)
            case 5 % Independent analysis of parameter sets for each axis - ...
                QR_Zeros(:,i+7)
                KFs = [K(:, QR_Zeros(:,i) ≥ ( i ∗ 10 - 9 ) & ( QR_Zeros(:,i) ≤ ...
                    i ∗ 10 ), i ), Kf(:,1:5,i)];

            case 6 % 1¬2 2¬3 3¬4 4¬55¬66¬6 axis group analysis(Note: For ...
                calculation convenience, the calculated value range in the 6th ...
                axis is 51¬70)
                KFs = [K(:, QR_Zeros(:,i) ≥ ( i ∗ 10 - 9 ) & ( QR_Zeros(:,i) ≤ ...
                    ( i + 1 ) ∗ 10 ), i ), Kf(:,1:5,i)];

            case 7  % 1¬3 2¬3 3 4¬65¬66¬6 axis group analysis
                if i ≤ 3
                    KFs = [K(:, QR_Zeros(:,i) ≥ ( i ∗ 10 - 9 ) & ( ...
                        QR_Zeros(:,i) ≤ 30 ), i ), Kf(:,1:5,i)];
                else
                    KFs = [K(:, QR_Zeros(:,i) ≥ ( i ∗ 10 - 9 ) & ( ...
                        QR_Zeros(:,i) ≤ 60 ), i ), Kf(:,1:5,i)];
                end

            case 8  % 1¬6 2¬6 3¬6 4¬65¬66¬6 axis group analysis
                KFs = [K(:, QR_Zeros(:,i) ≥ ( i ∗ 10 - 9 ) & ( QR_Zeros(:,i) ≤ ...
                    60 ), i ), Kf(:,1:5,i)];
        end

        [ KFs_CndNum_A(i, k), S, V ] = SVD_CndNum( KFs ); % go to the ...
            sub-function
```

```
            % matrix condition number comparison
            % If the condition number is too large (>100), save the corresponding SVD
            % matrix (variable name is automatically generated)
            % ------------------------------------------------------------
            % The principle of it is that the differences between the maximum ...
                value and
            % the minimum value on the diagonal of the S matrix are too large (3 ...
                orders
            % of magnitude here)
            % Then in the V matrix, look for the column of data corresponding to ...
                the minimum
            % value (generally the last column, because the result of the ...
                decomposition, the
            % diagonal elements of the S matrix are arranged from large to small, ...
                so the
            % minimum value is in the last column)
            % In the last column of the V matrix, find a value such that the value is
            % significantly larger than the other values (that is, the distance is ...
                very
            % long with all values are taken as absolute values), it indicates ...
                that the
            % parameter corresponding to this row needs to be eliminated ( it will ...
                have
            % a great impact on the identification results)
            % [The above steps cannot be written in MATLAB with code]
            if KFs_CndNum_A(i, k) ≥ 100
                eval(['J',num2str(k),num2str(i),'_S = S;']);
                eval(['J',num2str(k),num2str(i),'_V = V;']);
            end
        end
    end
```

Appendix F

The RMSD Values

This appendix shows the RMSD values listed in tables with the related statistic data and some figures. It should be noted that the values and the plots demonstrated in this appendix are obtained without the data coming from the low speed; except for the values in the Table F.1. The analyses related with RMSD are presented in Section 5.1.2, 5.1.3 and 5.1.4.

F.1 The Tables of RMSD

The tables listed in this section show the RMSD values of the verification. The values highlighted in yellow are grater than 10% except the standard deviation values. Furthermore, the statistical results of verification are attached with tables. The statistics data includes the mean, maximum and minimum values, the differences between the maximum and minimum values, the differences between the start and the end cycles, and the standard deviation.

Table F.1: The relative RMSD values

		Test	Cycles																							Mean		Minimum		Maximum		Diff of MAX/MIN		Diff of Start/End Cycle	Standard Deviation	
			C1	C2	C3	C4	C5	C6	C7	C8	C9	C10	C11	C12	C13	C14	C15	C16	C17	C18	C19	C20	C21	C22	C23	C24	Test	All Tests	Test	All Tests	Test	All Tests	Test	All Tests		Test	All Tests
Joint 1	Robot 1	T1	0.05327	0.05267	0.05265	0.05301	0.05314	0.05319	0.05317	0.05269	0.05294	0.05289	0.05298	0.05240	0.05366	0.05296	0.05289	0.05263	0.05285	0.05310	0.05283	0.05305	0.05250	0.05278	0.05246	0.05267	0.05289	0.05316	0.05240	0.04771	0.05366	0.05463	0.02353	0.12667	0.00721	0.0002837	0.0009653
		T2	0.04838	0.05266	0.05254	0.05254	0.05246	0.05332	0.05314	0.05333	0.05320	0.05336	0.05329	0.05307	0.05322	0.05314	0.05316	0.05321	0.05295	0.05314	0.05262	0.05326	0.05277	0.05326	0.05323	0.05346	0.05286		0.04838		0.05346		0.09501		0.09263	0.0009782	
		T3	0.04771	0.05292	0.05290	0.05269	0.05293	0.05311	0.05343	0.05314	0.05330	0.05326	0.05311	0.05271	0.05292	0.05305	0.05355	0.05351	0.05387	0.05387	0.05391	0.05413	0.05385	0.05383	0.05429	0.05364	0.05315		0.04771		0.05429		0.12120		0.11406	0.0012197	
		T4	0.04997	0.05371	0.05423	0.05463	0.05424	0.05379	0.05398	0.05406	0.05350	0.05352	0.05347	0.05363	0.05363	0.05381	0.05366	0.05378	0.05344	0.05442	0.05367	0.05444	0.05409	0.05383	0.05398	0.05405	0.05373		0.04997		0.05463		0.08537		0.07530	0.0008471	
	Robot 2	T1	0.04644	0.05470	0.05568	0.05471	0.05487	0.05478	0.05534	0.05463	0.05486	0.05423	0.05441	0.05406	0.05393	0.05388	0.05362	0.05344	0.05409	0.05423	0.05351	0.05387	0.05308	0.05419	0.05312	0.05410	0.05391	0.05349	0.04644	0.04507	0.05568	0.05568	0.16598	0.19059	0.16087	0.0016809	0.0017345
		T2	0.04507	0.05268	0.05468	0.05447	0.05439	0.05387	0.05392	0.05385	0.05372	0.05192	0.05359	0.05334	0.05331	0.05306	0.05330	0.05333	0.05284	0.05296	0.05312	0.05195	0.05315	0.05355	0.05379	0.05336	0.05305		0.04507		0.05468		0.17579		0.17716	0.0017897	
		T3	0.04617	0.05354	0.05505	0.05466	0.05439	0.05467	0.05433	0.05475	0.05486	0.05455	0.05490	0.05358	0.05354	0.05421	0.05324	0.05429	0.05366	0.05334	0.05312	0.05361	0.05368	0.05365	0.05399	0.05281	0.05369		0.04617		0.05505		0.16135		0.16299	0.0016853	
		T4	0.04577	0.05438	0.05398	0.05365	0.05404	0.05465	0.05476	0.05399	0.05381	0.05317	0.05307	0.05330	0.05364	0.05325	0.05357	0.05282	0.05323	0.05378	0.05389	0.05339	0.05401	0.05287	0.05337	0.05321	0.05332		0.04577		0.05476		0.16420		0.16497	0.0016520	
Joint 2	Robot 1	T1	0.07257	0.07361	0.07225	0.07374	0.07544	0.07364	0.07388	0.07420	0.07403	0.07514	0.07418	0.07333	0.07677	0.07601	0.07622	0.07475	0.07478	0.07628	0.07442	0.07422	0.07438	0.07624	0.07496	0.07603	0.07463	0.07302	0.07225	0.07023	0.07677	0.07983	0.05878	0.12026	0.02830	0.0011776	0.0016521
		T2	0.07331	0.07427	0.07023	0.07197	0.07110	0.07585	0.07253	0.07178	0.07304	0.07262	0.07254	0.07239	0.07090	0.07344	0.07272	0.07188	0.07319	0.07348	0.07277	0.07405	0.07206	0.07233	0.07316	0.07307	0.07270		0.07023		0.07585		0.07410		0.00845	0.0011393	
		T3	0.07379	0.07983	0.07083	0.07289	0.07175	0.07480	0.07158	0.07231	0.07285	0.07105	0.07277	0.07251	0.07166	0.07160	0.07229	0.07211	0.07271	0.07458	0.07170	0.07465	0.07256	0.07317	0.07198	0.07246	0.07285		0.07083		0.07983		0.11274		0.01271	0.0017857	
		T4	0.07342	0.07268	0.07149	0.07038	0.07293	0.07207	0.07278	0.07029	0.07032	0.07181	0.07184	0.07317	0.07225	0.07220	0.07115	0.07373	0.07088	0.07118	0.07140	0.07106	0.07370	0.07044	0.07244	0.07238	0.07192		0.07029		0.07373		0.04656		0.02050	0.0010497	
	Robot 2	T1	0.06264	0.05959	0.05948	0.05819	0.05866	0.05769	0.05765	0.05670	0.05819	0.05768	0.05702	0.05802	0.05794	0.05706	0.05748	0.05828	0.05840	0.05855	0.05716	0.05744	0.05780	0.05865	0.05832	0.05874	0.05822	0.05816	0.05670	0.05659	0.06264	0.06264	0.09479	0.09648	0.07047	0.0011616	0.0010447
		T2	0.06196	0.05930	0.05995	0.05794	0.05859	0.05795	0.05798	0.05753	0.05726	0.05773	0.05824	0.05743	0.05698	0.05731	0.05742	0.05773	0.05718	0.05876	0.05718	0.05781	0.05659	0.05845	0.05815	0.05748	0.05804		0.05659		0.06196		0.08668		0.06335	0.0011009	
		T3	0.06252	0.05887	0.05797	0.05684	0.05840	0.05799	0.05833	0.05856	0.05804	0.05908	0.05772	0.05786	0.05840	0.05861	0.05862	0.05904	0.05781	0.05854	0.05885	0.05676	0.05687	0.05772	0.05794	0.05860	0.05833		0.05676		0.06252		0.09207		0.06700	0.0010808	
		T4	0.06054	0.05873	0.05850	0.05861	0.05853	0.05721	0.05835	0.05802	0.05780	0.05758	0.05891	0.05786	0.05901	0.05846	0.05775	0.05709	0.05781	0.05748	0.05781	0.05744	0.05806	0.05752	0.05769	0.05689	0.05807		0.05689		0.06054		0.06028		0.04080	0.0007617	
Joint 3	Robot 1	T1	0.09873	0.10231	0.10204	0.10107	0.10166	0.10314	0.10284	0.10360	0.10517	0.10493	0.10563	0.10465	0.10603	0.10558	0.10640	0.10545	0.10558	0.10490	0.10617	0.10717	0.10622	0.10666	0.10524	0.10721	0.10452	0.10231	0.09873	0.09541	0.10721	0.10721	0.07910	0.11001	0.05863	0.0021032	0.0022453
		T2	0.09788	0.10029	0.10019	0.10096	0.10153	0.10001	0.10168	0.10340	0.10110	0.10139	0.10309	0.10225	0.10064	0.10290	0.10284	0.10243	0.10426	0.10288	0.10385	0.10328	0.10307	0.10347	0.10351	0.10522	0.10217		0.09788		0.10522		0.06981		0.04385	0.0016166	
		T3	0.09642	0.10007	0.10120	0.10125	0.10005	0.09997	0.10016	0.09934	0.10061	0.10197	0.10115	0.10276	0.10230	0.10170	0.10218	0.10286	0.10197	0.10222	0.10221	0.10143	0.10150	0.10259	0.10074	0.10338	0.10125		0.09642		0.10338		0.06735		0.05014	0.0014395	
		T4	0.09541	0.09863	0.09800	0.10002	0.09883	0.09997	0.10089	0.10028	0.10190	0.10251	0.10094	0.10282	0.10229	0.10112	0.10261	0.10299	0.10217	0.10177	0.10159	0.10205	0.10347	0.10262	0.10424	0.10379	0.10129		0.09541		0.10424		0.08466		0.06156	0.0020013	
	Robot 2	T1	0.08555	0.08456	0.08598	0.08529	0.08445	0.08375	0.08360	0.08462	0.08523	0.08422	0.08536	0.08521	0.08612	0.08553	0.08547	0.08494	0.08554	0.08641	0.08653	0.08615	0.08635	0.08711	0.08559	0.08632	0.08541	0.08583	0.08360	0.08360	0.08711	0.08810	0.04033	0.05108	0.00161	0.0008734	0.0009173
		T2	0.08471	0.08499	0.08574	0.08490	0.08520	0.08526	0.08465	0.08629	0.08413	0.08543	0.08555	0.08532	0.08436	0.08446	0.08551	0.08572	0.08512	0.08656	0.08514	0.08558	0.08561	0.08772	0.08739	0.08567	0.08546		0.08413		0.08772		0.04094		0.00890	0.0008437	
		T3	0.08583	0.08612	0.08571	0.08697	0.08548	0.08477	0.08623	0.08633	0.08611	0.08700	0.08547	0.08606	0.08631	0.08782	0.08604	0.08734	0.08707	0.08610	0.08632	0.08516	0.08709	0.08681	0.08757	0.08689	0.08636		0.08477		0.08782		0.03475		0.00617	0.0007492	
		T4	0.08572	0.08621	0.08653	0.08571	0.08476	0.08567	0.08476	0.08618	0.08560	0.08499	0.08689	0.08523	0.08624	0.08578	0.08510	0.08579	0.08641	0.08694	0.08669	0.08706	0.08660	0.08600	0.08810	0.08726	0.08609		0.08476		0.08810		0.03790		0.00434	0.0008172	
Joint 4	Robot 1	T1	0.14652	0.15576	0.15472	0.15582	0.15583	0.15387	0.15458	0.15283	0.15422	0.15340	0.15368	0.15547	0.15414	0.15331	0.15472	0.15518	0.15522	0.15388	0.15251	0.15437	0.15530	0.15299	0.15539	0.15435	0.15409	0.15503	0.14652	0.13804	0.15583	0.16012	0.05975	0.13792	0.05165	0.0018422	0.0031458
		T2	0.14252	0.15842	0.15993	0.15704	0.15623	0.15763	0.15656	0.15812	0.15602	0.15683	0.15832	0.15561	0.15637	0.15607	0.15808	0.15694	0.15559	0.15788	0.15604	0.15679	0.15662	0.15713	0.15487	0.15644	0.15634		0.14252		0.15993		0.10889		0.09695	0.0030826	
		T3	0.13804	0.15470	0.15749	0.15394	0.15445	0.15339	0.15373	0.15400	0.15515	0.15702	0.15505	0.15336	0.15438	0.15552	0.15533	0.15572	0.15520	0.15463	0.15386	0.15596	0.15480	0.15318	0.15676	0.15728	0.15429		0.13804		0.15749		0.12350		0.11774	0.0035975	
		T4	0.14193	0.15676	0.15730	0.15590	0.15415	0.15692	0.15435	0.15458	0.15407	0.15356	0.15375	0.15522	0.15530	0.15527	0.16012	0.15889	0.15686	0.15639	0.15621	0.15663	0.15693	0.15745	0.15451	0.15711	0.15542		0.14193		0.16012		0.11363		0.09509	0.0032327	
	Robot 2	T1	0.12280	0.14020	0.14167	0.14165	0.14215	0.14627	0.14496	0.14331	0.14614	0.14577	0.14633	0.14617	0.14751	0.14675	0.14722	0.14670	0.14639	0.14896	0.14643	0.14793	0.14514	0.14687	0.14779	0.14773	0.14470	0.14490	0.12280	0.12280	0.14896	0.15022	0.17562	0.18255	0.17837	0.0050740	0.0049555
		T2	0.12553	0.13843	0.14062	0.14333	0.14400	0.14646	0.14557	0.14536	0.14743	0.14724	0.14672	0.14749	0.14840	0.14726	0.14817	0.14980	0.14877	0.14854	0.14886	0.14774	0.14861	0.14992	0.14842	0.14794	0.14586		0.12553		0.14992		0.16268		0.16195	0.0050277	
		T3	0.12538	0.13942	0.14258	0.14447	0.14608	0.14323	0.14415	0.14640	0.14627	0.14663	0.14615	0.14770	0.14661	0.14840	0.14754	0.15022	0.14837	0.14911	0.14896	0.14797	0.14973	0.14849	0.14607	0.14827	0.14576		0.12538		0.15022		0.16536		0.16254	0.0048961	
		T4	0.12542	0.13804	0.13909	0.14173	0.14111	0.14303	0.14238	0.14336	0.14457	0.14323	0.14574	0.14527	0.14529	0.14540	0.14738	0.14614	0.14539	0.14346	0.14628	0.14449	0.14612	0.14447	0.14560	0.14613	0.14330		0.12542		0.14738		0.14901		0.14256	0.0043550	
Joint 5	Robot 1	T1	0.11696	0.11853	0.11229	0.09523	0.08910	0.09028	0.09059	0.08450	0.08680	0.08829	0.09902	0.10874	0.12004	0.11743	0.11312	0.08979	0.11448	0.11059	0.11546	0.10370	0.11006	0.10059	0.10166	0.10280	0.10334	0.10366	0.08450	0.08182	0.12004	0.13958	0.29605	0.41378	0.11651	0.0114328	0.0116144
		T2	0.10834	0.08707	0.08182	0.08719	0.08997	0.09245	0.08741	0.09047	0.09366	0.08660	0.09459	0.09739	0.09524	0.09500	0.09779	0.09331	0.09704	0.09706	0.09723	0.10068	0.09145	0.08993	0.09462	0.09408	0.09335		0.08182		0.10834		0.24475		0.13837	0.0053771	
		T3	0.11422	0.12143	0.09876	0.12006	0.09137	0.09893	0.09898	0.09693	0.10966	0.10643	0.10036	0.10195	0.11266	0.09923	0.09803	0.10427	0.09148	0.10415	0.09598	0.10102	0.09709	0.10120	0.09730	0.09878	0.10251		0.09137		0.12143		0.24753		0.10250	0.0077661	
		T4	0.11935	0.11826	0.11222	0.11439	0.11787	0.10941	0.10611	0.10608	0.10885	0.12244	0.11746	0.11593	0.11016	0.11399	0.12084	0.10961	0.11242	0.12006	0.12002	0.11022	0.10186	0.10784	0.13958	0.13566	0.11544		0.10186		0.13958		0.27023		0.03274	0.0085484	
	Robot 2	T1	0.07010	0.05201	0.05471	0.05222	0.05320	0.05126	0.05350	0.05383	0.05198	0.05316	0.05313	0.05237	0.05240	0.05244	0.05147	0.05233	0.05211	0.05354	0.05371	0.05317	0.05317	0.05369	0.05267	0.05292	0.05355	0.05353	0.05126	0.05126	0.07010	0.07010	0.26876	0.26876	0.23612	0.0035405	0.0030320
		T2	0.06683	0.05274	0.05452	0.05317	0.05308	0.05248	0.05181	0.05264	0.05175	0.05197	0.05287	0.05149	0.05182	0.05169	0.05222	0.05196	0.05272	0.05315	0.05316	0.05329	0.05272	0.05381	0.05397	0.05361	0.05331		0.05149		0.06683		0.22960		0.20229	0.0029239	
		T3	0.06655	0.05347	0.05397	0.05245	0.05335	0.05254	0.05355	0.05414	0.05267	0.05283	0.05242	0.05305	0.05373	0.05327	0.05362	0.05377	0.05358	0.05360	0.05287	0.05344	0.05486	0.05354	0.05424	0.05384	0.05397		0.05242		0.06655		0.21229		0.18895	0.0026861	
		T4	0.06646	0.05408	0.05440	0.05203	0.05198	0.05156	0.05283	0.05274	0.05269	0.05203	0.05173	0.05318	0.05215	0.05314	0.05215	0.05407	0.05260	0.05136	0.05281	0.05224	0.05254	0.05358	0.05350	0.05298	0.05328		0.05136		0.06646		0.22711		0.19823	0.0028575	
Joint 6	Robot 1	T1	0.05876	0.06394	0.06992	0.07134	0.07253	0.07282	0.07362	0.07509	0.07535	0.07449	0.07625	0.07720	0.07642	0.07748	0.07674	0.07656	0.07590	0.07781	0.07703	0.07767	0.07760	0.07795	0.07765	0.07725	0.07447	0.07460	0.05876	0.05876	0.07795	0.07906	0.24620	0.25682	0.26748	0.0045620	0.0043051
		T2	0.06342	0.06760	0.06843	0.06959	0.06988	0.07253	0.07327	0.07454	0.07570	0.07538	0.07616	0.07598	0.07681	0.07783	0.07739	0.07797	0.07906	0.07883	0.07778	0.07816	0.07899	0.07855	0.07892	0.07865	0.07506		0.06342		0.07906		0.19790		0.18361	0.0042413	
		T3	0.05961	0.06796	0.06922	0.07094	0.07362	0.07396	0.07480	0.07617	0.07622	0.07624	0.07632	0.07736	0.07708	0.07701	0.07701	0.07781	0.07694	0.07744	0.07795	0.07710	0.07798	0.07798	0.07766	0.07839	0.07511		0.05961		0.07839		0.23952		0.26005	0.0042335	
		T4	0.05934	0.06675	0.06974	0.07063	0.07059	0.07123	0.07284	0.07371	0.07468	0.07403	0.07490	0.07574	0.07575	0.07681	0.07661	0.07661	0.07551	0.07687	0.07755	0.07614	0.07609	0.07575	0.07549	0.07648	0.07374		0.05934		0.07755		0.23480		0.24271	0.0040235	
	Robot 2	T1	0.08275	0.09331	0.09556	0.09668	0.09488	0.09368	0.09532	0.09471	0.09654	0.09479	0.09452	0.09417	0.09562	0.09530	0.09507	0.09594	0.09541	0.09528	0.09609	0.09610	0.09526	0.09690	0.09702	0.09675	0.09490	0.09497	0.08275	0.08275	0.09702	0.09765	0.14708	0.15258	0.14689	0.0027077	0.0023419
		T2	0.08562	0.09571	0.09607	0.09549	0.09628	0.09520	0.09609	0.09701	0.09538	0.09576	0.09471	0.09428	0.09610	0.09540	0.09529	0.09423	0.09514	0.09559	0.09574	0.09552	0.09502	0.09603	0.09542	0.09548	0.09511		0.08562		0.09701		0.11740		0.11075	0.0020663	
		T3	0.08370	0.09658	0.09632	0.09659	0.09420	0.09654	0.09550	0.09497	0.09492	0.09623	0.09582	0.09610	0.09569	0.09371	0.09575	0.09552	0.09483	0.09583	0.09507	0.09590	0.09370	0.09460	0.09380	0.09462	0.09485		0.08370		0.09659		0.13350		0.13331	0.0024888	
		T4	0.08608	0.09765	0.09630	0.09689	0.09562	0.09453	0.09516	0.09538	0.09559	0.09516	0.09541	0.09541	0.09471	0.09474	0.09509	0.09452	0.09639	0.09554	0.09403	0.09525	0.09535	0.09443	0.09590	0.09551	0.09503		0.08608		0.09765		0.11847		0.10395	0.0020256	

Table F.2: The relative RMSD values calculated without low velocity data

		Tests	Cycles																								Mean		Minimum		Maximum		Diff of MAX/MIN		Diff of	Standard Deviation	
			C1	C2	C3	C4	C5	C6	C7	C8	C9	C10	C11	C12	C13	C14	C15	C16	C17	C18	C19	C20	C21	C22	C23	C24	Test	All Tests	Test	All Tests	Test	All Tests	Test	All Tests	Start/End Cycle	Test	All Tests
Joint 1	Robot 1	T1	0.05486	0.05274	0.05278	0.05329	0.05346	0.05361	0.05364	0.05314	0.05358	0.05328	0.05361	0.05296	0.05428	0.05361	0.05344	0.05329	0.05334	0.05372	0.05343	0.05368	0.05318	0.05342	0.05316	0.05339	0.05345	0.05367	0.05274	0.04922	0.05486	0.05486	0.03870	0.10293	0.02683	0.0004411	0.0008045
		T2	0.04980	0.05323	0.05276	0.05296	0.05283	0.05376	0.05374	0.05401	0.05381	0.05411	0.05396	0.05378	0.05403	0.05401	0.05390	0.05405	0.05365	0.05387	0.05331	0.05397	0.05354	0.05401	0.05403	0.05415	0.05355		0.04980		0.05415		0.08035		0.08737	0.0008975	
		T3	0.04922	0.05317	0.05317	0.05298	0.05330	0.05359	0.05387	0.05371	0.05396	0.05388	0.05357	0.05341	0.05366	0.05357	0.05394	0.05376	0.05435	0.05420	0.05445	0.05445	0.05418	0.05421	0.05484	0.05412	0.05365		0.04922		0.05484		0.10257		0.09967	0.0010501	
		T4	0.05170	0.05320	0.05415	0.05449	0.05426	0.05399	0.05412	0.05429	0.05390	0.05374	0.05377	0.05384	0.05394	0.05402	0.05399	0.05416	0.05372	0.05485	0.05407	0.05486	0.05447	0.05431	0.05425	0.05447	0.05402		0.05170		0.05486		0.05769		0.05357	0.0006143	
	Robot 2	T1	0.04538	0.05122	0.05143	0.05079	0.05145	0.05146	0.05185	0.05111	0.05180	0.05105	0.05149	0.05122	0.05119	0.05122	0.05102	0.05076	0.05110	0.05143	0.05072	0.05114	0.05056	0.05163	0.05055	0.05135	0.05095	0.05095	0.04538	0.04449	0.05185	0.05253	0.12471	0.15314	0.13142	0.0012372	0.0014190
		T2	0.04504	0.05036	0.05253	0.05230	0.05219	0.05171	0.05249	0.05215	0.05221	0.05019	0.05241	0.05198	0.05179	0.05167	0.05197	0.05213	0.05165	0.05167	0.05187	0.05049	0.05198	0.05230	0.05247	0.05213	0.05157		0.04504		0.05253		0.14268		0.15750	0.0015325	
		T3	0.04449	0.04910	0.05146	0.05128	0.05129	0.05055	0.05090	0.05126	0.05162	0.05174	0.05179	0.05049	0.05100	0.05126	0.05114	0.05124	0.05092	0.05094	0.05054	0.05084	0.05099	0.05083	0.05178	0.05013	0.05073		0.04449		0.05179		0.14096		0.12681	0.0014528	
		T4	0.04461	0.05077	0.05076	0.05076	0.05091	0.05147	0.05116	0.05088	0.05059	0.05067	0.05018	0.05056	0.05085	0.05039	0.05071	0.05065	0.05068	0.05132	0.05092	0.05097	0.05128	0.05031	0.05094	0.05028	0.05053		0.04461		0.05147		0.13324		0.12709	0.0013001	
Joint 2	Robot 1	T1	0.07815	0.07762	0.07651	0.07738	0.07958	0.07769	0.07811	0.07853	0.07854	0.07965	0.07881	0.07803	0.08179	0.08098	0.08124	0.07950	0.07958	0.08135	0.07927	0.07888	0.07921	0.08121	0.07991	0.08110	0.07928	0.07739	0.07651	0.07349	0.08179	0.08401	0.06452	0.12521	0.03772	0.0014345	0.0018840
		T2	0.07824	0.07736	0.07349	0.07580	0.07477	0.08021	0.07655	0.07603	0.07719	0.07662	0.07676	0.07649	0.07505	0.07793	0.07708	0.07629	0.07768	0.07802	0.07714	0.07859	0.07647	0.07674	0.07761	0.07756	0.07690		0.07349		0.08021		0.08373		0.00870	0.0013566	
		T3	0.07882	0.08401	0.07414	0.07675	0.07563	0.07920	0.07579	0.07668	0.07706	0.07531	0.07720	0.07673	0.07586	0.07593	0.07655	0.07663	0.07721	0.07910	0.07605	0.07940	0.07722	0.07771	0.07642	0.07687	0.07718		0.07414		0.08401		0.11751		0.02480	0.0019342	
		T4	0.07827	0.07601	0.07499	0.07416	0.07704	0.07622	0.07713	0.07447	0.07438	0.07611	0.07617	0.07749	0.07680	0.07671	0.07549	0.07843	0.07517	0.07551	0.07580	0.07560	0.07828	0.07468	0.07692	0.07692	0.07620		0.07416		0.07843		0.05435		0.01718	0.0012385	
	Robot 2	T1	0.06698	0.06201	0.06209	0.06080	0.06124	0.06015	0.05985	0.05907	0.06081	0.06026	0.05970	0.06058	0.06066	0.05950	0.06002	0.06110	0.06131	0.06143	0.05999	0.06024	0.06071	0.06156	0.06110	0.06158	0.06095	0.06089	0.05907	0.05901	0.06698	0.06698	0.11803	0.11888	0.08063	0.0015057	0.0013236
		T2	0.06610	0.06168	0.06229	0.06032	0.06103	0.06031	0.06036	0.05999	0.05963	0.06008	0.06081	0.06018	0.05954	0.05996	0.06015	0.06053	0.05975	0.06165	0.05996	0.06085	0.05946	0.06143	0.06128	0.06037	0.06074		0.05946		0.06610		0.10041		0.08661	0.0013601	
		T3	0.06689	0.06081	0.05994	0.05901	0.06063	0.06037	0.06093	0.06118	0.06037	0.06185	0.06054	0.06070	0.06124	0.06149	0.06122	0.06181	0.06072	0.06135	0.06197	0.05934	0.05964	0.06046	0.06099	0.06160	0.06104		0.05901		0.06689		0.11772		0.07906	0.0014615	
		T4	0.06432	0.06121	0.06062	0.06095	0.06120	0.05962	0.06103	0.06069	0.06039	0.06035	0.06190	0.06060	0.06201	0.06145	0.06040	0.05982	0.06070	0.06041	0.06073	0.06019	0.06106	0.06042	0.06050	0.05950	0.06084		0.05950		0.06432		0.07499		0.07499	0.0009633	
Joint 3	Robot 1	T1	0.10271	0.10497	0.10470	0.10419	0.10431	0.10645	0.10596	0.10625	0.10811	0.10778	0.10834	0.10755	0.10910	0.10894	0.10966	0.10885	0.10818	0.10817	0.10875	0.10992	0.10861	0.10940	0.10730	0.11020	0.10743	0.10517	0.10271	0.10014	0.11020	0.11020	0.06789	0.09129	0.07284	0.0020432	0.0021054
		T2	0.10255	0.10309	0.10369	0.10459	0.10433	0.10334	0.10416	0.10598	0.10456	0.10434	0.10584	0.10502	0.10326	0.10559	0.10549	0.10440	0.10671	0.10559	0.10693	0.10576	0.10561	0.10605	0.10594	0.10808	0.10504		0.10255		0.10808		0.05119		0.05395	0.0013360	
		T3	0.10076	0.10394	0.10368	0.10425	0.10324	0.10320	0.10275	0.10226	0.10333	0.10506	0.10388	0.10570	0.10516	0.10447	0.10448	0.10589	0.10449	0.10479	0.10503	0.10384	0.10351	0.10485	0.10377	0.10621	0.10411		0.10076		0.10621		0.05125		0.05402	0.0012133	
		T4	0.10014	0.10152	0.10077	0.10334	0.10186	0.10324	0.10417	0.10309	0.10487	0.10541	0.10354	0.10633	0.10523	0.10310	0.10493	0.10572	0.10447	0.10413	0.10392	0.10422	0.10664	0.10496	0.10672	0.10614	0.10410		0.10014		0.10672		0.06169		0.05993	0.0017736	
	Robot 2	T1	0.08844	0.08568	0.08727	0.08613	0.08547	0.08511	0.08551	0.08625	0.08677	0.08528	0.08611	0.08646	0.08709	0.08687	0.08705	0.08664	0.08744	0.08721	0.08788	0.08748	0.08721	0.08813	0.08729	0.08775	0.08677	0.08695	0.08511	0.08511	0.08844	0.08891	0.03762	0.04274	0.00779	0.0009217	0.0008366
		T2	0.08824	0.08617	0.08640	0.08605	0.08686	0.08647	0.08599	0.08748	0.08541	0.08655	0.08722	0.08667	0.08604	0.08655	0.08693	0.08706	0.08660	0.08787	0.08675	0.08741	0.08675	0.08891	0.08827	0.08742	0.08692		0.08541		0.08891		0.03939		0.00924	0.0008226	
		T3	0.08795	0.08644	0.08603	0.08732	0.08627	0.08563	0.08682	0.08696	0.08715	0.08786	0.08639	0.08667	0.08699	0.08884	0.08688	0.08804	0.08762	0.08715	0.08734	0.08624	0.08780	0.08756	0.08855	0.08782	0.08718		0.08563		0.08884		0.03613		0.00147	0.0008016	
		T4	0.08822	0.08647	0.08703	0.08676	0.08568	0.08615	0.08575	0.08649	0.08654	0.08619	0.08730	0.08610	0.08684	0.08639	0.08654	0.08649	0.08705	0.08753	0.08728	0.08805	0.08755	0.08676	0.08886	0.08782	0.08691		0.08568		0.08886		0.03578		0.00450	0.0007945	
Joint 4	Robot 1	T1	0.13051	0.12556	0.12389	0.12695	0.12770	0.12386	0.12560	0.12402	0.12574	0.12372	0.12364	0.12460	0.12392	0.12345	0.12398	0.12499	0.12500	0.12320	0.12387	0.12515	0.12500	0.12346	0.12520	0.12391	0.12487	0.12591	0.12320	0.12145	0.13051	0.13215	0.05595	0.08103	0.05053	0.0016433	0.0018558
		T2	0.12731	0.12815	0.12980	0.12604	0.12689	0.12741	0.12660	0.12674	0.12653	0.12834	0.12851	0.12476	0.12619	0.12546	0.12872	0.12590	0.12526	0.12820	0.12545	0.12718	0.12616	0.12713	0.12477	0.12730	0.12687		0.12476		0.12980		0.03877		0.00012	0.0013075	
		T3	0.12145	0.12359	0.12746	0.12476	0.12562	0.12387	0.12390	0.12349	0.12583	0.12769	0.12452	0.12318	0.12495	0.12598	0.12619	0.12618	0.12473	0.12544	0.12532	0.12612	0.12604	0.12468	0.12680	0.12902	0.12528		0.12145		0.12902		0.05868		0.06234	0.0016330	
		T4	0.12654	0.12741	0.12882	0.12617	0.12438	0.12773	0.12534	0.12385	0.12416	0.12495	0.12389	0.12619	0.12483	0.12516	0.13215	0.12912	0.12777	0.12796	0.12650	0.12736	0.12689	0.12851	0.12431	0.12837	0.12660		0.12385		0.13215		0.06287		0.01447	0.0020403	
	Robot 2	T1	0.10289	0.11125	0.11182	0.11116	0.11277	0.11408	0.11371	0.11099	0.11413	0.11366	0.11390	0.11271	0.11643	0.11624	0.11539	0.11468	0.11454	0.11716	0.11591	0.11610	0.11579	0.11539	0.11716	0.11712	0.11396	0.11428	0.10289	0.10289	0.11716	0.11835	0.12185	0.13068	0.13838	0.0030423	0.0030098
		T2	0.10574	0.11006	0.11047	0.11133	0.11423	0.11625	0.11488	0.11348	0.11464	0.11490	0.11411	0.11546	0.11834	0.11640	0.11585	0.11750	0.11760	0.11742	0.11805	0.11574	0.11670	0.11819	0.11661	0.11586	0.11499		0.10574		0.11834		0.10651		0.09579	0.0030127	
		T3	0.10555	0.11011	0.11233	0.11319	0.11454	0.11173	0.11208	0.11510	0.11438	0.11527	0.11597	0.11624	0.11692	0.11626	0.11587	0.11810	0.11755	0.11757	0.11704	0.11704	0.11764	0.11629	0.11435	0.11835	0.11498		0.10555		0.11835		0.10818		0.12130	0.0029731	
		T4	0.10442	0.10859	0.11086	0.11121	0.11064	0.11193	0.11154	0.11317	0.11480	0.11256	0.11571	0.11314	0.11372	0.11434	0.11737	0.11492	0.11517	0.11303	0.11525	0.11307	0.11607	0.11303	0.11608	0.11558	0.11318		0.10442		0.11737		0.11029		0.10679	0.0027978	
Joint 5	Robot 1	T1	0.10089	0.10336	0.09768	0.08753	0.08211	0.08400	0.08443	0.07869	0.08149	0.08214	0.08843	0.09914	0.11314	0.10941	0.10508	0.08466	0.10581	0.10258	0.10493	0.09282	0.09635	0.09189	0.09088	0.09241	0.09416	0.09428	0.07869	0.07475	0.11314	0.13136	0.30454	0.43094	0.08411	0.0099612	0.0105446
		T2	0.10103	0.07849	0.07475	0.07997	0.08274	0.08517	0.08094	0.08216	0.08604	0.07909	0.08561	0.08691	0.08710	0.08566	0.08909	0.08537	0.08925	0.08770	0.08867	0.09256	0.08451	0.08381	0.08774	0.08809	0.08552		0.07475		0.10103		0.26009		0.12807	0.0052305	
		T3	0.10600	0.10473	0.09089	0.10796	0.08422	0.09209	0.09207	0.09003	0.10126	0.09590	0.09246	0.09115	0.10199	0.09000	0.08942	0.09100	0.08495	0.09539	0.08872	0.09325	0.08702	0.09068	0.08769	0.08649	0.09314		0.08422		0.10796		0.21990		0.18410	0.0066267	
		T4	0.10966	0.09906	0.09634	0.10056	0.10056	0.09561	0.09477	0.09510	0.09575	0.11309	0.10748	0.10514	0.09910	0.10719	0.11433	0.09750	0.10270	0.11310	0.11157	0.09832	0.09120	0.09700	0.13136	0.12653	0.10429		0.09120		0.13136		0.30575		0.15387	0.0101336	
	Robot 2	T1	0.06895	0.04870	0.05101	0.04899	0.05005	0.04783	0.05053	0.04999	0.04928	0.05061	0.04994	0.04981	0.04934	0.04999	0.04866	0.04904	0.04858	0.05054	0.05033	0.05014	0.05041	0.05086	0.04995	0.05027	0.05058	0.05062	0.04783	0.04783	0.06895	0.06895	0.30635	0.30635	0.27092	0.0039971	0.0033333
		T2	0.06513	0.04960	0.05129	0.04970	0.04954	0.04957	0.04932	0.04980	0.04901	0.04847	0.05026	0.04869	0.04890	0.04877	0.04904	0.04891	0.04959	0.05063	0.05055	0.05070	0.04972	0.05144	0.05106	0.05085	0.05044		0.04847		0.06513		0.25568		0.21920	0.0032454	
		T3	0.06405	0.04990	0.04987	0.04910	0.05037	0.04940	0.05091	0.05111	0.04917	0.04989	0.04934	0.05062	0.05125	0.05065	0.05108	0.05138	0.05087	0.05102	0.04986	0.05058	0.05273	0.05073	0.05171	0.05117	0.05111		0.04910		0.06405		0.23334		0.20116	0.0028889	
		T4	0.06515	0.05041	0.05058	0.04812	0.04902	0.04874	0.05001	0.04989	0.04965	0.04920	0.04896	0.05020	0.04913	0.05045	0.04907	0.05171	0.04962	0.04814	0.05012	0.04931	0.04961	0.05109	0.05067	0.04982	0.05036		0.04812		0.06515		0.26142		0.23528	0.0032678	
Joint 6	Robot 1	T1	0.04925	0.05240	0.05645	0.05943	0.06029	0.06027	0.06169	0.06243	0.06335	0.06320	0.06423	0.06399	0.06452	0.06435	0.06495	0.06448	0.06392	0.06533	0.06472	0.06543	0.06610	0.06525	0.06597	0.06649	0.06244	0.06301	0.04925	0.04925	0.06649	0.06746	0.25930	0.26992	0.35008	0.0043232	0.0041395
		T2	0.05048	0.05527	0.05575	0.05686	0.05852	0.06070	0.06056	0.06271	0.06351	0.06363	0.06341	0.06449	0.06443	0.06543	0.06582	0.06536	0.06643	0.06665	0.06572	0.06499	0.06709	0.06638	0.06568	0.06629	0.06276		0.05048		0.06709		0.24759		0.31318	0.0043924	
		T3	0.05197	0.05630	0.05861	0.06040	0.06269	0.06287	0.06439	0.06441	0.06490	0.06476	0.06638	0.06482	0.06633	0.06511	0.06639	0.06591	0.06740	0.06611	0.06746	0.06696	0.06694	0.06668	0.06680	0.06708	0.06424		0.05197		0.06746		0.22959		0.29066	0.0038536	
		T4	0.04976	0.05539	0.05735	0.05888	0.05982	0.06035	0.06170	0.06237	0.06233	0.06300	0.06431	0.06401	0.06518	0.06557	0.06447	0.06484	0.06515	0.06588	0.06607	0.06523	0.06516	0.06478	0.06506	0.06547	0.06259		0.04976		0.06607		0.24686		0.31570	0.0039723	
	Robot 2	T1	0.07238	0.07841	0.08018	0.08191	0.08133	0.07998	0.08039	0.08100	0.08274	0.08191	0.08055	0.08164	0.08192	0.08127	0.08158	0.08447	0.08248	0.08217	0.08337	0.08210	0.08227	0.08286	0.08365	0.08261	0.08138	0.08153	0.07238	0.07238	0.08447	0.08447	0.14310	0.14310	0.14130	0.0023158	0.0018970
		T2	0.07436	0.08090	0.08141	0.08240	0.08226	0.08198	0.08228	0.08134	0.08116	0.08184	0.08122	0.08082	0.08205	0.08350	0.08184	0.08108	0.08174	0.08296	0.08260	0.08218	0.08330	0.08268	0.08109	0.08242	0.08164		0.07436		0.08350		0.10951		0.10841	0.0017200	
		T3	0.07331	0.08107	0.08242	0.08173	0.08190	0.08232	0.08226	0.08191	0.08193	0.08217	0.08164	0.08229	0.08244	0.08192	0.08220	0.08183	0.08181	0.08326	0.08178	0.08170	0.08044	0.08169	0.08257	0.08207	0.08161		0.07331		0.08326		0.11957		0.11949	0.0018459	
		T4	0.07425	0.08269	0.08160	0.08237	0.08235	0.08138	0.08247	0.08104	0.08250	0.08233	0.08191	0.08224	0.07985	0.08069	0.08328	0.08040	0.08286	0.08175	0.08067	0.08184	0.08148	0.08105	0.08205	0.08250	0.08148		0.07425		0.08328		0.10847		0.11116	0.0017581	

Table F.3: The relative RMSD values calculated from the cross verified with the identification results of Test 1 without low velocity data

Joint	Robot	Tests	C1	C2	C3	C4	C5	C6	C7	C8	C9	C10	C11	C12
Joint 1	Robot 1	T2	0.12358	0.08440	0.07276	0.06810	0.06498	0.06332	0.06129	0.06140	0.05968	0.05967	0.05955	0.05945
		T3	0.12454	0.08034	0.07240	0.06852	0.06638	0.06271	0.06154	0.06112	0.06032	0.06001	0.05979	0.05924
		T4	0.05490	0.06005	0.05766	0.05741	0.05699	0.05826	0.05791	0.05926	0.06000	0.06329	0.06183	0.06346
	Robot 2	T2	0.04806	0.05063	0.05245	0.05243	0.05191	0.05134	0.05253	0.05207	0.05192	0.05001	0.05237	0.05171
		T3	0.04806	0.04924	0.05163	0.05149	0.05139	0.05059	0.05110	0.05149	0.05141	0.05166	0.05199	0.05048
		T4	0.04748	0.05127	0.05097	0.05083	0.05090	0.05142	0.05150	0.05123	0.05080	0.05070	0.05075	0.05072
Joint 2	Robot 1	T2	0.08608	0.16901	0.13471	0.07902	0.07864	0.08092	0.07662	0.07579	0.07748	0.07636	0.07688	0.07644
		T3	0.08879	0.15356	0.12746	0.07945	0.07806	0.07952	0.07782	0.07651	0.07673	0.07562	0.07689	0.07733
		T4	0.08356	0.15018	0.12902	0.07905	0.07945	0.07777	0.08309	0.07415	0.07432	0.07649	0.07594	0.07822
	Robot 2	T2	0.06637	0.06184	0.06272	0.06054	0.06139	0.06054	0.06019	0.05994	0.05966	0.06022	0.06100	0.06047
		T3	0.06699	0.06099	0.06012	0.05921	0.06064	0.06046	0.06083	0.06112	0.06050	0.06226	0.06059	0.06111
		T4	0.06470	0.06141	0.06096	0.06104	0.06153	0.05994	0.06115	0.06071	0.06056	0.06120	0.06200	0.06062
Joint 3	Robot 1	T2	0.11480	0.10245	0.10618	0.10761	0.10875	0.10412	0.10521	0.10701	0.10796	0.10579	0.10581	0.10582
		T3	0.11341	0.10254	0.10643	0.10670	0.10775	0.10383	0.10326	0.10432	0.10676	0.10627	0.10556	0.10533
		T4	0.11522	0.10199	0.10144	0.10953	0.10447	0.10268	0.10488	0.10468	0.10825	0.10660	0.10536	0.10672
	Robot 2	T2	0.08886	0.08613	0.08659	0.08605	0.08644	0.08573	0.08620	0.08728	0.08586	0.08674	0.08708	0.08652
		T3	0.08842	0.08613	0.08594	0.08669	0.08671	0.08499	0.08672	0.08671	0.08718	0.08749	0.08635	0.08652
		T4	0.08903	0.08673	0.08733	0.08696	0.08631	0.08552	0.08594	0.08683	0.08696	0.08635	0.08708	0.08631
Joint 4	Robot 1	T2	0.13533	0.12968	0.13078	0.12805	0.13073	0.12983	0.12791	0.12713	0.12809	0.12904	0.13397	0.12873
		T3	0.13234	0.13387	0.12778	0.12686	0.12977	0.12693	0.12653	0.12699	0.12763	0.13134	0.12635	0.12565
		T4	0.13123	0.12791	0.12855	0.12639	0.12859	0.12926	0.13030	0.12378	0.12691	0.12709	0.12846	0.13044
	Robot 2	T2	0.10493	0.11218	0.11288	0.11200	0.11381	0.11675	0.11649	0.11479	0.11643	0.11546	0.11516	0.11475
		T3	0.10496	0.11299	0.11439	0.11373	0.11238	0.11374	0.11309	0.11422	0.11514	0.11538	0.11563	0.11593
		T4	0.10728	0.11318	0.11426	0.11506	0.11235	0.11545	0.11520	0.11540	0.11774	0.11429	0.11690	0.11431
Joint 5	Robot 1	T2	0.12296	0.09910	0.11449	0.08744	0.08355	0.08526	0.08232	0.08431	0.08697	0.08983	0.10072	0.09938
		T3	0.11262	0.11346	0.09241	0.14017	0.09034	0.11568	0.11076	0.11849	0.13301	0.12003	0.09952	0.09606
		T4	0.13657	0.12802	0.09933	0.13598	0.14809	0.15918	0.14079	0.16240	0.15671	0.20133	0.13058	0.12041
	Robot 2	T2	0.06699	0.05252	0.05626	0.05242	0.05250	0.04982	0.05106	0.04925	0.04943	0.04962	0.05062	0.04842
		T3	0.06636	0.05293	0.05540	0.05305	0.05305	0.05088	0.05190	0.05088	0.05036	0.05096	0.05000	0.05055
		T4	0.07130	0.05318	0.06053	0.05369	0.05191	0.04988	0.05096	0.04883	0.05013	0.04974	0.04922	0.05017
Joint 6	Robot 1	T2	0.05553	0.05740	0.05949	0.06173	0.06199	0.06136	0.06269	0.06512	0.06353	0.06526	0.06418	0.06697
		T3	0.06676	0.06122	0.07091	0.07507	0.07142	0.06570	0.06986	0.06788	0.06658	0.06809	0.06915	0.06917
		T4	0.07087	0.06453	0.06841	0.06945	0.06465	0.06572	0.06479	0.06742	0.06475	0.06791	0.06546	0.06875
	Robot 2	T2	0.07654	0.08263	0.08436	0.08506	0.08288	0.08212	0.08249	0.08275	0.08139	0.08190	0.08134	0.08064
		T3	0.07339	0.08101	0.08283	0.08142	0.08201	0.08197	0.08230	0.08214	0.08227	0.08239	0.08151	0.08189
		T4	0.08396	0.08863	0.08695	0.08900	0.08750	0.08525	0.08941	0.08841	0.08552	0.08645	0.08426	0.08426

Joint	Robot	Tests	C13	C14	C15	C16	C17	C18	C19	C20	C21	C22	C23	C24	Mean Test	Mean All Tests	Minimum Test	Minimum All Tests	Maximum Test	Maximum All Tests	Diff of MAX/MIN Test	Diff of MAX/MIN All Tests	Diff of Start/End Cycle	Standard Deviation Test	Standard Deviation All Tests
Joint 1	Robot 1	T2	0.05900	0.05902	0.05794	0.05746	0.05656	0.05669	0.05494	0.05622	0.05438	0.05529	0.05526	0.05517	0.06317		0.05438		0.12358		0.55998		0.55361	0.0145060	
		T3	0.05838	0.05776	0.05900	0.06184	0.06287	0.06280	0.06452	0.06475	0.06631	0.06319	0.06428	0.06497	0.06615	0.06364	0.05776	0.05438	0.12454	0.12454	0.53619	0.56338	0.47836	0.0133756	0.0115374
		T4	0.06175	0.06311	0.06159	0.06180	0.06352	0.06389	0.06395	0.06445	0.06651	0.06513	0.06490	0.06681	0.06160		0.05490		0.06681		0.17820		0.21684	0.0032317	
	Robot 2	T2	0.05157	0.05157	0.05165	0.05205	0.05148	0.05169	0.05160	0.05038	0.05192	0.05209	0.05227	0.05189	0.05157		0.04806		0.05253		0.08512		0.07964	0.0009771	
		T3	0.05116	0.05135	0.05086	0.05142	0.05101	0.05102	0.05045	0.05082	0.05108	0.05082	0.05179	0.05036	0.05095	0.05115	0.04806	0.04748	0.05199	0.05253	0.07545	0.09610	0.04789	0.0008460	0.0009152
		T4	0.05122	0.05076	0.05092	0.05089	0.05109	0.05160	0.05135	0.05145	0.05171	0.05051	0.05120	0.05101	0.05093		0.04748		0.05171		0.08174		0.07433	0.0007997	
Joint 2	Robot 1	T2	0.07499	0.07809	0.07732	0.07657	0.07816	0.07819	0.07729	0.07872	0.07660	0.07683	0.07840	0.07761	0.08403		0.07499		0.16901		0.55631		0.09841	0.0216008	
		T3	0.07603	0.07615	0.07687	0.07723	0.07741	0.07938	0.07597	0.07948	0.07723	0.07773	0.07632	0.07683	0.08310	0.08321	0.07562	0.07415	0.15356	0.16901	0.50756	0.56124	0.13469	0.0182801	0.0191029
		T4	0.07717	0.07745	0.07551	0.07842	0.07514	0.07639	0.07554	0.07561	0.07820	0.07486	0.07680	0.07766	0.08250		0.07415		0.15018		0.50622		0.07056	0.0180137	
	Robot 2	T2	0.05955	0.06027	0.06044	0.06047	0.05974	0.06175	0.06015	0.06117	0.05961	0.06146	0.06142	0.06041	0.06089		0.05955		0.06637		0.10273		0.08977	0.0014147	
		T3	0.06139	0.06173	0.06135	0.06184	0.06080	0.06135	0.06213	0.05956	0.05965	0.06064	0.06098	0.06157	0.06116	0.06108	0.05921	0.05921	0.06699	0.06699	0.11614	0.11614	0.08082	0.0014595	0.0013004
		T4	0.06214	0.06151	0.06063	0.05976	0.06077	0.06056	0.06094	0.06099	0.06244	0.06129	0.06207	0.05995	0.06120		0.05976		0.06470		0.07643		0.07340	0.0010140	
Joint 3	Robot 1	T2	0.10661	0.10535	0.10743	0.10624	0.10805	0.10643	0.10794	0.10727	0.10815	0.10898	0.10823	0.10909	0.10714		0.10245		0.11480		0.10762		0.04977	0.0022751	
		T3	0.10617	0.10614	0.10600	0.10688	0.10492	0.10555	0.10639	0.10635	0.10614	0.10865	0.10743	0.10767	0.10627	0.10664	0.10254	0.10144	0.11341	0.11522	0.09591	0.11966	0.05067	0.0020812	0.0023851
		T4	0.10762	0.10459	0.10741	0.10730	0.10676	0.10625	0.10683	0.10610	0.10847	0.10743	0.10777	0.10793	0.10651		0.10144		0.11522		0.11966		0.06325	0.0027635	
	Robot 2	T2	0.08662	0.08700	0.08728	0.08673	0.08684	0.08820	0.08688	0.08706	0.08696	0.08936	0.08763	0.08746	0.08698		0.08573		0.08936		0.04054		0.01583	0.0008717	
		T3	0.08711	0.08825	0.08703	0.08748	0.08718	0.08754	0.08739	0.08649	0.08754	0.08774	0.08828	0.08760	0.08706	0.08704	0.08499	0.08499	0.08842	0.08936	0.03883	0.04889	0.00932	0.0007943	0.0008071
		T4	0.08692	0.08661	0.08694	0.08647	0.08704	0.08769	0.08758	0.08760	0.08749	0.08778	0.08853	0.08764	0.08707		0.08552		0.08903		0.03942		0.01557	0.0007841	
Joint 4	Robot 1	T2	0.12497	0.12786	0.13191	0.13009	0.12765	0.13087	0.12696	0.12696	0.12789	0.13002	0.12717	0.12919	0.12920		0.12497		0.13533		0.07651		0.04532	0.0023225	
		T3	0.12579	0.12878	0.12863	0.12873	0.12586	0.12726	0.12722	0.12871	0.12813	0.12711	0.12735	0.12881	0.12810	0.12862	0.12565	0.12378	0.13387	0.13533	0.06140	0.08530	0.02668	0.0020428	0.0022479
		T4	0.12571	0.12641	0.13207	0.13112	0.12871	0.12974	0.12592	0.12875	0.12695	0.13279	0.12636	0.13196	0.12856		0.12378		0.13279		0.06786		0.00552	0.0023222	
	Robot 2	T2	0.12015	0.11747	0.11574	0.11792	0.11808	0.11790	0.11924	0.11735	0.11721	0.11845	0.11887	0.11839	0.11593		0.10493		0.12015		0.12670		0.12831	0.0032133	
		T3	0.11871	0.11703	0.11566	0.11841	0.11821	0.11824	0.11744	0.11881	0.11900	0.11728	0.11662	0.11966	0.11569	0.11557	0.10496	0.10493	0.11966	0.12015	0.12288	0.12670	0.14009	0.0031354	0.0028520
		T4	0.11644	0.11495	0.11732	0.11620	0.11523	0.11515	0.11626	0.11548	0.11630	0.11343	0.11677	0.11694	0.11508		0.10728		0.11774		0.08878		0.09003	0.0021328	
Joint 5	Robot 1	T2	0.10427	0.10150	0.09610	0.08680	0.09307	0.08603	0.09443	0.09945	0.08985	0.08304	0.09148	0.09024	0.09386		0.08232		0.12296		0.33055		0.26611	0.0101174	
		T3	0.11500	0.09180	0.09432	0.11455	0.08924	0.10308	0.09816	0.12293	0.10165	0.12107	0.13163	0.09360	0.10915	0.11212	0.08924	0.08232	0.14017	0.20133	0.36329	0.59113	0.16884	0.0147214	0.0245855
		T4	0.10611	0.11704	0.12730	0.11252	0.10401	0.12122	0.12133	0.10894	0.09442	0.12014	0.17443	0.17351	0.13335		0.09442		0.20133		0.53100		0.27047	0.0268214	
	Robot 2	T2	0.04932	0.04954	0.04913	0.04946	0.05056	0.05121	0.05093	0.05122	0.05032	0.05121	0.05086	0.05097	0.05140		0.04842		0.06699		0.27715		0.23917	0.0036907	
		T3	0.05142	0.05128	0.05141	0.05160	0.05154	0.05235	0.05018	0.05091	0.05188	0.05127	0.05253	0.05165	0.05226	0.05184	0.05000	0.04842	0.06636	0.07130	0.24653	0.32086	0.22169	0.0032208	0.0039035
		T4	0.04992	0.05043	0.04991	0.05221	0.05035	0.05020	0.04981	0.04972	0.04951	0.05104	0.05141	0.05060	0.05186		0.04883		0.07130		0.31521		0.29037	0.0047597	
Joint 6	Robot 1	T2	0.06687	0.06677	0.06801	0.06643	0.06788	0.06910	0.07021	0.06922	0.07122	0.06896	0.06914	0.06882	0.06533		0.05553		0.07122		0.22032		0.23928	0.0041408	
		T3	0.07153	0.06890	0.06936	0.06803	0.06957	0.06988	0.07120	0.06991	0.07229	0.07020	0.06982	0.06871	0.06922	0.06750	0.06122	0.05553	0.07507	0.07507	0.18443	0.26027	0.02924	0.0026175	0.0034681
		T4	0.06857	0.06857	0.06572	0.06763	0.06776	0.07007	0.07252	0.06952	0.07093	0.07010	0.06815	0.06835	0.06794		0.06453		0.07252		0.11023		0.03565	0.0022202	
	Robot 2	T2	0.08190	0.08390	0.08266	0.08169	0.08192	0.08313	0.08290	0.08245	0.08338	0.08287	0.08125	0.08287	0.08229		0.07654		0.08506		0.10017		0.08272	0.0015852	
		T3	0.08239	0.08273	0.08276	0.08212	0.08183	0.08325	0.08177	0.08185	0.08034	0.08188	0.08275	0.08259	0.08172	0.08309	0.07339	0.07339	0.08325	0.08941	0.11837	0.17915	0.12527	0.0018822	0.0024094
		T4	0.08207	0.08262	0.08486	0.08254	0.08546	0.08388	0.08319	0.08464	0.08417	0.08375	0.08475	0.08436	0.08525		0.08207		0.08941		0.08206		0.00475	0.0020994	

Table F.4: The relative RMSD values calculated from the cross verified with the identification results of Test 2 without low velocity data

		Tests	Cycles																								Mean		Minimum		Maximum		Diff of MAX/MIN		Diff of Start/End Cycle	Standard Deviation	
			C1	C2	C3	C4	C5	C6	C7	C8	C9	C10	C11	C12	C13	C14	C15	C16	C17	C18	C19	C20	C21	C22	C23	C24	Test	All Tests	Test	All Tests	Test	All Tests	Test	All Tests		Test	All Tests
Joint 1	Robot 1	T1	0.12585	0.08332	0.07227	0.06786	0.06530	0.06298	0.06074	0.06017	0.05939	0.05879	0.05891	0.05839	0.05879	0.05827	0.05697	0.05637	0.05626	0.05631	0.05504	0.05591	0.05386	0.05467	0.05435	0.05438	0.06271		0.05386		0.12585		0.57204		0.56790	0.0150127	
		T3	0.04917	0.05315	0.05305	0.05279	0.05337	0.05362	0.05388	0.05349	0.05419	0.05386	0.05365	0.05337	0.05349	0.06868	0.06815	0.07207	0.07260	0.07201	0.07172	0.07383	0.07137	0.06937	0.07019	0.07058	0.06132	0.06693	0.04917	0.04917	0.07383	0.12585	0.33400	0.60927	0.43528	0.0091773	0.0133520
		T4	0.10815	0.10365	0.08229	0.07558	0.07376	0.07484	0.07122	0.07360	0.07372	0.07850	0.07573	0.07838	0.07454	0.07666	0.07220	0.07181	0.07366	0.07320	0.07097	0.07301	0.07149	0.07167	0.07104	0.07271	0.07677		0.07097		0.10815		0.34378		0.32771	0.0094011	
	Robot 2	T1	0.04859	0.05174	0.05184	0.05121	0.05201	0.05206	0.05220	0.05146	0.05226	0.05141	0.05174	0.05175	0.05167	0.05151	0.05148	0.05088	0.05136	0.05164	0.05120	0.05141	0.05068	0.05193	0.05080	0.05164	0.05144		0.04859		0.05226		0.07025		0.06277	0.0007315	
		T3	0.04469	0.04905	0.05169	0.05163	0.05175	0.05108	0.05098	0.05162	0.05175	0.05185	0.05209	0.05090	0.05147	0.05149	0.05126	0.05159	0.05125	0.05128	0.05096	0.05108	0.05122	0.05118	0.05203	0.05068	0.05102	0.05115	0.04469	0.04469	0.05209	0.05226	0.14201	0.14487	0.13390	0.0014767	0.0012315
		T4	0.04487	0.05084	0.05104	0.05091	0.05117	0.05187	0.05144	0.05118	0.05103	0.05081	0.05077	0.05107	0.05148	0.05089	0.05126	0.05103	0.05133	0.05161	0.05194	0.05184	0.05191	0.05090	0.05152	0.05135	0.05100		0.04487		0.05194		0.13619		0.14444	0.0013569	
Joint 2	Robot 1	T1	0.08530	0.16986	0.13719	0.08057	0.08374	0.07865	0.07879	0.07901	0.07983	0.08048	0.07909	0.07844	0.08279	0.08114	0.08211	0.08007	0.08032	0.08195	0.07973	0.07946	0.07976	0.08155	0.08108	0.08133	0.08676		0.07844		0.16986		0.53822		0.04655	0.0211846	
		T3	0.07957	0.08966	0.07497	0.07731	0.07589	0.08009	0.07662	0.07655	0.07707	0.07575	0.07673	0.07745	0.07643	0.07676	0.07683	0.07743	0.07742	0.08062	0.07645	0.07980	0.07783	0.07764	0.07683	0.07670	0.07785	0.08058	0.07497	0.07432	0.08966	0.16986	0.16390	0.56248	0.03618	0.0028749	0.0129797
		T4	0.07916	0.07881	0.07561	0.07486	0.07808	0.07909	0.08109	0.07432	0.07619	0.07648	0.07583	0.07798	0.07804	0.07815	0.07679	0.07903	0.07557	0.07554	0.07614	0.07589	0.07865	0.07478	0.07768	0.07732	0.07713		0.07432		0.08109		0.08346		0.02327	0.0017157	
	Robot 2	T1	0.06724	0.06194	0.06255	0.06123	0.06122	0.05998	0.06009	0.05921	0.06096	0.06037	0.05988	0.06078	0.06085	0.05950	0.05991	0.06128	0.06140	0.06160	0.05996	0.06040	0.06087	0.06193	0.06114	0.06173	0.06108		0.05921		0.06724		0.11951		0.08200	0.0015598	
		T3	0.06738	0.06084	0.06007	0.05900	0.06034	0.06024	0.06103	0.06118	0.06055	0.06210	0.06059	0.06078	0.06140	0.06170	0.06118	0.06188	0.06078	0.06141	0.06195	0.05917	0.05966	0.06058	0.06085	0.06173	0.06110	0.06109	0.05900	0.05900	0.06738	0.06738	0.12439	0.12439	0.08390	0.0015672	0.0013729
		T4	0.06450	0.06135	0.06066	0.06114	0.06115	0.05983	0.06128	0.06068	0.06054	0.06073	0.06215	0.06093	0.06231	0.06132	0.06029	0.05983	0.06080	0.06057	0.06072	0.06044	0.06187	0.06091	0.06149	0.06030	0.06107		0.05983		0.06450		0.07245		0.06508	0.0009638	
Joint 3	Robot 1	T1	0.11664	0.10604	0.10660	0.10896	0.10808	0.10804	0.10694	0.10631	0.10814	0.10648	0.10855	0.10791	0.10852	0.10963	0.11052	0.11109	0.10874	0.10791	0.10816	0.11038	0.10973	0.10986	0.10852	0.10930	0.10879		0.10604		0.11664		0.09093		0.06291	0.0021513	
		T3	0.10006	0.10315	0.10371	0.10485	0.10402	0.10562	0.10297	0.10401	0.10349	0.10473	0.10567	0.10501	0.10457	0.10661	0.10450	0.10642	0.10371	0.10474	0.10501	0.10444	0.10284	0.10482	0.10401	0.10669	0.10440	0.10601	0.10006	0.09950	0.10669	0.11664	0.06211	0.14697	0.06623	0.0014109	0.0026632
		T4	0.09950	0.10264	0.10247	0.10448	0.10314	0.10384	0.10382	0.10459	0.10427	0.10507	0.10558	0.10601	0.10600	0.10450	0.10605	0.10638	0.10461	0.10584	0.10530	0.10485	0.10630	0.10590	0.10795	0.10691	0.10483		0.09950		0.10795		0.07824		0.07453	0.0017464	
	Robot 2	T1	0.08814	0.08576	0.08727	0.08620	0.08603	0.08590	0.08531	0.08650	0.08654	0.08519	0.08633	0.08696	0.08674	0.08648	0.08675	0.08703	0.08729	0.08691	0.08798	0.08825	0.08702	0.08771	0.08833	0.08789	0.08685		0.08519		0.08833		0.03562		0.00287	0.0008927	
		T3	0.08753	0.08612	0.08575	0.08661	0.08719	0.08569	0.08649	0.08699	0.08691	0.08739	0.08647	0.08671	0.08653	0.08779	0.08676	0.08776	0.08689	0.08714	0.08712	0.08668	0.08737	0.08728	0.08919	0.08757	0.08700	0.08693	0.08569	0.08519	0.08919	0.08937	0.03918	0.04676	0.00043	0.0007308	0.0007879
		T4	0.08788	0.08663	0.08696	0.08678	0.08663	0.08618	0.08570	0.08716	0.08638	0.08636	0.08718	0.08634	0.08627	0.08605	0.08667	0.08669	0.08667	0.08726	0.08725	0.08778	0.08730	0.08731	0.08937	0.08758	0.08693		0.08570		0.08937		0.04099		0.00335	0.0007582	
Joint 4	Robot 1	T1	0.13477	0.12817	0.12542	0.12570	0.12492	0.12356	0.12513	0.12435	0.12472	0.12581	0.12763	0.12189	0.12552	0.12148	0.12230	0.12360	0.12369	0.12278	0.12560	0.12619	0.12405	0.12144	0.12582	0.12264	0.12488		0.12144		0.13477		0.09891		0.09004	0.0027647	
		T3	0.12165	0.14373	0.13032	0.12516	0.12718	0.12611	0.12616	0.12576	0.12671	0.13096	0.12832	0.12232	0.12721	0.12687	0.12733	0.12699	0.12374	0.12520	0.12563	0.12829	0.12614	0.12460	0.12611	0.12759	0.12709	0.12649	0.12165	0.12144	0.14373	0.14373	0.15367	0.15511	0.04887	0.0041209	0.0033189
		T4	0.12605	0.13018	0.13021	0.12515	0.12709	0.13059	0.13093	0.12305	0.12526	0.12692	0.12762	0.12637	0.12706	0.12482	0.13044	0.12805	0.12638	0.12690	0.12558	0.12919	0.12538	0.12904	0.12618	0.13166	0.12751		0.12305		0.13166		0.06538		0.04449	0.0022887	
	Robot 2	T1	0.10427	0.10970	0.10974	0.11085	0.11328	0.11368	0.11223	0.10988	0.11328	0.11323	0.11301	0.11370	0.11487	0.11544	0.11552	0.11447	0.11414	0.11679	0.11484	0.11458	0.11540	0.11518	0.11504	0.11477	0.11325		0.10427		0.11679		0.10713		0.10064	0.0027150	
		T3	0.10546	0.11068	0.11200	0.11300	0.11274	0.11311	0.11129	0.11270	0.11337	0.11474	0.11457	0.11644	0.11674	0.11590	0.11573	0.11790	0.11779	0.11777	0.11610	0.11712	0.11843	0.11698	0.11426	0.11726	0.11467	0.11388	0.10546	0.10427	0.11843	0.11843	0.10949	0.11955	0.11186	0.0030072	0.0026867
		T4	0.10631	0.11009	0.11080	0.11383	0.11248	0.11441	0.11318	0.11340	0.11495	0.11335	0.11558	0.11433	0.11407	0.11366	0.11728	0.11551	0.11485	0.11451	0.11488	0.11363	0.11569	0.11314	0.11463	0.11469	0.11372		0.10631		0.11728		0.09355		0.07879	0.0021841	
Joint 5	Robot 1	T1	0.12174	0.12029	0.13383	0.09778	0.08324	0.08632	0.08948	0.08089	0.08349	0.09347	0.10740	0.11182	0.12941	0.12741	0.11717	0.08797	0.11477	0.10783	0.11347	0.09903	0.10214	0.09396	0.09340	0.09499	0.10380		0.08089		0.13383		0.39554		0.21972	0.0158360	
		T3	0.14160	0.14696	0.12632	0.16850	0.09290	0.11004	0.12588	0.11040	0.14106	0.14825	0.13302	0.11486	0.14399	0.10921	0.10955	0.10615	0.09754	0.10772	0.11214	0.10452	0.11497	0.12752	0.11454	0.08914	0.12070	0.12432	0.08914	0.08089	0.16850	0.23779	0.47096	0.65981	0.37047	0.0197650	0.0286416
		T4	0.17420	0.17044	0.14779	0.16245	0.15334	0.15087	0.15845	0.15318	0.16719	0.23779	0.16857	0.14758	0.13055	0.14964	0.14913	0.10665	0.11710	0.12816	0.13888	0.10039	0.10205	0.12571	0.16025	0.16239	0.14845		0.10039		0.23779		0.57783		0.06780	0.0288197	
	Robot 2	T1	0.07100	0.05294	0.05625	0.05161	0.05104	0.04890	0.05393	0.05085	0.04902	0.04962	0.04968	0.05012	0.04924	0.04982	0.04866	0.04868	0.04768	0.05028	0.05083	0.05008	0.04996	0.05117	0.05022	0.05020	0.05132		0.04768		0.07100		0.32850		0.29290	0.0045715	
		T3	0.06408	0.05083	0.05053	0.04974	0.05008	0.05022	0.05258	0.05152	0.05008	0.04984	0.04958	0.05082	0.05090	0.05072	0.05132	0.05100	0.05063	0.05190	0.05035	0.05045	0.05139	0.05150	0.05272	0.05150	0.05143	0.05111	0.04958	0.04768	0.06408	0.07100	0.22620	0.32850	0.19638	0.0028163	0.0036783
		T4	0.06648	0.05106	0.05182	0.04875	0.04867	0.04911	0.05092	0.04932	0.04988	0.04861	0.04873	0.05039	0.04923	0.04968	0.04976	0.05158	0.04945	0.04980	0.04967	0.04902	0.04879	0.05126	0.05158	0.05036	0.05058		0.04861		0.06648		0.26881		0.24247	0.0035340	
Joint 6	Robot 1	T1	0.05690	0.05499	0.06078	0.06464	0.06337	0.06094	0.06373	0.06529	0.06367	0.06450	0.06464	0.06576	0.06704	0.06528	0.06701	0.06573	0.06598	0.06793	0.06908	0.06958	0.07007	0.06762	0.06931	0.06922	0.06513		0.05499		0.07007		0.21520		0.21648	0.0037982	
		T3	0.05672	0.05742	0.06192	0.06411	0.06430	0.06387	0.06549	0.06476	0.06593	0.06511	0.06730	0.06510	0.06696	0.06585	0.06642	0.06600	0.06757	0.06635	0.06728	0.06714	0.06696	0.06672	0.06676	0.06702	0.06513	0.06461	0.05672	0.05499	0.06757	0.07007	0.16069	0.21520	0.18170	0.0028283	0.0031465
		T4	0.05733	0.05859	0.05978	0.06038	0.06007	0.06294	0.06194	0.06301	0.06390	0.06402	0.06449	0.06438	0.06525	0.06590	0.06447	0.06516	0.06550	0.06608	0.06614	0.06516	0.06516	0.06534	0.06507	0.06543	0.06356		0.05733		0.06614		0.13323		0.14137	0.0025363	
	Robot 2	T1	0.07599	0.08029	0.08267	0.08386	0.08192	0.08051	0.08057	0.08203	0.08273	0.08190	0.08070	0.08188	0.08224	0.08177	0.08248	0.08495	0.08292	0.08262	0.08371	0.08233	0.08241	0.08310	0.08386	0.08321	0.08211		0.07599		0.08495		0.10554		0.09501	0.0017300	
		T3	0.07739	0.08203	0.08311	0.08308	0.08244	0.08292	0.08224	0.08260	0.08234	0.08222	0.08132	0.08203	0.08266	0.08218	0.08211	0.08158	0.08166	0.08330	0.08182	0.08176	0.08026	0.08182	0.08259	0.08217	0.08198	0.08299	0.07739	0.07599	0.08330	0.08778	0.07094	0.13434	0.06176	0.0011738	0.0022181
		T4	0.07669	0.08414	0.08184	0.08333	0.08467	0.08372	0.08747	0.08377	0.08519	0.08682	0.08538	0.08487	0.08312	0.08479	0.08778	0.08491	0.08759	0.08589	0.08521	0.08639	0.08532	0.08541	0.08616	0.08667	0.08488		0.07669		0.08778		0.12631		0.13011	0.0022864	

Table F.5: The relative RMSD values calculated from the cross verified with the identification results of Test 3 without low velocity data

		Tests	C1	C2	C3	C4	C5	C6	C7	C8	C9	C10	C11	C12
Joint 1	Robot 1	T1	0.12720	0.07956	0.07181	0.06868	0.06634	0.06253	0.06083	0.06059	0.05953	0.05943	0.05940	0.05862
		T2	0.05010	0.05385	0.05296	0.05322	0.05290	0.05379	0.05373	0.05427	0.05363	0.05418	0.05393	0.05386
		T4	0.10947	0.09933	0.08155	0.07644	0.07486	0.07404	0.07133	0.07405	0.07396	0.07944	0.07653	0.07867
	Robot 2	T1	0.04881	0.05173	0.05161	0.05080	0.05151	0.05155	0.05232	0.05110	0.05211	0.05138	0.05143	0.05133
		T2	0.04490	0.05045	0.05233	0.05217	0.05179	0.05130	0.05251	0.05187	0.05212	0.05019	0.05218	0.05171
		T4	0.04475	0.05093	0.05077	0.05062	0.05075	0.05137	0.05146	0.05085	0.05091	0.05064	0.05046	0.05068
Joint 2	Robot 1	T1	0.08700	0.15050	0.12943	0.08031	0.08284	0.07901	0.08126	0.07982	0.08009	0.08076	0.07990	0.07904
		T2	0.07842	0.08325	0.07422	0.07659	0.07554	0.08172	0.07798	0.07669	0.07809	0.07683	0.07757	0.07709
		T4	0.07919	0.07727	0.07508	0.07510	0.07725	0.07727	0.07833	0.07464	0.07552	0.07610	0.07627	0.07779
	Robot 2	T1	0.06705	0.06197	0.06238	0.06134	0.06153	0.06020	0.06013	0.05925	0.06077	0.06023	0.05975	0.06081
		T2	0.06657	0.06173	0.06252	0.06044	0.06144	0.06052	0.06040	0.06004	0.05950	0.05990	0.06086	0.06013
		T4	0.06493	0.06129	0.06070	0.06127	0.06153	0.06009	0.06113	0.06073	0.06042	0.06050	0.06203	0.06099
Joint 3	Robot 1	T1	0.11820	0.10700	0.10697	0.10739	0.10683	0.10605	0.10644	0.10455	0.10794	0.10723	0.10705	0.10830
		T2	0.10332	0.10392	0.10380	0.10419	0.10363	0.10388	0.10441	0.10490	0.10452	0.10507	0.10430	0.10594
		T4	0.10007	0.10353	0.10287	0.10445	0.10206	0.10216	0.10393	0.10270	0.10404	0.10568	0.10386	0.10690
	Robot 2	T1	0.08904	0.08616	0.08755	0.08704	0.08514	0.08595	0.08583	0.08671	0.08676	0.08568	0.08635	0.08690
		T2	0.08888	0.08654	0.08671	0.08682	0.08601	0.08652	0.08649	0.08776	0.08579	0.08714	0.08723	0.08665
		T4	0.08803	0.08685	0.08721	0.08741	0.08578	0.08609	0.08598	0.08691	0.08685	0.08671	0.08708	0.08632
Joint 4	Robot 1	T1	0.14135	0.13308	0.12528	0.12564	0.12473	0.12178	0.12442	0.12439	0.12523	0.12272	0.12265	0.12280
		T2	0.13161	0.14438	0.13304	0.12622	0.12792	0.12706	0.12692	0.12593	0.12772	0.12555	0.13105	0.12616
		T4	0.12864	0.13579	0.12949	0.12465	0.12371	0.12617	0.12721	0.12163	0.12621	0.12386	0.12605	0.12793
	Robot 2	T1	0.10489	0.10948	0.11013	0.11137	0.11529	0.11270	0.11348	0.11282	0.11445	0.11418	0.11465	0.11393
		T2	0.10605	0.10969	0.11084	0.11174	0.11620	0.11526	0.11599	0.11613	0.11580	0.11574	0.11576	0.11550
		T4	0.10540	0.10908	0.11112	0.11329	0.11344	0.11246	0.11318	0.11502	0.11578	0.11345	0.11647	0.11367
Joint 5	Robot 1	T1	0.10721	0.11025	0.10037	0.12399	0.08819	0.11028	0.10437	0.10910	0.11714	0.10391	0.09597	0.10471
		T2	0.13861	0.12724	0.11280	0.14872	0.09123	0.10325	0.11506	0.10317	0.12861	0.13334	0.12474	0.11100
		T4	0.12069	0.10809	0.10079	0.11101	0.12670	0.11240	0.10609	0.11126	0.10650	0.15070	0.11475	0.11181
	Robot 2	T1	0.07139	0.05159	0.05584	0.05170	0.05155	0.04890	0.05114	0.05048	0.04825	0.04979	0.04964	0.04995
		T2	0.06525	0.04891	0.05105	0.04915	0.04996	0.04910	0.04879	0.04952	0.04836	0.04866	0.05017	0.04855
		T4	0.06583	0.05018	0.05138	0.04794	0.04913	0.04854	0.04961	0.04903	0.04901	0.04865	0.04838	0.05018
Joint 6	Robot 1	T1	0.06375	0.05743	0.06899	0.07429	0.06941	0.06298	0.06734	0.06603	0.06524	0.06673	0.06701	0.06811
		T2	0.05181	0.05581	0.05844	0.06017	0.06060	0.06149	0.06170	0.06267	0.06444	0.06448	0.06460	0.06522
		T4	0.05013	0.05635	0.05722	0.05933	0.06080	0.06076	0.06205	0.06243	0.06222	0.06306	0.06481	0.06391
	Robot 2	T1	0.07341	0.07896	0.08084	0.08235	0.08142	0.08113	0.08052	0.08115	0.08293	0.08244	0.08118	0.08219
		T2	0.07806	0.08230	0.08281	0.08518	0.08282	0.08368	0.08239	0.08230	0.08167	0.08228	0.08161	0.08113
		T4	0.08582	0.08772	0.08449	0.08887	0.08727	0.08809	0.08828	0.08746	0.08733	0.08905	0.08603	0.08525

		Tests	C13	C14	C15	C16	C17	C18	C19	C20	C21	C22	C23	C24	Mean		Minimum		Maximum		Diff of MAX/MIN		Diff of	Standard Deviation	
															Test	All Tests	Test	All Tests	Test	All Tests	Test	All Tests	Start/End Cycle	Test	All Tests
Joint 1	Robot 1	T1	0.05885	0.05731	0.05752	0.06107	0.06146	0.06154	0.06308	0.06364	0.06477	0.06177	0.06206	0.06346	0.06546		0.05731		0.12720		0.54943		0.50112	0.0140393	
		T2	0.05424	0.06897	0.06773	0.07229	0.07161	0.07121	0.07037	0.07311	0.07036	0.06856	0.06887	0.06981	0.06115	0.06504	0.05010	0.05010	0.07311	0.12720	0.31474	0.60613	0.39351	0.0086724	0.0132082
		T4	0.07441	0.05539	0.05440	0.05424	0.05401	0.05492	0.05417	0.05525	0.05451	0.05449	0.05421	0.05450	0.06851		0.05401		0.10947		0.50666		0.50218	0.0154174	
	Robot 2	T1	0.05118	0.05130	0.05137	0.05064	0.05107	0.05138	0.05085	0.05119	0.05051	0.05172	0.05055	0.05119	0.05119		0.04881		0.05232		0.06718		0.04888	0.0006742	
		T2	0.05140	0.05149	0.05192	0.05194	0.05142	0.05168	0.05172	0.05042	0.05189	0.05216	0.05226	0.05173	0.05140	0.05111	0.04490	0.04475	0.05251	0.05251	0.14486	0.14788	0.15207	0.0015075	0.0012364
		T4	0.05099	0.05066	0.05120	0.05077	0.05108	0.05157	0.05148	0.05149	0.05159	0.05056	0.05120	0.05073	0.05073		0.04475		0.05159		0.13268		0.13382	0.0013218	
Joint 2	Robot 1	T1	0.08255	0.08226	0.08231	0.08021	0.08000	0.08218	0.07956	0.08012	0.07959	0.08198	0.08057	0.08195	0.08597		0.07901		0.15050		0.47502		0.05801	0.0170036	
		T2	0.07514	0.07980	0.07747	0.07686	0.07784	0.07969	0.07762	0.07967	0.07700	0.07723	0.07839	0.07809	0.07787	0.08020	0.07422	0.07422	0.08325	0.15050	0.10839	0.50681	0.00423	0.0019576	0.0106079
		T4	0.07696	0.07696	0.07630	0.07929	0.07526	0.07848	0.07553	0.07608	0.07828	0.07533	0.07716	0.07720	0.07678		0.07464		0.07929		0.05860		0.02513	0.0013358	
	Robot 2	T1	0.06075	0.05931	0.05995	0.06131	0.06143	0.06155	0.06003	0.06071	0.06084	0.06189	0.06131	0.06163	0.06109		0.05925		0.06705		0.11638		0.08078	0.0015223	
		T2	0.05947	0.06006	0.06031	0.06056	0.05975	0.06175	0.06005	0.06110	0.05956	0.06134	0.06145	0.06047	0.06083	0.06101	0.05947	0.05925	0.06657	0.06705	0.10670	0.11638	0.09161	0.0014601	0.0013427
		T4	0.06222	0.06131	0.06046	0.05997	0.06079	0.06065	0.06079	0.06069	0.06215	0.06070	0.06169	0.05994	0.06112		0.05994		0.06493		0.07684		0.07684	0.0010309	
Joint 3	Robot 1	T1	0.10851	0.10768	0.11022	0.10987	0.10942	0.10798	0.10920	0.11034	0.11153	0.11107	0.10991	0.10962	0.10872		0.10455		0.11820		0.11552		0.07261	0.0026459	
		T2	0.10496	0.10381	0.10557	0.10457	0.10754	0.10570	0.10764	0.10531	0.10666	0.10641	0.10620	0.10841	0.10519	0.10624	0.10332	0.10007	0.10841	0.11820	0.04701	0.15335	0.04933	0.0013836	0.0027372
		T4	0.10664	0.10268	0.10605	0.10609	0.10548	0.10584	0.10513	0.10443	0.10741	0.10671	0.10902	0.10782	0.10481		0.10007		0.10902		0.08202		0.07736	0.0021294	
	Robot 2	T1	0.08725	0.08773	0.08704	0.08757	0.08816	0.08717	0.08845	0.08809	0.08749	0.08805	0.08764	0.08813	0.08716		0.08514		0.08904		0.04377		0.01018	0.0009649	
		T2	0.08652	0.08777	0.08730	0.08756	0.08743	0.08806	0.08709	0.08707	0.08724	0.08924	0.08780	0.08769	0.08722	0.08716	0.08579	0.08514	0.08924	0.08924	0.03866	0.04591	0.01341	0.0008112	0.0008161
		T4	0.08674	0.08704	0.08676	0.08686	0.08737	0.08721	0.08744	0.08737	0.08779	0.08755	0.08878	0.08783	0.08708		0.08578		0.08878		0.03375		0.00233	0.0006757	
Joint 4	Robot 1	T1	0.12480	0.12179	0.12274	0.12308	0.12463	0.12280	0.12564	0.12639	0.12481	0.12144	0.12596	0.12440	0.12511		0.12144		0.14135		0.14085		0.11992	0.0041697	
		T2	0.12565	0.12618	0.13099	0.12769	0.12639	0.12882	0.12529	0.12669	0.12651	0.12740	0.12606	0.12966	0.12837	0.12689	0.12529	0.12144	0.14438	0.14438	0.13222	0.15889	0.01478	0.0040155	0.0039548
		T4	0.12587	0.12337	0.13025	0.12864	0.12757	0.12740	0.12562	0.12868	0.12557	0.12987	0.12649	0.13166	0.12718		0.12163		0.13579		0.10429		0.02349	0.0030126	
	Robot 2	T1	0.11541	0.11593	0.11592	0.11509	0.11436	0.11667	0.11623	0.11482	0.11518	0.11461	0.11526	0.11593	0.11387		0.10489		0.11667		0.10096		0.10518	0.0026466	
		T2	0.11869	0.11687	0.11621	0.11806	0.11789	0.11728	0.11932	0.11587	0.11636	0.11758	0.11685	0.11712	0.11553	0.11433	0.10605	0.10489	0.11932	0.11932	0.11117	0.12087	0.10432	0.0030394	0.0028144
		T4	0.11383	0.11394	0.11696	0.11508	0.11403	0.11414	0.11542	0.11322	0.11470	0.11232	0.11452	0.11559	0.11359		0.10540		0.11696		0.09879		0.09668	0.0024290	
Joint 5	Robot 1	T1	0.12452	0.11547	0.11199	0.11006	0.11236	0.11421	0.11660	0.12014	0.10834	0.12074	0.13288	0.10043	0.11097		0.08819		0.13288		0.33635		0.06328	0.0098753	
		T2	0.13087	0.10434	0.10573	0.10007	0.09938	0.09899	0.11216	0.10143	0.11077	0.11935	0.11440	0.09108	0.11360	0.11311	0.09108	0.08819	0.14872	0.15867	0.38758	0.44420	0.34293	0.0151134	0.0136238
		T4	0.10091	0.11693	0.12039	0.10091	0.10539	0.11494	0.11711	0.10511	0.09723	0.09863	0.13724	0.15867	0.11476		0.09723		0.15867		0.38720		0.31463	0.0154647	
	Robot 2	T1	0.05007	0.04971	0.04860	0.04905	0.04828	0.04948	0.05026	0.05020	0.05148	0.05048	0.04941	0.04998	0.05114		0.04825		0.07139		0.32416		0.29990	0.0045863	
		T2	0.04961	0.04882	0.04901	0.04930	0.05014	0.04989	0.05057	0.05087	0.05125	0.05078	0.05022	0.05061	0.05036	0.05060	0.04836	0.04794	0.06525	0.07139	0.25879	0.32847	0.22428	0.0032855	0.0037796
		T4	0.04960	0.04969	0.04960	0.05197	0.04959	0.04877	0.04951	0.04921	0.05031	0.05050	0.05068	0.04996	0.05030		0.04794		0.06583		0.27175		0.24118	0.0034376	
Joint 6	Robot 1	T1	0.06993	0.06785	0.06801	0.06709	0.06641	0.06903	0.06893	0.06835	0.07155	0.06876	0.06912	0.06865	0.06754		0.05743		0.07429		0.22698		0.07688	0.0031696	
		T2	0.06508	0.06626	0.06602	0.06576	0.06634	0.06670	0.06604	0.06509	0.06738	0.06658	0.06583	0.06663	0.06355	0.06463	0.05181	0.05013	0.06738	0.07429	0.23098	0.32521	0.28589	0.0038639	0.0041561
		T4	0.06531	0.06545	0.06482	0.06488	0.06525	0.06578	0.06645	0.06525	0.06507	0.06504	0.06513	0.06573	0.06280		0.05013		0.06645		0.24564		0.31114	0.0038450	
	Robot 2	T1	0.08202	0.08172	0.08249	0.08510	0.08310	0.08246	0.08352	0.08216	0.08264	0.08288	0.08387	0.08308	0.08181		0.07341		0.08510		0.13738		0.13170	0.0021768	
		T2	0.08197	0.08334	0.08203	0.08136	0.08193	0.08303	0.08276	0.08219	0.08350	0.08260	0.08109	0.08233	0.08226	0.08346	0.07806	0.07341	0.08518	0.08905	0.08363	0.17560	0.05480	0.0012682	0.0026652
		T4	0.08223	0.08496	0.08769	0.08498	0.08780	0.08518	0.08410	0.08569	0.08554	0.08473	0.08627	0.08645	0.08630		0.08223		0.08905		0.07649		0.00734	0.0016830	

Table F.6: The relative RMSD values calculated from the cross verified with the identification results of Test 4 without low velocity data

Joint	Robot	Tests	C1	C2	C3	C4	C5	C6	C7	C8	C9	C10	C11	C12	C13	C14	C15	C16	C17	C18	C19	C20	C21	C22	C23	C24	Mean Test	Mean All Tests	Minimum Test	Minimum All Tests	Maximum Test	Maximum All Tests	Diff of MAX/MIN Test	Diff of MAX/MIN All Tests	Diff of Start/End Cycle	Standard Deviation Test	Standard Deviation All Tests
Joint 1	Robot 1	T1	0.05827	0.05795	0.05495	0.05503	0.05549	0.05684	0.05642	0.05708	0.05886	0.06194	0.06052	0.06207	0.06120	0.06199	0.06010	0.06057	0.06226	0.06199	0.06272	0.06254	0.06469	0.06362	0.06337	0.06513	0.06023		0.05495		0.06513		0.15628		0.11764	0.0030841	
		T2	0.10735	0.10332	0.08076	0.07400	0.07229	0.07400	0.07052	0.07288	0.07298	0.07807	0.07517	0.07807	0.07429	0.07635	0.07173	0.07164	0.07280	0.07182	0.06983	0.07158	0.07022	0.07078	0.07032	0.07176	0.07594	0.06802	0.06983	0.05373	0.10735	0.10823	0.34952	0.50355	0.33148	0.0094821	0.0121505
		T3	0.10823	0.09863	0.08011	0.07454	0.07376	0.07308	0.07074	0.07276	0.07367	0.07881	0.07576	0.07801	0.07359	0.05460	0.05433	0.05373	0.05417	0.05418	0.05441	0.05429	0.05418	0.05429	0.05502	0.05428	0.06788		0.05373		0.10823		0.50355		0.49843	0.0150869	
	Robot 2	T1	0.04803	0.05190	0.05168	0.05097	0.05177	0.05167	0.05199	0.05155	0.05213	0.05166	0.05135	0.05134	0.05115	0.05105	0.05120	0.05061	0.05086	0.05143	0.05042	0.05084	0.05033	0.05152	0.05038	0.05085	0.05111		0.04803		0.05213		0.07853		0.05869	0.0008328	
		T2	0.04487	0.05039	0.05236	0.05227	0.05198	0.05138	0.05228	0.05213	0.05204	0.05039	0.05206	0.05163	0.05133	0.05126	0.05170	0.05190	0.05123	0.05148	0.05140	0.05019	0.05176	0.05199	0.05212	0.05140	0.05131	0.05103	0.04487	0.04453	0.05236	0.05236	0.14295	0.14954	0.14546	0.0014971	0.0013107
		T3	0.04453	0.04907	0.05147	0.05145	0.05150	0.05067	0.05074	0.05155	0.05155	0.05188	0.05162	0.05045	0.05092	0.05102	0.05096	0.05127	0.05079	0.05105	0.05011	0.05051	0.05077	0.05064	0.05161	0.04973	0.05066		0.04453		0.05188		0.14176		0.11695	0.0014612	
Joint 2	Robot 1	T1	0.08233	0.15176	0.13060	0.08265	0.08273	0.07988	0.08489	0.07980	0.07983	0.08114	0.07998	0.07912	0.08356	0.08250	0.08242	0.07977	0.08024	0.08325	0.08016	0.07970	0.07974	0.08201	0.08030	0.08261	0.08629		0.07912		0.15176		0.47867		0.00348	0.0172615	
		T2	0.07865	0.08073	0.07405	0.07708	0.07621	0.08334	0.08087	0.07678	0.07926	0.07704	0.07771	0.07684	0.07669	0.08016	0.07888	0.07682	0.07850	0.07871	0.07834	0.07919	0.07701	0.07722	0.07842	0.07859	0.07821	0.08079	0.07405	0.07405	0.08334	0.15176	0.11145	0.51204	0.00086	0.0018829	0.0107182
		T3	0.07981	0.08596	0.07426	0.07804	0.07584	0.07995	0.07676	0.07694	0.07763	0.07563	0.07732	0.07708	0.07693	0.07594	0.07777	0.07769	0.07778	0.08246	0.07660	0.07951	0.07741	0.07818	0.07635	0.07708	0.07787		0.07426		0.08596		0.13611		0.03416	0.0023964	
	Robot 2	T1	0.06716	0.06199	0.06249	0.06092	0.06157	0.06009	0.06017	0.05948	0.06087	0.06083	0.05973	0.06066	0.06056	0.05960	0.06017	0.06148	0.06133	0.06148	0.06010	0.06063	0.06162	0.06274	0.06264	0.06207	0.06127		0.05948		0.06716		0.11443		0.07588	0.0015748	
		T2	0.06608	0.06184	0.06235	0.06031	0.06134	0.06053	0.06041	0.06019	0.05956	0.06020	0.06102	0.06058	0.05943	0.06018	0.06037	0.06075	0.05968	0.06162	0.06010	0.06087	0.05977	0.06188	0.06235	0.06113	0.06094	0.06115	0.05943	0.05898	0.06608	0.06733	0.10077	0.12407	0.07503	0.0013782	0.0014916
		T3	0.06733	0.06089	0.05999	0.05898	0.06065	0.06051	0.06089	0.06138	0.06048	0.06217	0.06062	0.06129	0.06127	0.06180	0.06139	0.06218	0.06070	0.06137	0.06206	0.05916	0.06015	0.06093	0.06192	0.06197	0.06125		0.05898		0.06733		0.12407		0.07967	0.0015547	
Joint 3	Robot 1	T1	0.12087	0.10515	0.10443	0.11039	0.10523	0.10720	0.10739	0.10496	0.10977	0.10693	0.10682	0.10815	0.10720	0.10913	0.10904	0.10987	0.10974	0.10639	0.10854	0.10959	0.10981	0.10825	0.10659	0.10931	0.10836		0.10443		0.12087		0.13603		0.09565	0.0031940	
		T2	0.10380	0.10203	0.10497	0.10404	0.10445	0.10440	0.10467	0.10554	0.10572	0.10480	0.10425	0.10535	0.10360	0.10472	0.10454	0.10406	0.10695	0.10455	0.10677	0.10524	0.10607	0.10591	0.10655	0.10807	0.10504	0.10588	0.10203	0.10114	0.10807	0.12087	0.05586	0.16321	0.04111	0.0012772	0.0027606
		T3	0.10114	0.10206	0.10528	0.10465	0.10382	0.10456	0.10330	0.10273	0.10451	0.10503	0.10380	0.10529	0.10384	0.10565	0.10350	0.10566	0.10403	0.10357	0.10393	0.10397	0.10334	0.10512	0.10548	0.10728	0.10423		0.10114		0.10728		0.05720		0.06067	0.0012976	
	Robot 2	T1	0.09012	0.08626	0.08776	0.08666	0.08540	0.08623	0.08568	0.08659	0.08698	0.08533	0.08666	0.08694	0.08742	0.08753	0.08684	0.08756	0.08798	0.08768	0.08842	0.08881	0.08740	0.08737	0.08776	0.08818	0.08723		0.08533		0.09012		0.05313		0.02151	0.0010924	
		T2	0.08972	0.08654	0.08674	0.08634	0.08612	0.08674	0.08633	0.08770	0.08570	0.08687	0.08750	0.08652	0.08664	0.08747	0.08710	0.08750	0.08718	0.08853	0.08699	0.08776	0.08713	0.08856	0.08787	0.08769	0.08722	0.08720	0.08570	0.08533	0.08972	0.09012	0.04477	0.05313	0.02259	0.0008885	0.0009131
		T3	0.08853	0.08632	0.08603	0.08681	0.08645	0.08579	0.08662	0.08669	0.08731	0.08750	0.08666	0.08656	0.08711	0.08847	0.08666	0.08787	0.08735	0.08756	0.08722	0.08695	0.08777	0.08682	0.08865	0.08784	0.08715		0.08579		0.08865		0.03230		0.00779	0.0007662	
Joint 4	Robot 1	T1	0.13499	0.12536	0.12467	0.12730	0.12789	0.12640	0.12615	0.12574	0.12401	0.12370	0.12216	0.12396	0.12376	0.12502	0.12501	0.12434	0.12533	0.12419	0.12621	0.12437	0.12593	0.12513	0.12356	0.12511	0.12543		0.12216		0.13499		0.09506		0.07323	0.0024003	
		T2	0.13044	0.12920	0.13158	0.12841	0.13212	0.13402	0.12942	0.12791	0.12576	0.12680	0.12780	0.12643	0.12448	0.12970	0.13282	0.12781	0.12698	0.12948	0.12725	0.12555	0.12813	0.12978	0.12484	0.13132	0.12867	0.12705	0.12448	0.12216	0.13402	0.13499	0.07120	0.09506	0.00670	0.0025236	0.0027431
		T3	0.12305	0.13422	0.12803	0.12673	0.12810	0.12862	0.12490	0.12639	0.12572	0.12911	0.12342	0.12418	0.12492	0.12899	0.12888	0.12763	0.12554	0.12633	0.12758	0.12665	0.12785	0.12785	0.12514	0.12921	0.12704		0.12305		0.13422		0.08324		0.05009	0.0023713	
	Robot 2	T1	0.11103	0.11278	0.11673	0.11387	0.11657	0.11573	0.11502	0.11414	0.11629	0.11561	0.11647	0.11559	0.11732	0.11696	0.11827	0.11695	0.11697	0.11698	0.11691	0.11573	0.11709	0.11652	0.11804	0.11689	0.11602		0.11103		0.11827		0.06125		0.05283	0.0016620	
		T2	0.11068	0.11210	0.11613	0.11374	0.11725	0.11777	0.11716	0.11688	0.11652	0.11690	0.11724	0.11668	0.12019	0.11768	0.11848	0.11969	0.12046	0.11743	0.11988	0.11661	0.11829	0.11946	0.11961	0.11824	0.11729	0.11655	0.11068	0.10926	0.12046	0.12046	0.08125	0.09303	0.06835	0.0023891	0.0022693
		T3	0.10926	0.11205	0.11761	0.11442	0.11481	0.11375	0.11256	0.11520	0.11498	0.11600	0.11701	0.11695	0.11802	0.11701	0.11764	0.11914	0.11962	0.11756	0.11726	0.11748	0.11938	0.11804	0.11707	0.11926	0.11634		0.10926		0.11962		0.08662		0.09156	0.0025510	
Joint 5	Robot 1	T1	0.12909	0.13035	0.10213	0.12646	0.13418	0.15044	0.13286	0.15155	0.14637	0.18126	0.11189	0.11410	0.11910	0.12198	0.12133	0.09965	0.10958	0.11634	0.11505	0.10128	0.09762	0.11362	0.14715	0.14687	0.12584		0.09762		0.18126		0.46143		0.13776	0.0203077	
		T2	0.16807	0.15806	0.13266	0.14831	0.14047	0.14085	0.14719	0.14345	0.15942	0.21993	0.14990	0.13309	0.11843	0.13264	0.12679	0.09165	0.10179	0.10475	0.11757	0.09260	0.09318	0.11159	0.13072	0.13148	0.13311	0.12093	0.09165	0.08737	0.21993	0.21993	0.58326	0.60273	0.21770	0.0285254	0.0244954
		T3	0.11534	0.11386	0.09606	0.11849	0.11313	0.10610	0.10213	0.10551	0.10999	0.13721	0.09703	0.09640	0.10351	0.09996	0.09760	0.09205	0.08737	0.09829	0.09166	0.10101	0.09320	0.09113	0.10000	0.12506	0.10384		0.08737		0.13721		0.36322		0.08420	0.0118860	
	Robot 2	T1	0.07766	0.05194	0.06076	0.05434	0.05194	0.04925	0.05196	0.05159	0.04891	0.05083	0.05050	0.05025	0.04998	0.05071	0.04820	0.04894	0.04852	0.04966	0.05143	0.05065	0.05118	0.05139	0.04948	0.05030	0.05210		0.04820		0.07766		0.37930		0.35228	0.0059853	
		T2	0.06924	0.04927	0.05202	0.05027	0.05021	0.04943	0.04902	0.05046	0.04906	0.04974	0.05090	0.04879	0.04940	0.04972	0.04850	0.04913	0.05039	0.05007	0.05137	0.05109	0.05081	0.05169	0.05029	0.05084	0.05090	0.05157	0.04850	0.04820	0.06924	0.07766	0.29953	0.37930	0.26582	0.0040169	0.0045764
		T3	0.06762	0.05031	0.05108	0.05011	0.05072	0.04990	0.05145	0.05219	0.04994	0.05095	0.05007	0.05084	0.05101	0.05159	0.05072	0.05125	0.05108	0.05103	0.05106	0.05086	0.05238	0.05165	0.05189	0.05135	0.05171		0.04990		0.06762		0.26206		0.24066	0.0034522	
Joint 6	Robot 1	T1	0.07060	0.06168	0.06815	0.07017	0.06519	0.06569	0.06496	0.06782	0.06640	0.06852	0.06525	0.06872	0.06822	0.06748	0.06632	0.06773	0.06664	0.06978	0.07166	0.06992	0.07205	0.07029	0.06899	0.06965	0.06799		0.06168		0.07205		0.14384		0.01340	0.0024260	
		T2	0.05544	0.05784	0.05819	0.05814	0.05917	0.06332	0.06105	0.06328	0.06545	0.06541	0.06376	0.06552	0.06472	0.06623	0.06610	0.06599	0.06632	0.06699	0.06637	0.06516	0.06758	0.06691	0.06575	0.06643	0.06380	0.06548	0.05544	0.05356	0.06758	0.07205	0.17965	0.25656	0.19835	0.0035095	0.0036465
		T3	0.05356	0.05714	0.05913	0.06116	0.06363	0.06350	0.06494	0.06478	0.06528	0.06514	0.06682	0.06499	0.06662	0.06536	0.06681	0.06596	0.06734	0.06629	0.06787	0.06726	0.06706	0.06677	0.06675	0.06714	0.06464		0.05356		0.06787		0.21084		0.25353	0.0035428	
	Robot 2	T1	0.08402	0.08493	0.08563	0.08823	0.08675	0.08409	0.08698	0.08801	0.08559	0.08556	0.08297	0.08429	0.08390	0.08297	0.08290	0.08649	0.08521	0.08461	0.08552	0.08439	0.08507	0.08516	0.08592	0.08400	0.08513		0.08290		0.08823		0.06044		0.00027	0.0014487	
		T2	0.07733	0.08252	0.08219	0.08377	0.08482	0.08412	0.08685	0.08405	0.08396	0.08594	0.08472	0.08374	0.08457	0.08719	0.08605	0.08564	0.08639	0.08707	0.08671	0.08628	0.08712	0.08658	0.08480	0.08601	0.08493	0.08539	0.07733	0.07733	0.08719	0.08823	0.11311	0.12359	0.11225	0.0021711	0.0016982
		T3	0.08569	0.08593	0.08511	0.08723	0.08708	0.08775	0.08757	0.08802	0.08678	0.08812	0.08508	0.08501	0.08440	0.08628	0.08607	0.08591	0.08634	0.08664	0.08471	0.08514	0.08421	0.08518	0.08637	0.08567	0.08610		0.08421		0.08812		0.04443		0.00028	0.0011336	

F.2 The Figures of RMSD

Figure F.1 and F.2 are the plots of RMSD values obtained from the self verification, which the verification is established based the identification results of itself. The rest figures (from Figure F.3 to Figure F.10) are the plots of RMSD values calculated from the cross verification, which the verification is established based the identification results of other tests.

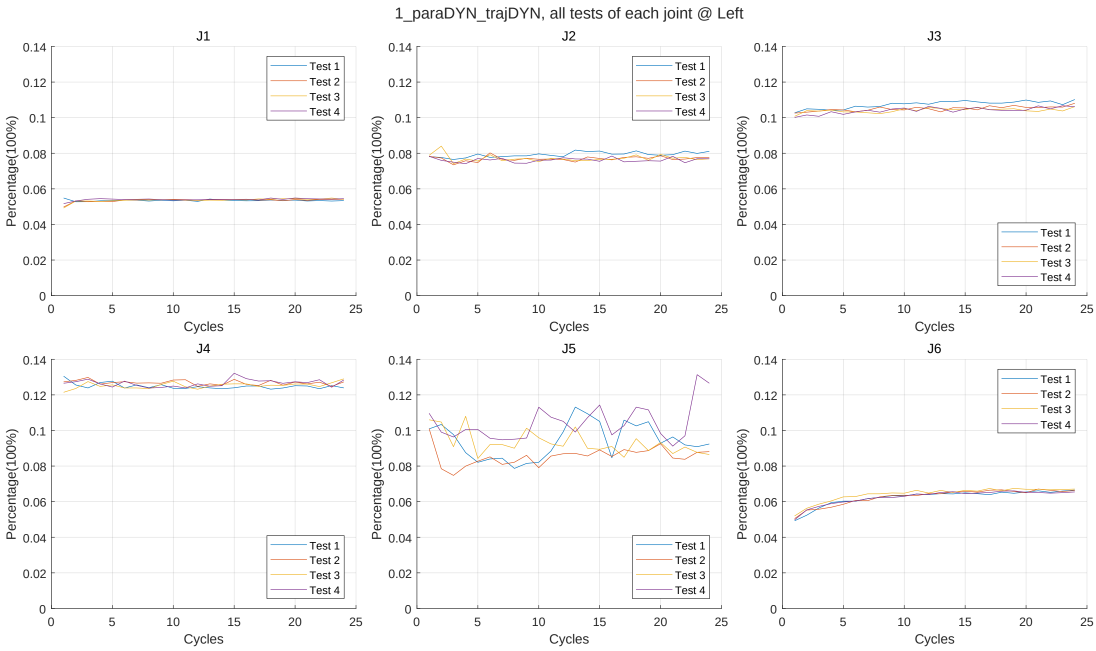

Figure F.1: The RMSD values versus cycles of the self verifications

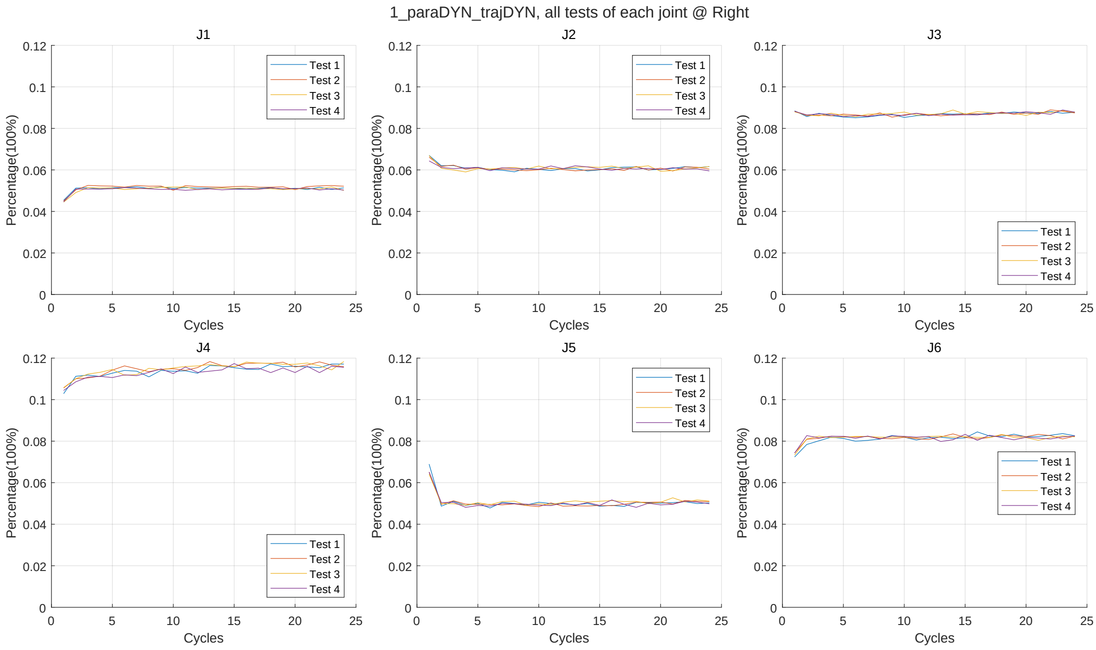

Figure F.2: The RMSD values versus cycles of the self verifications

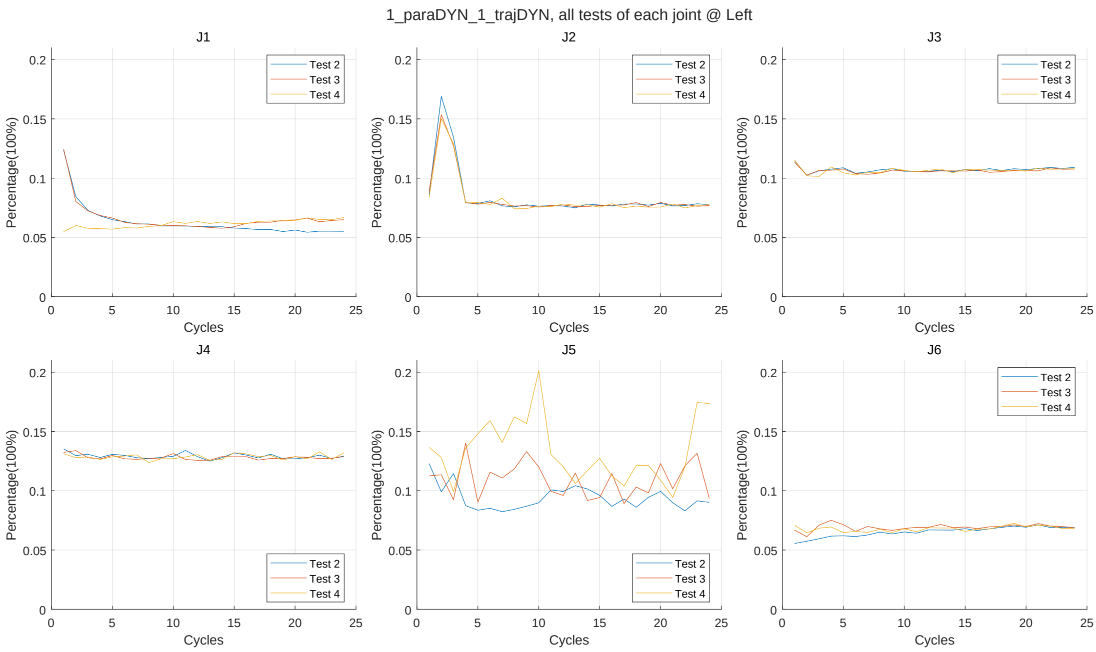

Figure F.3: The RMSD values versus cycles, calculated from the cross verifications based the identification results of Test 1 of Robot 1

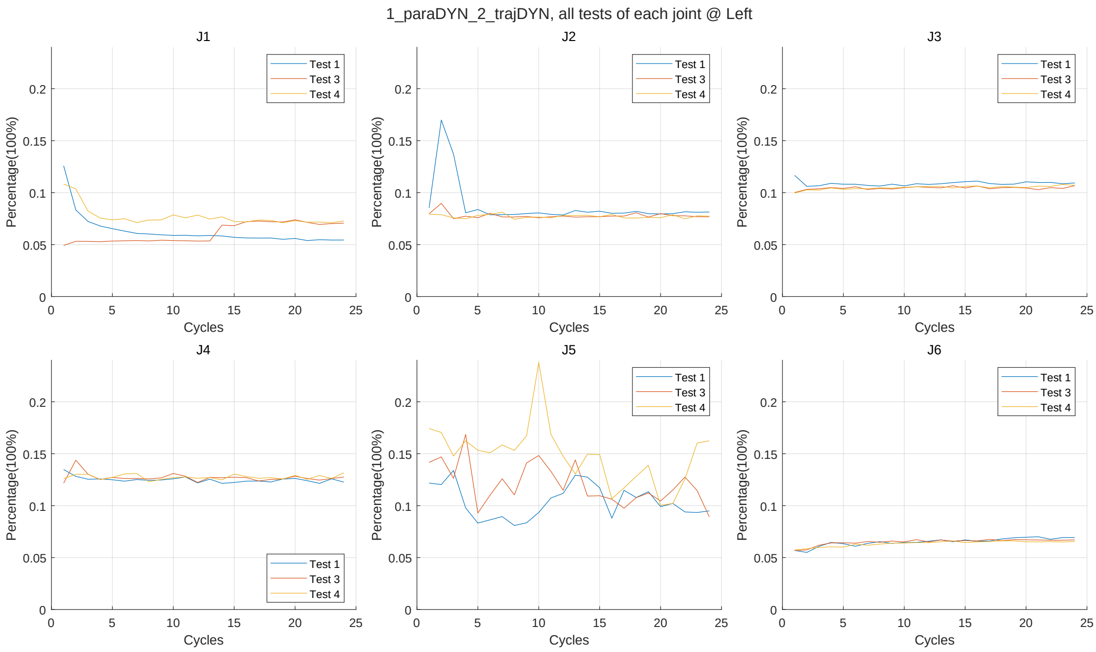

Figure F.4: The RMSD values versus cycles, calculated from the cross verifications based the identification results of Test 2 of Robot 1

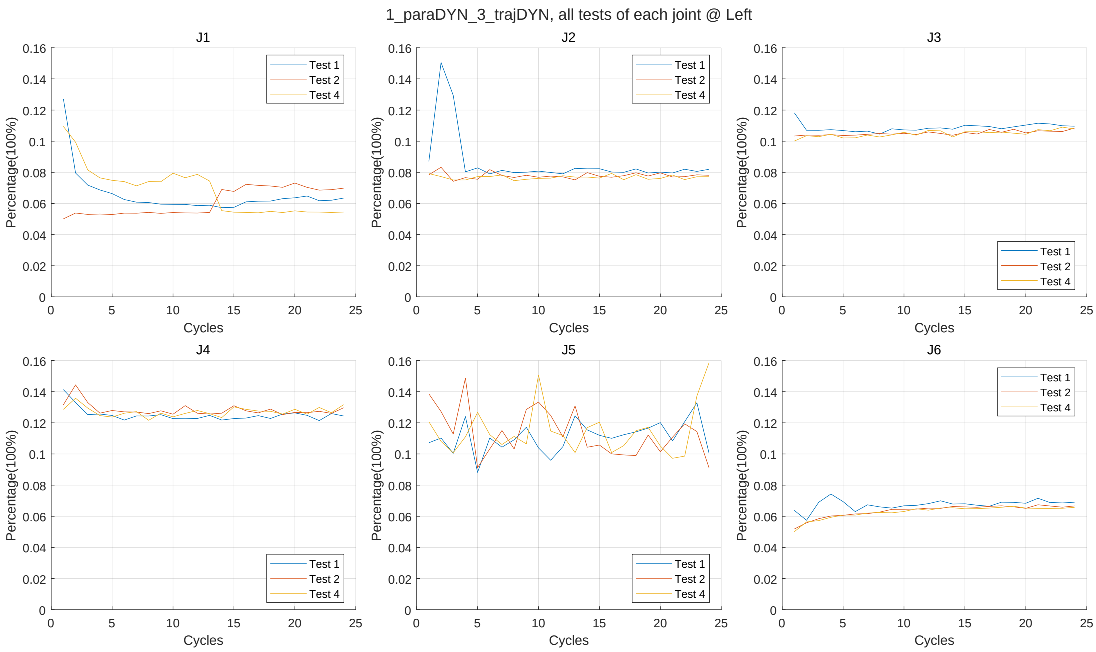

Figure F.5: The RMSD values versus cycles, calculated from the cross verifications based the identification results of Test 3 of Robot 1

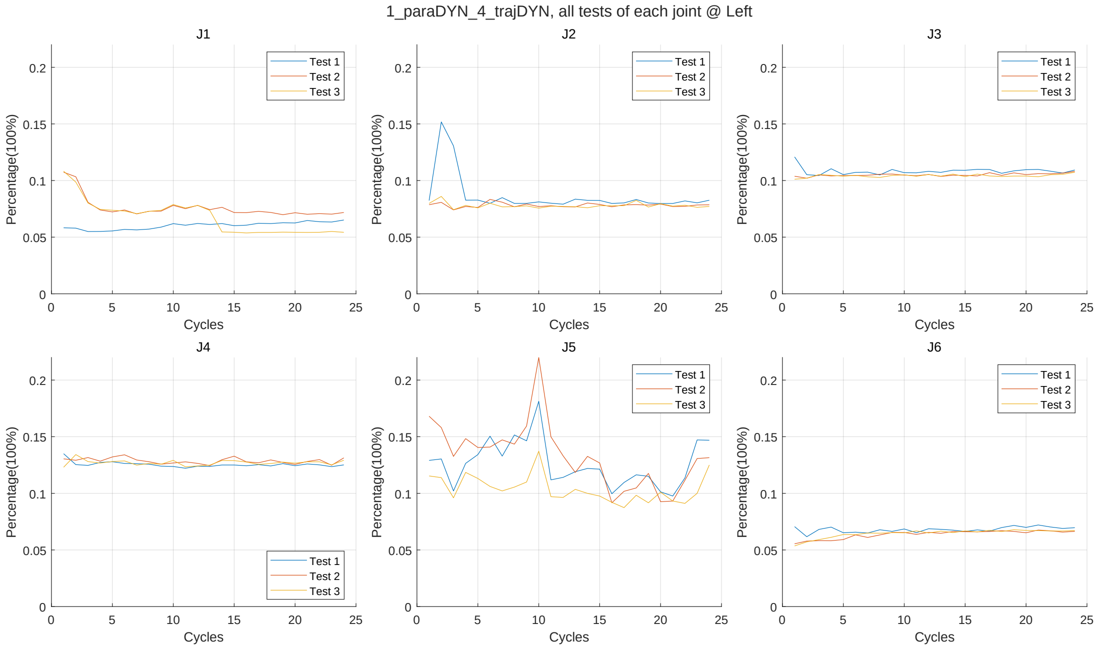

Figure F.6: The RMSD values versus cycles, calculated from the cross verifications based the identification results of Test 4 of Robot 1

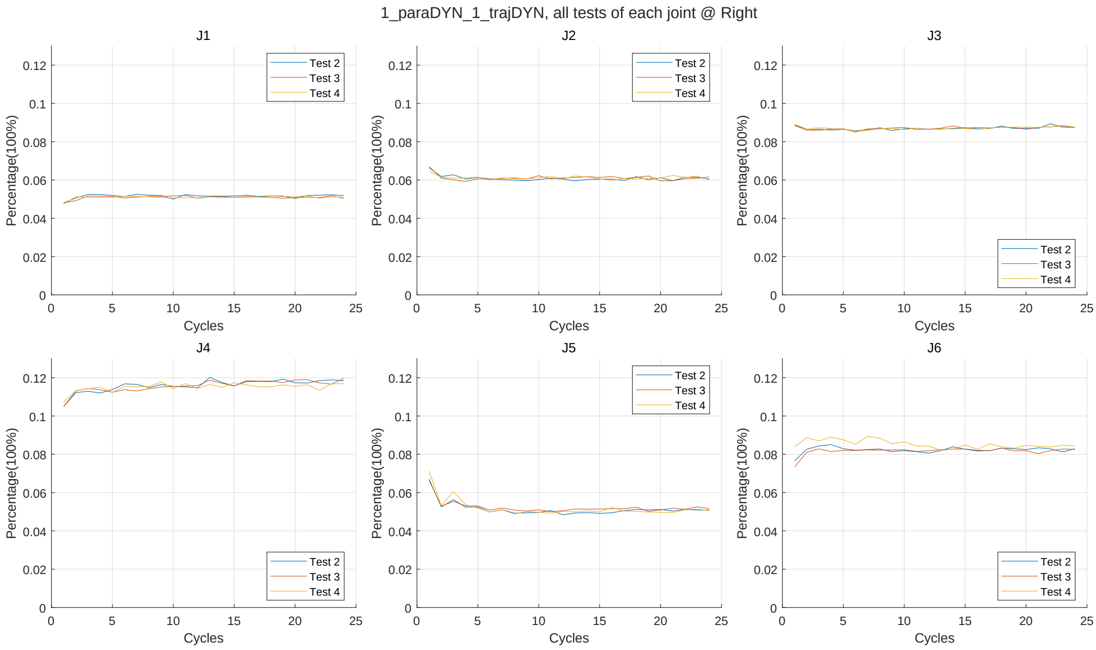

Figure F.7: The RMSD values versus cycles, calculated from the cross verifications based the identification results of Test 1 of Robot 2

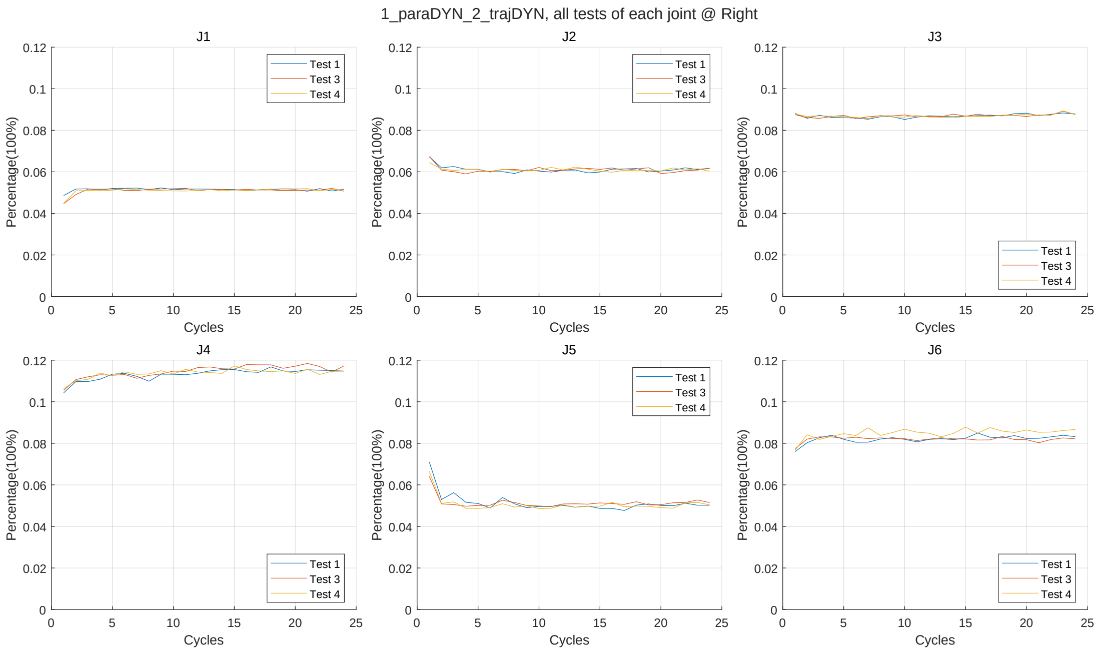

Figure F.8: The RMSD values versus cycles, calculated from the cross verifications based the identification results of Test 2 of Robot 2

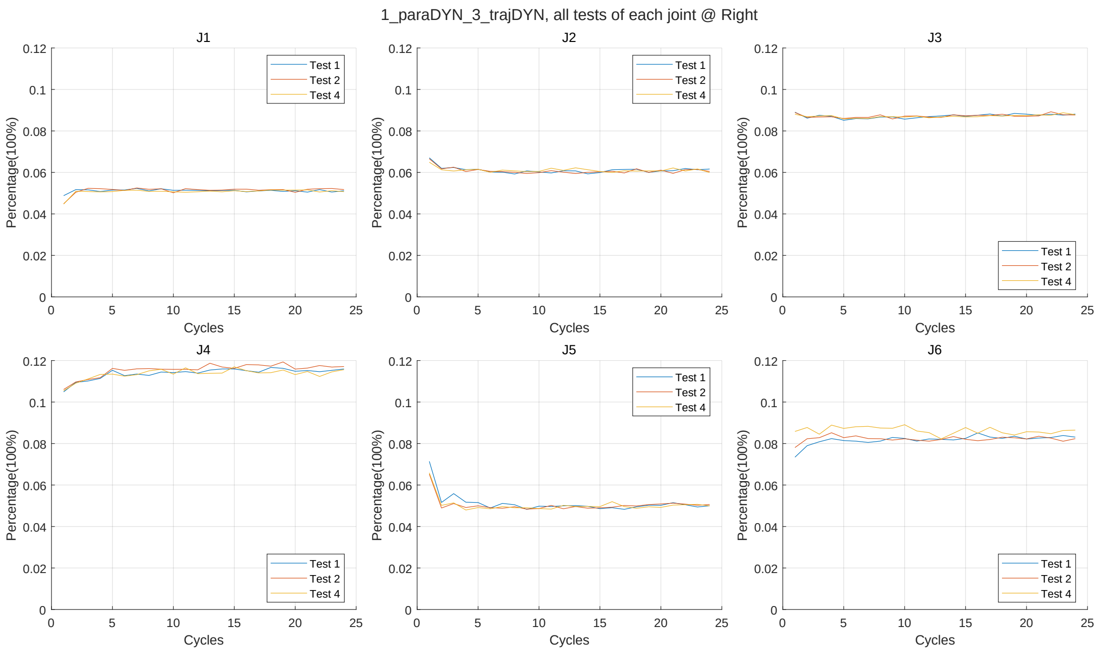

Figure F.9: The RMSD values versus cycles, calculated from the cross verifications based the identification results of Test 3 of Robot 2

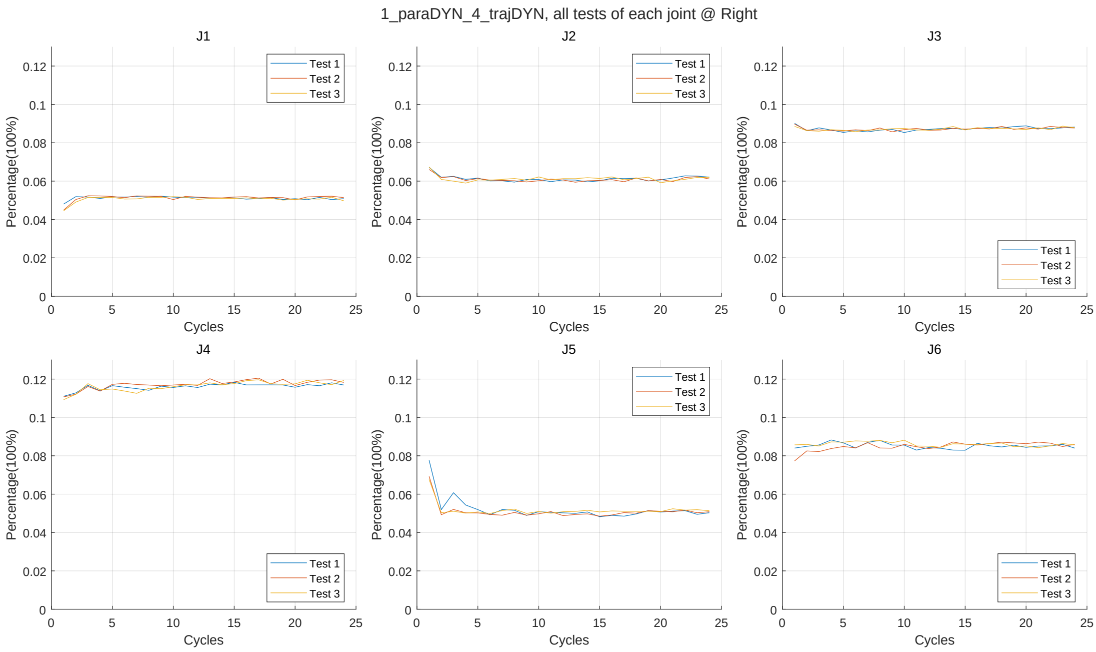

Figure F.10: The RMSD values versus cycles, calculated from the cross verifications based the identification results of Test 4 of Robot 2

Appendix G

The Identification Results Of The Dynamic Parameters

The figures shown in this appendix are the dynamic parameter identification results of both robots, which are used for the analysis in Section 5.1.1 and 5.1.5.1. The subplot A of all figures are the plots with the y-axis labelled automatically, and the subplots B of all figures are the plots with the widening scale of y-axis, which the scaling are chosen with the values multiplied by 0.5. It should be pointed that some dynamic parameters have the same plots between two subplots because the original y-axis range of the right subplot meets the requirements of multiply by 0.5.

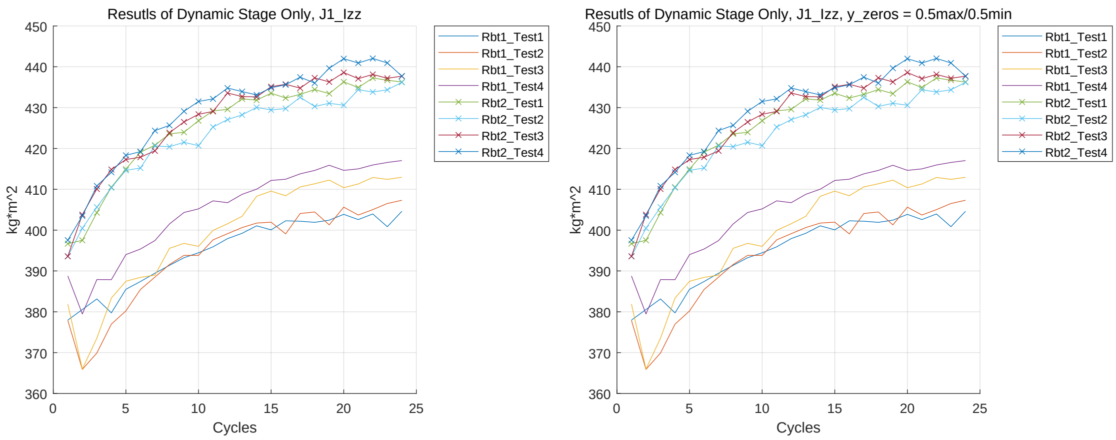

(a) Labelled automatically (b) Labelled with the widening scale of y-axis

Figure G.1: I_{zz} of Joint 1

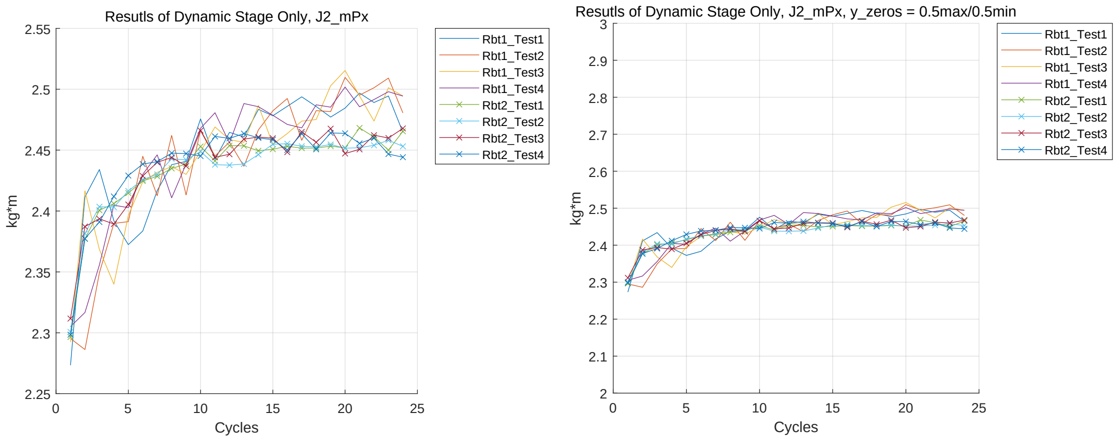

(a) Labelled automatically (b) Labelled with the widening scale of y-axis

Figure G.2: mP_x of Joint 2

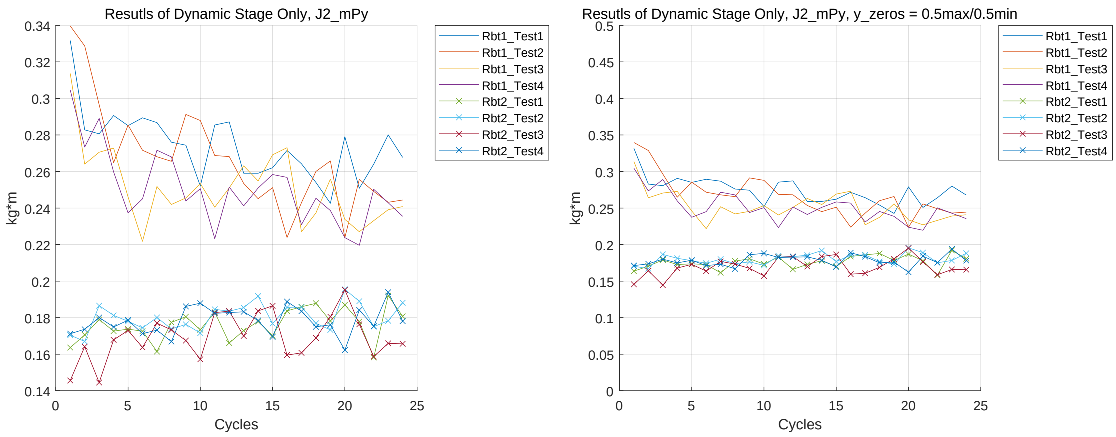

(a) Labelled automatically (b) Labelled with the widening scale of y-axis

Figure G.3: mP_y of Joint 2

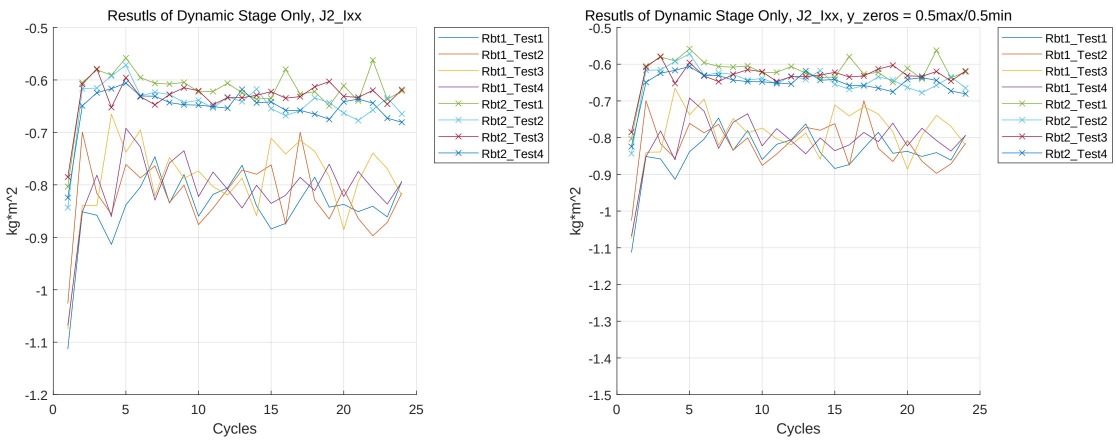

(a) Labelled automatically (b) Labelled with the widening scale of y-axis

Figure G.4: I_{xx} of Joint 2

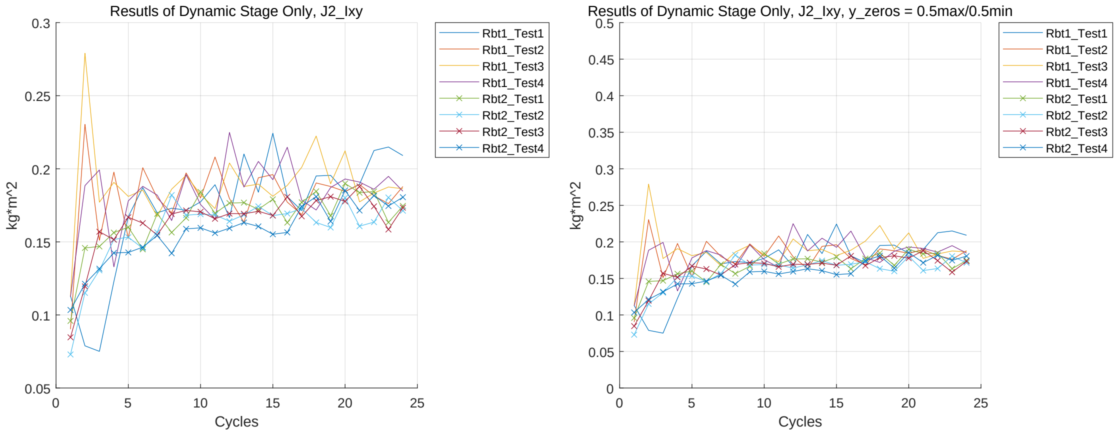

(a) Labelled automatically (b) Labelled with the widening scale of y-axis

Figure G.5: I_{xy} of Joint 2

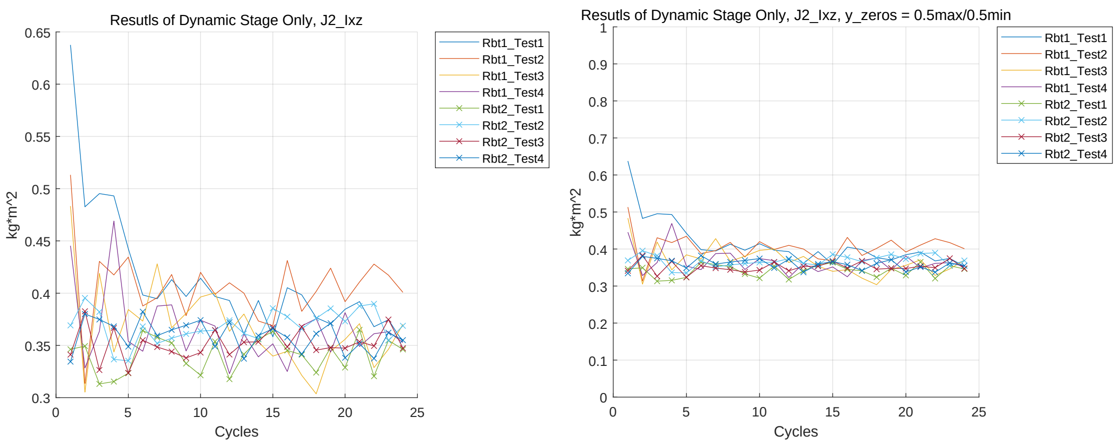

(a) Labelled automatically (b) Labelled with the widening scale of y-axis

Figure G.6: I_{xz} of Joint 2

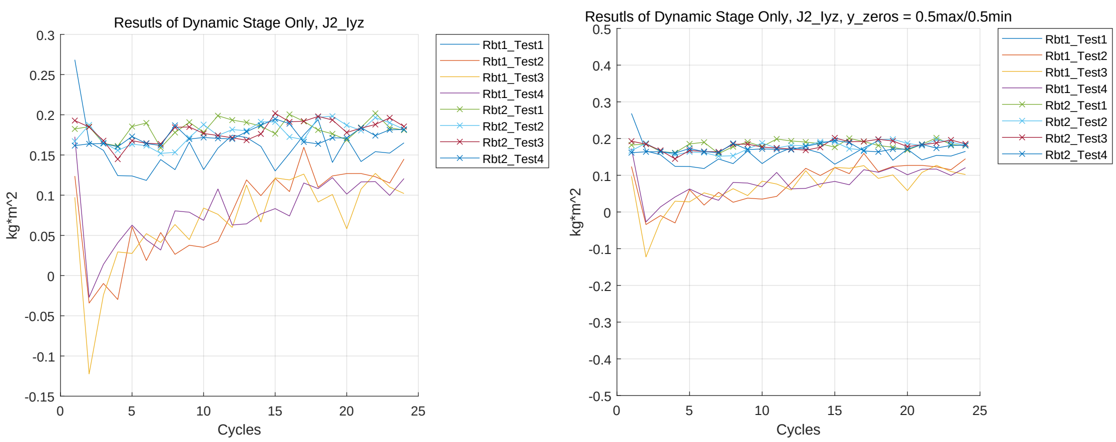

(a) Labelled automatically (b) Labelled with the widening scale of y-axis

Figure G.7: I_{yz} of Joint 2

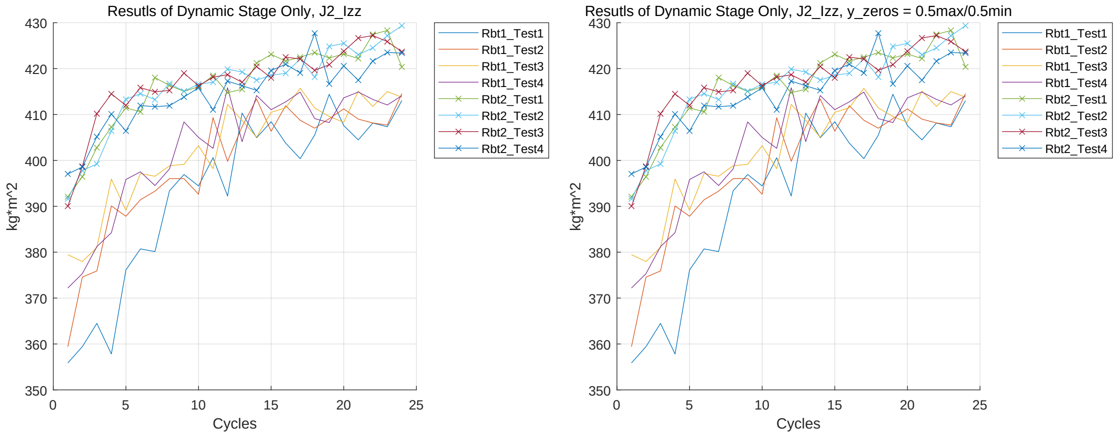

(a) Labelled automatically (b) Labelled with the widening scale of y-axis

Figure G.8: I_{zz} of Joint 2

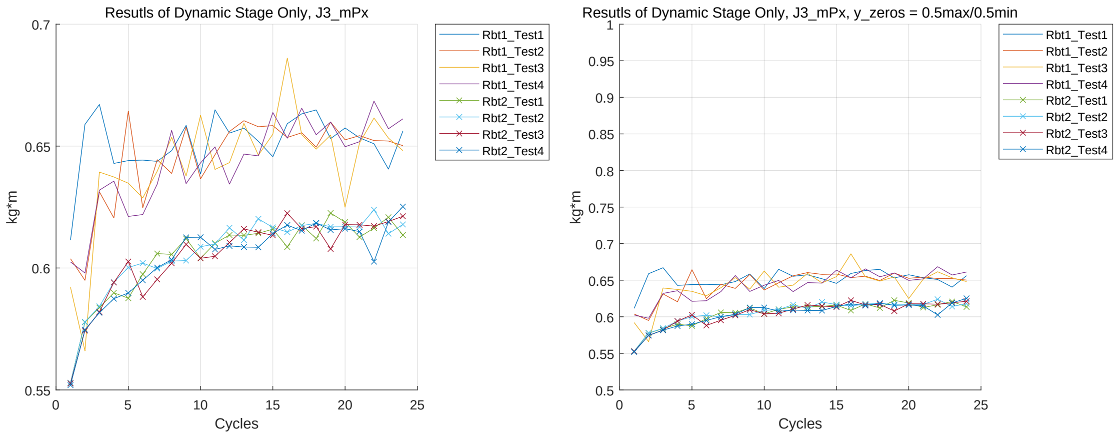

(a) Labelled automatically (b) Labelled with the widening scale of y-axis

Figure G.9: mP_x of Joint 3

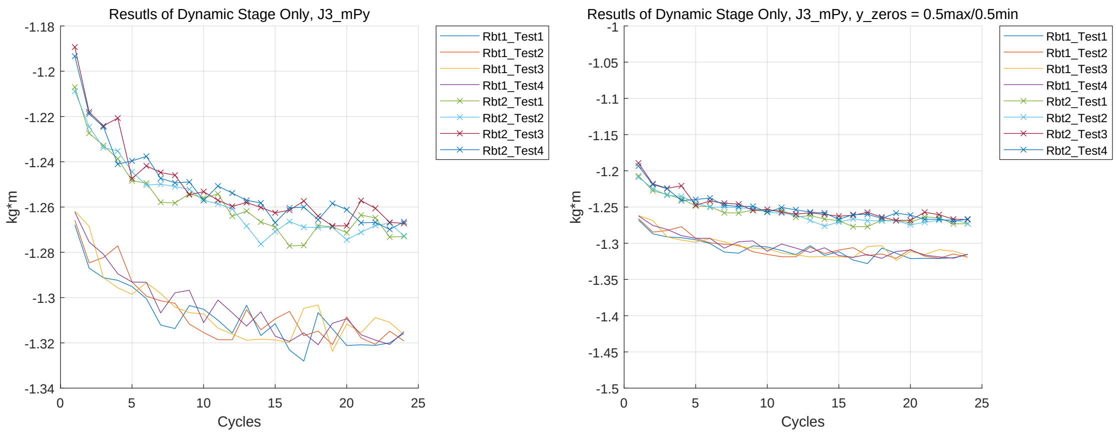

(a) Labelled automatically (b) Labelled with the widening scale of y-axis

Figure G.10: mP_y of Joint 3

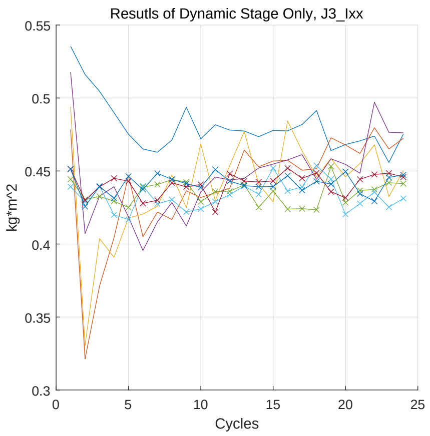

(a) Labelled automatically

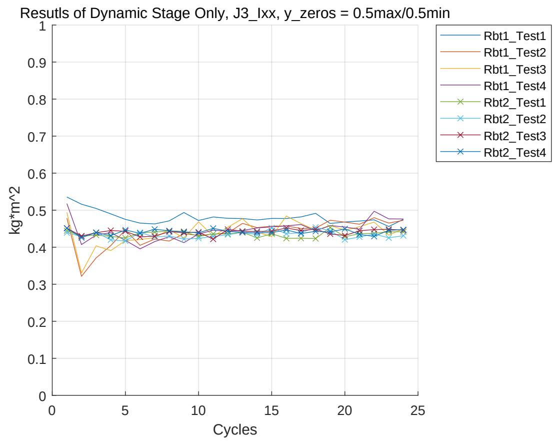

(b) Labelled with the widening scale of y-axis

Figure G.11: I_{xx} of Joint 3

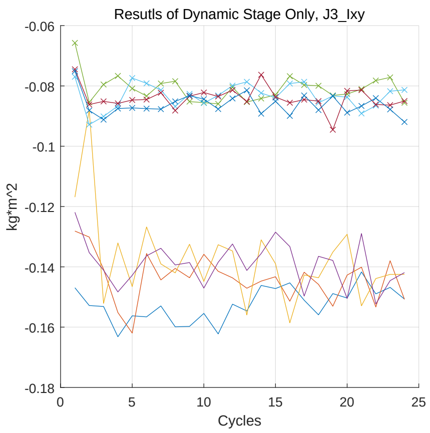

(a) Labelled automatically

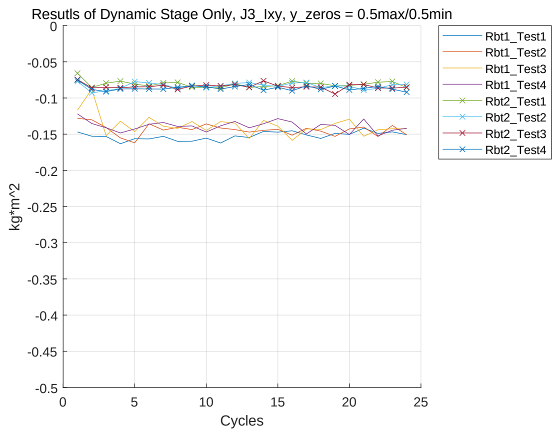

(b) Labelled with the widening scale of y-axis

Figure G.12: I_{xy} of Joint 3

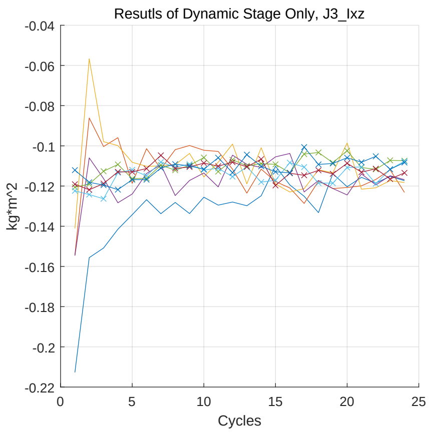

(a) Labelled automatically

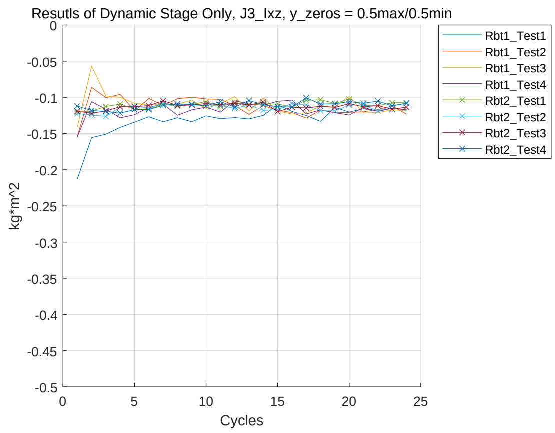

(b) Labelled with the widening scale of y-axis

Figure G.13: I_{xz} of Joint 3

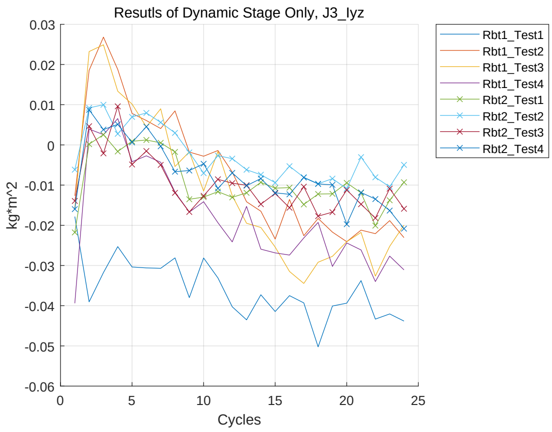

(a) Labelled automatically

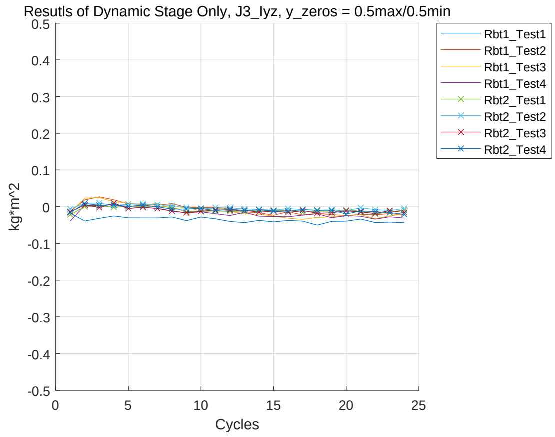

(b) Labelled with the widening scale of y-axis

Figure G.14: I_{yz} of Joint 3

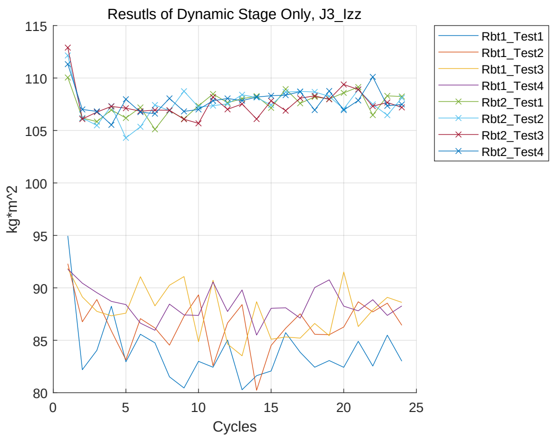

(a) Labelled automatically

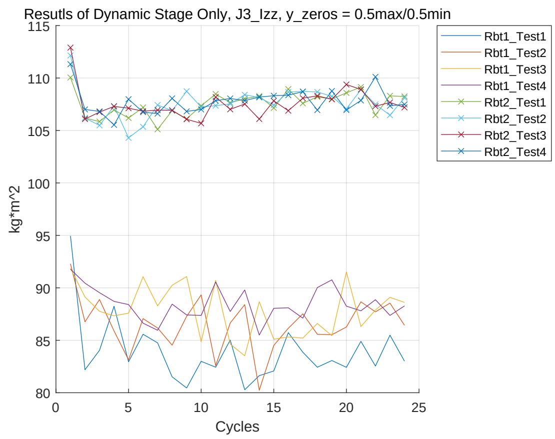

(b) Labelled with the widening scale of y-axis

Figure G.15: I_{zz} of Joint 3

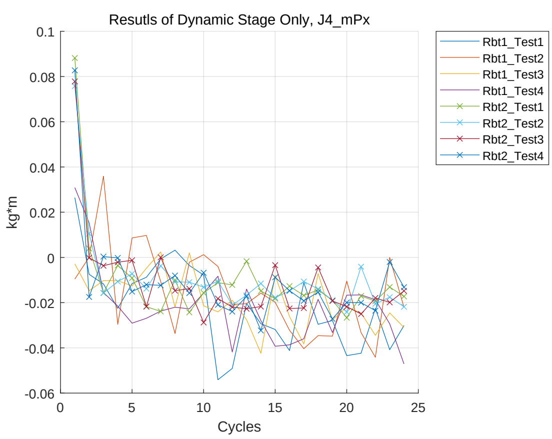

(a) Labelled automatically

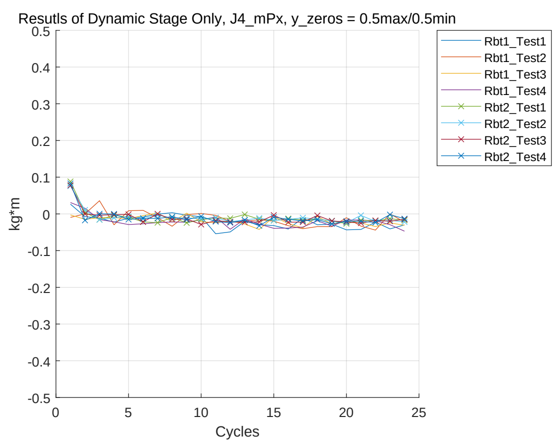

(b) Labelled with the widening scale of y-axis

Figure G.16: mP_x of Joint 4

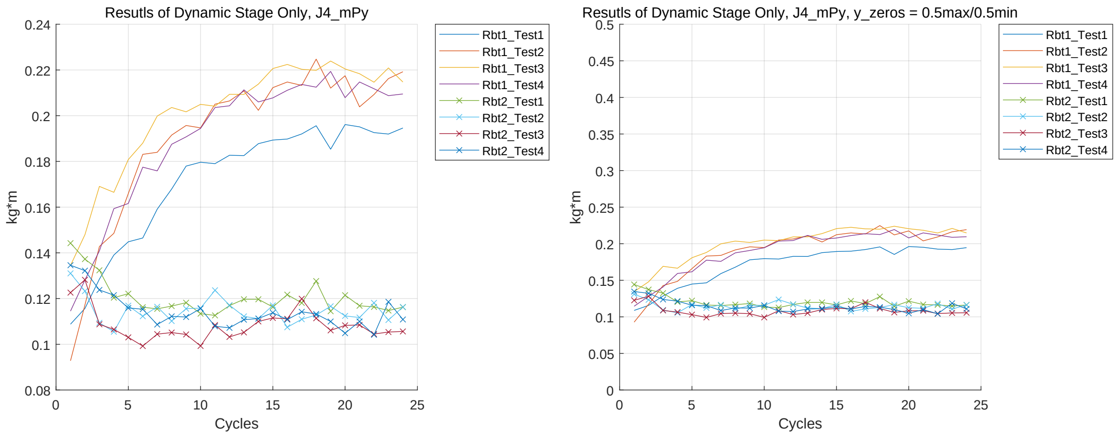

(a) Labelled automatically (b) Labelled with the widening scale of y-axis

Figure G.17: mP_y of Joint 4

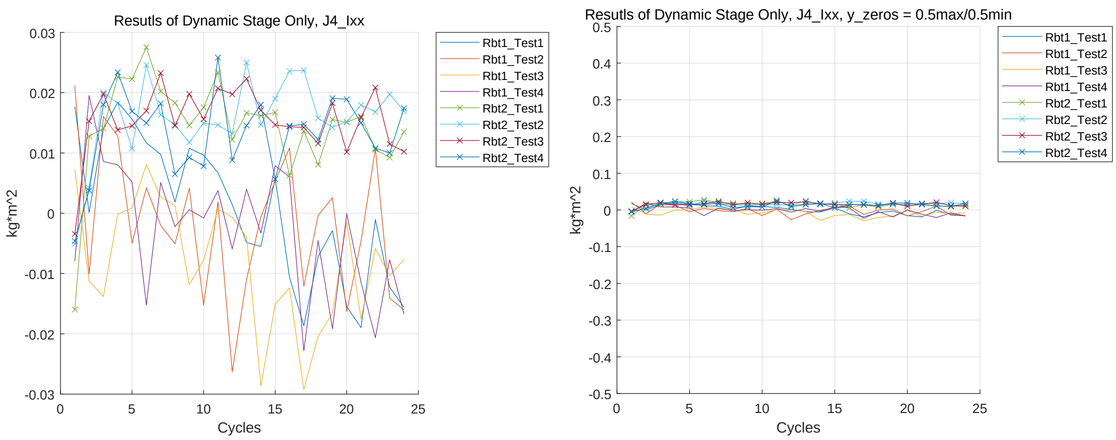

(a) Labelled automatically (b) Labelled with the widening scale of y-axis

Figure G.18: I_{xx} of Joint 4

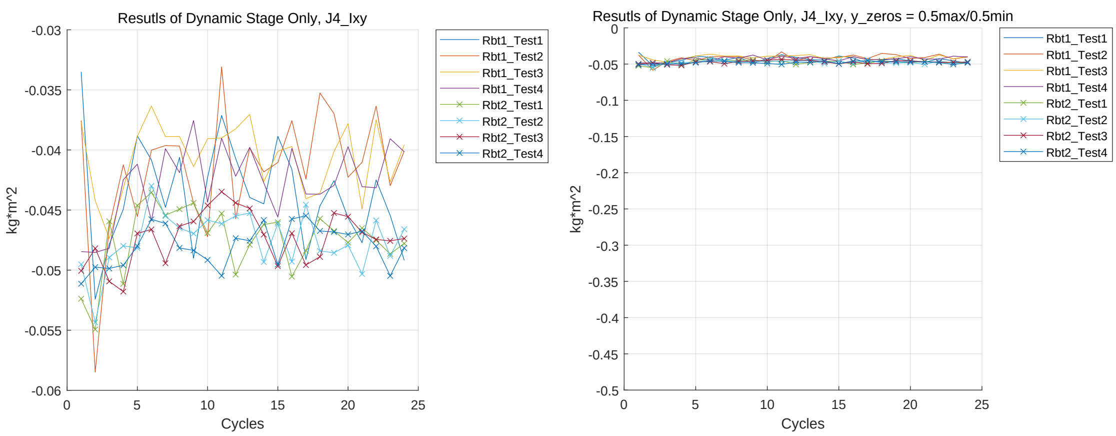

(a) Labelled automatically (b) Labelled with the widening scale of y-axis

Figure G.19: I_{xy} of Joint 4

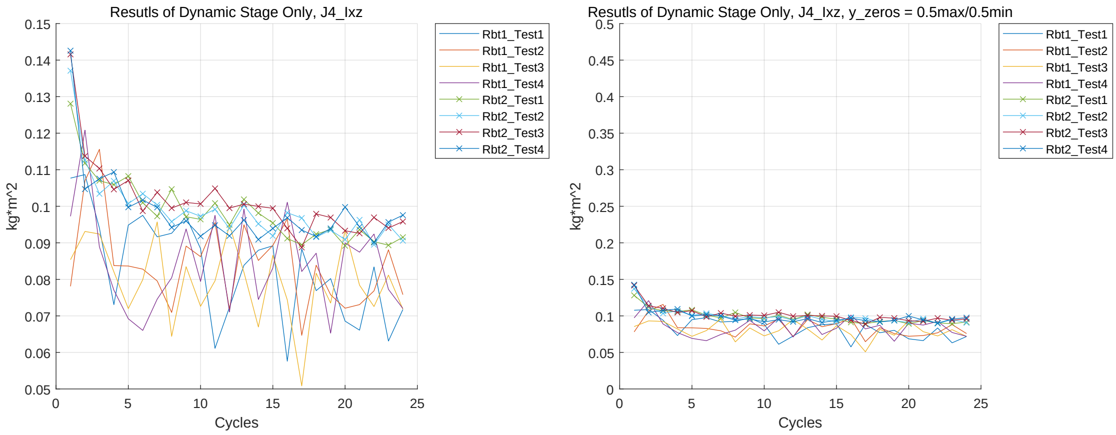

(a) Labelled automatically (b) Labelled with the widening scale of y-axis

Figure G.20: I_{xz} of Joint 4

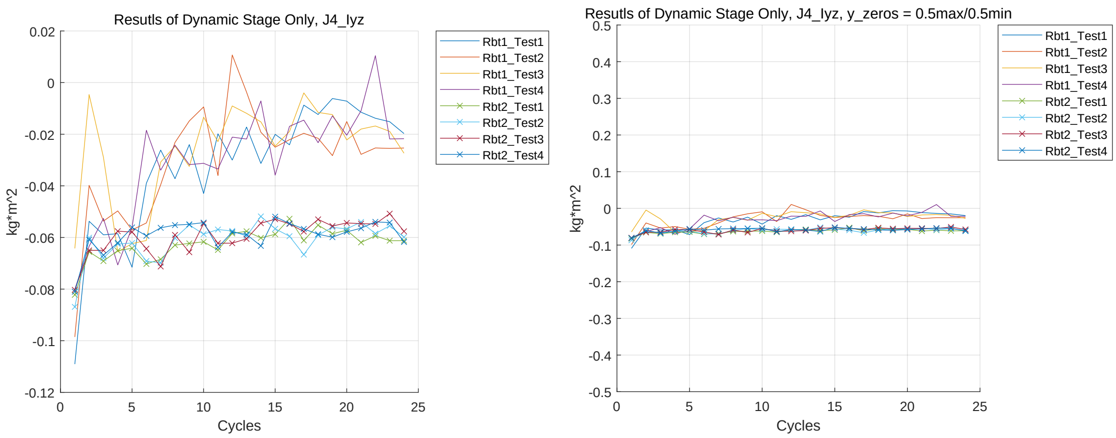

(a) Labelled automatically (b) Labelled with the widening scale of y-axis

Figure G.21: I_{yz} of Joint 4

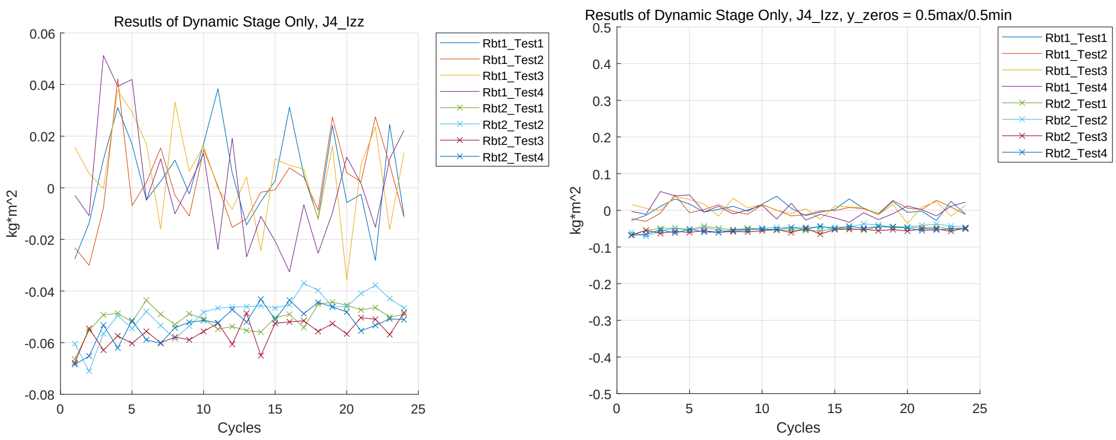

(a) Labelled automatically (b) Labelled with the widening scale of y-axis

Figure G.22: I_{zz} of Joint 4

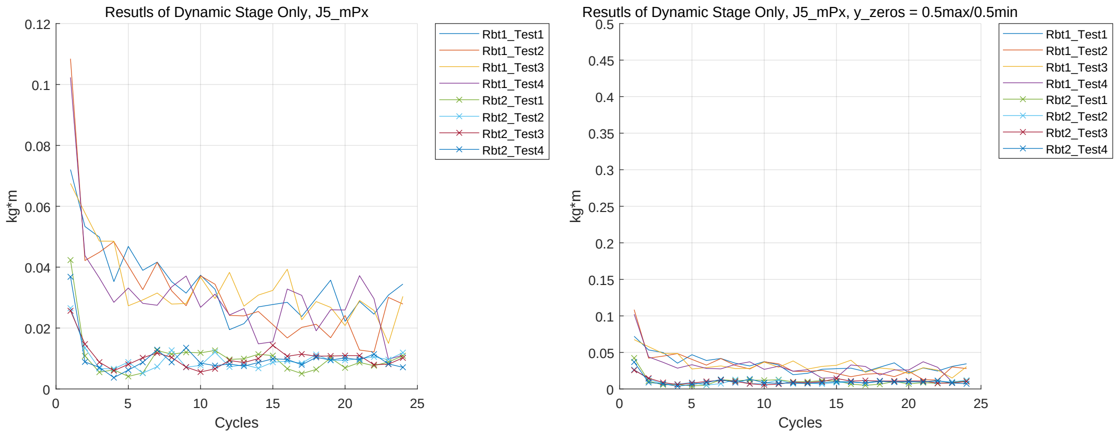

(a) Labelled automatically (b) Labelled with the widening scale of y-axis

Figure G.23: mP_x of Joint 5

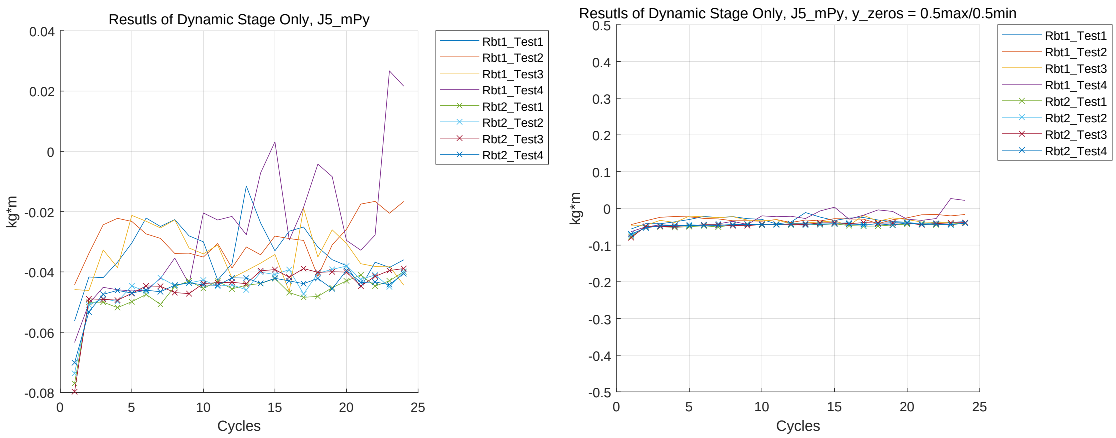

(a) Labelled automatically (b) Labelled with the widening scale of y-axis

Figure G.24: mP_y of Joint 5

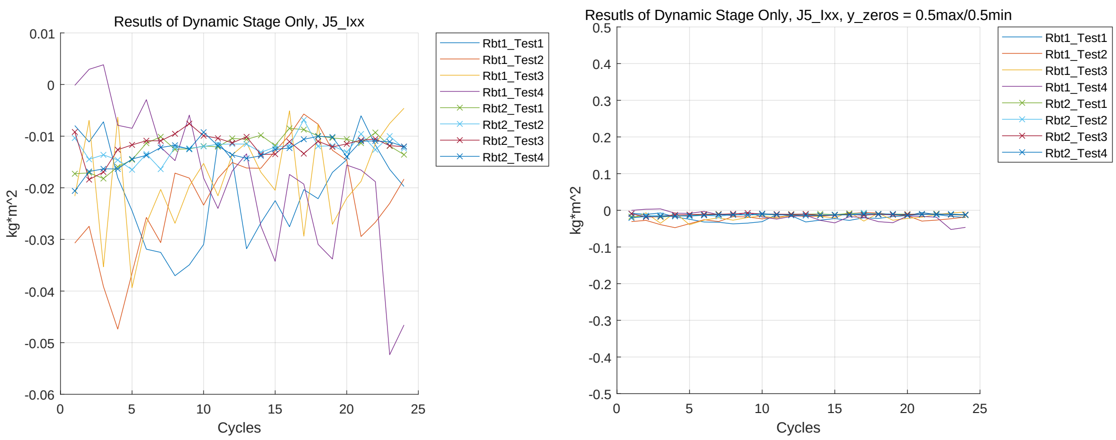

(a) Labelled automatically (b) Labelled with the widening scale of y-axis

Figure G.25: I_{xx} of Joint 5

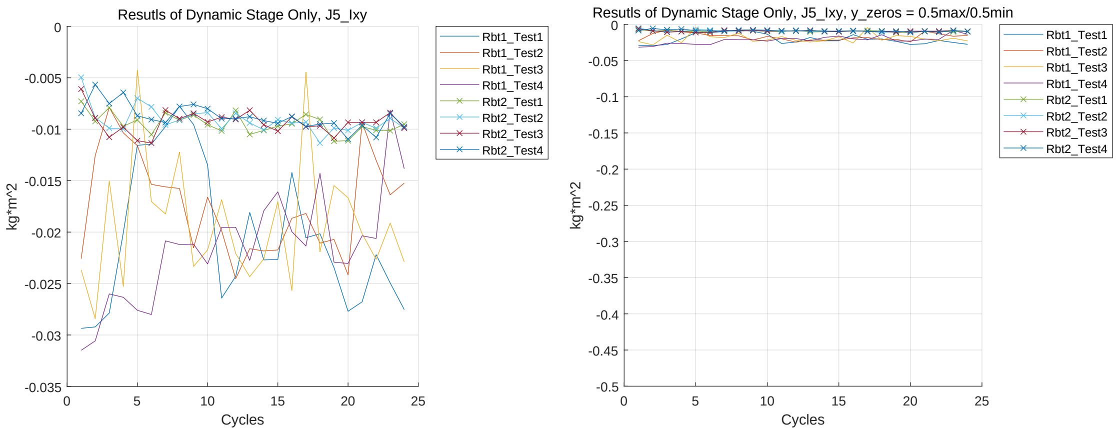

(a) Labelled automatically (b) Labelled with the widening scale of y-axis

Figure G.26: I_{xy} of Joint 5

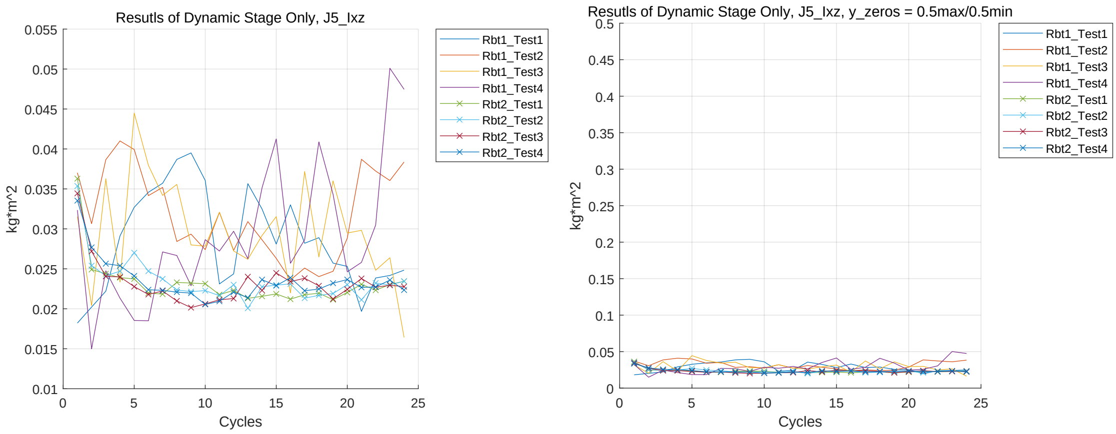

(a) Labelled automatically (b) Labelled with the widening scale of y-axis

Figure G.27: I_{xz} of Joint 5

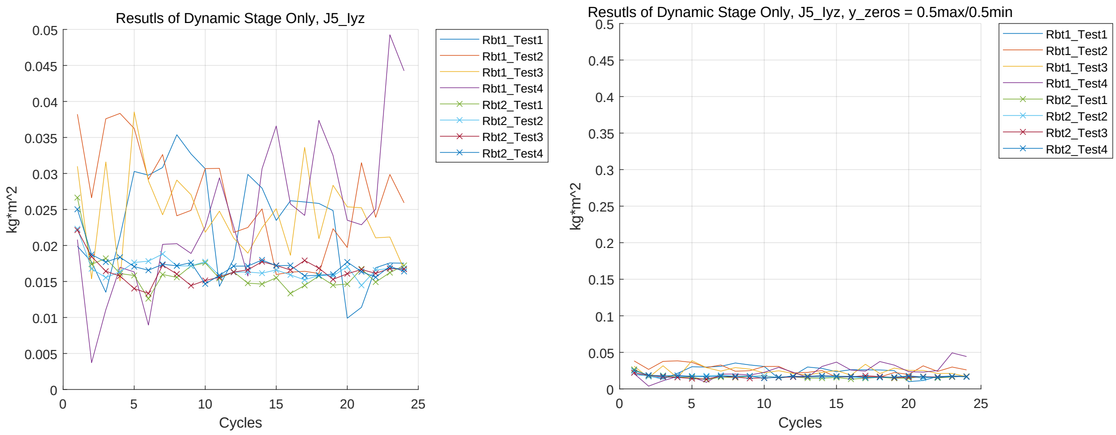

(a) Labelled automatically (b) Labelled with the widening scale of y-axis

Figure G.28: I_{yz} of Joint 5

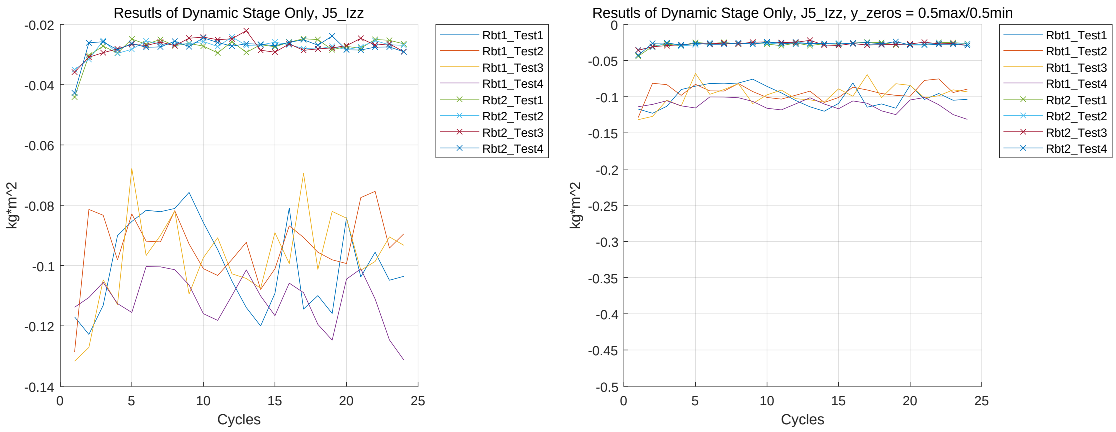

(a) Labelled automatically (b) Labelled with the widening scale of y-axis

Figure G.29: I_{zz} of Joint 5

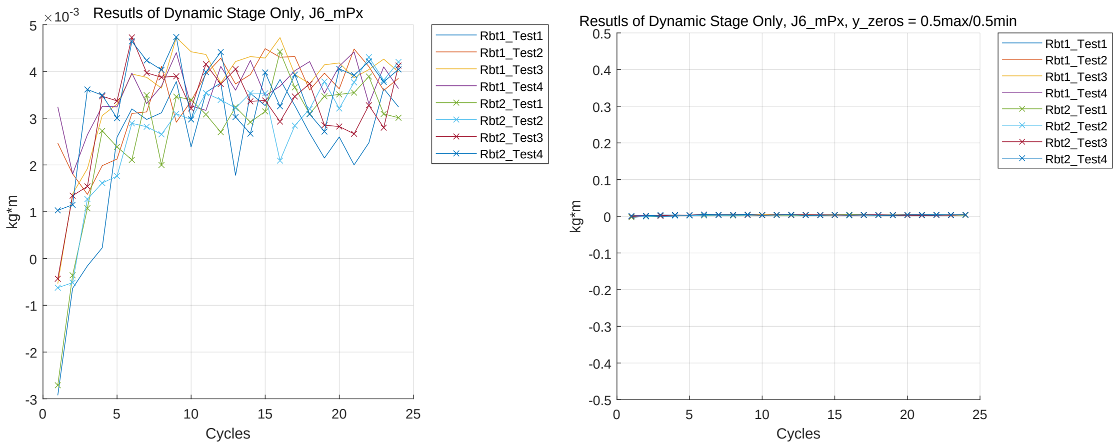

(a) Labelled automatically (b) Labelled with the widening scale of y-axis

Figure G.30: mP_x of Joint 6

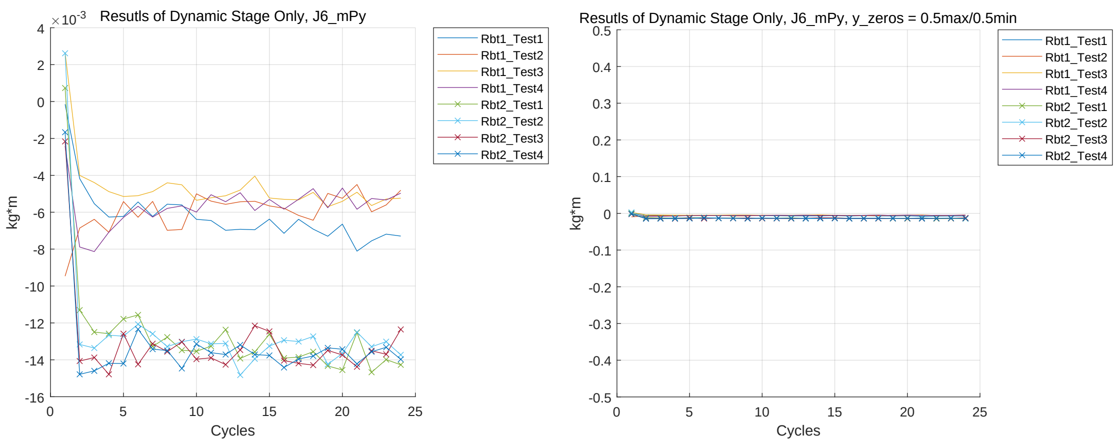

(a) Labelled automatically (b) Labelled with the widening scale of y-axis

Figure G.31: mP_y of Joint 6

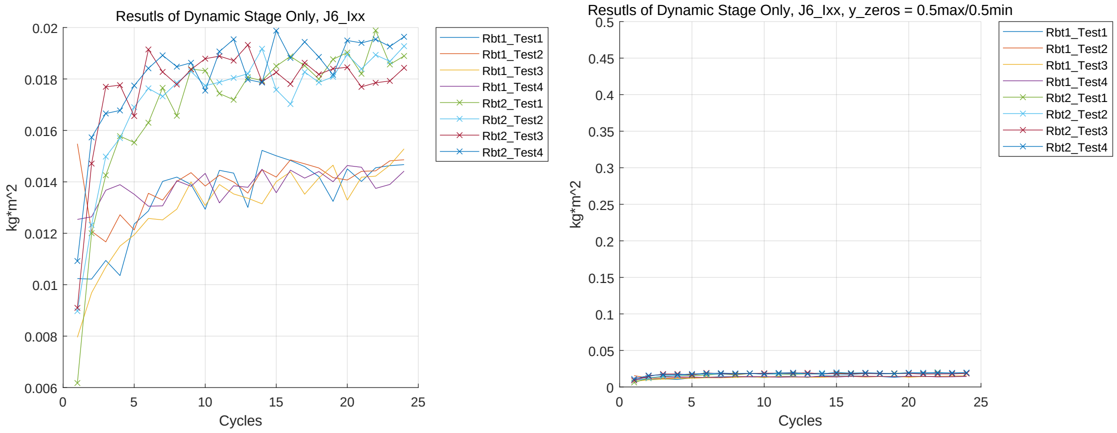

(a) Labelled automatically (b) Labelled with the widening scale of y-axis

Figure G.32: I_{xx} of Joint 6

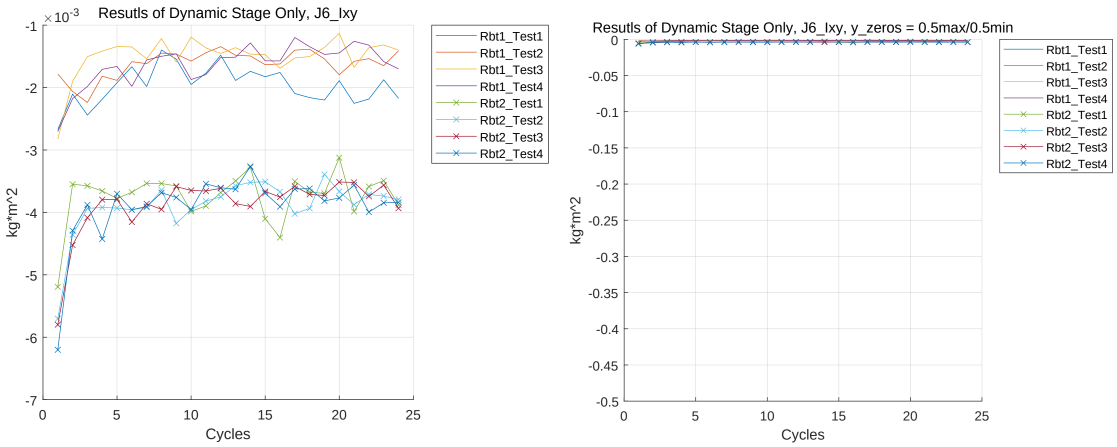

(a) Labelled automatically (b) Labelled with the widening scale of y-axis

Figure G.33: I_{xy} of Joint 6

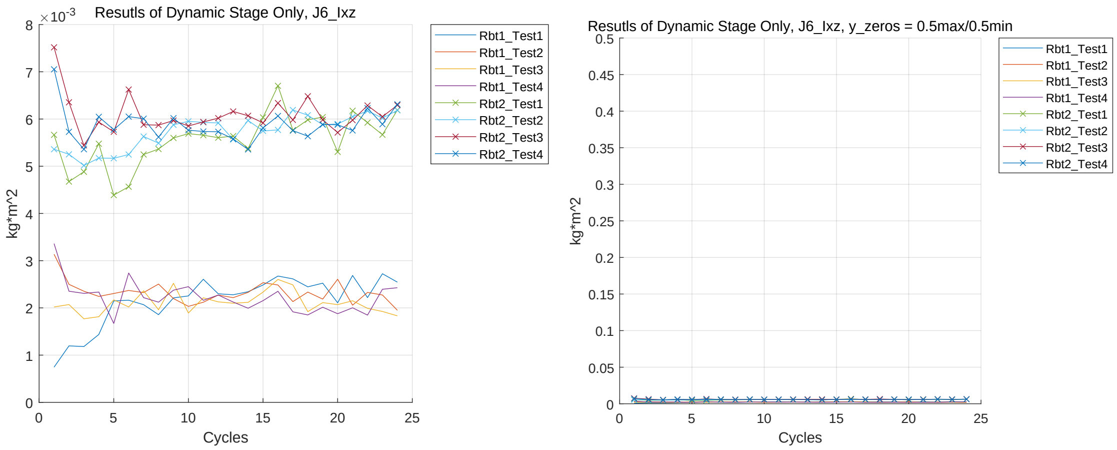

(a) Labelled automatically (b) Labelled with the widening scale of y-axis

Figure G.34: I_{xz} of Joint 6

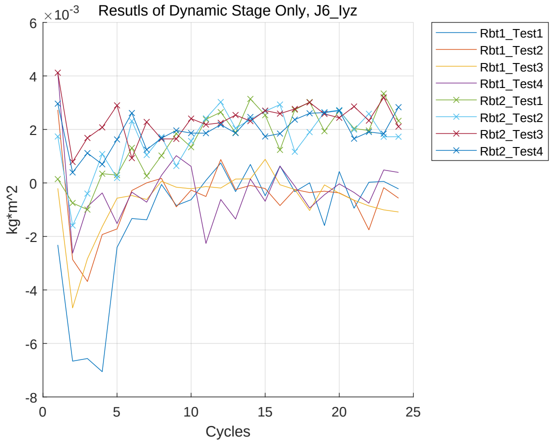

(a) Labelled automatically

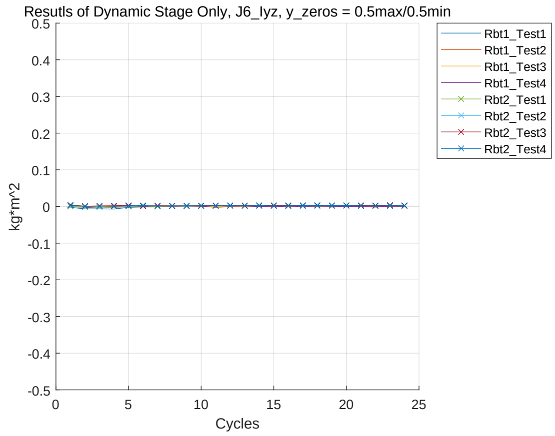

(b) Labelled with the widening scale of y-axis

Figure G.35: I_{yz} of Joint 6

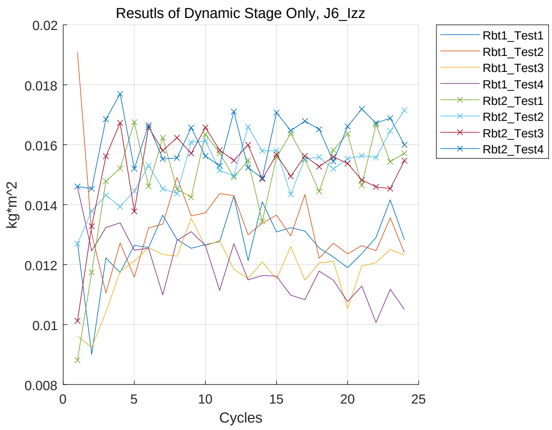

(a) Labelled automatically

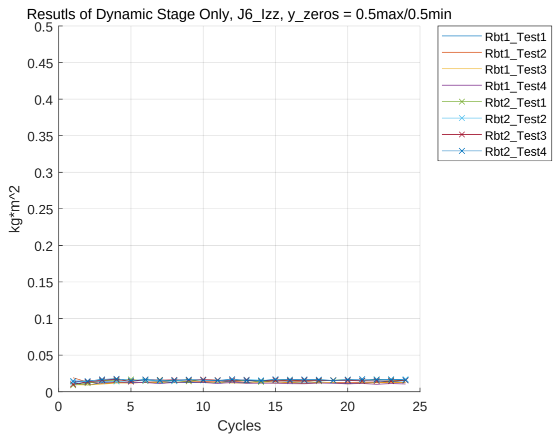

(b) Labelled with the widening scale of y-axis

Figure G.36: I_{zz} of Joint 6

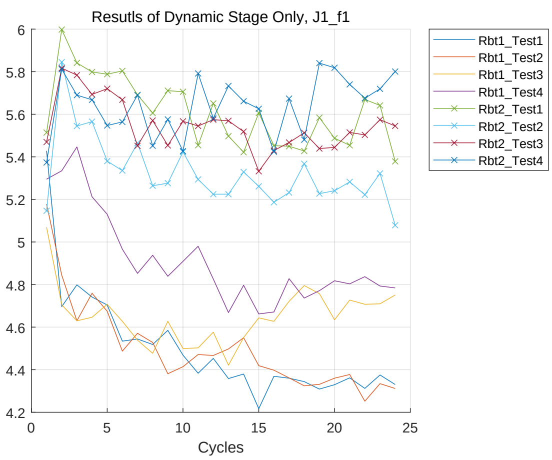

(a) Labelled automatically

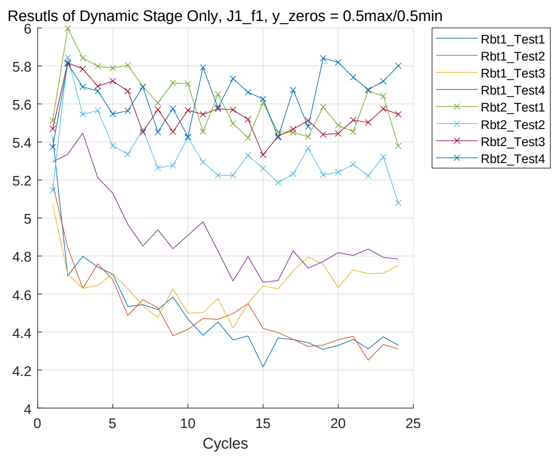

(b) Labelled with the widening scale of y-axis

Figure G.37: f_1 of Joint 1

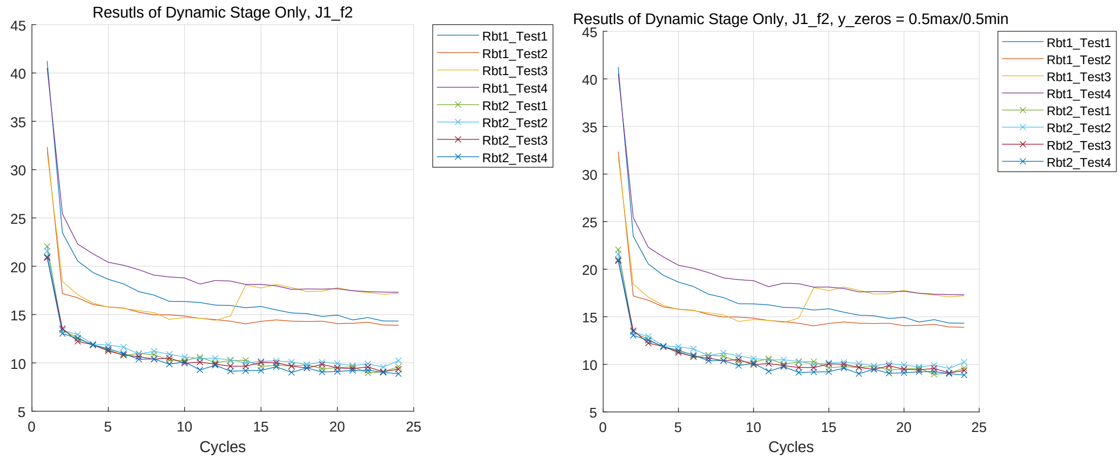

(a) Labelled automatically (b) Labelled with the widening scale of y-axis

Figure G.38: f_2 of Joint 1

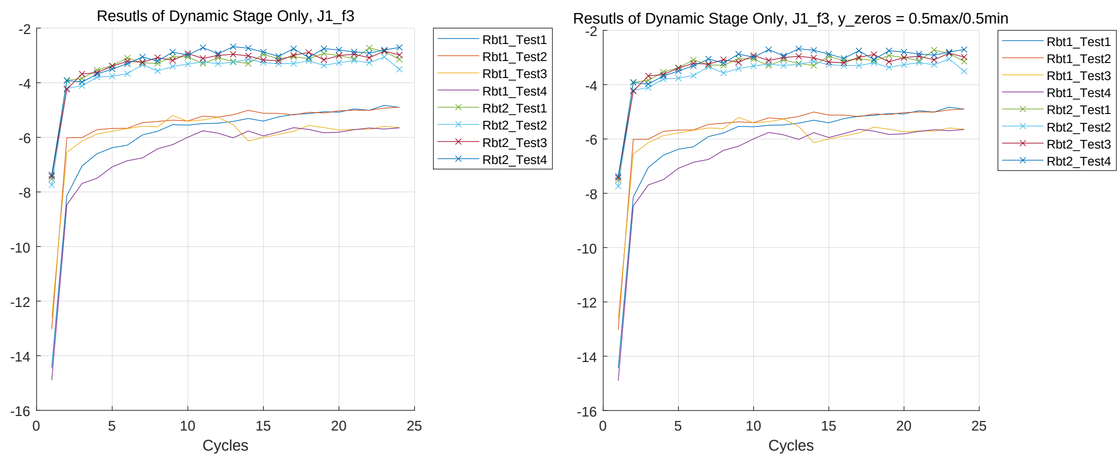

(a) Labelled automatically (b) Labelled with the widening scale of y-axis

Figure G.39: f_3 of Joint 1

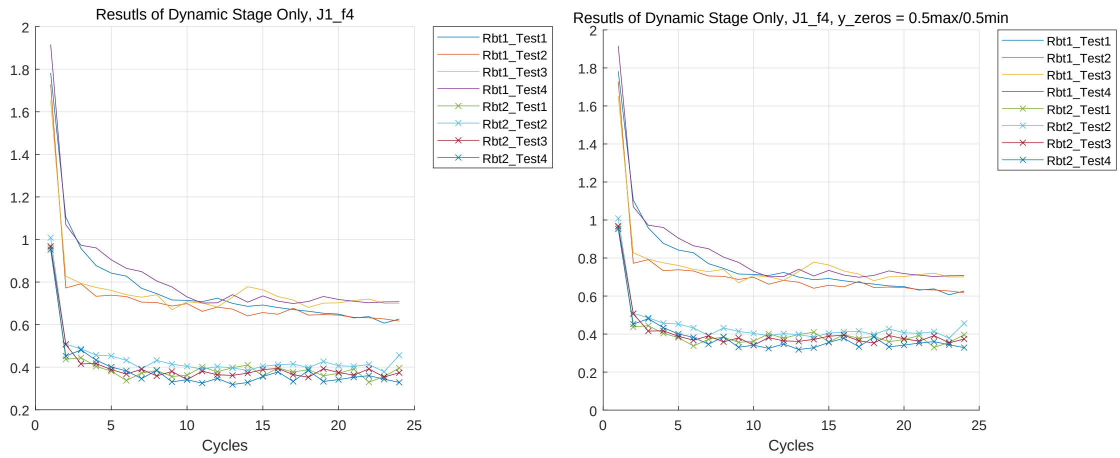

(a) Labelled automatically (b) Labelled with the widening scale of y-axis

Figure G.40: f_4 of Joint 1

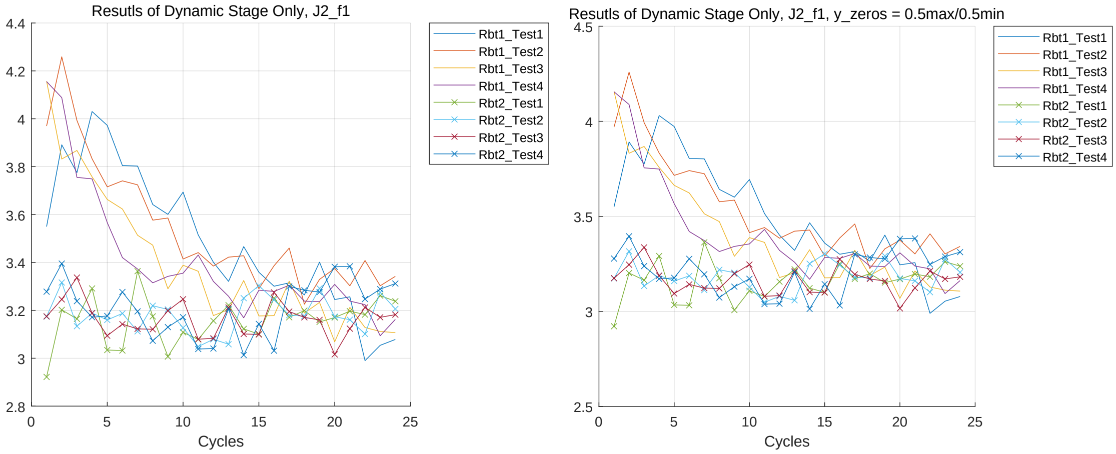

(a) Labelled automatically

(b) Labelled with the widening scale of y-axis

Figure G.41: f_1 of Joint 2

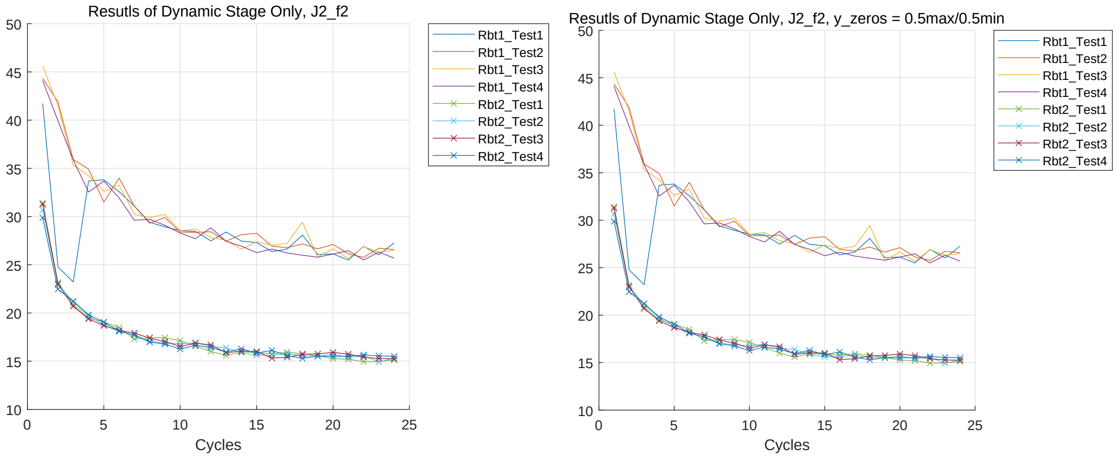

(a) Labelled automatically

(b) Labelled with the widening scale of y-axis

Figure G.42: f_2 of Joint 2

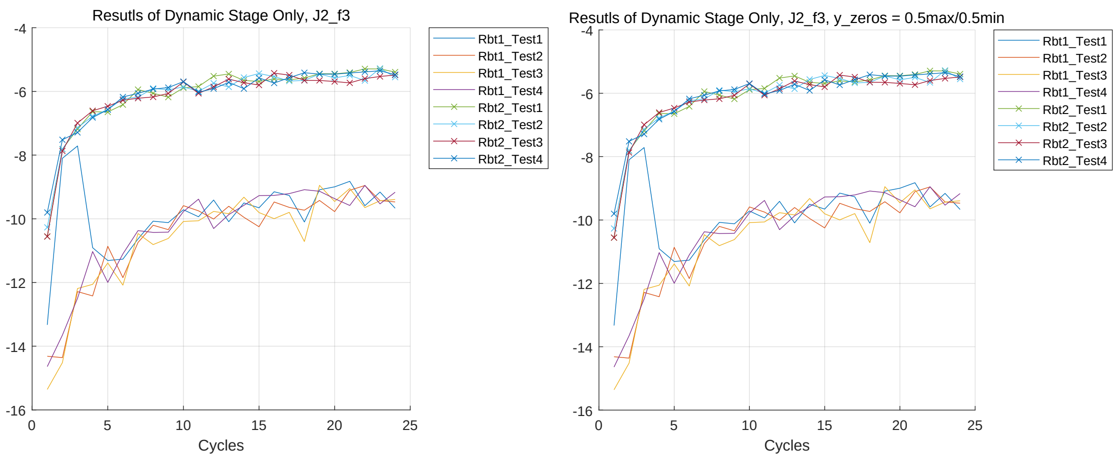

(a) Labelled automatically

(b) Labelled with the widening scale of y-axis

Figure G.43: f_3 of Joint 2

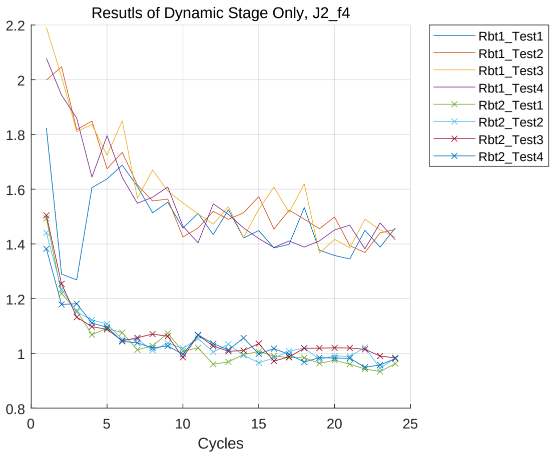

(a) Labelled automatically

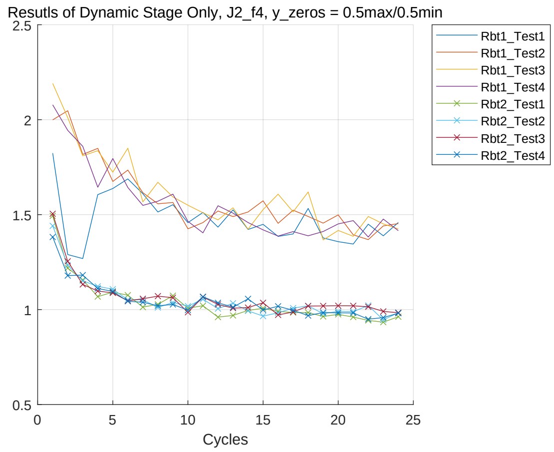

(b) Labelled with the widening scale of y-axis

Figure G.44: f_4 of Joint 2

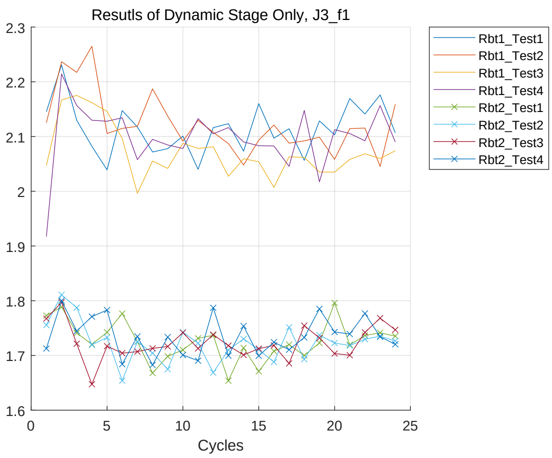

(a) Labelled automatically

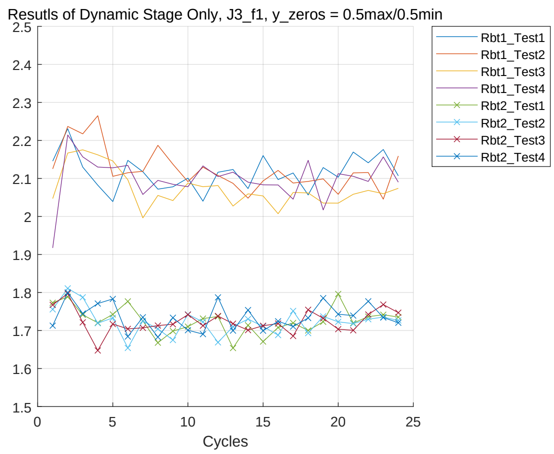

(b) Labelled with the widening scale of y-axis

Figure G.45: f_1 of Joint 3

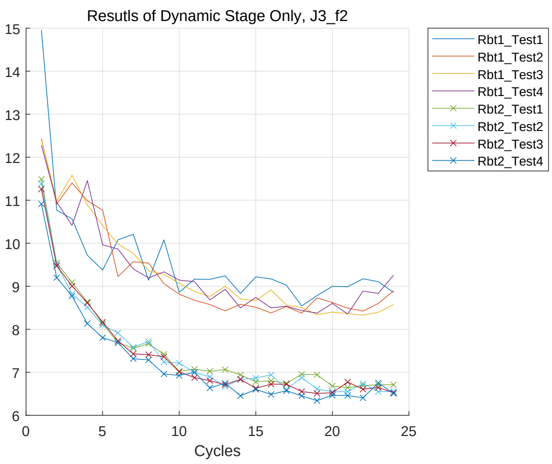

(a) Labelled automatically

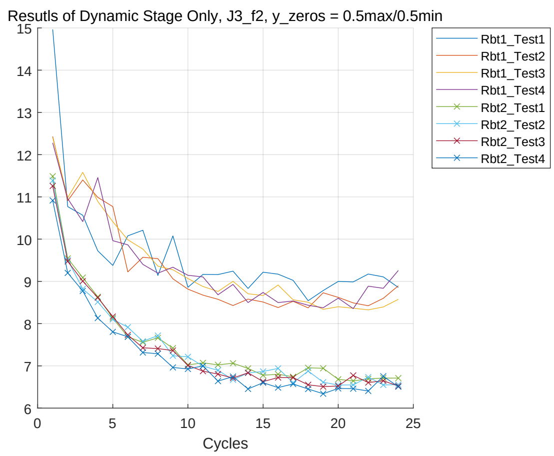

(b) Labelled with the widening scale of y-axis

Figure G.46: f_2 of Joint 3

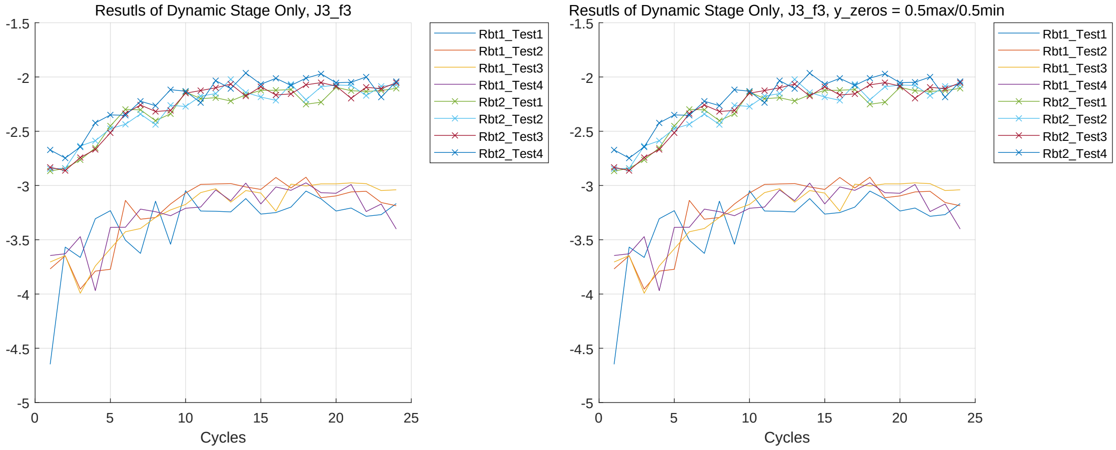

(a) Labelled automatically (b) Labelled with the widening scale of y-axis

Figure G.47: f_3 of Joint 3

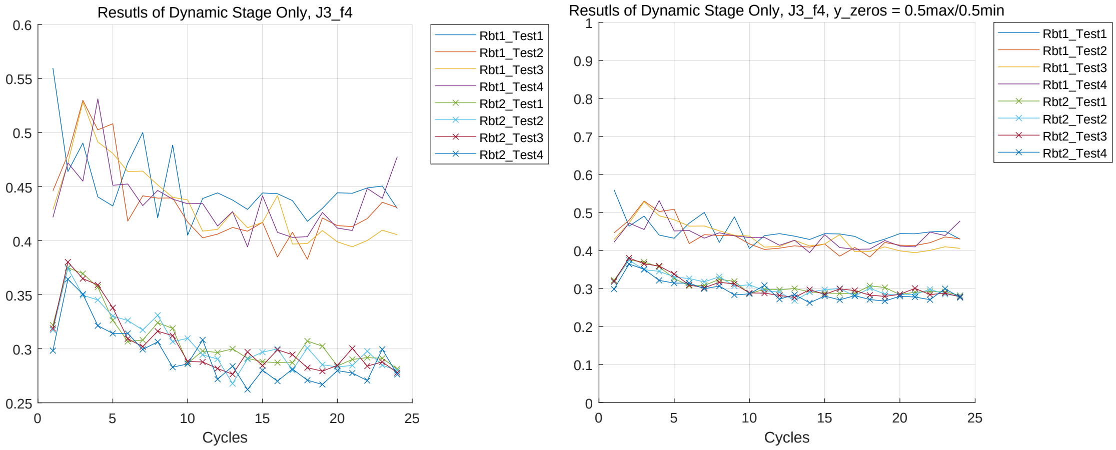

(a) Labelled automatically (b) Labelled with the widening scale of y-axis

Figure G.48: f_4 of Joint 3

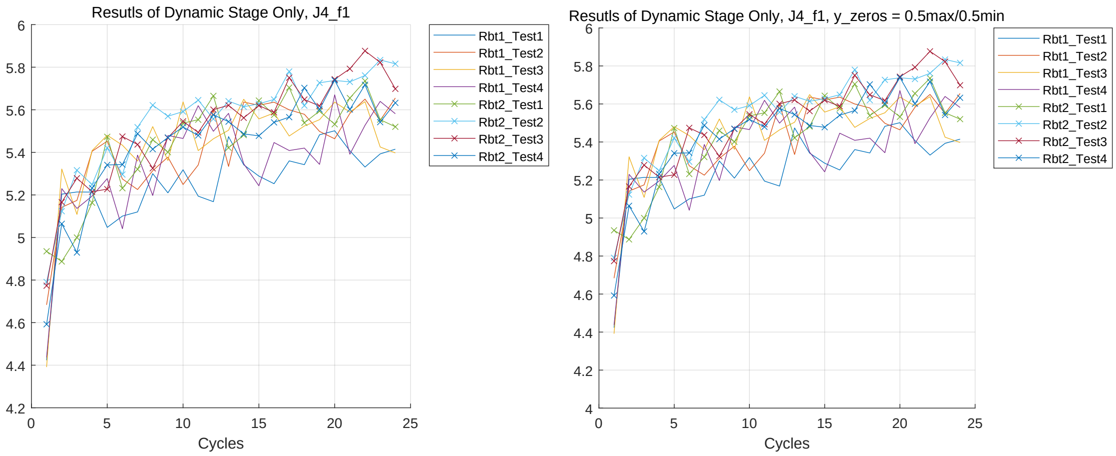

(a) Labelled automatically (b) Labelled with the widening scale of y-axis

Figure G.49: f_1 of Joint 4

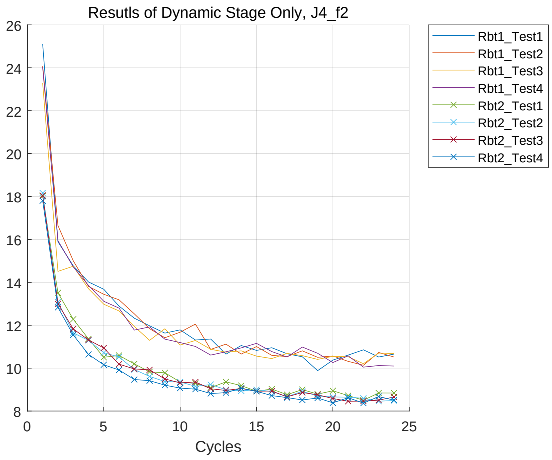

(a) Labelled automatically

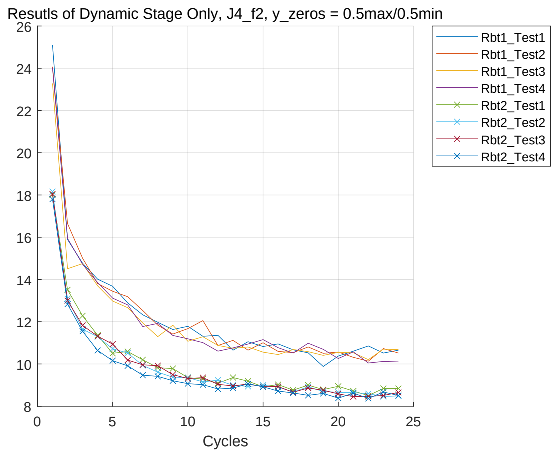

(b) Labelled with the widening scale of y-axis

Figure G.50: f_2 of Joint 4

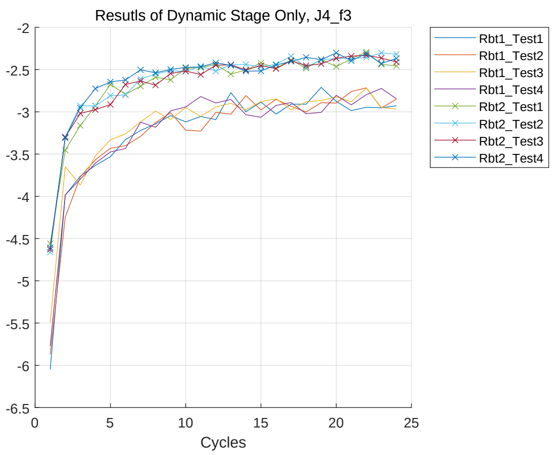

(a) Labelled automatically

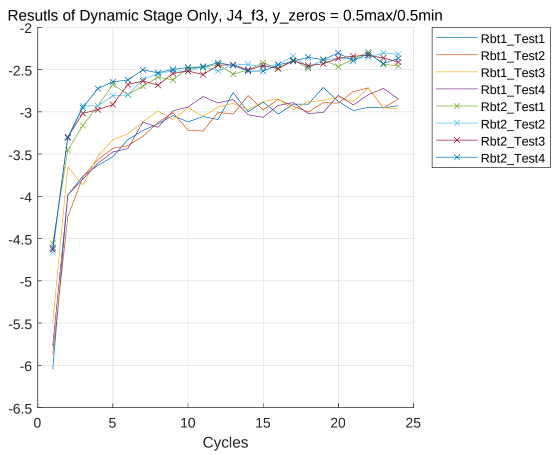

(b) Labelled with the widening scale of y-axis

Figure G.51: f_3 of Joint 4

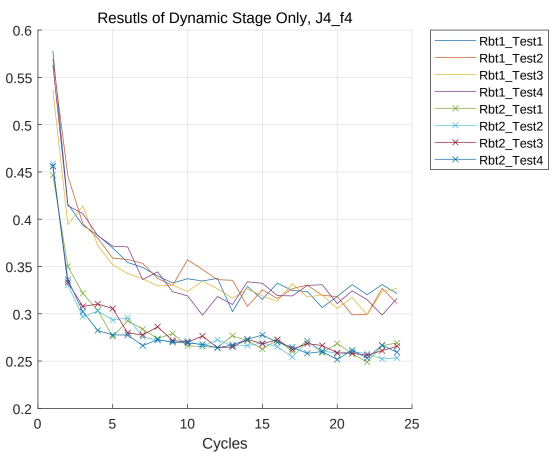

(a) Labelled automatically

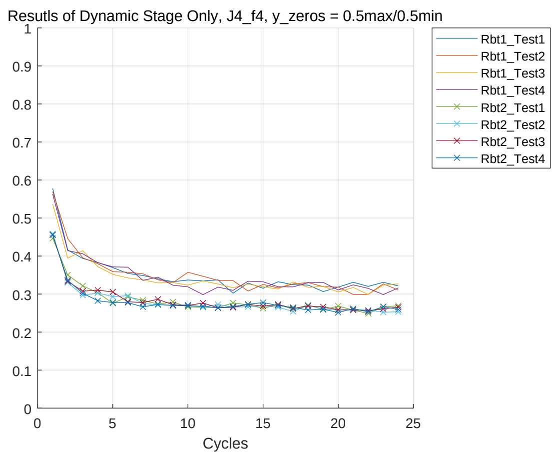

(b) Labelled with the widening scale of y-axis

Figure G.52: f_4 of Joint 4

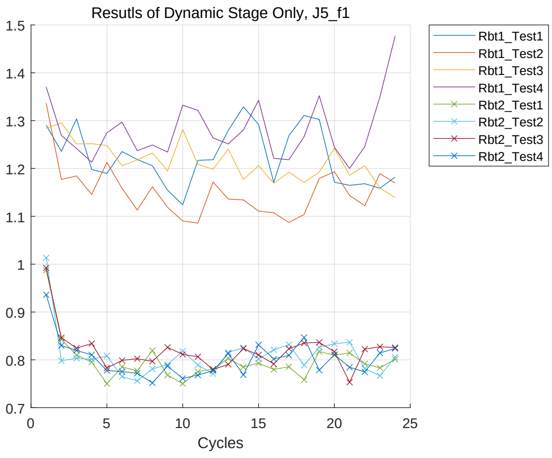

(a) Labelled automatically

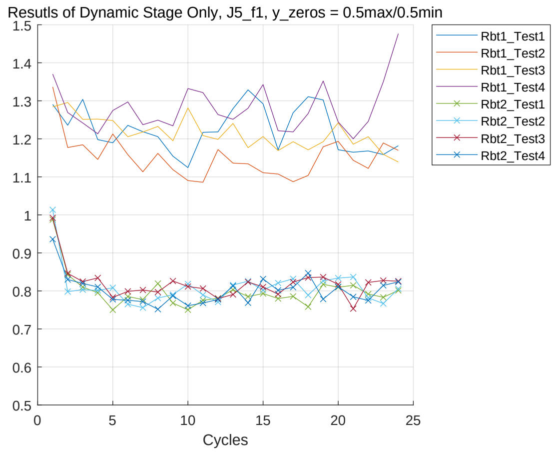

(b) Labelled with the widening scale of y-axis

Figure G.53: f_1 of Joint 5

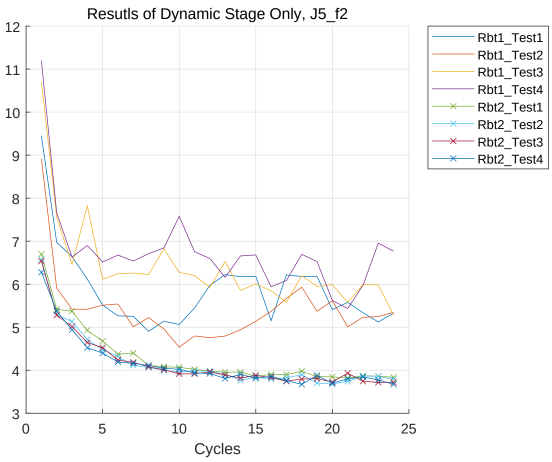

(a) Labelled automatically

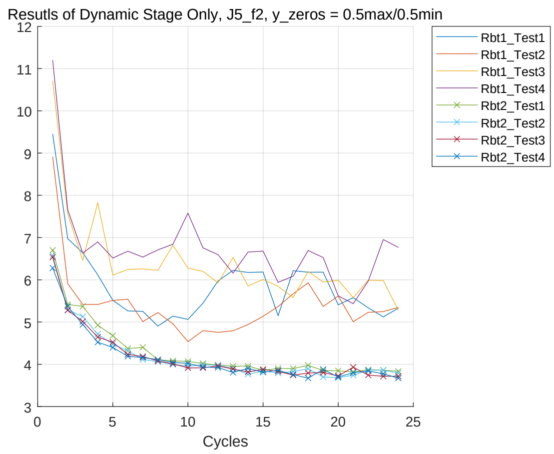

(b) Labelled with the widening scale of y-axis

Figure G.54: f_2 of Joint 5

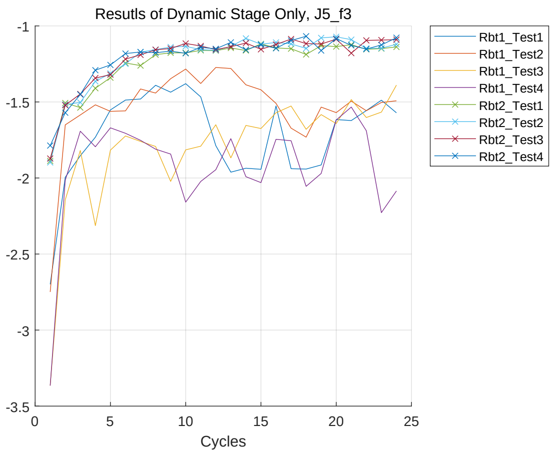

(a) Labelled automatically

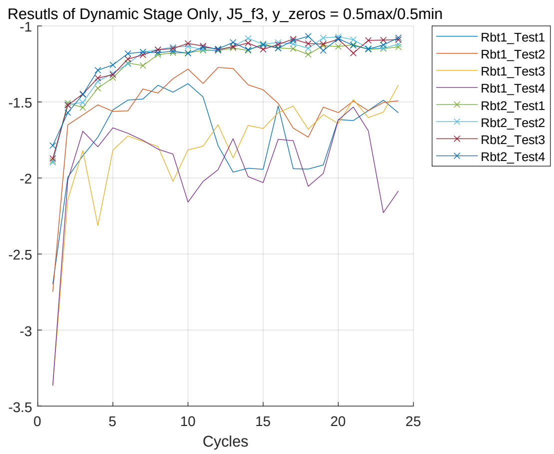

(b) Labelled with the widening scale of y-axis

Figure G.55: f_3 of Joint 5

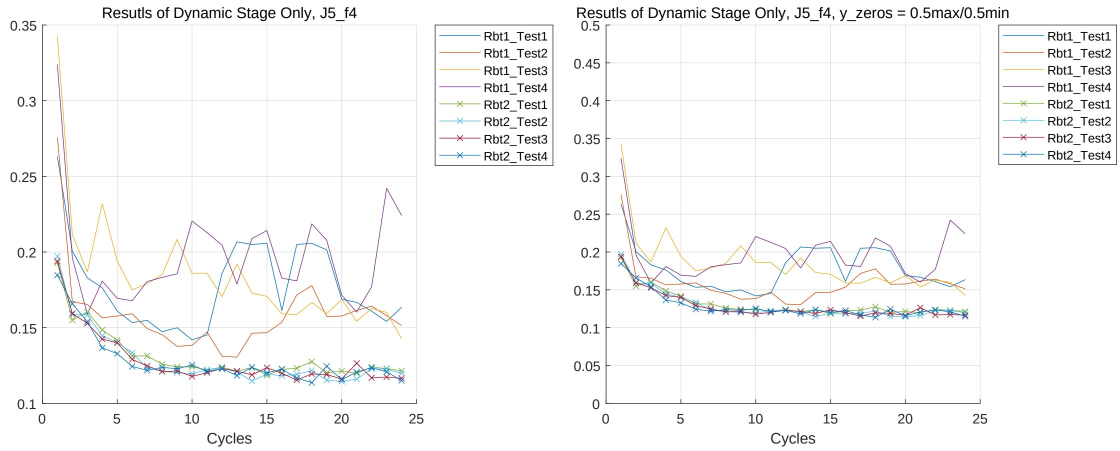

(a) Labelled automatically

(b) Labelled with the widening scale of y-axis

Figure G.56: f_4 of Joint 5

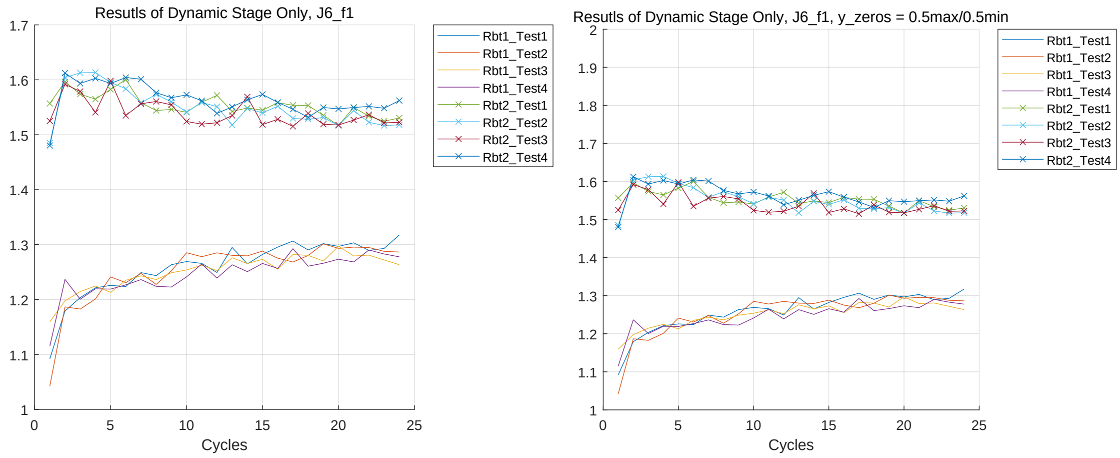

(a) Labelled automatically

(b) Labelled with the widening scale of y-axis

Figure G.57: f_1 of Joint 6

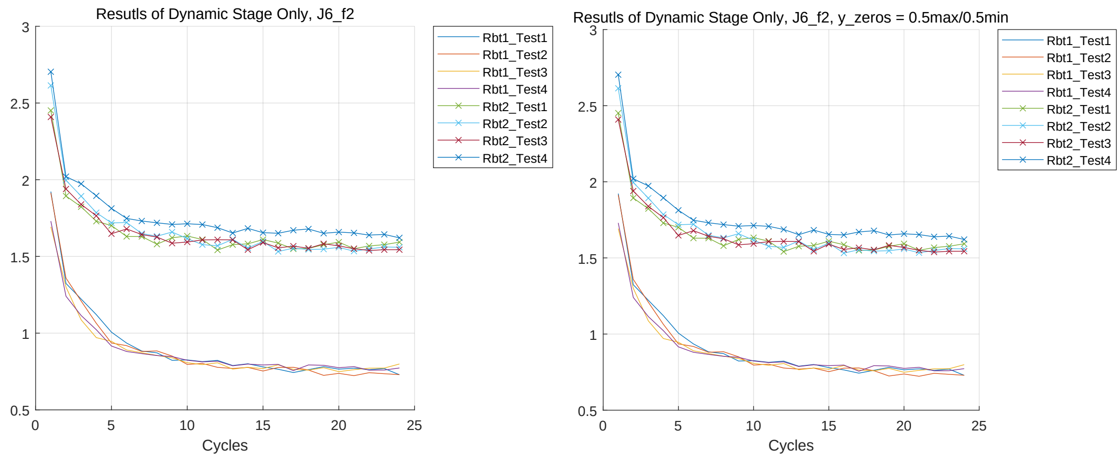

(a) Labelled automatically

(b) Labelled with the widening scale of y-axis

Figure G.58: f_2 of Joint 6

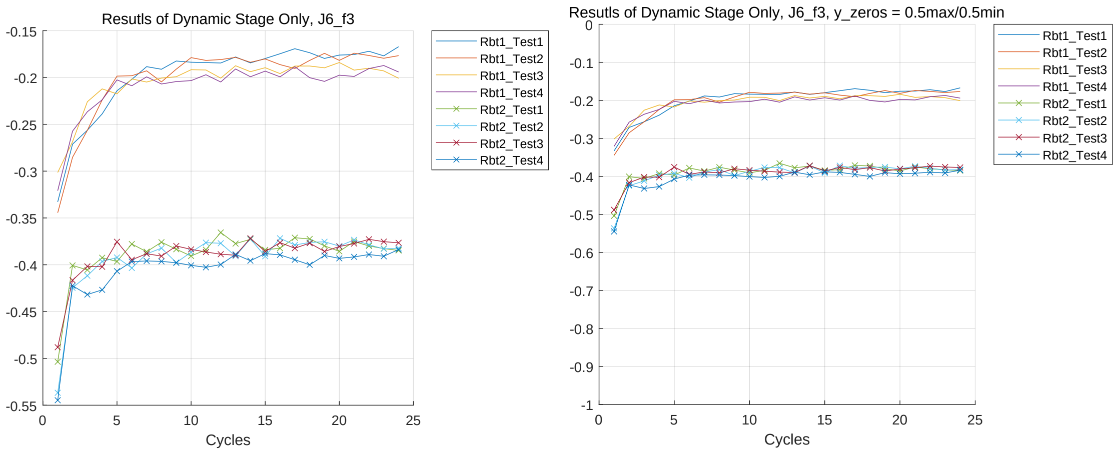

(a) Labelled automatically (b) Labelled with the widening scale of y-axis

Figure G.59: f_3 of Joint 6

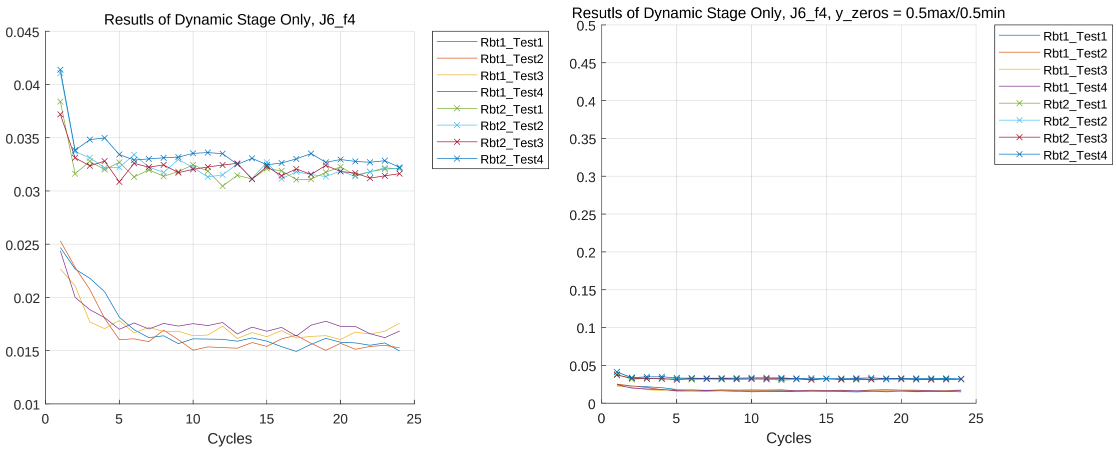

(a) Labelled automatically (b) Labelled with the widening scale of y-axis

Figure G.60: f_4 of Joint 6

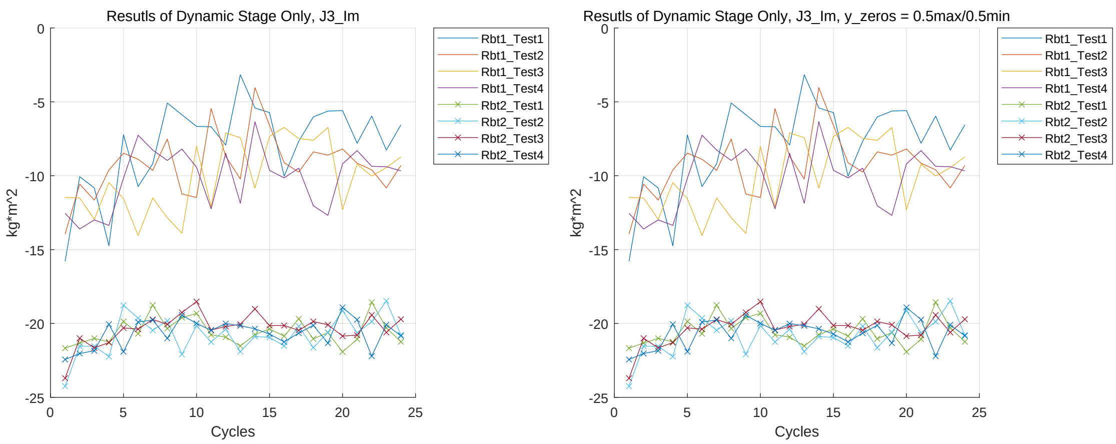

(a) Labelled automatically (b) Labelled with the widening scale of y-axis

Figure G.61: I_m of Joint 3

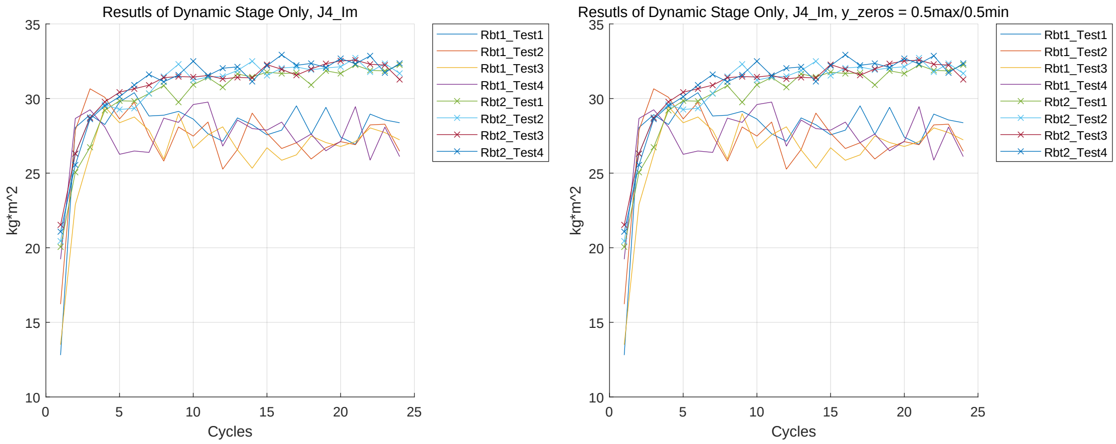

(a) Labelled automatically (b) Labelled with the widening scale of y-axis

Figure G.62: I_m of Joint 4

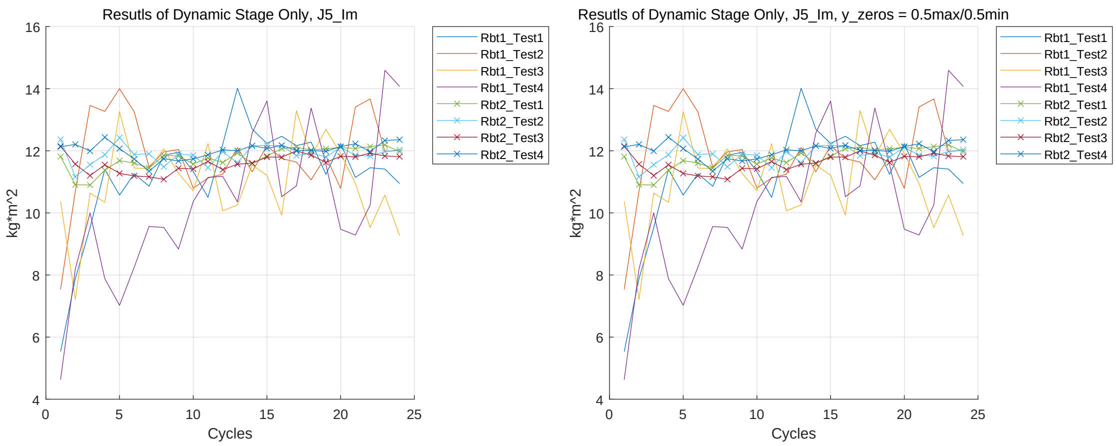

(a) Labelled automatically (b) Labelled with the widening scale of y-axis

Figure G.63: I_m of Joint 5

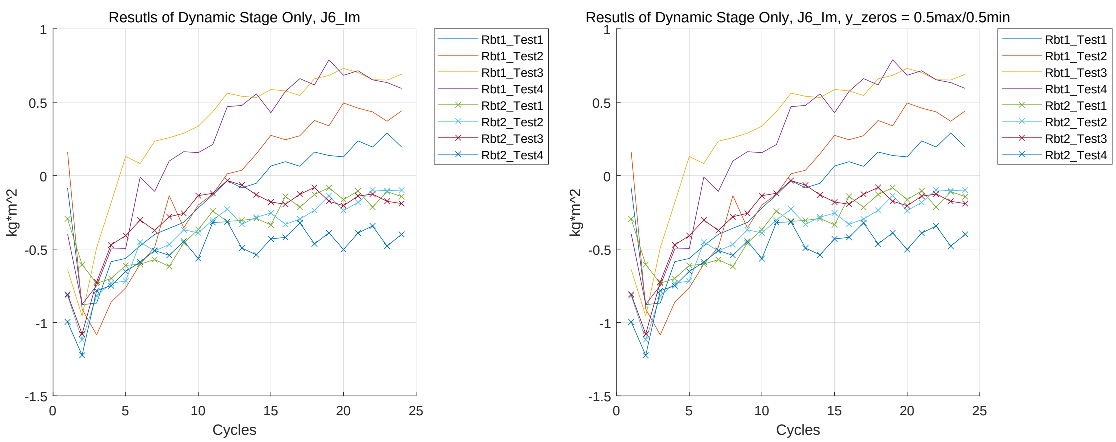

(a) Labelled automatically (b) Labelled with the widening scale of y-axis

Figure G.64: I_m of Joint 6

Appendix H

The Statistics Data Of The Identification Results

The tables shown in this section contain the statistics results of all dynamic parameters and are used to analysis in Section 5.1.5.1. To make the tables more clear, the titles of “Minimum”, “Maximum”, “Difference between Minimum and Maximum”, “Differences between Start and End Cycles” and “Standard Deviation” have been noted as “MIN”, “MAX”, “D/MM”, “D/SE” and “Sdv” respectively.

Table H.1: The statistics data of the identification results (1/8)

				All Cycles						The cycles without 1st 5 cycles					
				Mean	MIN	MAX	D/MM	D/SE	Sdv	Mean	MIN	MAX	D/MM	D/SE	Sdv
1	J1_Izz	Robot 1	T1	395.0708	377.9726	404.6069	0.0658	0.0705	8.6134	398.6718	387.4123	404.6069	0.0425	0.0444	5.2102
			T2	394.2585	365.8972	407.3106	0.1017	0.0778	12.1522	399.5416	385.4614	407.3106	0.0536	0.0567	6.2626
			T3	399.3032	365.9901	412.9436	0.1137	0.0813	13.6214	404.7900	388.4364	412.9436	0.0593	0.0631	8.2498
			T4	405.1108	379.4690	417.0318	0.0901	0.0727	11.0691	409.7180	395.3692	417.0318	0.0519	0.0548	6.5554
		Robot 2	T1	425.3887	396.6843	437.2569	0.0928	0.0998	12.3072	430.8098	419.0915	437.2569	0.0415	0.0410	5.5211
			T2	423.1736	393.5597	436.1905	0.0977	0.1083	11.3952	427.9718	415.2093	436.1905	0.0481	0.0505	5.8352
			T3	427.1423	393.5951	438.5863	0.1026	0.1121	12.1928	432.2010	417.8618	438.5863	0.0473	0.0475	6.3375
			T4	428.9708	397.5389	442.0354	0.1007	0.1011	12.3984	434.2622	419.2267	442.0354	0.0516	0.0441	6.2522
2	J2_mPx	Robot 1	T1	2.4475	2.2733	2.4969	0.0895	0.0842	0.0524	2.4661	2.3836	2.4969	0.0454	0.0340	0.0299
			T2	2.4420	2.2862	2.5097	0.0890	0.0807	0.0618	2.4683	2.4126	2.5097	0.0387	0.0146	0.0289
			T3	2.4460	2.2924	2.5154	0.0887	0.0882	0.0537	2.4680	2.4240	2.5154	0.0363	0.0291	0.0268
			T4	2.4480	2.3051	2.5018	0.0786	0.0821	0.0560	2.4719	2.4108	2.5018	0.0364	0.0264	0.0249
		Robot 2	T1	2.4345	2.2966	2.4682	0.0695	0.0735	0.0367	2.4492	2.4247	2.4682	0.0176	0.0168	0.0113
			T2	2.4331	2.3007	2.4581	0.0640	0.0662	0.0345	2.4468	2.4258	2.4581	0.0132	0.0113	0.0092
			T3	2.4374	2.3117	2.4678	0.0633	0.0675	0.0365	2.4532	2.4288	2.4678	0.0158	0.0161	0.0113
			T4	2.4387	2.2984	2.4641	0.0672	0.0634	0.0374	2.4537	2.4385	2.4641	0.0104	0.0023	0.0086
3	J2_mPy	Robot 1	T1	0.2740	0.2426	0.3317	0.2686	0.1928	0.0185	0.2687	0.2426	0.2894	0.1617	0.0748	0.0139
			T2	0.2665	0.2238	0.3397	0.3411	0.2805	0.0281	0.2568	0.2238	0.2913	0.2315	0.1003	0.0181
			T3	0.2511	0.2218	0.3137	0.2929	0.2323	0.0201	0.2453	0.2218	0.2730	0.1877	0.0857	0.0142
			T4	0.2505	0.2196	0.3046	0.2789	0.2268	0.0203	0.2446	0.2196	0.2717	0.1916	0.0391	0.0142
		Robot 2	T1	0.1761	0.1582	0.1921	0.1763	0.1045	0.0085	0.1772	0.1582	0.1921	0.1763	0.0470	0.0090
			T2	0.1804	0.1670	0.1955	0.1458	0.1041	0.0072	0.1814	0.1716	0.1955	0.1223	0.0788	0.0069
			T3	0.1697	0.1445	0.1952	0.2597	0.1380	0.0124	0.1725	0.1572	0.1952	0.1945	0.0118	0.0108
			T4	0.1782	0.1622	0.1939	0.1633	0.0401	0.0075	0.1789	0.1622	0.1939	0.1633	0.0399	0.0081
4	J2_Ixx	Robot 1	T1	-0.8427	-1.1130	-0.7464	0.4910	0.2875	0.0694	-0.8237	-0.8840	-0.7464	0.1843	0.0139	0.0377
			T2	-0.8213	-1.0264	-0.6997	0.4669	0.2055	0.0686	-0.8186	-0.8971	-0.6998	0.2818	0.0364	0.0507
			T3	-0.7895	-1.0746	-0.6653	0.6152	0.2368	0.0813	-0.7785	-0.8856	-0.6953	0.2737	0.1796	0.0502
			T4	-0.8085	-1.0680	-0.6921	0.5431	0.2565	0.0691	-0.7973	-0.8442	-0.7278	0.1599	0.0911	0.0343
		Robot 2	T1	-0.6187	-0.8033	-0.5581	0.4394	0.2268	0.0459	-0.6164	-0.6493	-0.5623	0.1547	0.0431	0.0214
			T2	-0.6459	-0.8433	-0.5717	0.4752	0.2118	0.0485	-0.6454	-0.6773	-0.6175	0.0968	0.0549	0.0166
			T3	-0.6317	-0.7851	-0.5789	0.3562	0.2122	0.0369	-0.6284	-0.6473	-0.6030	0.0735	0.0213	0.0118
			T4	-0.6525	-0.8243	-0.6061	0.3602	0.1743	0.0410	-0.6495	-0.6806	-0.6181	0.1012	0.0793	0.0161

Table H.2: The statistics data of the identification results (2/8)

				All Cycles						The cycles without 1st 5 cycles					
				Mean	MIN	MAX	D/MM	D/SE	Sdv	Mean	MIN	MAX	D/MM	D/SE	Sdv
5	J2_Ixy	Robot 1	T1	0.1735	0.0751	0.2243	0.6653	0.8505	0.0392	0.1898	0.1666	0.2243	0.2572	0.1171	0.0173
			T2	0.1806	0.0903	0.2304	0.6082	1.0812	0.0258	0.1848	0.1634	0.2081	0.2146	0.0642	0.0115
			T3	0.1892	0.1127	0.2790	0.5962	0.6540	0.0274	0.1895	0.1674	0.2224	0.2475	0.0050	0.0131
			T4	0.1831	0.1124	0.2249	0.5002	0.6430	0.0234	0.1886	0.1646	0.2249	0.2680	0.0178	0.0152
		Robot 2	T1	0.1662	0.0959	0.1899	0.4951	0.8204	0.0197	0.1728	0.1449	0.1899	0.2371	0.2047	0.0111
			T2	0.1587	0.0729	0.1820	0.5993	1.3489	0.0238	0.1677	0.1456	0.1820	0.2001	0.1767	0.0088
			T3	0.1638	0.0847	0.1879	0.5493	1.0473	0.0215	0.1711	0.1546	0.1879	0.1772	0.0649	0.0080
			T4	0.1569	0.1034	0.1852	0.4418	0.7466	0.0198	0.1645	0.1422	0.1852	0.2322	0.2337	0.0124
6	J2_Ixz	Robot 1	T1	0.4122	0.3533	0.6375	0.4459	0.4459	0.0621	0.3864	0.3533	0.4143	0.1474	0.1129	0.0181
			T2	0.4062	0.3136	0.5132	0.3890	0.2191	0.0349	0.4020	0.3689	0.4313	0.1447	0.0336	0.0185
			T3	0.3668	0.3037	0.4834	0.3717	0.2342	0.0401	0.3615	0.3037	0.4280	0.2906	0.0083	0.0294
			T4	0.3651	0.3230	0.4689	0.3112	0.2079	0.0338	0.3581	0.3230	0.3888	0.1692	0.0242	0.0191
		Robot 2	T1	0.3409	0.3132	0.3649	0.1418	0.0002	0.0167	0.3439	0.3177	0.3649	0.1293	0.0496	0.0156
			T2	0.3684	0.3353	0.3954	0.1519	0.0010	0.0155	0.3696	0.3520	0.3898	0.0970	0.0017	0.0117
			T3	0.3513	0.3237	0.3826	0.1540	0.0181	0.0139	0.3522	0.3380	0.3747	0.0980	0.0215	0.0099
			T4	0.3590	0.3345	0.3823	0.1250	0.0615	0.0142	0.3584	0.3373	0.3823	0.1176	0.0712	0.0132
7	J2_Iyz	Robot 1	T1	0.1572	0.1184	0.2684	0.5590	0.3849	0.0305	0.1544	0.1184	0.1939	0.3896	0.3946	0.0192
			T2	0.0783	-0.0342	0.1596	1.2143	0.1704	0.0563	0.0930	0.0188	0.1596	0.8821	6.7013	0.0437
			T3	0.0697	-0.1223	0.1271	1.9624	0.0486	0.0556	0.0876	0.0412	0.1271	0.6758	0.9559	0.0290
			T4	0.0807	-0.0269	0.1726	1.1559	0.3012	0.0418	0.0881	0.0318	0.1218	0.7387	1.7129	0.0267
		Robot 2	T1	0.1829	0.1590	0.2018	0.2123	0.0080	0.0115	0.1847	0.1590	0.2018	0.2123	0.0469	0.0109
			T2	0.1773	0.1520	0.1982	0.2333	0.0887	0.0142	0.1798	0.1520	0.1982	0.2333	0.1250	0.0139
			T3	0.1804	0.1448	0.2018	0.2825	0.0381	0.0134	0.1827	0.1638	0.2018	0.1886	0.1266	0.0113
			T4	0.1734	0.1603	0.1948	0.1770	0.1236	0.0098	0.1757	0.1618	0.1948	0.1695	0.1060	0.0096
8	J2_Izz	Robot 1	T1	393.3510	355.8586	414.4113	0.1413	0.1606	18.5070	401.4059	380.1329	414.4113	0.0827	0.0849	9.7060
			T2	399.2003	359.4052	414.5698	0.1331	0.1535	14.0913	404.8964	391.4186	414.5698	0.0558	0.0591	7.4715
			T3	402.7142	377.9599	415.7144	0.0908	0.0904	11.5533	407.4524	396.5497	415.7144	0.0461	0.0419	6.6260
			T4	403.0448	372.1880	415.8227	0.1049	0.1126	13.1438	408.6457	394.5189	415.8227	0.0512	0.0417	6.5612
		Robot 2	T1	416.2713	392.0812	428.3185	0.0846	0.0721	9.1046	420.0267	410.5936	428.3185	0.0414	0.0238	4.5538
			T2	416.2688	391.6136	429.3532	0.0879	0.0964	9.3161	420.1095	413.2470	429.3532	0.0375	0.0358	4.5383
			T3	417.1380	390.0389	427.1992	0.0870	0.0863	8.3807	420.3124	414.9353	427.1992	0.0287	0.0189	3.8523
			T4	414.7046	397.0552	427.6990	0.0716	0.0663	7.5208	417.6654	411.0373	427.6990	0.0390	0.0278	4.5984
9	J3_mPx	Robot 1	T1	0.6513	0.6115	0.6671	0.0834	0.0731	0.0118	0.6530	0.6386	0.6649	0.0396	0.0185	0.0079
			T2	0.6448	0.5950	0.6643	0.1044	0.0768	0.0180	0.6506	0.6247	0.6604	0.0540	0.0407	0.0091
			T3	0.6425	0.5660	0.6861	0.1749	0.0947	0.0236	0.6500	0.6249	0.6861	0.0891	0.0308	0.0135
			T4	0.6434	0.5980	0.6684	0.1055	0.0974	0.0186	0.6501	0.6219	0.6684	0.0696	0.0631	0.0123
		Robot 2	T1	0.6053	0.5529	0.6225	0.1118	0.1096	0.0164	0.6124	0.5975	0.6225	0.0403	0.0269	0.0061
			T2	0.6066	0.5529	0.6239	0.1137	0.1174	0.0162	0.6131	0.5998	0.6239	0.0387	0.0263	0.0068
			T3	0.6050	0.5527	0.6225	0.1121	0.1240	0.0169	0.6113	0.5882	0.6225	0.0551	0.0562	0.0091
			T4	0.6042	0.5520	0.6252	0.1171	0.1326	0.0169	0.6114	0.5950	0.6252	0.0483	0.0507	0.0074
10	J3_mPy	Robot 1	T1	-1.3082	-1.3280	-1.2678	0.0475	0.0378	0.0139	-1.3138	-1.3280	-1.3004	0.0212	0.0118	0.0076
			T2	-1.3058	-1.3208	-1.2658	0.0434	0.0421	0.0151	-1.3124	-1.3208	-1.2994	0.0165	0.0152	0.0068
			T3	-1.3052	-1.3237	-1.2618	0.0491	0.0434	0.0153	-1.3111	-1.3237	-1.2934	0.0234	0.0178	0.0080
			T4	-1.3041	-1.3208	-1.2622	0.0464	0.0418	0.0154	-1.3104	-1.3208	-1.2932	0.0213	0.0169	0.0084
		Robot 2	T1	-1.2576	-1.2771	-1.2070	0.0581	0.0546	0.0170	-1.2646	-1.2771	-1.2494	0.0222	0.0188	0.0081
			T2	-1.2570	-1.2764	-1.2089	0.0558	0.0528	0.0173	-1.2643	-1.2764	-1.2499	0.0212	0.0179	0.0086
			T3	-1.2504	-1.2684	-1.1893	0.0665	0.0655	0.0194	-1.2584	-1.2684	-1.2418	0.0214	0.0205	0.0077
			T4	-1.2508	-1.2699	-1.1934	0.0641	0.0613	0.0181	-1.2580	-1.2699	-1.2376	0.0261	0.0234	0.0085
11	J3_Ixx	Robot 1	T1	0.4806	0.4559	0.5355	0.1487	0.1123	0.0178	0.4743	0.4559	0.4937	0.0766	0.0220	0.0093
			T2	0.4400	0.3213	0.4797	0.3302	0.0126	0.0367	0.4494	0.4050	0.4797	0.1557	0.1665	0.0207
			T3	0.4400	0.3306	0.4939	0.3307	0.0885	0.0341	0.4485	0.4205	0.4842	0.1317	0.0708	0.0186
			T4	0.4466	0.3955	0.5179	0.2362	0.0805	0.0279	0.4475	0.3955	0.4971	0.2043	0.2038	0.0238
		Robot 2	T1	0.4351	0.4234	0.4532	0.0657	0.0068	0.0079	0.4358	0.4234	0.4532	0.0657	0.0055	0.0081
			T2	0.4329	0.4167	0.4538	0.0816	0.0182	0.0096	0.4340	0.4204	0.4538	0.0735	0.0193	0.0093
			T3	0.4411	0.4218	0.4519	0.0666	0.0125	0.0079	0.4409	0.4218	0.4519	0.0666	0.0420	0.0081
			T4	0.4413	0.4257	0.4513	0.0567	0.0087	0.0067	0.4419	0.4293	0.4510	0.0479	0.0228	0.0055
12	J3_Ixy	Robot 1	T1	-0.1525	-0.1632	-0.1417	0.1517	0.0255	0.0055	-0.1519	-0.1622	-0.1417	0.1450	0.0377	0.0055
			T2	-0.1439	-0.1620	-0.1281	0.2640	0.1767	0.0078	-0.1441	-0.1533	-0.1356	0.1307	0.1119	0.0053
			T3	-0.1377	-0.1586	-0.0879	0.8031	0.2191	0.0144	-0.1405	-0.1586	-0.1268	0.2506	0.1239	0.0087
			T4	-0.1390	-0.1523	-0.1219	0.2494	0.1641	0.0075	-0.1393	-0.1523	-0.1285	0.1854	0.0408	0.0070
		Robot 2	T1	-0.0810	-0.0859	-0.0657	0.3075	0.3019	0.0045	-0.0818	-0.0859	-0.0768	0.1195	0.0268	0.0031
			T2	-0.0832	-0.0928	-0.0770	0.2061	0.0565	0.0041	-0.0828	-0.0891	-0.0786	0.1333	0.0273	0.0030
			T3	-0.0840	-0.0945	-0.0745	0.2689	0.1413	0.0038	-0.0843	-0.0945	-0.0763	0.2388	0.0058	0.0036
			T4	-0.0862	-0.0920	-0.0751	0.2241	0.2241	0.0036	-0.0863	-0.0920	-0.0814	0.1290	0.0506	0.0028
13	J3_Ixz	Robot 1	T1	-0.1310	-0.2127	-0.1101	0.9319	0.4485	0.0206	-0.1236	-0.1338	-0.1101	0.2147	0.0747	0.0072
			T2	-0.1133	-0.1542	-0.0861	0.7905	0.2015	0.0137	-0.1139	-0.1287	-0.0998	0.2887	0.2142	0.0088
			T3	-0.1102	-0.1411	-0.0567	1.4886	0.1621	0.0152	-0.1127	-0.1230	-0.0986	0.2471	0.0731	0.0079
			T4	-0.1172	-0.1546	-0.1038	0.4898	0.2443	0.0105	-0.1149	-0.1247	-0.1038	0.2018	0.0271	0.0065
		Robot 2	T1	-0.1103	-0.1206	-0.1024	0.1774	0.1095	0.0046	-0.1089	-0.1162	-0.1024	0.1340	0.0754	0.0036
			T2	-0.1142	-0.1263	-0.1077	0.1735	0.1204	0.0052	-0.1128	-0.1188	-0.1077	0.1038	0.0631	0.0039
			T3	-0.1127	-0.1219	-0.1047	0.1634	0.0474	0.0042	-0.1115	-0.1197	-0.1047	0.1428	0.0194	0.0035
			T4	-0.1110	-0.1218	-0.1006	0.2103	0.0338	0.0051	-0.1093	-0.1168	-0.1006	0.1610	0.0730	0.0038

Table H.3: The statistics data of the identification results (3/8)

				All Cycles						The cycles without 1st 5 cycles					
				Mean	MIN	MAX	D/MM	D/SE	Sdv	Mean	MIN	MAX	D/MM	D/SE	Sdv
14	J3_Iyz	Robot 1	T1	-0.0360	-0.0502	-0.0178	1.8170	1.4575	0.0072	-0.0379	-0.0502	-0.0281	0.7869	0.4323	0.0059
			T2	-0.0073	-0.0241	0.0268	1.8982	0.8196	0.0154	-0.0123	-0.0241	0.0085	3.8472	4.8040	0.0111
			T3	-0.0115	-0.0345	0.0249	2.3837	0.2681	0.0179	-0.0174	-0.0345	0.0090	4.8374	5.4503	0.0130
			T4	-0.0181	-0.0394	0.0065	7.0143	0.2108	0.0127	-0.0213	-0.0340	-0.0027	11.5102	10.4404	0.0087
		Robot 2	T1	-0.0091	-0.0218	0.0025	9.5669	0.5727	0.0068	-0.0104	-0.0201	0.0012	17.4370	8.6142	0.0052
			T2	-0.0028	-0.0109	0.0100	2.0911	0.1932	0.0067	-0.0048	-0.0109	0.0080	2.3695	1.6244	0.0053
			T3	-0.0100	-0.0182	0.0096	2.8974	0.1386	0.0071	-0.0123	-0.0182	-0.0015	10.9075	9.3915	0.0044
			T4	-0.0076	-0.0208	0.0087	3.3877	0.3037	0.0079	-0.0097	-0.0208	0.0045	5.5951	5.5951	0.0060
15	J3_Izz	Robot 1	T1	83.8558	80.2832	94.9495	0.1545	0.1258	2.9938	83.1668	80.2832	85.7274	0.0635	0.0300	1.6871
			T2	86.5038	80.2403	92.2948	0.1306	0.0635	2.4621	86.2699	80.2403	89.3271	0.1017	0.0073	2.2032
			T3	87.8249	83.5209	91.8600	0.0908	0.0354	2.4466	87.5858	83.5209	91.5062	0.0873	0.0268	2.5635
			T4	88.4538	85.4983	91.7778	0.0684	0.0382	1.5500	88.1063	85.4983	90.7594	0.0580	0.0189	1.4281
		Robot 2	T1	107.5389	105.1102	110.0484	0.0449	0.0164	1.1787	107.6684	105.1102	109.1375	0.0369	0.0098	1.0139
			T2	107.5948	104.2960	112.1501	0.0700	0.0360	1.5284	107.7278	105.3502	108.8903	0.0325	0.0262	0.9206
			T3	107.5403	105.6798	112.8990	0.0639	0.0505	1.4495	107.4109	105.6798	109.3831	0.0339	0.0034	0.9524
			T4	107.7769	105.5349	111.3217	0.0520	0.0344	1.1970	107.7888	106.6055	110.1088	0.0318	0.0069	0.8759
16	J4_mPx	Robot 1	T1	-0.0216	-0.0541	0.0265	3.0441	2.1373	0.0191	-0.0259	-0.0541	0.0032	17.8573	2.4272	0.0172
			T2	-0.0151	-0.0442	0.0359	2.2308	1.3145	0.0191	-0.0194	-0.0442	0.0097	5.5422	3.2756	0.0157
			T3	-0.0188	-0.0424	0.0024	18.3375	9.9202	0.0122	-0.0211	-0.0424	0.0024	18.3375	5.4568	0.0127
			T4	-0.0216	-0.0471	0.0309	2.5253	2.5253	0.0170	-0.0262	-0.0471	-0.0083	4.6611	0.7492	0.0107
		Robot 2	T1	-0.0103	-0.0266	0.0882	1.3021	1.1956	0.0221	-0.0163	-0.0266	-0.0017	14.7764	0.2084	0.0058
			T2	-0.0093	-0.0241	0.0758	1.3185	1.2882	0.0195	-0.0146	-0.0241	-0.0037	5.4459	0.5801	0.0056
			T3	-0.0110	-0.0288	0.0778	1.3696	1.1901	0.0210	-0.0176	-0.0288	0.0001	519.4270	0.3188	0.0076
			T4	-0.0110	-0.0323	0.0827	1.3904	1.1591	0.0215	-0.0165	-0.0323	-0.0020	14.9890	0.0930	0.0075
17	J4_mPy	Robot 1	T1	0.1718	0.1088	0.1961	0.4453	0.7888	0.0268	0.1835	0.1465	0.1961	0.2530	0.3285	0.0133
			T2	0.1910	0.0928	0.2247	0.5871	1.3624	0.0341	0.2061	0.1831	0.2247	0.1853	0.1974	0.0117
			T3	0.2012	0.1345	0.2239	0.3994	0.5969	0.0246	0.2122	0.1880	0.2239	0.1603	0.1422	0.0097
			T4	0.1905	0.1145	0.2194	0.4779	0.8293	0.0295	0.2036	0.1759	0.2194	0.1983	0.1804	0.0125
		Robot 2	T1	0.1204	0.1126	0.1442	0.2191	0.1941	0.0077	0.1175	0.1126	0.1277	0.1177	0.0001	0.0035
			T2	0.1148	0.1055	0.1310	0.1949	0.1122	0.0056	0.1141	0.1075	0.1236	0.1308	0.0361	0.0037
			T3	0.1084	0.0992	0.1282	0.2259	0.1385	0.0068	0.1069	0.0992	0.1199	0.1724	0.0643	0.0047
			T4	0.1141	0.1041	0.1346	0.2261	0.1763	0.0075	0.1111	0.1041	0.1186	0.1217	0.0390	0.0037
18	J4_Ixx	Robot 1	T1	0.0004	-0.0190	0.0184	2.0287	1.8818	0.0118	-0.0029	-0.0190	0.0117	2.6251	2.3361	0.0104
			T2	-0.0020	-0.0263	0.0212	2.2413	1.7566	0.0117	-0.0044	-0.0263	0.0108	3.4299	4.7904	0.0103
			T3	-0.0081	-0.0292	0.0081	4.6161	2.0510	0.0101	-0.0093	-0.0292	0.0081	4.6161	1.9483	0.0103
			T4	-0.0029	-0.0228	0.0195	2.1687	1.1011	0.0107	-0.0054	-0.0228	0.0079	3.8894	0.0982	0.0097
		Robot 2	T1	0.0145	-0.0160	0.0275	1.5803	1.8453	0.0082	0.0153	0.0063	0.0275	0.7712	0.5094	0.0051
			T2	0.0159	-0.0051	0.0250	1.2035	4.3330	0.0065	0.0175	0.0117	0.0250	0.5304	0.3102	0.0040
			T3	0.0155	-0.0034	0.0232	1.1483	3.9642	0.0055	0.0164	0.0102	0.0232	0.5628	0.3993	0.0040
			T4	0.0133	-0.0046	0.0258	1.1781	4.7850	0.0067	0.0138	0.0057	0.0258	0.7804	0.1627	0.0052
19	J4_Ixy	Robot 1	T1	-0.0437	-0.0524	-0.0335	0.5647	0.4683	0.0044	-0.0437	-0.0492	-0.0371	0.3249	0.2047	0.0035
			T2	-0.0415	-0.0585	-0.0331	0.7674	0.0679	0.0051	-0.0404	-0.0472	-0.0331	0.4270	0.0021	0.0035
			T3	-0.0405	-0.0474	-0.0363	0.3032	0.0497	0.0029	-0.0401	-0.0449	-0.0363	0.2360	0.0888	0.0025
			T4	-0.0426	-0.0485	-0.0376	0.2923	0.1715	0.0031	-0.0418	-0.0459	-0.0376	0.2220	0.1251	0.0024
		Robot 2	T1	-0.0475	-0.0549	-0.0435	0.2619	0.0877	0.0027	-0.0469	-0.0505	-0.0435	0.1607	0.0976	0.0019
			T2	-0.0475	-0.0543	-0.0430	0.2640	0.0590	0.0023	-0.0469	-0.0503	-0.0430	0.1705	0.0838	0.0019
			T3	-0.0473	-0.0518	-0.0435	0.1911	0.0537	0.0022	-0.0467	-0.0497	-0.0435	0.1424	0.0162	0.0018
			T4	-0.0480	-0.0511	-0.0455	0.1246	0.0581	0.0017	-0.0476	-0.0505	-0.0455	0.1101	0.0522	0.0015
20	J4_Ixz	Robot 1	T1	0.0832	0.0576	0.1087	0.4699	0.3337	0.0142	0.0799	0.0576	0.0975	0.4092	0.2641	0.0125
			T2	0.0842	0.0647	0.1156	0.4404	0.0292	0.0118	0.0817	0.0647	0.0966	0.3304	0.0843	0.0093
			T3	0.0795	0.0508	0.0957	0.4688	0.1586	0.0107	0.0781	0.0508	0.0957	0.4688	0.1011	0.0110
			T4	0.0845	0.0653	0.1208	0.4597	0.2597	0.0132	0.0829	0.0653	0.1011	0.3542	0.0907	0.0109
		Robot 2	T1	0.0987	0.0892	0.1281	0.3037	0.2855	0.0090	0.0952	0.0892	0.1047	0.1479	0.0937	0.0046
			T2	0.0991	0.0895	0.1371	0.3473	0.3393	0.0098	0.0957	0.0895	0.1034	0.1348	0.1242	0.0038
			T3	0.1015	0.0887	0.1416	0.3732	0.3231	0.0103	0.0978	0.0887	0.1049	0.1539	0.0291	0.0040
			T4	0.0987	0.0901	0.1426	0.3682	0.3157	0.0106	0.0950	0.0901	0.1017	0.1142	0.0406	0.0032
21	J4_Iyz	Robot 1	T1	-0.0316	-0.1091	-0.0062	16.6549	0.8190	0.0244	-0.0214	-0.0429	-0.0062	5.9511	0.4936	0.0109
			T2	-0.0302	-0.0985	0.0107	10.2136	0.7427	0.0218	-0.0224	-0.0544	0.0107	6.0843	0.5338	0.0136
			T3	-0.0259	-0.0656	-0.0040	15.3931	0.5742	0.0187	-0.0209	-0.0612	-0.0040	14.2947	0.5529	0.0123
			T4	-0.0298	-0.0801	0.0104	8.7052	0.7286	0.0212	-0.0206	-0.0358	0.0104	4.4495	0.1750	0.0110
		Robot 2	T1	-0.0625	-0.0822	-0.0528	0.5586	0.2554	0.0060	-0.0607	-0.0703	-0.0528	0.3316	0.1285	0.0041
			T2	-0.0609	-0.0869	-0.0519	0.6759	0.3110	0.0073	-0.0590	-0.0698	-0.0519	0.3467	0.1341	0.0048
			T3	-0.0594	-0.0803	-0.0508	0.5815	0.2825	0.0067	-0.0579	-0.0712	-0.0508	0.4030	0.1046	0.0053
			T4	-0.0590	-0.0810	-0.0519	0.5593	0.2377	0.0059	-0.0574	-0.0638	-0.0519	0.2285	0.0401	0.0033
22	J4_Izz	Robot 1	T1	0.0039	-0.0282	0.0384	1.7342	0.6090	0.0179	0.0040	-0.0282	0.0384	1.7342	1.2663	0.0169
			T2	0.0011	-0.0300	0.0422	1.7121	0.5096	0.0164	0.0028	-0.0153	0.0274	1.5581	6.4313	0.0123
			T3	0.0059	-0.0358	0.0377	1.9489	0.1300	0.0179	0.0028	-0.0358	0.0331	2.0819	0.1952	0.0175
			T4	0.0010	-0.0326	0.0512	1.6365	8.5888	0.0224	-0.0050	-0.0326	0.0222	2.4667	5.5933	0.0167
		Robot 2	T1	-0.0507	-0.0663	-0.0436	0.5224	0.2604	0.0049	-0.0498	-0.0559	-0.0436	0.2823	0.1260	0.0039
			T2	-0.0486	-0.0710	-0.0370	0.9223	0.2292	0.0077	-0.0460	-0.0585	-0.0370	0.5822	0.0283	0.0053
			T3	-0.0560	-0.0678	-0.0484	0.4027	0.2871	0.0050	-0.0548	-0.0650	-0.0484	0.3446	0.1305	0.0044
			T4	-0.0527	-0.0685	-0.0431	0.5872	0.2539	0.0065	-0.0507	-0.0603	-0.0431	0.3975	0.1326	0.0047

Table H.4: The statistics data of the identification results (4/8)

				All Cycles						The cycles without 1st 5 cycles					
				Mean	MIN	MAX	D/MM	D/SE	Sdv	Mean	MIN	MAX	D/MM	D/SE	Sdv
23	J5_mPx	Robot 1	T1	0.0345	0.0195	0.0721	0.7298	0.5221	0.0118	0.0301	0.0195	0.0417	0.5326	0.1160	0.0062
			T2	0.0319	0.0121	0.1085	0.8880	0.7428	0.0192	0.0254	0.0121	0.0416	0.7078	0.1450	0.0080
			T3	0.0333	0.0150	0.0675	0.7781	0.5495	0.0118	0.0290	0.0150	0.0393	0.6191	0.0401	0.0058
			T4	0.0305	0.0098	0.1023	0.9046	0.8919	0.0175	0.0257	0.0098	0.0372	0.7376	0.6064	0.0081
		Robot 2	T1	0.0103	0.0041	0.0423	0.9027	0.7425	0.0073	0.0094	0.0050	0.0126	0.6019	1.0762	0.0025
			T2	0.0098	0.0052	0.0265	0.8047	0.5505	0.0041	0.0091	0.0052	0.0127	0.5919	1.3021	0.0020
			T3	0.0104	0.0056	0.0257	0.7830	0.6024	0.0040	0.0098	0.0056	0.0143	0.6111	0.0024	0.0021
			T4	0.0100	0.0037	0.0368	0.8990	0.8069	0.0061	0.0094	0.0071	0.0135	0.4739	0.1861	0.0017
24	J5_mPy	Robot 1	T1	-0.0332	-0.0562	-0.0115	3.8909	0.3601	0.0094	-0.0310	-0.0451	-0.0115	2.9236	0.6272	0.0083
			T2	-0.0291	-0.0442	-0.0166	1.6657	0.6238	0.0074	-0.0290	-0.0415	-0.0166	1.4992	0.3923	0.0071
			T3	-0.0342	-0.0465	-0.0189	1.4641	0.0321	0.0081	-0.0335	-0.0465	-0.0189	1.4641	0.9151	0.0076
			T4	-0.0257	-0.0634	0.0267	3.3752	1.3411	0.0223	-0.0193	-0.0460	0.0267	2.7253	1.4695	0.0203
		Robot 2	T1	-0.0471	-0.0770	-0.0399	0.9285	0.4815	0.0071	-0.0448	-0.0508	-0.0399	0.2720	0.1590	0.0027
			T2	-0.0448	-0.0736	-0.0380	0.9347	0.4586	0.0071	-0.0425	-0.0473	-0.0380	0.2433	0.1422	0.0027
			T3	-0.0449	-0.0797	-0.0389	1.0513	0.5125	0.0082	-0.0422	-0.0472	-0.0389	0.2137	0.1292	0.0027
			T4	-0.0454	-0.0701	-0.0395	0.7750	0.4217	0.0059	-0.0434	-0.0466	-0.0395	0.1790	0.1194	0.0018
25	J5_Ixx	Robot 1	T1	-0.0208	-0.0370	-0.0061	5.1094	1.4832	0.0093	-0.0226	-0.0370	-0.0061	5.1094	0.3808	0.0091
			T2	-0.0218	-0.0474	-0.0057	7.2906	0.4034	0.0103	-0.0180	-0.0306	-0.0057	4.3587	0.2886	0.0070
			T3	-0.0182	-0.0393	-0.0046	7.5511	0.7871	0.0096	-0.0172	-0.0294	-0.0046	5.3837	0.8289	0.0077
			T4	-0.0179	-0.0523	0.0038	14.6853	294.5798	0.0143	-0.0222	-0.0523	-0.0029	16.8128	14.8539	0.0127
		Robot 2	T1	-0.0121	-0.0182	-0.0085	1.1448	0.2135	0.0027	-0.0109	-0.0136	-0.0085	0.6002	0.1960	0.0014
			T2	-0.0123	-0.0165	-0.0068	1.4113	0.1976	0.0021	-0.0119	-0.0164	-0.0068	1.3948	0.0781	0.0019
			T3	-0.0117	-0.0184	-0.0076	1.4304	0.3069	0.0023	-0.0112	-0.0136	-0.0076	0.7888	0.1043	0.0014
			T4	-0.0130	-0.0206	-0.0092	1.2305	0.4166	0.0026	-0.0120	-0.0143	-0.0092	0.5485	0.1241	0.0015
26	J5_Ixy	Robot 1	T1	-0.0205	-0.0294	-0.0078	2.7754	0.0623	0.0069	-0.0197	-0.0277	-0.0078	2.5620	1.4047	0.0066
			T2	-0.0173	-0.0245	-0.0079	2.1133	0.3251	0.0048	-0.0185	-0.0245	-0.0093	1.6243	0.0078	0.0039
			T3	-0.0192	-0.0284	-0.0043	5.6557	0.0330	0.0060	-0.0192	-0.0257	-0.0045	4.7613	0.3442	0.0050
			T4	-0.0215	-0.0315	-0.0082	2.8550	0.5606	0.0053	-0.0197	-0.0280	-0.0082	2.4292	0.5061	0.0043
		Robot 2	T1	-0.0095	-0.0112	-0.0073	0.5314	0.3038	0.0010	-0.0097	-0.0112	-0.0082	0.3661	0.0963	0.0009
			T2	-0.0091	-0.0113	-0.0050	1.2858	0.9949	0.0013	-0.0094	-0.0113	-0.0078	0.4481	0.2638	0.0008
			T3	-0.0093	-0.0113	-0.0061	0.8608	0.6223	0.0011	-0.0093	-0.0113	-0.0081	0.3927	0.1282	0.0008
			T4	-0.0088	-0.0110	-0.0057	0.9369	0.1551	0.0012	-0.0092	-0.0110	-0.0076	0.4456	0.0776	0.0009
27	J5_Ixz	Robot 1	T1	0.0285	0.0182	0.0395	0.5389	0.3636	0.0062	0.0296	0.0197	0.0395	0.5017	0.2818	0.0059
			T2	0.0318	0.0236	0.0410	0.4239	0.0364	0.0056	0.0303	0.0236	0.0387	0.3898	0.1231	0.0050
			T3	0.0298	0.0164	0.0445	0.6311	0.4795	0.0063	0.0294	0.0164	0.0380	0.5674	0.5674	0.0054
			T4	0.0293	0.0150	0.0501	0.7007	0.4668	0.0087	0.0311	0.0185	0.0501	0.6306	1.5647	0.0084
		Robot 2	T1	0.0231	0.0211	0.0363	0.4174	0.3539	0.0030	0.0222	0.0211	0.0234	0.0983	0.0665	0.0008
			T2	0.0235	0.0201	0.0354	0.4324	0.3367	0.0029	0.0225	0.0201	0.0247	0.1878	0.0509	0.0011
			T3	0.0232	0.0202	0.0344	0.4149	0.3387	0.0028	0.0224	0.0202	0.0245	0.1769	0.0452	0.0012
			T4	0.0235	0.0205	0.0335	0.3874	0.3335	0.0026	0.0225	0.0205	0.0239	0.1402	0.0015	0.0009
28	J5_Iyz	Robot 1	T1	0.0230	0.0099	0.0354	0.7200	0.1186	0.0072	0.0236	0.0099	0.0354	0.7200	0.4108	0.0075
			T2	0.0265	0.0160	0.0383	0.5836	0.3218	0.0071	0.0242	0.0160	0.0326	0.5106	0.1119	0.0056
			T3	0.0244	0.0151	0.0385	0.6084	0.4619	0.0059	0.0239	0.0167	0.0336	0.5037	0.4243	0.0043
			T4	0.0241	0.0037	0.0492	0.9243	1.1266	0.0106	0.0269	0.0089	0.0492	0.8183	3.9453	0.0098
		Robot 2	T1	0.0161	0.0126	0.0266	0.5267	0.3535	0.0026	0.0154	0.0126	0.0176	0.2825	0.3659	0.0013
			T2	0.0168	0.0145	0.0223	0.3523	0.2460	0.0015	0.0165	0.0145	0.0188	0.2317	0.0557	0.0010
			T3	0.0165	0.0133	0.0221	0.3975	0.2454	0.0017	0.0162	0.0133	0.0179	0.2554	0.2524	0.0011
			T4	0.0172	0.0147	0.0250	0.4142	0.3450	0.0019	0.0167	0.0147	0.0180	0.1851	0.0100	0.0009
29	J5_Izz	Robot 1	T1	-0.0996	-0.1228	-0.0757	0.6220	0.1149	0.0149	-0.0980	-0.1200	-0.0757	0.5849	0.2680	0.0144
			T2	-0.0935	-0.1287	-0.0754	0.7076	0.3047	0.0113	-0.0931	-0.1079	-0.0754	0.4315	0.0264	0.0085
			T3	-0.0973	-0.1317	-0.0678	0.9419	0.2921	0.0151	-0.0942	-0.1094	-0.0695	0.5756	0.0351	0.0101
			T4	-0.1113	-0.1313	-0.1003	0.3084	0.1532	0.0084	-0.1112	-0.1313	-0.1003	0.3084	0.3084	0.0093
		Robot 2	T1	-0.0276	-0.0441	-0.0248	0.7802	0.4001	0.0039	-0.0267	-0.0295	-0.0248	0.1896	0.0052	0.0014
			T2	-0.0274	-0.0350	-0.0242	0.4475	0.2312	0.0022	-0.0267	-0.0284	-0.0242	0.1725	0.0567	0.0010
			T3	-0.0273	-0.0358	-0.0221	0.6210	0.1890	0.0027	-0.0265	-0.0292	-0.0221	0.3219	0.0755	0.0019
			T4	-0.0274	-0.0427	-0.0239	0.7909	0.3196	0.0035	-0.0268	-0.0291	-0.0239	0.2185	0.0542	0.0014
30	J6_mPx	Robot 1	T1	0.0023	-0.0029	0.0038	1.7641	2.1078	0.0017	0.0030	0.0018	0.0038	0.5353	0.0130	0.0006
			T2	0.0034	0.0014	0.0045	0.6945	0.5627	0.0009	0.0038	0.0029	0.0045	0.3509	0.2424	0.0005
			T3	0.0036	-0.0005	0.0047	1.1134	8.4428	0.0012	0.0041	0.0036	0.0047	0.2294	0.0111	0.0003
			T4	0.0036	0.0018	0.0044	0.5911	0.1198	0.0006	0.0038	0.0032	0.0044	0.2830	0.0838	0.0004
		Robot 2	T1	0.0027	-0.0027	0.0044	1.6128	2.1104	0.0015	0.0032	0.0020	0.0044	0.5479	0.4267	0.0006
			T2	0.0028	-0.0006	0.0043	1.1449	7.7356	0.0013	0.0033	0.0021	0.0043	0.5140	0.4546	0.0005
			T3	0.0032	-0.0004	0.0047	1.0915	10.5442	0.0011	0.0035	0.0027	0.0047	0.4360	0.1272	0.0006
			T4	0.0035	0.0010	0.0047	0.7827	2.9290	0.0009	0.0038	0.0027	0.0047	0.4364	0.1290	0.0006
31	J6_mPy	Robot 1	T1	-0.0062	-0.0081	-0.0001	53.9259	48.3894	0.0015	-0.0067	-0.0081	-0.0054	0.4902	0.3400	0.0007
			T2	-0.0059	-0.0095	-0.0045	1.1045	0.4921	0.0010	-0.0057	-0.0070	-0.0045	0.5521	0.2336	0.0007
			T3	-0.0047	-0.0057	0.0027	3.1379	2.9642	0.0016	-0.0051	-0.0057	-0.0040	0.4113	0.0265	0.0004
			T4	-0.0056	-0.0081	-0.0024	2.3656	1.0557	0.0011	-0.0055	-0.0063	-0.0047	0.3358	0.1249	0.0004
		Robot 2	T1	-0.0126	-0.0147	0.0007	21.0242	20.4729	0.0030	-0.0135	-0.0147	-0.0116	0.2686	0.2336	0.0008
			T2	-0.0125	-0.0148	0.0026	6.6648	6.2457	0.0033	-0.0132	-0.0148	-0.0121	0.2282	0.1374	0.0006
			T3	-0.0131	-0.0148	-0.0022	5.8395	4.7139	0.0024	-0.0136	-0.0144	-0.0122	0.1833	0.1328	0.0007
			T4	-0.0133	-0.0148	-0.0017	7.8986	7.4097	0.0025	-0.0136	-0.0145	-0.0123	0.1723	0.1322	0.0005

Table H.5: The statistics data of the identification results (5/8)

				All Cycles						The cycles without 1st 5 cycles					
				Mean	MIN	MAX	D/MM	D/SE	Sdv	Mean	MIN	MAX	D/MM	D/SE	Sdv
32	J6_Ixx	Robot 1	T1	0.0135	0.0102	0.0152	0.3287	0.4329	0.0016	0.0142	0.0129	0.0152	0.1546	0.1399	0.0007
			T2	0.0139	0.0117	0.0155	0.2464	0.0401	0.0010	0.0142	0.0133	0.0149	0.1056	0.0963	0.0005
			T3	0.0130	0.0080	0.0153	0.4794	0.9208	0.0017	0.0138	0.0125	0.0153	0.1807	0.2152	0.0007
			T4	0.0138	0.0125	0.0146	0.1432	0.1498	0.0006	0.0140	0.0131	0.0146	0.1081	0.1047	0.0005
		Robot 2	T1	0.0170	0.0062	0.0199	0.6894	2.0586	0.0029	0.0182	0.0163	0.0199	0.1804	0.1592	0.0009
			T2	0.0173	0.0090	0.0193	0.5345	1.1480	0.0023	0.0182	0.0170	0.0193	0.1168	0.0930	0.0006
			T3	0.0177	0.0091	0.0193	0.5291	1.0257	0.0020	0.0184	0.0177	0.0193	0.0844	0.0372	0.0005
			T4	0.0182	0.0109	0.0199	0.4506	0.7983	0.0019	0.0189	0.0175	0.0199	0.1172	0.0665	0.0007
33	J6_Ixy	Robot 1	T1	-0.0020	-0.0027	-0.0014	0.9105	0.1868	0.0003	-0.0019	-0.0023	-0.0014	0.6111	0.3044	0.0003
			T2	-0.0016	-0.0022	-0.0013	0.6643	0.2080	0.0002	-0.0015	-0.0018	-0.0013	0.3350	0.1095	0.0001
			T3	-0.0015	-0.0028	-0.0011	1.4954	0.5045	0.0003	-0.0014	-0.0017	-0.0011	0.4948	0.0364	0.0002
			T4	-0.0016	-0.0027	-0.0012	1.2581	0.3714	0.0003	-0.0015	-0.0020	-0.0012	0.6532	0.1414	0.0002
		Robot 2	T1	-0.0037	-0.0052	-0.0031	0.6623	0.2526	0.0004	-0.0037	-0.0044	-0.0031	0.4097	0.0552	0.0003
			T2	-0.0039	-0.0057	-0.0034	0.6821	0.3350	0.0004	-0.0038	-0.0042	-0.0034	0.2313	0.0418	0.0002
			T3	-0.0039	-0.0058	-0.0035	0.6506	0.3217	0.0005	-0.0037	-0.0042	-0.0035	0.1822	0.0530	0.0002
			T4	-0.0039	-0.0062	-0.0033	0.9004	0.3809	0.0005	-0.0037	-0.0040	-0.0033	0.2244	0.0297	0.0002
34	J6_Ixz	Robot 1	T1	0.0022	0.0007	0.0027	0.7264	2.4167	0.0005	0.0024	0.0019	0.0027	0.3183	0.1770	0.0002
			T2	0.0023	0.0019	0.0031	0.3783	0.3783	0.0002	0.0023	0.0019	0.0026	0.2522	0.1770	0.0002
			T3	0.0021	0.0018	0.0026	0.3203	0.0931	0.0002	0.0021	0.0018	0.0026	0.2962	0.0929	0.0002
			T4	0.0022	0.0017	0.0034	0.5030	0.2780	0.0003	0.0022	0.0018	0.0027	0.3256	0.1138	0.0002
		Robot 2	T1	0.0056	0.0044	0.0067	0.3453	0.0928	0.0005	0.0057	0.0046	0.0067	0.3187	0.3556	0.0005
			T2	0.0057	0.0050	0.0062	0.1898	0.1539	0.0004	0.0059	0.0052	0.0062	0.1523	0.1784	0.0002
			T3	0.0061	0.0054	0.0075	0.2762	0.1629	0.0004	0.0061	0.0057	0.0066	0.1375	0.0499	0.0002
			T4	0.0059	0.0054	0.0071	0.2407	0.1049	0.0003	0.0058	0.0054	0.0063	0.1517	0.0432	0.0002
35	J6_Iyz	Robot 1	T1	-0.0013	-0.0071	0.0007	10.4869	0.9037	0.0023	-0.0003	-0.0016	0.0007	3.1384	0.8324	0.0007
			T2	-0.0006	-0.0037	0.0027	2.3506	1.2089	0.0012	-0.0004	-0.0018	0.0009	3.0076	1.0130	0.0005
			T3	-0.0007	-0.0047	0.0009	6.2891	4.3601	0.0011	-0.0003	-0.0011	0.0009	2.2300	1.3005	0.0005
			T4	-0.0003	-0.0026	0.0041	1.6372	0.9048	0.0013	-0.0003	-0.0023	0.0010	3.2186	2.1393	0.0008
		Robot 2	T1	0.0016	-0.0010	0.0033	1.2986	15.3372	0.0012	0.0021	0.0003	0.0033	0.9221	0.7728	0.0008
			T2	0.0017	-0.0016	0.0030	1.5269	0.0050	0.0011	0.0021	0.0006	0.0030	0.7905	0.2532	0.0007
			T3	0.0023	0.0008	0.0041	0.8092	0.4889	0.0007	0.0024	0.0009	0.0032	0.7099	1.2703	0.0005
			T4	0.0019	0.0004	0.0030	0.8676	0.0444	0.0007	0.0021	0.0012	0.0028	0.5610	0.0836	0.0004
36	J6_Izz	Robot 1	T1	0.0127	0.0090	0.0143	0.3693	0.0076	0.0010	0.0129	0.0119	0.0143	0.1670	0.0205	0.0007
			T2	0.0134	0.0111	0.0191	0.4210	0.3510	0.0015	0.0133	0.0122	0.0149	0.1811	0.0629	0.0008
			T3	0.0118	0.0092	0.0135	0.3182	0.2811	0.0010	0.0121	0.0105	0.0135	0.2222	0.0203	0.0006
			T4	0.0119	0.0101	0.0146	0.3094	0.2799	0.0011	0.0116	0.0101	0.0131	0.2312	0.1630	0.0008
		Robot 2	T1	0.0150	0.0088	0.0168	0.4742	0.7838	0.0017	0.0154	0.0134	0.0167	0.1933	0.0753	0.0009
			T2	0.0152	0.0127	0.0171	0.2598	0.3510	0.0010	0.0156	0.0143	0.0171	0.1634	0.1205	0.0007
			T3	0.0152	0.0101	0.0167	0.3948	0.5280	0.0014	0.0155	0.0145	0.0166	0.1237	0.0673	0.0006
			T4	0.0161	0.0145	0.0177	0.1789	0.0951	0.0009	0.0162	0.0149	0.0172	0.1339	0.0394	0.0007
37	J1_f1	Robot 1	T1	4.4958	4.2167	5.4280	0.2232	0.2022	0.2516	4.3964	4.2167	4.5848	0.0803	0.0450	0.0954
			T2	4.4967	4.2519	5.1785	0.1789	0.1674	0.2064	4.4124	4.2519	4.5710	0.0698	0.0391	0.0885
			T3	4.6521	4.4210	5.0691	0.1279	0.0628	0.1317	4.6260	4.4210	4.7953	0.0781	0.0267	0.1070
			T4	4.9124	4.6619	5.4463	0.1440	0.0965	0.2168	4.8147	4.6619	4.9798	0.0638	0.0366	0.0920
		Robot 2	T1	5.6097	5.3787	5.9978	0.1032	0.0245	0.1615	5.5628	5.3787	5.8037	0.0732	0.0732	0.1241
			T2	5.3224	5.0787	5.8448	0.1311	0.0131	0.1603	5.2766	5.0787	5.4650	0.0707	0.0481	0.0868
			T3	5.5485	5.3322	5.8166	0.0833	0.0138	0.1170	5.5095	5.3322	5.6680	0.0592	0.0217	0.0753
			T4	5.6402	5.3735	5.8402	0.0799	0.0795	0.1367	5.6460	5.4240	5.8402	0.0713	0.0425	0.1327
38	J1_f2	Robot 1	T1	17.5642	14.3273	41.2369	0.6526	0.6526	5.4959	15.7002	14.3273	18.1752	0.2117	0.2117	1.0636
			T2	15.5475	13.8972	32.3553	0.5705	0.5705	3.6876	14.4754	13.8972	15.6816	0.1138	0.1138	0.4745
			T3	17.1639	14.4062	31.7808	0.5467	0.4586	3.3813	16.4586	14.4062	18.1219	0.2050	0.0994	1.4015
			T4	19.8272	17.3108	40.5248	0.5728	0.5728	4.7990	18.2063	17.3108	20.1045	0.1390	0.1390	0.8020
		Robot 2	T1	10.8538	8.9510	22.0535	0.5941	0.5647	2.6155	9.9610	8.9510	10.9695	0.1840	0.1092	0.5802
			T2	11.1639	9.5642	21.5798	0.5568	0.5257	2.4312	10.3284	9.5642	11.6255	0.1773	0.1196	0.5286
			T3	10.7218	9.0853	20.8768	0.5648	0.5521	2.4010	9.8718	9.0853	10.8245	0.1607	0.1362	0.4660
			T4	10.4502	8.8769	20.9830	0.5769	0.5769	2.5310	9.5226	8.8769	10.9706	0.1908	0.1908	0.5784
39	J1_f3	Robot 1	T1	-6.0070	-14.4364	-4.8289	1.9896	0.6603	1.9557	-5.3456	-6.2875	-4.8289	0.3021	0.2201	0.3721
			T2	-5.6212	-13.0272	-4.8974	1.6600	0.6241	1.6093	-5.1824	-5.6671	-4.8974	0.1572	0.1358	0.2032
			T3	-6.0004	-12.5938	-5.2033	1.4204	0.5519	1.4348	-5.6354	-6.1349	-5.2033	0.1790	0.0065	0.2305
			T4	-6.6168	-14.8954	-5.6458	1.6383	0.6205	1.9197	-5.9564	-6.8580	-5.6458	0.2147	0.1758	0.3630
		Robot 2	T1	-3.3692	-7.5206	-2.7255	1.7594	0.5820	0.9255	-3.0883	-3.2968	-2.7255	0.2096	0.0170	0.1537
			T2	-3.6064	-7.7394	-3.0565	1.5321	0.5468	0.9273	-3.3126	-3.6671	-3.0565	0.1998	0.0435	0.1453
			T3	-3.3489	-7.4277	-2.8410	1.6145	0.5983	0.9215	-3.0529	-3.2456	-2.8410	0.1424	0.0724	0.1178
			T4	-3.2300	-7.3724	-2.6803	1.7506	0.6327	0.9580	-2.8986	-3.3055	-2.6803	0.2333	0.1808	0.1752
40	J1_f4	Robot 1	T1	0.7778	0.6069	1.7821	0.6595	0.6487	0.2434	0.6896	0.6069	0.8278	0.2668	0.2436	0.0541
			T2	0.7242	0.6167	1.7288	0.6433	0.6433	0.2190	0.6640	0.6167	0.7317	0.1572	0.1572	0.0313
			T3	0.7674	0.6700	1.6528	0.5947	0.5760	0.1924	0.7162	0.6700	0.7782	0.1390	0.0536	0.0274
			T4	0.8262	0.6990	1.9158	0.6351	0.6308	0.2544	0.7371	0.6990	0.8643	0.1912	0.1815	0.0503
		Robot 2	T1	0.4065	0.3298	0.9614	0.6569	0.5877	0.1213	0.3751	0.3298	0.4102	0.1961	0.1748	0.0221
			T2	0.4448	0.3786	1.0083	0.6245	0.5475	0.1241	0.4086	0.3786	0.4562	0.1701	0.0556	0.0185
			T3	0.4069	0.3417	0.9681	0.6470	0.6135	0.1238	0.3721	0.3417	0.3942	0.1332	0.0167	0.0152
			T4	0.3891	0.3187	0.9523	0.6654	0.6547	0.1271	0.3484	0.3187	0.3857	0.1739	0.1407	0.0212

Table H.6: The statistics data of the identification results (6/8)

				All Cycles						The cycles without 1st 5 cycles					
				Mean	MIN	MAX	D/MM	D/SE	Sdv	Mean	MIN	MAX	D/MM	D/SE	Sdv
41	J2_f1	Robot 1	T1	3.4887	2.9899	4.0302	0.2581	0.1328	0.2910	3.3953	2.9899	3.8046	0.2141	0.1909	0.2366
			T2	3.5379	3.2256	4.2587	0.2426	0.1581	0.2645	3.4283	3.2256	3.7407	0.1377	0.1066	0.1393
			T3	3.3900	3.0687	4.1570	0.2618	0.2526	0.2884	3.2675	3.0687	3.6230	0.1530	0.1425	0.1504
			T4	3.4028	3.0938	4.1552	0.2554	0.2390	0.2735	3.2818	3.0938	3.4311	0.0983	0.0754	0.0865
		Robot 2	T1	3.1583	2.9219	3.3636	0.1313	0.1082	0.0976	3.1676	3.0071	3.3636	0.1060	0.0678	0.0839
			T2	3.1821	3.0487	3.3162	0.0807	0.0101	0.0740	3.1788	3.0487	3.3031	0.0770	0.0059	0.0763
			T3	3.1646	3.0160	3.3368	0.0961	0.0022	0.0716	3.1532	3.0160	3.2747	0.0790	0.0126	0.0639
			T4	3.2105	3.0132	3.3952	0.1125	0.0104	0.1147	3.1996	3.0132	3.3838	0.1095	0.0108	0.1198
42	J2_f2	Robot 1	T1	28.5754	23.2129	41.7296	0.4437	0.3465	3.8375	27.8209	25.4920	32.5727	0.2174	0.1628	1.7968
			T2	30.0690	25.7700	44.3467	0.4189	0.4007	4.8894	28.0571	25.7700	33.9983	0.2420	0.2183	1.9680
			T3	30.0390	25.6470	45.6382	0.4380	0.4199	4.9986	27.9789	25.6470	33.2600	0.2289	0.2040	1.9258
			T4	29.4418	25.4915	44.0952	0.4219	0.4174	4.7920	27.3940	25.4915	31.9289	0.2016	0.1954	1.7472
		Robot 2	T1	17.5127	14.9538	31.4099	0.5239	0.5186	3.5954	16.1216	14.9538	18.4786	0.1907	0.1817	0.9963
			T2	17.5224	14.9353	30.6671	0.5130	0.5011	3.4319	16.1692	14.9353	18.0610	0.1731	0.1528	0.8692
			T3	17.5561	15.2509	31.2694	0.5123	0.5123	3.4880	16.2283	15.2509	18.1983	0.1620	0.1620	0.8974
			T4	17.4845	15.2918	29.8801	0.4882	0.4811	3.2590	16.1692	15.2918	18.1455	0.1573	0.1456	0.7891
43	J2_f3	Robot 1	T1	-9.8168	-13.3300	-7.7126	0.7284	0.2748	1.1416	-9.6971	-11.2672	-8.8231	0.2770	0.1420	0.6040
			T2	-10.4803	-14.3589	-8.9552	0.6034	0.3385	1.5015	-9.8570	-11.8478	-8.9552	0.3230	0.2007	0.6477
			T3	-10.6163	-15.3576	-8.9490	0.7161	0.3883	1.6256	-9.9623	-12.0831	-8.9490	0.3502	0.2226	0.7386
			T4	-10.3166	-14.6403	-8.9499	0.6358	0.3740	1.5043	-9.6730	-11.1014	-8.9499	0.2404	0.1744	0.5905
		Robot 2	T1	-6.1075	-10.5555	-5.2916	0.9947	0.4892	1.1377	-5.6709	-6.4162	-5.2916	0.2125	0.1596	0.3105
			T2	-6.1320	-10.2677	-5.2793	0.9449	0.4593	1.0636	-5.7161	-6.2347	-5.2793	0.1810	0.1095	0.2569
			T3	-6.1765	-10.5563	-5.4269	0.9452	0.4804	1.0886	-5.7761	-6.2757	-5.4269	0.1564	0.1259	0.2610
			T4	-6.0895	-9.8019	-5.3519	0.8315	0.4416	0.9834	-5.6919	-6.1751	-5.3519	0.1538	0.1136	0.2597
44	J2_f4	Robot 1	T1	1.4784	1.2686	1.8237	0.3044	0.2002	0.1299	1.4661	1.3451	1.6880	0.2032	0.1359	0.0897
			T2	1.5797	1.3683	2.0470	0.3315	0.2732	0.1838	1.5014	1.3683	1.7346	0.2111	0.1625	0.0844
			T3	1.6061	1.3665	2.1908	0.3762	0.3497	0.2059	1.5249	1.3665	1.8496	0.2611	0.2297	0.1144
			T4	1.5535	1.3821	2.0783	0.3350	0.3190	0.1896	1.4717	1.3821	1.6430	0.1588	0.1385	0.0786
		Robot 2	T1	1.0364	0.9338	1.4933	0.3747	0.3555	0.1188	0.9919	0.9338	1.0757	0.1319	0.1054	0.0387
			T2	1.0498	0.9456	1.4407	0.3437	0.3173	0.1056	1.0074	0.9456	1.0545	0.1033	0.0646	0.0303
			T3	1.0613	0.9719	1.5045	0.3540	0.3464	0.1119	1.0207	0.9719	1.0707	0.0923	0.0598	0.0297
			T4	1.0444	0.9494	1.3821	0.3131	0.2903	0.0946	1.0061	0.9494	1.0676	0.1107	0.0603	0.0332
45	J3_f1	Robot 1	T1	2.1145	2.0392	2.2308	0.0859	0.0180	0.0451	2.1116	2.0401	2.1760	0.0625	0.0189	0.0374
			T2	2.1232	2.0454	2.2649	0.0969	0.0159	0.0552	2.1057	2.0454	2.1871	0.0648	0.0208	0.0351
			T3	2.0724	1.9963	2.1751	0.0822	0.0132	0.0474	2.0547	1.9963	2.0964	0.0477	0.0107	0.0260
			T4	2.0988	1.9172	2.2143	0.1342	0.0902	0.0562	2.0961	2.0172	2.1565	0.0646	0.0207	0.0342
		Robot 2	T1	1.7262	1.6539	1.7961	0.0792	0.0212	0.0352	1.7192	1.6539	1.7961	0.0792	0.0232	0.0342
			T2	1.7230	1.6540	1.8108	0.0866	0.0166	0.0346	1.7129	1.6540	1.7514	0.0556	0.0438	0.0264
			T3	1.7236	1.6475	1.7971	0.0832	0.0116	0.0307	1.7219	1.6855	1.7682	0.0468	0.0250	0.0216
			T4	1.7352	1.6827	1.8001	0.0652	0.0045	0.0347	1.7280	1.6827	1.7871	0.0584	0.0216	0.0320
46	J3_f2	Robot 1	T1	9.5846	8.5427	14.9641	0.4291	0.4082	1.2850	9.1910	8.5427	10.2102	0.1633	0.1213	0.4515
			T2	9.2719	8.3731	12.4306	0.3264	0.2844	1.1461	8.7381	8.3731	9.5710	0.1252	0.0357	0.3657
			T3	9.3387	8.3266	12.4082	0.3289	0.3089	1.1366	8.8342	8.3266	9.9845	0.1660	0.1412	0.4805
			T4	9.3230	8.3562	12.2787	0.3195	0.2460	1.0304	8.8778	8.3562	9.8645	0.1529	0.0615	0.4143
		Robot 2	T1	7.4997	6.6433	11.4874	0.4217	0.4158	1.1609	7.0056	6.6433	7.6866	0.1357	0.1270	0.3386
			T2	7.4259	6.5463	11.3863	0.4251	0.4242	1.1636	6.9419	6.5463	7.9151	0.1729	0.1717	0.4149
			T3	7.3708	6.5089	11.2586	0.4219	0.4207	1.1731	6.8620	6.5089	7.7313	0.1581	0.1564	0.3604
			T4	7.2037	6.3410	10.9153	0.4191	0.4039	1.1030	6.7402	6.3410	7.6884	0.1753	0.1537	0.3688
47	J3_f3	Robot 1	T1	-3.3402	-4.6477	-3.0481	0.5248	0.3186	0.3271	-3.2499	-3.6255	-3.0481	0.1894	0.0962	0.1542
			T2	-3.2275	-3.9549	-2.9239	0.3527	0.1545	0.3118	-3.0804	-3.3107	-2.9239	0.1323	0.0156	0.1093
			T3	-3.2415	-3.9927	-2.9759	0.3417	0.1796	0.2945	-3.1119	-3.4263	-2.9759	0.1514	0.1129	0.1425
			T4	-3.2473	-3.9687	-2.9757	0.3337	0.0671	0.2449	-3.1492	-3.4008	-2.9757	0.1429	0.0047	0.1297
		Robot 2	T1	-2.3027	-2.8665	-2.0953	0.3681	0.2658	0.2409	-2.1941	-2.4026	-2.0953	0.1467	0.0845	0.0894
			T2	-2.2867	-2.8465	-2.0222	0.4076	0.2720	0.2411	-2.1838	-2.4385	-2.0222	0.2059	0.1493	0.1215
			T3	-2.2721	-2.8624	-2.0522	0.3948	0.2753	0.2570	-2.1531	-2.3374	-2.0522	0.1390	0.1218	0.0917
			T4	-2.1974	-2.7472	-1.9638	0.3989	0.2360	0.2276	-2.0999	-2.3529	-1.9638	0.1982	0.1323	0.1076
48	J3_f4	Robot 1	T1	0.4505	0.4051	0.5597	0.2763	0.2323	0.0326	0.4434	0.4051	0.5000	0.1899	0.0893	0.0229
			T2	0.4324	0.3827	0.5298	0.2776	0.0346	0.0375	0.4164	0.3827	0.4415	0.1330	0.0302	0.0165
			T3	0.4328	0.3943	0.5282	0.2535	0.0543	0.0353	0.4203	0.3943	0.4643	0.1508	0.1260	0.0228
			T4	0.4363	0.3943	0.5312	0.2576	0.1331	0.0296	0.4285	0.3943	0.4776	0.1744	0.0557	0.0210
		Robot 2	T1	0.3079	0.2814	0.3750	0.2497	0.1258	0.0264	0.2968	0.2814	0.3240	0.1316	0.0826	0.0118
			T2	0.3059	0.2678	0.3744	0.2847	0.1179	0.0260	0.2961	0.2678	0.3310	0.1909	0.1419	0.0164
			T3	0.3044	0.2764	0.3802	0.2730	0.1282	0.0290	0.2918	0.2764	0.3162	0.1259	0.1013	0.0119
			T4	0.2932	0.2622	0.3643	0.2801	0.0738	0.0259	0.2835	0.2622	0.3142	0.1653	0.1208	0.0150
49	J4_f1	Robot 1	T1	5.2542	4.4232	5.5014	0.1960	0.2242	0.2150	5.3157	5.1005	5.5014	0.0729	0.0616	0.1184
			T2	5.4184	4.6835	5.6552	0.1718	0.2075	0.2264	5.4835	5.2253	5.6552	0.0760	0.0721	0.1530
			T3	5.4345	4.3913	5.6493	0.2227	0.2291	0.2546	5.5115	5.3590	5.6493	0.0514	0.0067	0.0967
			T4	5.3567	4.4368	5.6700	0.2175	0.2580	0.2574	5.4362	5.0412	5.6700	0.1109	0.1071	0.1598
		Robot 2	T1	5.4409	4.8874	5.7353	0.1478	0.1185	0.2369	5.5328	5.2314	5.7353	0.0879	0.0552	0.1281
			T2	5.5515	4.7909	5.8337	0.1788	0.2140	0.2452	5.6493	5.2960	5.8337	0.0922	0.0982	0.1237
			T3	5.5144	4.7734	5.8767	0.1877	0.1938	0.2517	5.6150	5.3249	5.8767	0.0939	0.0409	0.1427
			T4	5.4416	4.5923	5.7388	0.1998	0.2265	0.2628	5.5495	5.3426	5.7388	0.0690	0.0543	0.1019

Table H.7: The statistics data of the identification results (7/8)

				All Cycles						The cycles without 1st 5 cycles					
				Mean	MIN	MAX	D/MM	D/SE	Sdv	Mean	MIN	MAX	D/MM	D/SE	Sdv
50	J4_f2	Robot 1	T1	12.2622	9.8810	25.1033	0.6064	0.5756	3.1294	11.0966	9.8810	12.8918	0.2335	0.1736	0.7456
			T2	12.2509	10.1337	24.0739	0.5791	0.5631	3.0016	11.1077	10.1337	13.1834	0.2313	0.2023	0.8114
			T3	11.9620	10.2057	23.2804	0.5616	0.5413	2.7443	10.9405	10.2057	12.6649	0.1942	0.1569	0.6219
			T4	12.0514	10.0466	24.0300	0.5819	0.5798	2.9697	10.9246	10.0466	12.7972	0.2149	0.2110	0.6902
		Robot 2	T1	10.0282	8.5044	18.0151	0.5279	0.5094	2.0951	9.2108	8.5044	10.5897	0.1969	0.1653	0.5413
			T2	9.8772	8.4582	18.1631	0.5343	0.5326	2.1110	9.0602	8.4582	10.5170	0.1958	0.1928	0.5274
			T3	9.8828	8.4542	18.0467	0.5315	0.5206	2.0975	9.0560	8.4542	10.1830	0.1698	0.1503	0.5221
			T4	9.6556	8.3692	17.8030	0.5299	0.5222	2.0386	8.8820	8.3692	9.9119	0.1556	0.1418	0.4050
51	J4_f3	Robot 1	T1	-3.2445	-6.0470	-2.7110	1.2306	0.5158	0.6751	-2.9951	-3.3293	-2.7110	0.2281	0.1206	0.1483
			T2	-3.2432	-5.8711	-2.7163	1.1614	0.5146	0.6622	-2.9975	-3.4012	-2.7163	0.2522	0.1621	0.1841
			T3	-3.1642	-5.4980	-2.7192	1.0219	0.4607	0.5695	-2.9511	-3.2611	-2.7192	0.1993	0.0907	0.1212
			T4	-3.2044	-5.7707	-2.7234	1.1189	0.5067	0.6388	-2.9617	-3.4351	-2.7234	0.2613	0.1713	0.1647
		Robot 2	T1	-2.6719	-4.5602	-2.2929	0.9889	0.4612	0.4825	-2.4918	-2.7938	-2.2929	0.2185	0.1205	0.1188
			T2	-2.6378	-4.6625	-2.3020	1.0254	0.5027	0.4936	-2.4569	-2.8007	-2.3020	0.2166	0.1720	0.1180
			T3	-2.6619	-4.6295	-2.3309	0.9861	0.4790	0.4856	-2.4763	-2.6847	-2.3309	0.1518	0.0989	0.1064
			T4	-2.6100	-4.6087	-2.3025	1.0016	0.4864	0.4786	-2.4421	-2.6232	-2.3025	0.1393	0.0977	0.0816
52	J4_f4	Robot 1	T1	0.3492	0.3022	0.5780	0.4771	0.4439	0.0558	0.3284	0.3022	0.3543	0.1470	0.0928	0.0131
			T2	0.3493	0.2988	0.5694	0.4752	0.4543	0.0571	0.3281	0.2988	0.3574	0.1638	0.1306	0.0177
			T3	0.3421	0.2989	0.5366	0.4430	0.3911	0.0492	0.3232	0.2989	0.3425	0.1274	0.0461	0.0106
			T4	0.3453	0.2984	0.5630	0.4699	0.4382	0.0558	0.3237	0.2984	0.3707	0.1949	0.1468	0.0165
		Robot 2	T1	0.2836	0.2490	0.4466	0.4425	0.3972	0.0411	0.2689	0.2490	0.2925	0.1489	0.0797	0.0099
			T2	0.2808	0.2523	0.4586	0.4498	0.4474	0.0421	0.2662	0.2523	0.2957	0.1469	0.1432	0.0100
			T3	0.2839	0.2562	0.4559	0.4380	0.4173	0.0414	0.2685	0.2562	0.2862	0.1050	0.0507	0.0079
			T4	0.2793	0.2516	0.4559	0.4481	0.4312	0.0414	0.2658	0.2516	0.2776	0.0934	0.0655	0.0072
53	J5_f1	Robot 1	T1	1.2245	1.1243	1.3287	0.1539	0.0842	0.0592	1.2195	1.1243	1.3287	0.1539	0.0433	0.0613
			T2	1.1514	1.0858	1.3365	0.1876	0.1249	0.0538	1.1356	1.0858	1.1933	0.0901	0.0097	0.0350
			T3	1.2146	1.1391	1.2956	0.1208	0.1128	0.0408	1.2010	1.1391	1.2813	0.1110	0.0551	0.0330
			T4	1.2814	1.2000	1.4766	0.1873	0.0776	0.0639	1.2834	1.2000	1.4766	0.1873	0.1385	0.0664
		Robot 2	T1	0.7985	0.7502	0.9876	0.2404	0.1886	0.0460	0.7884	0.7503	0.8193	0.0842	0.0204	0.0192
			T2	0.8096	0.7560	1.0133	0.2540	0.2050	0.0491	0.8003	0.7560	0.8367	0.0964	0.0528	0.0258
			T3	0.8191	0.7532	0.9921	0.2408	0.1678	0.0427	0.8094	0.7532	0.8364	0.0994	0.0335	0.0210
			T4	0.8010	0.7518	0.9360	0.1968	0.1200	0.0384	0.7921	0.7518	0.8468	0.1122	0.0623	0.0263
54	J5_f2	Robot 1	T1	5.8674	4.9047	9.4510	0.4810	0.4361	0.9432	5.5853	4.9047	6.2241	0.2120	0.0124	0.4772
			T2	5.4020	4.5356	8.9148	0.4912	0.4003	0.8290	5.1830	4.5356	5.9302	0.2352	0.0348	0.3565
			T3	6.3917	5.2795	10.7096	0.5070	0.5070	1.0775	6.0386	5.2795	6.8209	0.2260	0.1545	0.3484
			T4	6.7537	5.4351	11.1974	0.5146	0.3957	1.0761	6.4835	5.4351	7.5789	0.2829	0.0134	0.5049
		Robot 2	T1	4.2813	3.8184	6.7004	0.4301	0.4279	0.6948	3.9821	3.8184	4.4000	0.1322	0.1236	0.1674
			T2	4.1768	3.6810	6.5748	0.4401	0.4235	0.6655	3.8980	3.6810	4.3177	0.1475	0.1222	0.1561
			T3	4.1620	3.7167	6.5360	0.4313	0.4312	0.6530	3.8891	3.7167	4.2347	0.1223	0.1222	0.1525
			T4	4.1408	3.6720	6.2776	0.4151	0.4150	0.6112	3.8877	3.6720	4.1895	0.1235	0.1234	0.1568
55	J5_f3	Robot 1	T1	-1.7199	-2.6989	-1.3799	0.9559	0.4177	0.2959	-1.6550	-1.9616	-1.3799	0.4216	0.0563	0.2178
			T2	-1.5382	-2.7493	-1.2733	1.1592	0.4572	0.2852	-1.4658	-1.7314	-1.2733	0.3598	0.0426	0.1266
			T3	-1.8022	-3.3649	-1.3893	1.4220	0.5871	0.3916	-1.6735	-2.0220	-1.3893	0.4553	0.1940	0.1476
			T4	-1.9258	-3.3654	-1.5336	1.1944	0.3803	0.3569	-1.8780	-2.2278	-1.5336	0.4527	0.2223	0.1929
		Robot 2	T1	-1.2413	-1.8874	-1.1182	0.6879	0.3970	0.1810	-1.1637	-1.2609	-1.1182	0.1276	0.0850	0.0372
			T2	-1.2138	-1.8976	-1.0717	0.7707	0.4094	0.1898	-1.1335	-1.2494	-1.0717	0.1658	0.1030	0.0407
			T3	-1.2090	-1.8722	-1.0862	0.7236	0.4176	0.1820	-1.1321	-1.2182	-1.0862	0.1215	0.1050	0.0372
			T4	-1.2064	-1.7869	-1.0680	0.6731	0.3970	0.1687	-1.1367	-1.1818	-1.0680	0.1066	0.0883	0.0357
56	J5_f4	Robot 1	T1	0.1778	0.1419	0.2631	0.4606	0.3788	0.0290	0.1728	0.1419	0.2067	0.3134	0.0659	0.0244
			T2	0.1586	0.1305	0.2758	0.5267	0.4509	0.0277	0.1518	0.1305	0.1778	0.2659	0.0489	0.0126
			T3	0.1844	0.1428	0.3425	0.5832	0.5832	0.0393	0.1714	0.1428	0.2084	0.3149	0.1843	0.0154
			T4	0.1980	0.1591	0.3240	0.5089	0.3082	0.0348	0.1959	0.1603	0.2421	0.3379	0.3360	0.0227
		Robot 2	T1	0.1312	0.1185	0.1928	0.3853	0.3700	0.0173	0.1236	0.1185	0.1314	0.0977	0.0753	0.0034
			T2	0.1286	0.1144	0.1971	0.4196	0.3925	0.0192	0.1204	0.1144	0.1333	0.1419	0.1018	0.0042
			T3	0.1282	0.1154	0.1939	0.4050	0.3990	0.0182	0.1204	0.1154	0.1291	0.1061	0.0971	0.0037
			T4	0.1280	0.1137	0.1847	0.3844	0.3772	0.0169	0.1209	0.1137	0.1254	0.0929	0.0751	0.0035
57	J6_f1	Robot 1	T1	1.2592	1.0922	1.3175	0.1710	0.2063	0.0506	1.2789	1.2237	1.3175	0.0712	0.0766	0.0252
			T2	1.2538	1.0423	1.3014	0.1991	0.2343	0.0569	1.2756	1.2275	1.3014	0.0567	0.0453	0.0212
			T3	1.2515	1.1595	1.2969	0.1060	0.0896	0.0318	1.2646	1.2351	1.2969	0.0477	0.0229	0.0168
			T4	1.2456	1.1152	1.2926	0.1372	0.1457	0.0372	1.2581	1.2227	1.2926	0.0540	0.0417	0.0215
		Robot 2	T1	1.5536	1.5169	1.6003	0.0521	0.0169	0.0206	1.5480	1.5169	1.6003	0.0521	0.0436	0.0182
			T2	1.5501	1.4851	1.6133	0.0795	0.0222	0.0333	1.5416	1.5168	1.5838	0.0423	0.0415	0.0198
			T3	1.5398	1.5152	1.5980	0.0518	0.0016	0.0243	1.5327	1.5152	1.5689	0.0342	0.0080	0.0162
			T4	1.5641	1.4804	1.6123	0.0818	0.0553	0.0289	1.5608	1.5317	1.6042	0.0452	0.0261	0.0189
58	J6_f2	Robot 1	T1	0.9079	0.7290	1.9226	0.6208	0.6208	0.2660	0.7996	0.7290	0.9352	0.2206	0.2206	0.0519
			T2	0.8915	0.7229	1.9138	0.6223	0.6189	0.2697	0.7849	0.7229	0.9185	0.2130	0.2058	0.0581
			T3	0.8799	0.7491	1.6929	0.5575	0.5281	0.2144	0.7958	0.7491	0.8901	0.1584	0.1025	0.0406
			T4	0.8869	0.7558	1.7300	0.5631	0.5533	0.2151	0.8032	0.7558	0.8804	0.1415	0.1221	0.0367
		Robot 2	T1	1.6567	1.5416	2.4514	0.3711	0.3502	0.1899	1.5874	1.5416	1.6331	0.0560	0.0227	0.0288
			T2	1.6723	1.5320	2.6144	0.4140	0.4033	0.2326	1.5857	1.5320	1.7212	0.1099	0.0937	0.0505
			T3	1.6537	1.5387	2.4090	0.3613	0.3591	0.1886	1.5837	1.5387	1.6790	0.0835	0.0804	0.0383
			T4	1.7615	1.6212	2.7035	0.4003	0.4003	0.2261	1.6774	1.6212	1.7477	0.0724	0.0724	0.0350

Table H.8: The statistics data of the identification results (8/8)

				All Cycles						The cycles without 1st 5 cycles					
				Mean	MIN	MAX	D/MM	D/SE	Sdv	Mean	MIN	MAX	D/MM	D/SE	Sdv
59	J6_f3	Robot 1	T1	-0.1973	-0.3329	-0.1671	0.9922	0.4980	0.0396	-0.1801	-0.2020	-0.1671	0.2088	0.1728	0.0082
			T2	-0.2000	-0.3445	-0.1740	0.9794	0.4872	0.0407	-0.1837	-0.2047	-0.1740	0.1762	0.1083	0.0083
			T3	-0.2045	-0.3015	-0.1840	0.6384	0.3339	0.0272	-0.1938	-0.2048	-0.1840	0.1132	0.0035	0.0059
			T4	-0.2087	-0.3209	-0.1872	0.7143	0.3952	0.0286	-0.1983	-0.2088	-0.1872	0.1155	0.0704	0.0063
		Robot 2	T1	-0.3879	-0.5036	-0.3656	0.3776	0.2361	0.0264	-0.3796	-0.3906	-0.3656	0.0686	0.0182	0.0063
			T2	-0.3928	-0.5367	-0.3717	0.4439	0.2877	0.0333	-0.3824	-0.4034	-0.3717	0.0852	0.0524	0.0087
			T3	-0.3895	-0.4881	-0.3717	0.3132	0.2286	0.0235	-0.3823	-0.3947	-0.3717	0.0618	0.0460	0.0066
			T4	-0.4049	-0.5447	-0.3837	0.4195	0.2955	0.0322	-0.3940	-0.4027	-0.3837	0.0495	0.0326	0.0051
60	J6_f4	Robot 1	T1	0.0170	0.0149	0.0247	0.3953	0.3933	0.0026	0.0159	0.0149	0.0170	0.1200	0.1170	0.0005
			T2	0.0167	0.0150	0.0253	0.4061	0.3967	0.0026	0.0156	0.0150	0.0169	0.1122	0.0524	0.0005
			T3	0.0172	0.0160	0.0227	0.2926	0.2249	0.0015	0.0167	0.0160	0.0176	0.0874	0.0547	0.0004
			T4	0.0177	0.0162	0.0244	0.3346	0.3094	0.0016	0.0171	0.0162	0.0178	0.0867	0.0436	0.0004
		Robot 2	T1	0.0320	0.0305	0.0384	0.2066	0.1630	0.0015	0.0317	0.0305	0.0325	0.0614	0.0260	0.0005
			T2	0.0325	0.0311	0.0411	0.2416	0.2190	0.0020	0.0319	0.0311	0.0334	0.0676	0.0398	0.0006
			T3	0.0322	0.0309	0.0372	0.1706	0.1498	0.0012	0.0319	0.0311	0.0326	0.0457	0.0298	0.0005
			T4	0.0335	0.0322	0.0414	0.2215	0.2215	0.0018	0.0330	0.0322	0.0336	0.0413	0.0208	0.0004
61	J3_Im	Robot 1	T1	-7.8609	-15.7940	-3.1690	3.9839	0.5848	2.9861	-6.8420	-10.7323	-3.1690	2.3866	0.3890	1.8424
			T2	-9.2062	-13.9417	-4.0425	2.4488	0.3325	2.0577	-8.7736	-11.4755	-4.0425	1.8387	0.0472	1.8688
			T3	-10.0566	-14.0571	-6.7298	1.0888	0.2388	2.3782	-9.6529	-14.0571	-6.7298	1.0888	0.3792	2.4951
			T4	-10.1510	-13.6053	-6.3521	1.1418	0.2293	2.0288	-9.5243	-12.6824	-6.3521	0.9966	0.3324	1.6861
		Robot 2	T1	-20.5611	-21.9182	-18.5651	0.1806	0.0200	0.8747	-20.4395	-21.9182	-18.5651	0.1806	0.0263	0.8926
			T2	-20.7796	-24.2454	-18.4781	0.3121	0.1431	1.2501	-20.5462	-22.0870	-18.4781	0.1953	0.0576	0.9301
			T3	-20.3222	-23.7068	-18.5229	0.2799	0.1684	1.0068	-19.9882	-20.8542	-18.5229	0.1259	0.0326	0.6037
			T4	-20.6358	-22.4407	-18.9138	0.1865	0.0714	0.9398	-20.3673	-22.2088	-18.9138	0.1742	0.0470	0.7568
62	J4_Im	Robot 1	T1	27.8146	12.8065	30.3894	0.5786	1.2158	3.3088	28.4081	26.9266	30.3894	0.1139	0.0662	0.9010
			T2	27.1838	16.2208	30.6505	0.4708	0.6315	2.6933	27.3126	25.2677	29.7500	0.1507	0.1104	1.1386
			T3	26.5195	13.5007	29.4464	0.5415	1.0169	3.0884	27.1569	25.3306	28.9860	0.1261	0.0533	0.9708
			T4	27.4281	19.2291	29.7607	0.3539	0.3578	2.1003	27.7255	25.8745	29.7607	0.1306	0.0141	1.2003
		Robot 2	T1	30.2372	20.0550	32.2549	0.3782	0.6083	2.7629	31.3051	29.7517	32.2549	0.0776	0.0815	0.7405
			T2	30.6933	20.4440	32.7177	0.3751	0.5499	2.6523	31.7007	29.3429	32.7177	0.1031	0.0798	0.7794
			T3	30.8018	21.5308	32.5722	0.3390	0.4525	2.4039	31.7108	30.6541	32.5722	0.0589	0.0202	0.5506
			T4	30.9637	21.0762	32.9276	0.3599	0.5351	2.6578	32.0137	30.9007	32.9276	0.0616	0.0470	0.5824
63	J5_Im	Robot 1	T1	11.2152	5.5336	14.0131	0.6051	0.9780	1.6833	11.8028	10.5018	14.0131	0.2506	0.0280	0.8132
			T2	11.8581	7.5398	13.9995	0.4614	0.5937	1.3399	11.8753	10.7906	13.6686	0.2106	0.0931	0.8219
			T3	11.0004	7.2167	13.2908	0.4570	0.1060	1.3411	11.1676	9.2722	13.2908	0.3024	0.1899	1.0663
			T4	10.2974	4.6306	14.5905	0.6826	2.0394	2.3224	11.0215	8.2571	14.5905	0.4341	0.7045	1.8396
		Robot 2	T1	11.7700	10.8976	12.1890	0.1059	0.0134	0.3521	11.8843	11.4449	12.1890	0.0610	0.0316	0.2279
			T2	11.8877	11.1607	12.4209	0.1015	0.0269	0.2878	11.8911	11.4577	12.1723	0.0587	0.0125	0.2047
			T3	11.6051	11.0807	12.1474	0.0878	0.0275	0.2877	11.6199	11.0807	11.9973	0.0764	0.0556	0.2715
			T4	12.0172	11.3429	12.4359	0.0879	0.0190	0.2451	11.9778	11.3429	12.3586	0.0822	0.0533	0.2501
64	J6_Im	Robot 1	T1	-0.1453	-0.8784	0.2907	4.0221	3.3149	0.3410	-0.0267	-0.4772	0.2907	2.6418	1.4094	0.2328
			T2	-0.0608	-1.0841	0.4948	3.1909	1.7115	0.4904	0.1051	-0.6018	0.4948	2.2162	1.7327	0.3379
			T3	0.3170	-0.9567	0.7304	2.3098	2.0807	0.4587	0.5131	0.0826	0.7304	0.8869	7.3622	0.1874
			T4	0.2229	-0.8760	0.7889	2.1105	2.4990	0.5012	0.4403	-0.1070	0.7889	1.1356	61.5745	0.2691
		Robot 2	T1	-0.3479	-0.7330	-0.0823	7.9071	0.5143	0.2105	-0.2844	-0.6184	-0.0823	6.5141	0.7622	0.1718
			T2	-0.3964	-1.1171	-0.0973	10.4803	0.8795	0.2662	-0.2796	-0.5128	-0.0973	4.2698	0.7831	0.1249
			T3	-0.2824	-1.0786	-0.0335	31.1848	0.7649	0.2565	-0.1730	-0.3730	-0.0335	10.1308	0.3718	0.0844
			T4	-0.5361	-1.2236	-0.3146	2.8899	0.5989	0.2180	-0.4453	-0.5890	-0.3146	0.8723	0.3217	0.0858

Appendix I

The Identification Results Of Excitation Trajectory Of Robot 1

The figures shown in this appendix represent the dynamic parameter identification results of Robot LEFT, which are mentioned in Section 5.1.5.2. Also the identified results of the selected cycles are shown here. The left sub-figures are the plots with the y-axis labelled automatically, and the right sub-figures are the plots with y-axis labelled multiplied by 0.5. It should be pointed that the identified friction coefficients are not presented due to the non-physical parameters. Additionally, it should be noticed that some parameters have the same plots between two sub-figures because the original y-axis range of the right sub-figure meet the requirements of multiple 0.5.

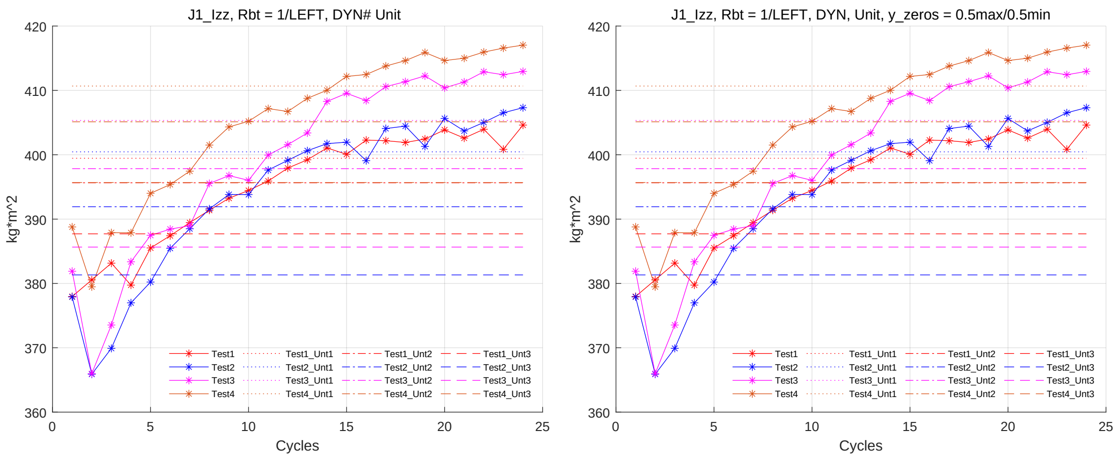

(a) Labelled automatically

(b) Labelled with the widening scale of y-axis

Figure I.1: I_{zz} of Joint 1 of the Robot LEFT with the identified results of selected cycles

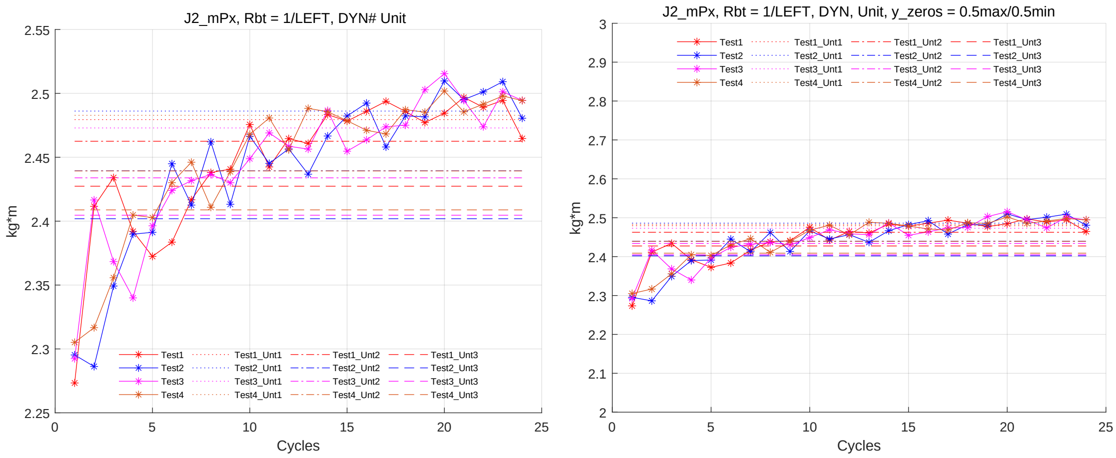

(a) Labelled automatically (b) Labelled with the widening scale of y-axis

Figure I.2: mP_x of Joint 2 of the Robot LEFT with the identified results of selected cycles

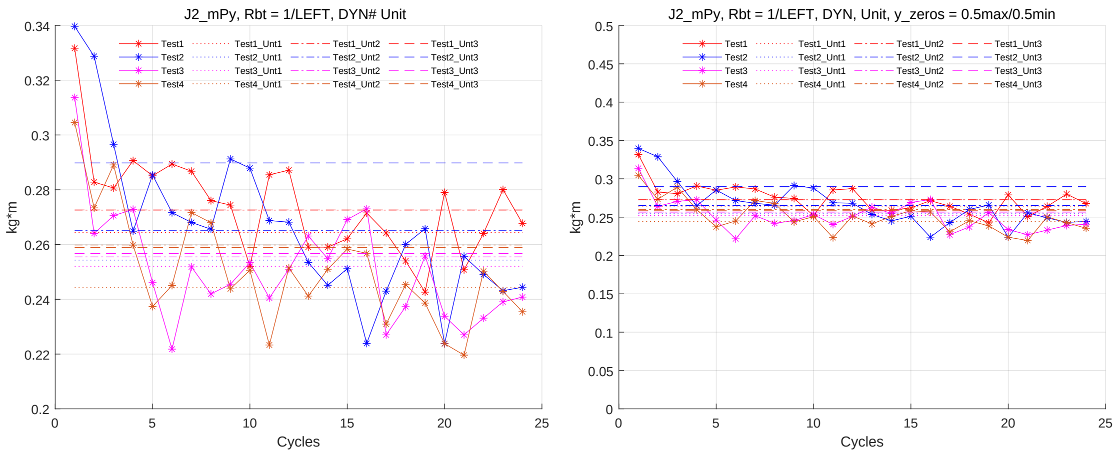

(a) Labelled automatically (b) Labelled with the widening scale of y-axis

Figure I.3: mP_y of Joint 2 of the Robot LEFT with the identified results of selected cycles

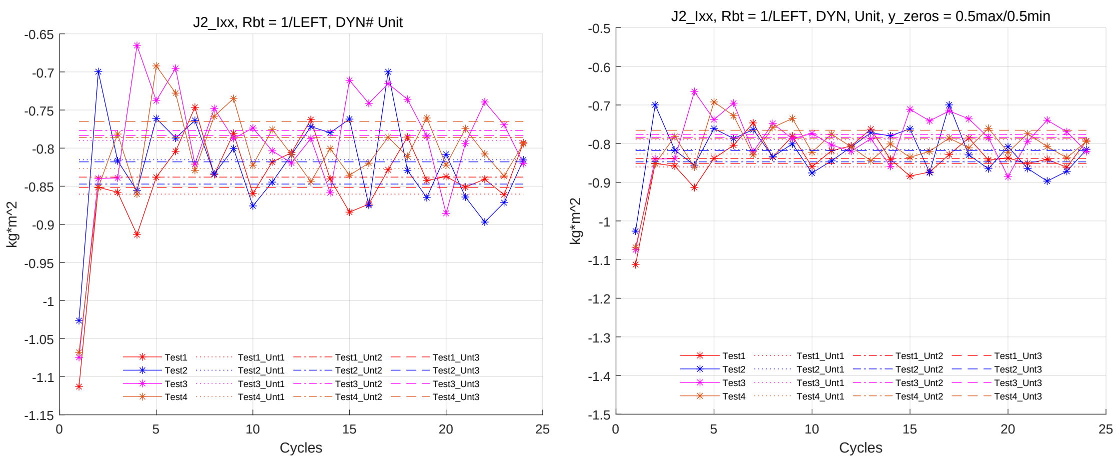

(a) Labelled automatically (b) Labelled with the widening scale of y-axis

Figure I.4: I_{xx} of Joint 2 of the Robot LEFT with the identified results of selected cycles

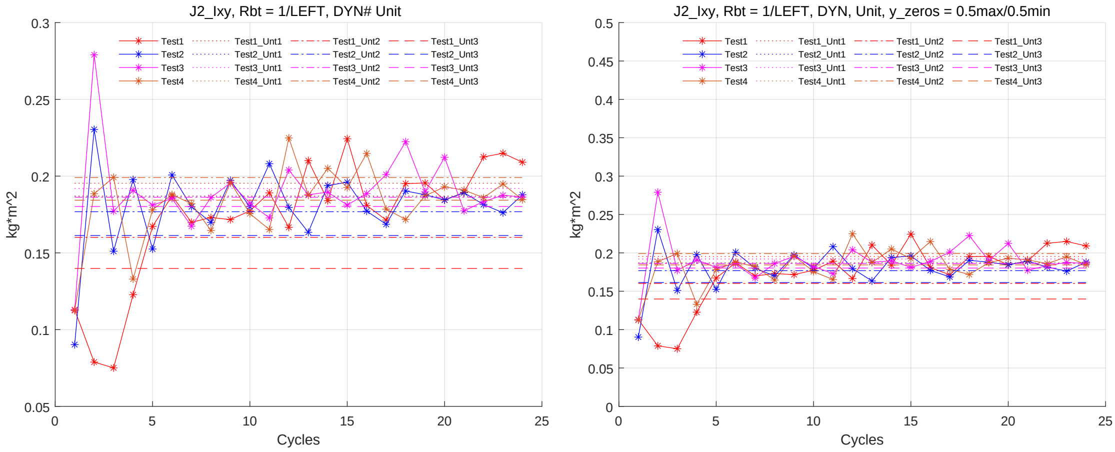

(a) Labelled automatically (b) Labelled with the widening scale of y-axis

Figure I.5: I_{xy} of Joint 2 of the Robot LEFT with the identified results of selected cycles

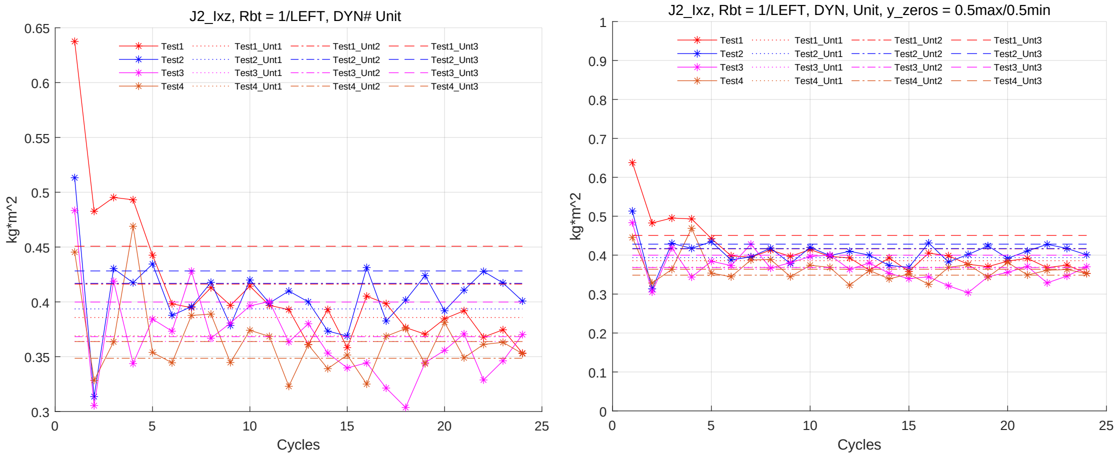

(a) Labelled automatically (b) Labelled with the widening scale of y-axis

Figure I.6: I_{xz} of Joint 2 of the Robot LEFT with the identified results of selected cycles

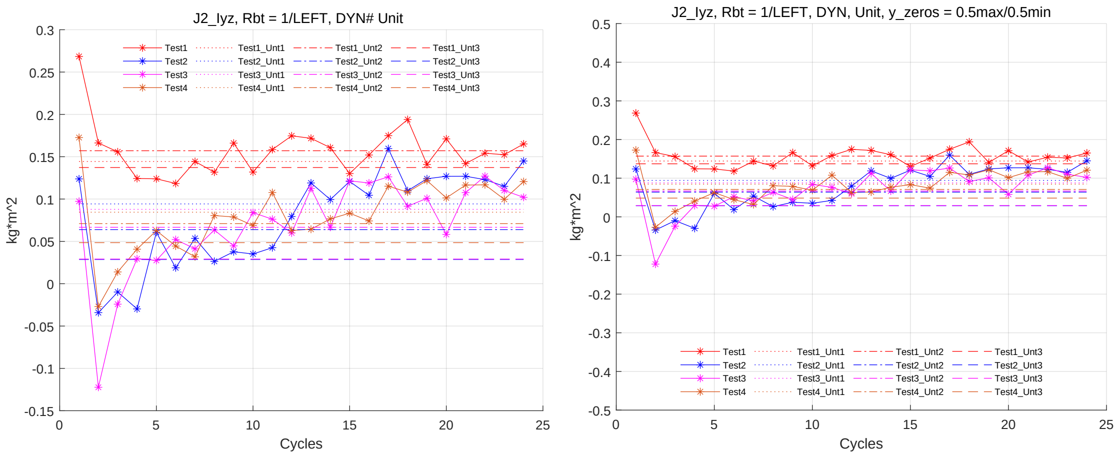

(a) Labelled automatically (b) Labelled with the widening scale of y-axis

Figure I.7: I_{yz} of Joint 2 of the Robot LEFT with the identified results of selected cycles

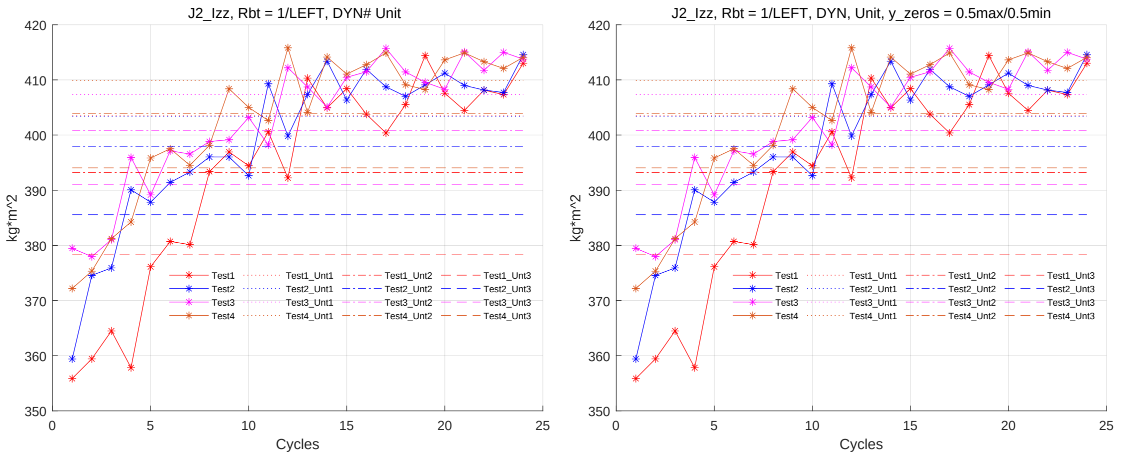

(a) Labelled automatically (b) Labelled with the widening scale of y-axis

Figure I.8: I_{zz} of Joint 2 of the Robot LEFT with the identified results of selected cycles

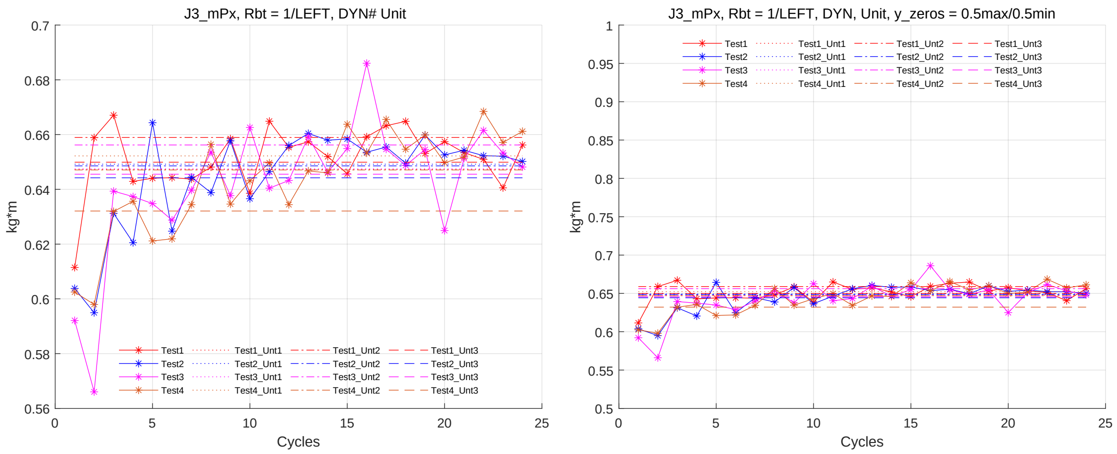

(a) Labelled automatically (b) Labelled with the widening scale of y-axis

Figure I.9: mP_x of Joint 3 of the Robot LEFT with the identified results of selected cycles

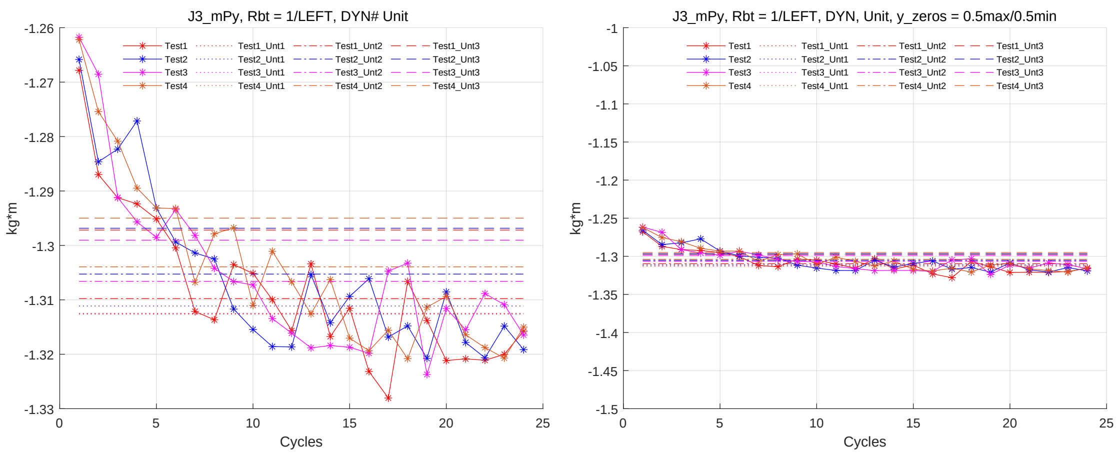

(a) Labelled automatically (b) Labelled with the widening scale of y-axis

Figure I.10: mP_y of Joint 3 of the Robot LEFT with the identified results of selected cycles

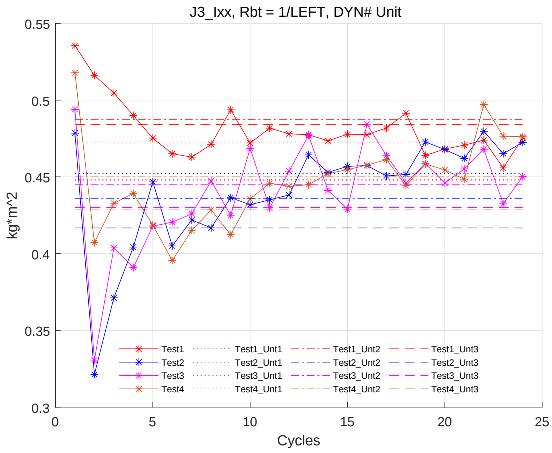

(a) Labelled automatically

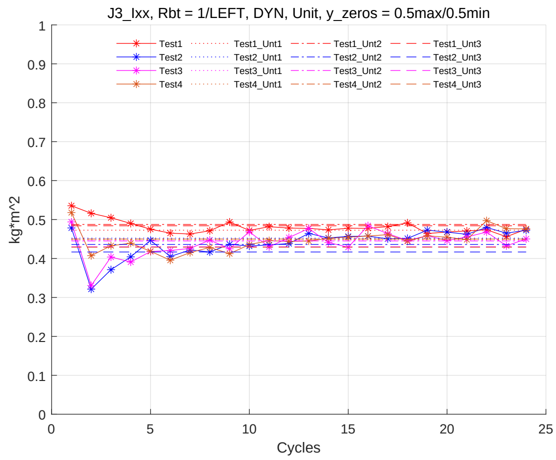

(b) Labelled with the widening scale of y-axis

Figure I.11: I_{xx} of Joint 3 of the Robot LEFT with the identified results of selected cycles

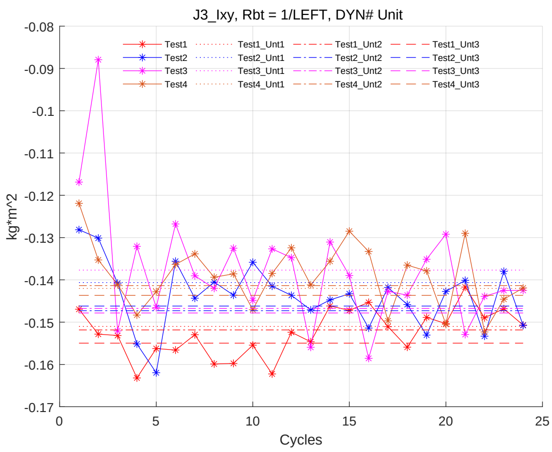

(a) Labelled automatically

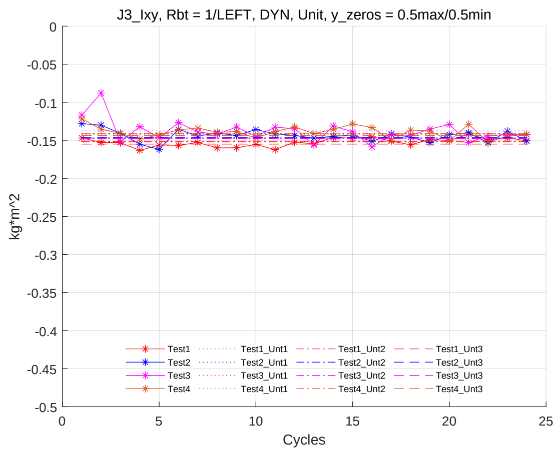

(b) Labelled with the widening scale of y-axis

Figure I.12: I_{xy} of Joint 3 of the Robot LEFT with the identified results of selected cycles

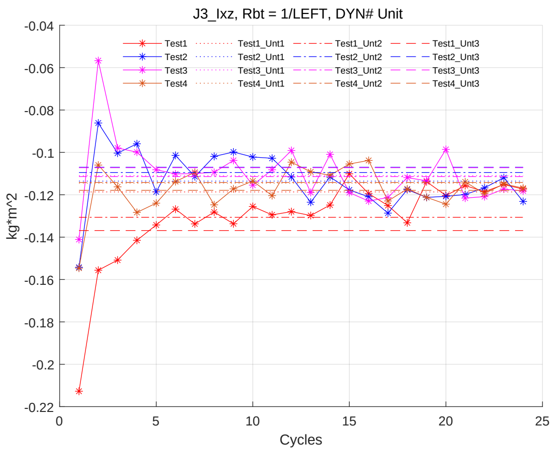

(a) Labelled automatically

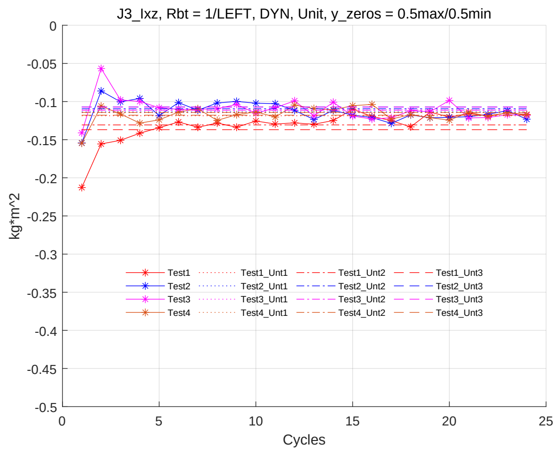

(b) Labelled with the widening scale of y-axis

Figure I.13: I_{xz} of Joint 3 of the Robot LEFT with the identified results of selected cycles

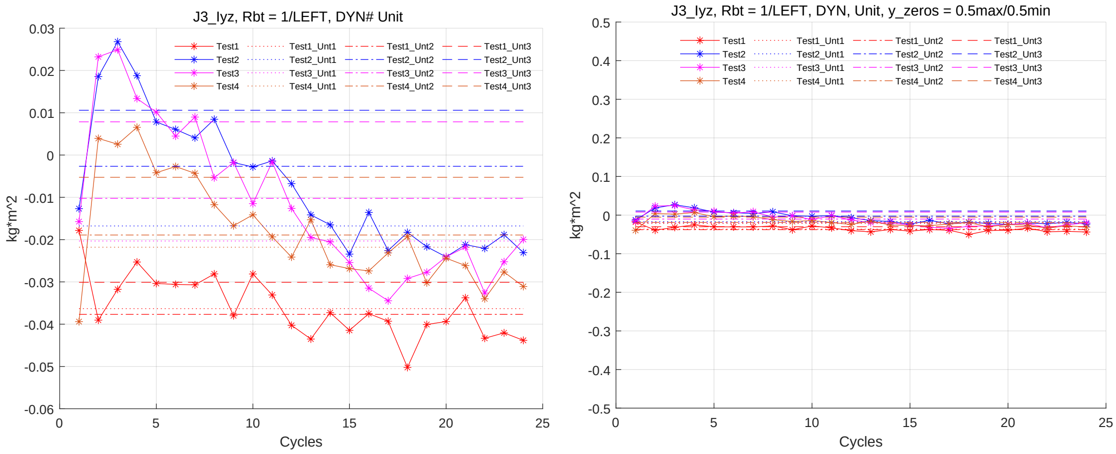

(a) Labelled automatically (b) Labelled with the widening scale of y-axis

Figure I.14: I_{yz} of Joint 3 of the Robot LEFT with the identified results of selected cycles

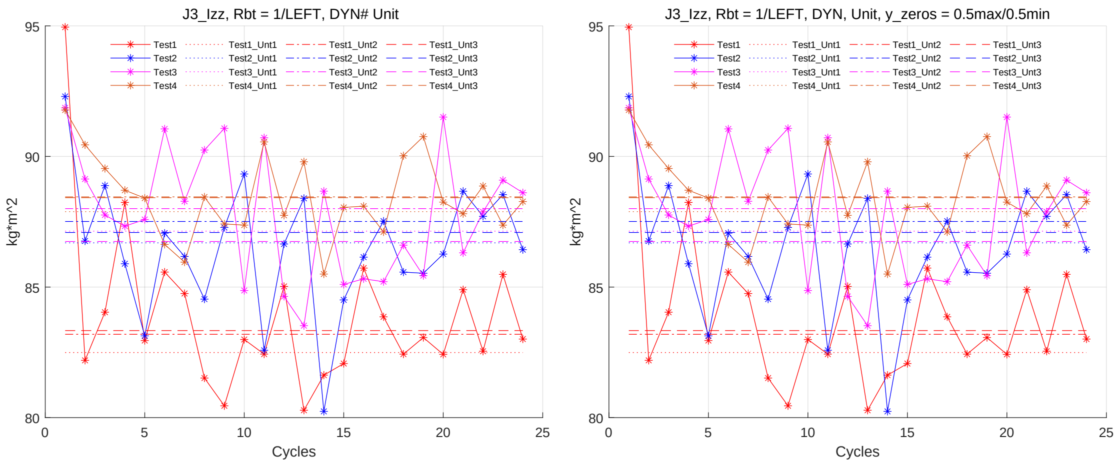

(a) Labelled automatically (b) Labelled with the widening scale of y-axis

Figure I.15: I_{zz} of Joint 3 of the Robot LEFT with the identified results of selected cycles

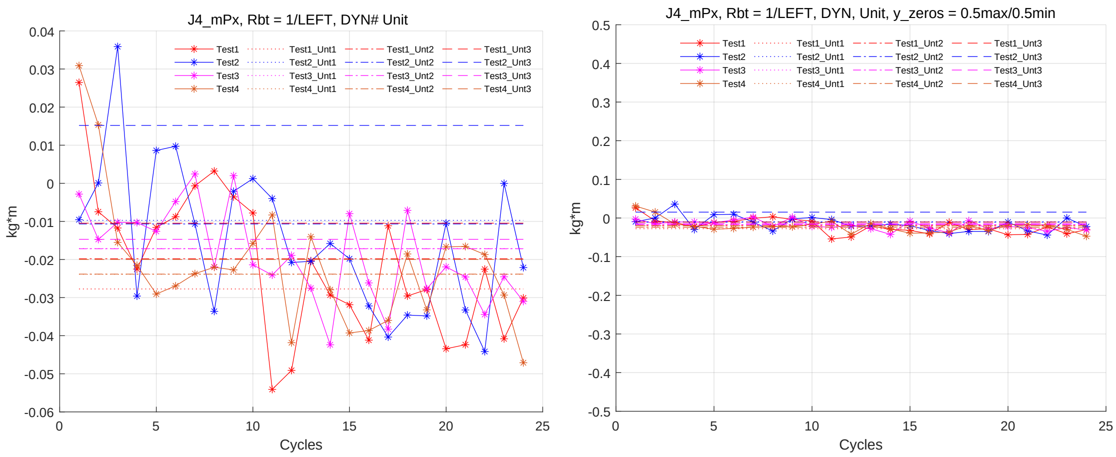

(a) Labelled automatically (b) Labelled with the widening scale of y-axis

Figure I.16: mP_x of Joint 4 of the Robot LEFT with the identified results of selected cycles

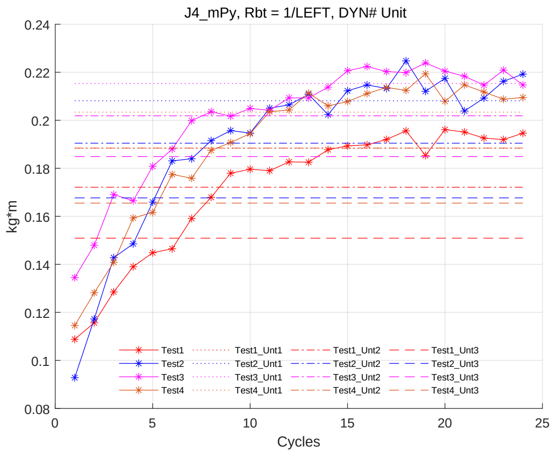

(a) Labelled automatically

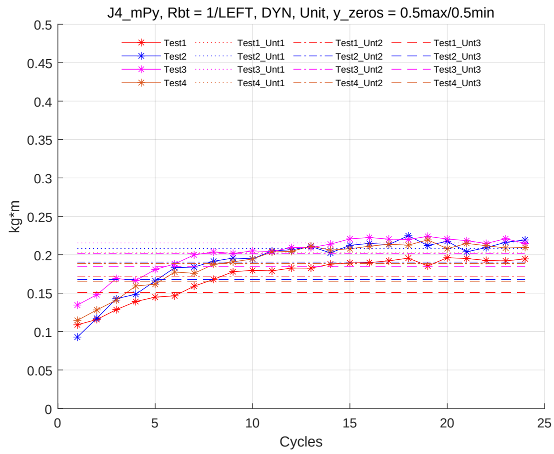

(b) Labelled with the widening scale of y-axis

Figure I.17: mP_y of Joint 4 of the Robot LEFT with the identified results of selected cycles

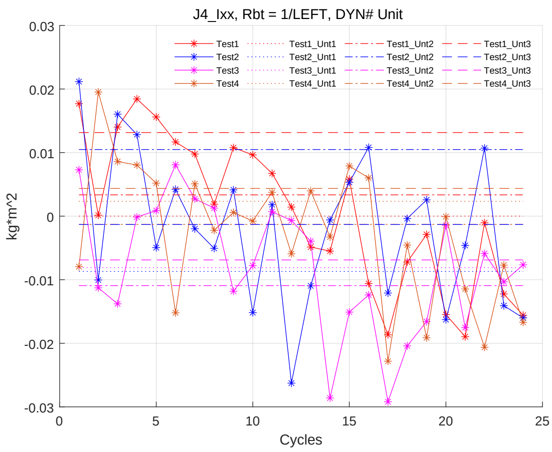

(a) Labelled automatically

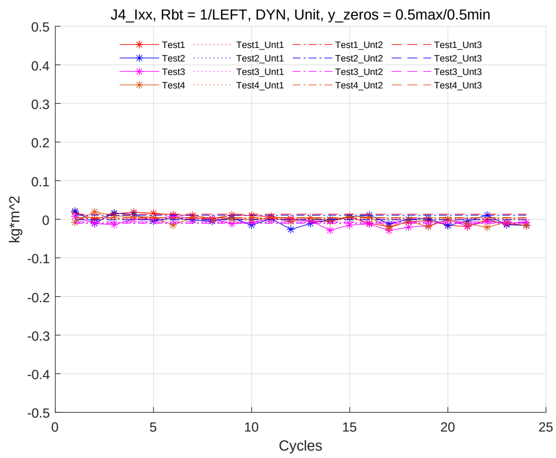

(b) Labelled with the widening scale of y-axis

Figure I.18: I_{xx} of Joint 4 of the Robot LEFT with the identified results of selected cycles

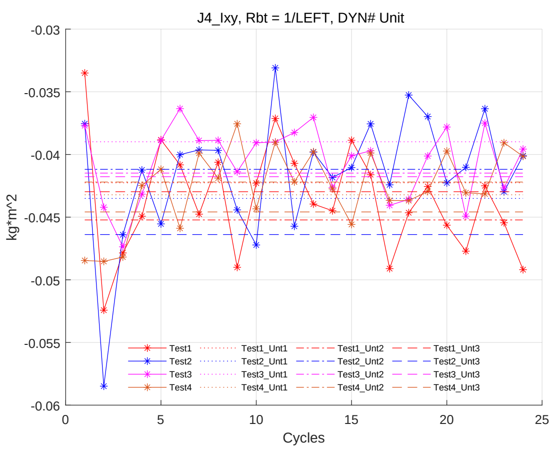

(a) Labelled automatically

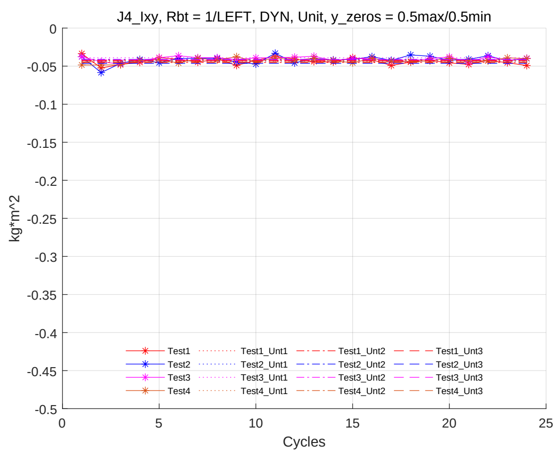

(b) Labelled with the widening scale of y-axis

Figure I.19: I_{xy} of Joint 4 of the Robot LEFT with the identified results of selected cycles

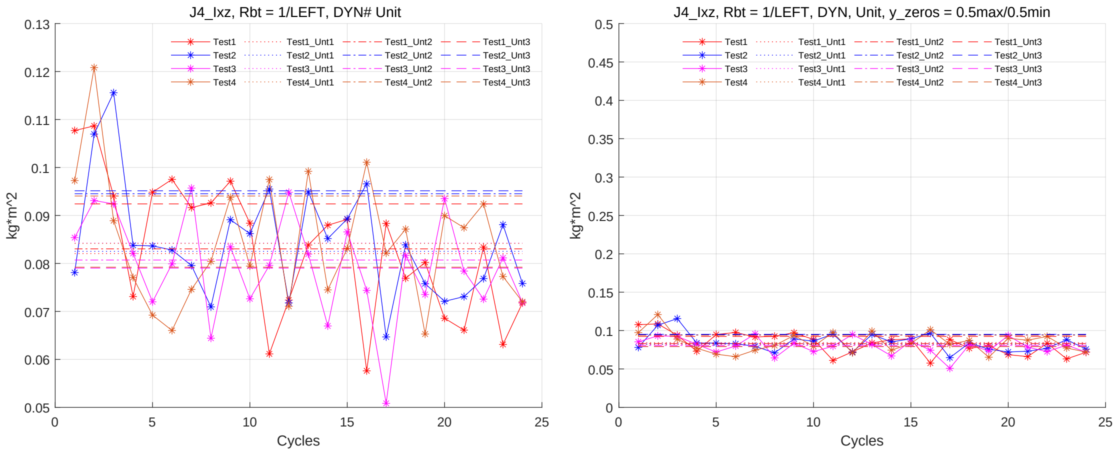

(a) Labelled automatically (b) Labelled with the widening scale of y-axis

Figure I.20: I_{xz} of Joint 4 of the Robot LEFT with the identified results of selected cycles

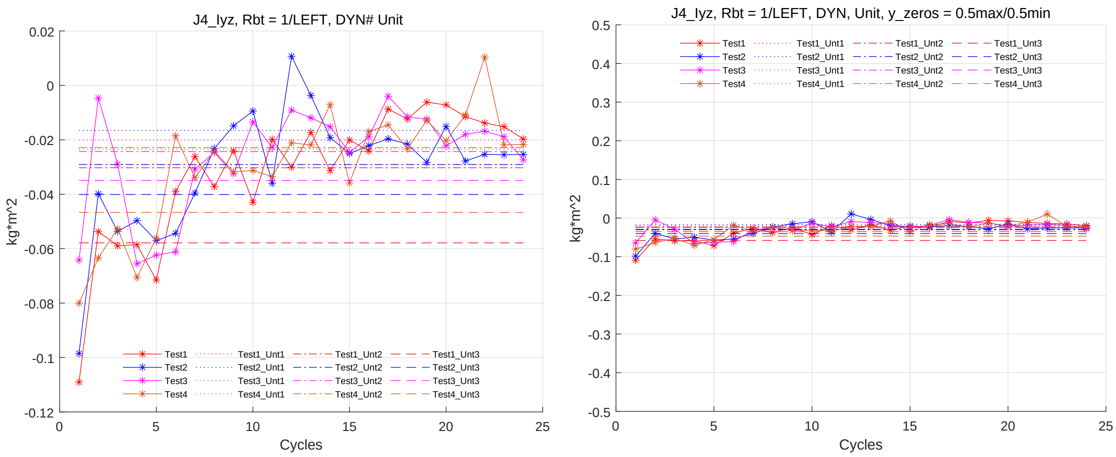

(a) Labelled automatically (b) Labelled with the widening scale of y-axis

Figure I.21: I_{yz} of Joint 4 of the Robot LEFT with the identified results of selected cycles

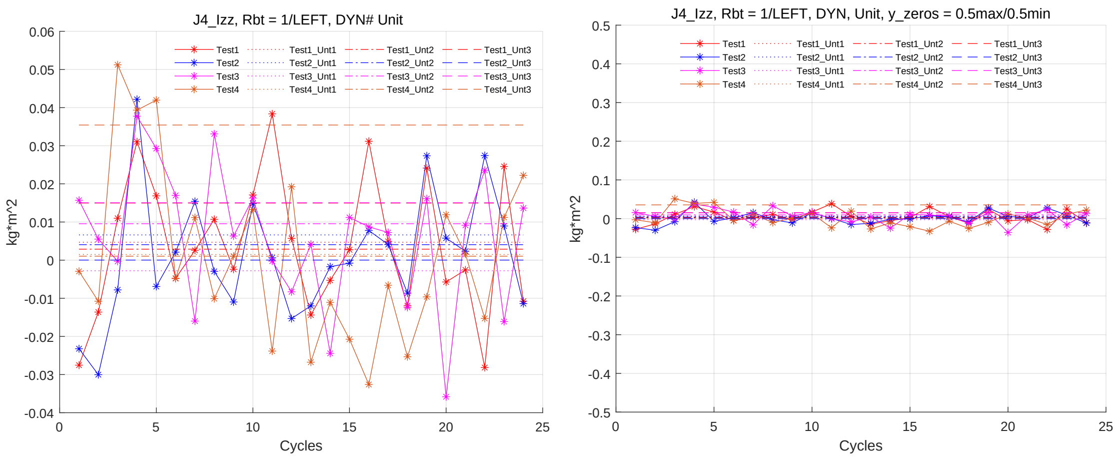

(a) Labelled automatically (b) Labelled with the widening scale of y-axis

Figure I.22: I_{zz} of Joint 4 of the Robot LEFT with the identified results of selected cycles

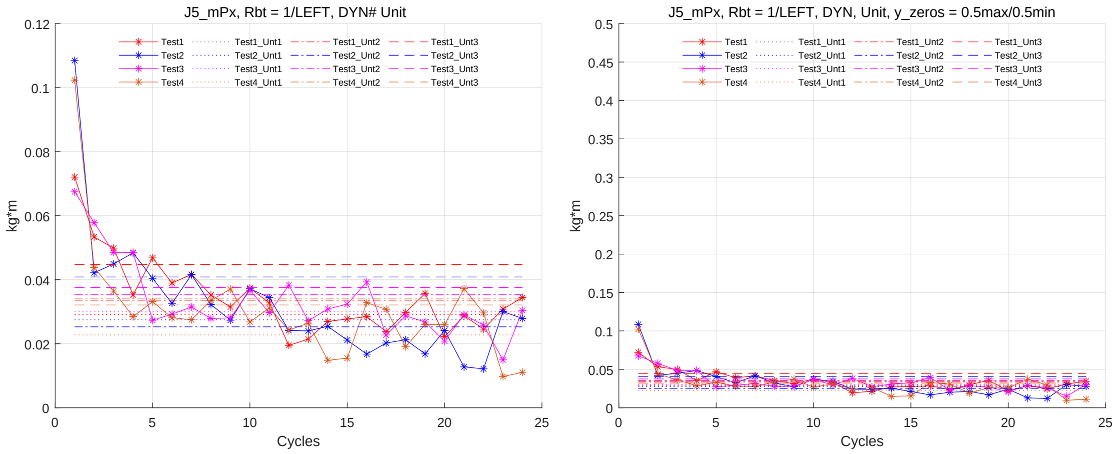

(a) Labelled automatically

(b) Labelled with the widening scale of y-axis

Figure I.23: mP_x of Joint 5 of the Robot LEFT with the identified results of selected cycles

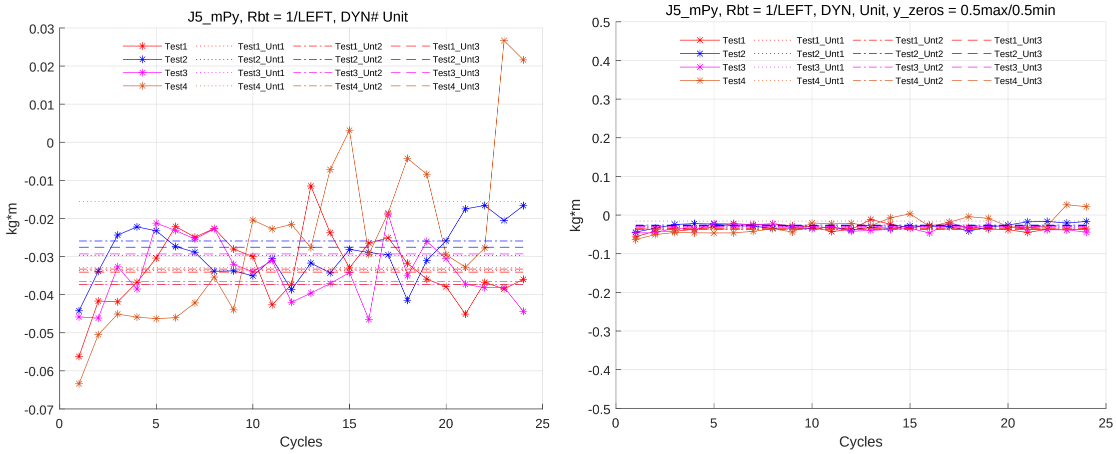

(a) Labelled automatically

(b) Labelled with the widening scale of y-axis

Figure I.24: mP_y of Joint 5 of the Robot LEFT with the identified results of selected cycles

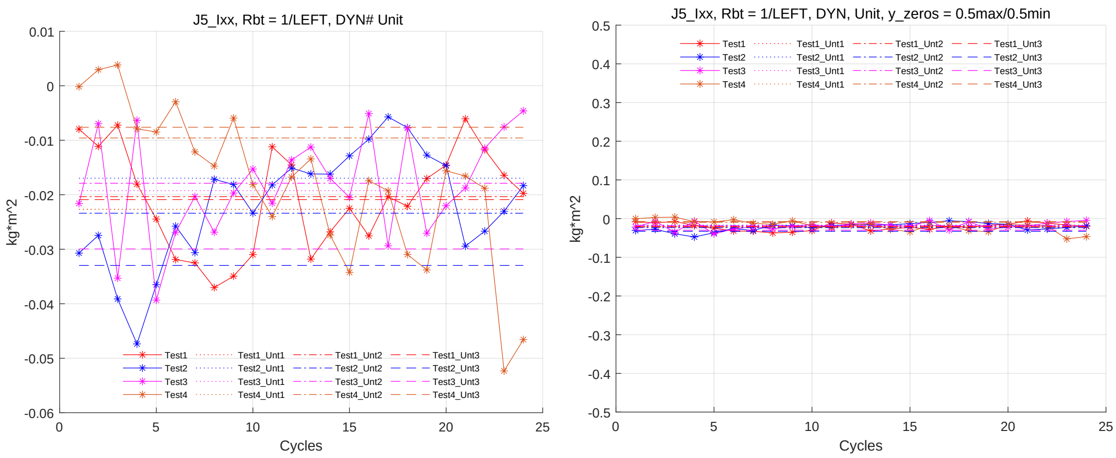

(a) Labelled automatically

(b) Labelled with the widening scale of y-axis

Figure I.25: I_{xx} of Joint 5 of the Robot LEFT with the identified results of selected cycles

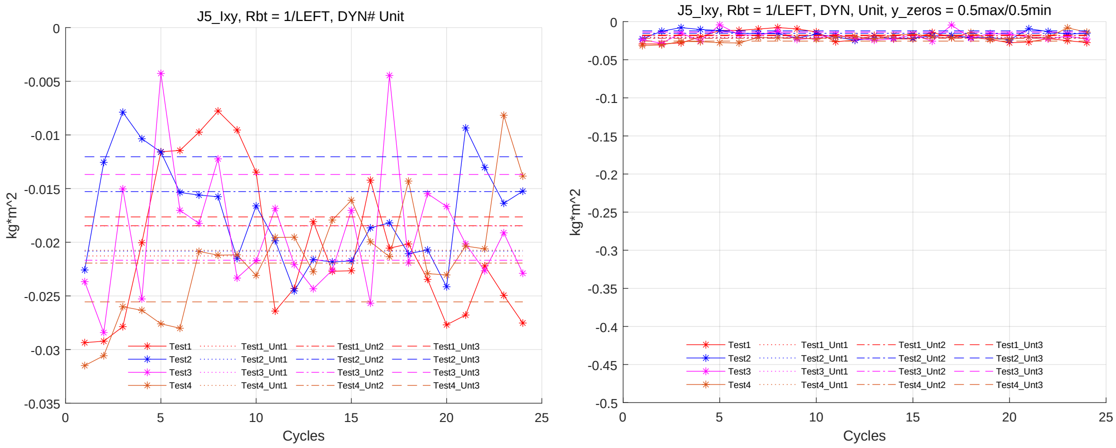

(a) Labelled automatically (b) Labelled with the widening scale of y-axis

Figure I.26: I_{xy} of Joint 5 of the Robot LEFT with the identified results of selected cycles

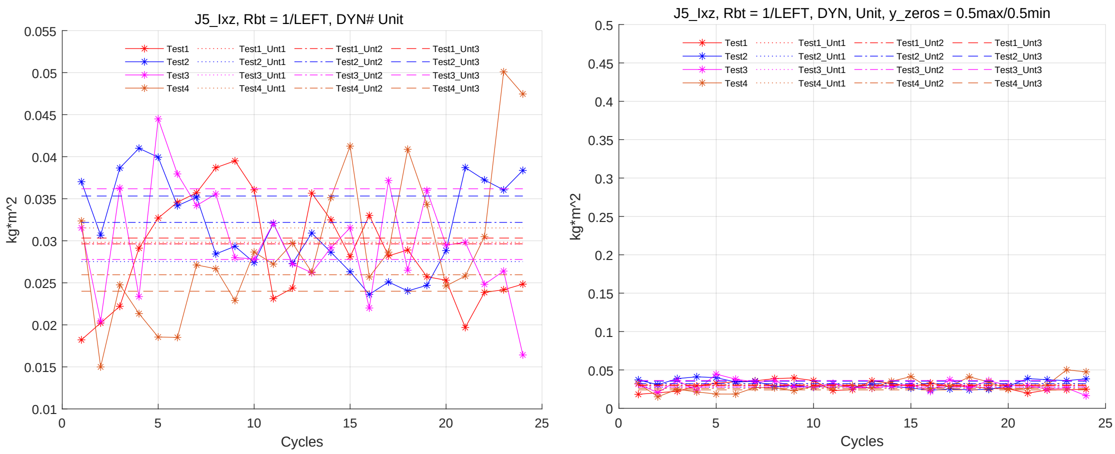

(a) Labelled automatically (b) Labelled with the widening scale of y-axis

Figure I.27: I_{xz} of Joint 5 of the Robot LEFT with the identified results of selected cycles

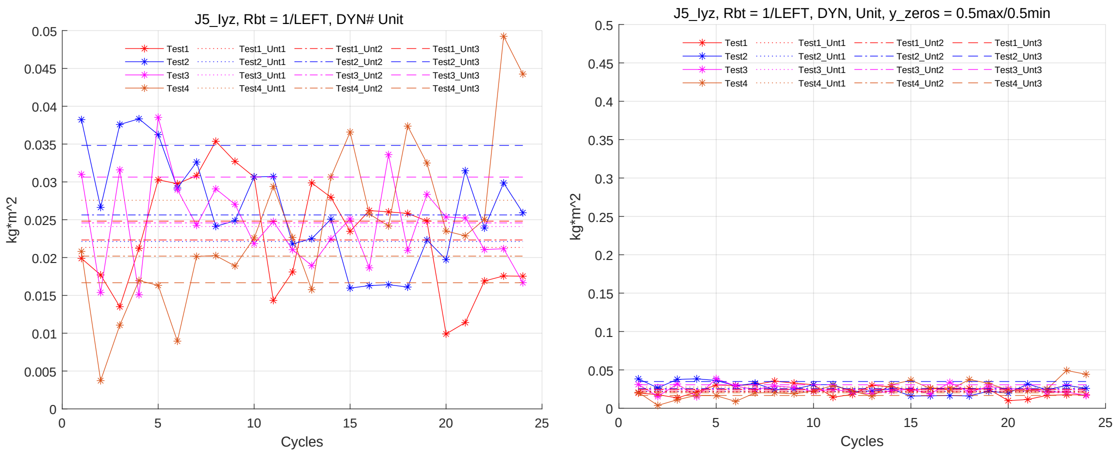

(a) Labelled automatically (b) Labelled with the widening scale of y-axis

Figure I.28: I_{yz} of Joint 5 of the Robot LEFT with the identified results of selected cycles

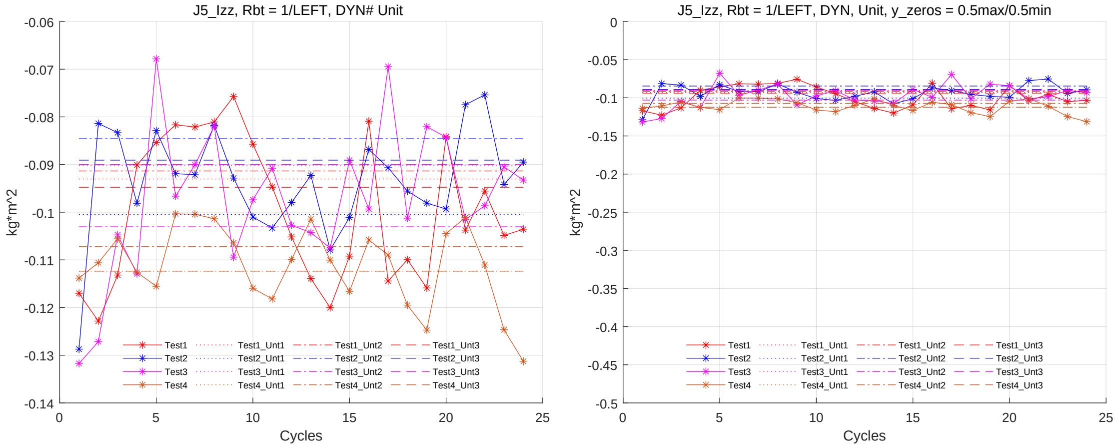

(a) Labelled automatically (b) Labelled with the widening scale of y-axis

Figure I.29: I_{zz} of Joint 5 of the Robot LEFT with the identified results of selected cycles

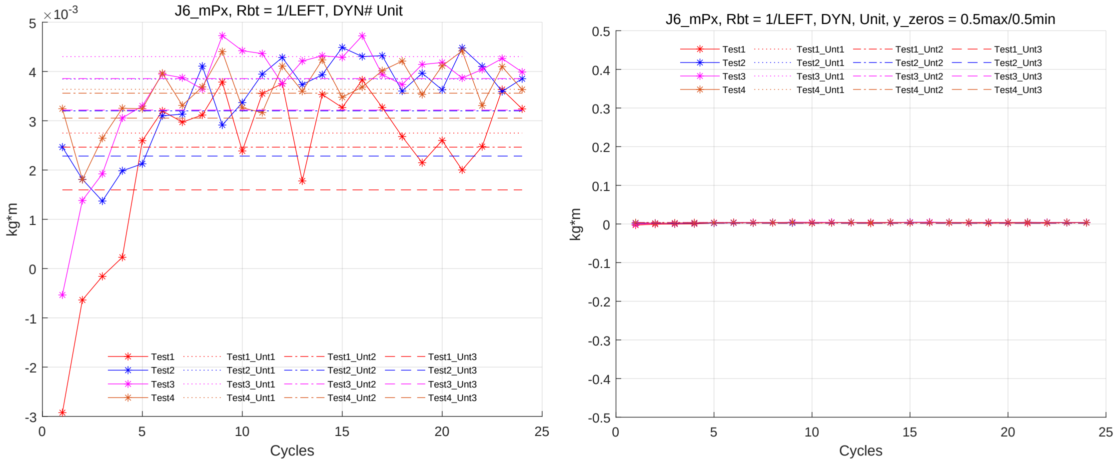

(a) Labelled automatically (b) Labelled with the widening scale of y-axis

Figure I.30: mP_x of Joint 6 of the Robot LEFT with the identified results of selected cycles

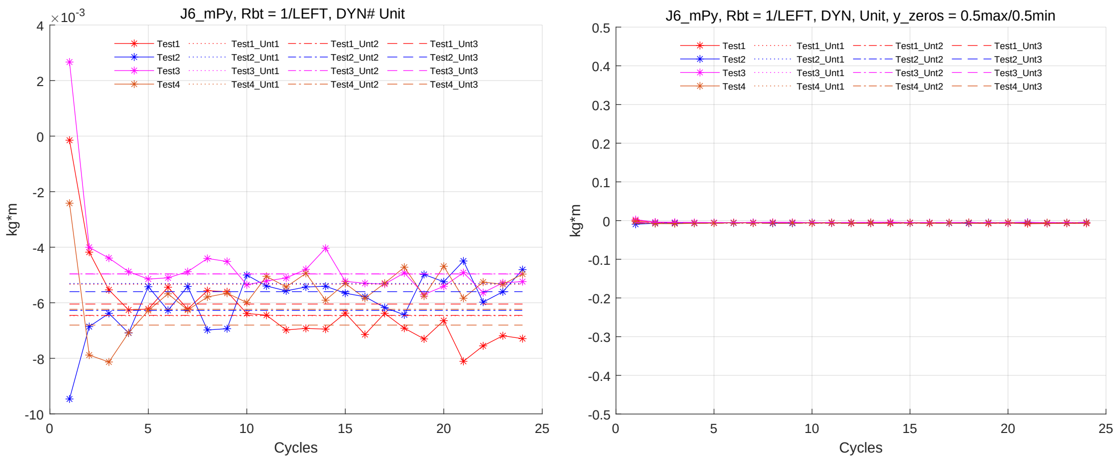

(a) Labelled automatically (b) Labelled with the widening scale of y-axis

Figure I.31: mP_y of Joint 6 of the Robot LEFT with the identified results of selected cycles

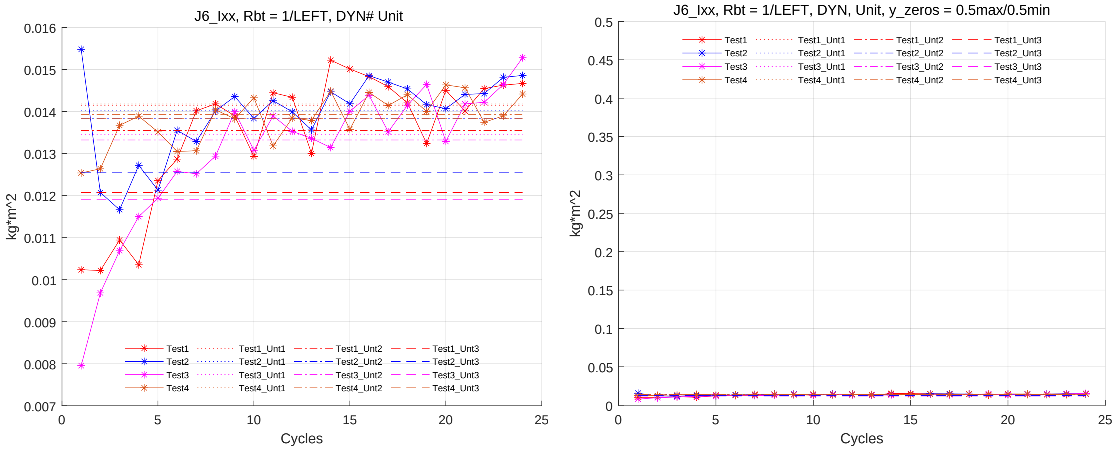

(a) Labelled automatically

(b) Labelled with the widening scale of y-axis

Figure I.32: I_{xx} of Joint 6 of the Robot LEFT with the identified results of selected cycles

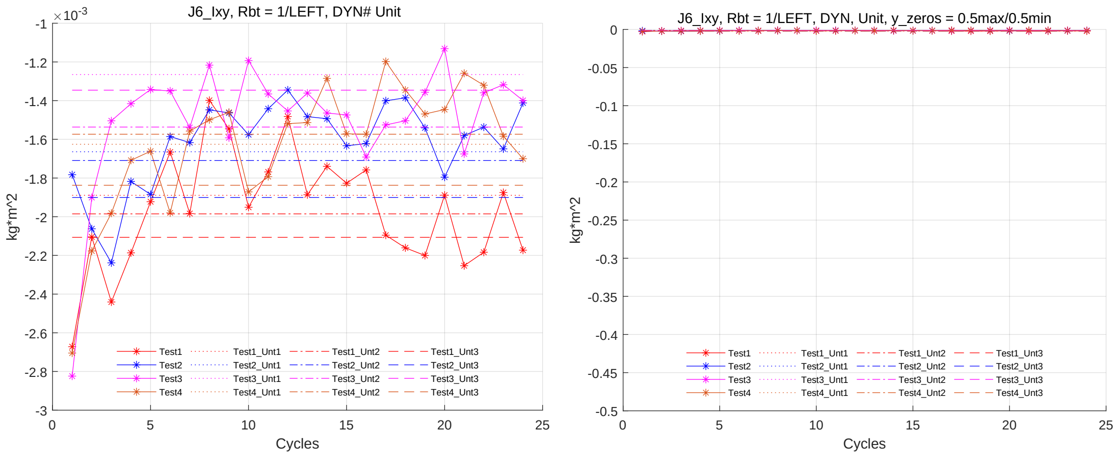

(a) Labelled automatically

(b) Labelled with the widening scale of y-axis

Figure I.33: I_{xy} of Joint 6 of the Robot LEFT with the identified results of selected cycles

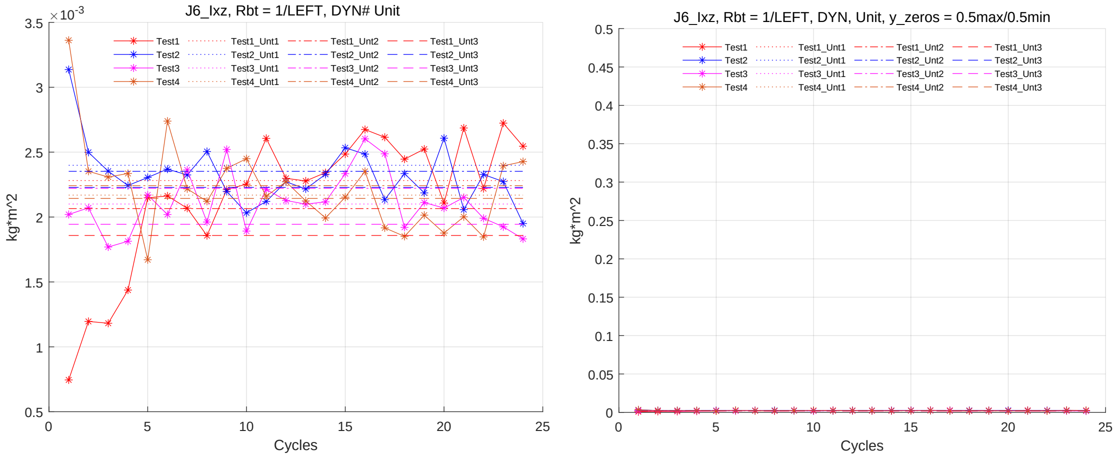

(a) Labelled automatically

(b) Labelled with the widening scale of y-axis

Figure I.34: I_{xz} of Joint 6 of the Robot LEFT with the identified results of selected cycles

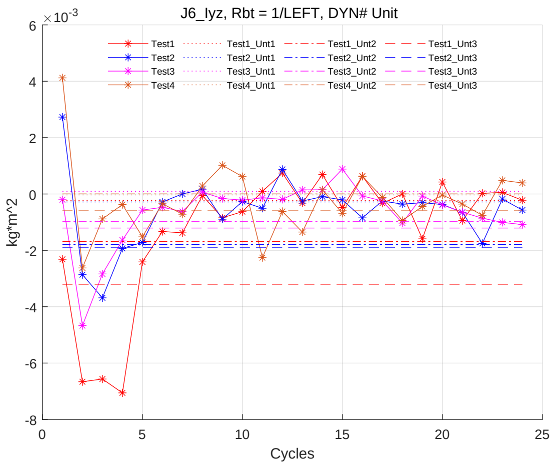

(a) Labelled automatically

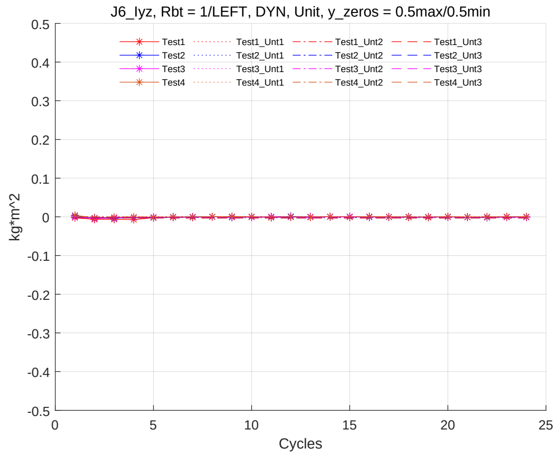

(b) Labelled with the widening scale of y-axis

Figure I.35: I_{yz} of Joint 6 of the Robot LEFT with the identified results of selected cycles

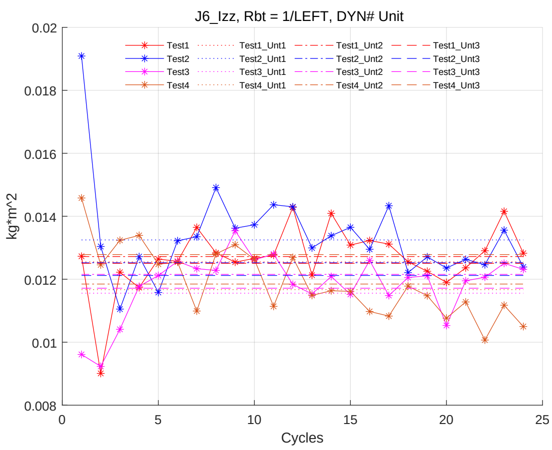

(a) Labelled automatically

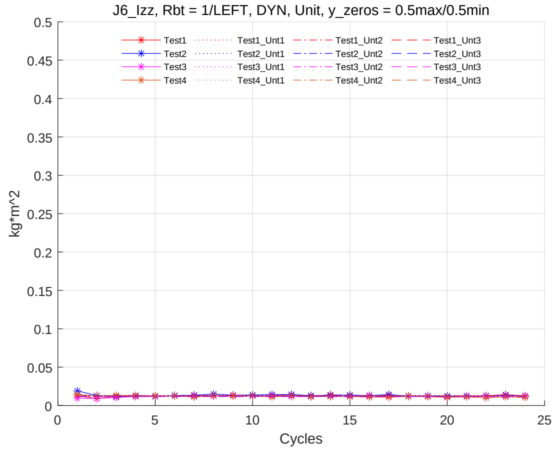

(b) Labelled with the widening scale of y-axis

Figure I.36: I_{zz} of Joint 6 of the Robot LEFT with the identified results of selected cycles

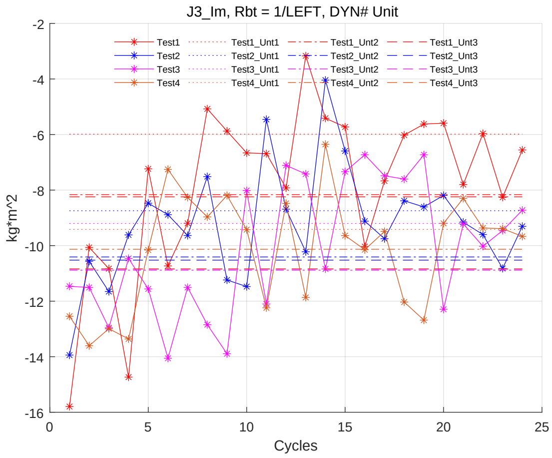

(a) Labelled automatically

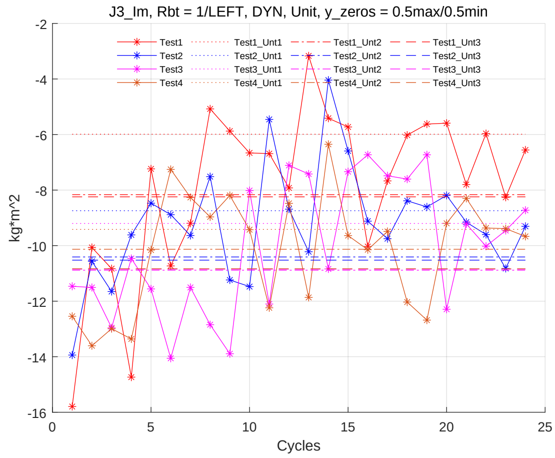

(b) Labelled with the widening scale of y-axis

Figure I.37: I_m of Joint 3 of the LEFT Robot with the identified results of selected cycles

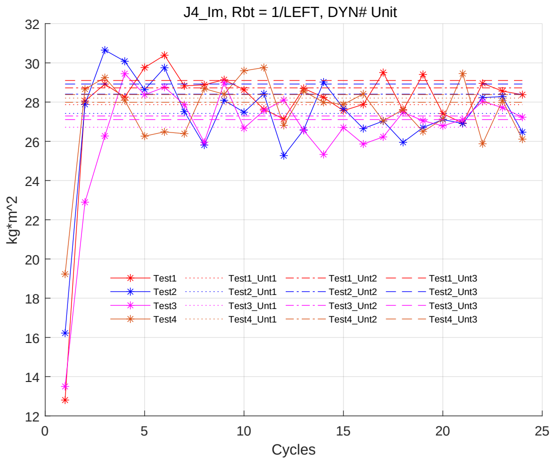

(a) Labelled automatically

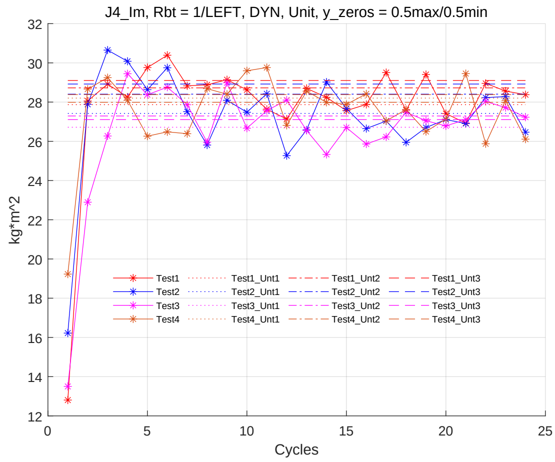

(b) Labelled with the widening scale of y-axis

Figure I.38: I_m of Joint 4 of the LEFT Robot with the identified results of selected cycles

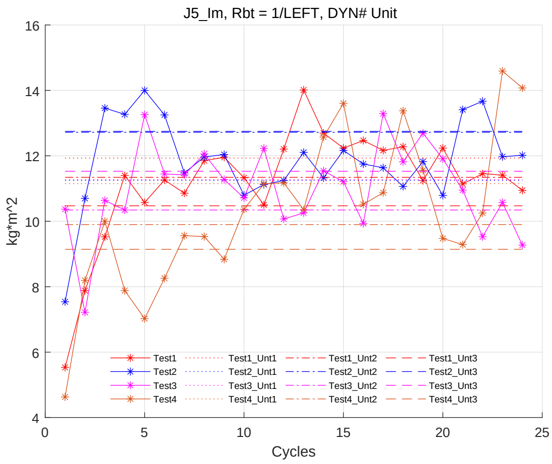

(a) Labelled automatically

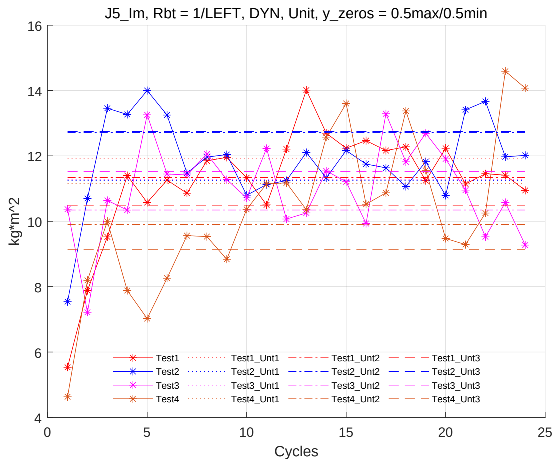

(b) Labelled with the widening scale of y-axis

Figure I.39: I_m of Joint 5 of the LEFT Robot with the identified results of selected cycles

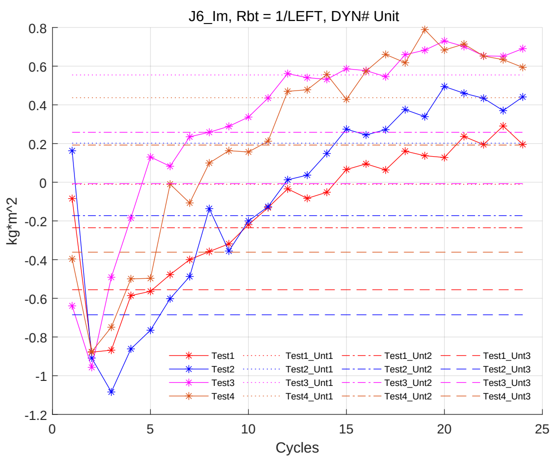

(a) Labelled automatically

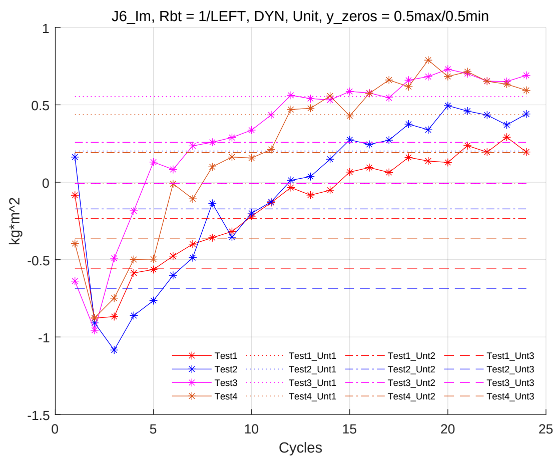

(b) Labelled with the widening scale of y-axis

Figure I.40: I_m of Joint 6 of the LEFT Robot with the identified results of selected cycles

Appendix J

The Identification Results Of Excitation Trajectory Of Robot 2

The figures shown in this appendix represent the dynamic parameter identification results of Robot RIGHT, which are mentioned in Section 5.1.5.2. Also the identified results of the selected cycles are shown here. The left sub-figures are the plots with the y-axis labelled automatically, and the right sub-figures are the plots with y-axis labelled multiplied by 0.5. It should be pointed that the identified friction coefficients are not presented due to the non-physical parameters. Additionally, it should be noticed that some parameters have the same plots between two sub-figures because the original y-axis range of the right sub-figure meet the requirements of multiple 0.5.

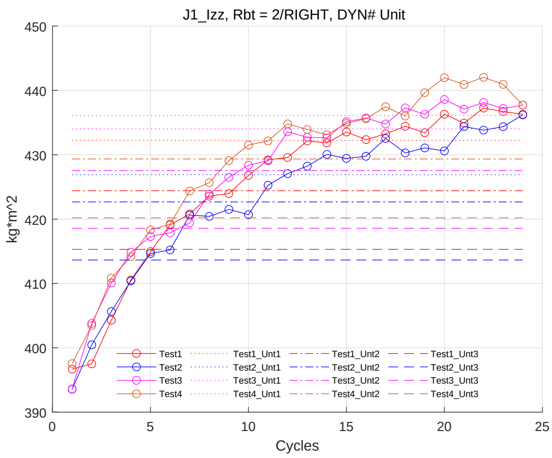

(a) Labelled automatically

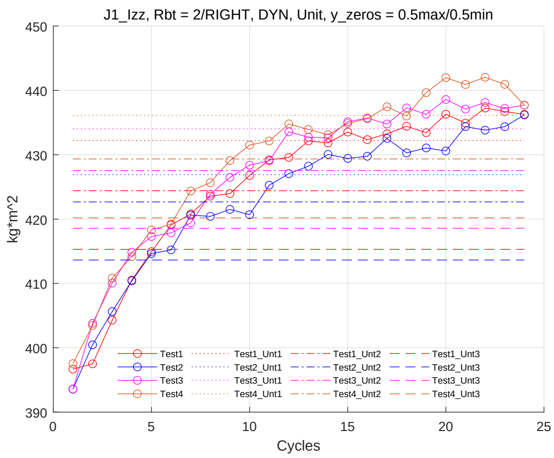

(b) Labelled with the widening scale of y-axis

Figure J.1: I_{zz} of Joint 1 of the Robot RIGHT with the identified results of selected cycles

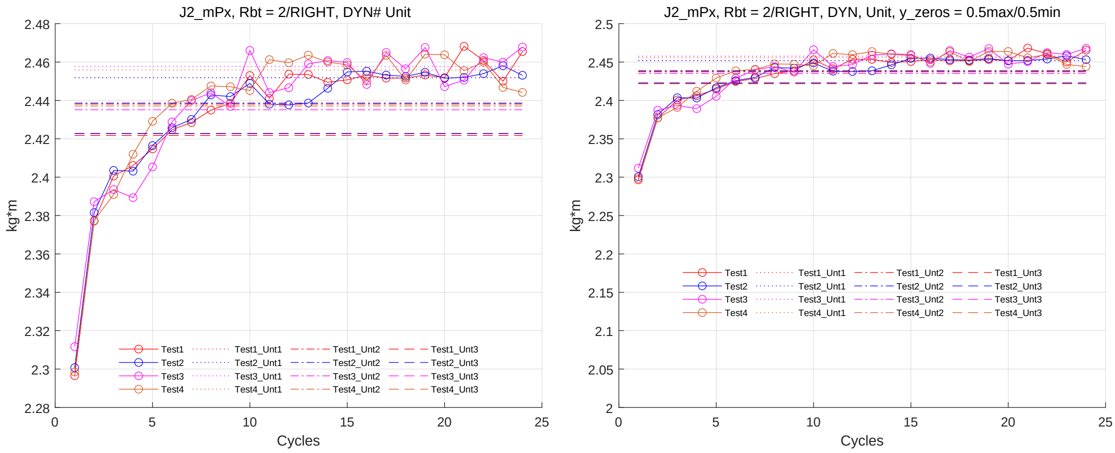

(a) Labelled automatically
(b) Labelled with the widening scale of y-axis

Figure J.2: mP_x of Joint 2 of the Robot RIGHT with the identified results of selected cycles

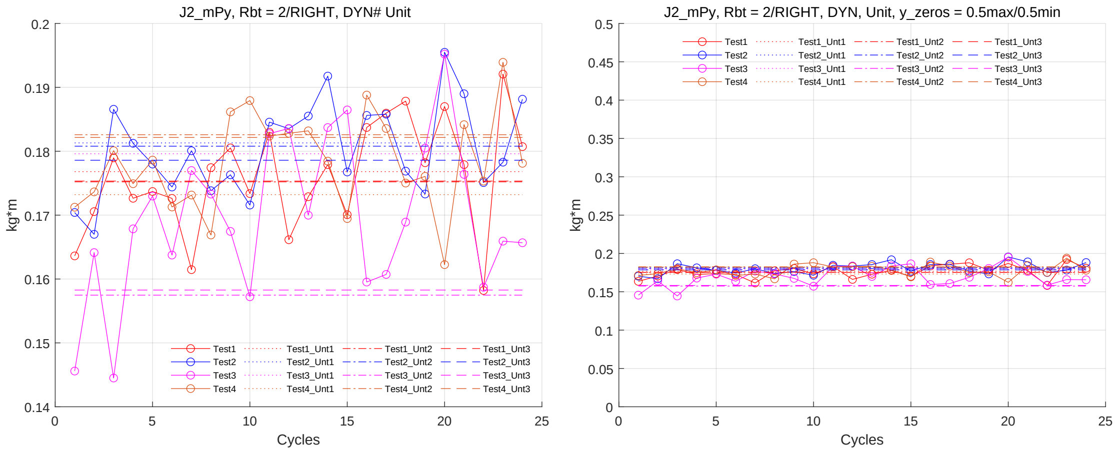

(a) Labelled automatically
(b) Labelled with the widening scale of y-axis

Figure J.3: mP_y of Joint 2 of the Robot RIGHT with the identified results of selected cycles

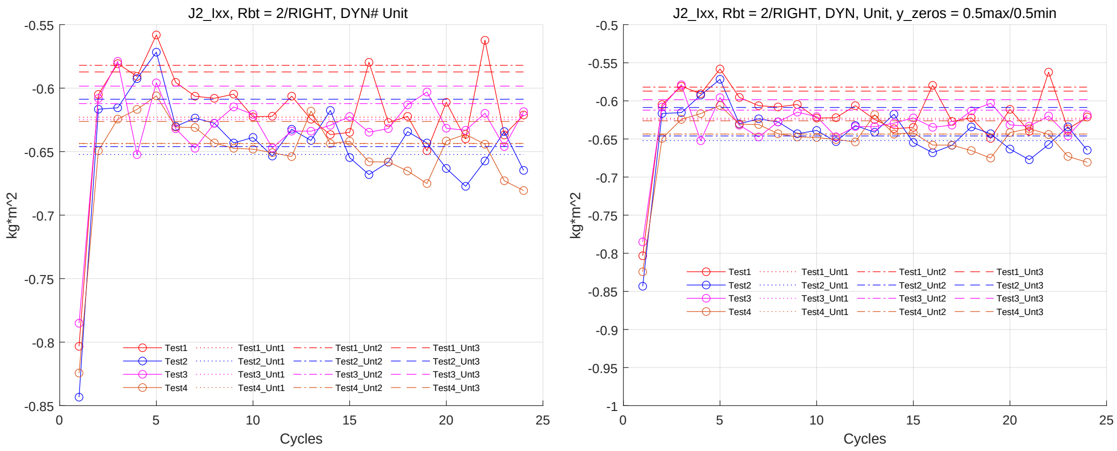

(a) Labelled automatically
(b) Labelled with the widening scale of y-axis

Figure J.4: I_{xx} of Joint 2 of the Robot RIGHT with the identified results of selected cycles

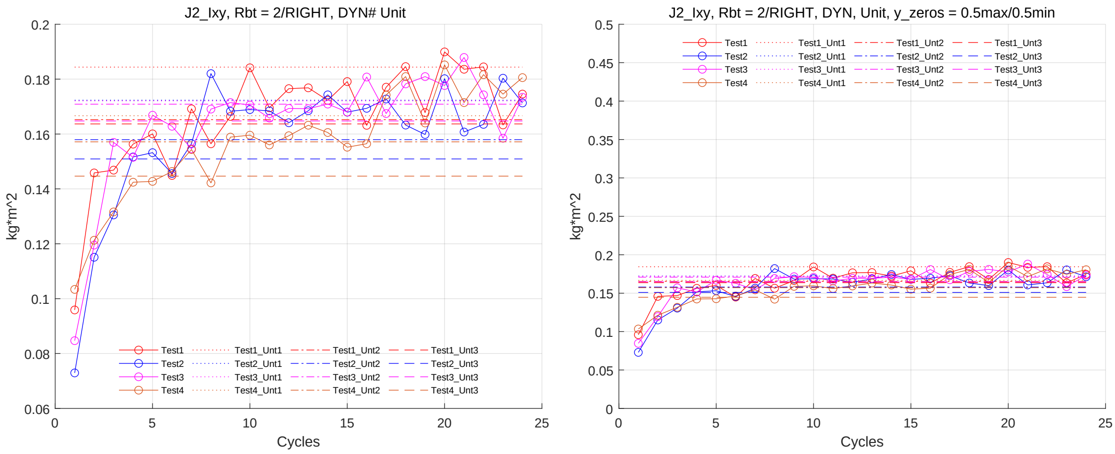

(a) Labelled automatically (b) Labelled with the widening scale of y-axis

Figure J.5: I_{xy} of Joint 2 of the Robot RIGHT with the identified results of selected cycles

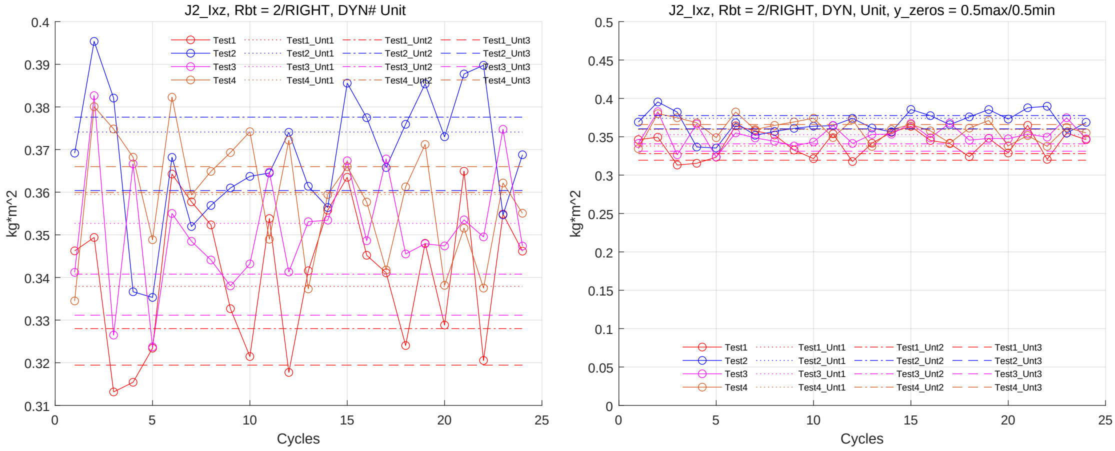

(a) Labelled automatically (b) Labelled with the widening scale of y-axis

Figure J.6: I_{xz} of Joint 2 of the Robot RIGHT with the identified results of selected cycles

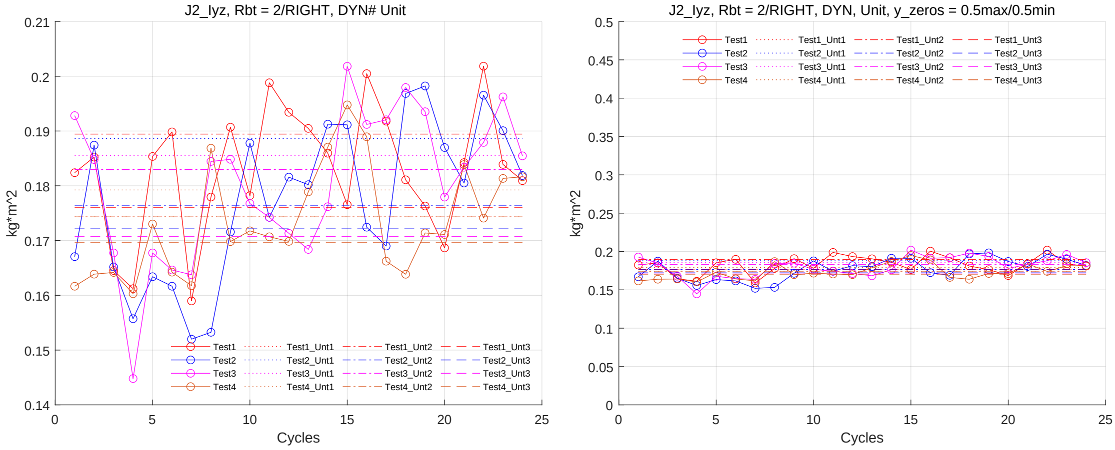

(a) Labelled automatically (b) Labelled with the widening scale of y-axis

Figure J.7: I_{yz} of Joint 2 of the Robot RIGHT with the identified results of selected cycles

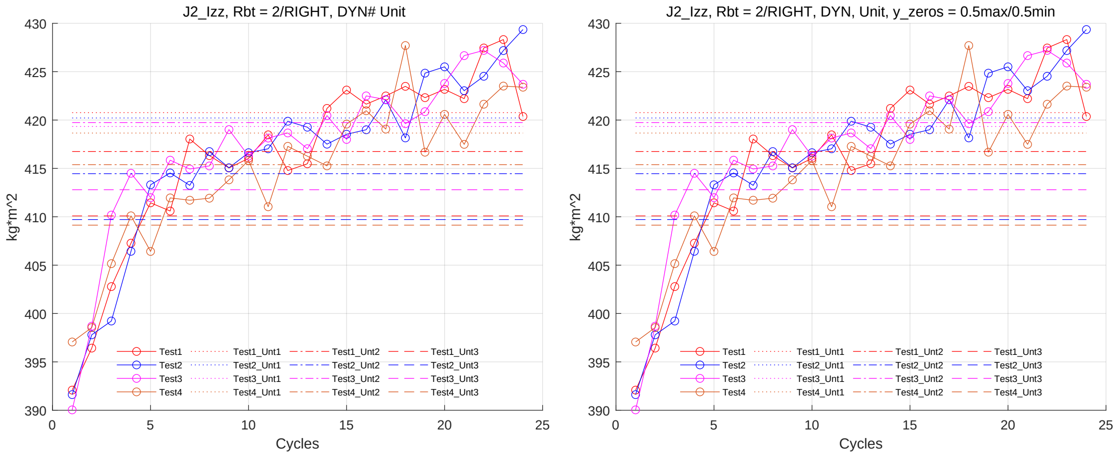

(a) Labelled automatically (b) Labelled with the widening scale of y-axis

Figure J.8: I_{zz} of Joint 2 of the Robot RIGHT with the identified results of selected cycles

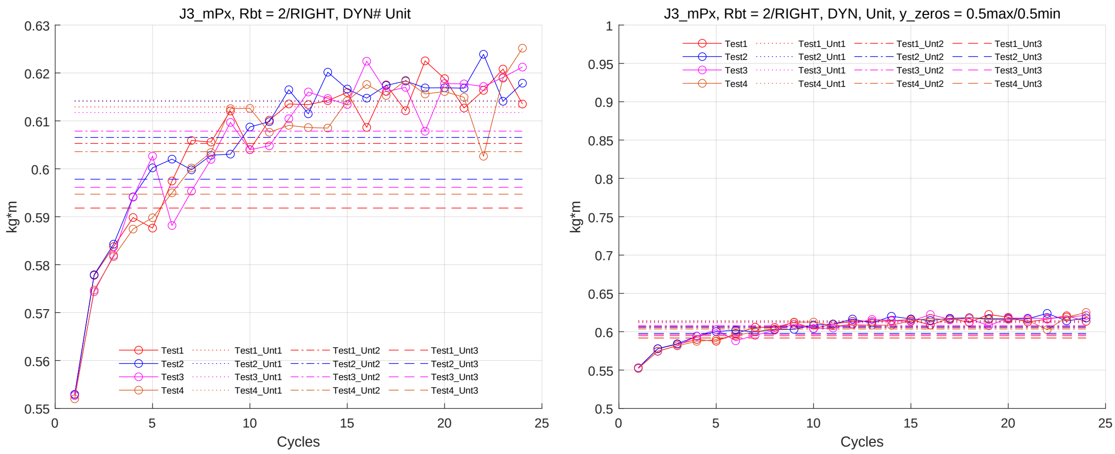

(a) Labelled automatically (b) Labelled with the widening scale of y-axis

Figure J.9: mP_x of Joint 3 of the Robot RIGHT with the identified results of selected cycles

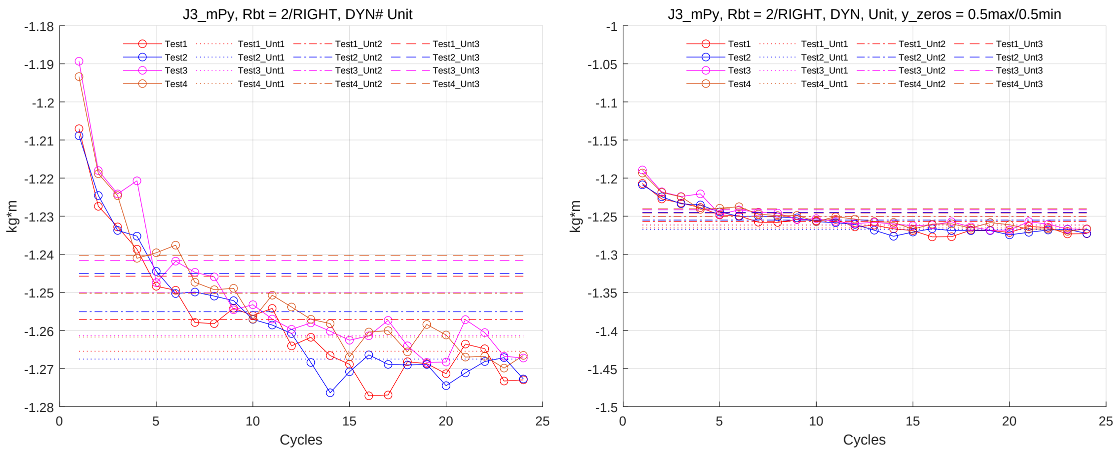

(a) Labelled automatically (b) Labelled with the widening scale of y-axis

Figure J.10: mP_y of Joint 3 of the Robot RIGHT with the identified results of selected cycles

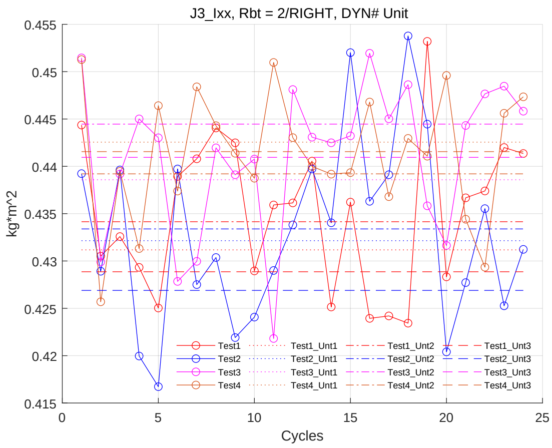

(a) Labelled automatically

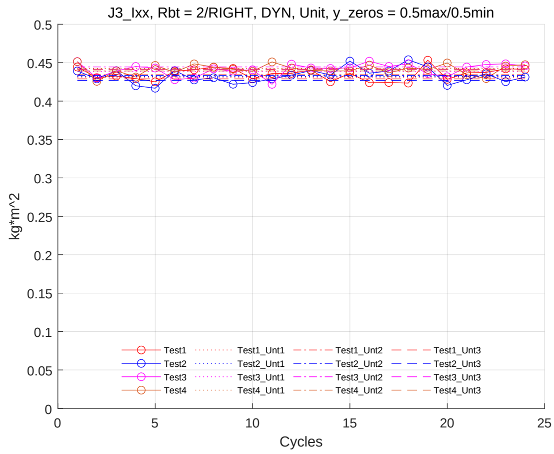

(b) Labelled with the widening scale of y-axis

Figure J.11: I_{xx} of Joint 3 of the Robot RIGHT with the identified results of selected cycles

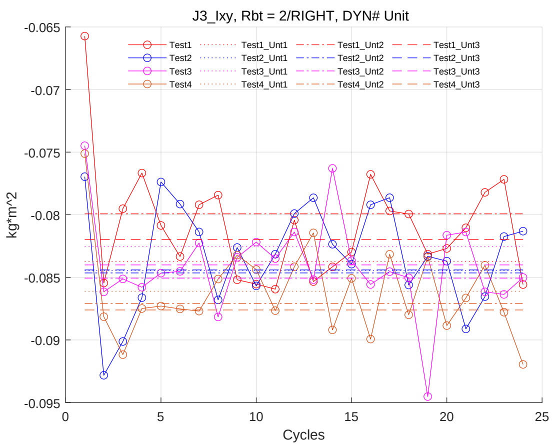

(a) Labelled automatically

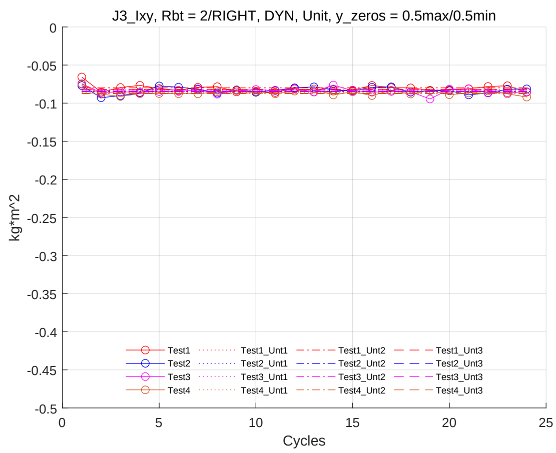

(b) Labelled with the widening scale of y-axis

Figure J.12: I_{xy} of Joint 3 of the Robot RIGHT with the identified results of selected cycles

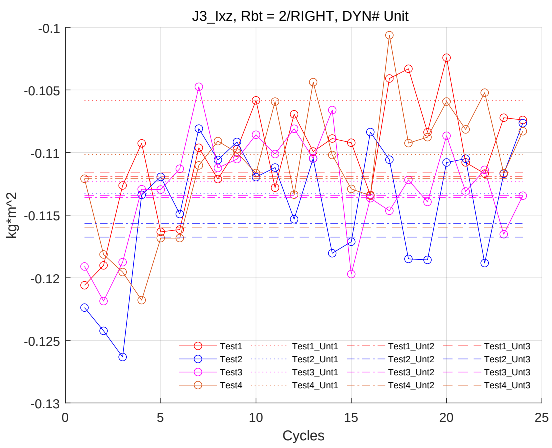

(a) Labelled automatically

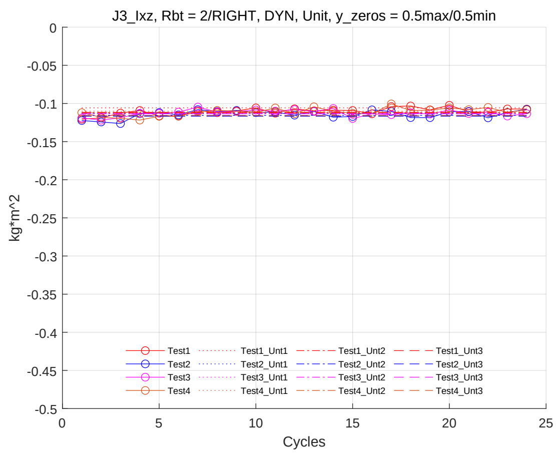

(b) Labelled with the widening scale of y-axis

Figure J.13: I_{xz} of Joint 3 of the Robot RIGHT with the identified results of selected cycles

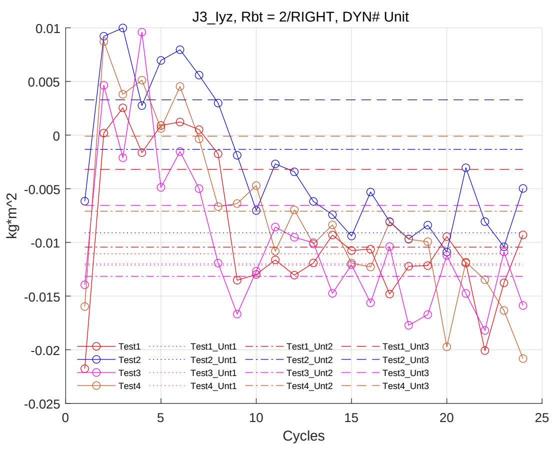

(a) Labelled automatically

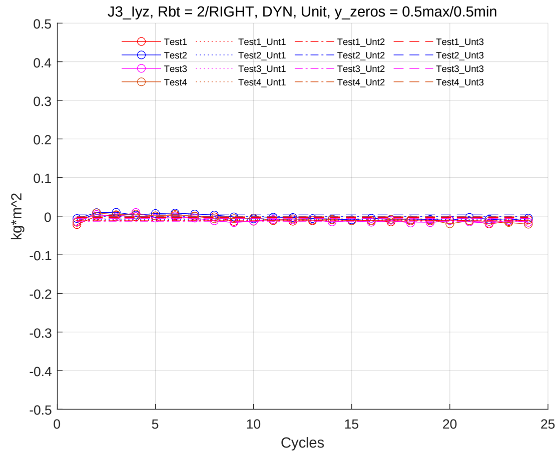

(b) Labelled with the widening scale of y-axis

Figure J.14: I_{yz} of Joint 3 of the Robot RIGHT with the identified results of selected cycles

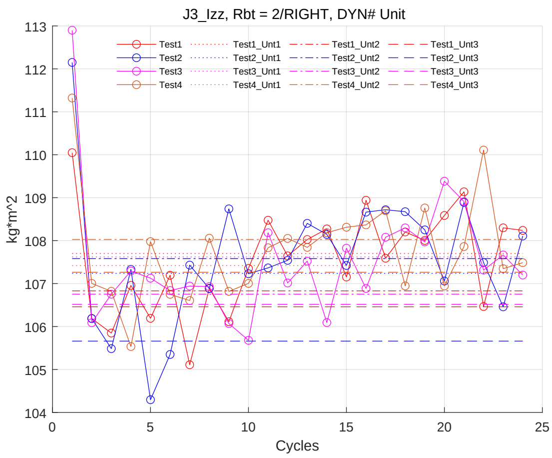

(a) Labelled automatically

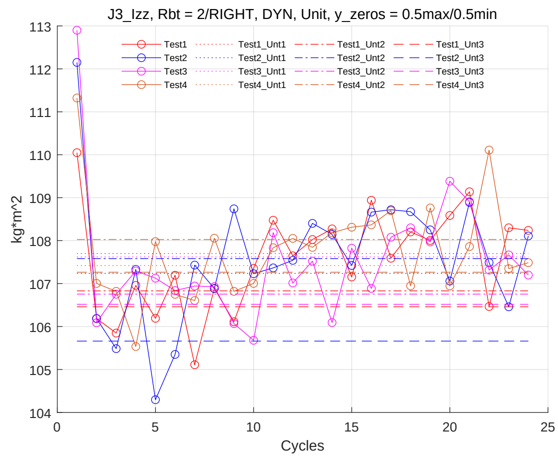

(b) Labelled with the widening scale of y-axis

Figure J.15: I_{zz} of Joint 3 of the Robot RIGHT with the identified results of selected cycles

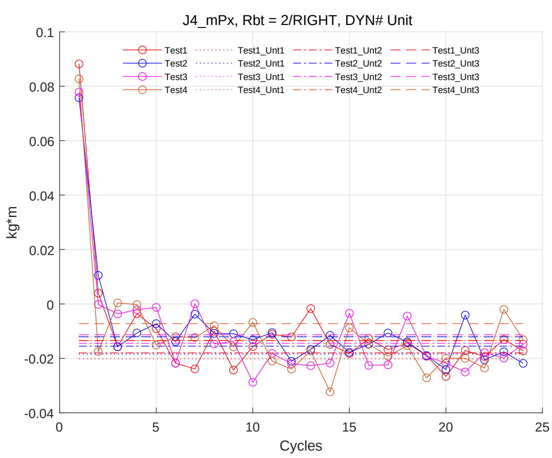

(a) Labelled automatically

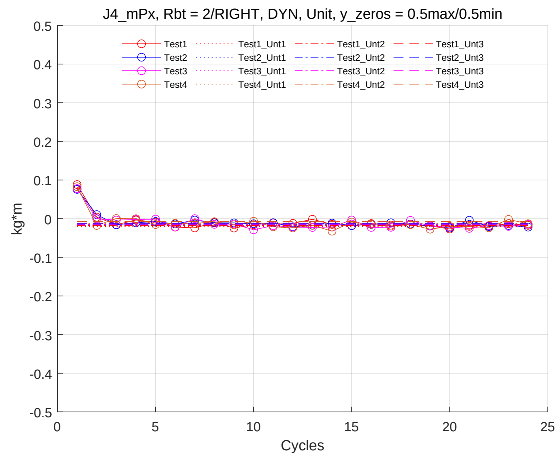

(b) Labelled with the widening scale of y-axis

Figure J.16: mP_x of Joint 4 of the Robot RIGHT with the identified results of selected cycles

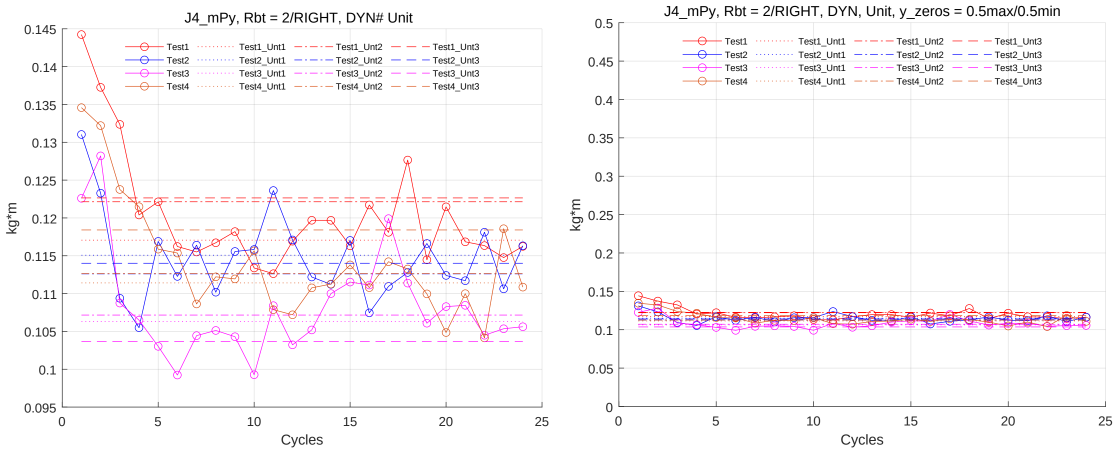

(a) Labelled automatically (b) Labelled with the widening scale of y-axis

Figure J.17: mP_y of Joint 4 of the Robot RIGHT with the identified results of selected cycles

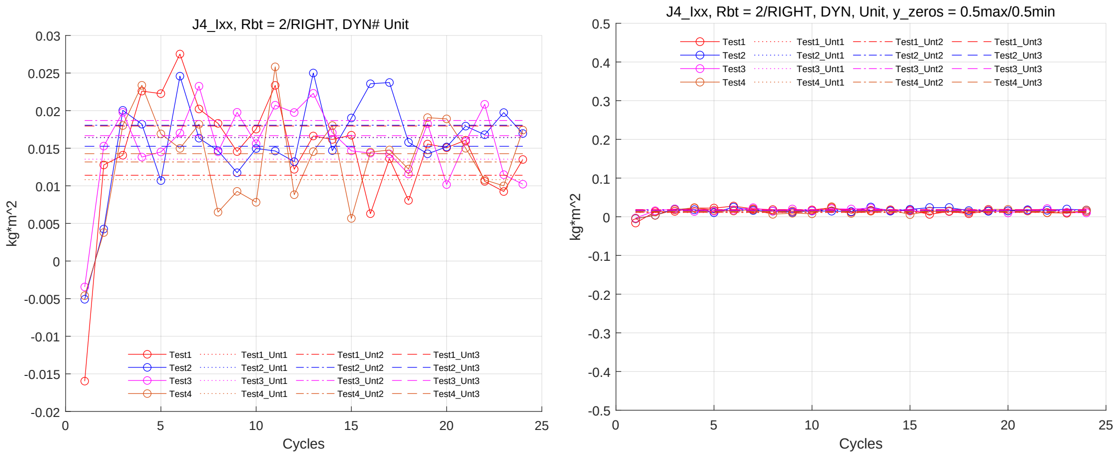

(a) Labelled automatically (b) Labelled with the widening scale of y-axis

Figure J.18: I_{xx} of Joint 4 of the Robot RIGHT with the identified results of selected cycles

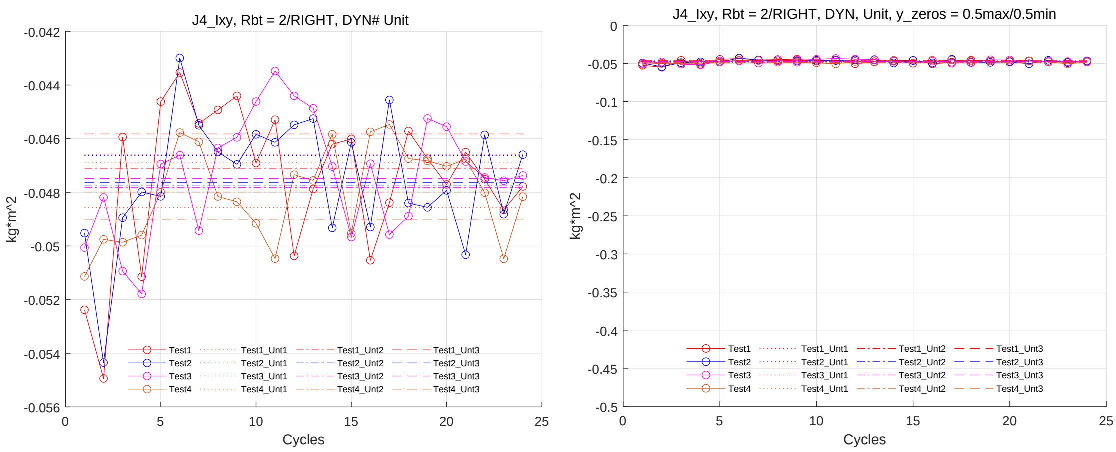

(a) Labelled automatically (b) Labelled with the widening scale of y-axis

Figure J.19: I_{xy} of Joint 4 of the Robot RIGHT with the identified results of selected cycles

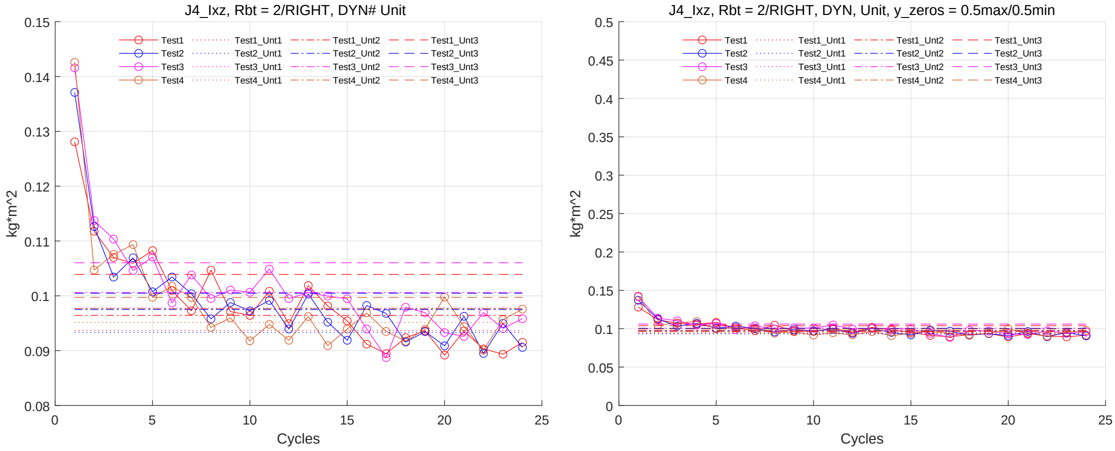

(a) Labelled automatically (b) Labelled with the widening scale of y-axis

Figure J.20: I_{xz} of Joint 4 of the Robot RIGHT with the identified results of selected cycles

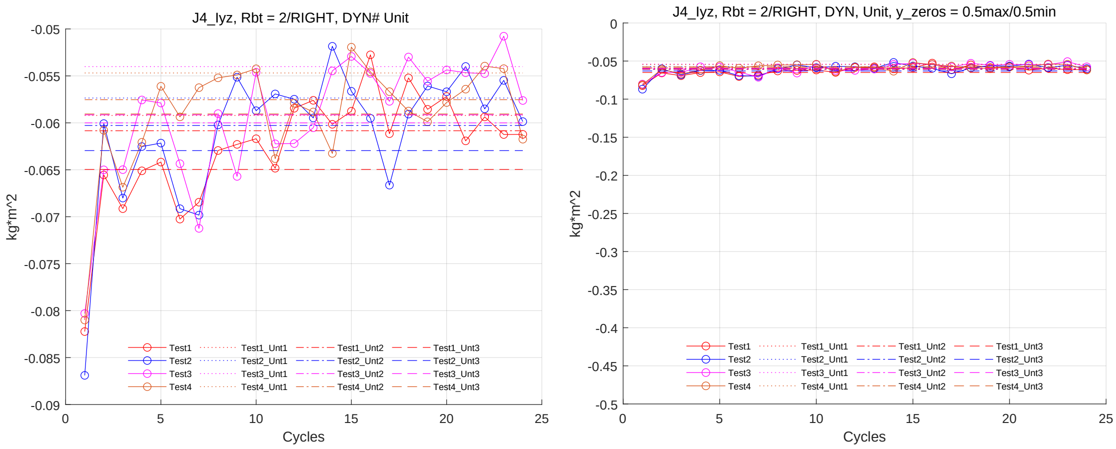

(a) Labelled automatically (b) Labelled with the widening scale of y-axis

Figure J.21: I_{yz} of Joint 4 of the Robot RIGHT with the identified results of selected cycles

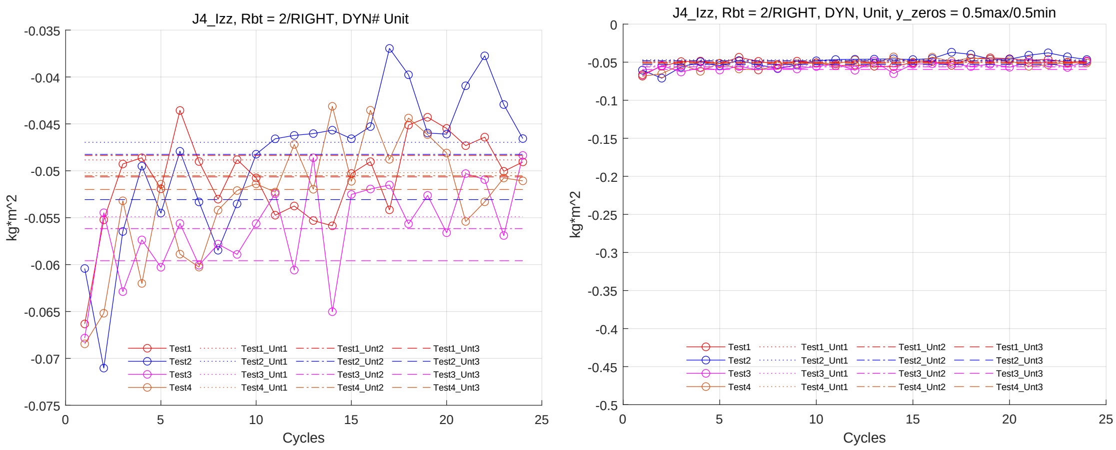

(a) Labelled automatically (b) Labelled with the widening scale of y-axis

Figure J.22: I_{zz} of Joint 4 of the Robot RIGHT with the identified results of selected cycles

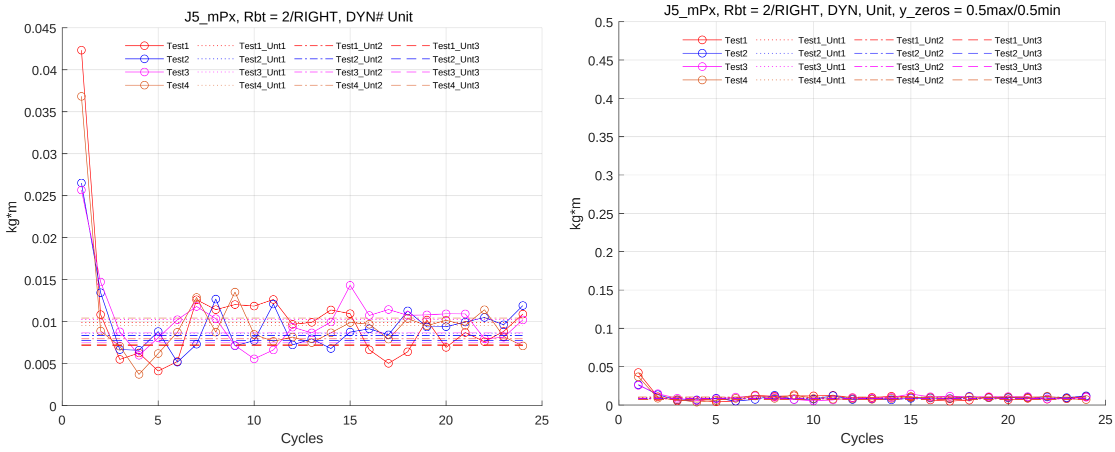

(a) Labelled automatically (b) Labelled with the widening scale of y-axis

Figure J.23: mP_x of Joint 5 of the Robot RIGHT with the identified results of selected cycles

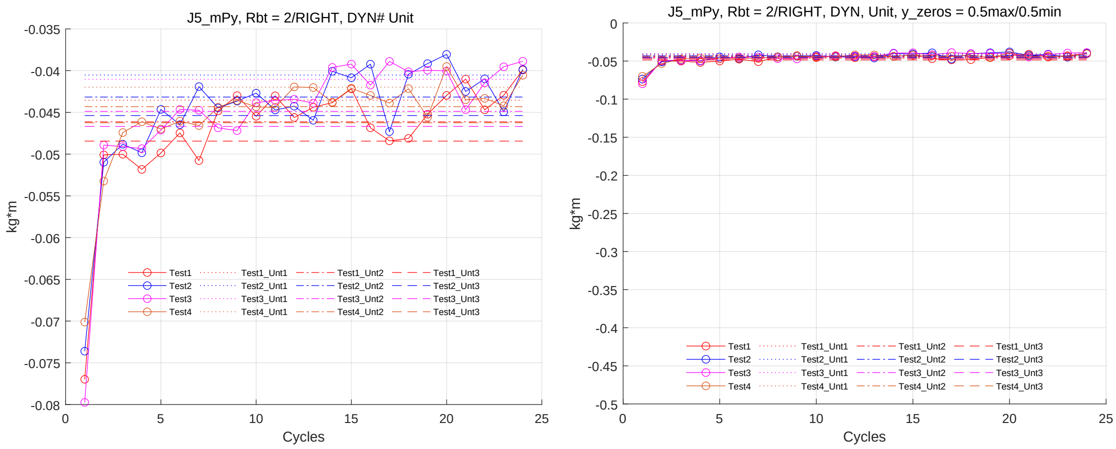

(a) Labelled automatically (b) Labelled with the widening scale of y-axis

Figure J.24: mP_y of Joint 5 of the Robot RIGHT with the identified results of selected cycles

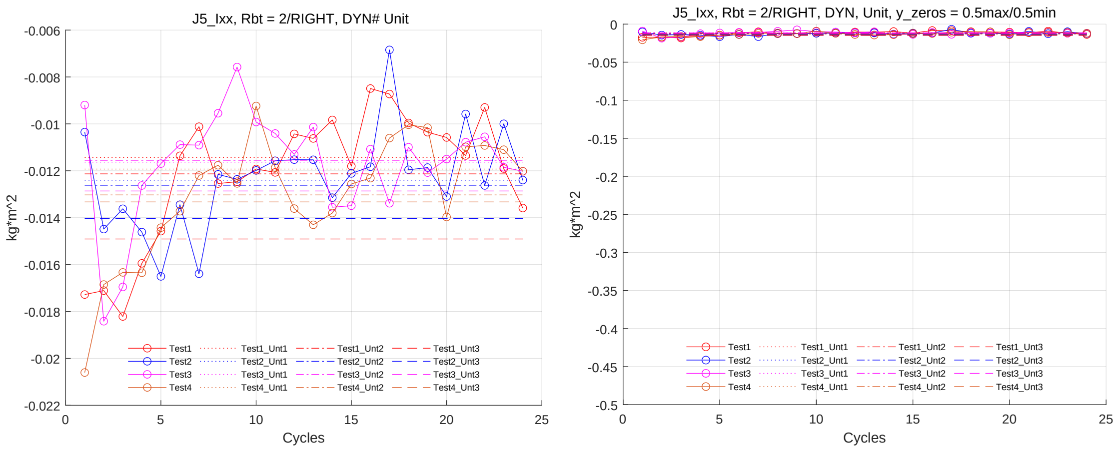

(a) Labelled automatically (b) Labelled with the widening scale of y-axis

Figure J.25: I_{xx} of Joint 5 of the Robot RIGHT with the identified results of selected cycles

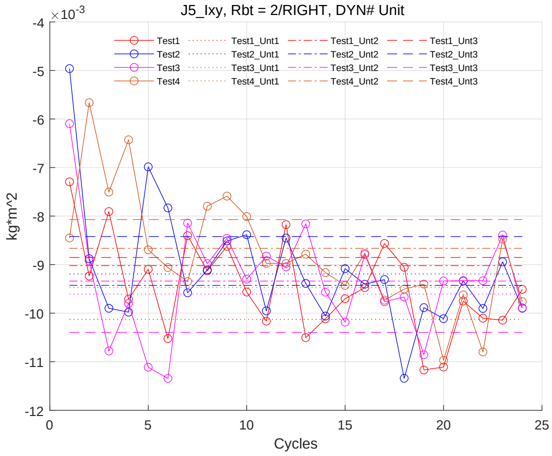

(a) Labelled automatically

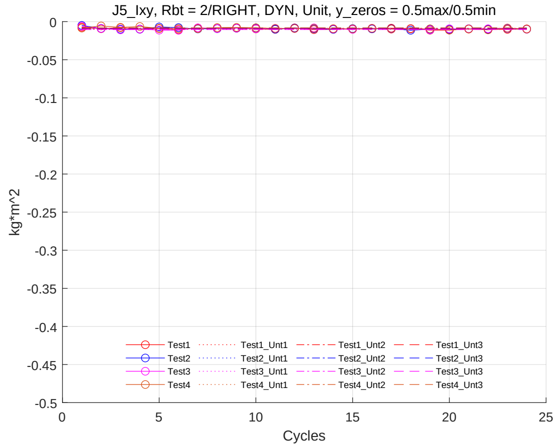

(b) Labelled with the widening scale of y-axis

Figure J.26: I_{xy} of Joint 5 of the Robot RIGHT with the identified results of selected cycles

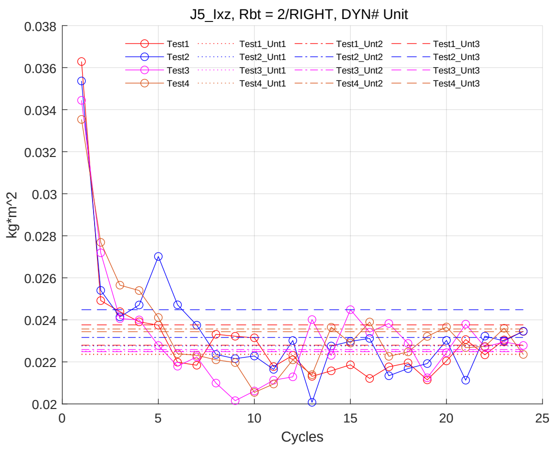

(a) Labelled automatically

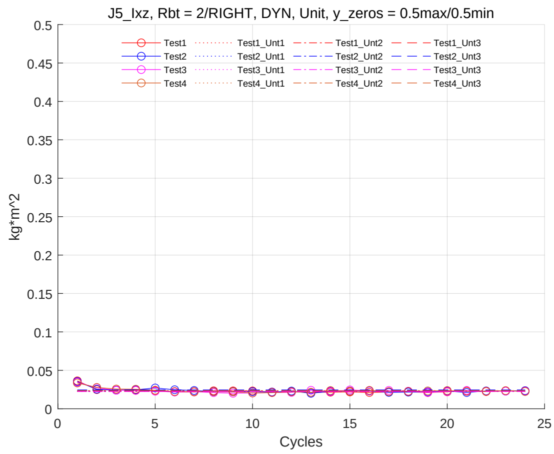

(b) Labelled with the widening scale of y-axis

Figure J.27: I_{xz} of Joint 5 of the Robot RIGHT with the identified results of selected cycles

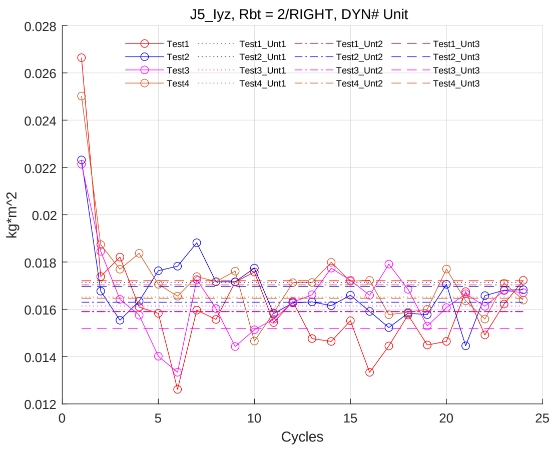

(a) Labelled automatically

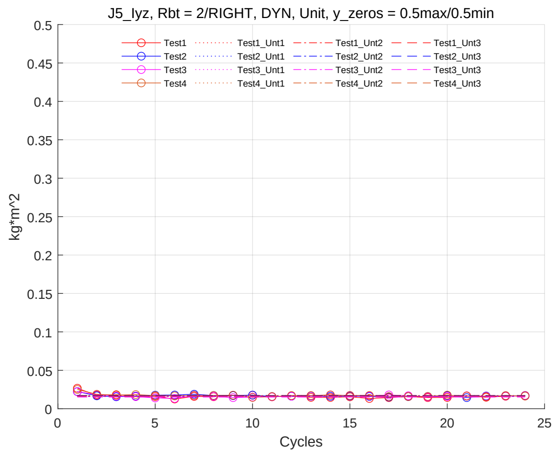

(b) Labelled with the widening scale of y-axis

Figure J.28: I_{yz} of Joint 5 of the Robot RIGHT with the identified results of selected cycles

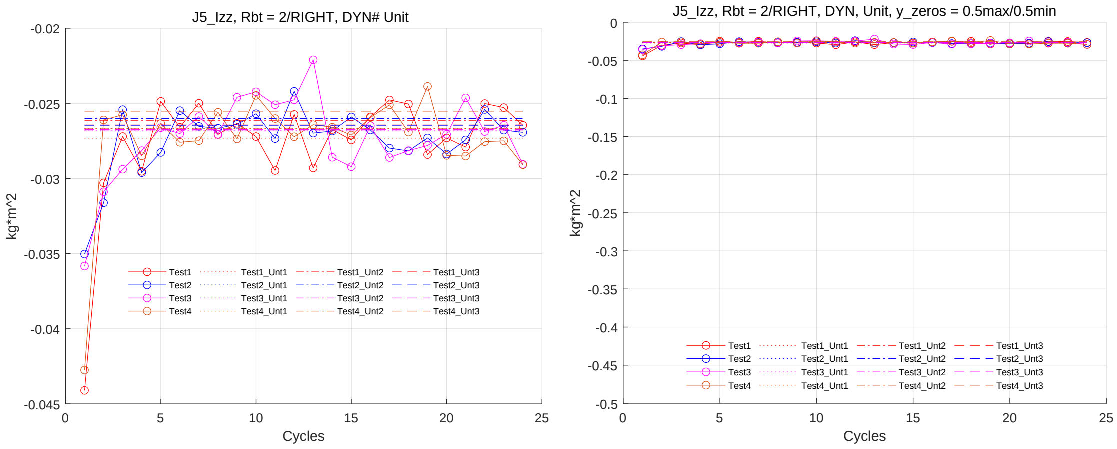

(a) Labelled automatically (b) Labelled with the widening scale of y-axis

Figure J.29: I_{zz} of Joint 5 of the Robot RIGHT with the identified results of selected cycles

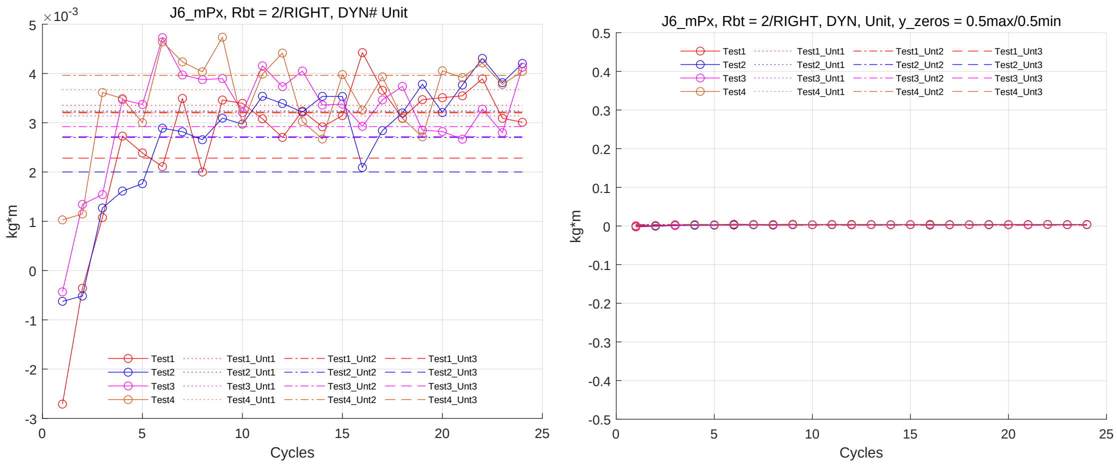

(a) Labelled automatically (b) Labelled with the widening scale of y-axis

Figure J.30: mP_x of Joint 6 of the Robot RIGHT with the identified results of selected cycles

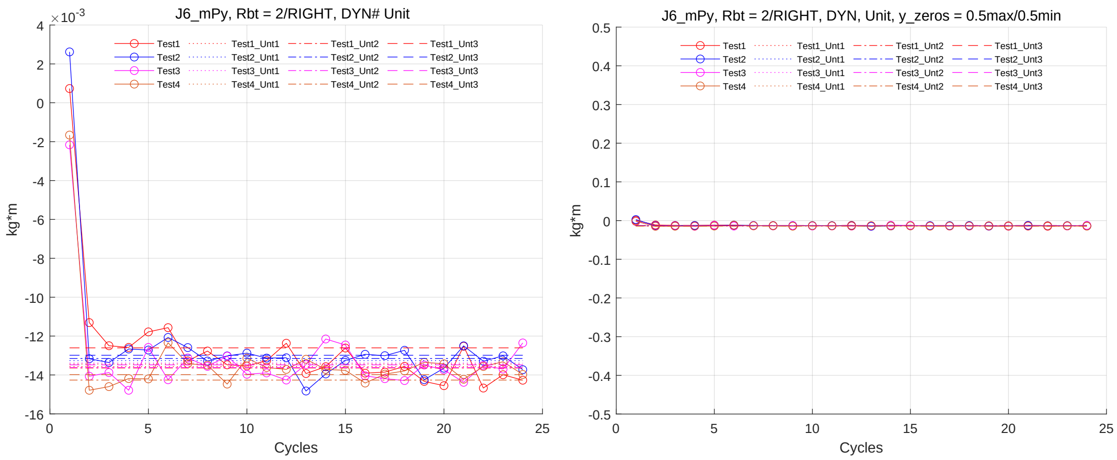

(a) Labelled automatically (b) Labelled with the widening scale of y-axis

Figure J.31: mP_y of Joint 6 of the Robot RIGHT with the identified results of selected cycles

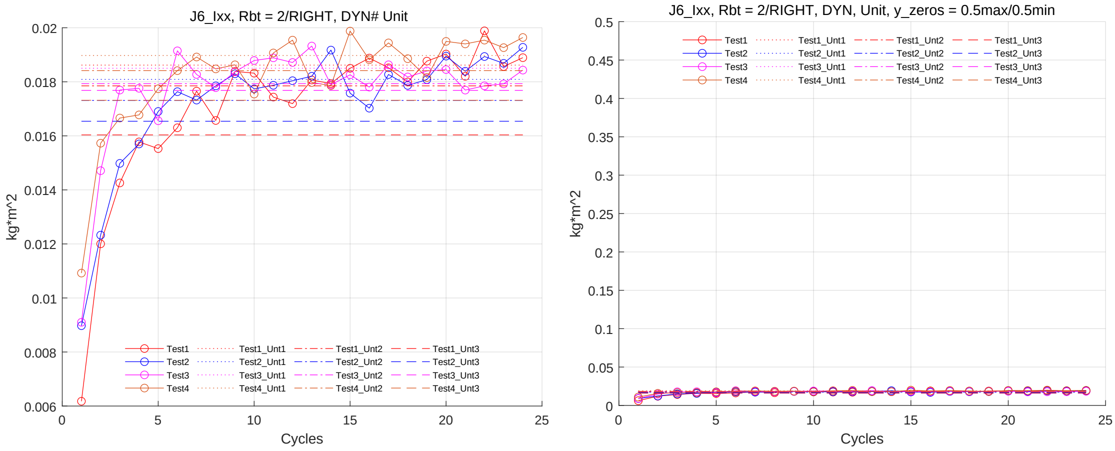

(a) Labelled automatically

(b) Labelled with the widening scale of y-axis

Figure J.32: I_{xx} of Joint 6 of the Robot RIGHT with the identified results of selected cycles

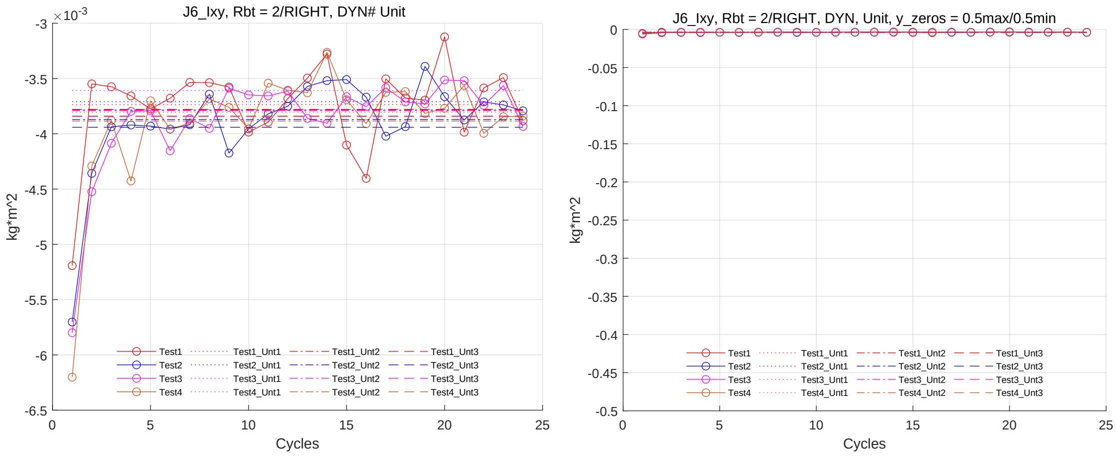

(a) Labelled automatically

(b) Labelled with the widening scale of y-axis

Figure J.33: I_{xy} of Joint 6 of the Robot RIGHT with the identified results of selected cycles

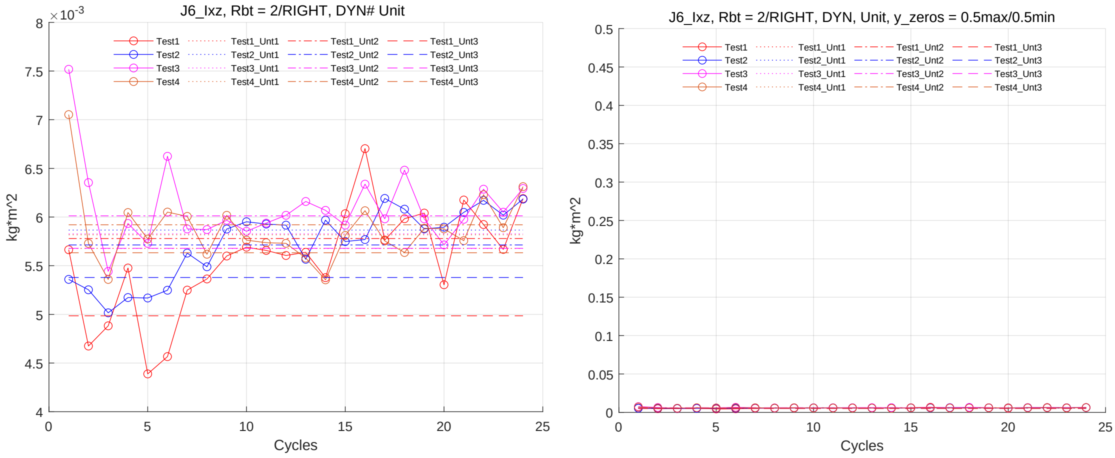

(a) Labelled automatically

(b) Labelled with the widening scale of y-axis

Figure J.34: I_{xz} of Joint 6 of the Robot RIGHT with the identified results of selected cycles

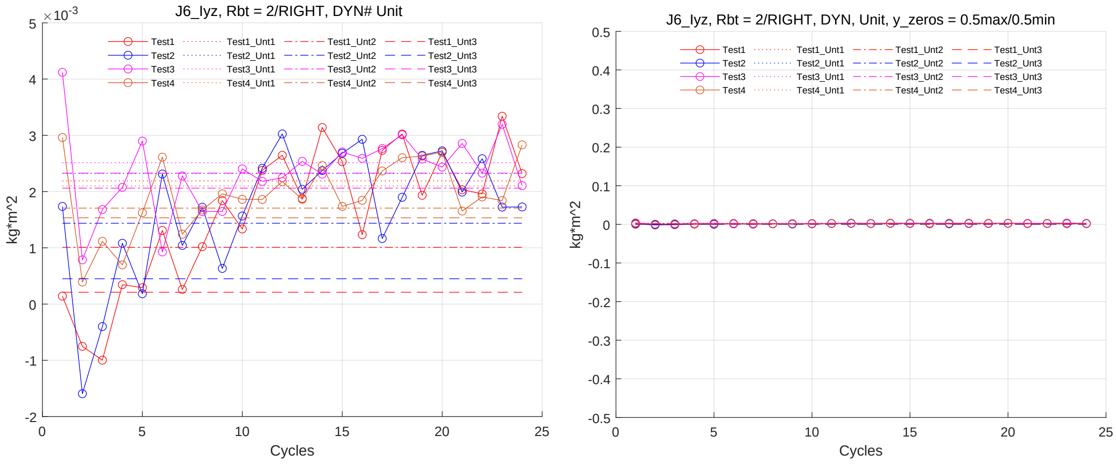

(a) Labelled automatically

(b) Labelled with the widening scale of y-axis

Figure J.35: I_{yz} of Joint 6 of the Robot RIGHT with the identified results of selected cycles

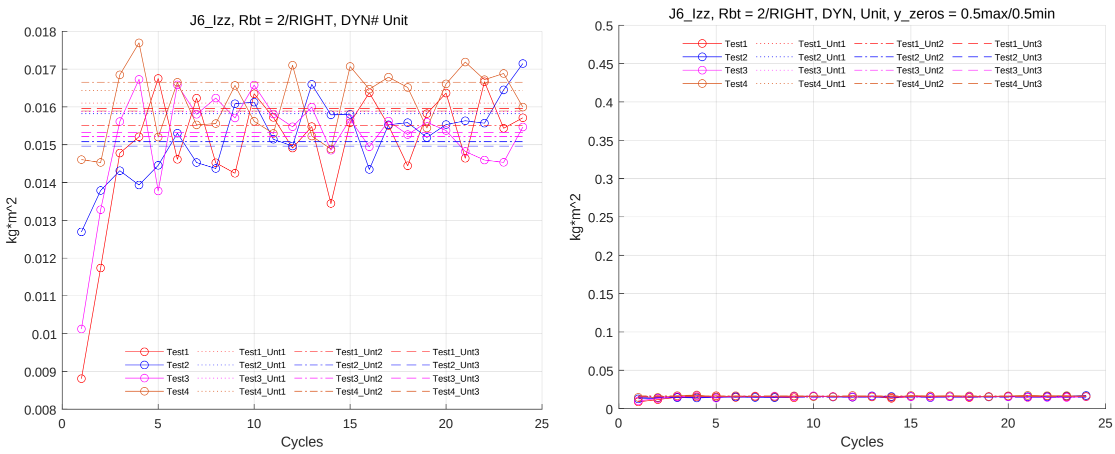

(a) Labelled automatically

(b) Labelled with the widening scale of y-axis

Figure J.36: I_{zz} of Joint 6 of the Robot RIGHT with the identified results of selected cycles

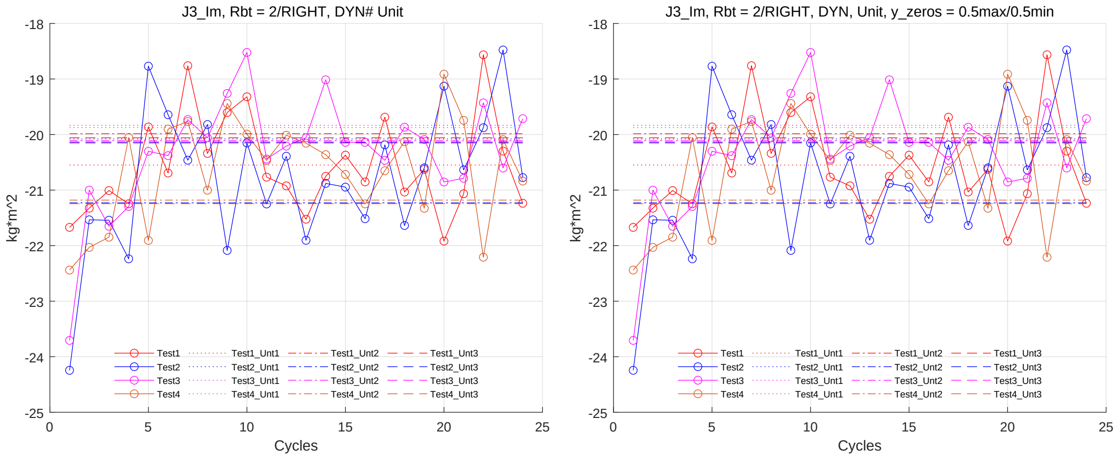

(a) Labelled automatically

(b) Labelled with the widening scale of y-axis

Figure J.37: I_m of Joint 3 of the RIGHT Robot with the identified results of selected cycles

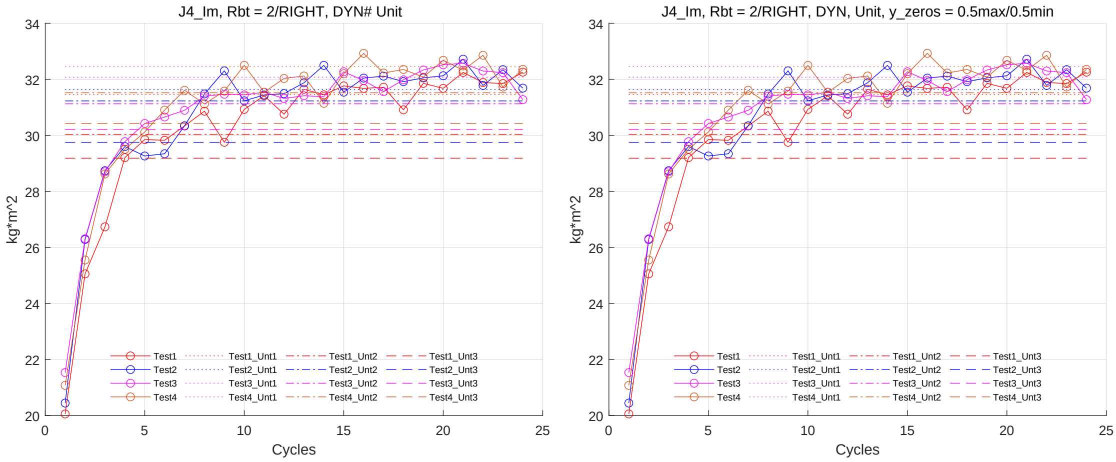

(a) Labelled automatically (b) Labelled with the widening scale of y-axis

Figure J.38: I_m of Joint 4 of the RIGHT Robot with the identified results of selected cycles

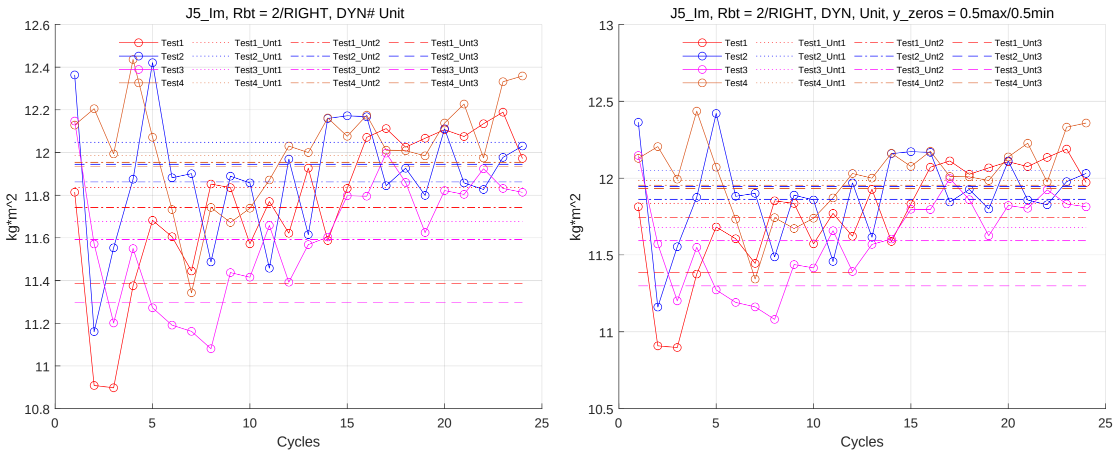

(a) Labelled automatically (b) Labelled with the widening scale of y-axis

Figure J.39: I_m of Joint 5 of the RIGHT Robot with the identified results of selected cycles

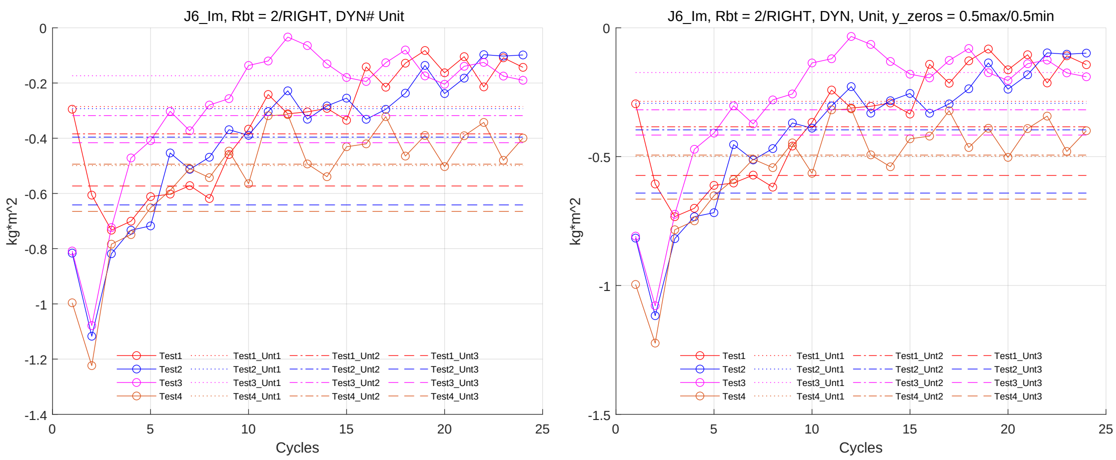

(a) Labelled automatically (b) Labelled with the widening scale of y-axis

Figure J.40: I_m of Joint 6 of the RIGHT Robot with the identified results of selected cycles

Appendix K

The Verification Results Of The Excitation Trajectory

The figures in this appendix indicate the identification results of the excitation trajectory of all joints from one test of the Robot RIGHT, which are used in Section 5.1.1 and 5.1.2. They are shown with the measured torque and the estimated torque, marked with blue curve and red curve respectively. The green curve is the scaled velocity corresponded to the torque output. These figures are demonstrated cycle by cycle.

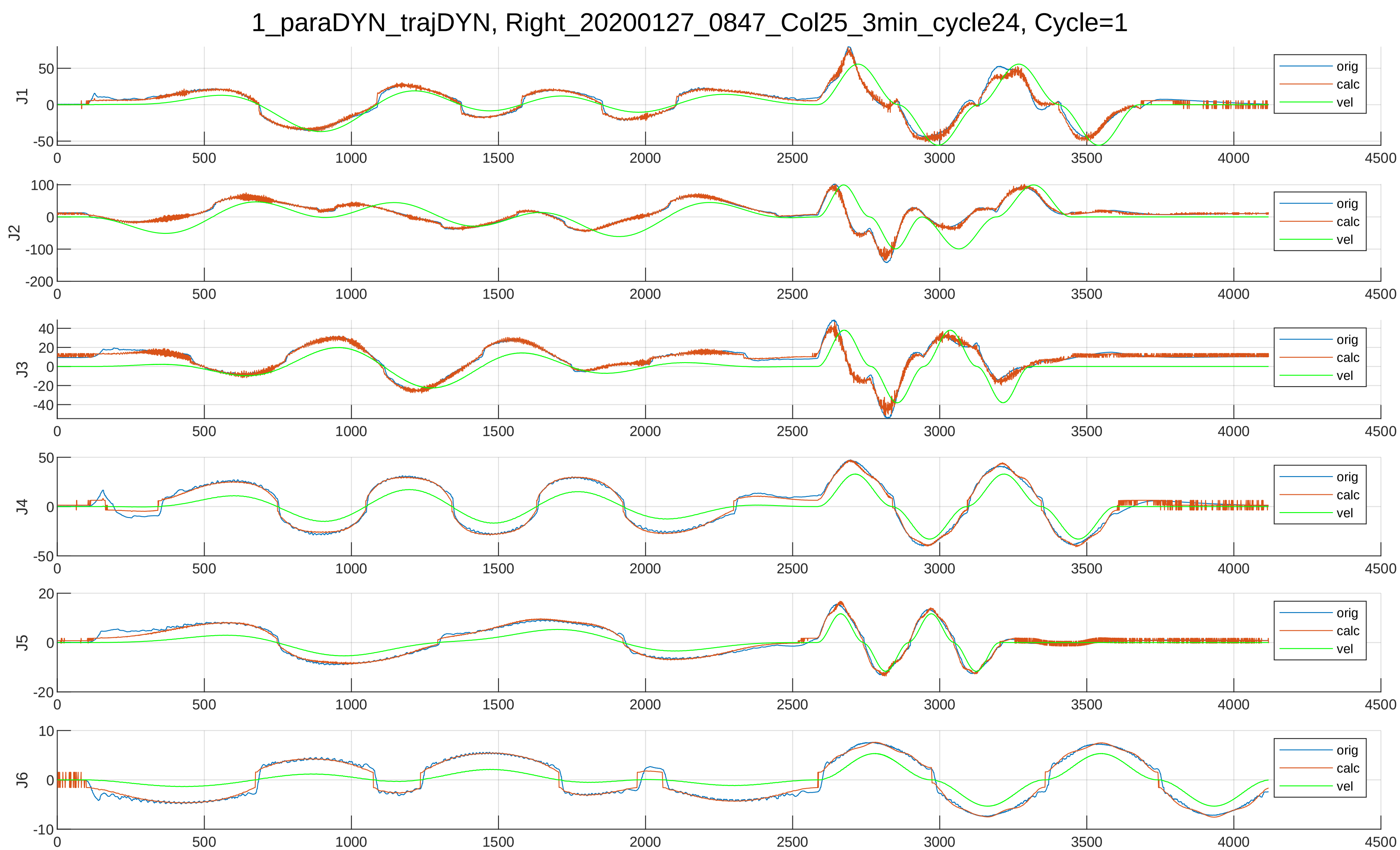

Figure K.1: The identification results of the excitation trajectory stage in the 1st cycle of Robot 2

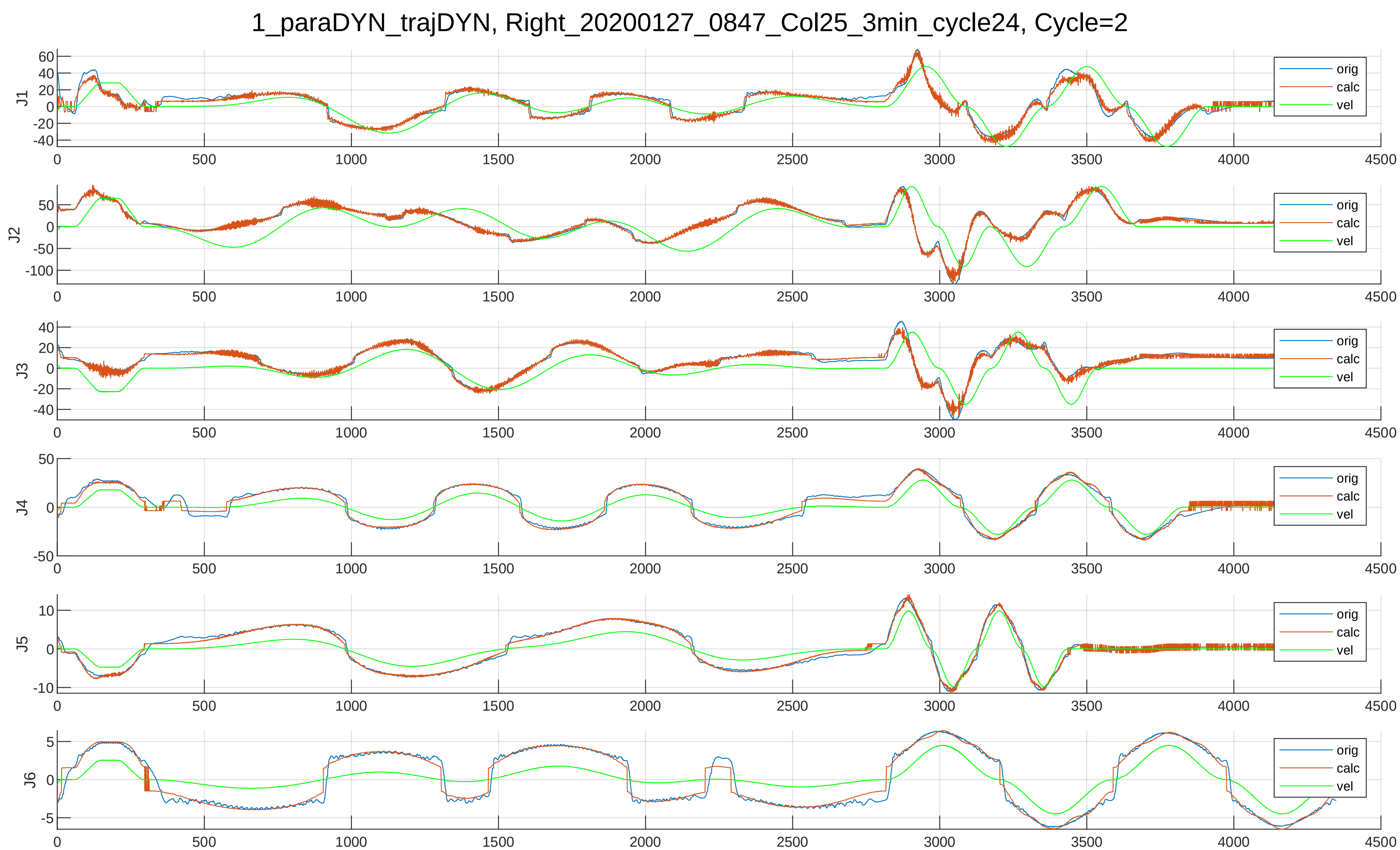

Figure K.2: The identification results of the excitation trajectory stage in the 2$^{\text{nd}}$ cycle of Robot 2

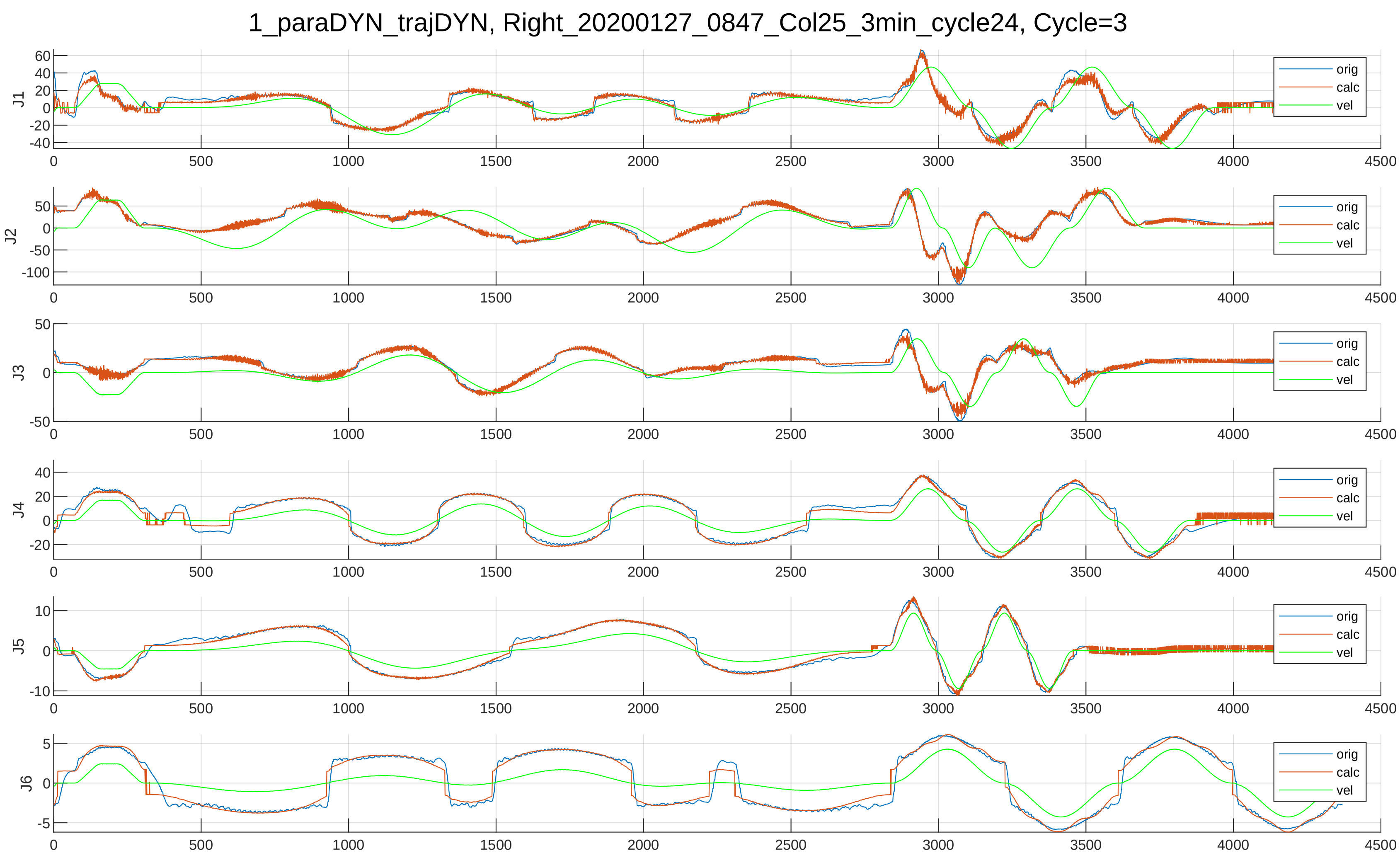

Figure K.3: The identification results of the excitation trajectory stage in the 3rd cycle of Robot 2

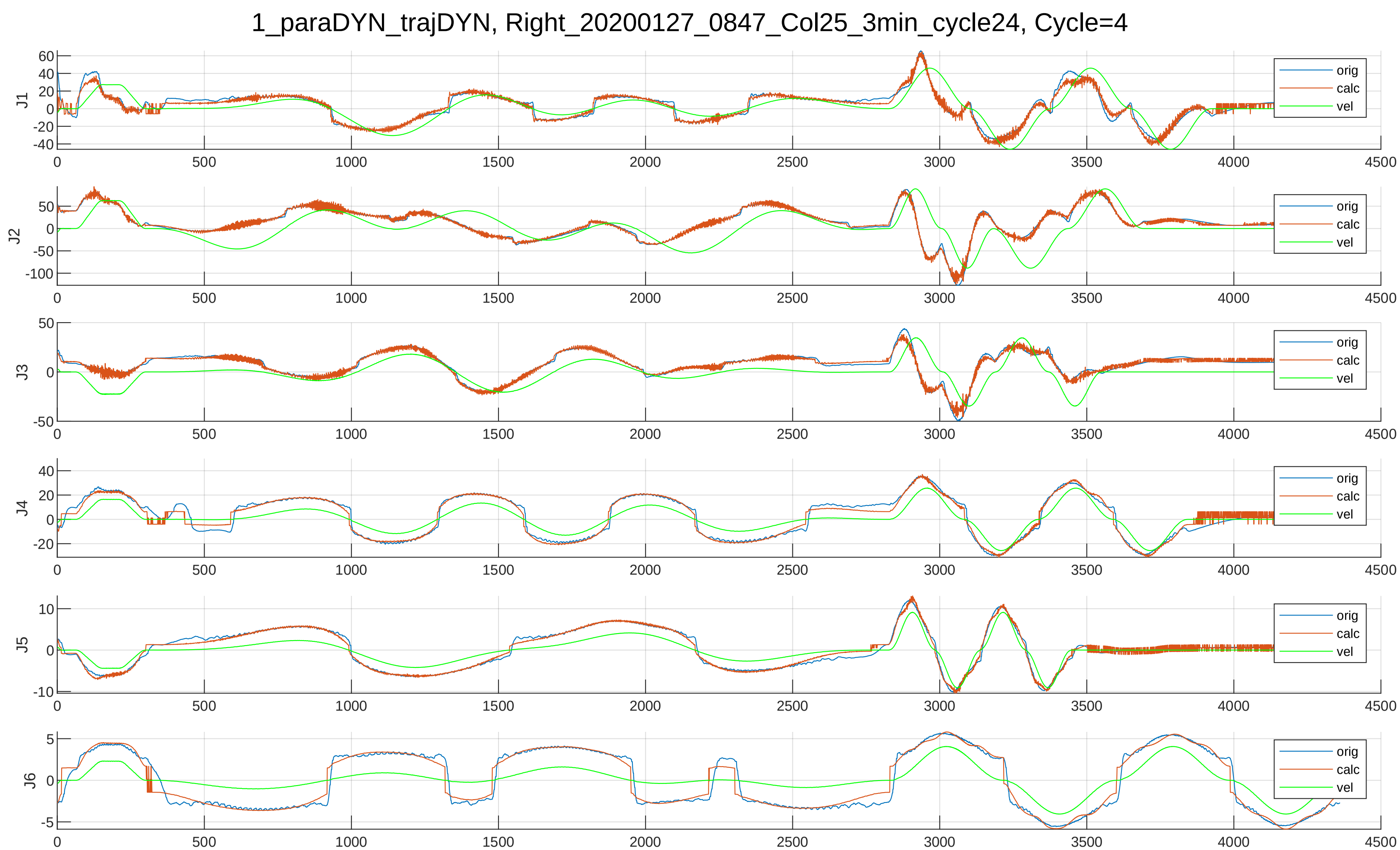

Figure K.4: The identification results of the excitation trajectory stage in the 4th cycle of Robot 2

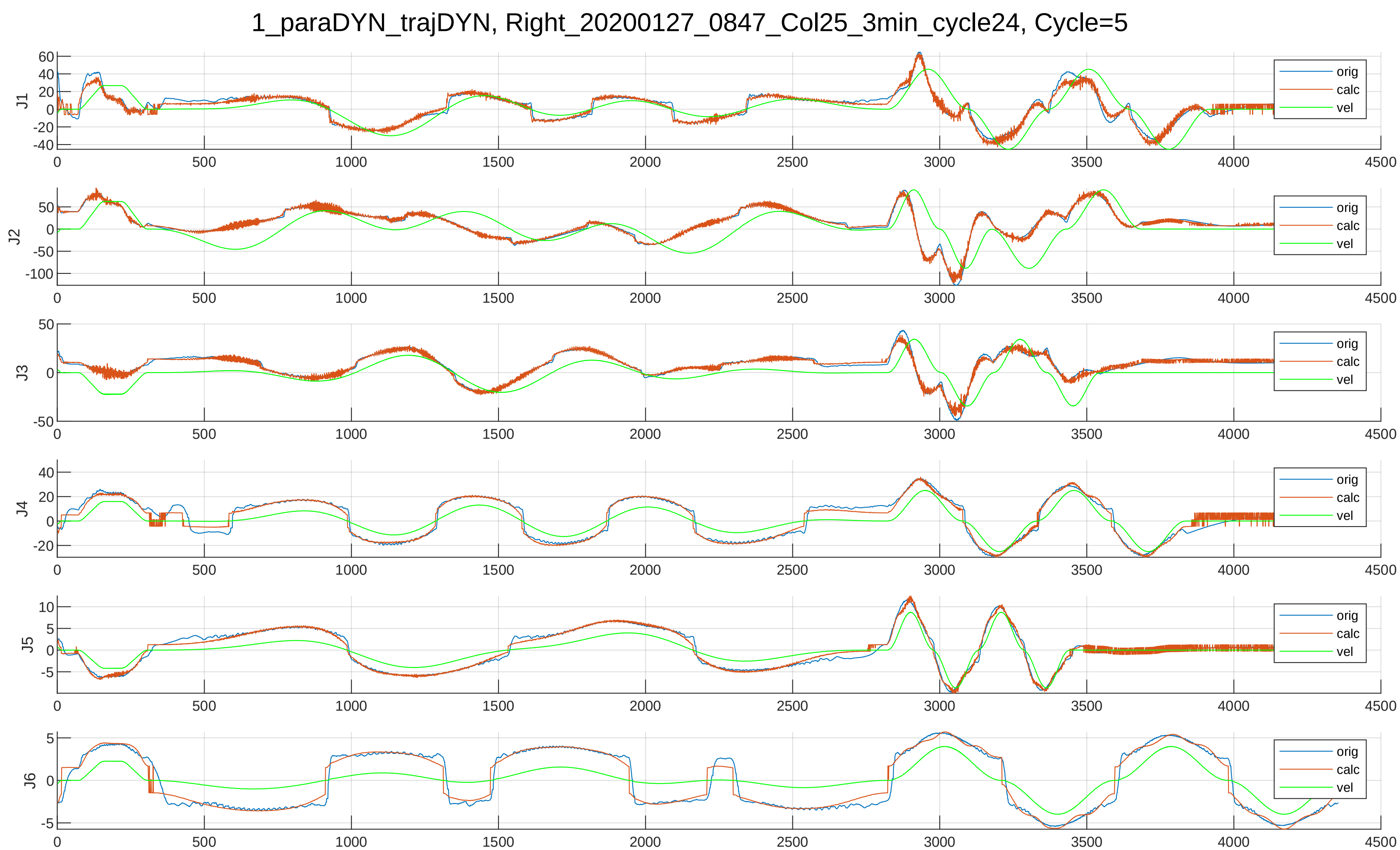

Figure K.5: The identification results of the excitation trajectory stage in the 5th cycle of Robot 2

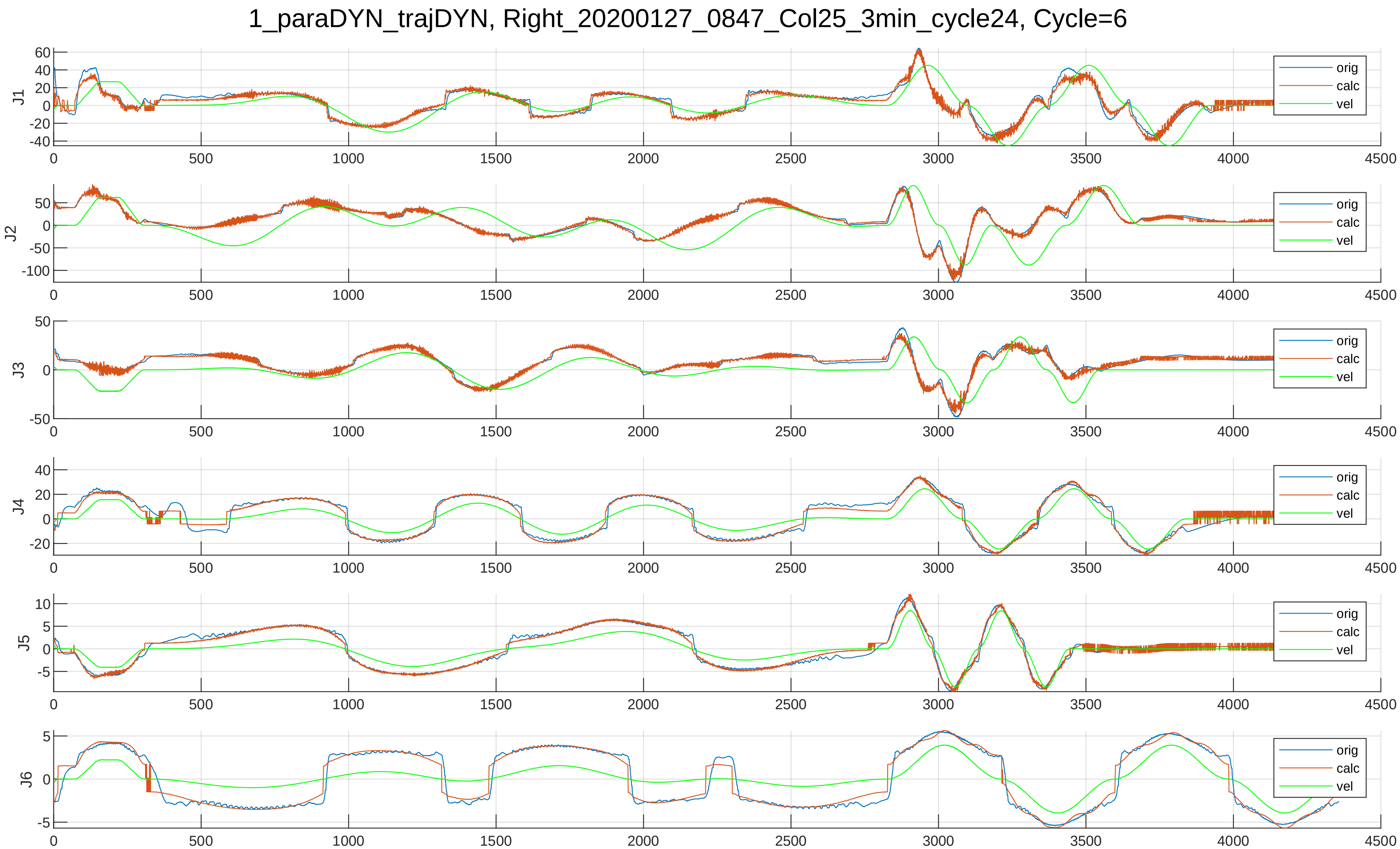

Figure K.6: The identification results of the excitation trajectory stage in the 6^{th} cycle of Robot 2

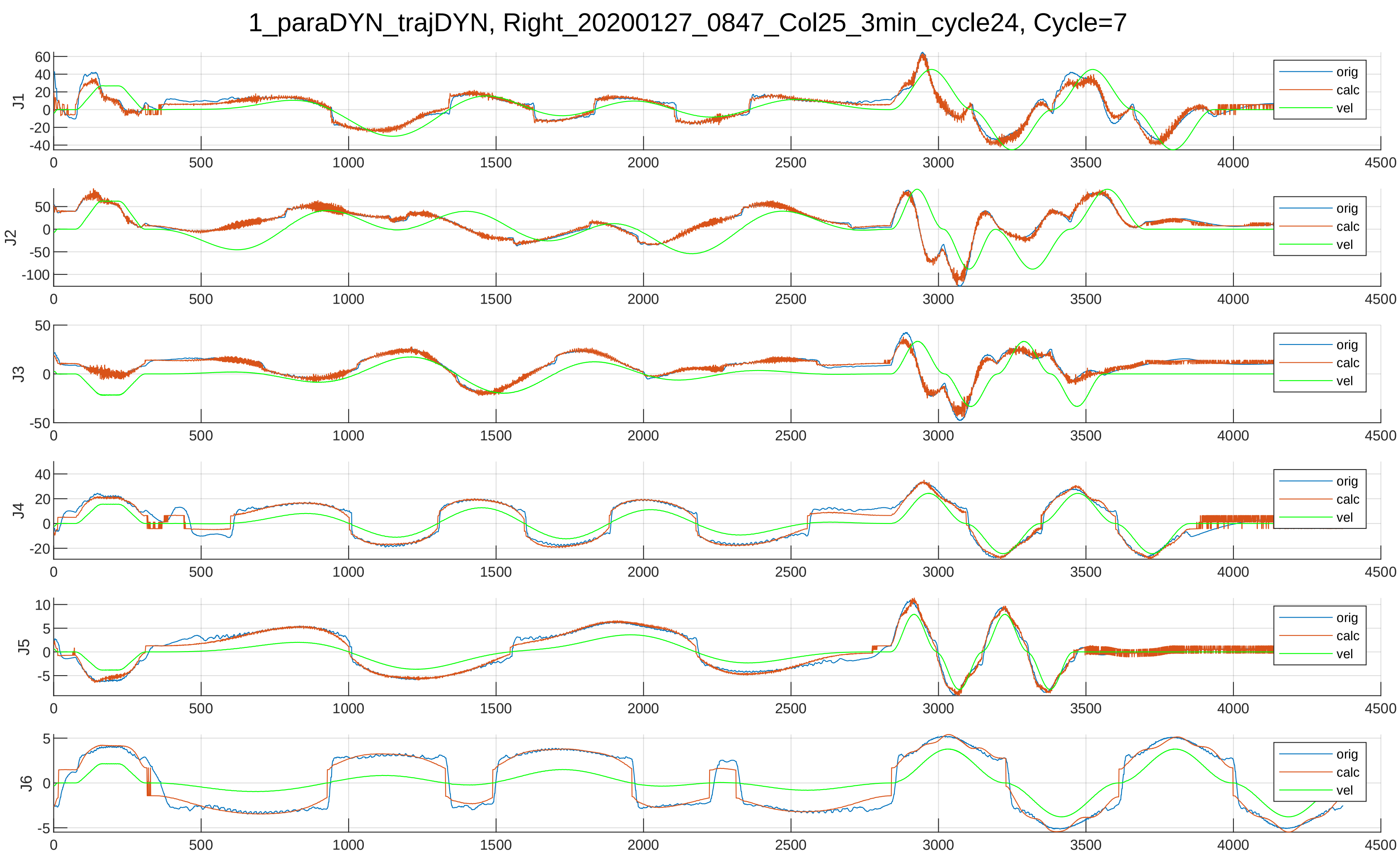

Figure K.7: The identification results of the excitation trajectory stage in the 7th cycle of Robot 2

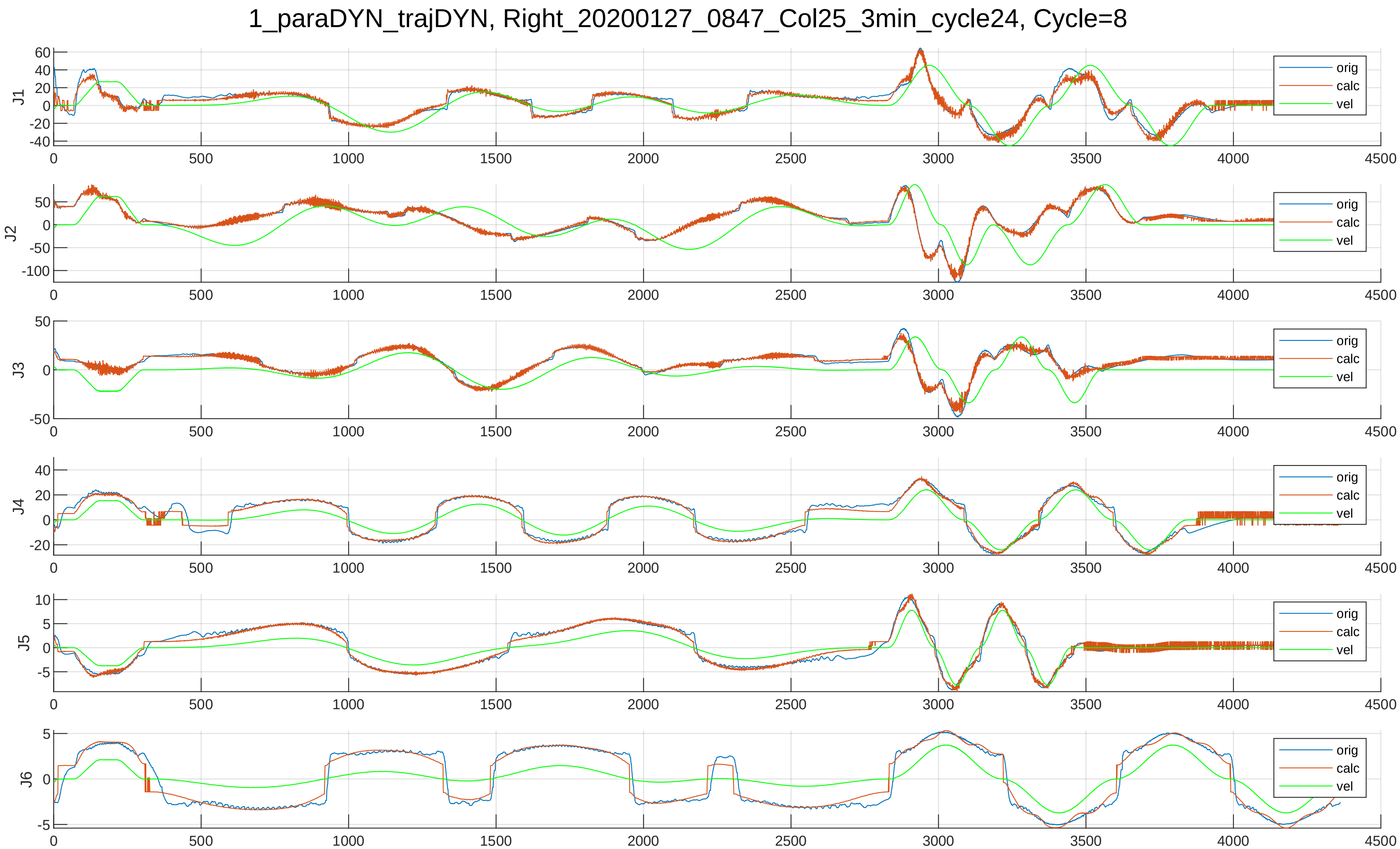

Figure K.8: The identification results of the excitation trajectory stage in the 8th cycle of Robot 2

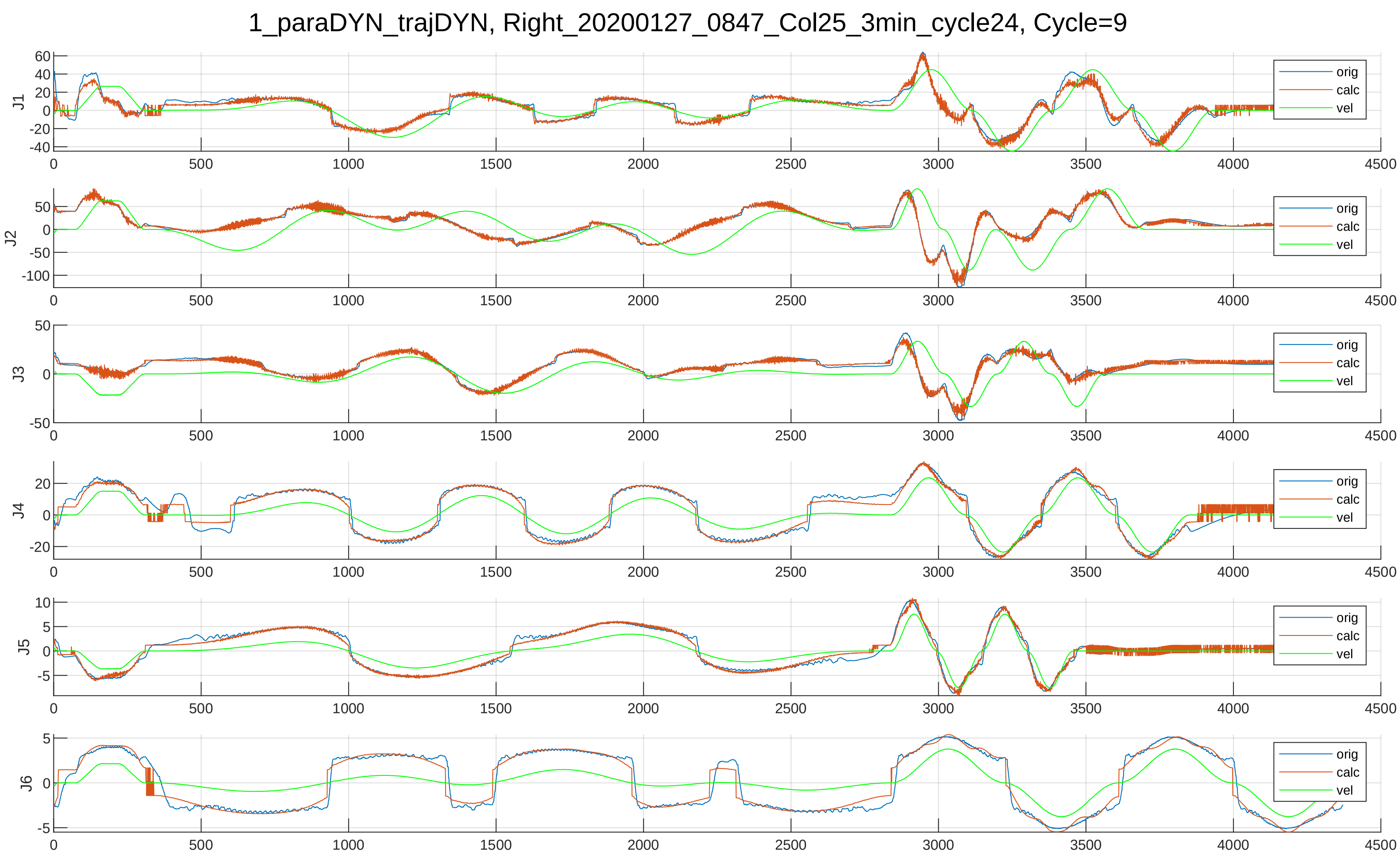

Figure K.9: The identification results of the excitation trajectory stage in the 9^{th} cycle of Robot 2

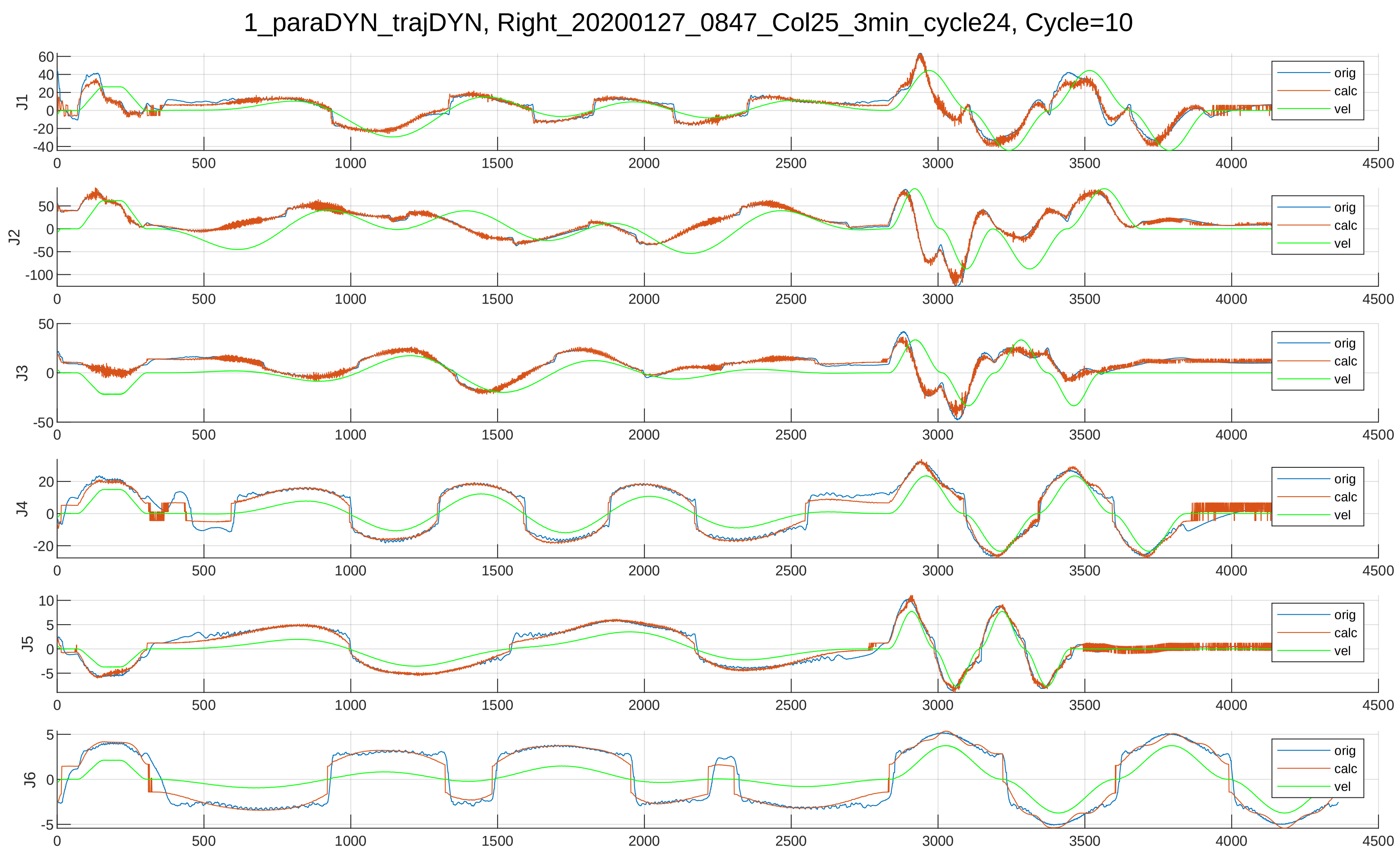

Figure K.10: The identification results of the excitation trajectory stage in the 10^{th} cycle of Robot 2

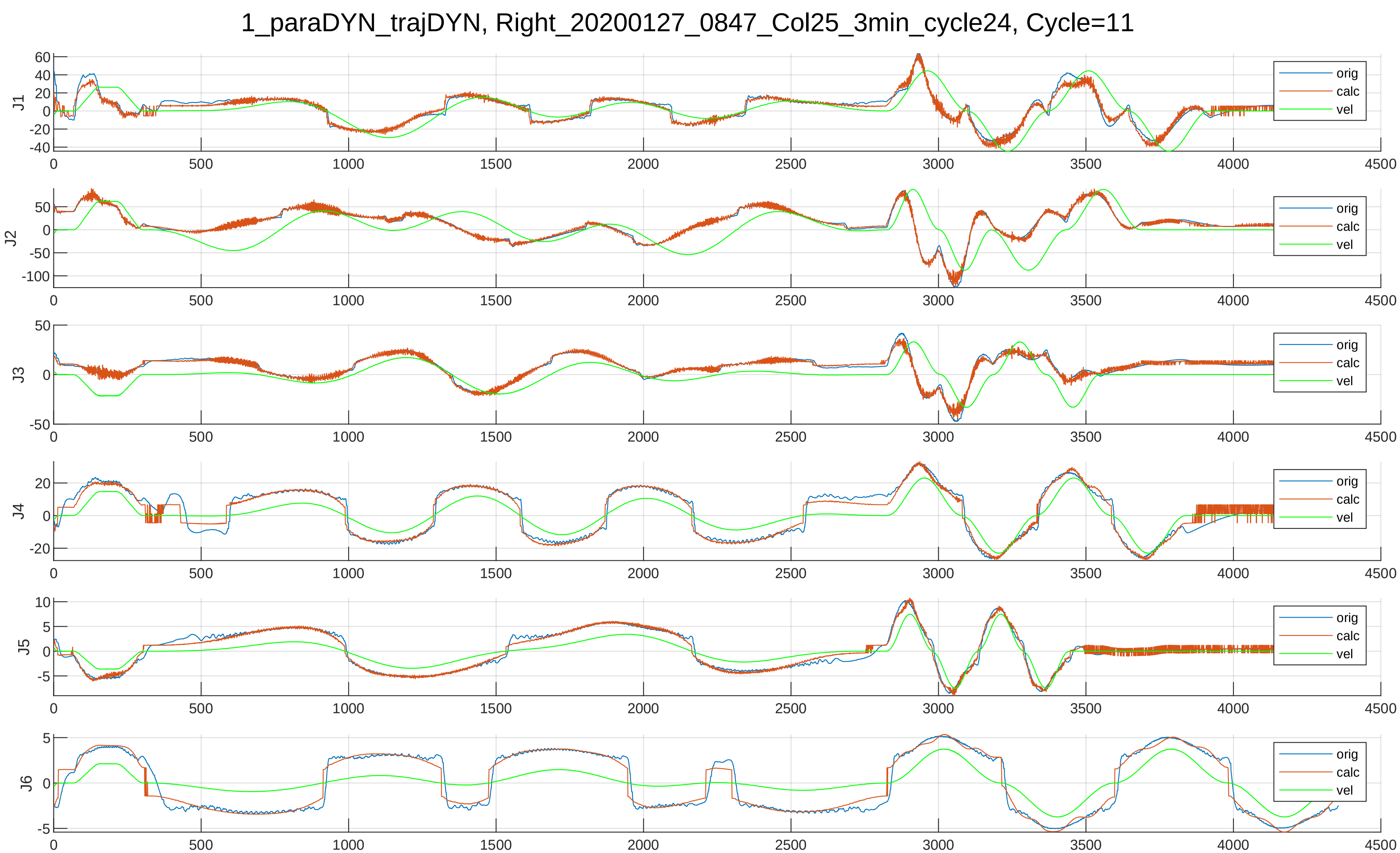

Figure K.11: The identification results of the excitation trajectory stage in the 11$^{\text{th}}$ cycle of Robot 2

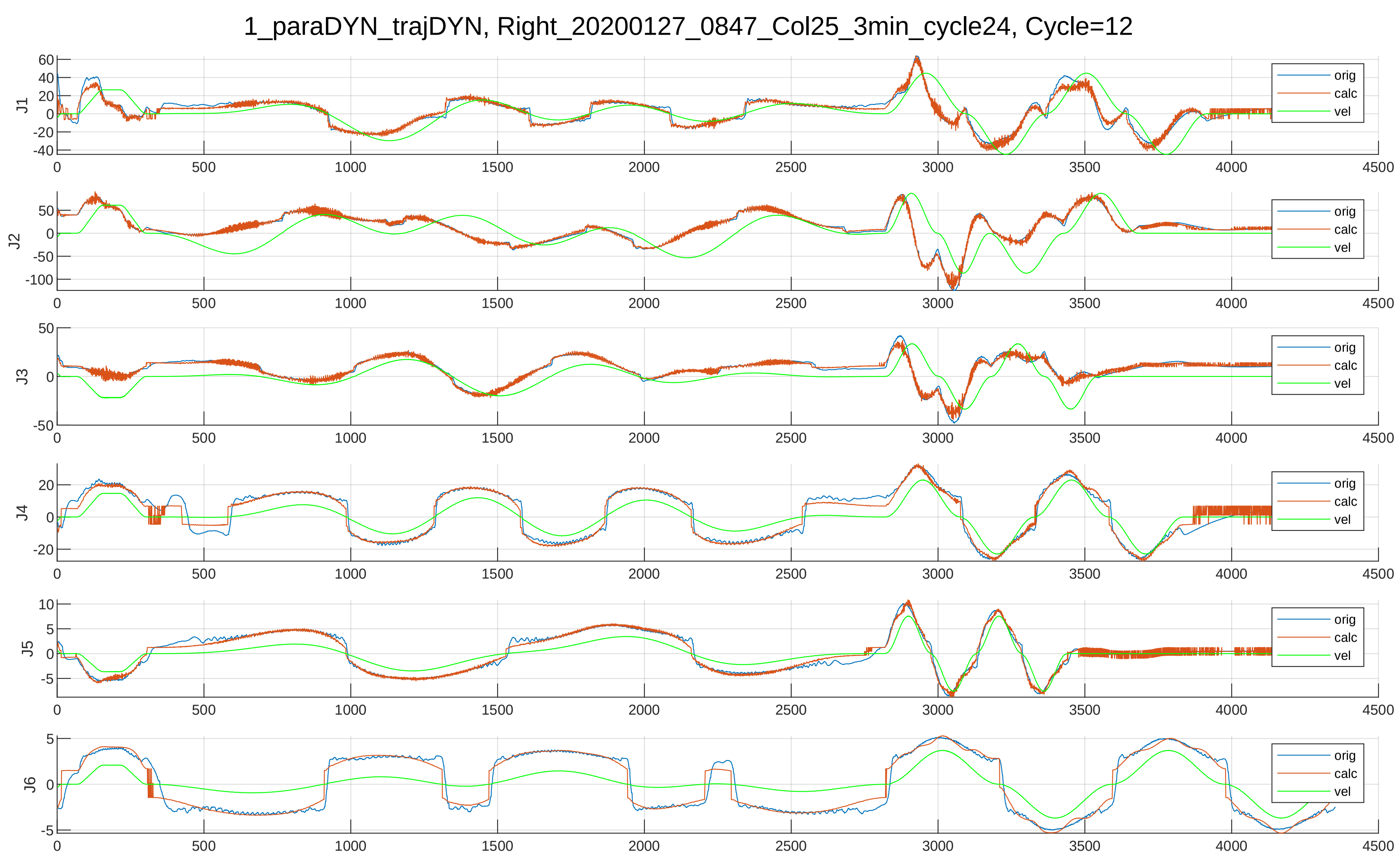

Figure K.12: The identification results of the excitation trajectory stage in the 12th cycle of Robot 2

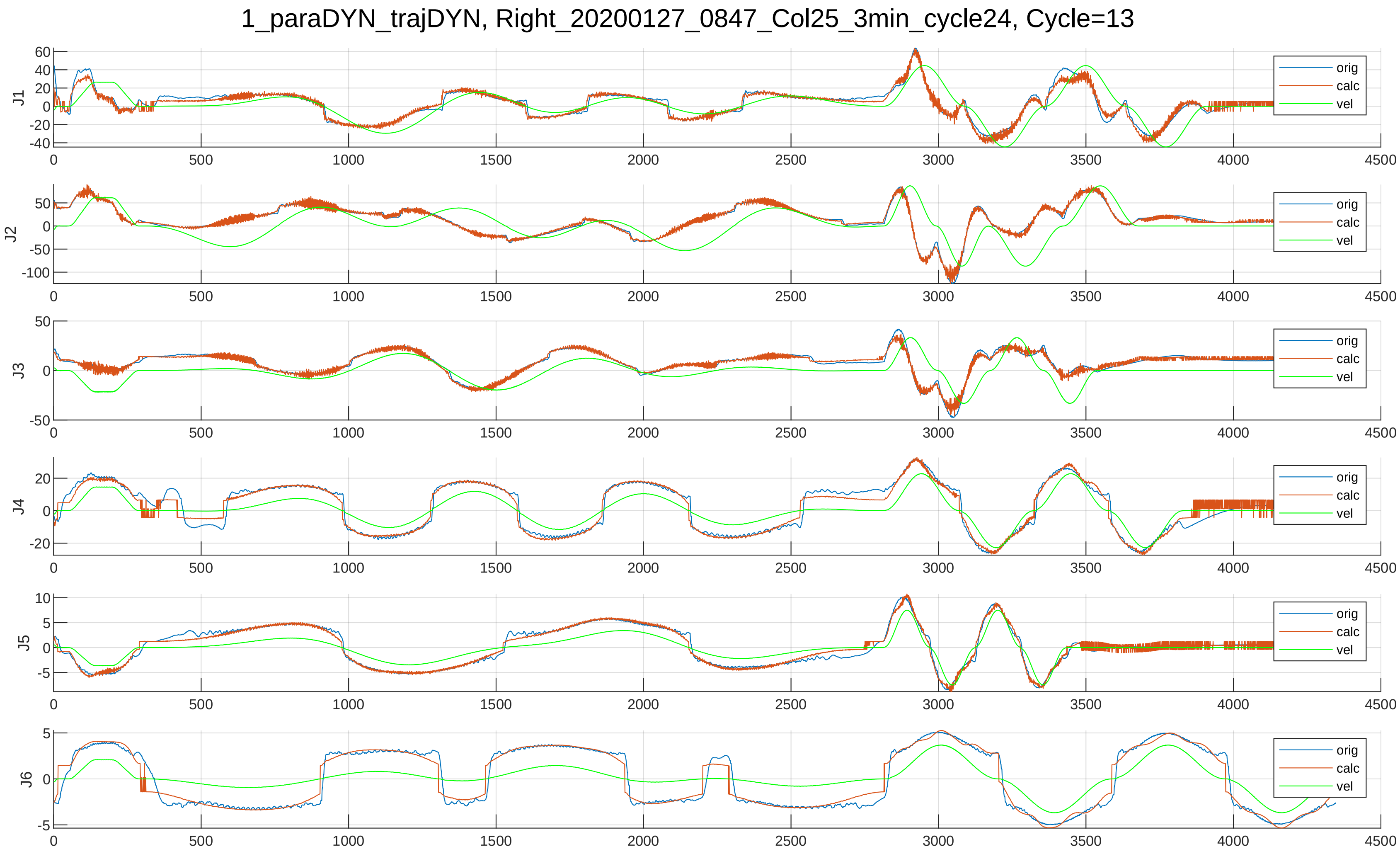

Figure K.13: The identification results of the excitation trajectory stage in the 13th cycle of Robot 2

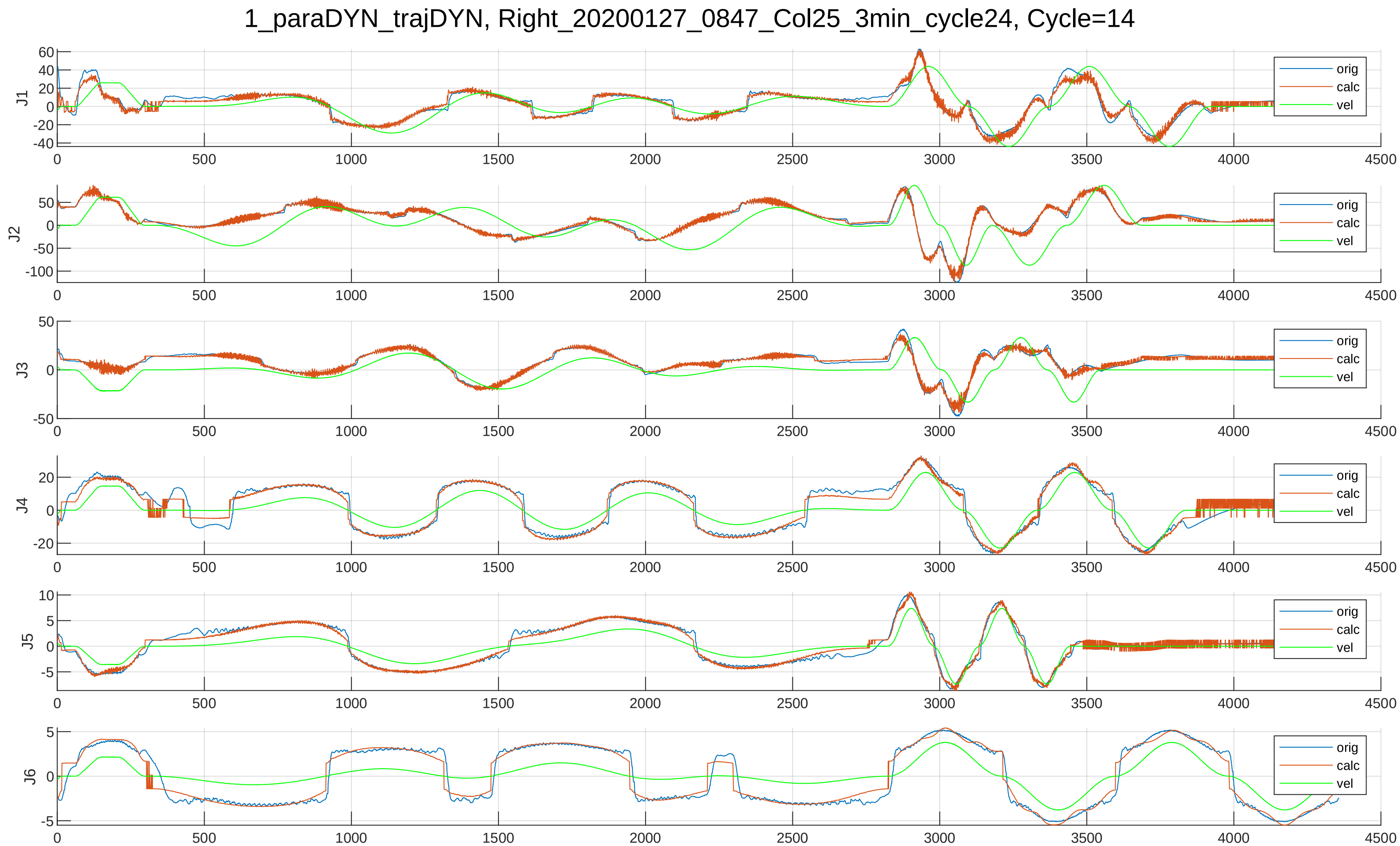

Figure K.14: The identification results of the excitation trajectory stage in the 14th cycle of Robot 2

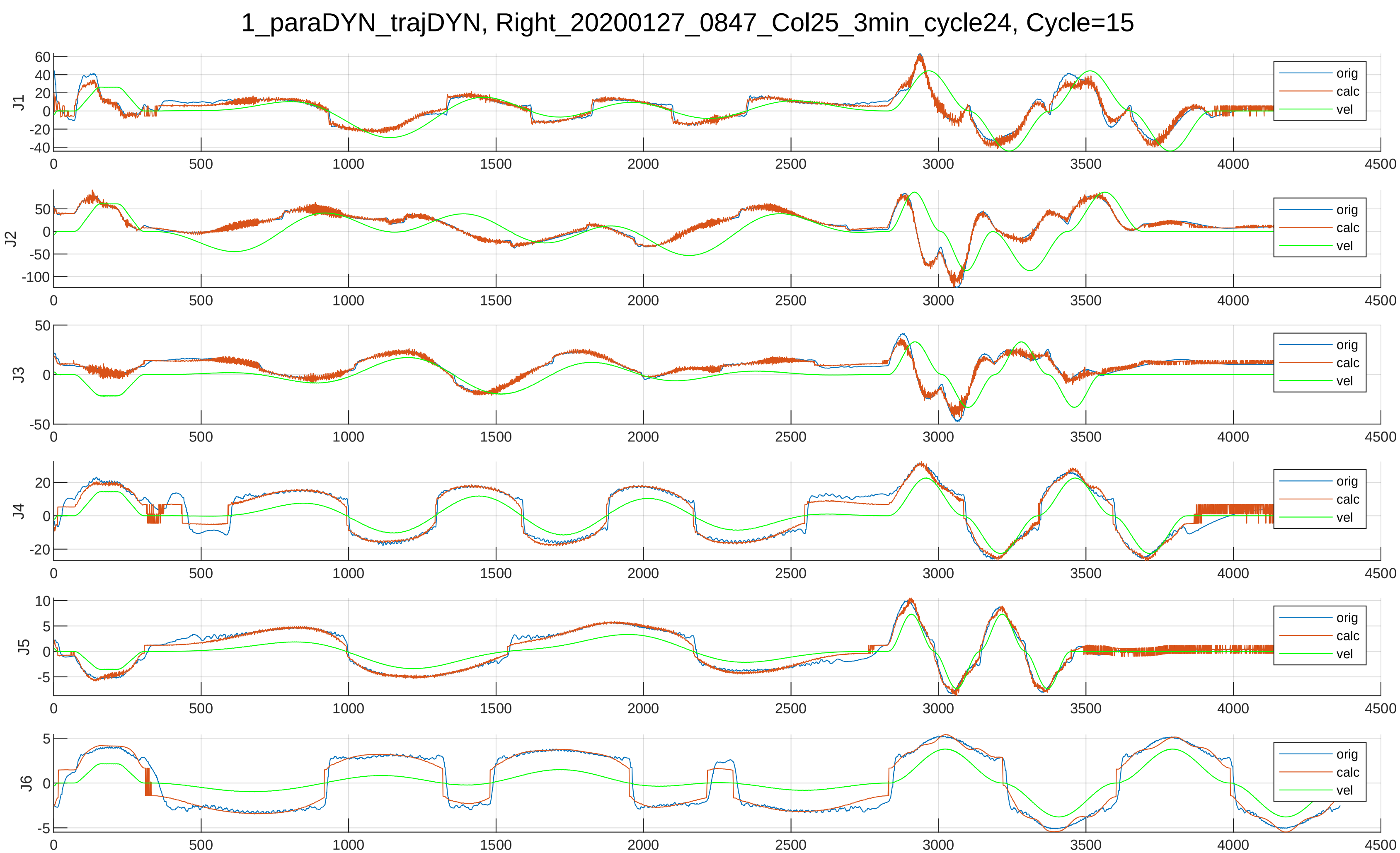

Figure K.15: The identification results of the excitation trajectory stage in the 15^{th} cycle of Robot 2

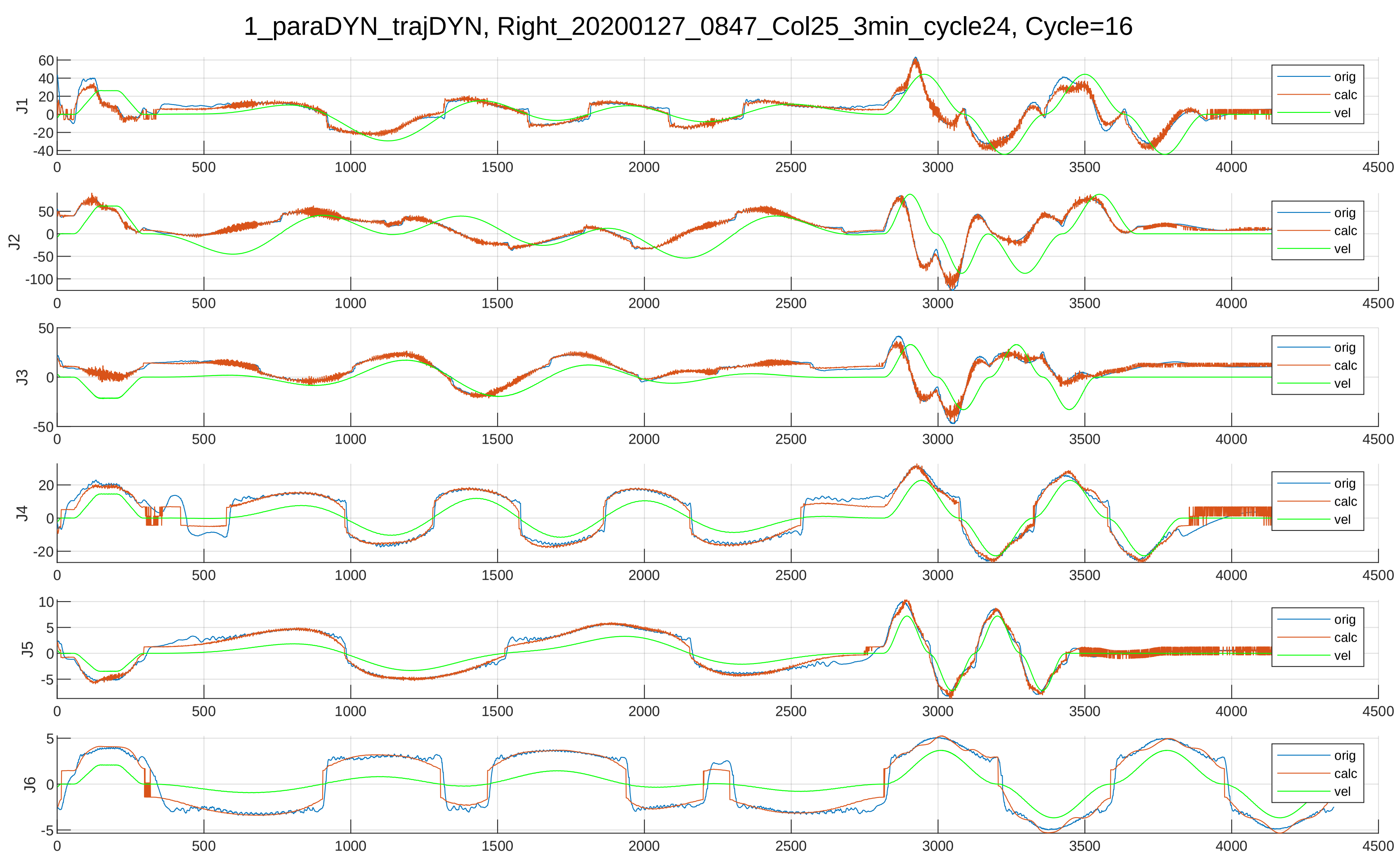

Figure K.16: The identification results of the excitation trajectory stage in the 16$^{\mathrm{th}}$ cycle of Robot 2

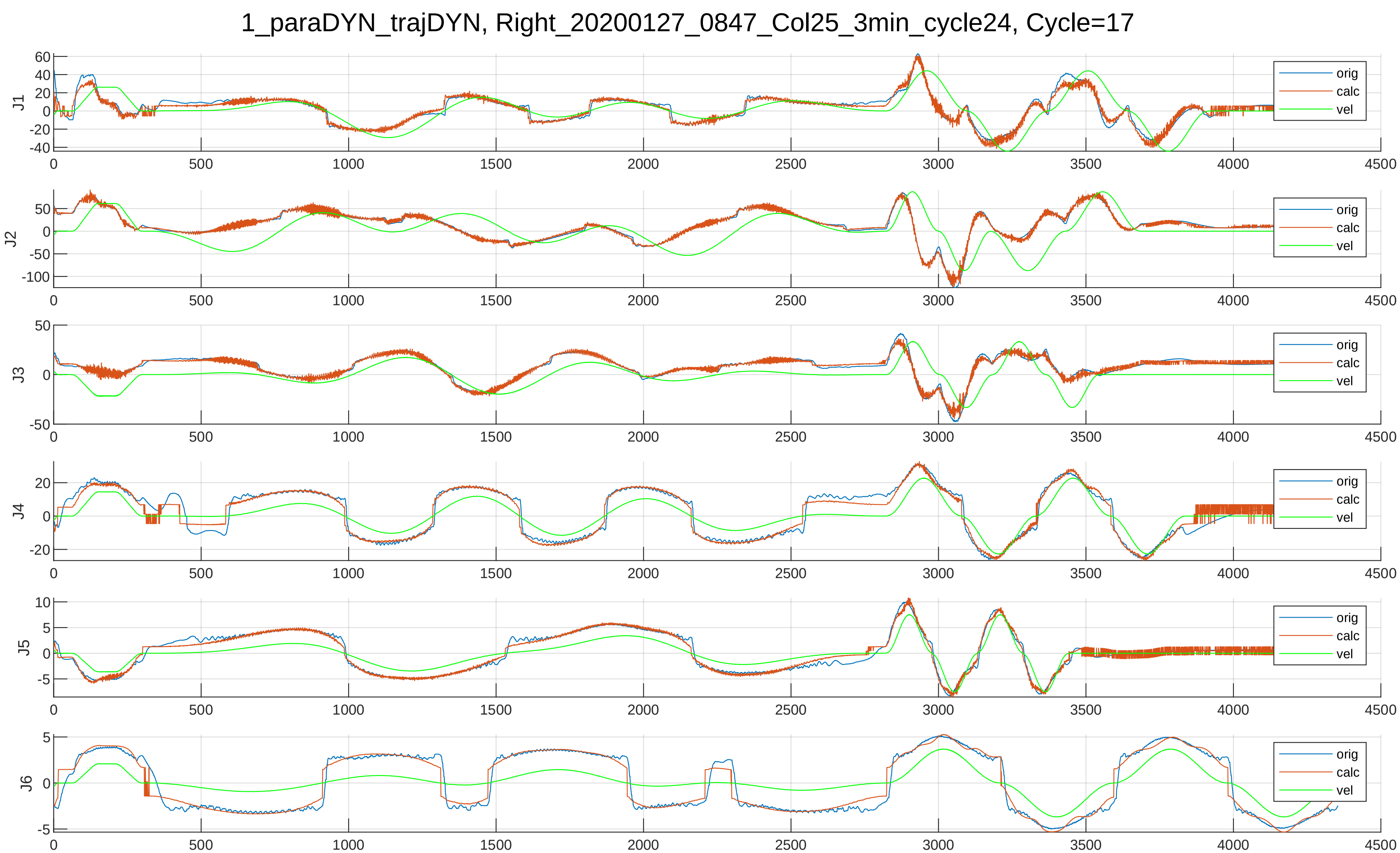

Figure K.17: The identification results of the excitation trajectory stage in the 17th cycle of Robot 2

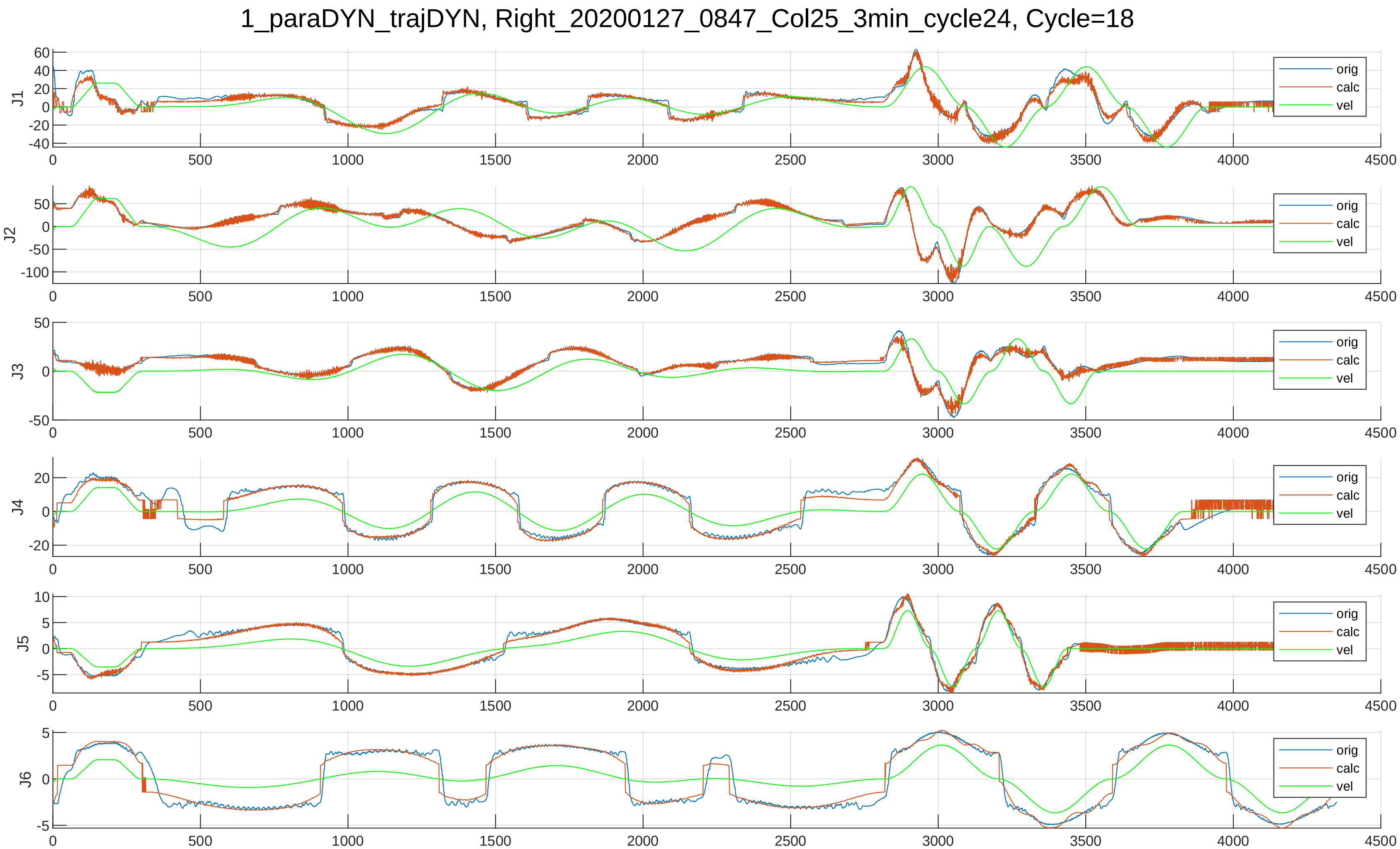

Figure K.18: The identification results of the excitation trajectory stage in the 18$^{\text{th}}$ cycle of Robot 2

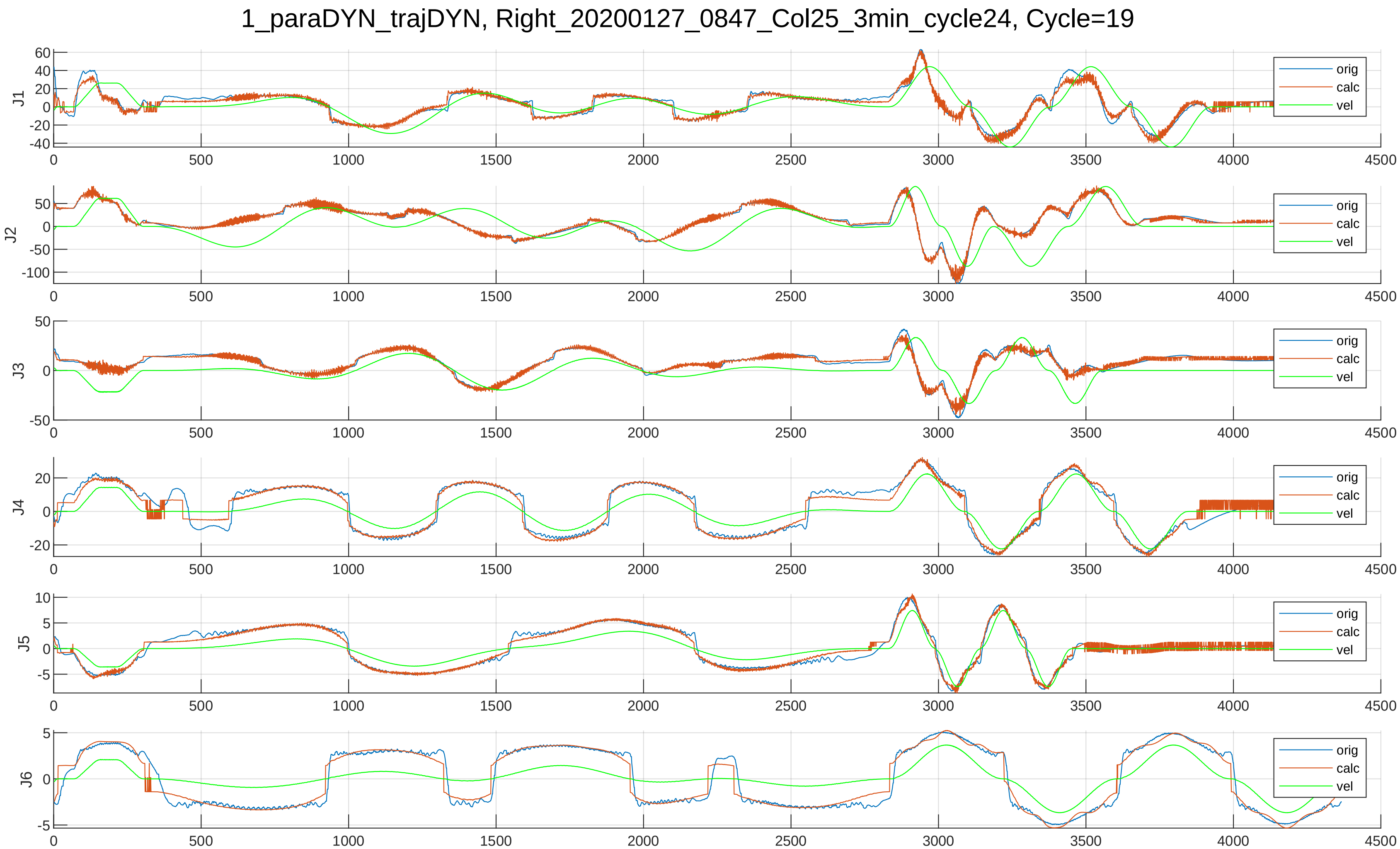

Figure K.19: The identification results of the excitation trajectory stage in the 19th cycle of Robot 2

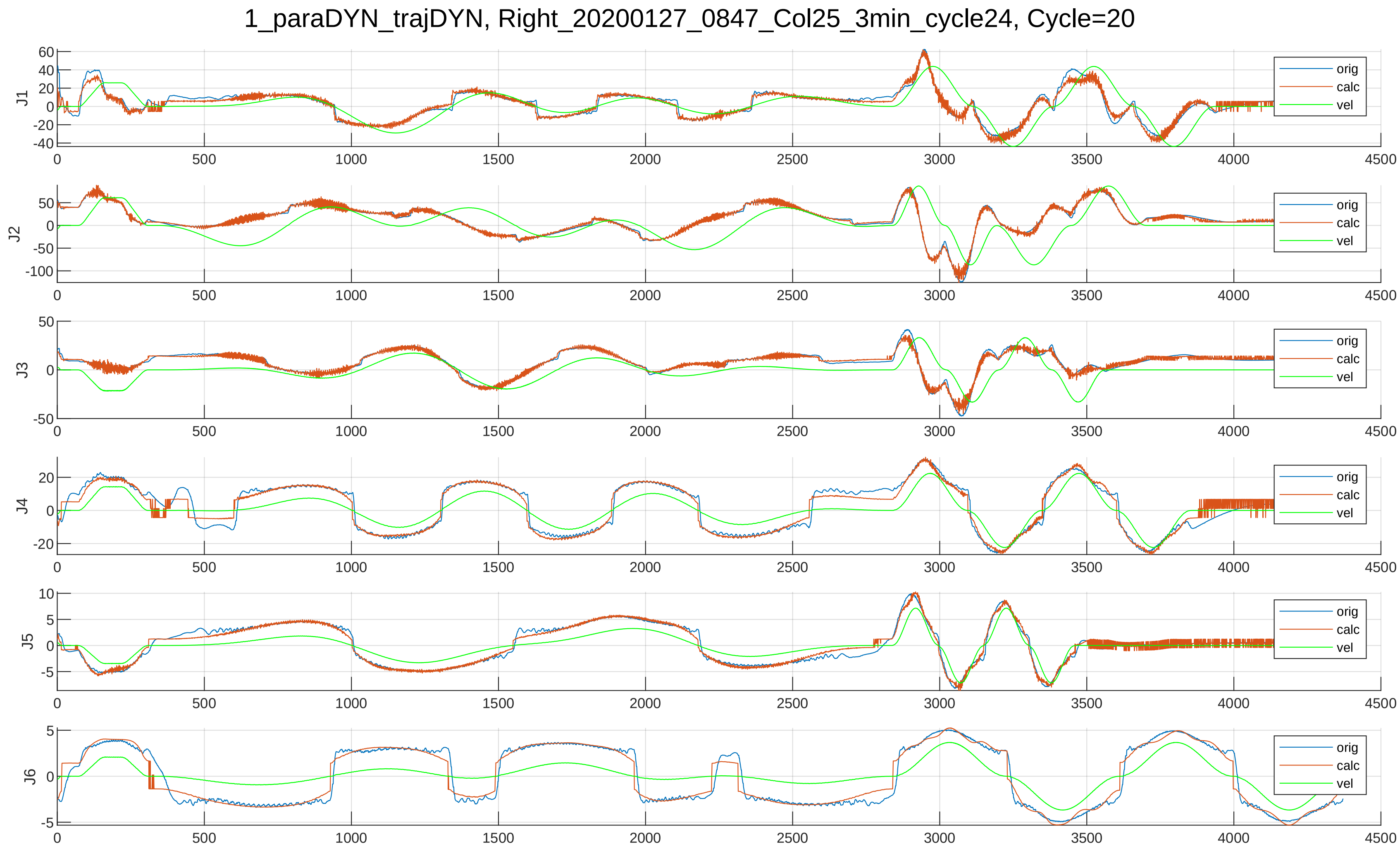

Figure K.20: The identification results of the excitation trajectory stage in the 20th cycle of Robot 2

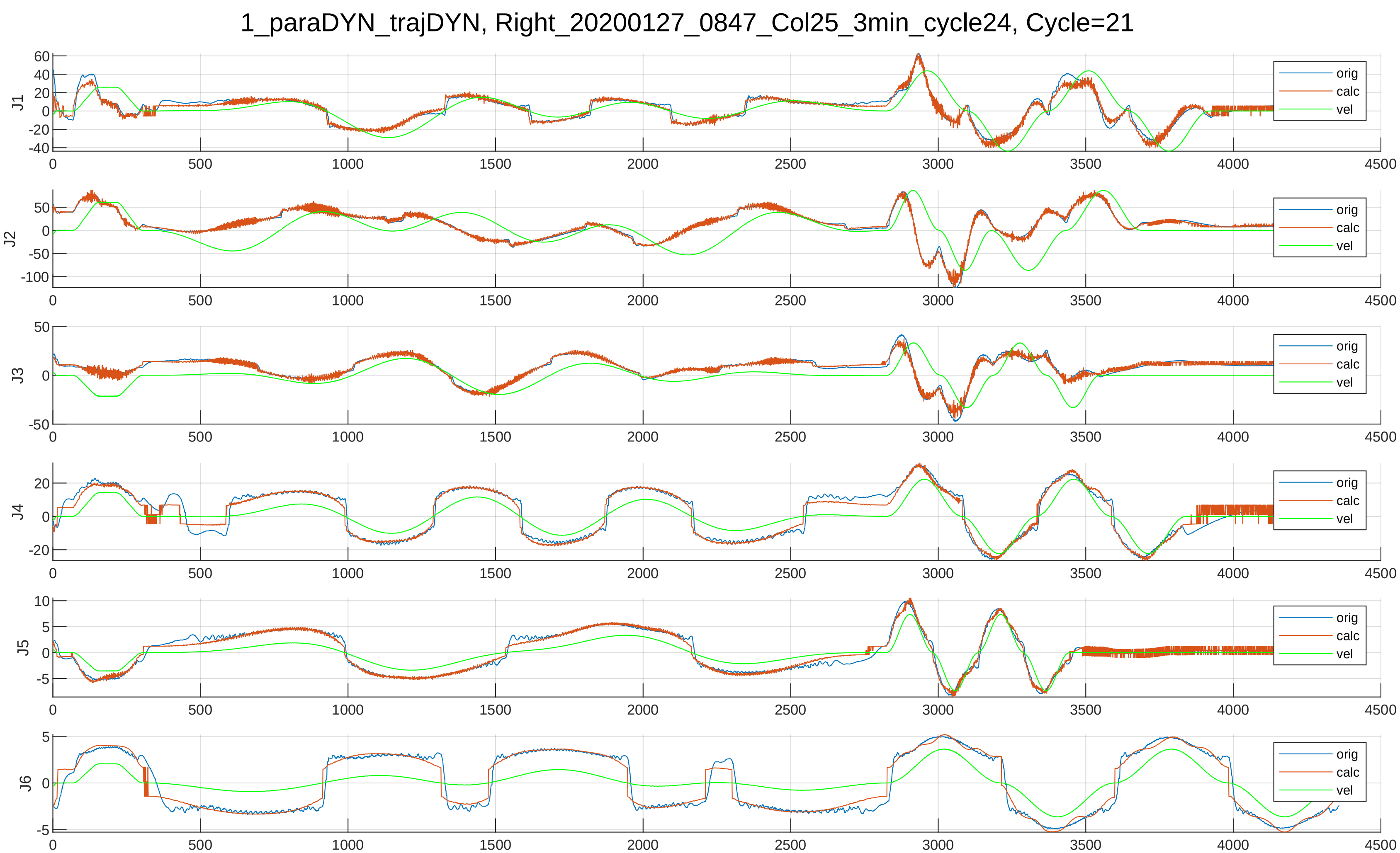

Figure K.21: The identification results of the excitation trajectory stage in the 21^{st} cycle of Robot 2

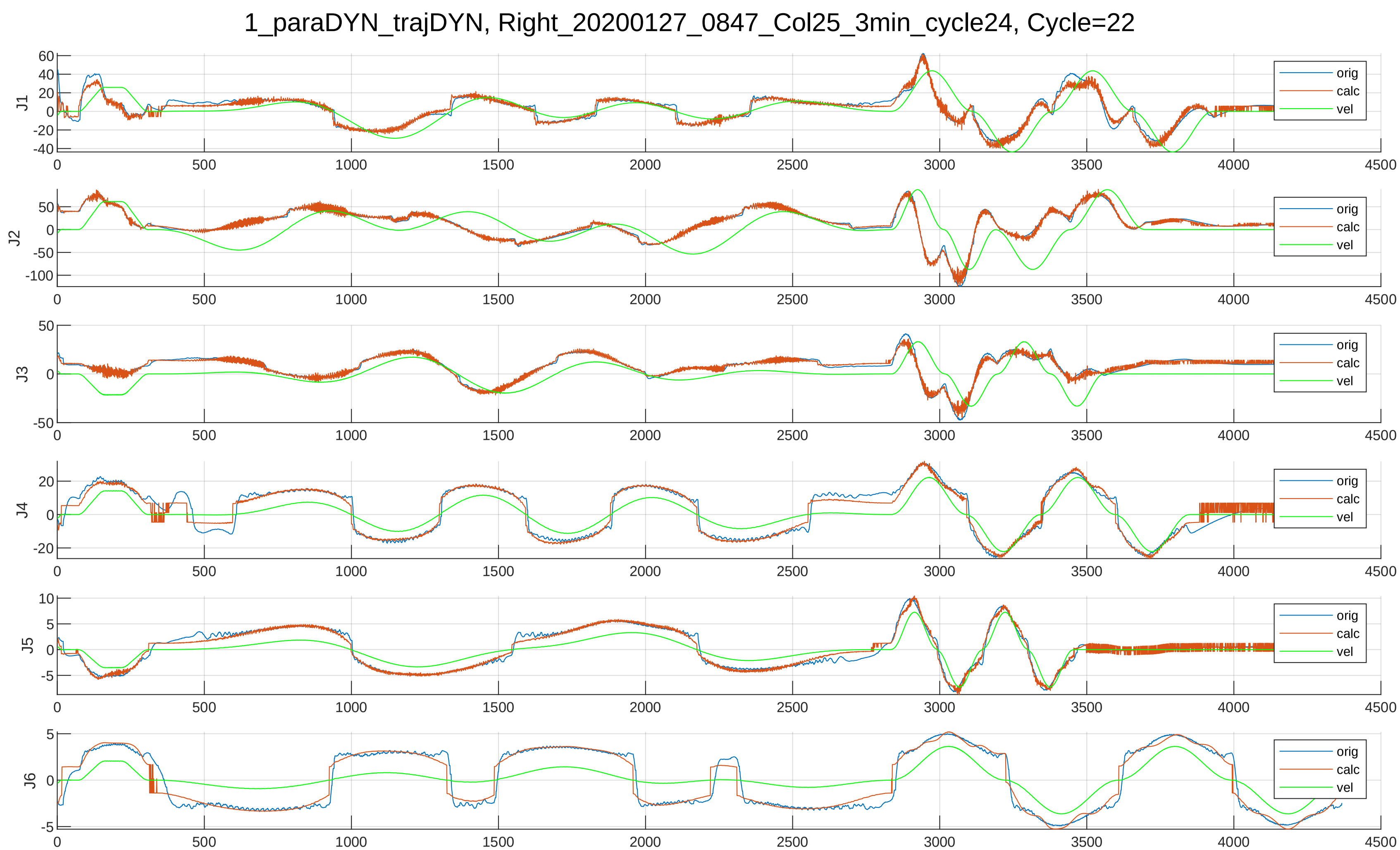

Figure K.22: The identification results of the excitation trajectory stage in the 22^{nd} cycle of Robot 2

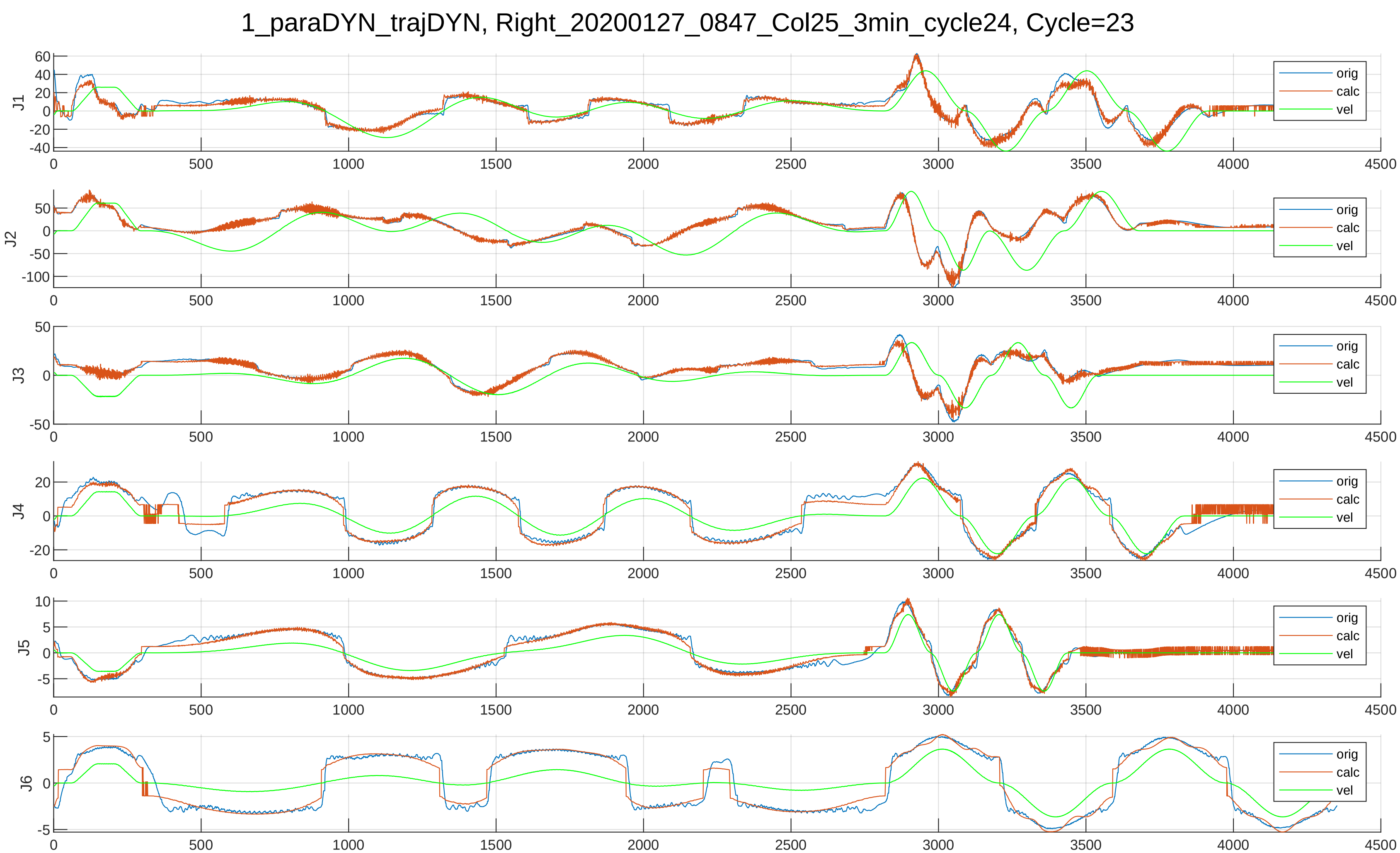

Figure K.23: The identification results of the excitation trajectory stage in the 23rd cycle of Robot 2

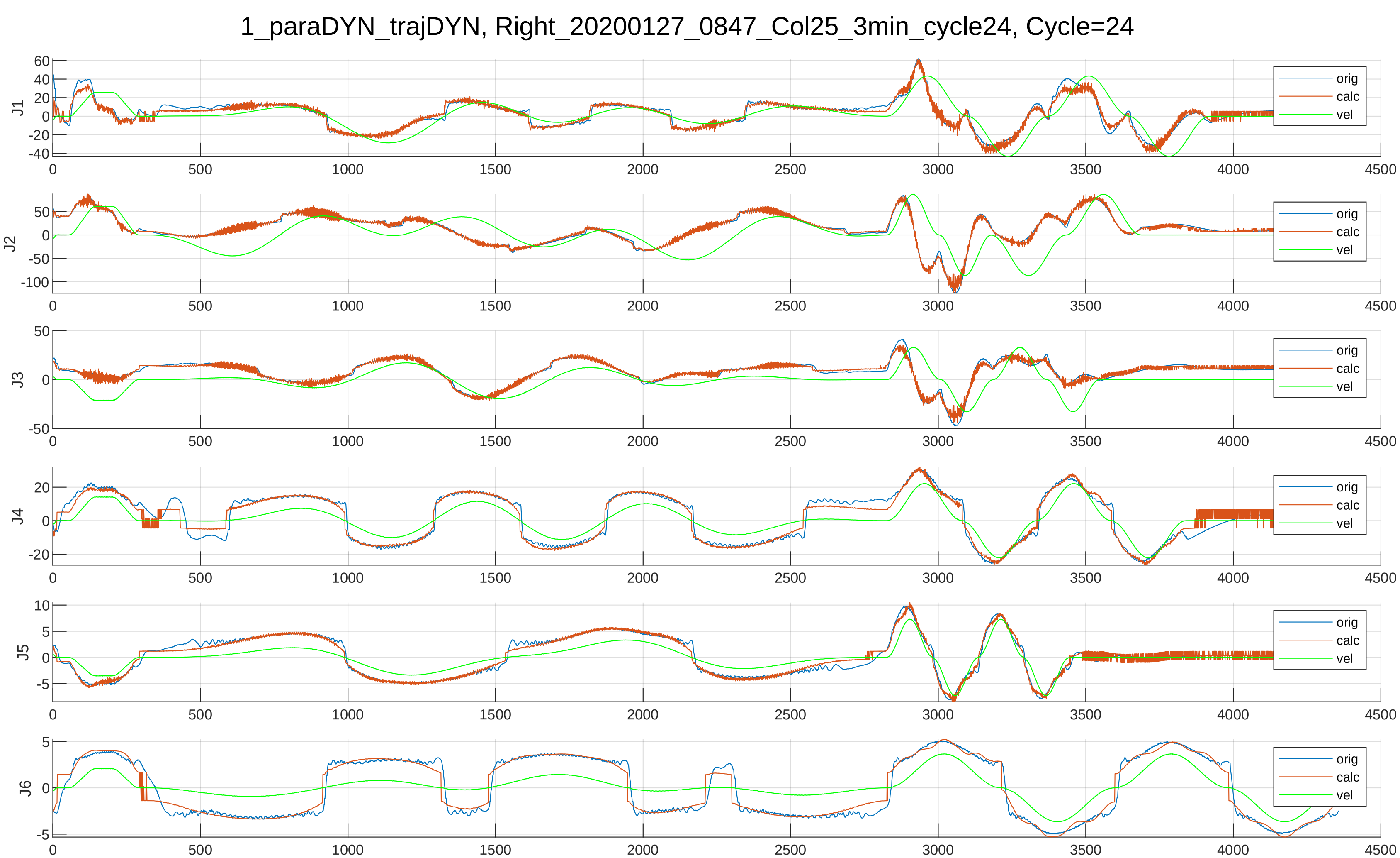

Figure K.24: The identification results of the excitation trajectory stage in the 24$^{\text{th}}$ cycle of Robot 2

Appendix L

The Verification Results Of One Cycle In The Test Trajectory

The figures in this appendix indicate the identification results of all joints in one cycle from a test of the Robot RIGHT, which are used in Section 5.1.1 and 5.1.2. They are shown with the measured torque and the estimated torque, marked with blue curve and red curve respectively. The green curve is the scaled velocity corresponded to the torque output. These figures are demonstrated cycle by cycle.

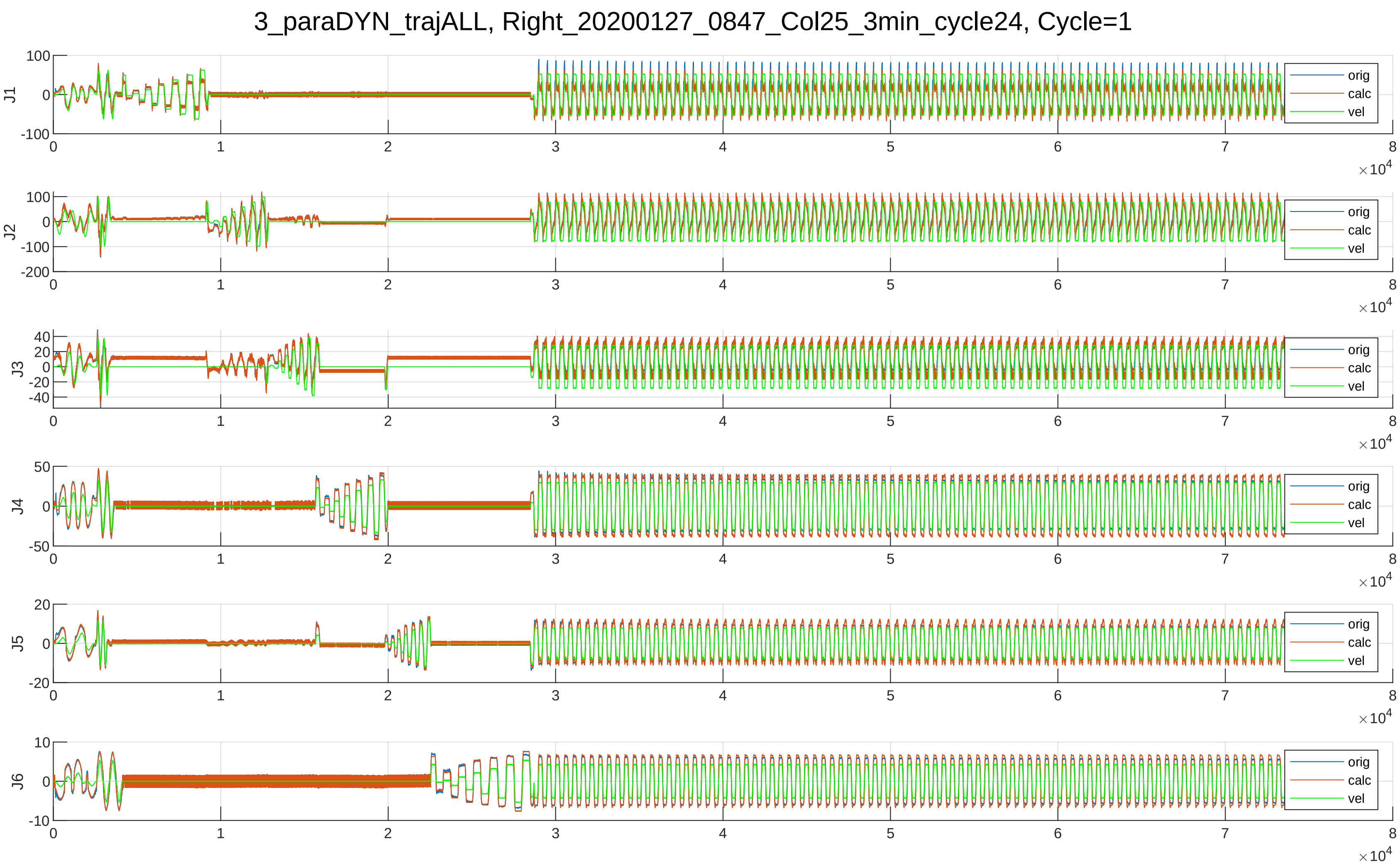

Figure L.1: The identification results of the all trajectory stage in the 1^{st} cycle of Robot 2

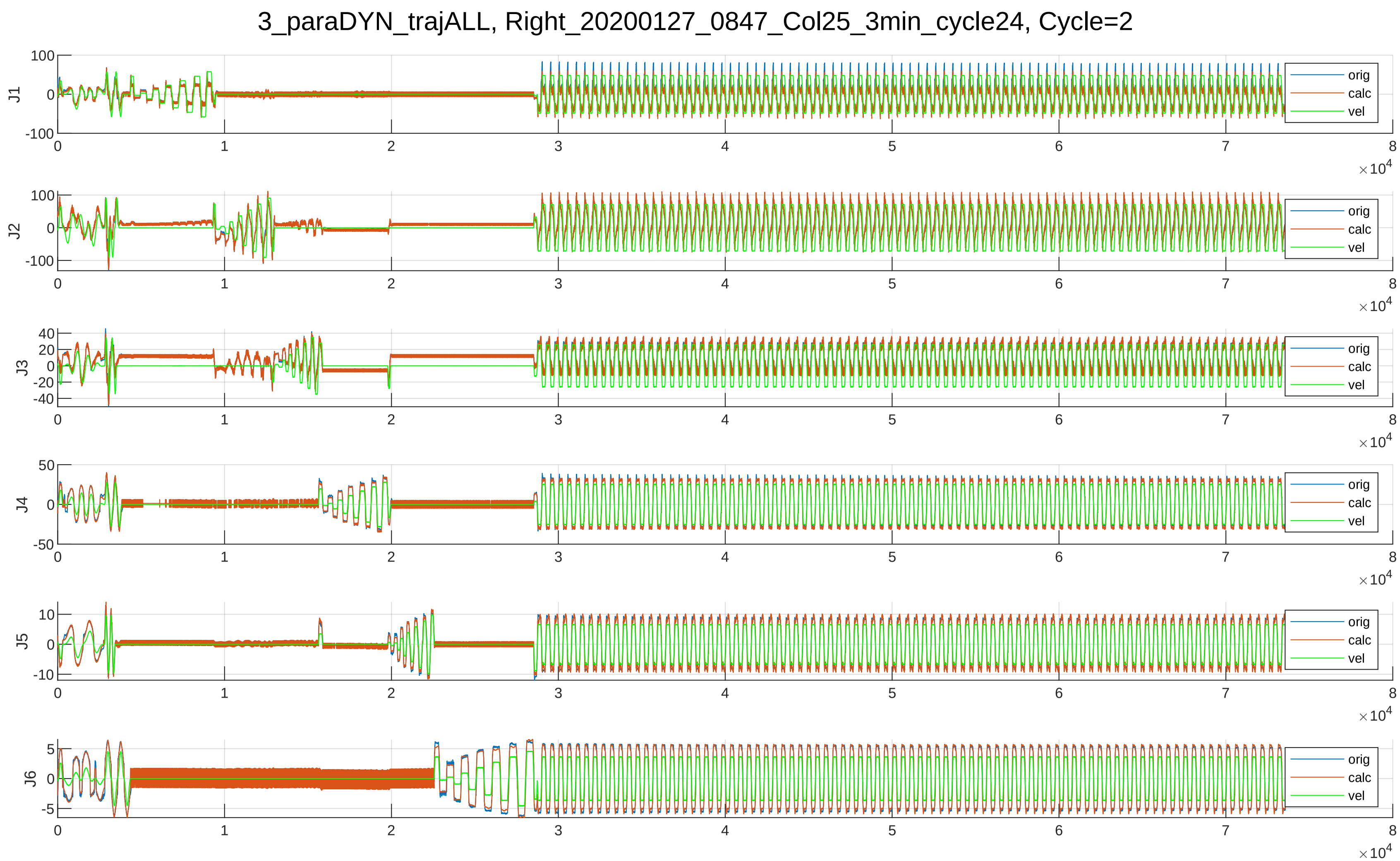

Figure L.2: The identification results of the all trajectory stage in the 2nd cycle of Robot 2

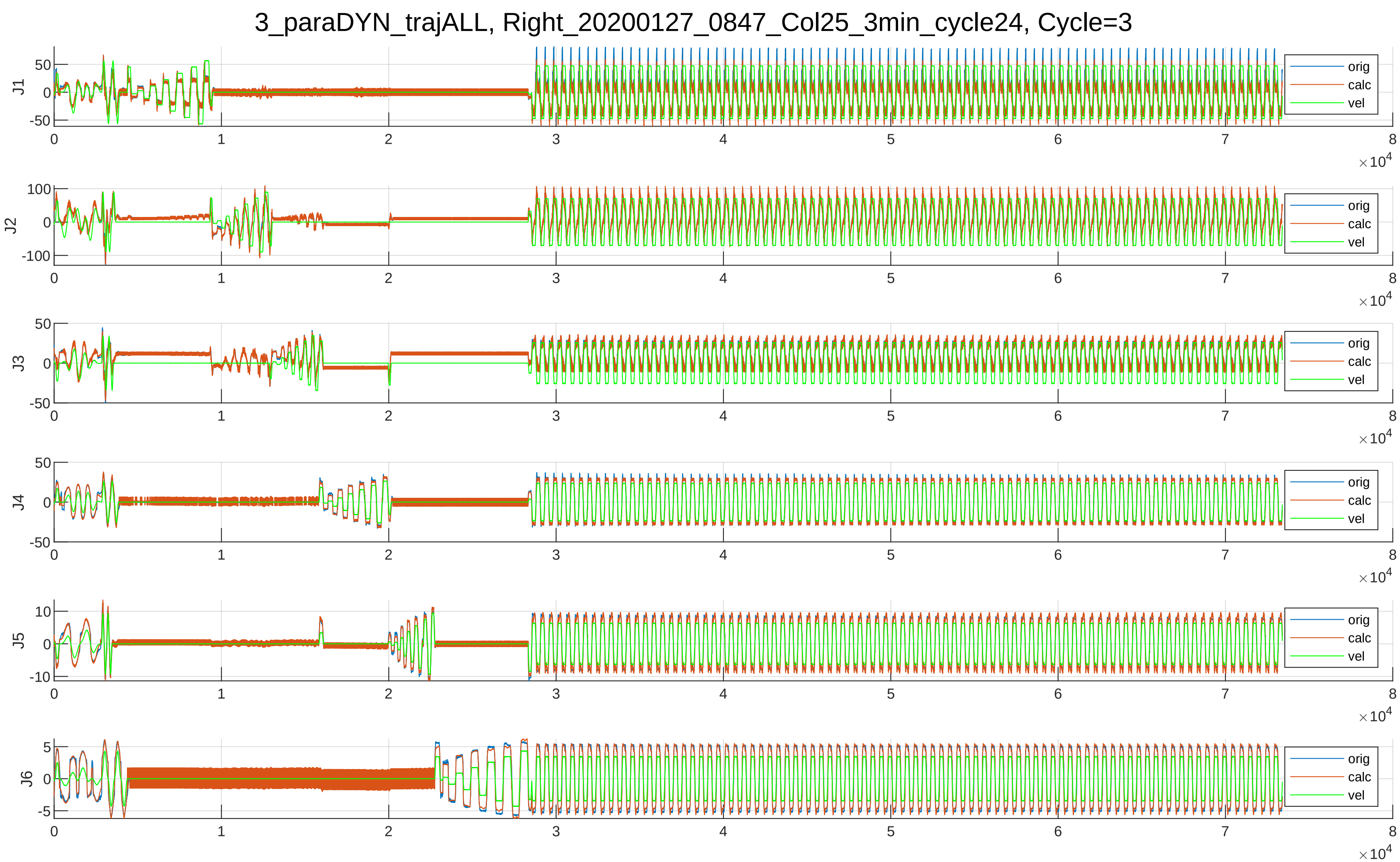

Figure L.3: The identification results of the all trajectory stage in the 3rd cycle of Robot 2

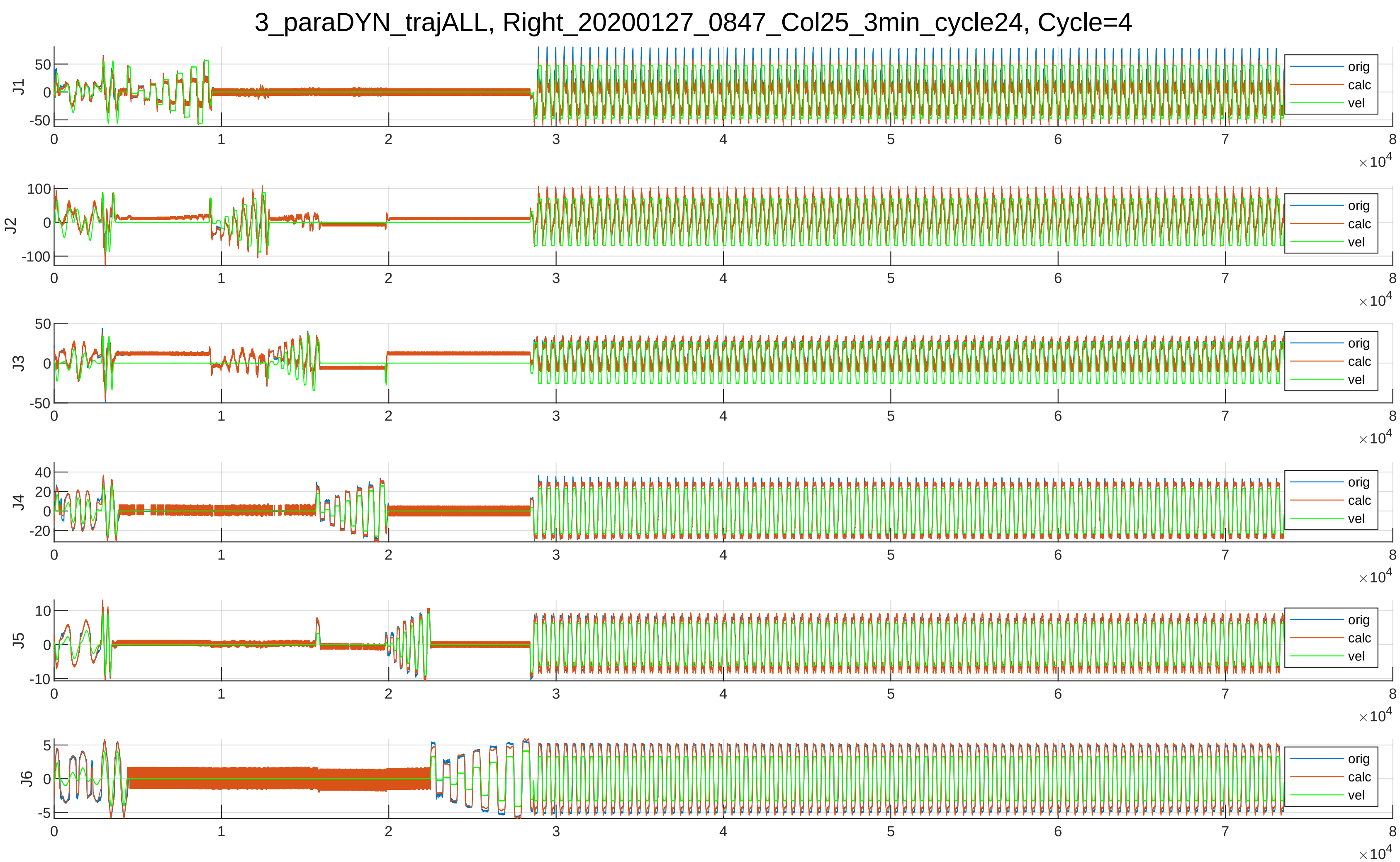

Figure L.4: The identification results of the all trajectory stage in the 4^{th} cycle of Robot 2

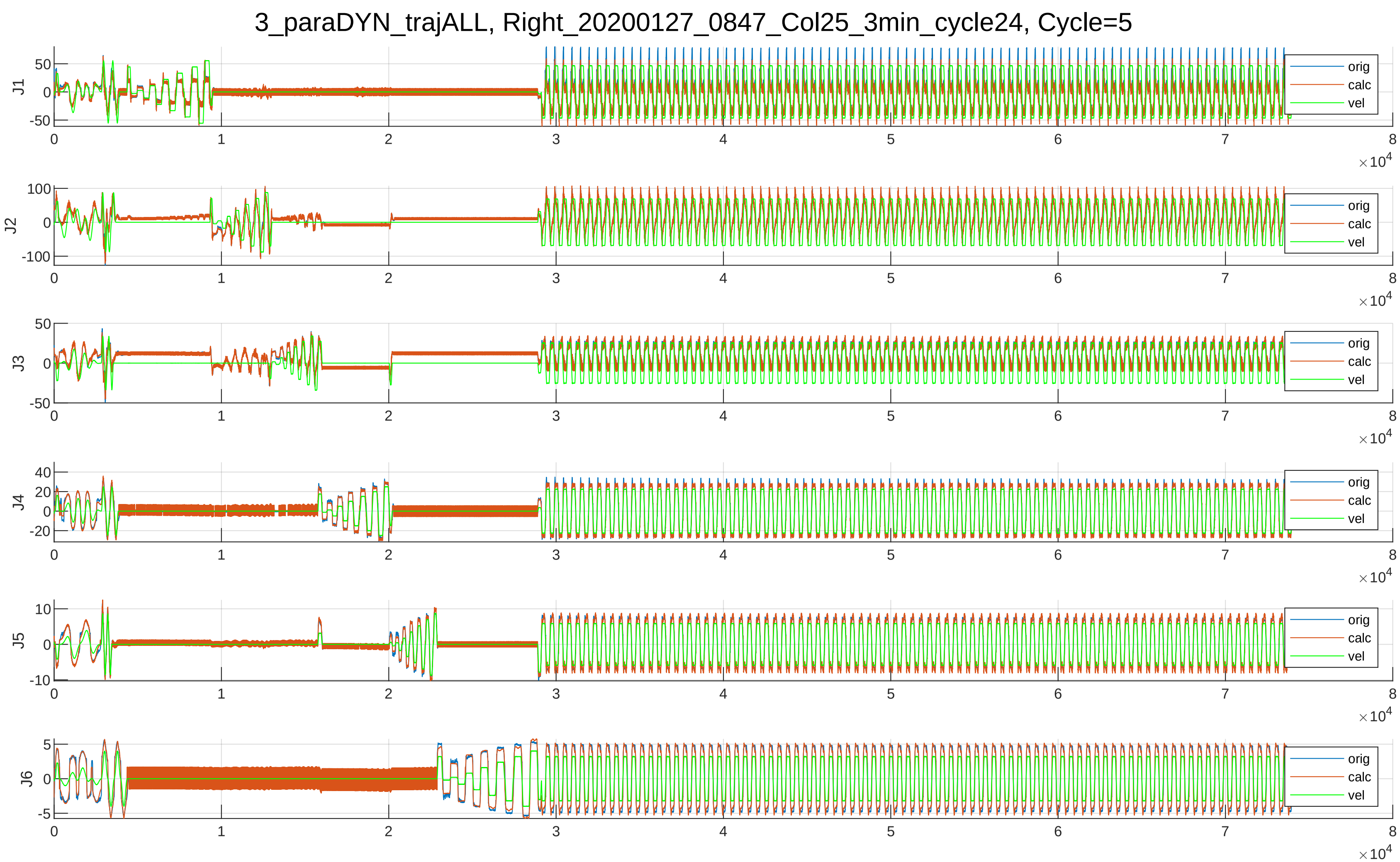

Figure L.5: The identification results of the all trajectory stage in the 5th cycle of Robot 2

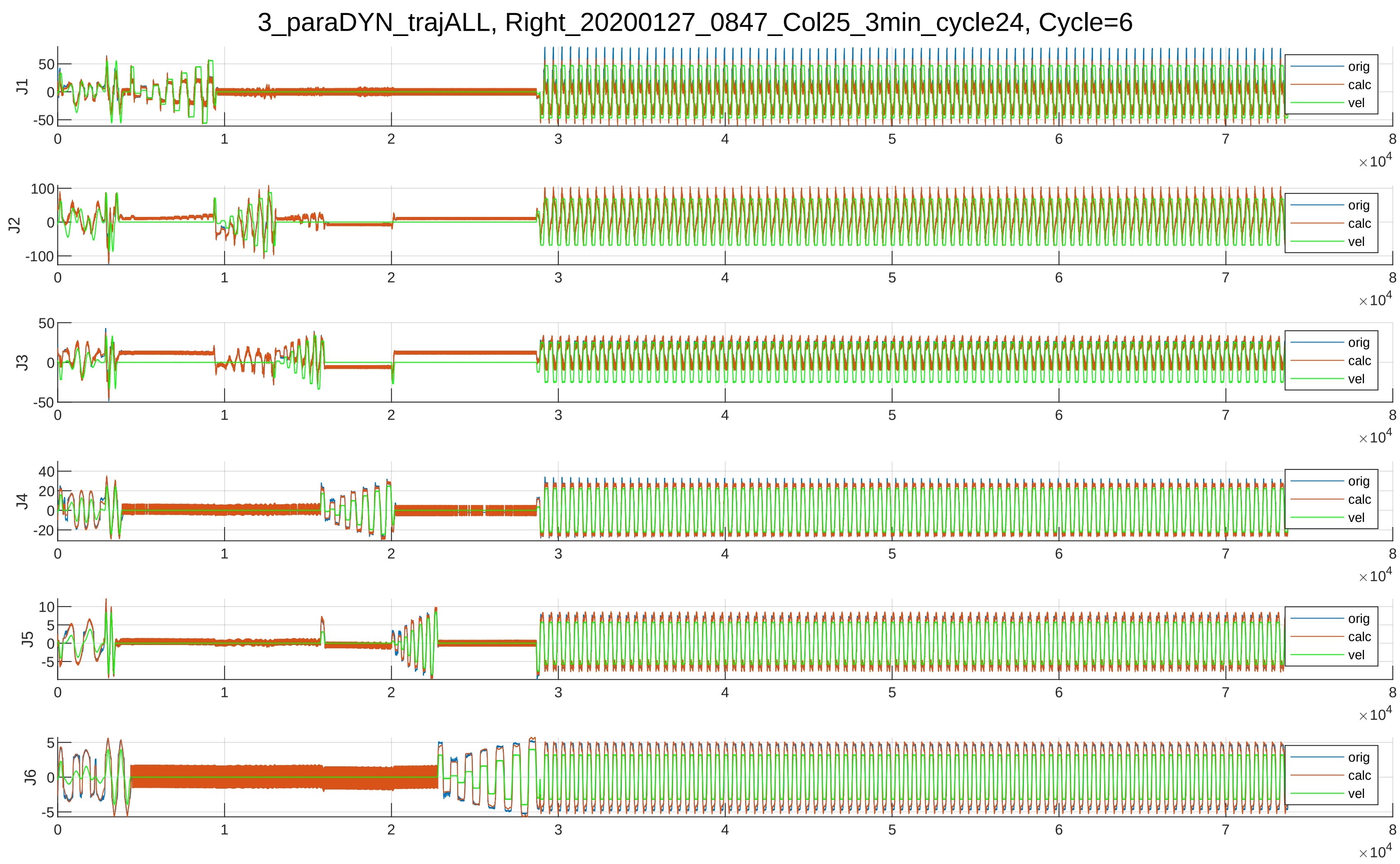

Figure L.6: The identification results of the all trajectory stage in the 6^{th} cycle of Robot 2

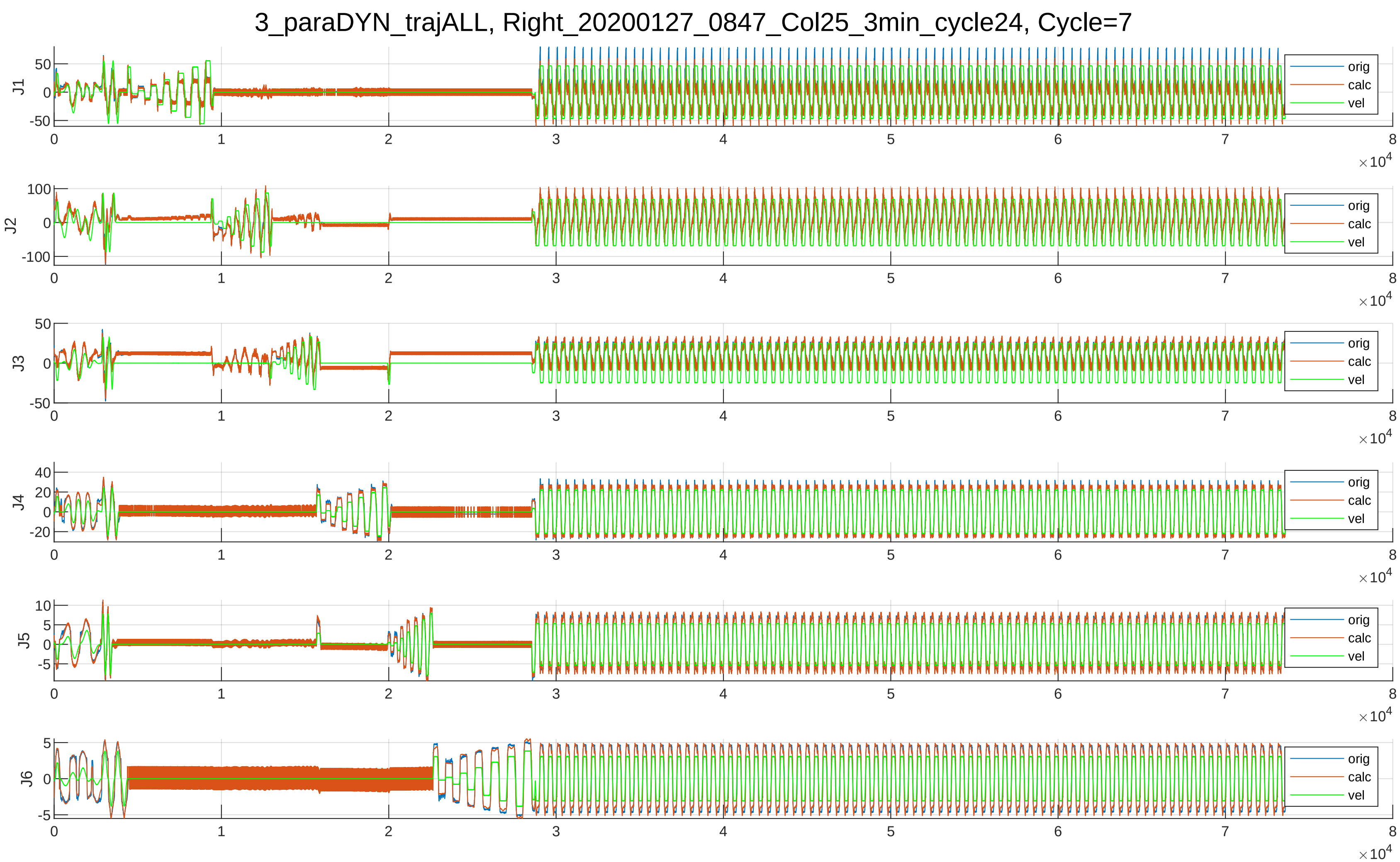

Figure L.7: The identification results of the all trajectory stage in the 7^{th} cycle of Robot 2

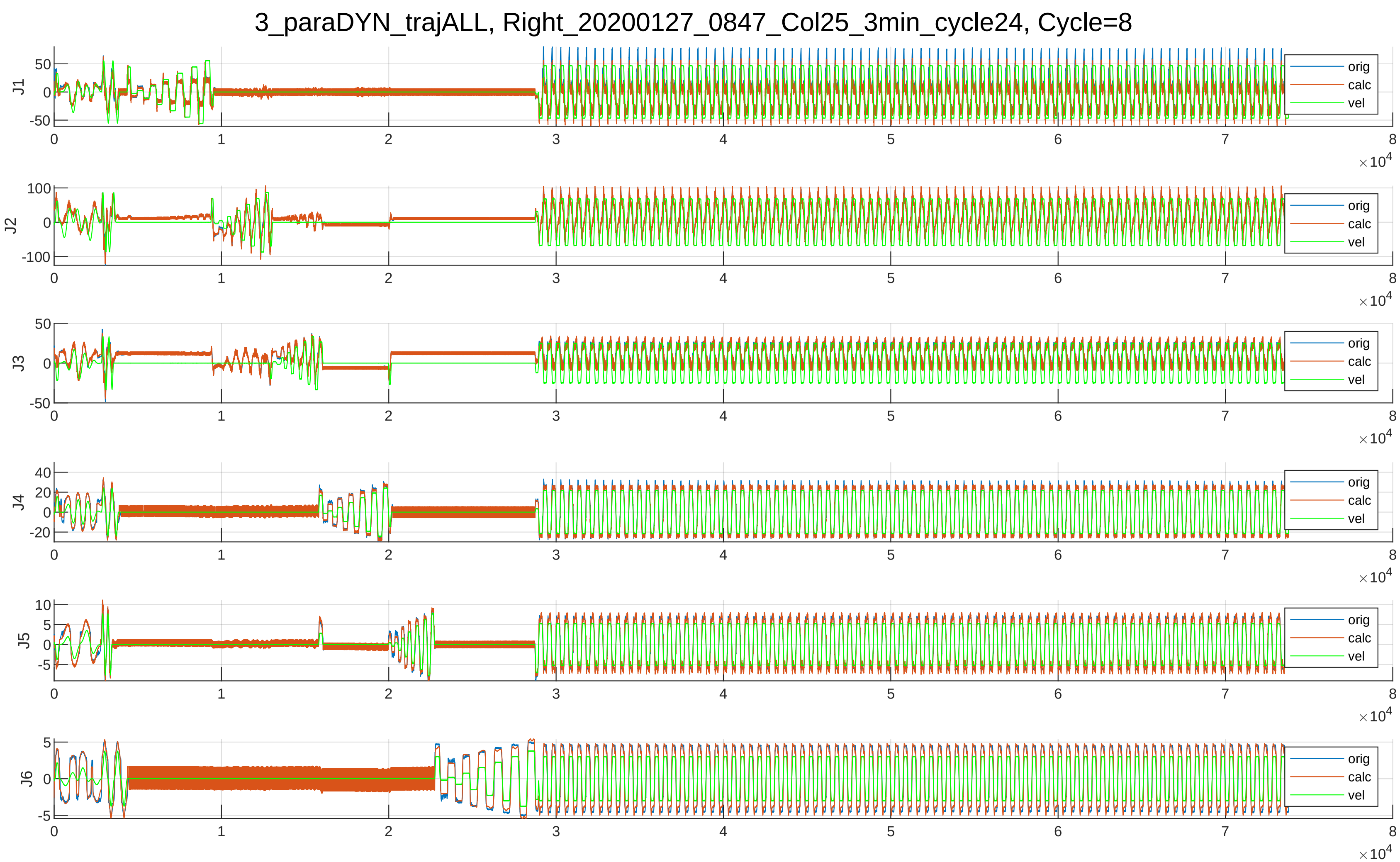

Figure L.8: The identification results of the all trajectory stage in the 8th cycle of Robot 2

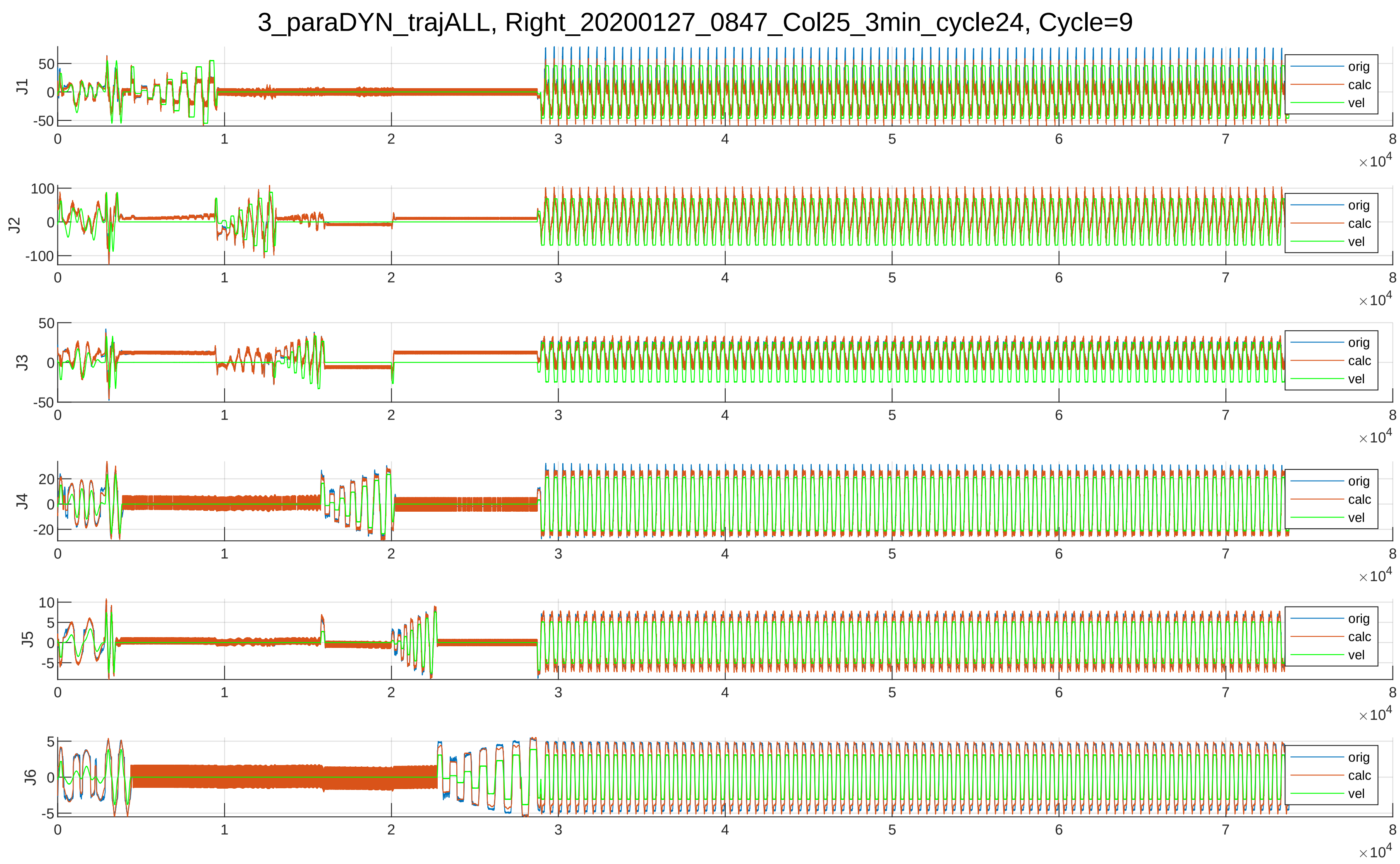

Figure L.9: The identification results of the all trajectory stage in the 9th cycle of Robot 2

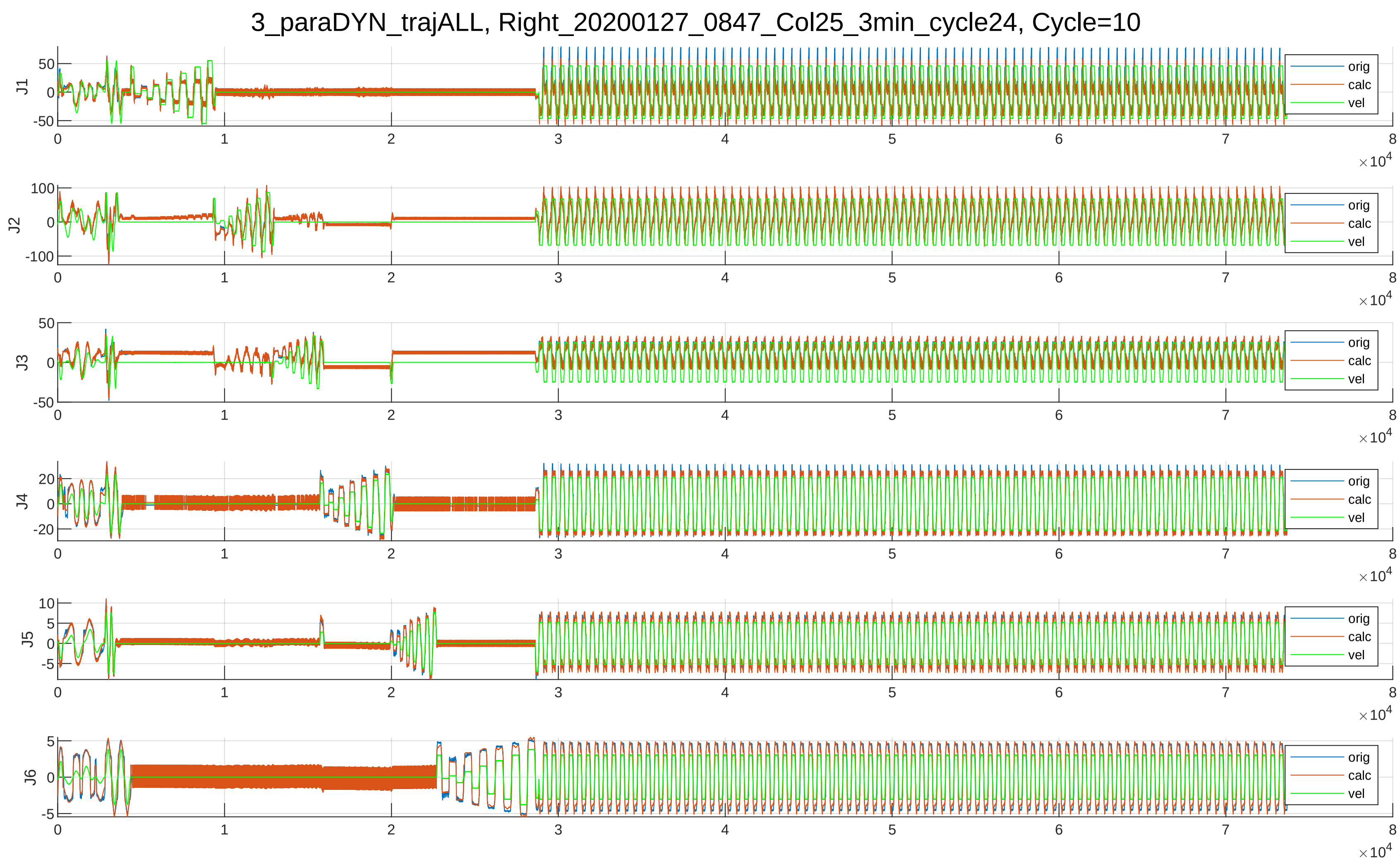

Figure L.10: The identification results of the all trajectory stage in the 10^{th} cycle of Robot 2

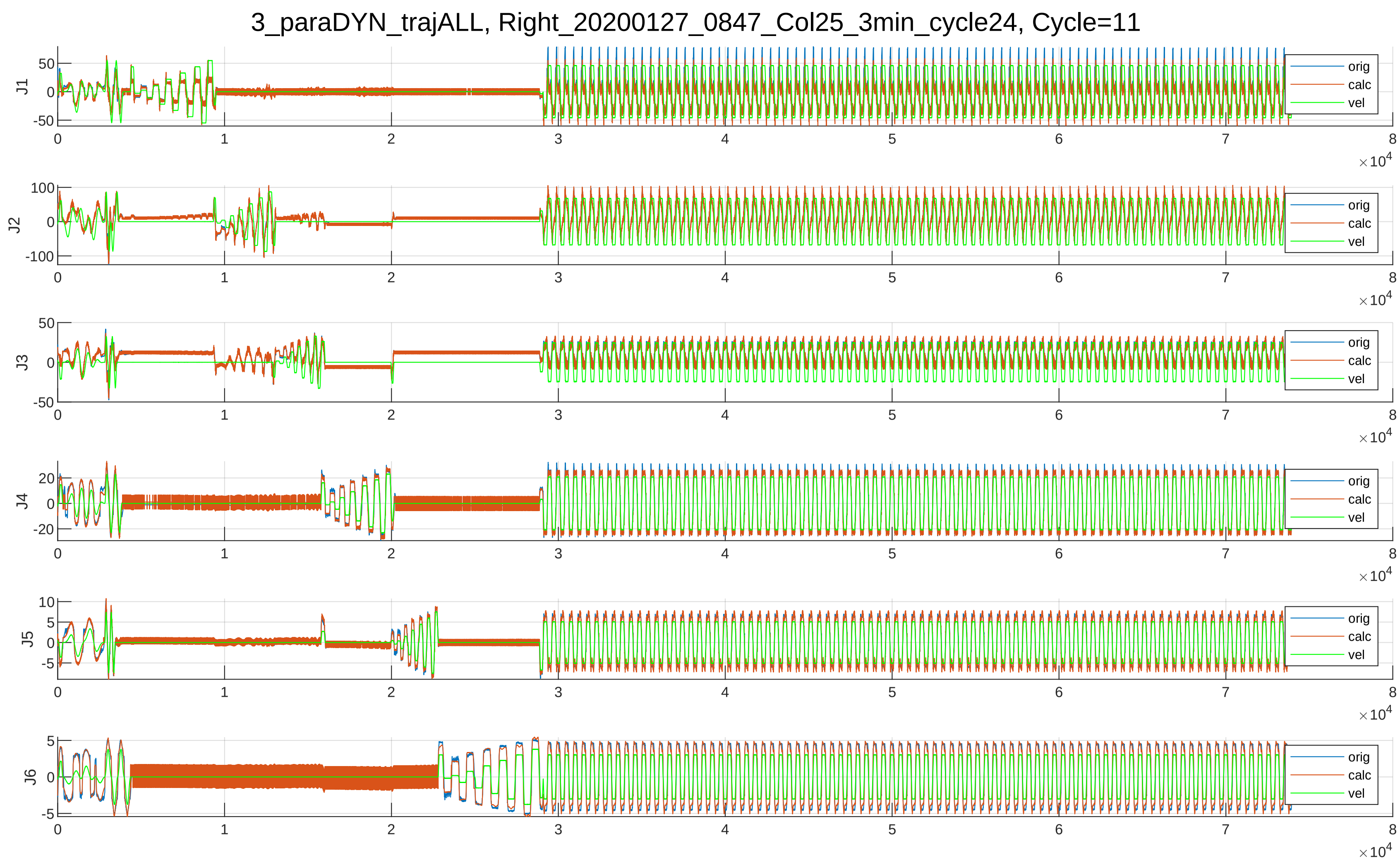

Figure L.11: The identification results of the all trajectory stage in the 11^{th} cycle of Robot 2

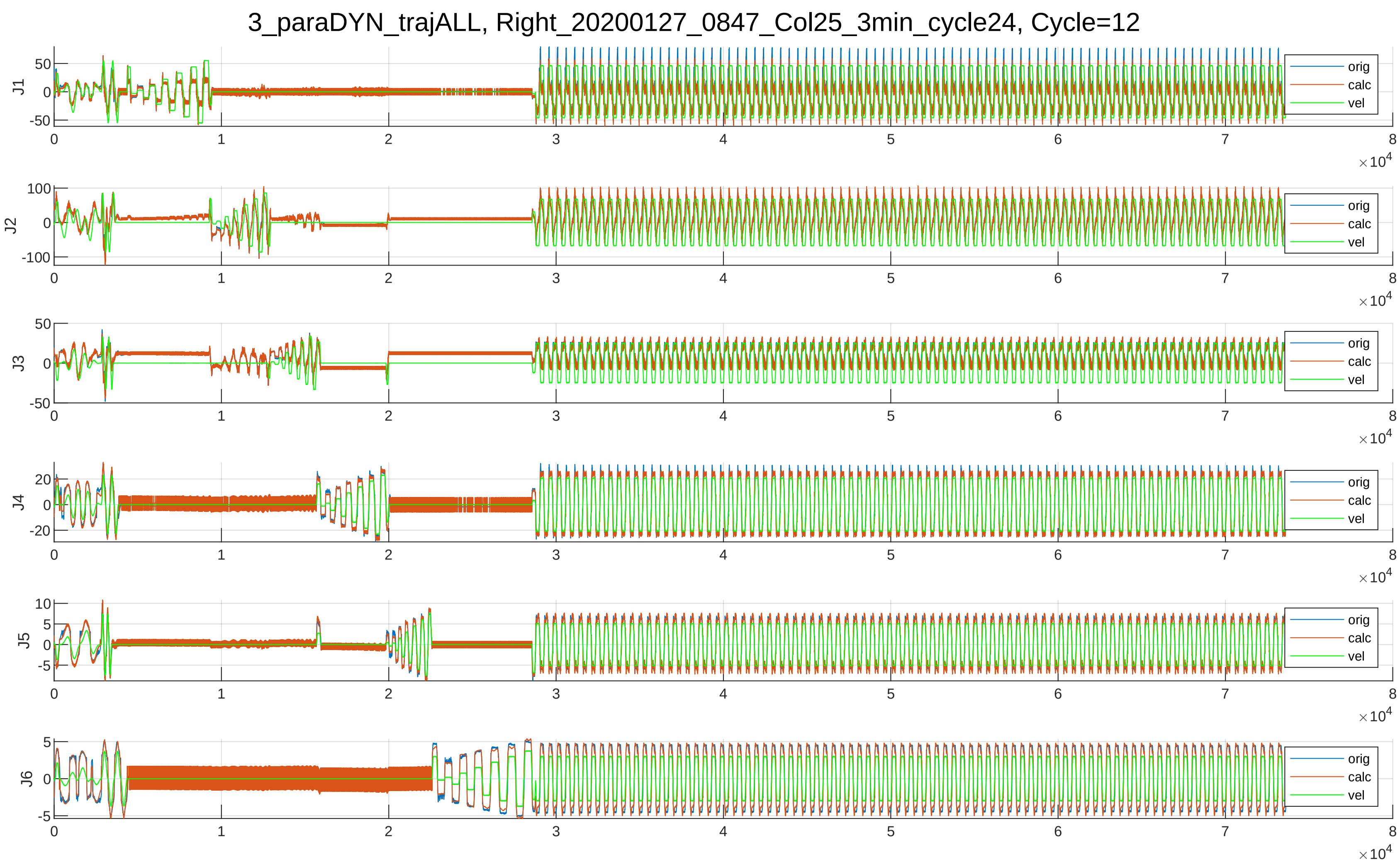

Figure L.12: The identification results of the all trajectory stage in the 12th cycle of Robot 2

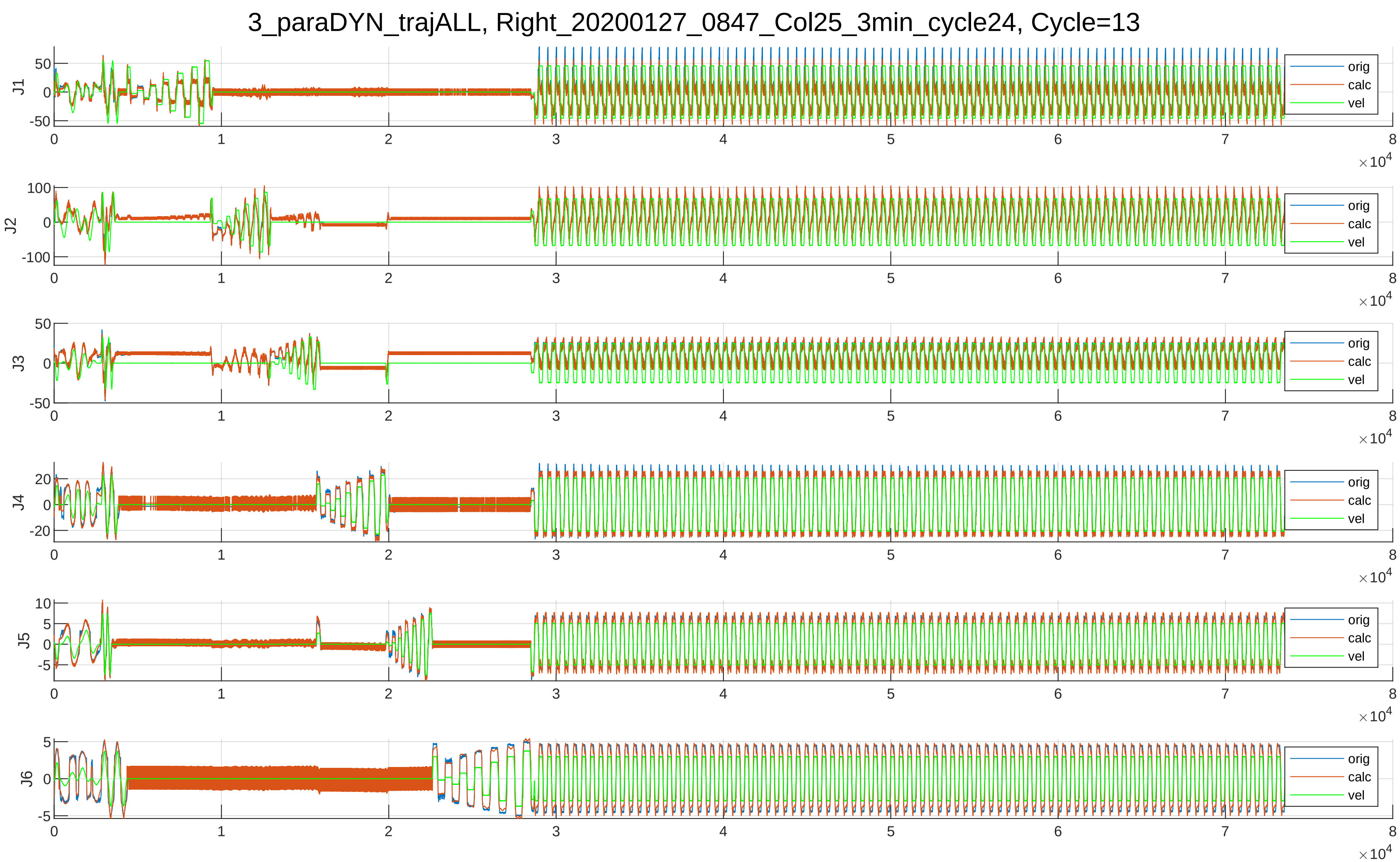

Figure L.13: The identification results of the all trajectory stage in the 13th cycle of Robot 2

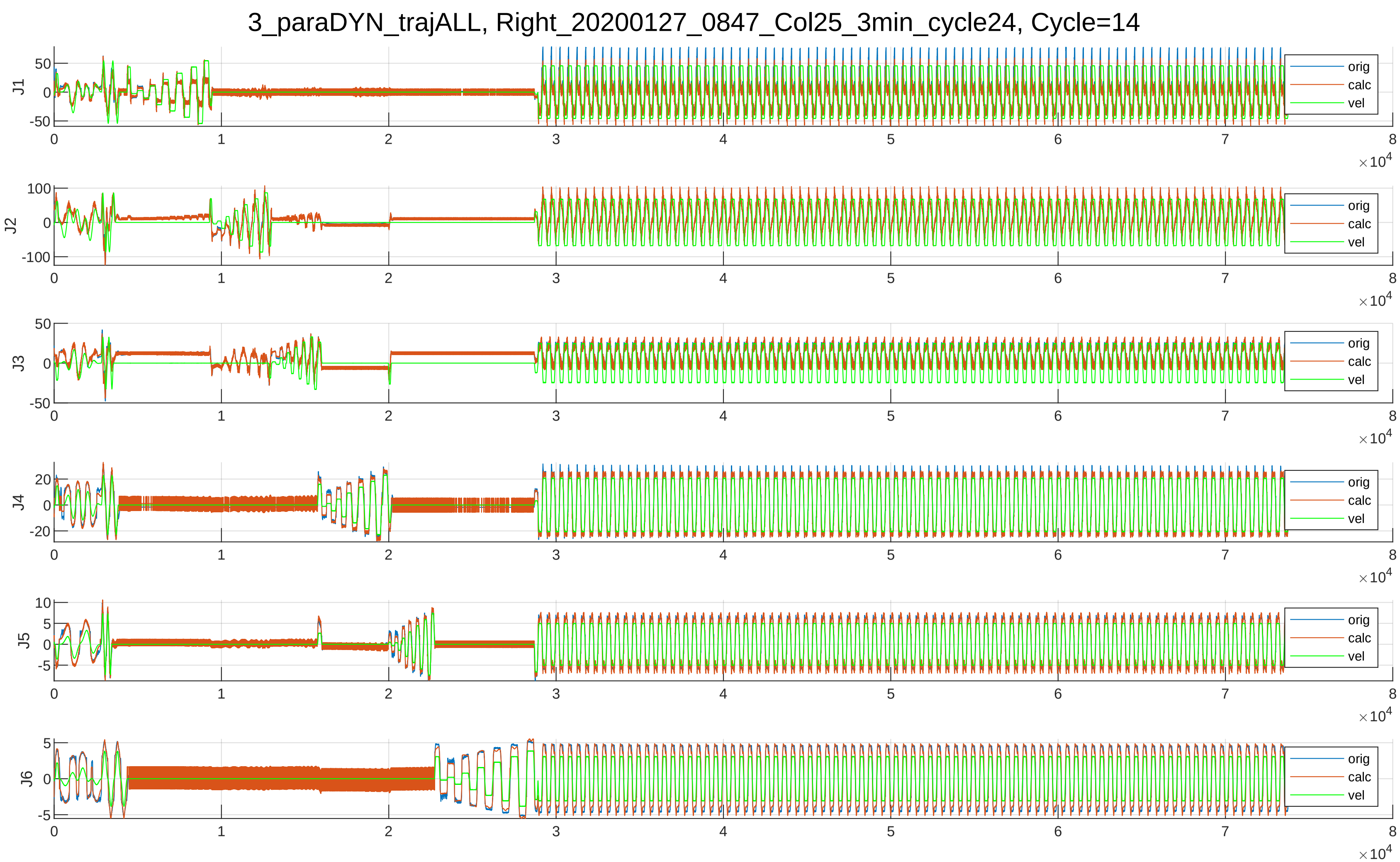

Figure L.14: The identification results of the all trajectory stage in the 14th cycle of Robot 2

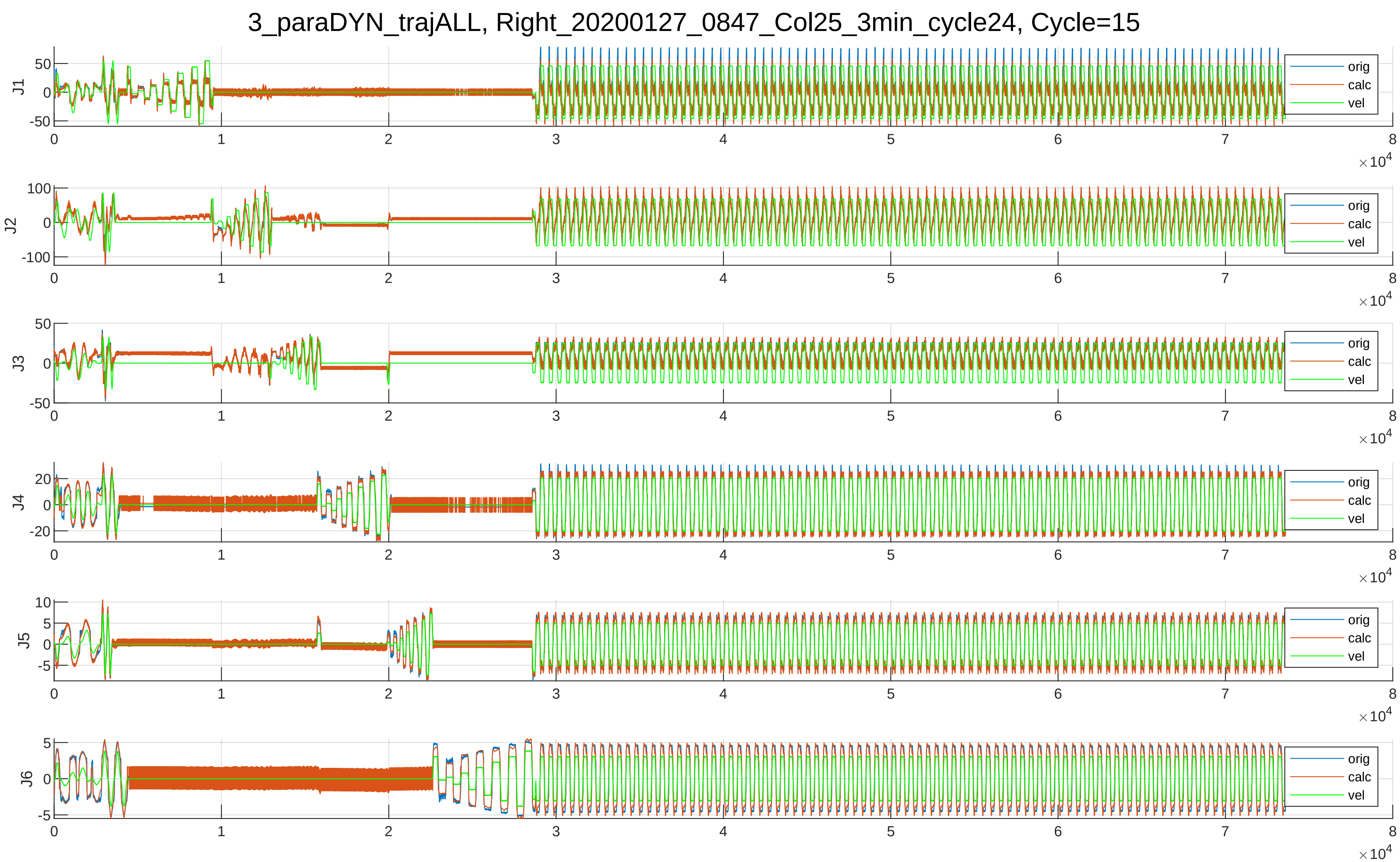

Figure L.15: The identification results of the all trajectory stage in the 15^{th} cycle of Robot 2

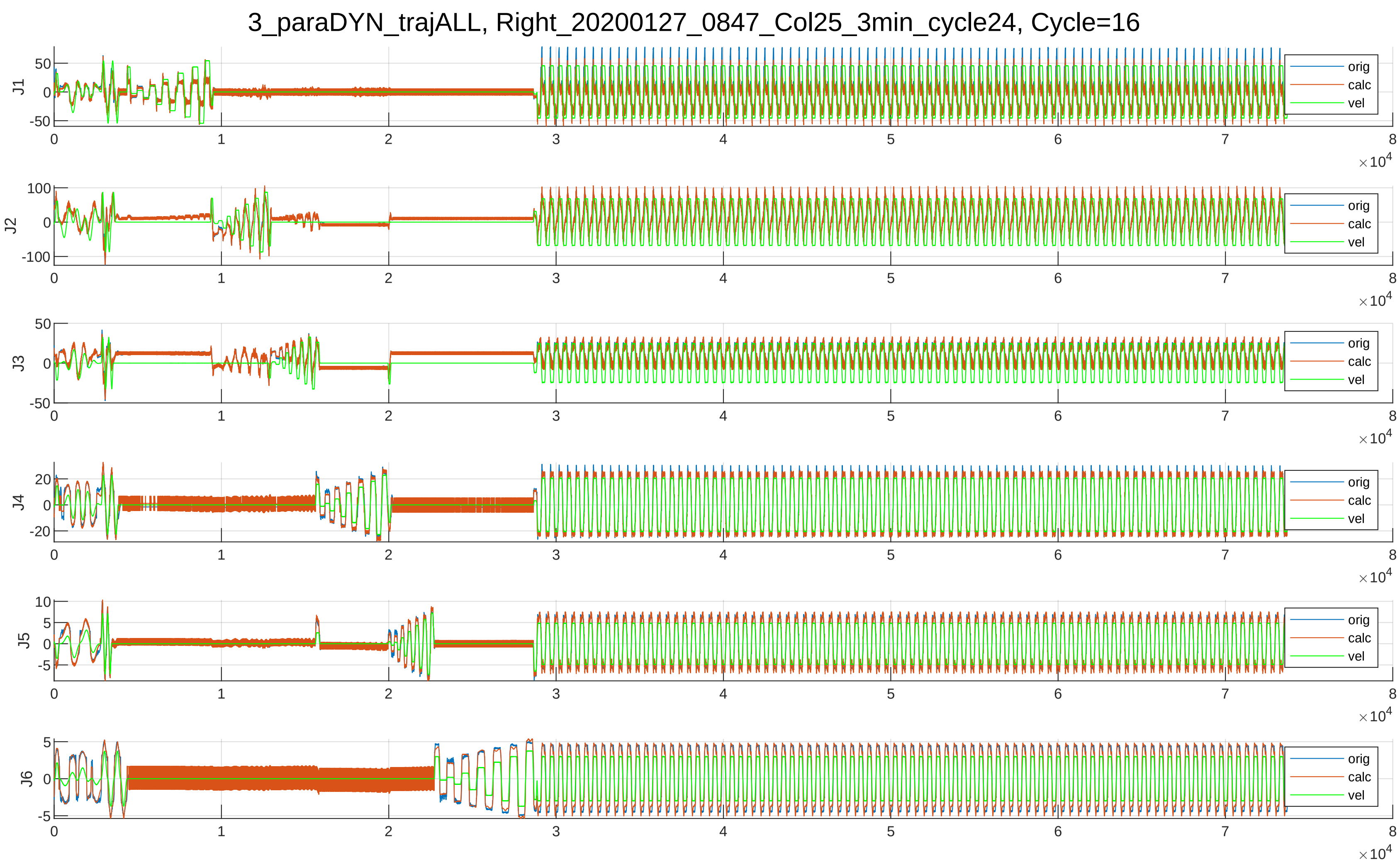

Figure L.16: The identification results of the all trajectory stage in the 16th cycle of Robot 2

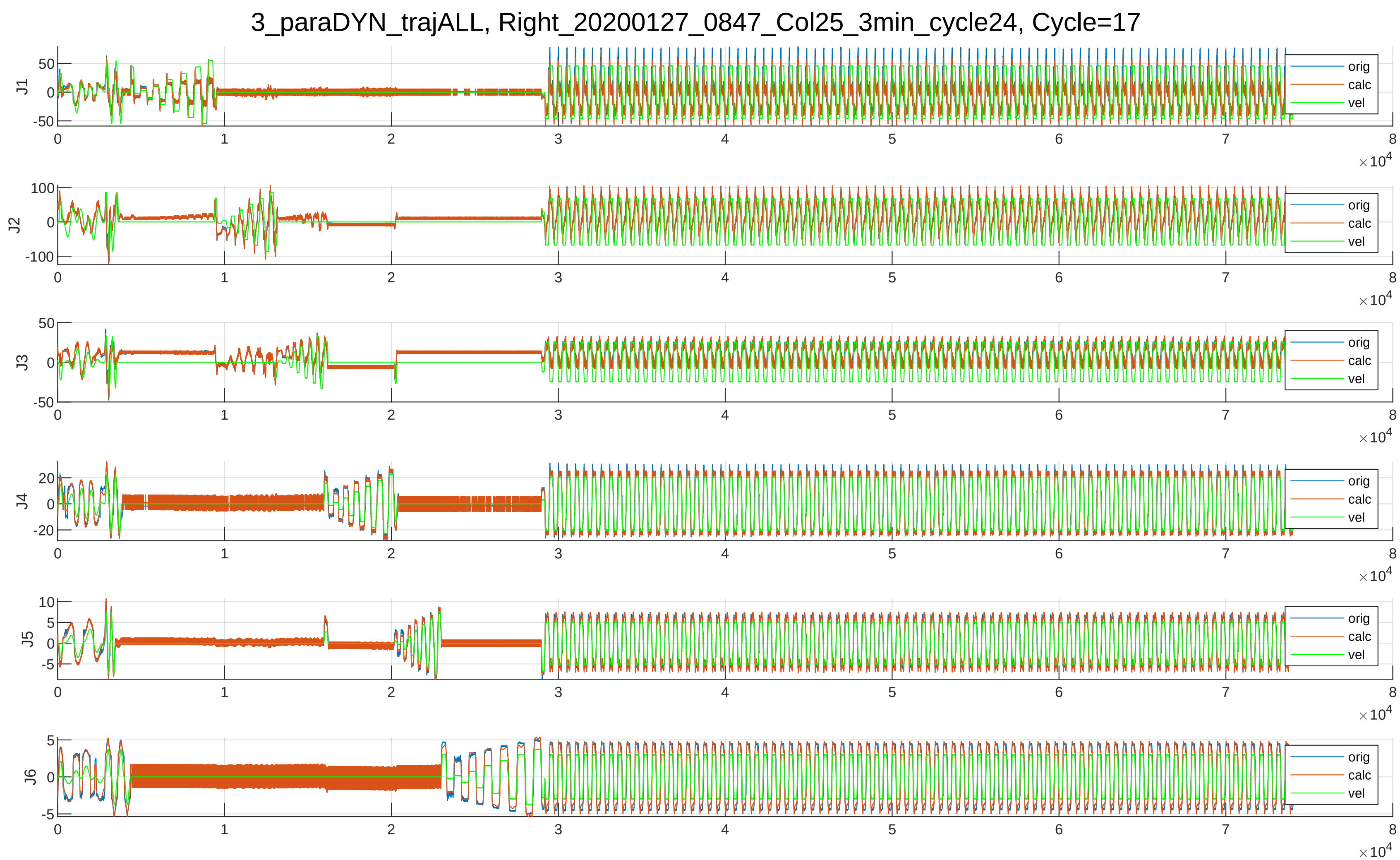

Figure L.17: The identification results of the all trajectory stage in the 17$^{\text{th}}$ cycle of Robot 2

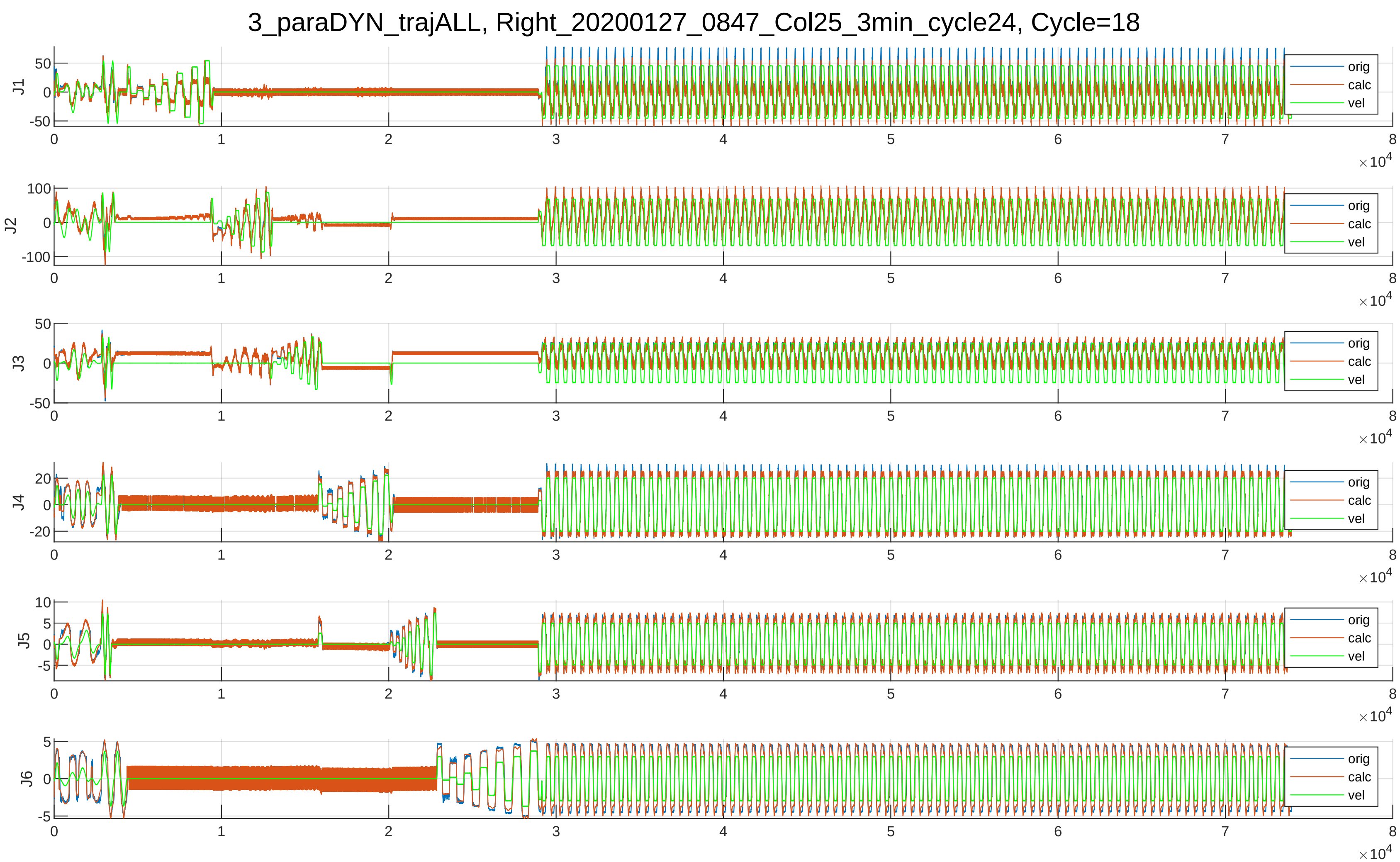

Figure L.18: The identification results of the all trajectory stage in the 18th cycle of Robot 2

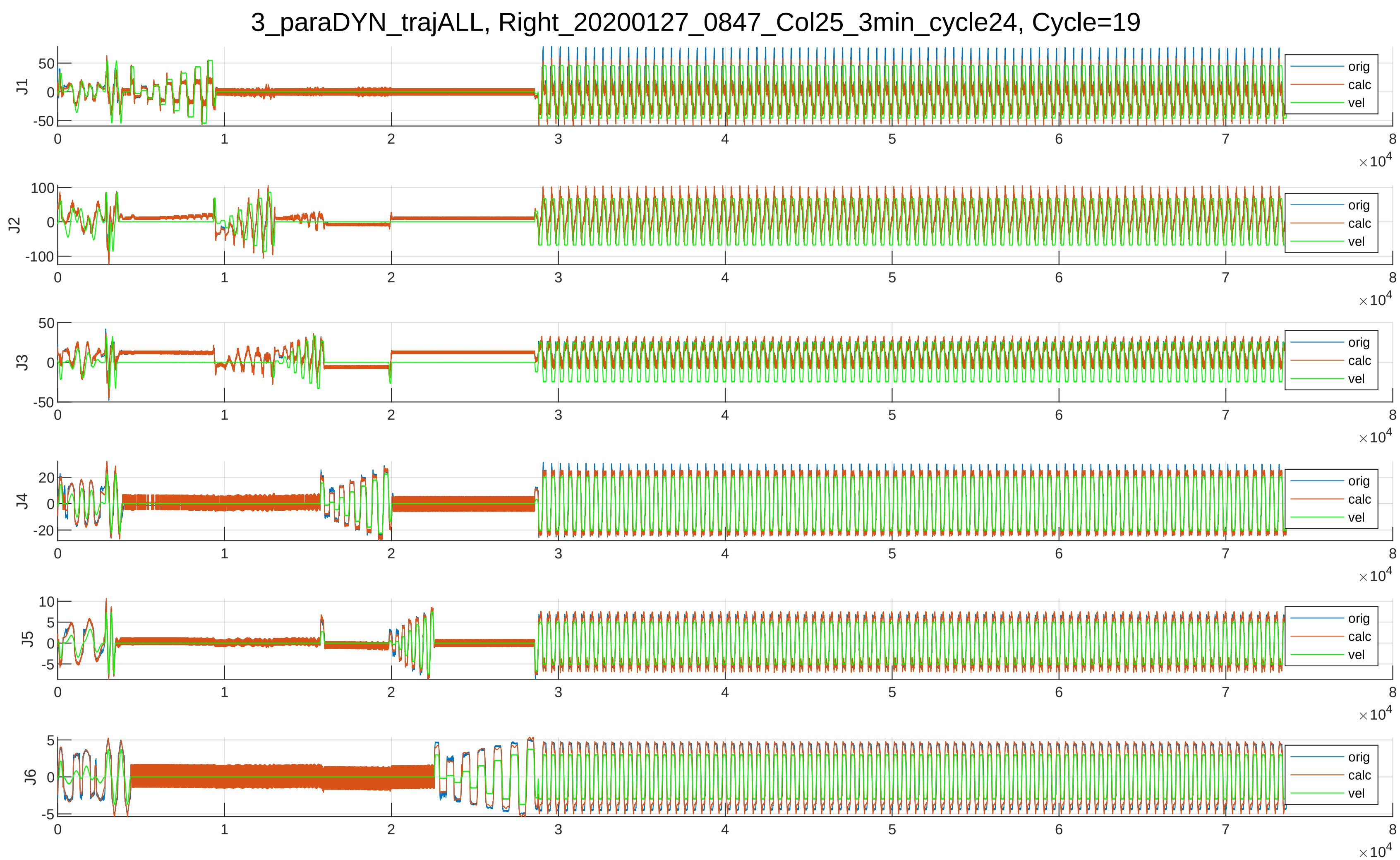

Figure L.19: The identification results of the all trajectory stage in the 19$^{\text{th}}$ cycle of Robot 2

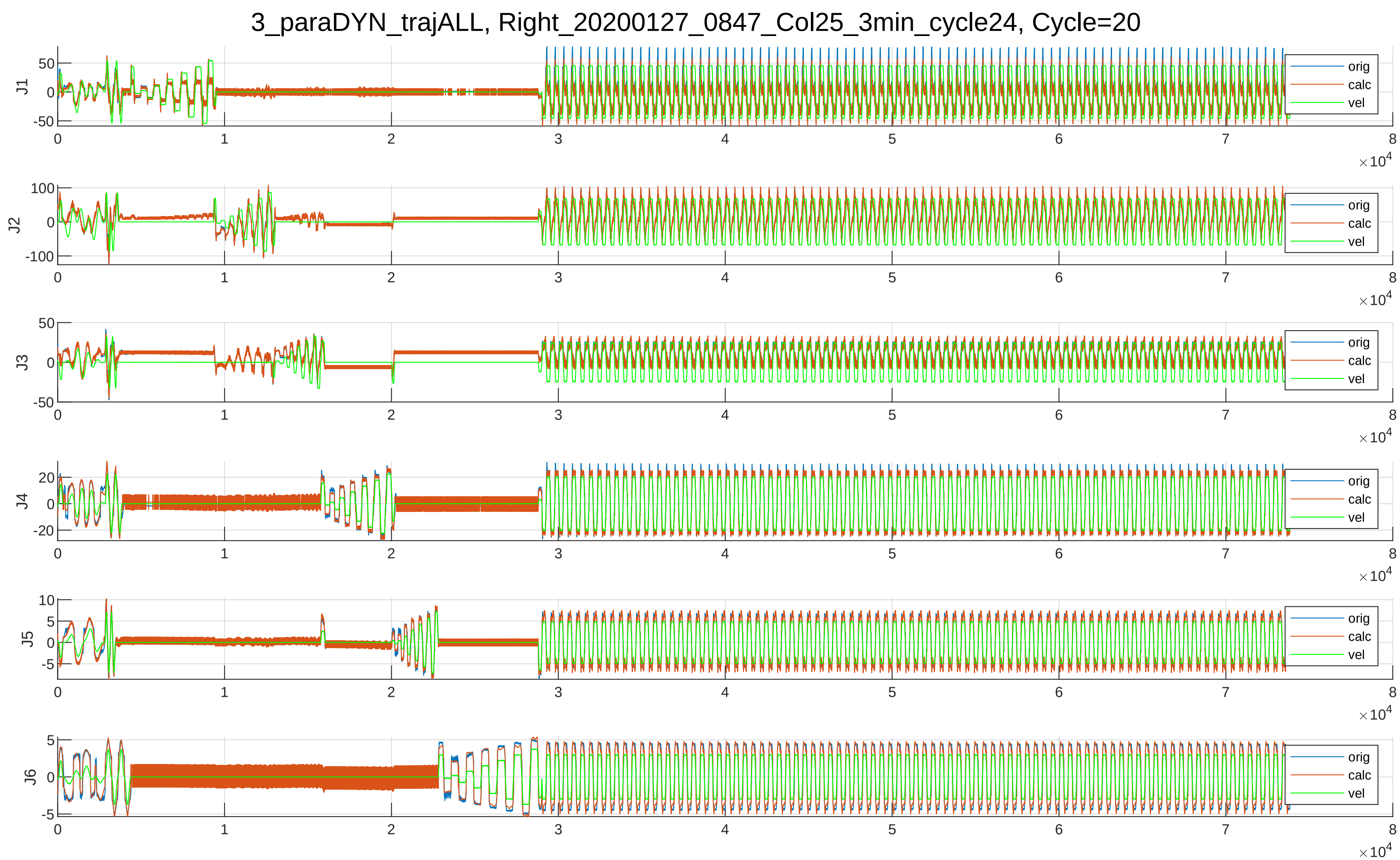

Figure L.20: The identification results of the all trajectory stage in the 20th cycle of Robot 2

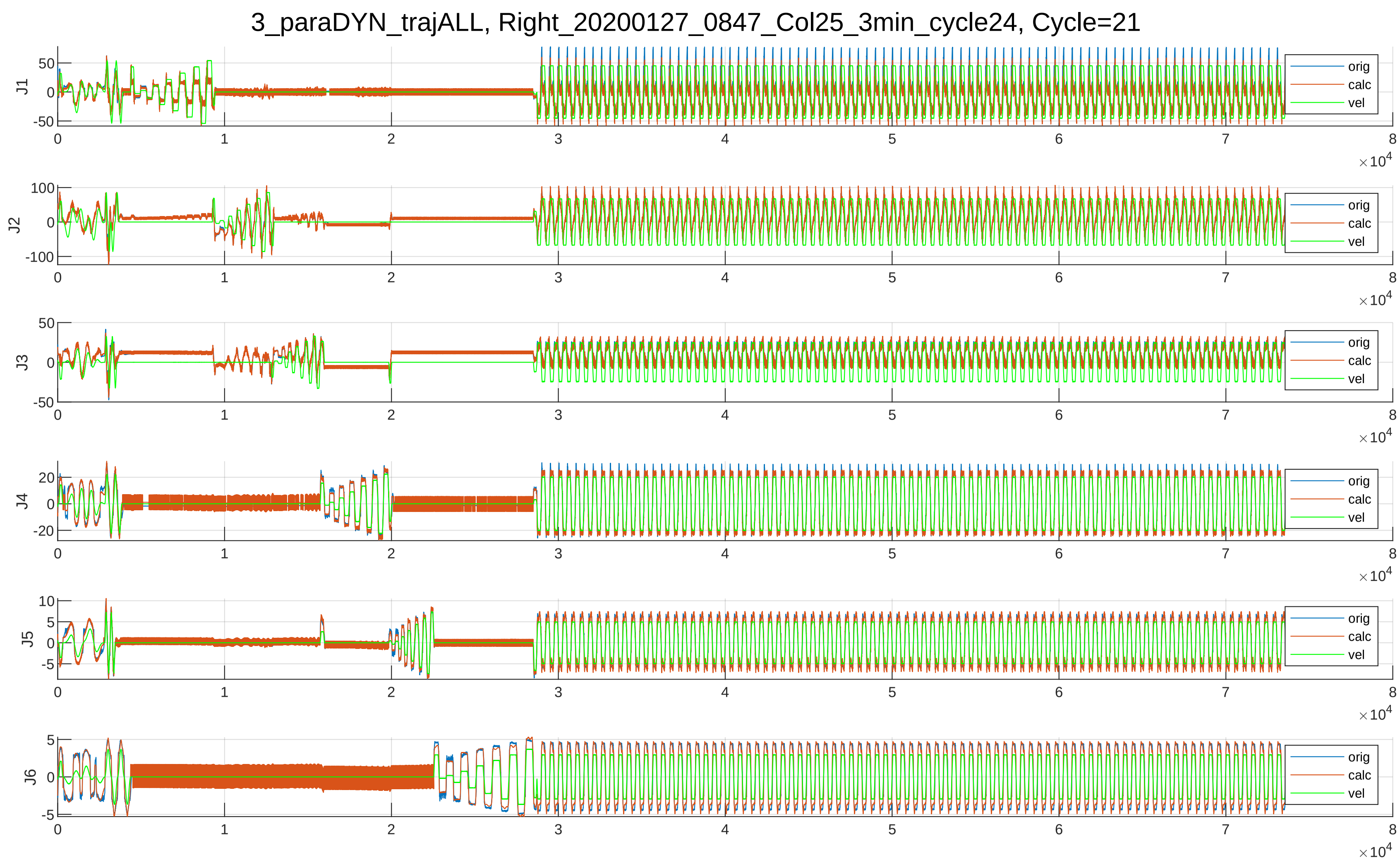

Figure L.21: The identification results of the all trajectory stage in the 21^{st} cycle of Robot 2

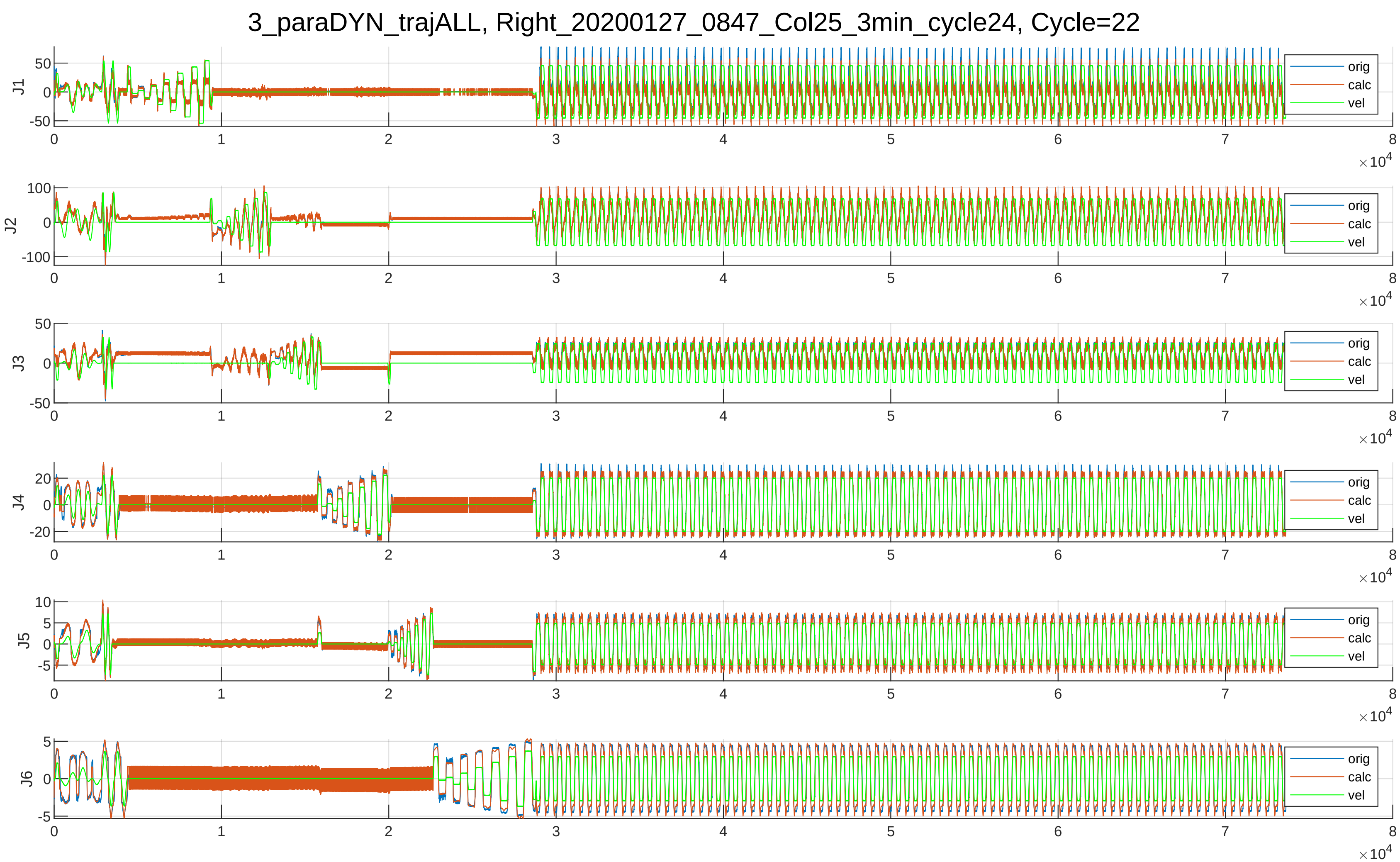

Figure L.22: The identification results of the all trajectory stage in the 22^{nd} cycle of Robot 2

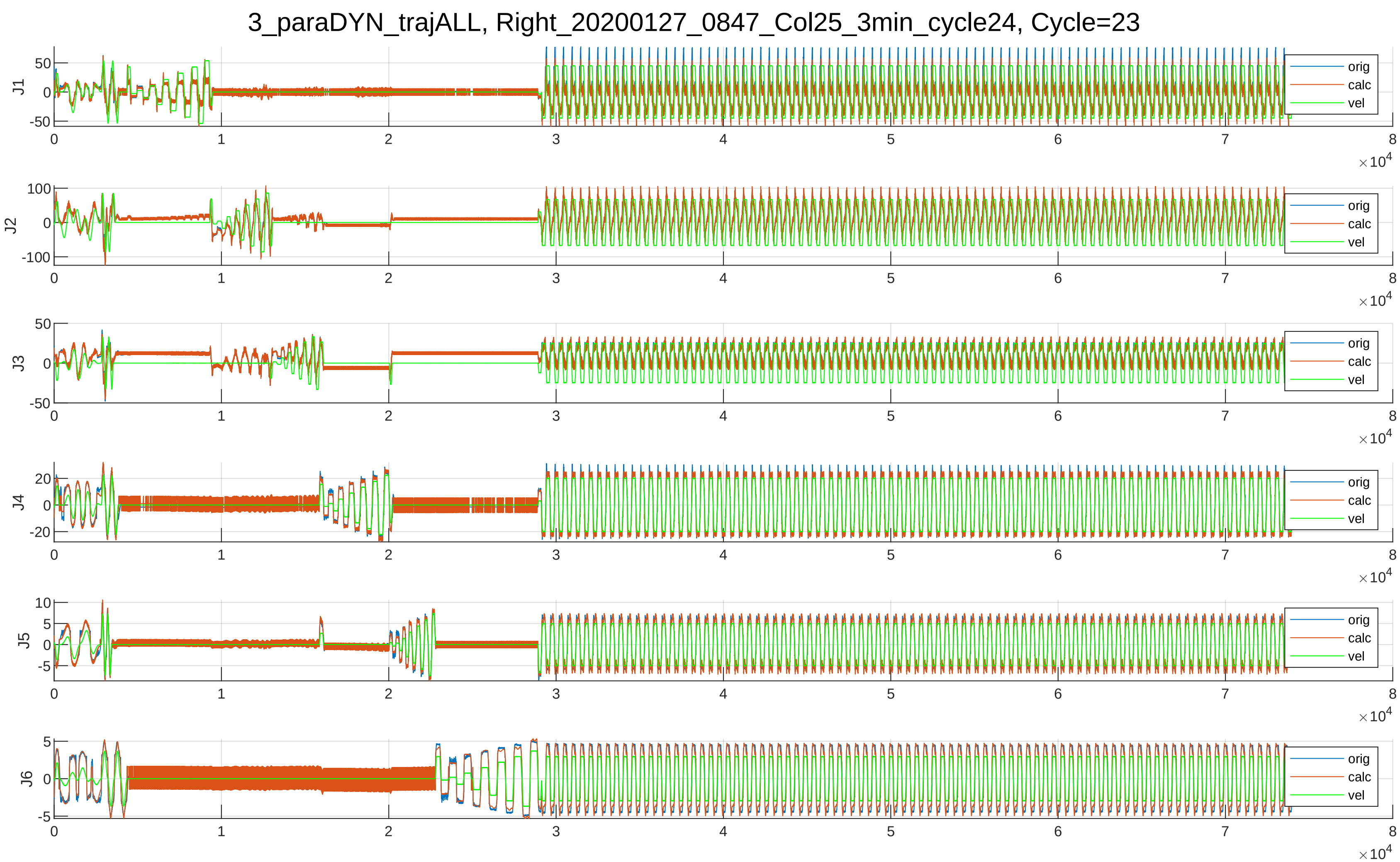

Figure L.23: The identification results of the all trajectory stage in the 23rd cycle of Robot 2

Appendix M

The Friction Measurement

In this appendix, the figures represent the plots of friction measurement of all tests. It should be pointed that all plots come from the data obtain with the velocity of 60%, and the plots of Joint 2 and 3 are shown without the gravity effect. The related discussions are presented in Section 5.2.2.

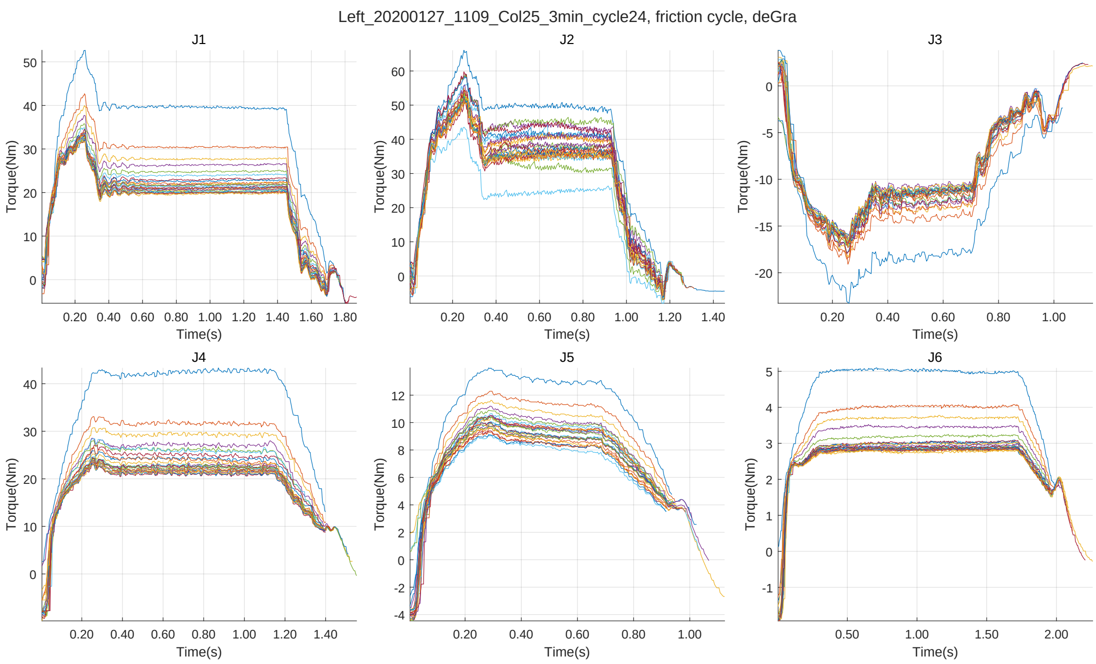

Figure M.1: The friction measurement results of the Test 1 of the Robot 1

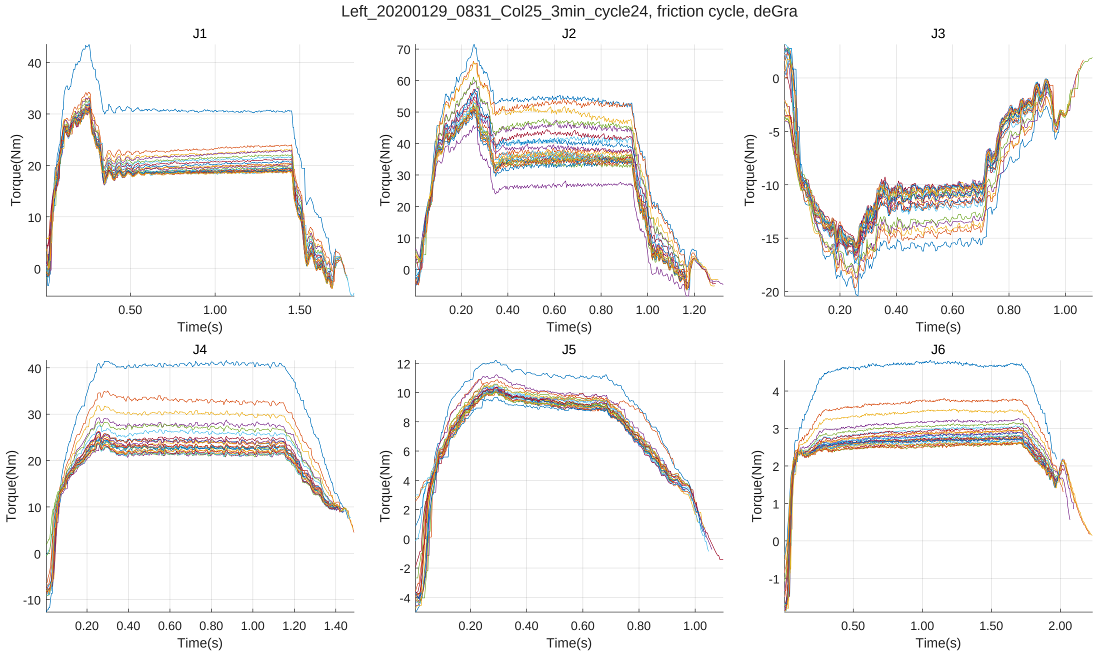

Figure M.2: The friction measurement results of the Test 2 of the Robot 1

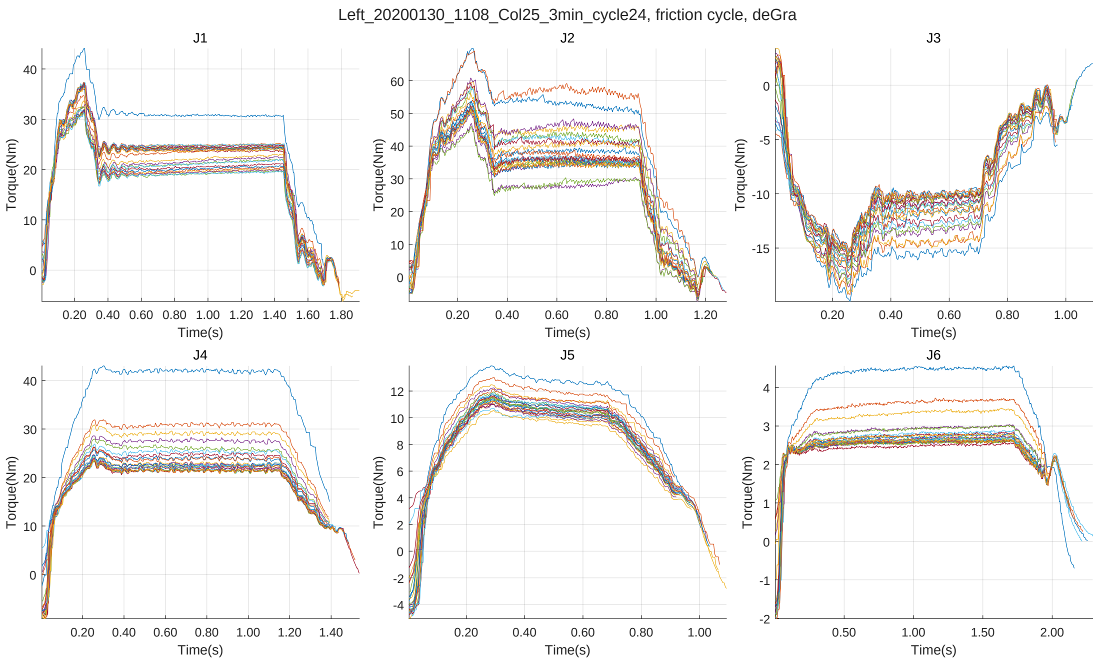

Figure M.3: The friction measurement results of the Test 3 of the Robot 1

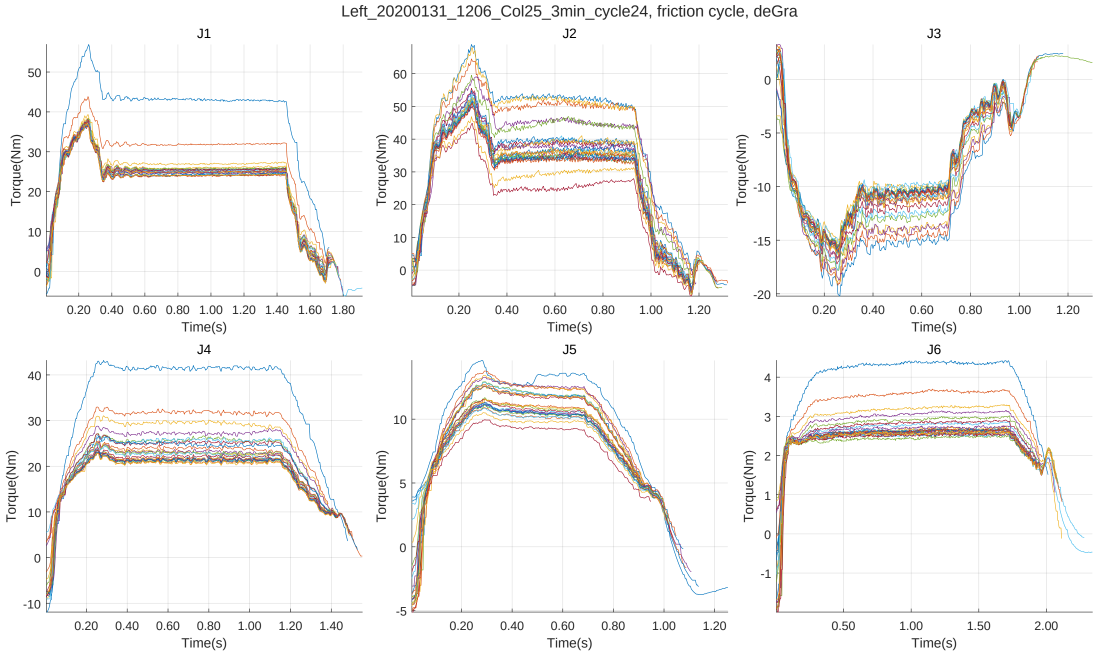

Figure M.4: The friction measurement results of the Test 4 of the Robot 1

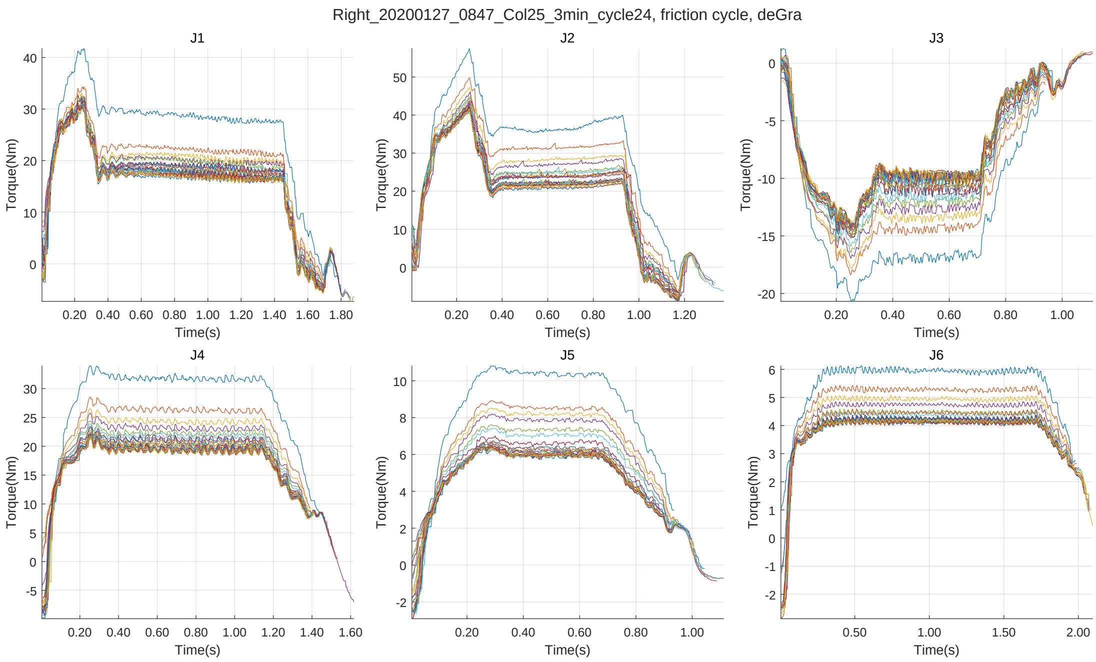

Figure M.5: The friction measurement results of the Test 1 of the Robot 2

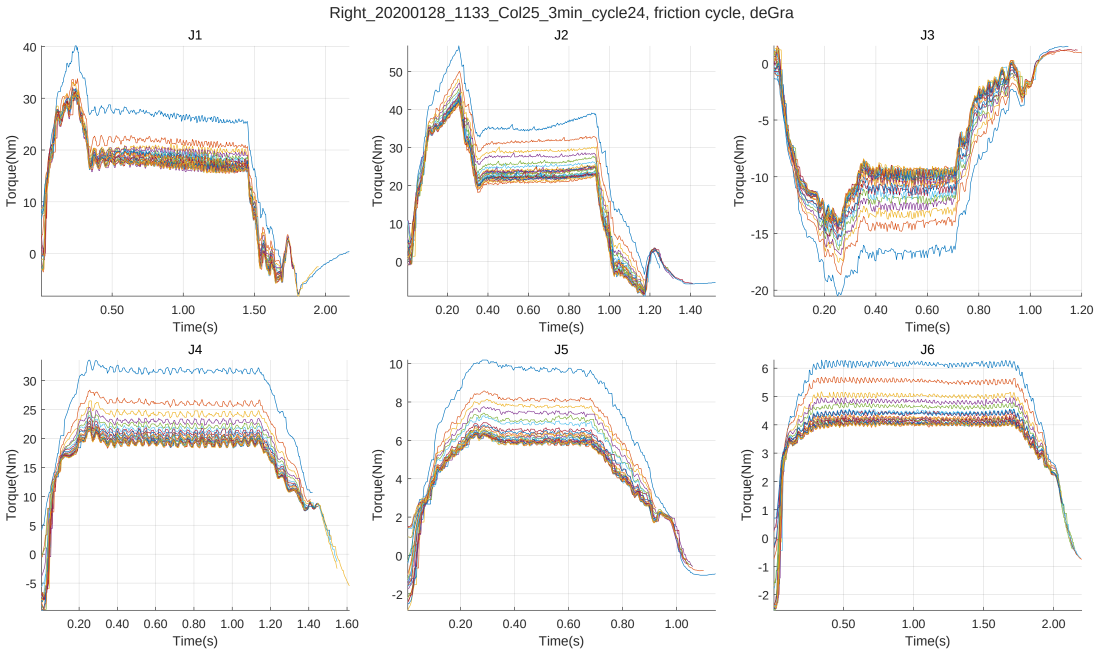

Figure M.6: The friction measurement results of the Test 2 of the Robot 2

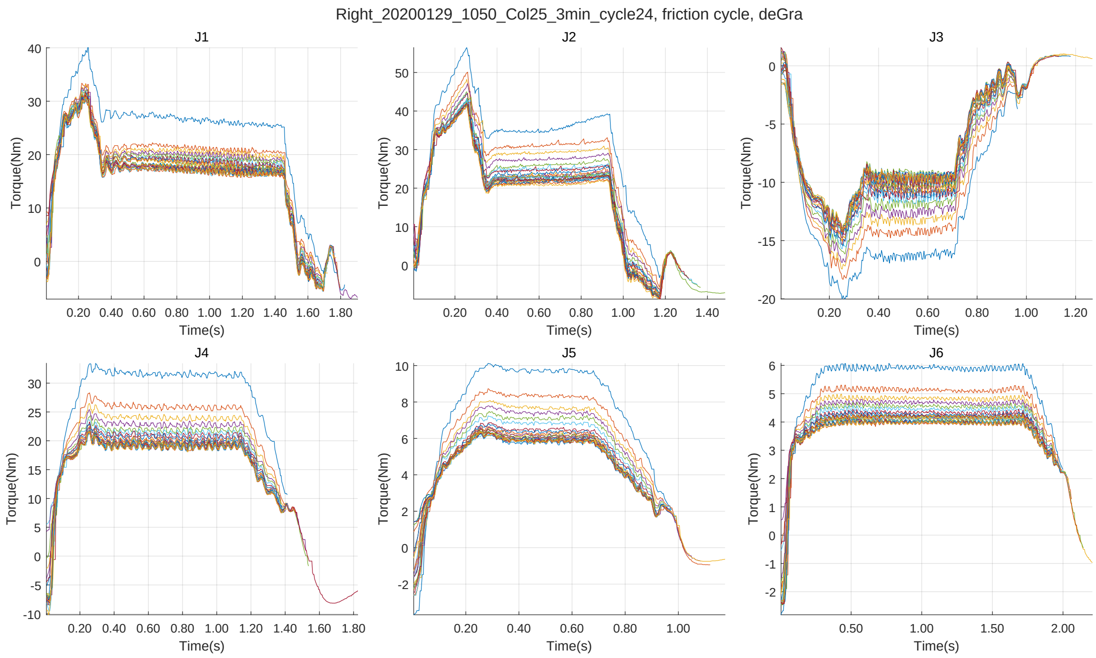

Figure M.7: The friction measurement results of the Test 3 of the Robot 2

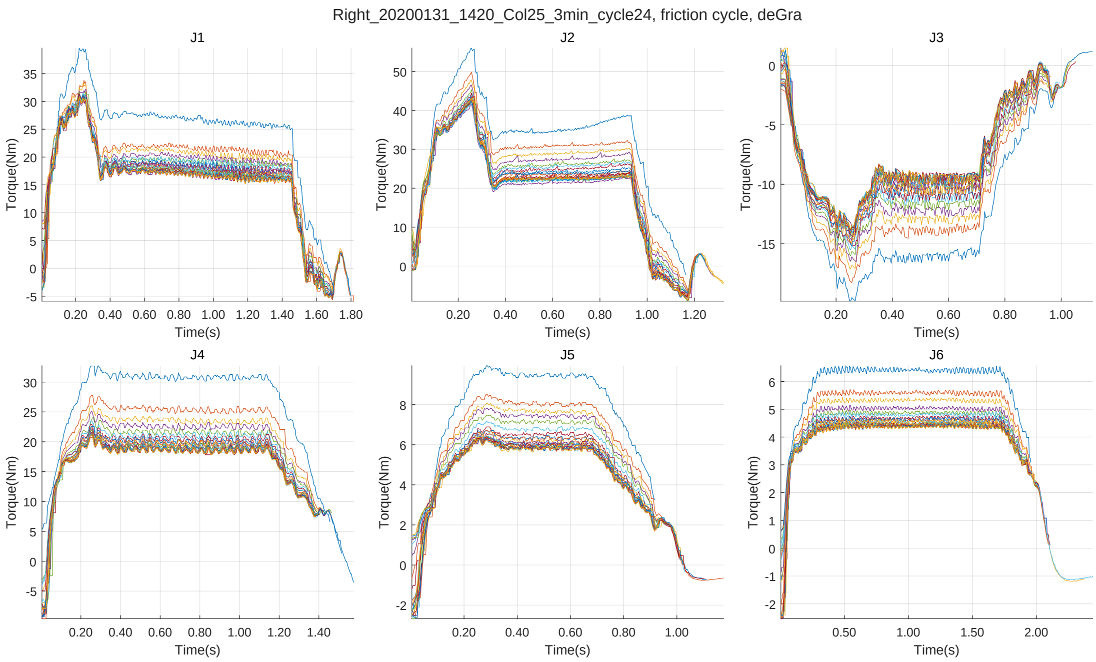

Figure M.8: The friction measurement results of the Test 4 of the Robot 2

Appendix N

The Curve Fitting Results Of Fiction Measurement

This appendix shows the figures and tables of the curve fitting results of all tests. They are listed and separated based on the robot used. It should be pointed that all figures and tables in this appendix come from the data obtain with the velocity of 60%. Moreover, the curve fitting results of the mixed data are provided. The related discussions are presented in Section 5.2.4.

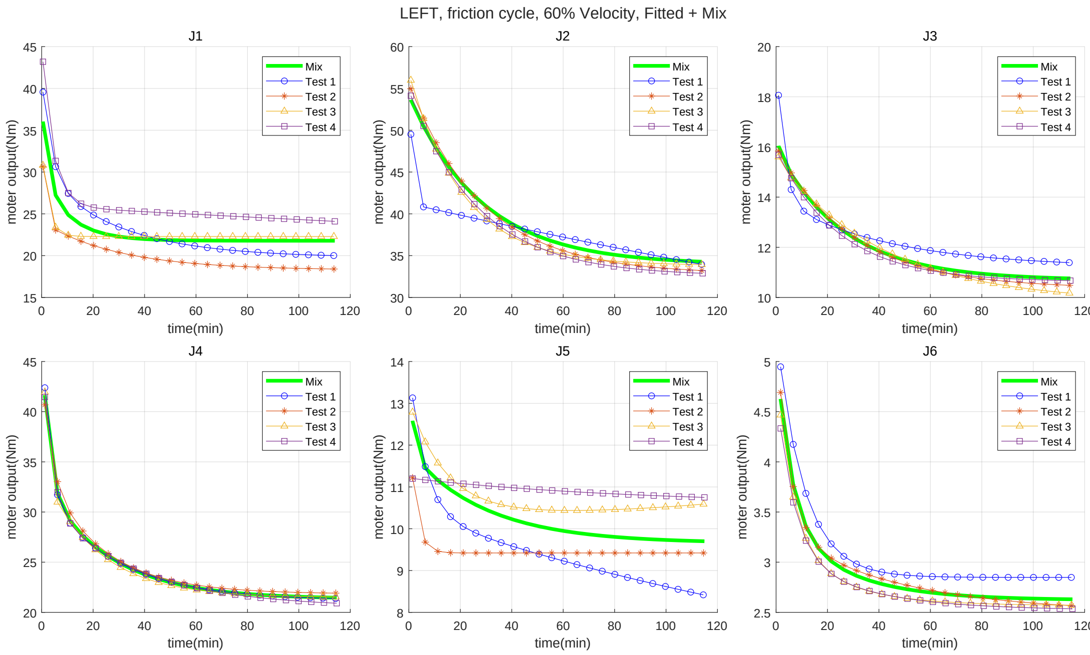

Figure N.1: The curve fitting results of Robot 1, the curve fitting results of the mixed data are included

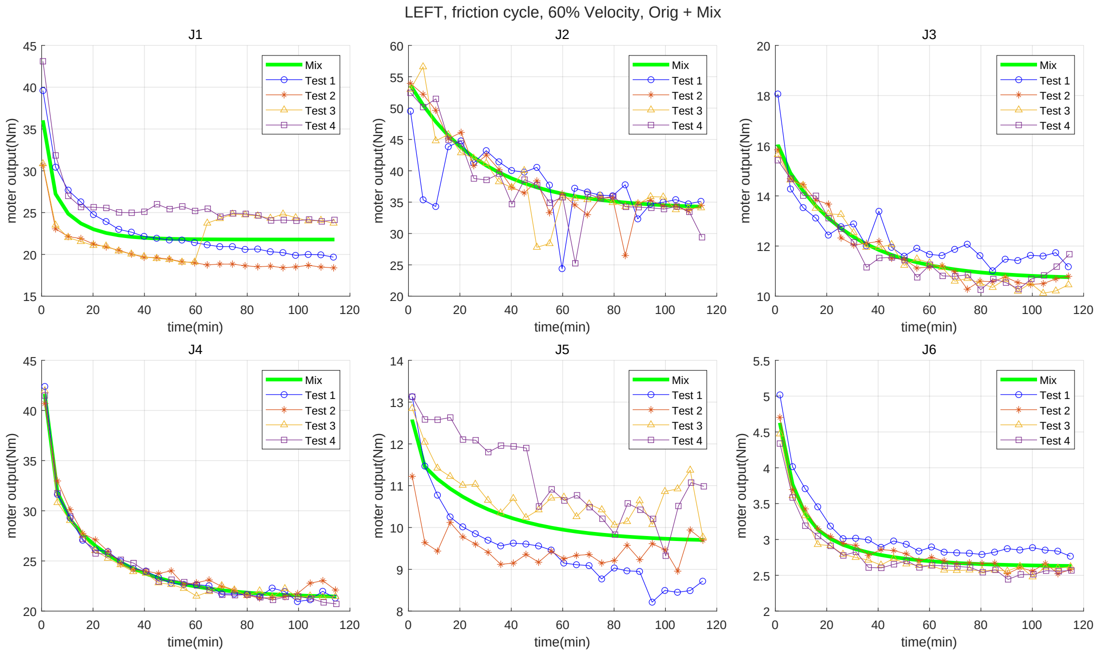

Figure N.2: The friction measure results of Robot 1, the curve fitting results of the mixed data are included

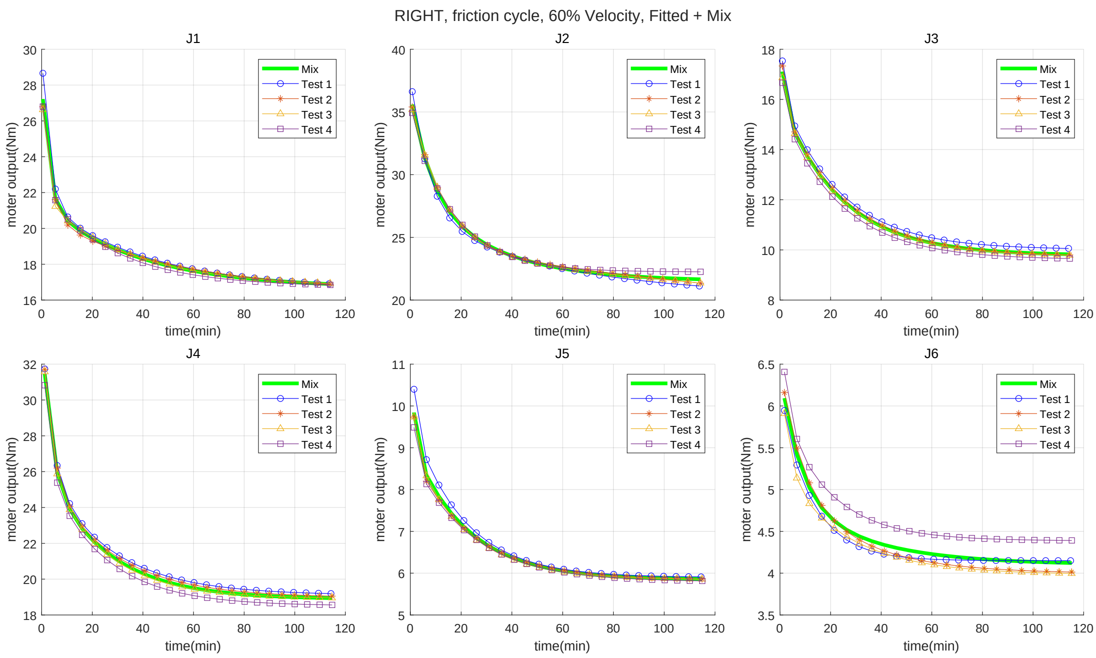

Figure N.3: The curve fitting results of Robot 2, the curve fitting results of the mixed data are included

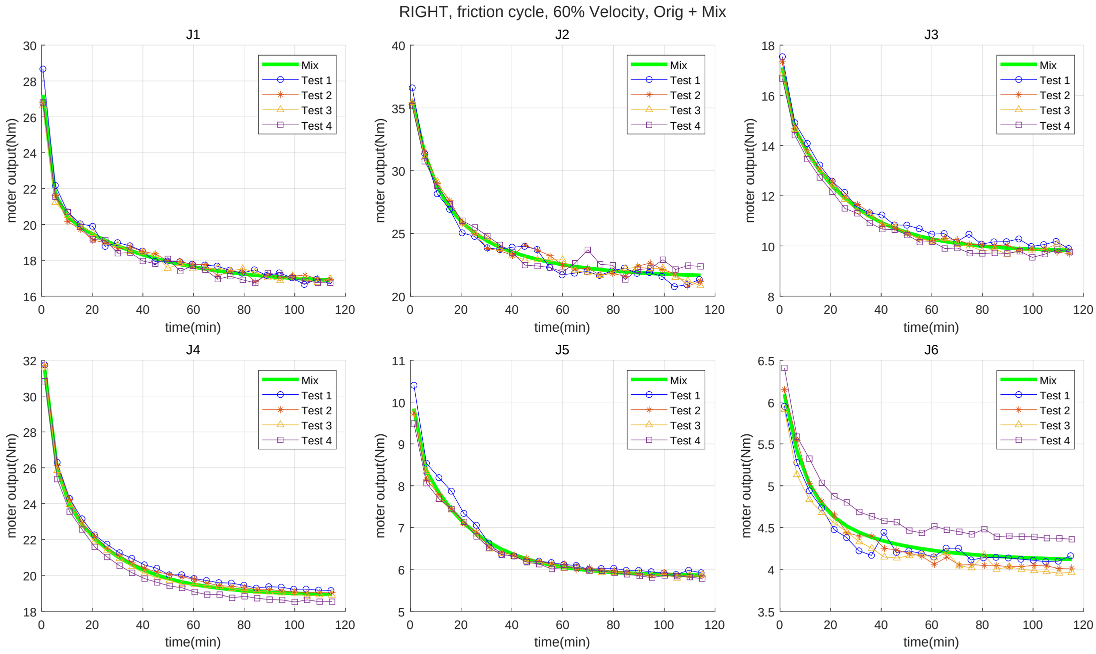

Figure N.4: The friction measure results of Robot 2, the curve fitting results of the mixed data are included

Table N.1: The coefficient values of curve fitting results based the data of velocity 60%

		Robot 1					Robot 2				
		a	b	t_1	c	t_2	a	b	t_1	c	t_2
J1	Test 1	19.77026	9.73214	0.03265	11.67983	0.26982	16.60894	4.87445	0.02442	8.56154	0.34612
	Test 2	18.27142	5.74287	0.03330	16.97301	1.91256	16.43789	4.23503	0.01983	7.13872	0.30589
	Test 3	22.28989	10.40884	0.41645	0.00075	0.62944	16.73945	4.91514	0.02848	6.72405	0.58940
	Test 4	0.00010	25.90156	0.00063	19.41412	0.23147	16.74283	5.34110	0.03470	6.11869	0.49903
	Mix	21.78051	7.69488	0.09112	8.58167	0.44921	16.66632	4.76634	0.02673	7.04924	0.38493
J2	Test 1	0.00061	41.22656	0.00171	91.01516	3.15342	20.25689	6.46293	0.01768	11.05555	0.13452
	Test 2	32.79851	22.73072	0.03497	0.02162	0.03537	1.22552	22.78061	0.00109	12.10573	0.07892
	Test 3	1.38558	32.43925	0.00000	22.95347	0.04728	11.58601	12.10697	0.00188	12.18326	0.07421
	Test 4	32.57238	22.17582	0.03723	0.59863	21.84848	22.23717	12.31519	0.05791	15.24718	3.74801
	Mix	33.28272	0.63420	0.00000	20.26215	0.03546	21.49307	7.59125	0.03352	7.37318	0.12803
J3	Test 1	11.20058	2.72219	0.02342	5.89466	0.35741	10.01373	6.35484	0.04344	8.42142	1.85479
	Test 2	10.36020	5.60232	0.03338	2.53509	4.12087	9.73987	6.28627	0.04018	8.05008	1.75232
	Test 3	9.79920	5.71317	0.02393	4.23101	3.12396	9.73268	6.16768	0.04148	2.08807	0.58102
	Test 4	10.62322	5.26603	0.04107	1.33444	7.31144	9.61073	6.09544	0.04280	2.10070	0.59052
	Mix	10.68824	5.26739	0.03766	3.15259	2.56492	9.77537	6.23555	0.04202	2.92480	0.82751
J4	Test 1	21.19655	11.06320	0.03591	16.84452	0.37939	19.10495	7.17766	0.03863	7.98374	0.26564
	Test 2	21.83026	12.48219	0.04392	9.99550	0.29249	18.96849	7.21557	0.03879	8.13319	0.27017
	Test 3	21.47913	12.67422	0.04701	128.49383	2.24793	18.90628	7.82414	0.04458	7.87270	0.33366
	Test 4	20.49632	10.61168	0.02832	15.25196	0.28822	18.50941	7.93419	0.04381	7.39567	0.35792
	Mix	21.32332	11.72613	0.03905	14.66988	0.39107	18.87610	7.54541	0.04150	7.79821	0.30128
J5	Test 1	5.45197	4.93189	0.00444	3.51922	0.16437	5.89756	3.85085	0.04930	19.59727	2.13811
	Test 2	9.42068	3.12297	0.39177	4.89889	4.33250	5.84252	3.11477	0.04363	17.04609	1.99486
	Test 3	10.24828	0.05854	-0.01534	2.73915	0.06943	5.84192	3.25441	0.04718	1.72386	0.49068
	Test 4	10.57930	0.66012	0.01167	-0.02900	0.02265	5.79326	3.07698	0.04302	14.80664	2.04065
	Mix	9.65410	2.19311	0.03346	2.20435	0.67999	5.84707	3.34512	0.04628	6.96687	1.45718
J6	Test 1	2.84830	2.47387	0.09353	8.47239	7.29263	4.14913	1.92346	0.07792	33.80185	3.22148
	Test 2	2.49551	0.80493	0.02117	1.97865	0.18930	3.99559	1.16797	0.03625	1.32515	0.12231
	Test 3	2.56731	0.69286	0.04451	1.66920	0.16200	3.98294	1.27476	0.03925	1.23148	0.29293
	Test 4	2.52090	0.59806	0.03237	1.62864	0.15007	4.38703	1.55022	0.05083	1.08628	0.33498
	Mix	2.62189	0.81188	0.03963	1.69208	0.17465	4.09768	0.82804	0.03083	1.51205	0.12662

Appendix O

The Fiction And Velocities

This appendix shows the figures of friction versus velocities in different cycles of all tests, which is discussed in Section 5.2.3. In these plots, the sequence of curves from the 1st cycle to the end cycle is marked with an arrow from the “cold” to “hot” state.

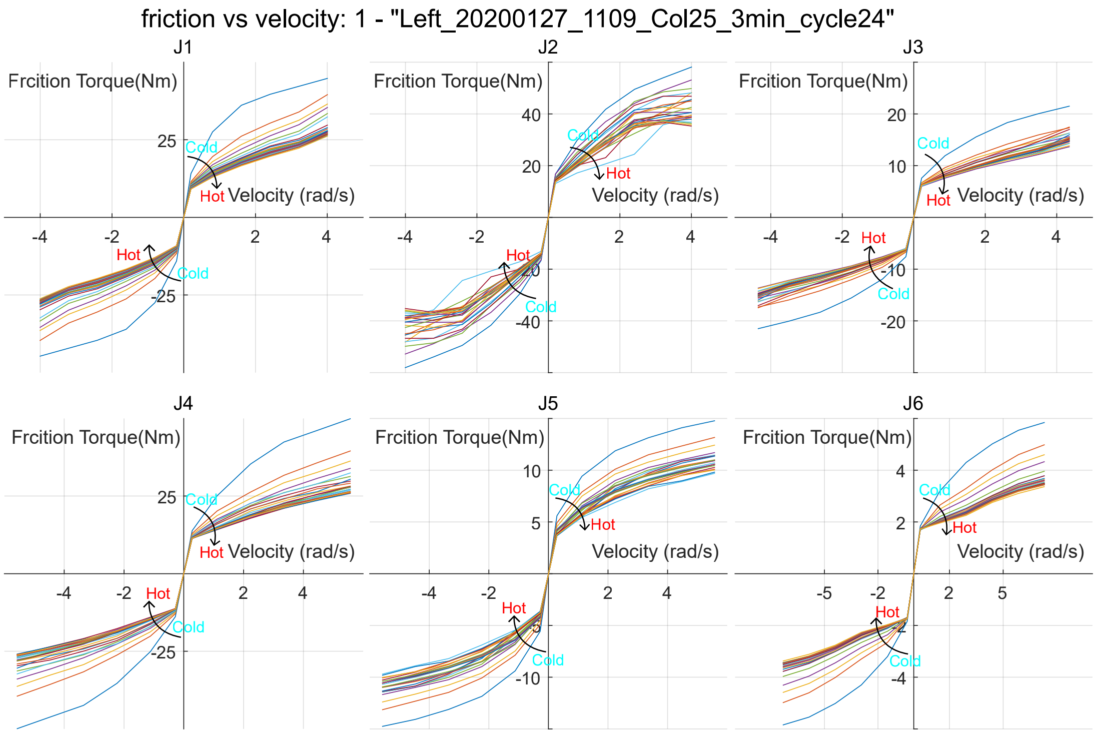

Figure O.1: The friction versus velocities in diffident cycles of all joints of Test 1 of Robot 1

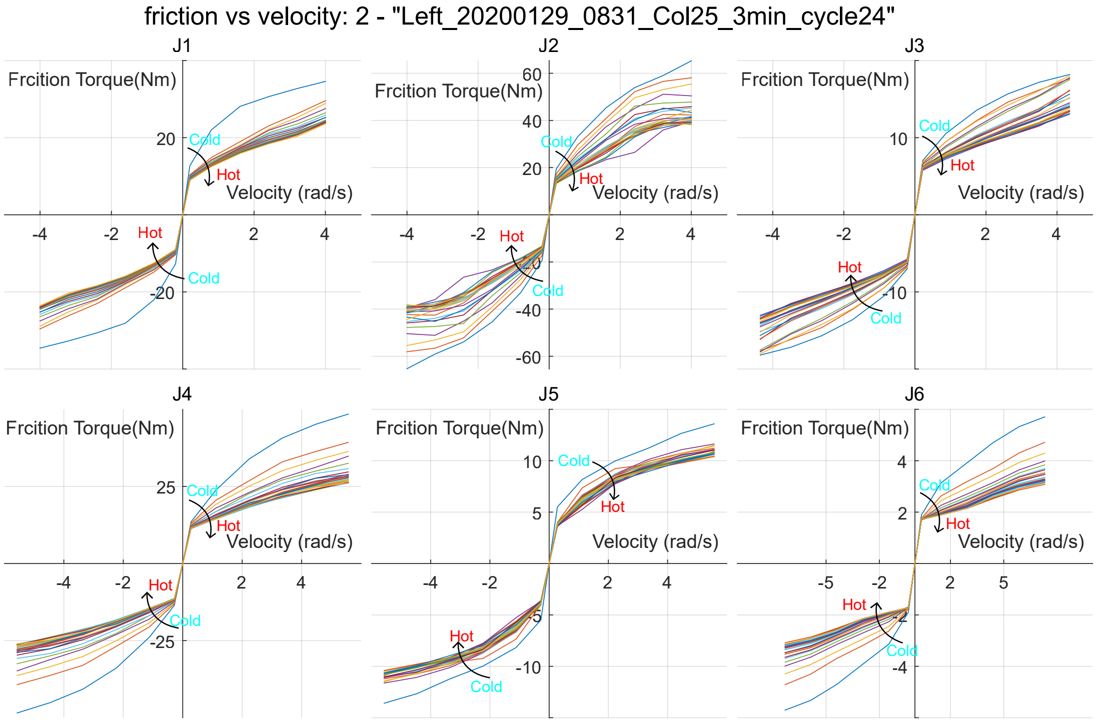

Figure O.2: The friction versus velocities in diffident cycles of all joints of Test 2 of Robot 1

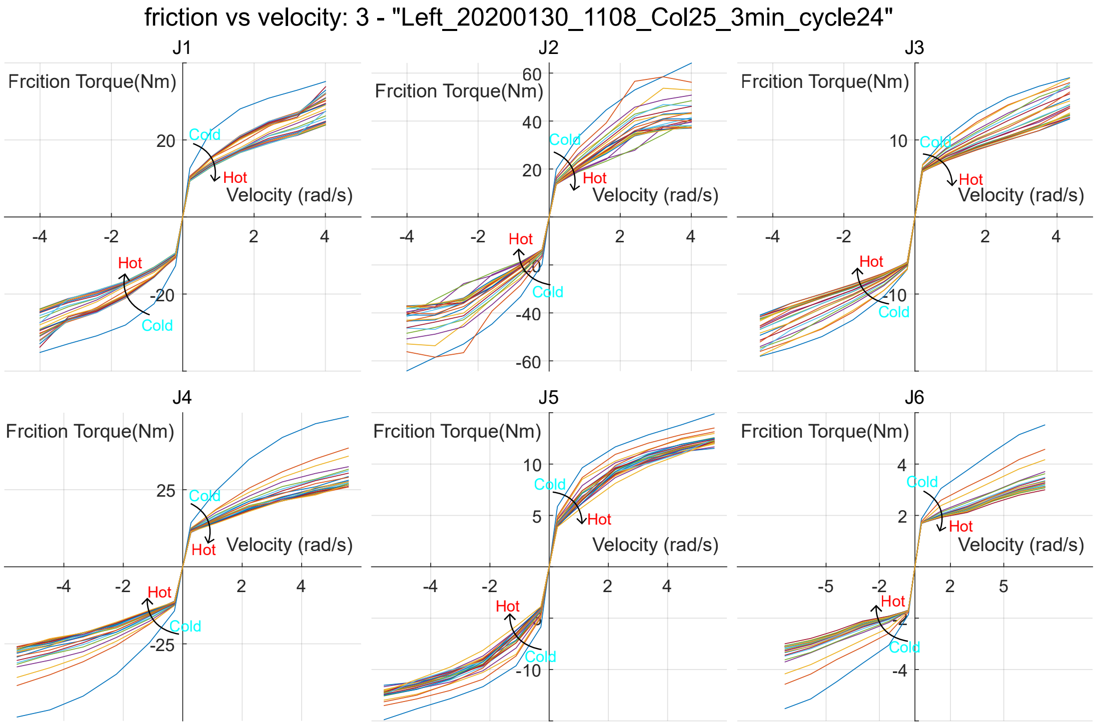

Figure O.3: The friction versus velocities in diffident cycles of all joints of Test 3 of Robot 1

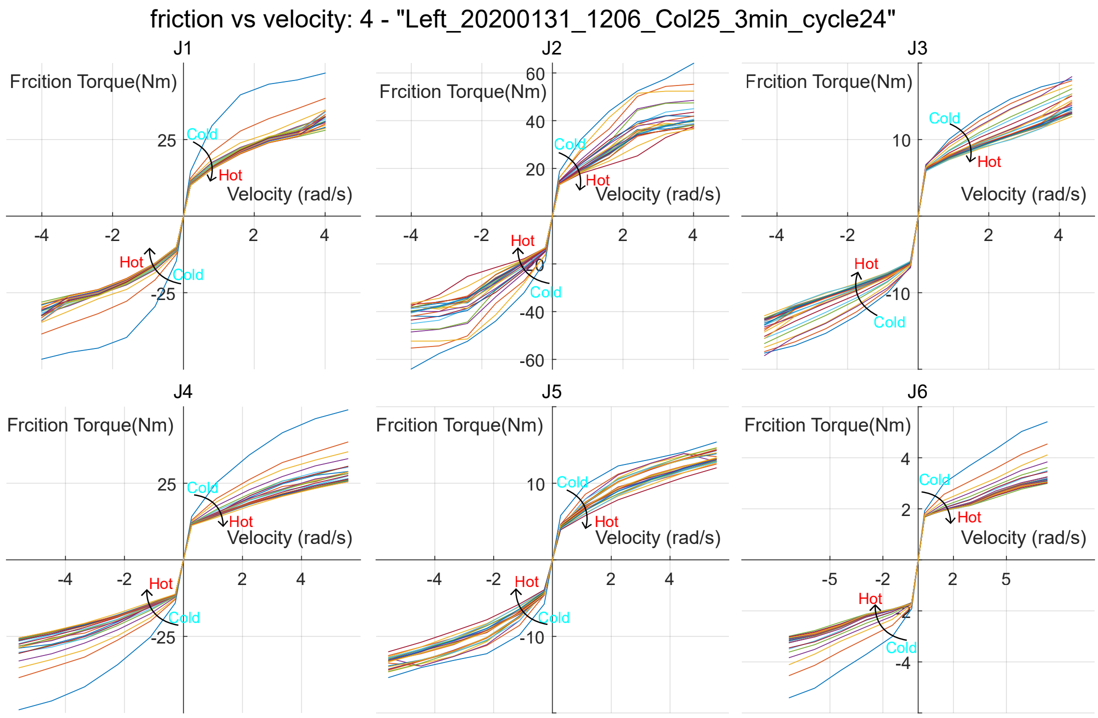

Figure O.4: The friction versus velocities in diffident cycles of all joints of Test 4 of Robot 1

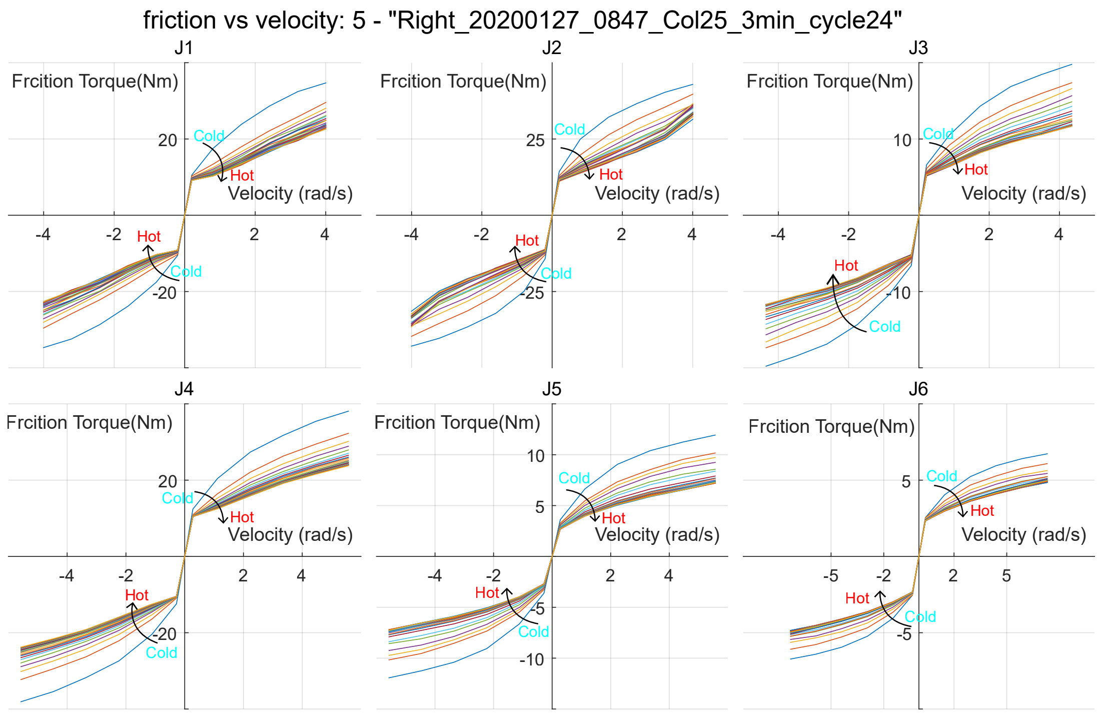

Figure O.5: The friction versus velocities in diffident cycles of all joints of Test 1 of Robot 2

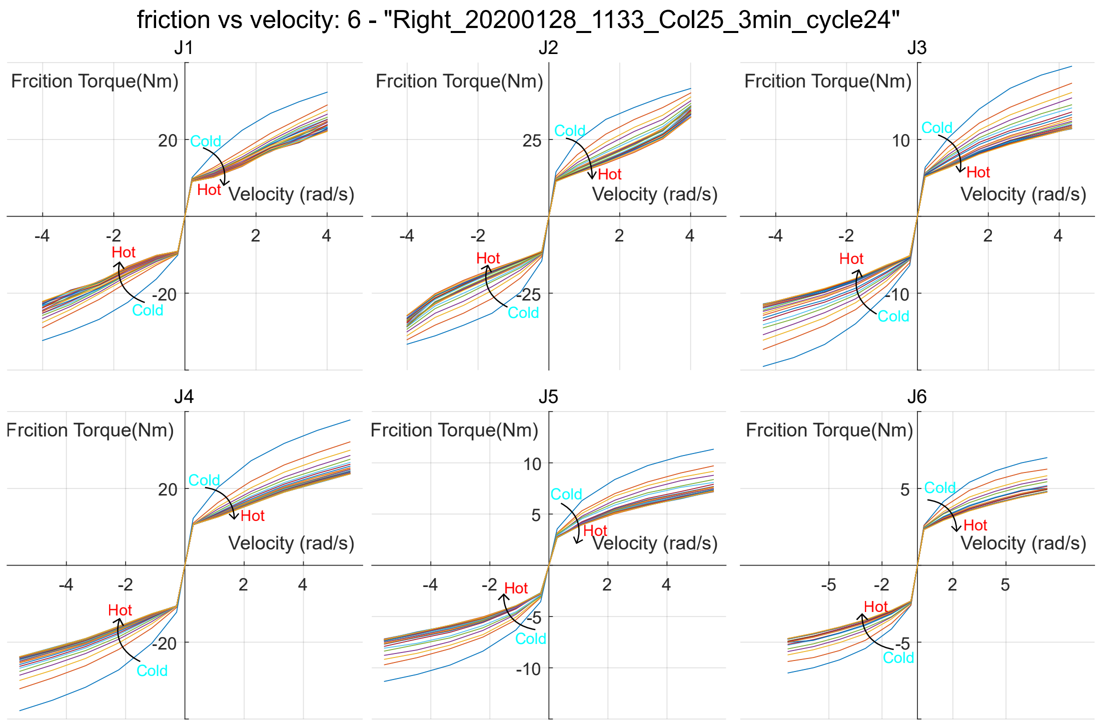

Figure O.6: The friction versus velocities in diffident cycles of all joints of Test 2 of Robot 2

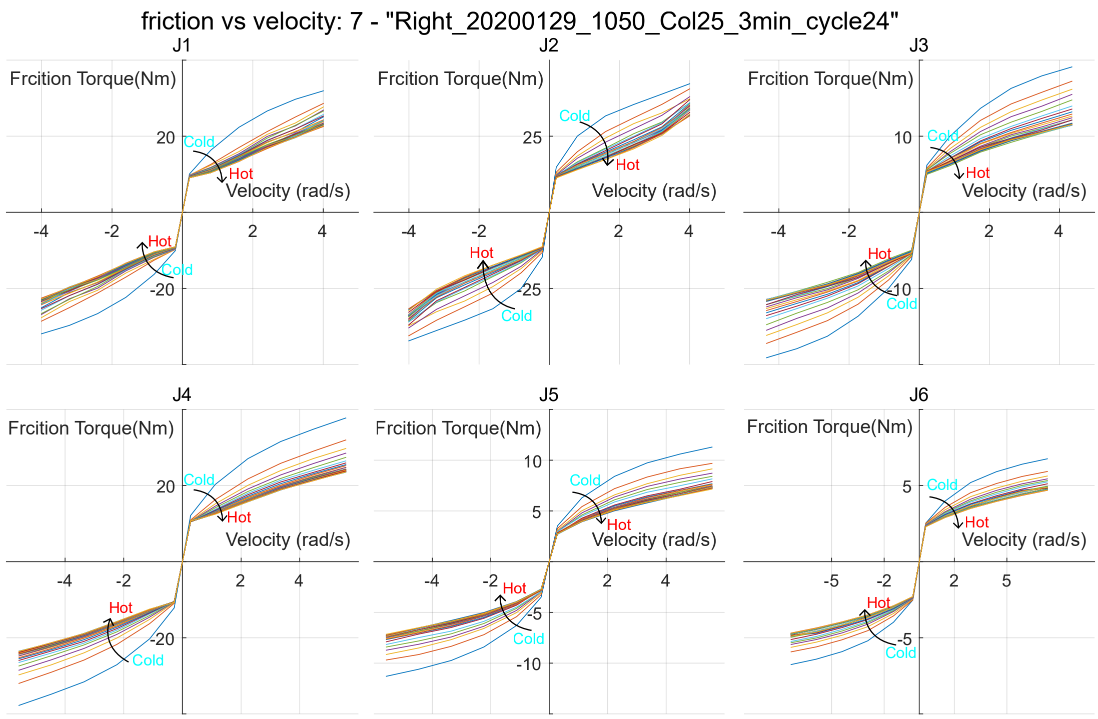

Figure O.7: The friction versus velocities in diffident cycles of all joints of Test 3 of Robot 2

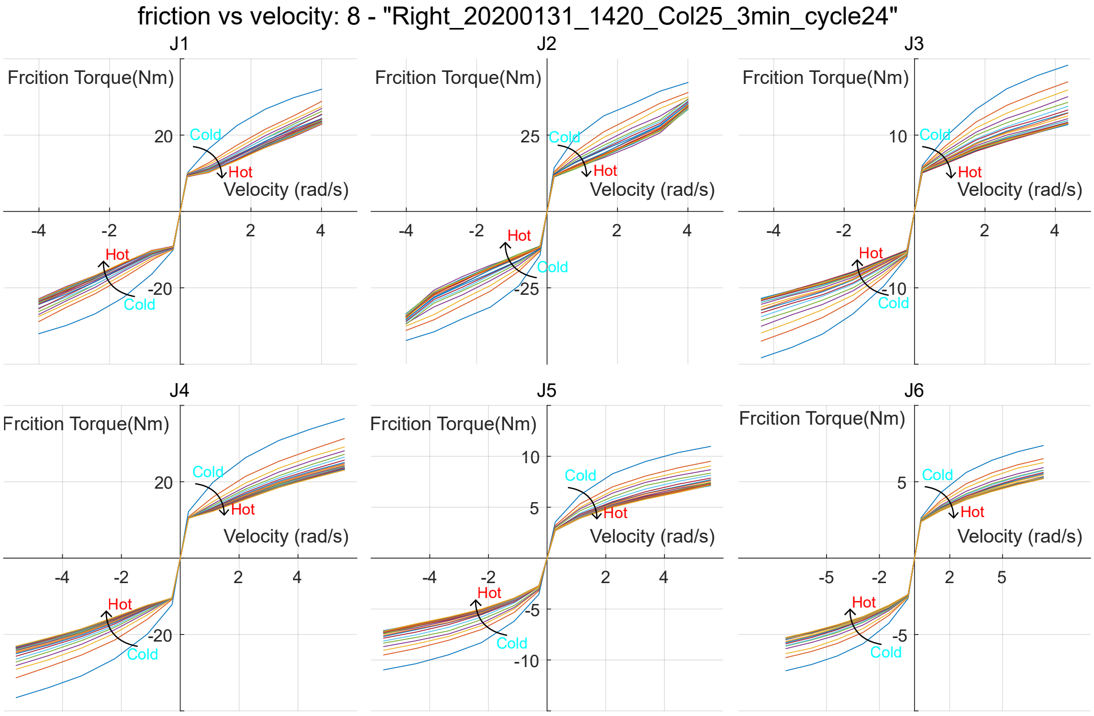

Figure O.8: The friction versus velocities in diffident cycles of all joints of Test 4 of Robot 2